UNITED STATES AIR FORCE

SUMMER FACULTY RESEARCH PROGRAM

1986

PROGRAM MANAGEMENT REPORT

UNIVERSAL ENERGY SYSTEMS, INC.

VOLUME 2 of 3

PROGRAM DIRECTOR, U.E.S.
RODNEY C. DARRAH

PROGRAM ADMINISTRATOR, U.E.S.
SUSAN K. ESPY

PROGRAM MANAGER, A.F.O.S.R.
MAJOR RICHARD KORKA

SUBMITTED TO

AIR FORCE OFFICE OF SCIENTIFIC RESEARCH

BOLLING AIR FORCE BASE

WASHINGTON, DC

DECEMBER 1986

SECURITY CLASSIFICATION OF THIS PAGE

AD-A202 789

(1)

REPORT DOCUMENTATION PAGE

1a. REPORT SECURITY CLASSIFICATION UNCLASSIFIED	1b. RESTRICTIVE MARKINGS
2a. SECURITY CLASSIFICATION AUTHORITY	3. DISTRIBUTION/AVAILABILITY OF REPORT APPROVED FOR PUBLIC RELEASE; Distribution Unlimited
2b. DECLASSIFICATION/DOWNGRADING SCHEDULE	
4. PERFORMING ORGANIZATION REPORT NUMBER(S)	5. MONITORING ORGANIZATION REPORT NUMBER(S) AFOSR-TR- 87-0308
6a. NAME OF PERFORMING ORGANIZATION Universal Energy Systems, Inc 6b. OFFICE SYMBOL (If applicable)	7a. NAME OF MONITORING ORGANIZATION AFOSR/XOT
6c. ADDRESS (City, State and ZIP Code) 4401 Dayton-Xenia Road Dayton, OH 45432	7b. ADDRESS (City, State and ZIP Code) Building 410 Bolling AFB, DC 20332-6448
8a. NAME OF FUNDING/SPONSORING ORGANIZATION AFOSR 8b. OFFICE SYMBOL (If applicable) XOT	9. PROCUREMENT INSTRUMENT IDENTIFICATION NUMBER F49620-85-C-0013
8c. ADDRESS (City, State and ZIP Code) Building 410 Bolling AFB, DC 20332	10. SOURCE OF FUNDING NOS. PROGRAM ELEMENT NO.: 61102F PROJECT NO.: 3396 TASK NO.: D5 WORK UNIT NO.:
11. TITLE (Include Security Classification) USAF Summer Faculty Research Program - Volume 2 - 1986 Program Management Report	
12. PERSONAL AUTHOR(S) Rodney C. Darrah, Susan K. Espy	
13a. TYPE OF REPORT Annual 13b. TIME COVERED FROM _____ TO _____	14. DATE OF REPORT (Yr., Mo., Day) December 1986 15. PAGE COUNT
16. SUPPLEMENTARY NOTATION	
17. COSATI CODES FIELD / GROUP / SUB. GR.	18. SUBJECT TERMS (Continue on reverse if necessary and identify by block number)
19. ABSTRACT (Continue on reverse if necessary and identify by block number) See Attached	
20. DISTRIBUTION/AVAILABILITY OF ABSTRACT UNCLASSIFIED/UNLIMITED XX SAME AS RPT. ☐ DTIC USERS ☐	21. ABSTRACT SECURITY CLASSIFICATION UNCLASSIFIED
22a. NAME OF RESPONSIBLE INDIVIDUAL Major Richard W. Kopka, Program Manager	22b. TELEPHONE NUMBER (Include Area Code) 202-767-4970 22c. OFFICE SYMBOL XOT

89 1 23 007

DD FORM 1473, 83 APR EDITION OF 1 JAN 73 IS OBSOLETE

88 12 28 064

SECURITY CLASSIFICATION OF THIS PAGE

USAF SUMMER FACULTY RESEARCH PROGRAM - 1986

The United States Air Force Summer Faculty Research Program - (USAF-SFRP) is a program designed to introduce university, college, and technical institute faculty members to Air Force research. This is accomplished by the faculty member being selected on a nationally advertised, competitive basis for a ten-week assignment during the summer intersession period to perform research at Air Force laboratories/centers and research activities. Each assignment is in a subject area and at an Air Force facility mutually agreed upon by the faculty member and the Air Force. In addition to compensation and travel, cost of living allowances are also paid. The USAF-SFRP is sponsored by the Air Force Office of Scientific Research, Air Force Systems Command, United States Air Force, and is conducted by Universal Energy Systems, Inc.

The specific objectives of the 1986 USAF-SFRP are:

(1) To provide a productive means for scientists and engineers holding advanced degrees to participate in research at various Air Force research activities;

(2) To stimulate continuing professional association among the scholars and their professional peers in the Air Force;

(3) To further the research objectives of the United States Air Force;

(4) To enhance the research productivity and capabilities of scientists and engineers especially as these relate to Air Force technical interests.

During the summer of 1986, 158 faculty members participated in the USAF-SFRP. These researchers were assigned to approximately 25 USAF laboratories/centers and research activities across the country. A Management Report along with a three volume Technical Report consisting of a compilation of the final reports written by the assigned faculty members describing their summer research efforts is provided by the contractor, Universal Energy Systems.

UNITED STATES AIR FORCE

SUMMER FACULTY RESEARCH PROGRAM

1986

PROGRAM TECHNICAL REPORT

UNIVERSAL ENERGY SYSTEMS, INC.

VOLUME II of III

Program Director, UES
Rodney C. Darrah

Program Administrator, UES
Susan K. Espy

Program Manager, AFOSR
Major Richard Kopka

Submitted to

Air Force Office of Scientific Research

Bolling Air Force Base

Washington, DC

December 1986

TABLE OF CONTENTS

PREFACE

The United States Air Force Summer Faculty Research Program (USAF-SFRP) is a program designed to introduce university, college, and technical institute faculty members to Air Force research. This is accomplished by the faculty members being selected on a nationally advertised competitive basis for a ten-week assignment during the summer intersession period to perform research at Air Force laboratories/centers. Each assignment is in a subject area and at an Air Force facility mutually agreed upon by the faculty members and the Air Force. In addition to compensation, travel and cost of living allowances are also paid. The USAF-SFRP is sponsored by the Air Force Office of Scientific Research, Air Force Systems Command, United States Air Force, and is conducted by Universal Energy Systems, Inc.

The specific objectives of the 1986 USAF-SFRP are:

(1) To provide a productive means for Scientists and Engineers holding Ph.D. degrees to participate in research at the Air Force Weapons Laboratory;

(2) To stimulate continuing professional association among the Scholars and their professional peers in the Air Force;

(3) To further the research objectives of the United States Air Force;

(4) To enhance the research productivity and capabilities of Scientists and Engineers especially as these relate to Air Force technical interests.

During the summer of 1986, 158-faculty members participated. These researchers were assigned to 25 USAF laboratories/centers across the country. This three volume document is a compilation of the final reports written by the assigned faculty members about their summer research efforts.

Pg. xxxix

LIST OF 1986 PARTICIPANTS

LIST OF PARTICIPANTS

NAME/ADDRESS	DEGREE, SPECIALTY, LABORATORY ASSIGNED
Dr. John E. Ahlquist Assistant Professor Dept. of Meteorology Florida State University Tallahassee, FL 32306-3034 (904) 644-1558.	Degree: Ph.D., Meteorology, 1981 Specialty: Meteorology Assigned: AFGL
Dr. Rasphal S. Ahluwalia Associate Professor Dept. of Industrial Eng. West Virginia University Morgantown, WV (304) 293-4607	Degree: Ph.D., Systems Eng., 1977 Specialty: Systems Engineering Assigned: AAMRL
Dr. David R. Anderson Assistant Professor Dept. of Chemistry University of Colorado Austin Bluffs Parkway Colorado Springs, CO 80907 (303) 570-9578	Degree: Ph.D., Organic Chemistry, 1978 Specialty: Organic Chemistry Assigned: FJSRL
Dr. David M. Barnhart Professor Dept. of Physical Sciences Eastern Montana College 1500 North 30th Street Billings, MT 59101-0298 (406) 657-2028	Degree: Ph.D., Chemistry, 1964 Specialty: Chemistry Assigned: FJSRL
Dr. Frank P. Battles Professor Mass. Maritime Academy Basic Science Dept. Buzzards Bay, MA 02532 (617) 224-8388	Degree: Ph.D., Physics, 1969 Specialty: Physics Assigned: AFGL
Dr. Georges A. Becus Associate Professor University of Cincinnati Aero. Engineering and Engineering Mechanics Cincinnati, OH 45221 (513) 475-6115	Degree: Ph.D., Engineering Science, 1973 Specialty: Engineering Services Assigned: FDL

Dr. Rex L. Berney
Associate Professor
University of Dayton
Physics Department
300 College Park
Dayton, OH 45469
(513) 299-3012 or 299-2311

Degree: Ph.D., Solid State Physics, 1978
Specialty: Solid State Physics
Assigned: AL

Dr. Albert W. Biggs
Professor
University of Alabama
in Huntsville
Electrical Engineering
Engineering Bldg 263-B
(ECE Dept.)
Huntsville, AL 35899
(205) 895-6459

Degree: Ph.D., Electrical Engineering, 1965
Specialty: Electrical Engineering
Assigned: WL

Dr. Phillip A. Bishop
Assistant Professor
Director of Human Performance
Laboratory
The University of Alabama
P O Box 1967
Area of HPER
University, AL 35486
(205) 348-8370

Degree: Ed.D., Exercise Physiology, 1983
Specialty: Exercise Physiology
Assigned: SAM

Dr. Patricia T. Boggs
Assistant Professor
of Management Science
Wright State University
Dayton, OH 45435
(513) 873-2080 or 2290

Degree: D.B.A., Decision Science, 1984
Specialty: Decision Science
Assigned: HRL/LR

Dr. James A. Brown
Assistant Professor
Tougaloo College
c/o History Dept.
Tougaloo, MS 39174
(601) 957-3623

Degree: M.A., History, 1966
Specialty: History
Assigned: WL

Dr. Clifford G. Burgess
Assistant Professor
Univ. of Southern Mississippi
Computer Science Department
Sou. Station Box 5106
Hattiesburg, MS 39406
(601) 266-4949

Degree: Ph.D., Computer Science, 1985
Specialty: Computer Science
Assigned: SAM

Dr. Jeffrey D. Camm
Assistant Professor
University of Cincinnati
Quantitative Analysis/IS
ML #130
Cincinnati, OH 45221
(513) 475-3621

Degree: Ph.D., Management Science, 1984
Specialty: Management Science
Assigned: BRMC

Dr. Thomas A. Carney
Assistant Professor
Dept. of Meteorology
Florida State University
404 Love Building
Tallahassee, FL 32306
(904) 644-6806

Degree: Ph.D., Meteorology, 1984
Specialty: Meteorology
Assigned: ESC

Dr. George D. Catalano
Associate Professor
Mechanical Engineeering Dept.
Louisiana State University
Baton Rouge, LA 70803-6413
(504) 388-5792

Degree: Ph.D., Aerospace Engineering, 1977
Specialty: Aerospace Engineering
Assigned: AD

Dr. Bor-Chin Chang
Assistant Professor
Electrical Engineering Dept.
Bradley University
Peoria, IL 61625
(309) 676-7611

Degree: Ph.D., Electrical Engineering, 1983
Specialty: Electrical Engineering
Assigned: FDL

Dr. Garvin Chastain
Associate Professor
Boise State University
Dept. of Psychology
1910 University Drive
Boise, ID 83704
(208) 385-2855

Degree: Ph.D., Human Experimental Psychology, 1976
Specialty: Human Experimental Psychology
Assigned: HRL/OT

Dr. Shive K. Chaturvedi
Assistant Professor
Civil Engineering
Ohio State University
470 Hitchcock Hall
Columbus, OH 43210
(614) 422-2617

Degree: Ph.D., Mechanical Engineering, 1979
Specialty: Mechanical Engineering
Assigned: ML

Dr. Hoffman H. Chen
Associate Professor
Grambling State University
Department of Chemistry
Grambling, LA 71245
(318) 274-2260

Degree: Ph.D., Organic Chemistry, 1976
Specialty: Mechanical Engineering
Assigned: SAM

Dr. Lea D. Chen
Assistant Professor
The University of Iowa
Dept. of Mechanical Eng.
Iowa City, IA 52242
(319) 353-5695

Degree: Ph.D., Mechanical Engineering, 1981
Specialty: Organic Chemistry
Assigned: APL

Dr. Wu C. Cheng
Associate Professor
Physics Department
Paine College
1235 Fifteenth Street
Augusta, GA 30910-2799
(404) 722-4471

Degree: Ph.D., Physical Chemistry, 1954
Specialty: Physical Chemistry
Assigned: FJSRL

Dr. John Y. Cheung
Associate Professor
University of Oklahoma
School of Electrical Eng.
and Computer Science
202 W. Boyd, Room 219
Oklahoma City, OK 73170
(405) 325-4324

Degree: Ph.D., Electrical Engineering, 1975
Specialty: Electrical Engineering
Assigned: AL

Dr. Derald Chriss
Assistant Professor
Southern University
Chemistry Dept.
Southern Branch P.O.
Baton Rouge, LA 70813
(504) 771-2000

Degree: M.A., Chemistry, 1981
Specialty: Physical and Analytical Chemistry
Assigned: ML

Dr. Wolfgang Christian
Assistant Professor
Dept. of Physics
Davidson College
Davidson, NC 28036
(704) 892-2000

Degree: Ph.D., Physics, 1975
Specialty: Physics
Assigned: AFGL

Dr. Jacob N. Chung
Associate Professor
Washington State University
Dept. of Mechanical Engineering
Pullman, WA 99164-2920
(509) 335-3222

Degree: Ph.D., Mechanical Engineering, 1979
Specialty: Mechanical Engineering
Assigned: APL

Dr. Brenda J. Claiborne
Assistant Professor
University of Texas,
San Antonio
Div. of Life Sciences
San Antonio, TX 78285
(512) 691-4458

Degree: Ph.D., Biology, 1981
Specialty: Biology
Assigned: SAM

Dr. Donald F. Collins
Physics Chairman
Warren Wilson College
Physics Department
Box 5117
701 Warren Wilson Road
Swannanoa, NC 28778
(704) 298-3325

Degree: Ph.D., Physics, 1970
Specialty: Physics
Assigned: AFGL

Dr. William T. Cooper
Assistant Professor
Chemistry Dept.
Florida State University
Tallahassee, FL 32306-3006
(904) 644-6875 or 644-3810

Degree: Ph.D., Chemistry, 1981
Specialty: Chemistry
Assigned: ESC

Dr. Richard H Cox
Professor
Kansas State University
Center for Human Motor
Performance
203 Ahearn
Manhattan, KS 66502
(913) 532-6765

Degree: Ph.D., Motor Learning and Control, 1973
Specialty: Motor Learning & Control
Assigned: HRL/MO

Dr. William Day
Associate Professor
Dept. of Computer Science
and Engineering
Auburn University
244 Payne Street
Auburn, AL 36830
(205) 826-4330

Degree: Ph.D., Mathematics, 1969
Specialty: Mathematics
Assigned: RADC

Dr. Vito G. DelVecchio
Professor of Biology
University of Scranton
Scranton, PA 18510
(717) 961-6117

Degree: Ph.D., Biochemical Genetics, 1967
Specialty: Biochemistry, Genetics
Assigned: SAM

Dr. Shirshak K. Dhali
Assistant Professor
Dept. of Electrical Engineering
Southern Illinois University
Carbondale, IL 62901
(618) 536-2364

Degree: Ph.D., Electrical Engineering, 1984
Specialty: Electrical Engineering
Assigned: APL

Dr. Lokesh R. Dharani
Assistant Professor
University of Missouri-Rolla
Dept. of Engineering Mechanics
Rolla, MO 65401-0249
(314) 341-4586

Degree: Ph.D., Engineering Mechanics, 1982
Specialty: Engineering Mechanics
Assigned: ML

Dr. Peter O. Disimile
Assistant Professor
Aerospace Engineering and Engineering Mechanics
University of Cincinnati
Mail Location 70
Cincinnati, OH 45221
(513) 475-2936

Degree: Ph.D., Fluid Mechanics, 1984
Specialty: Fluid Mechanics
Assigned: FDL

Dr. Michael L. Doria
Associate Professor of Mechanical Engineering
Valparaiso University
Valparaiso, IN 46383
(219) 464-5104

Degree: Ph.D., Mechanics, 1968
Specialty: Mechanics
Assigned: FDL

Dr. George R. Doyle, Jr.
Associate Professor
University of Dayton
Mechanical Engineering Dept.
300 College Park Drive
Dayton, OH 45469
(513) 229-2995

Degree: Ph.D., Mechanical Engineering, 1973
Specialty: Mechanical Engineering
Assigned: FDL

Dr. Franklin E. Eastep
Professor
Aerospace Engineering
University of Dayton
300 College Park Drive
Dayton, OH 45469
(513) 229-2241

Degree: Ph.D., Aero and Astro, 1968
Specialty: Aero and Astro
Assigned: FDL

Dr. Thaddeus J. Englert
Assistant Professor
University of Wyoming
Dept. of Electrical Eng.
University Station
Laramie, WY 82071
(307) 766-6321

Degree: Ph.D., Physics, 1982
Specialty: Physics
Assigned: FJSRL

Dr. Dennis R. Flentge
Assistant Professor
Cedarville College
Math/Science Department
Box 601
Cedarville, OH 45314
(513) 766-2211

Degree: Ph.D., Physical Chemistry, 1974
Specialty: Physical Chemistry
Assigned: APL

Dr. Mark A. Fulk
Assistant Professor
University of Florida
Computer & Information Sciences
512 Weil Hall
Gainesville, FL 32611
(904) 392-9219

Degree: Ph.D., Computer Science, 1986
Specialty: Computer Science
Assigned: AD

Dr. Patrick T. Gannon, Sr.
Assistant Professor
Dept. of Meteorology
Lyndon State College
Vail Hill
Lyndonville, VT 05851
(302) 626-9371

Degree: Ph.D., Atmospheric Science, 1977
Specialty: Atmospheric Science
Assigned: AFGL

Dr. John K. George
Professor of Chemistry
Mary Washington College
Fredericksburg, VA 22401
(703) 899-4320

Degree: Ph.D., Physical Chemistry, 1976
Specialty: Physical Chemistry
Assigned: FJSRL

Dr. Albert C. Giere
Assistant Professor
Physics Department
Oakwood College
Huntsville, AL 35806
(205) 837-1630

Degree: Ph.D., Mathematical Physics, 1965
Specialty: Mathematical Physics
Assigned: AEDC

Dr. Doris O. Ginn
Associate Professor
Dept. of English and Modern Foreign
1400 John R. Lynch Street
Jackson, MS 39217
(601) 968-2116

Degree: Ph.D., Linguistics, 1979
Specialty: Linguistics
Assigned: HRL/ID

Dr. Thomas A. Gosink
Research Associate Professor
University of Alaska
Geophysical Institute
Fairbanks, AK 99776-0800
(907) 786-1800

Degree: Ph.D., Organic Chemistry, 1965
Specialty: Organic Chemistry
Assigned: SAM

Dr. Raghava G. Gowda
Assistant Professor
Dept. of Computer Science
University of Dayton
300 College Park Drive
Dayton, OH 45469
(513) 229-3808

Degree: A.B.D., Electrical Engineering, 1982
Specialty: Electrical Engineering
Assigned: HRL/LR

Dr. Gerald R. Graves
Assistant Professor
Industrial Engineering
Louisiana State University
3128 CEBA
Baton Rouge, LA 70803
(504) 388-5112

Degree: Ph.D. Industrial Engineering, 1985
Specialty: Industrial Engineering
Assigned: ML

Dr. Ronald L. Greene
Associate Professor
University of New Orleans
Dept. of Physics
3726 Piedmont Drive
New Orleans, LA 70122
(504) 286-6714

Degree: Ph.D., Physics, 1971
Specialty: Physics
Assigned: AL

Dr. William M. Grissom
Instructor
Physics Dept.
Morehouse College
830 Westview Dr., S.W.
Dansby Hall, Suite 131
Atlanta, GA 30314
(404) 681-2800

Degree: MSE Mechanical Engineering, 1978
Specialty: Mechanical Engineering
Assigned: RPL

Dr. William A. Grosky
Associate Professor
Computer Science Dept.
Wayne State University
Detroit, MI 48202
(313) 577-2477

Degree: Ph.D., Engineering and Applied Science, 1971
Specialty: Eng. & Applied Science
Assigned: AL

Dr. Thomas R. Gulledge
Assistant Professor
Quantitative Business Analysis
Louisiana State University
3190 CEBA, QBA
Baton Rouge, LA 70803
(504) 388-2506

Degree: Ph.D., Engineering Management, 1981
Specialty: Engineering Management
Assigned: BRMC

Dr. Ramesh C. Gupta
Professor of Mathematics
University of Maine at Orono
Dept. of Mathematics
Orono, MN 04469
(207) 581-3913

Degree: Ph.D., Mathematical Statistics, 1970
Specialty: Mathematical Statistics
Assigned: SAM

Dr. Fabian C. Hadipriono
Assistant Professor
The Ohio State University
Civil Engineering Dept.
2070 Neil Avenue
Columbus, OH 43210
(614) 422-8518

Degree: Ph.D., Engineering, Civil Engineering, 1982
Specialty: Engineering, Civil Engineering
Assigned: WL

Dr. Frank O. Hadlock
Professor and Chairman
Florida Atlantic University
Dept. of Mathematics
Boca Raton, FL 33431
(305) 393-3342

Degree: Ph.D., Mathematics, 1966
Specialty: Mathematics
Assigned: SAM

Dr. Prabhat Hajela
Assistant Professor
Engineering Sciences
University of Flordia
231 Aero Engineering Bldg.
Gainesville, FL 32611
(904) 392-0961

Degree: Ph.D., Aeronautics and Astronautics, 1982
Specialty: Aeronautics & Astronautics
Assigned: AD

Dr. Patrick R. Hannon
Assistant Professor
Helth & Physical Education
Northern Arizona University
Box 6012, HPR Dept.
Flagstaff, AZ 86011
(602) 523-4122

Degree: Ed.D., Exercise Science, 1980
Specialty: Education, Exercise Science
Assigned: AAMRL

Dr. Donald F. Hanson
Associate Professor
University of Mississippi
Dept. of Electrical Engineering
University, MS 38677
(601) 232-5389

Degree: Ph.D., Electrical Eng. (Electromagnetics), 1976
Specialty: Electrical Engineering, Electromagnetic Electronics
Assigned: RADC

Dr. Gerald F. Harris
Director
Biomedical Engineering
Shriners Hospital
2211 N. Oak Park Avenue
Chicago, IL 60635
(312) 622-5400

Degree: Ph.D., Biomedical Engr., 1981
Specialty: Biomedical Engineering, Biomechanics
Assigned: AAMRL

Dr. Edward J. Hass
Assistant Professor
Franklin and Marshall College
Whitely Psychology Lab.
Box 3003
Lancaster, PA 17604
(717) 291-4202

Degree: Ph.D., Psychology, 1983
Specialty: Psychology
Assigned: HRL/OT

Dr. Doyle E. Hasty
Associate Professor
Engineering/Physics
Motlow State College
P O Box 860
Tullahoma, TN 37330
(615) 455-8511

Degree: M.S., Engineering Administration, 1974
Specialty: Engineering Administration
Assigned: AEDC

Dr. Michael A. Hayes
Assistant Professor
Dept. of Physics
Dartmouth College
Hanover, NH 03755
(603) 646-2973

Degree: Ph.D., Plasma Physics, 1981
Specialty: Plasma Physics
Assigned: AFGL

Dr. James C. Ho
Professor of Physics & Chemistry
Wichita State University
Wichita, KS 67208
(316) 689-3190

Degree: Ph.D., Chemistry, 1966
Specialty: Chemistry
Assigned: APL

Dr. Peter F. Hoffman
Assistant Professor
Dept. of Mathematics
University of Colorado
Box 170, UCD
Denver, CO 80202
(303) 556-4808

Degree: Ph.D., Applied Mathematics, 1985
Specialty: Applied Mathematics
Assigned: AEDC

Dr. Robert R. Hoffman
Assistant Professor
Dept. of Psychology
Adelphi University
Garden City, NY 11530
(516) 663-1055

Degree: Ph.D., Experimental Psychology, 1976
Specialty: Experimental Psychology
Assigned: ESD

Dr. Clifford C. Houk
Professor of Chemistry
Director Industrial Hygiene Program
Ohio University
Dept. of Chemistry
Athens, OH 45701-2979
(614) 594-6205

Degree: Ph.D., Inorganic Chemistry, 1966
Specialty: Inorganic Chemistry
Assigned: OEHL

Dr. Ming-Shing Hung
Associate Professsor
Dept. of Administrative Sciences
Kent State University
Kent, OH 44242
(216) 672-2750

Degree: Doctor of Business Admin., Management Science, 1973
Specialty: Business Administration, Management Science
Assigned: LC

Dr. John M. Jobe
Assistant Professor
Decision Sciences Dept.
Miami University of Ohio
229 Culler Hall
(513) 529-7291

Degree: Ph.D., Statistics, 1984
Specialty: Statistics
Assigned: RADC

Dr. Glen Johnson
Associate Professor
Mechanical and Materials Engineering
Vanderbilt University
Box 8-B
Nashville, TN 37235
(615) 322-0414

Degree: Ph.D., Mechanical Engineering, 1978
Specialty: Mechanical Engineering
Assigned: AEDC

Dr. Betty Jones
Associate Professor
Dir. of the EM Institute
830 Westview Dr., S.W.
Atlanta, GA 30314
(404) 681-2800

Degree: Ph.D., Biology, 1978
Specialty: Biology
Assigned: SAM

Dr. Jeremy C. Jones
Assistant Professor
University of West Florida
Systems Science
USF LIB 630 CS & Eng
Tampa, FL 33620
(813) 974-2114

Degree: M.S., Physics, 1968
M.S., Math, 1966
Specialty: Physics, Math
Assigned: AD

Dr. Marvin S. Keener
Professor of Mathematics
Oklahoma State University
Math Department
Stillwater, OK 74078
(405) 624-5789

Degree: Ph.D., Mathematics, 1970
Specialty: Mathematics
Assigned: AD

Dr. Yong S. Kim
Assistant Professor
Dept. of Civil Engineering
The Catholic Univ. of America
Washington, DC 20064
(202) 635-5163

Degree: Ph.D., Civil Engineering, 1984
Specialty: Civil Engineering
Assigned: ESC

Dr. Joel R. Klink
Professor
Univ. of Wisconsin-Eau Claire
Chemistry Dept.
Eau Claire, WI 54701
(715) 836-5518

Degree: Ph.D., Organic Chemistry, 1964
Specialty: Organic Chemistry
Assigned: RPL

Dr. Stephan E. Kolitz
Assistant Professor
University of Massachusetts
Management Sciences Dept.
Boston, MA 02125
(617) 929-8051

Degree: Ph.D., Operations Research, 1983
Specialty: Operations Research
Assigned: ESD

Dr. Philipp G. Kornreich
Professor
Dept. of Electrical Engineering
and Computer Engineering
Syracuse University
Syracuse, NY 13244
(315) 423-4447

Degree: Ph.D., Electrical Eng., 1967
Specialty: Electrical Engineering
Assigned: RADC

Dr. Mou-Liang Kung
Associate Professor
Math and Computer Science
Norfolk State University
2401 Corprew Avenue
Norfolk, VA 23504
(804) 623-8820

Degree: Ph.D., Math, 1974
M.S., Computer Science, 1985
Specialty: Mathematics
Assigned: RADC

Dr. Charles E. Lance
Assistnat Professor
University of Georgia
Dept. of Psychology
Athens, GA 30602
(404) 542-4439

Degree: Ph.D., Psychology, 1985
Specialty: Psychology
Assigned: HRL/ID

Dr. David I. Lawson
Assistant Professor
Mathematics and Computer Science
Stetson University
Box 8348
DeLand, FL 32720
(904) 734-4121

Degree: M.A., Mathematics, 1968
Specialty: Mathematics
Assigned: AD

Dr. Paul S.T. Lee
Associate Professor
Dept. of Business Admin.
N.C. A&T State University
1601 E. Market Street
Greensboro, NC 27410
(919) 379-7656

Degree: Ph.D., Quantitative Methods and Research Economics, 1973
Specialty: Quantitative Methods and Research Economics
Assigned: FDL

Dr. C. Randal Lishawa
Physics Instructor
Dept. of Chemistry and Physics
Jefferson State University
Birmingham, AL 35243
(205) 853-1200

Degree: Ph.D., Physical Chemistry, 1981
Specialty: Physical Chemistry
Assigned: AFGL

Dr. Cheng Liu
Associate Professor
Dept. of Engr. Tech.
University of North Carolina
Charlotte, NC 28223
(704) 597-4191

Degree: M.S., Civil Engineering, 1963
Specialty: Civil Engineering
Assigned: ESC

Dr. James C. LoPresto
Professor of Astronomy
Edinboro University
Dept. of Physics
Edbinboro, PA 16444
(814) 732-2469

Degree: Ph.D., Astronomy, 1974
Specialty: Astronomy
Assigned: AFGL

Dr. Stephen L. Loy
Assistant Professor
Iowa State University
Management
374 Carver
Ames, IA 50010
(515) 294-8108

Degree: DBA, MIS, 1986
Specialty: Management Information System
Assigned: HRL/LR

Dr. Nancy I. Lyons
Associate Professor
Dept. of Statistics
University of Georgia
Statistics Building
Athens, GA 30602
(404) 542-5232

Degree: Ph.D., Statistics, 1975
Specialty: Statistics
Assigned: LMC

Dr. Robert L. Manicke
Assistant Professor
U.S. Naval Academy
Math Department
Attn: 9E
Annapolis, MD 21402
(301) 267-3603

Degree: Ph.D., Statistics, 1980
Specialty: Statistics
Assigned: AAMRL

Dr. Arthur A. Mason
Professor of Physics
The University of Tennessee
Space Institute
Tullahoma, TN 37388
(615) 455-0631

Degree: Ph.D., Physics, 1963
Specialty: Physics
Assigned: AEDC

Dr. Curtis W. McDonald
Professor of Chemistry
Dept. of Chemistry
Texas Southern University
3100 Cleborne
Houston, TX 77004
(713) 527-7003

Degree: Ph.D., Chemistry, 1962
Specialty: Chemistry
Assignged: OEHL

Dr. Gopal M. Mehrotra
Assistant Professor
Wright State University
Materials Science and
Engineering Program
Systems Engineering
Dayton, OH 45435
(513) 873-2481

Degree: Ph.D., Metallurgy, 1975
Specialty: Metallurgy
Assigned: ML

Dr. Jorge L. Mendoza
Associate Professor
Texas A&M University
Psychology Department
College Station, TX 77843
(409) 845-0880

Degree: Ph.D., Psychology, 1974
Specialty: Psychology
Assigned: HRL/MO

Dr. Shreenivas Moorthy
Associate Professor
Texas A&I University
Electrical Engineering &
Computer Science
Campus Box 192
Kingsville, TN 78363
(512) 595-2004

Degree: Ph.D., Electrical
Engineering, 1972
Specialty: Electrical Engineering
Assigned: HRL/LR

Dr. Mary L. Morton-Gibson
Assistant Professor
Physics Department
The Citadel
Charleston, SC 29409
(803) 792-6943

Degree: Ph.D., Physiology and Biophysics, 1970
Specialty: Physiology and Biophysics
Assigned: SAM

Dr. Rex C. Moyer
Associate Professor
Trinity University
Biology Dept.
715 Stadium Drive
San Antonio, TX 78284
(512) 736-7242

Degree: Ph.D., Microbiology, 1965
Specialty: Microbiology
Assgined: SAM

Dr. V. Dakshina Murty
Associate Professor
University of Portland
School of Engineering
Portland, OR 97203
(503) 283-7379

Degree: Ph.D., Engineering Mechanics, 1982
Specialty: Engineering Mechanics
Assigned: FDL

Dr. Richard W. Nau
Professor of Math and
Computer Science
Carleton College
Northfield, MN 55057
(607) 663-4361

Degree: Ph.D., Applied Math and Computer Science, 1970
Specialty: Applied Math and Computer Science
Assigned: WL

Dr. Henry Nebel
Associate Professor
Alfred University
Physics Department
Alfred, NY 14802
(607) 871-2208

Degree: Ph.D., Physics, 1967
Specialty: Physics
Assigned: AFGL

Dr. Robert M. Nehs
Associate Professor
Dept. of Mathematical Sciences
Texas Southern University
3100 Cleburne Avenue
Houston, TX 77004
(713) 527-7915

Degree: Ph.D., Mathematics, 1980
Specialty: Mathematics
Assigned: AFGL

Dr. Douglas L. Oliver
Assistant Professor
University of Toledo
Toledo, OH 43606
(419) 537-2885

Degree: Ph.D., Mechanical Engineering, 1985
Specialty: Mechanical Engineering
Assigned: APL

Dr. Philip D. Olivier
Assistant Professor
University of Texas at San Antonio
Division of Engineering
San Antonio, TX 78285
(512) 691-5565

Degree: Ph.D., Electrical Engineering, 1980
Specialty: Electrical Engineering
Assigned: HRL/ID

Dr. Harvey L. Paige
Associate Professor
Alfred University
Dept. of Chemistry
Alfred, NY 14802
(607) 871-2201

Degree: Ph.D., Inorganic Chemistry, 1969
Specialty: Inorganic Chemistry
Assigned: ML

Dr. Parsottam J. Patel
Associate Professor
Meharry Medical College
Dept. of Microbiology
Nashville, TN 37208
(615) 327-6760

Degree: Ph.D., Microbiology, 1976
Specialty: Microbiology
Assigned: SAM

Dr. Robert A. Patsiga
Professor
Dept. of Chemistry
Indiana Univ. of Pennsylvania
Indiania, PA 15705
(412) 357-2210

Degree: Ph.D., Organic and Polymer Chemistry, 1962
Specialty: Organic Polymer Chemistry
Assigned: ML

Dr. Martin A. Patt
Associate Professor
University of Lowell
Dept. of Electrical Engineering
1 University Avenue
Lowell, MA 01854
(617) 452-5000

Degree: M.S., Science, Electrical Engineering, 1964
Specialty: Electrical Engineering
Assigned: AFGL

Dr. Jacqueline G. Paver
Research Associate
Duke University
Biomedical Engineering Dept.
136 Engineering Building
Durham, NC 27706
(919) 684-6185

Degree: Ph.D., Biomedical Engineering, 1984
Specialty: Biomechanical Engineering
Assigned: AAMRL

Dr. Alexandru A. Pelin
Associate Professor
of Computer Science
Florida International University
Dept. of Mathematical Sciences
Tamiami Campus
Miami, FL 33199
(305) 554-3386

Degree: Ph.D., Computer Science, 1977
Specialty: Computer Science
Assigned: WL

Dr. Bernard J. Piersma
Professor of Chemistry
Houghton College
Houghton, NY 14744
(716) 567-2211

Degree: Ph.D., Physical Chemistry, 1965
Specialty: Physical Chemistry
Assigned: FJSRL

Dr. Leonard Price
Professor of Chemistry
Xavier University of Louisiana
Chemistry Department
7325 Palmetto Street
New Orleans, LA 70125

Degree: Ph.D., Organic Chemistry, 1962
Specialty: Organic Chemistry
Assigned: SAM

Dr. Craig G. Prohazka
Assistant Professor
University of Lowell
Dept. of Electrical Engineering
Lowell, MA 01854
(617) 452-5000

Degree: Ph.D., Electrical Engineering, 1981
Specialty: Electrical Engineering
Assigned: RADC

Dr. L. Rai Pujara
Assistant Professor
Electrical Systems Engineering
Wright State University
Dayton, OH 45435
(513) 873-2456

Degree: Ph.D., Mathematics, 1971
Specialty: Electrical Sys. Engineering
Assigned: FDL

Dr. Richard S. Quimby
Assistant Professor
Worcester Polytechnic Institute
Dept. of Physics
100 Institute Road
Worcester, MA 01609
(617) 793-5490

Degree: Ph.D., Physics, 1979
Specialty: Physics
Assigned: RADC

Dr. Singiresu S. Rao
Associate Professor
School of Mechanical Engineering
Purdue University
West Lafayette, IN 47907
(317) 494-9766

Degree: Ph.D., Engineering Design, 1971
Specialty: Engineering Design
Assigned: FDL

Dr. Ralph J. Rascati
Associate Professor
Kennesaw College
Biology Department
Marietta, GA 30061
(404) 529-2878

Degree: Ph.D., Biochemistry, 1975
Specialty: Biochemistry
Assigned: OEHL

Dr. Kuldip S. Rattan
Associate Professor
Dept. of Electrical Systems Engineering
Wright State University
Dayton, OH 45435
(513) 873-2497

Degree: Ph.D., Electrical Engineering, 1975
Specialty: Electrical Engineering
Assigned: AAMRL

Dr. Barbara Rice
Associate Professor
Mathematics Dept.
Alabama A&M University
P O Box 326
Normal, AL 35762
(205) 859-7448

Degree: Ph.D., Mathematics, 1965
Specialty: Mathematics
Assigned: AD

Dr. Dan B. Rinks
Assistant Professor
Louisiana State University
Dept. of Quantitative Business Analysis
3180 CEBA
Baton Rouge, LA 70803
(504) 388-5318

Degree: Ph.D., Quantitative Management Science, 1978
Specialty: Quantitative Mgmt. Science
Assigned: LMC

Dr. William P. Robey
Assistant Professor
Electronics & Computer Technology
Oklahoma State University
202CR
Stillwater, OK 74078
(405) 624-5716

Degree: B.S., Engineering Physics, 1968
Specialty: Engineering Physics
Assigned: AFGL

Dr. Kenneth C. Russell
Professor
Massachusetts Institute of Technology
Materials Science
Nuclear Engineering
Room 13-5066
77 Massachusetts Avenue
Cambridge, MA 02139
(617) 253-3328

Degree: Ph.D., Metall. Engineering, 1964
Specialty: Metallurgy Engineering
Assigned: ML

Dr. Sally A. Sage
Assistant Professor
West Georgia College
Dept. of Math/Computer Science
Carrollton, GA 30118
(404) 834-1380

Degree: M.S., Computer Science, 1979
Specialty: Computer Science
Assigned: AD

Dr. Mo Samimy
Assistant Professor
Ohio State University
Mechanical Engineering Dept.
206 W. 18th Avenue
Columbus, OH 43210
(614) 422-6988

Degree: Ph.D., Mechanical Engineering, 1984
Specialty: Mechanical Engineering
Assigned: APL

Dr. John F. Schaefer
Associate Professor
Dept. of Electrical Engineering
The Citadel
Charleston, SC 29409
(803) 792-4899

Degree: Ph.D., Electrical Engineering, 1965
Specialty: Electrical Engineering
Assigned: ESC

Dr. John R. Schneider
Professor of Physics
University of Dayton
Physics Department
Dayton, OH 45469
(513) 229-1000

Degree: Ph.D., Physics, 1965
Specialty: Physics
Assigned: ML

Dr. Richard M. Schori
Professor of Mathematics
Oregon State University
Math Department
Corvallis, OR 97331
(503) 754-4686

Degree: Ph.D., Mathematics, 1964
Specialty: Mathematics
Assigned: SAM

Dr. William D. Schulz
Professor
Eastern Kentucky University
Dept. of Chemistry
Moore 337, EKU
Richmond, KY 40475
(606) 622-1463

Degree: Ph.D., Analytical Chemistry, 1975
Specialty: Analytical Chemistry
Assigned: ESC

Dr. Meckinley Scott
Professor
University of Alabama
Mathematics Department
Box 1416
University, AL 35486
(206) 348-1985

Degree: Ph.D., Statistics, 1964
Specialty: Statistics
Assigned: AD

Dr. Martin A. Shadday, Jr.
Assistant Professor
University of South Carolina
Mechanical Engineering
College of Engineering
Columbia, SC 29208
(803) 777-7118

Degree: Ph.D., Mechanical Engineering, 1982
Specialty: Mechanical Engineering
Assigned: WL

Dr. Nisar Shaikh
Assistant Professor
University of Nebraska-Lincoln
Dept. of Engineering Mechanics
212 Bancroft Hall
Lincoln, NE 68588-0437
(402) 472-2384

Degree: Ph.D., Applied Mechanics, 1982
Specialty: Applied Mathematics
Assigned: ML

Dr. Dolores C. Shockley
Associate Professor
Meharry Medical College
Dept. of Pharmacology
1005 D.B. Todd Blvd.
Nashville, TN 37208
(615) 327-6510

Degree: Ph.D., Pharmacology, 1955
Specialty: Pharmacology
Assigned: SAM

Dr. William D. Shontz
Associate Professor
Montana State University
Department of Psychology
Bozeman, MT 59717
(406) 994-5180

Degree: Ph.D., Experimental Psychology, 1967
Specialty: Psychology
Assigned: AFHRL/OTE

Dr. William D. Siuru, Jr.
Senior Research Associate
Space and Flight Systems Lab.
University of Colorado at Colorado Springs
1867 Austin Bluffs Parkway
Colorado Springs, CO 80907
(303) 593-3573

Degree: Ph.D., Mechanical Engineering, 1975
Specialty: Mechanical Engineering
Assigned: FJSRL

Dr. Boghos D. Sivazlian
Professor
The University of Florida
Dept. of Industrial and Systems Engineering
303 Weil Hall
Gainesville, FL 32611
(904) 392-1464

Degree: Ph.D., Operations Research, 1966
Specialty: Operations Research
Assigned: AD

Dr. Siavash H. Sohrab
Assistant Professor
Dept. of Mechanical and Nuclear Engineering
Northwestern University
Technical Institute
Evanston, IL 60201
(312) 491-3572

Degree: Ph.D., Engineering Physics, 1981
Specialty: Engineering Physics
Assigned: RPL

Dr. Stuart R. Stock
Assistant Professor
Georgia Institute of Technology
School of Materials Engineering
Atlanta, GA 30332-0245
(404) 894-6882

Degree: Ph.D., Metallurgy, 1983
Specialty: Metallurgy
Assigned: ML

Dr. James E. Sturm
Professor
Dept. of Chemistry #6
Lehigh University
Bethlehem, PA 18015
(215) 861-3477

Degree: Ph.D., Physical Chemistry, 1957
Specialty: Physical Chemistry
Assigned: AFGL

Dr. Edgar C. Tacker
Professor of Electrical Eng.
University of Tulsa
600 S. College
Tulsa, OK 74104
(918) 592-6000

Degree: Ph.D., Electrical Engineering, 1964
Specialty: Electrical Engineering
Assigned: AAMRL

Dr. Nicholas E. Takach
Assistant Professor
Dept. of Chemistry
University of Tulsa
600 S. College
Tulsa, OK 74104
(918) 592-6000

Degree: Ph.D., Chemistry, 1979
Specialty: Chemistry
Assigned: RPL

Dr. Arjun Tan
Assistant Professor
Alabama A&M University
Physics Dept.
Box 447
Normal, AL 35762
(205) 859-7470

Degree: Ph.D., Physics, 1979
Specialty: Physics
Assigned: AEDC

Dr. Robert P. Taylor
Assistant Professor
Mech. and Nuclear Engr. Dept.
Mississippi State University
Drawer ME
Mississippi State, MS 39762
(601) 325-7316

Degree: Ph.D., Mechanical Engineering, 1983
Specialty: Mechanical Engineering
Assigned: APL

Dr. Ken Tomiyama
Assistant Professor
Pennsylvania State University
Dept. of Electrical Engineering
121 E.E. East
University Park, PA 16802
(814) 865-7667

Degree: Ph.D., System Science, 1977
Specialty: System Science
Assigned: AL

Dr. Phillip D. Tomporowski
Assistant Professor
Dept. of Psychology
University of Alabama
Box 2968
University, AL 35486
(205) 348-1936

Degree: Ph.D., Experimental Psychology, 1977
Specialty: Experimental Psychology
Assigned: HRL/MO

Dr. Timothy R. Troutt
Assistant Professor
Washington State University
Dept. of Mechanical Engineering
Sloan Hall 201
Pullman, WA 99164-2920
(509) 335-4375

Degree: Ph.D., Mechanical Engineering, 1978
Specialty: Mechanical Engineering
Assigned: FJSRL

Dr. C. Randall Truman
Assistant Professor
Mechanical Engineering
University of New Mexico
Albuquerque, NM 87131
(505) 277-6296

Degree: Ph.D., Mechanical Engineering, 1983
Specialty: Mechanical Engineering
Assigned: WL

Dr. Roy M. Ventullo
Associate Professor
Dept. of Biology
University of Dayton
300 College Park
Dayton, OH 45469-0001
(513) 229-2503

Degree: Ph.D., Microbiology, 1978
Specialty: Microbiology
Assigned: ESC

Dr. Doris J. Walker-Dalhouse
Director of Independent/
Home-Study Programs
Associate Professor of Reading
Jackson State University
P O Box 17120
Jackson, MS 39217
(601) 968-9684

Degree: Ph.D., Reading Education, 1977
Specialty: Reading Education
Assigned: HRL/ID

Dr. Donald W. Welch
Research Scientist
Texas A&M University
Hyperbaric Laboratory
College Station, TX 77843
(409) 845-4027

Degree: Doctorate, Microbiology, 1985
Specialty: Microbiology
Assigned: WHMC

Dr. Albert R. Wellens
Associate Professor and
Associate Chairman
Dept. of Psychology
University of Miami
P O Box 248185
Coral Gables, FL 33158
(305) 284-2814

Degree: Ph.D., Experimental Social Psychology, 1972
Specialty: Experimental Social Psychology
Assigned: AAMRL

Dr. Stephen T. Welstead
Assistant Professor
University of Alabama
in Huntsville
Dept. of Mathematics
Huntsville, AL 35899
(205) 895-6470

Degree: Ph.D., Applied Mathematics, 1982
Specialty: Applied Mathematics
Assigned: RADC

Dr. Shih-sung Wen
Professor of Psychology
Psychology Department
Jackson State University
1325 J.R. Lynch Street
Jackson, MS 39217
(601) 968-2371

Degree: Ph.D., Educational Psychology, 1971
Specialty: Educational Psychology,
Assigned: SAM

Dr. Stanley J. Whidden
Researcher
JESM Baromedical Research
Institute
4400 Gen. Meyer Avenue, 114
New Orleans, LA 70117
(504) 363-7656

Degree: Ph.D., Physiology, Pharmacology, 1978
Specialty: Hyperbaric Medicine,
Assigned: SAM

Dr. Dennis W. Whitson
Professor of Physics
Indiana Univ. of Pennsylvania
Physics Department
Indiana, PA 15705
(412) 357-2589

Degree: Ph.D., Physics, 1969
Specialty: Physics
Assigned: AL

Dr. Shirley A. Williams
Assistant Professor
Jackson State University
Jackson, MS 39217
(601) 968-2586

Degree: Ph.D., Physiology and Biophysics, 1985
Specialty: Physiology and Biophysics
Assigned: OEHL

Dr. Billy R. Wooten
Professor
Dept. of Psychology
Brown University
Providence, RI 02906
(401) 863-2330

Degree: Ph.D. of Philosophy, Psychology, 1970
Specialty: Philosophy, Psychology
Assigned: HRL/OT

Dr. Daniel W. Yannitell
Associate Professor
Mechanical Engineering Dept.
Louisiana State University
Baton Rouge, LA 70803
(504) 388-5972

Degree: Ph.D., Theoretical and Applied Mechanics, 1967
Specialty: Theoretical and Applied Mechanics
Assigned: RPL

Dr. Tsun-wai G. Yip
Assistant Professor
Aero-Astro Engineering Dept.
Ohio State University
2300 West Case Road
Columbus, OH 43220
(614) 422-1241

Degree: Ph.D., Aero-Astro Engineering, 1984
Specialty: Aeronautics-Astronautics Engineering
Assigned: FDL

Dr. Robert L. Yolton
Associate Professor of Psychophysiology
Pacific University
College of Optometry
Forest Grove, OR 97116
(503) 357-6151

Degree: Ph.D., Psychology, 1975
Doctor of Optometry, 1975
Specialty: Psychology, Optometry
Assigned: AAMRL

Dr. Richard W. Young
Associate Professor
Aerospace Engineering and Engineering Mechanics
University or Cincinnati
ML 70
Cincinnati, OH 45242
(513) 475-3014

Degree: Ph.D., Applied Mechanics, 1975
Specialty: Applied Mechanics
Assigned: FDL

Dr. Ajmal Yousuff
Assistant Professor
Drexel University
Dept. of Mechanical Enginnering and Mechanics
Philadelphia, PA 19104
(215) 895-1868

Degree: Ph.D., Aeronautics, 1983
Specialty: Aeronautics
Assigned: FDL

Dr. David D. Zeigler
Adjunct Faculty
North Texas State University
Biology Department
Denton, TX 76203
(817) 565-3622

Degree: Ph.D., Zoology, 1984
Specialty: Zoology
Assigned: AD

Dr. Henry Zmuda
Assistant Professor
Stevens Institute of Technology
Electrical Engineering Dept.
Castle Point Station
Hoboken, NJ 07030
(201) 420-5507

Degree: Ph.D., Electrical Engineering, 1984
Specialty: Electrical Engineering
Assigned: RADC

Dr. George W. Zobrist
Professor of Computer Science
Dept. of Computer Science
University of Missouri-Rolla
Rolla, MO 65401
(314) 341-4836

Degree: Ph.D., Electrical Engineering, 1965
Specialty: Electrical Engineering
Assigned: AL

PARTICIPANT LABORATORY ASSIGNMENT

C. PARTICIPANT LABORATORY ASSIGNMENT (Page 1)

1986 USAF/UES SUMMER FACULTY RESEARCH PROGRAM

AERO PROPULSION LABORATORY (AFWAL/APL)
(Wright-Patterson Air Force Base)

1. Lea Chen
2. Jacob Chung
3. Shirshak Dhali
4. Dennis Flentge
5. James Ho
6. Douglas Oliver
7. Mo Samimy
8. Robert Taylor

ARMAMENT LABORATORY (AD)
(Eglin Air Force Base)

1. George D. Catalano
2. Mark A. Fulk
3. Jeremy C. Jones
4. Marvin S. Keener
5. David I. Lawson
6. Barbara C. Rice
7. Sally A. Sage
8. Meckinley Scott
9. Boghos D. Sivazlian
10. David D. Zeigler
11. Probhat Hajela

ARMSTRONG AEROSPACE MEDICAL RESEARCH LABORATORY (AAMRL)
(Wright-Patterson Air Force Base)

1. Rashpal S. Ahluwalia
2. Patrick R. Hannon
3. Gerald F. Harris
4. Robert L. Manicke
5. Jacqueline G. Paver
6. Kuldip S. Rattan
7. Edgar C. Tacker
8. Albert R. Wellens
9. Robert L. Yolton

ARNOLD ENGINEERING DEVELOPMENT CENTER (AEDC)
(Arnold Air Force Station)

1. Albert C. Giere
2. Doyle E. Hasty
3. Peter E. Hoffman
4. Glen E. Johnson
5. Arthur A. Mason
6. Arjun Tan

AVIONICS LABORATORY (AFWAL/AL)
(Wright-Patterson Air Force Base)

1. Rex L. Berney
2. John Y. Cheung
3. Ronald L. Greene
4. William Grosky
5. Ken Tomiyama
6. Dennis W. Whitson
7. George W. Zobrist

BUSINESS RESEARCH MANAGEMENT CENTER (BRMC)
(Wright-Patterson Air Force Base)

1. Jeffrey Camm
2. Thomas Gulledge

C. PARTICIPANT LABORATORY ASSIGNMENT (Page 2)

ELECTRONICS SYSTEMS DIVISION (ESD)
(Hanscom Air Force Base)

1. Robert Hoffman
2. Stephan Kolitz

ENGINEERING AND SERVICES CENTER (ESC)
(Tyndall Air Force Base)

1. Thomas Carney
2. William Cooper
3. Yong Kim
4. Cheng Liu
5. John Schaefer
6. William Schulz
7. Roy Ventullo

FLIGHT DYNAMICS LABORATORY (AFWAL/FDL)
(Wright-Patterson Air Force Base)

1. George Becus
2. Bor-Chin Chang
3. Peter Disimile
4. Michael Doria
5. George Doyle
6. Franklin Eastep
7. Paul Lee
8. V. Dakshina Murty
9. L. Pujara
10. Singiresu Rao
11. Tsun-Wai Yip
12. Warren Young
13. Ajmal Yousuff

FRANK J. SEILER RESEARCH LABORATORY (FJSRL)
(USAF Academy)

1. David Anderson
2. David Barnhart
3. Wu Cheng
4. Thaddeus Englert
5. John George
6. Bernard Piersma
7. William Siuru
8. Timothy Troutt

GEOPHYSICS LABORATORY (AFGL)
(Hanscom Air Force Base)

1. Jon Ahlquist
2. Frank Battles
3. Wolfgang Christian
4. Donald Collins
5. Patrick Gannon
6. Michael Hayes
7. C. Lishawa
8. James LoPresto
9. Henry Nebel
10. Robert Nehs
11. Martin Patt
12. William Robey
13. James Sturm

HUMAN RESOURCES LABORATORY/ID (HRL/ID)
(Lowry Air Force Base)

1. Doris Ginn
2. Charles Lance
3. Philip Olivier
4. Doris Walker-Dalhouse

HUMAN RESOURCES LABORATORY/LR (HRL/LR)
(Wright-Patterson Air Force Base)

1. Patricia Boggs
2. Raghava Gowda
3. Stephen Loy
4. Shreenivas Moorthy

C. PARTICIPANT LABORATORY ASSIGNMENT (Page 3)

HUMAN RESOURCES LABORATORY/MO (HRL/MO)
(Brooks Air Force Base)
1. Richard Cox
2. Jorge Mendoza
3. Phillip Tomporowski

HUMAN RESOURCES LABORATORY/OT (HRL/OT)
(Williams Air Force Base)
1. Garvin Chastain
2. Edward Hass
3. William Shontz
4. Billy Wooten

LOGISTICS COMMAND (LC)
(Wright-Patterson Air Force Base)
1. Ming-Shing Hung

LOGISTICS MANAGEMENT CENTER (LMC)
(Gunter Air Force Base)
1. Nancy Lyons
2. Dan Rinks

MATERIALS LABORATORY (AFWAL/ML)
(Wright-Patterson Air Force Base)
1. Shive Chaturvedi
2. Derald Chriss
3. Lokesh Dharani
4. Gerald Graves
5. Gopal Mehrota
6. Harvey Paige
7. Robert Patsiga
8. Kenneth Russell
9. James Schneider
10. Nisar Shaikh
11. Stuart Stock

OCCUPATIONAL AND ENVIRONMENTAL HEALTH LABORATORY (OEHL)
(Brooks Air Force Base)
1. Clifford Houk
2. Curtis McDonald
3. Ralph Rascati
4. Shirley Williams

ROCKET PROPULSION LABORATORY (RPL)
(Edwards Air Force Base)
1. William Grissom
2. Joel Klink
3. Siavash Sohrab
4. Nicholas Takach
5. Danial Yannitell

C. PARTICIPANT LABORATORY ASSIGNMENT (Page 4)

ROME AIR DEVELOPMENT CENTER (RADC)
(Griffiss Air Force Base)

1. William Day
2. Donald Hanson
3. John Jobe
4. Philipp Kornreich
5. Mou-Liang Kung
6. Craig Prohazka
7. Richard Quimby
8. Stephen Welstead
9. Henry Zmuda

SCHOOL OF AEROSPACE MEDICINE (SAM)
(Brooks Air Force Base)

1. Vito Del Vecchio
2. Phillip Bishop
3. Clifford Burgess
4. Hoffman Chen
5. Brenda Claiborne
6. Thomas Gosink
7. Ramesh Gupta
8. Frank Hadlock
9. Betty Jones
10. Mary Morton-Gibson
11. Rex Moyer
12. Parsottam Patel
13. Leonard Price
14. Richard Schori
15. Dolores Shockley
16. Shih-sung Wen
17. Stanley Whidden

WEAPONS LABORATORY (WL)
(Kirtland Air Force Base)

1. Albert Biggs
2. James Brown
3. Fabian Hadipriono
4. Richard Nau
5. Alexandru Pelin
6. Martin Shadday
7. C. Truman

WILLFORD HALL MEDICAL CENTER
(Lackland Air Force Base)

1. Donald Welch

RESEARCH REPORTS

RESEARCH REPORTS

1986 SUMMER FACULTY RESEARCH PROGRAM

Technical Report Number Volume I	Title	Professor
1	Weather Forecast Evaluation by Decomposition of the Wind Field into Rotational and Divergent Components	Dr. Jon E. Ahlquist
2	Specification of a Vision Based Navigation System for a Mobile Robot	Dr. Rashpal S. Ahluwalia
3	An EPR Study of the Intermediate Radicals Produced in the Catalyzed and Uncatalyzed Thermal Decomposition of Dinitrotoluenes	Dr. David R. Anderson
4	An EPR and HPLC Study of the Mecnanisms and Kinetics of TNT with Various Reagents	Dr. David M. Barnhart
5	Atmospheric Turbulence Effects on Optical Beams	Dr. Frank P. Battles
6	Some Issues in the Modeling and Control of Large Flexible Space Structures	Dr. Georges A. Becus
7	Fresnel Drag Unit and Registration Optics for the Ring Laser Gyro	Dr. Rex L. Berney
8	Corrugated Waveguides for Slow Waves	Dr. Albert W. Biggs
9	Work Capacity Increased in High Ambient Temperature Chemical Warfare Environments Through Use of Intermittent Work and Individual Liquid Cooling	Dr. Phillip A. Bishop
10	Factors Impacting Adaptation of Decision Support Systems: An Interdisciplinary Approach	Dr. Patricia T. Boggs
11	American Ballistic Missile Defense, 1955-1979	Dr. James A. Brown

73	The Synthesis of Fluorodinitroethy-Initraminoalkyl Nitrates and Compatibility Studies of GAP-Nitrate and TAEI	Dr. Joel R. Klink
74	Reliability in Satellite Communication Networks	Dr. Stephan E. Kolitz
75	Investigation of Vapor Deposited Aluminum Alloy Films	Dr. Philipp G. Kornreich
76	Modification of Priority Handling Algorithm in the Integrated Node Network	Dr. Mou-Liang Kung
77	Ability, Experience and Task Characteristic Predictors of Performance	Dr. Charles E. Lance
78	Multiaperture Optical Systems and Neural Networks Capable of the Detection of Motion, Speed, Direction and Distance	Dr. David I. Lawson
79	Experimental Design and Transparency Durability Prediction	Dr. Paul S.T. Lee
80	Ion-Molecule Reactions of H_2O^+/H_2O, N_2^+/CO_2, and N^+/CO_2	Dr. C. Randal Lishawa
81	Study of Rutting of Asphalt Pavement Under High Tire Pressure and Temperature	Dr. Cheng Liu
82	Selected Spectral Studies of the Sun	Dr. James C. LoPresto
83	Visual Problem-Structuring and Hemispheric Processes of the Human Brain	Dr. Stephen L. Loy
84	Review and Evaluation of a Refueling Capability Assessment Model	Dr. Nancy I. Lyons
85	Statistical Pattern Recognition Modelling of Visual Perceptions	Dr. Robert L. Manicke
86	An Experimental Design to Verify the AFGL FASCOD2 for Water Vapor and Carbon Dioxide at Low Temperatures and Pressures	Dr. Arthur A. Mason
87	The Determination of Lead in Blood	Dr. Curtis W. McDonald

1986 USAF-UES SUMMER FACULTY RESEARCH PROGRAM

Sponsored by the
AIR FORCE OFFICE OF SCIENTIFIC RESEARCH

Conducted by the
Universal Energy Systems, Inc.

Simulation of the Cardiac Conduction System

Prepared by: Dr. Frank Hadlock, Professor of Mathematics
Mathematics Department
Florida Atlantic University
Boca Raton, Fl. 33431
Research performed at:
Clinical Sciences Division
School of Aerospace Medicine
Brooks AFB, San Antonio Tx
With: Dr. Sherwood Samn
Date: August 1, 1986
Contract: F49620-85-0013

Simulation of the Cardiac Conduction System

by
Frank Hadlock

ABSTRACT

A synchronous discrete event simulation model was developed to simulate the wave of cardiac depolarization of the ventricular portion of the human heart. The model employs a discrete geometrical model of the heart, based on one millimeter cubical cells, and a discrete set of conduction states which the cells can assume. The eventual output of the simulation is EKG signals or body surface potentials. The model is sampled synchronously at time steps appropriate for the intended output.

1 INTRODUCTION

By way of background, the research project described in this report is concerned with the computer simulation of the cardiac conduction system. The eventual objective is the generation of EKG signals, vectorcardiogram signals or body surface potential maps. This project was selected as being one of mutual interest to the Air Force and the investigator. For their part, the Air Force is interested in inexpensive,

noninvasive methods for the early detection of coronary artery disease [5]. To be able to interpret body surface potential maps correctly, a quantitative theory for their genesis is needed. The development of a cardiac conduction simulation model with the eventual generation of body surface potential maps will be an aid to the formulation of such a theory. For the author's part, the research project was relevant to past algorithm and software development experience, and to ongoing research interests. From 1979 through 1981 the author was associated with the development of an ambulatory arrythmia monitor as contractor for DataMedix, Inc. of Boca Raton, Fl. From 1981 through 1982, while on leave from his university, the author acted as Director of Advanced Software Development at DataMedix. During this time he had major responsibility for the development and testing of algorithms for EKG data compression and for QRS classification. As an outgrowth of this experience, he has become interested in measures of similarity, particularly Levenshtein distance, which might be applied to waveform comparison. With respect to Levenshtein distance, he has developed fast algorithms for its computation, and has interests in working on its application to EKG interpretation.

2 OBJECTIVES OF THE RESEARCH EFFORT

For over the past twenty years, medical researchers have been working on various simulation models as an aid in understanding the cardiac conduction system. A possible application of such a simulation model is as a diagnostic aid. By modifying the normal heart geometry to reflect suspected conduction defects such as ischemia, output from the simulation can be compared with the patient's EKG, vectorcardiogram, or body surface potential map. Close agreement will tend to corroborate the diagnosis as to conduction defects.

By way of background we will briefly describe and compare four discrete event simulation models developed in the past. We begin with one due to Moe [4] which is concerned with modelling circus rhythms in the atria. The geometry is 2 dimensional, with hexagonal tissue units. The model is finite state, with each tissue unit being in one of 5 possible states during the simulation period. The 5 states are as follows. First is an absolute refractory state, assumed after firing and during which the cell is incapable of being fired again. Next, in order of normal assumption, are three relative refractory states, during which the cells can be triggered to fire again, but at a reduction in conduction velocity proportional to the remaining time in relative refractory. Finally there is a rest state. Time is descretized by employing 5 ms time units. While this model introduces some useful concepts, it concerns itself with

simulation of the atria and utilizes a two dimensional geometry.

The next model, due to Eifler and Plonsey [3] uses a complicated cell shape : an elongated rhombic duodecahedron. As in the model due to Moe, et al, this model discretizes the states which can be assumed by a tissue unit. They assume only three states : rest, absolute and relative refractory. On the other hand, their model is sophisticated with regard to providing for different conduction velocities between units, depending on whether the units are axial or lateral neighbors.

The third model, due to Selvester and Solomon [6], uses a cube as a cell shape. There model provides for two states, rest and absolute refractory. Since the model only makes one pass, the absolute refractory state can be used for vacant cells. Despite its simplicity, the model is very slow and does not provide for modeling re-entrant rhythms.

The fourth model, due to Samn [5], is an asynchronous simulation model. It may be viewed as a generaiization of Moe's method to 3 dimensions, using a time ordered priority queue to store events. While it has the capacity to model re-entrant rhythms, the overhead necessary to maintain the event queue in order of event priority tends to make the model slow.

The specific objective of this project was to develop a synchronous simulation model which would be capable of modelling re-entrant rhythms and would be relatively fast.

3 BASIC ASSUMPTIONS FOR THE SIMULATION MODEL

3.1 Geometric Aspects Of The Model

Physically, the heart is modeled as a 3-dimensional rectangular array, 100 cubical units in each dimension, each cube being one mm on an edge. Each cube of tissue, or cell, is assumed to be homogeneous as to tissue type, and hence as to conduction properties. Each cell can excite all neighboring, non- vacant cells, where a neighbor is considered to be any cell which has a side, edge or point in common. Consequently a cell can have as many as 26 neighbors. It should be pointed out that this is contrary to the assumptions made in the model due to Eifler and Plonsey, who permit only reduced communication between lateral neighbors. Only ventricles and His/Purkinje fibres are incorporated in the current heart geometry file. However the model provides for additional types, which might be utilized to represent different levels of ischemia. Test data is taken from a digitized version of a human heart, fixed in agar on autopsy and sliced into 100 slices along its verticle axis.

3.2 Electrophysiological Aspects Of The Model

Each type of tissue is assumed to be characterized by its own action potential wave form with the duration of the absolute refractory period being a function of the last RR interval (actually the cells last firing and its current firing) and relative refractory period a function only of cell type. While the only sample heart geometry currently available to us provides only two cell types (Purkinje and ventrucular), the computer implementation of the model has the potential for accepting heart geometries which include up to five additional types, corresponding to various levels of ischemia.

Conduction velocity is also dependant on cell type, with the maximum velocity assumed to be 2 meters/second. This assumption is reflected later in the choice of the smallest simulation time unit, chosen so that wave of depolarization never propagates across more that a single single cell during the time unit. Besides cell type, conduction velocity is dependent on cell state, with the velocity varying directly with the time a cell has spent in the relative refractory state, (if it was in relative refractory) and achieving its maximum if the cell was in the rest state.

The conduction states used in this model are as follows. First of all, absolute refractory refers to the period immediately after firing during which a cell cannot be activated again. In this model, this period is divided into

two states: absolute-refractory-1 (corresponding to the upstroke of the action potential) and absolute-refractory-2 (the remainder of the period). By unfired and to-fire, will be meant the status of not having been scheduled to fire and the status of having been scheduled to fire. The model divides the state of relative-refractory-unfired into fourteen periods, corresponding to the remaining time in relative refractory, and the same for relative-refractory-to-fire. Finally there are two separate states, rest-unfired and rest-to-fire to represent a cell's being in rest and unscheduled to-fire, and being in rest and being scheduled to-fire. This totals thirty two distinct states used to represent the state-time information about a cell.

4 COMPUTER IMPLEMENTATION OF THE MODEL

4.1 A Synchronous Computer Model For Cardiac Conduction: An Overview

One of the basic decisions which must be made in developing a simulation model is whether to use a synchronous or an asynchronous approach. In the synchronous approach, a basic simulation time unit is chosen and the system is examined periodically in increments of this time unit. For our application, the electrophysiological state of the conduction system at the end of the next time unit must be computed from its current state.

In the asynchronous approach, significant events are stored in a priority queue ordered by time of occurrence. The next event to occur is obtained from the head of the queue. Processing the event may schedule other events to occur, which must be entered in the event queue according to time of occurrence.

In both approaches, time and state information must be maintained. The asynchronous approach will be more efficient if the simulation output is never needed except at the time of occurrence of significant events or with less frequency. If output is needed with less frequency, then generation of output can be designated as a significant event and be scheduled by itself or by other events. An improvement in efficiency is then realized if the asynchronous approach results in sampling the system less frequently than the synchronous approach, and the overhead involved with maintainig the priority queue is offset by this savings. For our application, the signal needed to generate an electrocardiogram, vectorcardiogram, or body surface potential map is sampled periodically. Typical sampling rates are 2 ms or 4 ms sampling. This would suggest using a synchronous simulation model, with time step chosen so that the rate with which the system state is sampled is sufficiently high so as to obtain the desired degree of accuracy of the simulation output.

4.2 Static Representation Of Heart Geometry, Cell Type And State

The CELL array is a 100x100x100 array, which simultaneously defines the heart geometry as well as the type and state of individual tissue units (cells). It also, alternately stores the time of last firing and the time till firing. In its current form, two bytes of information are allocated to each cell. The two bytes are partitioned into three fields. Field-1 (8 bits) stores the time of last firing while the cell is in certain states, and stores the time till next firing during the other states. Field-2 (3 bits) stores the cell type while Field-3 (5 bits) stores state-time information. The 5 bit state-time code is shown in the table below.

State	Code
Absolute-refractory-1	00000
Relative-refractory-unfired	00001
.	.
.	.
Relative-refractory-unfired	01110
Absolute-refractory-2	01111
Rest-unfired	10000
Relative-refractory-to-fire	10001
.	.
.	.
Relative-refractory-to-fire	11110
Rest-to-fire	11111

Note that the use of sequential codes for the relative-refractory-unfired (and for the relative-refractory-to-fire) states facilitate next state computation. The last 4 bits determine the number of relative-refractory- unfired time units remaining for the cell (14 for a cell with state code 01110). Since Field 3 is the least significant, decrementing CELL(x,y,z) changes cell x,y,z to its next relative-refractory-unfired state (or next relative-refractory-to-fire state). Note that if x,y,z is relative-refractory-unfired with one relative-refractory-unfired time unit remaining (code = 0000) its state temporarily becomes absolute-refractory-1. After decrementing, a comparison is performed to see if a transition to rest-unfired (or rest-to-fire) is in order. Thus the code selection, placing absolute-refractory-1 below relative-refractory-unfired and rest-unfired below relative-refractory-to-fire as buffers, permits decrementing without first testing; without the buffers information in other fields would be affected.

4.3 Dynamic Representation Of State-Time Information

To make the model efficient, it is necessary to utilize a redundant representation of the conduction system. The CELL array is complete in that it contains all the information necessary to perform the simulation. At the same time, it requires 2,000,000 bytes of information. Thus, if only CELL were available, the model would require on the order of 200 million instructions to be executed to simulate a single

cycle. To avoid this, special purpose [Alist structures, designed to minimize the number of page faults, have been adopted. Because the kind of processing which takes place in each state differs, and because the need for simultaneous transfer of information with the CELL array differs, the list structures differ from one state to the next. The dynamic structures introduced to provide efficient processing of cells in each state are described as follows:

Description of List Structure

Absolute-refractory-1: REF1-CRC is an unordered circular buffer of records. Each record contains the x,y,z coordinates of a cell in this state, along with its remaining time in this state, and time in absolute-refractory-2. Input is from WVE-LST and from the head of REF1-CRC. Cells at the head of REF1-CRC are processed and either go the tail of REF1-CRC or to REF2-STK. Processing is a 1 ms intervals.

Absolute-refractory-2 and Relative-refractory-unfired: REF2-STK is a series of stacks, one for each Z-plane. Each record contains x,y coordinates along with the time remaining in its current state is from REF1-CRC. A single link implementation is used and deleted cells pass to the rest state and are only accounted for in the CELL array. Processing is at 8 ms intervals. Rest-to-fire and Relative-refractory-to-fire: WVE-LST is a series of stacks, one for each Z-plane. Further, there is a current version and a next version. The stacks are implemented as linear arrays (no pointers). Each record contains x,y coordinates and the time the cell was last fired (obtained from Field 1 of CELL). The top stack element is processed by decrementing its remaining to-fire time in CELL. If fired, the coordinate information goes to FIRE-DIR and FIRE-COORD structure else the

record is copied to the top of the corresponding stack of the next version of WVE-LST. Input is accomplished by processing FIRE-DIR and FIRE-COORD to determine new cells triggered to-fire. Processing is at .5 ms intervals with relative-refractory-to-fire times updated with the same frequency as relative-refractory-unfired. Next and current versions of WVE-LST are interchanged (i.e., designations are interchanged).

4.4 Propagation Of The Wave Front

Propagation of the wave front is accomplished by processing cell records on WVE-LST which represent cells in either Rest-to-fire or Relative- refractory-to-fire. Since WVE-LST is organized as a series of stacks indexed by Z-plane, the z coordinate is automatically determined. After retrieving the x,y coordinates, Field 1 of CELL(x,y,z) is decremented, adjusting the remaining time-to-fire. If this time is non-zero, the cell record is copied to the head of the corresponding stack for the next version of WVE-LST. Otherwise the coordinate information is read into FIRE-DIR and FIRE-COORD which maintains a series of unordered lists corresponding to Z-planes of cells just fired. Next each Z-plane is processed as follows. For every cell above, on the same plane, or below, which just fired, its neighbers on the Z-plane are tested. Any non-vacant cells in rest-to-fire or relative-refractory-to-fire have new firing times computed, these replacing the old ones (in CELL) if they earlier firing times. Cells in relative- refractory-unfired or rest-unfired are changed to the appropriate states and

added to the next version of WVE-LST.

5 RECOMMENDATIONS

A Fortran 77 implementation of this model was developed after the decision to adopt a synchronous approach. The initial part of the summer fellowship period was spent considering alternative strategies for speeding up the asynchronous model. Some alternatives were to employ a fishpear data structure to facilitate maintenance of the priority queue. Another alternative was suggested by the observation that scheduling times (relative to the present) assumed only a small set of values, suggesting that the priority queue be organized as a series of constant time queues. Inserting an invent into the priority queue would be accomplished by pushing it on the stack (queue) indexed by its time of occurrence (relative to the present).

However, because it was recognized that simulation output was needed in synchronous fashion, it was decided to take a synchronous approach. The first version was a test version and was developed for a two dimensional geometry. It took only seconds to propagate a wave front through what corresponded to a quarter of a single plane of the three dimensional geometry due to Sylvester (less than .25 %). The current version should be tested. If it probes to be more efficient than the asynchronous model due to Samn, then the code to generate body surface potentials can be added at the end of the 2 ms loop.

Acknowledgements

I would like to thank the Air Force Systems Command and the Air Force Office of Scientific Research for sponsorship of my research. The research project on which I worked was both meaningful and interesting, I hope that the results can be used in the continuing search for more effective, noninvasive techniques for diagnosing coronary artery disease. I found the USAF School of Aerospace Medicine at Brooks Air Force Base to be an intellectually stimulating environment and want to particularly express my appreciation for the helpful exchange of ideas with both Dr. Sherwood Samn and Colonel Gil Tolan. I would also like to thank Dr. Schwartz for his help in determining realistic estimates for conduction parameters.

References

1. Cohn, R. L., Rush, S., and Lepeschkin, E.: Theoretical analyses and computer simulation of ECG ventricular gradient and recovery waveforms. IEEE Trans. Bio- Med., Vol. BME-29, pp. 413-423, 1982

2. Cuffin, B. N., and Geselowistz, D.S.: Studies of the electrocardiogram using realistic cardiac and torso models. IEEE TRANS. BioMed Eng., Vol. BME-24, pp. 242-252, 1977

3. Eifler, W. J., and Plonsey, R.: A cellular model for the simulation of act- ivation in the ventricular myocardium. J. Electrocardiology, 8(2), pp. 117-128, 1975

4. Moe, G. K., Rheinboldt, W. C., and Abildskov, J. A. : A computer model of atrial fibrillation. Am. Heart J. 67, pp. 200-229, 1964

5. Samn, S. : An asynchronous, finite state model for ventricular depolariztion. Unpublished.

6. Selvester, M.D., and Solomon, J.C. : Optimal ECG electrode sites and criteria for detectection of asymptomatic coronary artery disease at rest and with excercise. Unpublished report.

1986 USAF-UES SUMMER FACULTY RESEARCH PROGRAM

GRADUATE STUDENT SUMMER SUPPORT PROGRAM

Sponsored by the

AIR FORCE OFFICE OF SCIENTIFIC RESEARCH

Conducted by the

Universal Energy Systems, Inc.

FINAL REPORT

A Framework of an Optimum Synthesis Environment for the Hydrocode EPIC-2

Prepared by:	Prabhat Hajela
Academic Rank:	Assistant Professor
Department and University:	Department of Engineering Sciences University of Florida, Gainesville, Florida
Research Location:	Eglin Air Force Base, Armament Laboratory, Clusters and Warheads Branch, Computational Mechanics Group
USAF Researcher:	Mr. M.E. Gunger
Date:	July 12, 1986
Contract No:	F49620-85-C-0013

A Framework of an Optimum Synthesis Environment for the Hydrocode EPIC-2

by

Prabhat Hajela

ABSTRACT

The present study seeks to examine the efficacy of a mathematical nonlinear programming approach for the optimal synthesis of structures subjected to high strain-rate plastic deformations. Efficient methods of constraint representation are implemented to reduce the dimensionality of the optimization problem, where the latter is an outcome of the transient nature of the response functions. A Lagrangian discretized domain approach is used for the solution of the equations of motion and is coupled to a feasible usable search direction algorithm to form an optimization programming system. The optimum sizing of a projectile shell for survival in a high velocity impact, provides the test problem for this study. A stepwise linearization of the design space is attempted for computational efficiency, with encouraging results.

Acknowledgements

The author would like to acknowledge the support of the Air Force Systems Command and the Air Force Office of Scientific Research for their support of this effort. The author would also like to thank the Eglin Air Force Base Armament Laboratory for extending the use of their research facilities. The invaluable assistance from Mr. M. E. Nixon and Lt. D. L. May is gratefully acknowledged. Discussions with Messrs. M. E. Gunger and W. H. Cook were extremely useful in identifying pertinent characteristics of the problem examined in this study.

I. Introduction

I obtained my Ph.d Degree from Stanford University in July 1982. As a graduate student, I investigated efficient methods of automated structural synthesis, an area in which I first developed interest during a summer program at NASA Langley Research Center. I continued to work in optimum design methods during a one-year postdoctoral assignment at UCLA and consider it my primary field of research interest. The application areas at the Eglin AFB Armanent Laboratory provided some challenging extensions in the field of optimum structural synthesis. Formost amongst these is the design of structures characterized by nonlinear analysis and a variable geometry of the computational domain.

II. Objectives of the Research Effort

Significant advances in digital computing capabilities, coupled with parallel development of more efficient methods of analysis, have contributed to the emergence of automated structural synthesis as a viable design tool. Early contributions to the concept of optimum structural design can be found in publications of Maxwell [1] and Michell [2]. The 1950's witnessed the development of the simultaneous failure mode theory [3], in which a structure was considered optimal if it failed in each of the several failure modes at the same load condition. The contemporary approach to the optimum structural synthesis problem can be traced to the pioneering efforts of Schmit [4]. The past two decades have witnessed considerable research activity in the field and has resulted in the emergence of two distinct approaches - the optimality criteria methods [5] and the nonlinear programming technique [6]. An extensive review of the literature in this period is documented in [7]. Of the optimality criteria and the nonlinear programming strategies, the latter is considered a more general approach, and is used in the work described in this report.

The nonlinear programming approach has enjoyed considerable success in the design of elastic structural systems subjected to static load conditions. The methodology involves the coupling of a mathematical nonlinear programming algorithm to an analysis procedure for a given problem domain, to obtain an optimization programming system [8]. Despite the apparent success of this approach, there are several drawbacks that

must be considered in its implementation. Strictly speaking, the problem of optimal structural synthesis is one of repetitive analysis of candidate designs, to obtain the best in terms of a prescribed set of conditions. Rather than use a random selection of the trial designs, the optimization algorithm provides a systematic search procedure. Furthermore, the search for new designs is terminated when certain mathematically determined conditions for optimality, such as the Kuhn-Tucker conditions [9], are satisfied. The search techniques for constrained optimization problems need the gradients of the constraints and the objective function, in addition to the function values. Hence, in the presence of a large number of design variables and constraints, such methods become extremely inefficient from a computational standpoint.

Several approaches have been suggested to circumvent the problems of large dimensionality described above. One approach to reduce the computer resource requirements is to substitute the detailed analysis of the structure by an approximate analysis of a reduced order model. Such methods have been proposed and implemented with a great degree of success. The other approach is to simplify the design space itself by reducing the number of design variables and constraints that the optimization algorithm has to contend with. Design variable linking is a process that allows the user to limit the number of design variables in the optimization. Constraint deletion and cumulative constraint representations permit a further reduction in the dimensionality of the design space. Additional savings in computational effort can be achieved by constructing high quality explicit approximations to the design space. A detailed description of these concepts is available in [10,11,12].

The developments described above have been largely confined to the design of statically loaded, elastic structural systems. Constraints obtained from a dynamic loading environment have largely been of the form in which the natural frequencies of the structure are constrained to lie in some prespecified pockets [13]. Transient response constraints [14], and constraints from a random loading environment [15] have received little attention in this effort. Also included in the latter category is the optimum design of structures which exhibit geometric or material nonlinearities.

The primary focus of the work described in this effort was to assess the applicability of optimization methods in the design of structures that undergo significant plastic deformations under dynamic loads. This includes the development of an optimization programming system for the task. An additional task was to identify the problem areas typical of this class of structures, where the analysis is inherently nonlinear and does not lend itself conveniently to the approximation concepts developed in context of optimum design of elastic systems. The test problem chosen for this task was a shell colliding against a rigid wall with a prescribed velocity, resulting in severe plastic deformations in the structure. An interesting feature of the proposed problem is its resemblance to a shape optimization problem, a subject that has received considerable recent attention [16,17]. Subsequent sections of this report describe the structural optimization problem, the implementation of the cumulative constraint concept to circumvent the parametric nature of the design constraints, the description of the optimization programming system and preliminary results for the test problem. Shortcomings in the present approach are also identified.

III. Mathematical Problem Statement

The general statement for a nonlinear programming optimum design problem can be written as follows.

$$\text{Minimize} \quad W(\bar{d}) \tag{1}$$

$$\text{Subject to} \quad g_j(\bar{d}) \leq 0 \qquad j=1,2,\ldots m \tag{2}$$

$$h_k(\bar{d}) = 0 \qquad k=1,2,\ldots p \tag{3}$$

$$d_i^{\ell} \leq d_i \leq d_i^{u} \qquad i=1,2,\ldots n \tag{4}$$

Here, $W(\bar{d})$ is the objective function and in structural optimization problems, is typically the structural weight; $g_j(\bar{d})$ and $h_k(\bar{d})$ are the inequality and equality constraints that prescribe bounds on the response quantities of interest. The constraints are generally defined in a normalized manner as follows.

$$g_j(\bar{d}) = \frac{z(\bar{d})}{z_{all}} - 1 \leq 0 \tag{5}$$

Here, $z(\bar{d})$ is the response quantity to be constrained and in structural design would typically be the element stress, nodal displacement, natural

frequency of the structure or a buckling load parameter; z_{all} is the prescribed bound on this response quantity. The vector $\overline{d}$ represents the design variables that are to be optimally assigned in the optimization algorithm and are generally the element member sizes, material properties or geometry definition parameters. The individual components d_i of the design variable vector have prescribed lower and upper bounds d_i^{ℓ} and d_i^{u}, respectively. These permit specification of limits on design variable changes to achieve the desired objective. It is important to note that the objective and constraint functions are, for most realistic structural design problems, implicit functions of the design variables. The sensitivity of these functions for the design variables must be obtained by numerical techniques.

IV. The Feasible Usable Algorithm

The optimization algorithm adopted in the present work is based on the feasible directions approach of Zoutendijk [18] and is the basis of a constrained minimization program CONMIN [19]. The basic approach of this technique is described herein for completeness. Consider the scalar objective function $W(\overline{d})$ that is to be minimized subject to the constraints $g_j(\overline{d}) \leq 0$, $j=1,2,\ldots,m$, where W and g_j are general nonlinear functions of the design variables. The feasible directions approach is in the category of direct methods for constrained optimization and proceeds towards the optimum in a sequence of design variable update cycles of the form

$$d_i^{j+1} = d_i^j + \alpha^* S^j \tag{6}$$

where, S^j is the direction of search established by the algorithm and α^* is the step size that must be taken in the direction of the proposed search. The search direction is deemed to be feasible if a small move in that direction from the current design does not cause an increased violation in the constraints. For linear and convex constraints, this can be mathematically stated as

$$S^T \nabla g_j \leq 0 \tag{7}$$

where the equality condition is applicable in the case of linear and outward-curving constraints. Further, the direction is considered to be

both feasible and usable, if in addition to (7), the following inequality is also valid.

$$S^T \nabla F < 0 \qquad (8)$$

This represents an improvement in the objective function for a minimization problem. A geometric interpretation of this approach is shown in Figure 1. The inequalities (7) and (8) result in a feasible-usable sector in the design space in which the search must proceed. The step size selection for the algorithm is based on a one dimensional search along this direction. The basic technique used in CONMIN is to minimize W along a steepest descent direction until one of the constraint boundaries is encountered. The search then proceeds along this boundary till the objective function can no longer decrease. The significance of objective and constraint function sensitivity for the purpose of optimization is abundantly clear from this discussion.

V. High Velocity Impact Computations - EPIC 2

The analysis for the design problem considered in this study is complex, and involves the transient dynamic response of a continuum. The ability to model arbitrary geometries of the continuum is of absolute essence in any automated design environment, and hence a discrete numerical approach is preferred. The EPIC-2 computer program is configured to obtain solutions for dynamic response analyses in impact and detonation problems, for plane strain and axi-symmetric situations. Furthermore, it has the capability to model strain hardening and high strain rate effects that are typical of the problem under consideration. The geometry of the domain is discretized into triangular elements, with lumped masses at each node. The displacements within the elements are assumed to vary linearly between the nodes, giving the triangular elements the semblance of constant strain triangles in the finite element method. The solution grid is Lagrangian in that it moves with the material during elastic and plastic flow. For an initial set of prescribed displacements and velocities, the strains and strain rates are determined by considering the spatial derivatives of the former. The strains are then used to determine the stresses using the constitutive laws. Once the element and nodal stresses are established, the corresponding nodal forces and and

nodal accelerations can also be determined. New estimates of the nodal velocity are obtained by a linear extrapolation of the velocity at the previous time step and from the acceleration determined for that step. This process is repeated for the time period of interest and a time history of the quantities of interest such as strains, stresses and pressures are stored for postprocessing. Additional details on the theoretical and computational aspects of EPIC-2 are available in [20].

VI. Efficient Methods of Constraint Representation

The pressure and strain information available from EPIC-2 is a function of time and the design constraints to limit these responses to allowable values during some predetermined initial period of impact, can be written as follows

$$|\varepsilon_i(\bar{d},t)|/\varepsilon_{all} - 1 \leq 0 \qquad (9)$$

$$|p_j(\bar{d},t)|/p_{all} - 1 \leq 0 \qquad (10)$$

where, p_{all} and ε_{all} are the upper bounds on the pressure within the explosive and the strains in the structural shell, respectively. The constraints denoted by (9) and (10) are parametric in time and a maximum response cannot be determined by either a close form evaluation or a functional maximization, particularly in the case of the pressure, which is a nonconvex function of time. A discrete sampling of the response is therefore used to represent the pressure and strain constraints. To avoid the problem of misrepresenting the maximum response, a large number of closely spaced points must be considered in the solution. This, coupled to the sizeable number of elements that one must include in a relatively coarse model of the structure, would result in an inordinately large number of design constraints for the problem.

This problem can be addressed by recourse to the cumulative constraint formulation which allows the user to denote a large number of design constraints by a single representative measure. For the design constraints g_j, $j=1,2,\ldots,m$, the representative cumulative constraint g is written as follows

$$\Omega = \begin{cases} -\varepsilon + \sum_{j=1}^{m} \langle g_j \rangle^r & \text{if } \Omega > \psi \\ -\varepsilon + \frac{1}{\rho} \mathrm{Ln}\left(\sum_{j=1}^{m} \exp(\rho g_j) \right) & \text{if } \Omega < \psi \end{cases} \qquad (11)$$

where $$\langle g_j \rangle = \begin{cases} g_i & \text{if } g_i > 0 \\ 0 & \text{if } g_i < 0 \end{cases}$$

where, 'ψ' is a preselected parameter (order 10^{-1}) that allows transition from one formulation to the other and is chosen such that the change occurs close to the constraint boundary; r is a constraint smoothing factor typically chosen as 2 but is reduced as the constraint approaches the boundary; 'ρ' is the constraint participation factor and its numerical value is typically of order 100. The constraint participation factor is such that the most critical constraint dominates the cumulative function. If a smaller value of ρ is chosen, a smear of a larger number of constraints can be obtained in the cumulative constraint. Discussions pertaining to the mathematical validity of the constraint representation are available in [21].

VII. Implementation of the Programming System

A. Program Structure.

The analysis and optimization programs described in the preceeding sections were coupled into an automated synthesis environment by a sequence of pre- and post-processor programs. The flow between these programs and the other processors was controlled in the Command Language feature of DEC systems, and is best illustrated in the annotated flowchart shown in Figure 2. This section of the report describes the specific tasks of each module in the flowchart, including a description of the data files that are necessary in the present implementation.

A typical input runstream for the program EPIC-2 can be broken down into three segments. The first deals with input information pertaining to the task that is to be performed, i.e., whether the program is to be run as a preprocessor only, or if dynamic response computations are required. It also contains input on what information is to be saved for post-processing. The second portion of a typical runstream is devoted to the definition of the geometry of the problem domain and a third segment

details element connectivity information and additional information pertaining to velocity of impact and time for which response must be tabulated. In a typical synthesis procedure, it is the geometry of the structure that is generally changed to achieve the desired objectives.

The program PREEPIC is the preprocessor to EPIC-2, and is configured to generate new geometry information for the program in a desired format. It makes use of the design variables, which in the present problem are r or z coordinates of nodes, and computes the location of other node points in a grid, the order of which is predetermined and not allowed to vary. The design variable data is contained in a data file DESIGN which also contains lower and upper bounds on the design variables. Other parameters that describe the geometry of the structure but do not change in the resizing, are contained in another data file GEOM. All data files in the present task are unformatted for ease of programming.

The optimization algorithm requires not only the function information for the pressures and strains, but also the sensitivities of these response quantities for each design variable. This sensitivity is obtained by a first order finite difference approximation, by perturbing each design variable, one at a time. Hence, for n design variables, the analysis to obtain the response sensitivities must be repeated n+1 times. The parameter that identifies the variable to be perturbed is in the data file NDVNCON, which also contains information on the number of design variables and constraints, the number of explosive and structural elements, and the step size for the finite difference approximation.

Each new runstream created by the preprocessor is executed by EPIC and the output information is postprocessed in the program POSTEPIC. Here, the cumulative constraints for the strain and pressure constraints are computed and stored in a data file CONFUN for computing the sensitivity information. The latter information is obtained in program GRAD and transferred to the optimization program CONOPT in a data file GGRAD. The program CONOPT contains the call to the constrained minimization program CONMIN and also provides the latter with objective function and constraint information as required. The flow chart illustrating the execution of the optimization program is shown in Figure 3.

For purposes of computational efficiency, the nonlinear optimization problem was replaced by a sequence of piecewise linear approximations. Consider the case of a general nonlinear objective function $F(\bar{x})$ to be minimized subject to nonlinear inequality constraints $g_j(\bar{x})$, j=1,2,...,m, and prescribed lower and upper bounds on the design variable vector, x_i^{ℓ} and x_i^{u}, respectively. At any given point in the design space, the objective and constraint functions can be assumed to be linear for small changes in the design variable vector. The function sensitivities can be obtained at the given point and updated values of the functions can be written as follows.

$$F(\bar{x} + \Delta\bar{x}) = F(\bar{x}) + \nabla F(\bar{x}).\Delta\bar{x} \tag{12}$$

$$g_j(\bar{x} + \Delta\bar{x}) = g_j(\bar{x}) + \nabla g_j(\bar{x}).\Delta\bar{x} \tag{13}$$

The validity of these approximations is ensured if the change in the design variable vector is restricted to be a small one. One possible approach of ensuring this is to permit a ±20% change in each component of the design vector for any piecewise cycle. The optimization problem statement for such a repetitive piecewise linear approximation can be stated as follows.

Minimize	$F(\bar{x})$	(14)
Subject to	$g_j(\bar{x}) \leq 0$	(15)
	$0.8\ x_i \leq x_i \leq 1.2\ x_i$	(16)
	$x_i^{\ell} \leq x_i \leq x_i^{u}$	(17)

This process is repeated till the constraints are satisfied and the objective function does not show an appreciable change in successive iterations.

B. The Test Problem Description.

The projectile shown in Figure 4 is chosen as a test problem to assess the validity of the programming system implemented in this study. The projectile has a steel shell and is packed with an explosive charge.

It impacts a rigid target, normal to the surface and at a prescribed velocity. The rigid target assumption was made to reduce the complexity of the analysis problem as would be introduced if the projectile were allowed to penetrate the target. The impact causes severe plastic deformations to develop in the structural shell and also introduces a pressure pulse into the explosive charge. The optimum design requirements were formulated to maximize the total internal volume and hence the explosive carrying capacity of the shell. The design constraints include an upper bound on the plastic strains at any point in the shell and on the maximum pressure in the explosive. An additional constraint was imposed requiring the ratio of the explosive weight to the structural weight to be above some prespecified value.

A mathematical statement of this problem can be formulated as follows

$$\text{Maximize } V \equiv \text{Minimize } (-V(\bar{x})) \tag{18}$$

where V is the internal volume of the shell

$$\text{Subject to } g_1 \equiv \Omega_1(\varepsilon_i, \varepsilon_{all}) \leq 0 \tag{19}$$

$$g_2 \equiv \Omega_2(p_i, p_{all}) \leq 0 \tag{20}$$

$$g_3 \equiv 0.675\, W_{exp}/W_{str} - 1 \leq 0 \tag{21}$$

In the above expressions, the values of ε_{all} and p_{all} are 0.5 and 0.725×10^6 psi, respectively; W_{exp} and W_{str} are weights of the explosive and the structural shell. The time duration of impact for which these conditions are to be satisfied was chosen as 80 μsecs. The constant 0.675 of (21) was selected on the basis of typical explosive to structure weight ratio in a 500lb class warhead. The design variables selected for this study are designated as x_i, i=1,2,...,5, in Figure 4.

VIII. Numerical Results

Numerical results for the problem described in the preceeding section, were obtained for two specific cases. The first, involves a fixed external geometry and variation of the first three design variables only. This permits a change in the internal geometry of the shell. To obtain a better understanding of the design space, parametric variations of the design variables were attempted to observe their influence on the

IX. Concluding Remarks

The report describes the preliminary implementation of an optimum synthesis methodology for the sizing of structures that are subject to high strain rate deformations. The use of hydrocodes for analysis appears to be a logical choice for this class of problems. In the current application, the hydrocode EPIC-2 was coupled to a feasible usable search directions program CONMIN, to obtain the synthesis procedure. Numerical testing of the proposed method indicates the potential for using such techniques in the design process. Extension of the current work to include target penetration and the associated time dependent pressure boundary condition on the shell, is a natural choice. Despite the encouraging results obtained in this effort, there are several issues that need to be addressed at a fundamental level.

At the very outset, it is important to emphasize the considerable investment of computational resource required for hydrocodes to run in a repetitive analysis mode. For the class of problems examined in this effort, it appears that the constraint functions can be approximated by explicit linear or quadratic functions. Approximate analysis procedures, similar to the reduced basis concepts in the synthesis of elastic structural systems, must be explored in some detail. The design problems that are most likely to be addressed in such an environment, includes the element of shape change in the basic configuration. This is a relatively new discipline in the field of automated synthesis and requires a focused effort in context of this problem. The response sensitivities generated by perturbing the nodal coordinate system also include the effect of a reorienting grid system. This effect must be isolated to obtain better convergence characteristics in the optimization process. The current set up is somewhat limited in that the order of the grid is not allowed to vary in the optimization. This places a restriction on the allowable changes in the design variable. A variable order, adaptable grid for the analysis problem is seen as a possible solution to this problem.

Ongoing research on this subject is expected to address some of the problems outlined above and will be reported in other publications.

X. References

1. Maxwell, C., Scientific Papers, Vol. 2, 1869.

2. Michell, A.G.M., "The Limits of Economy of Material in Frame Structures," Philosophical Magazine, Series 6, Vol. 8, 1904.

3. Cox, H.L., The Design of Structures of Least Weight, Pergamon, New York, 1956.

4. Schmit, L.A., "Structural Design by Systematic Synthesis," Proceedings of the 2nd Conference on Electronic Computation, ASCE, New York, 105-122, 1960.

5. Berke, L. and Venkayya, V.B., "Review of Optimality Criteria Approaches to Structural Optimization," presented at the ASME Winter Annual Meeting, New York, November 1974.

6. Schmit, L.A. and Pope, G.G., "Introduction and Basic Concepts: Structural Design Applications of Mathematical Programming Techniques," AGARDograph 149, Chapter 1, 1971.

7. Schmit, L.A., "Structural Synthesis - Its Genesis and Development," AIAA Journal, Vol. 19, No. 10, October 1981.

8. Rogers, J.L., Jr., Sobieski, J.E., and Bhat, R.B., "An Implementation of the Programming Structural Synthesis System (PROSSS)," NASA TM-83180, December 1981.

9. Rao, S.S., Optimization - Theory and Applications, Wiley Eastern, New Delhi, 1979.

10. Schmit, L.A. and Miura, H., "Approximation Concepts for Efficient Structural Synthesis," NASA CR-2552, March 1976.

11. Schmit, L.A., "Some Approximation Concepts for Structural Synthesis," AIAA Journal, Vol. 12, No. 5, 1974.

12. Hajela, P., and Sobieski, J.E., "The Controlled Growth Method - A Tool for Structural Optimization," AIAA Journal, Vol. 20, No. 10, October 1982.

13. Fox, R.L., and Kapoor, M.P., "Structural Optimization in the Dynamic Response Regime," AIAA Journal, Vol. 8, No. 10, October 1970.

14. Mills-Curran, W.C., "Optimization of Structures Subjected to Periodic Loads," Ph. D. Thesis, University of California, Los Angeles, California, 1983.

15. Hajela, P., "Optimal Airframe Synthesis for Gust Loads," NASA Contractor Report CR-178947, February 1986.

15. Ramakrishnan, C.V. and Francavilla, A., "Structural Shape Optimization using Penalty Functions," Journal of Structural Mechanics, 3(4), 1975.

17. Bennett, J.A., and Botkin, M.E., "Structural Shape Optimization with Geometric Description and Adaptive Mesh Refinement," AIAA Journal, Vol. 23, No. 3, March 1985.

18. Zoutendijk, G., "Methods of Feasible Directions," Elsevier Publishing Company, Amsterdam, 1960.

19. Vanderplaats, G.N., "CONMIN - A Fortran Program for Constrained Function Minimization, Users Manual," NASA TM X-62282, August 1973.

20. Jonnson, G.R., "EPIC-2, A Computer Program for Elastic-Plastic Impact Computations in 2 Dimensions Plus Spin," Contractor Report ARBRL-CR-00373, June 1978.

21. Hajela, P., "Techniques in Optimum Structural Synthesis with Static and Dynamic Constraints," Ph. D. Thesis, Stanford University, July 1982.

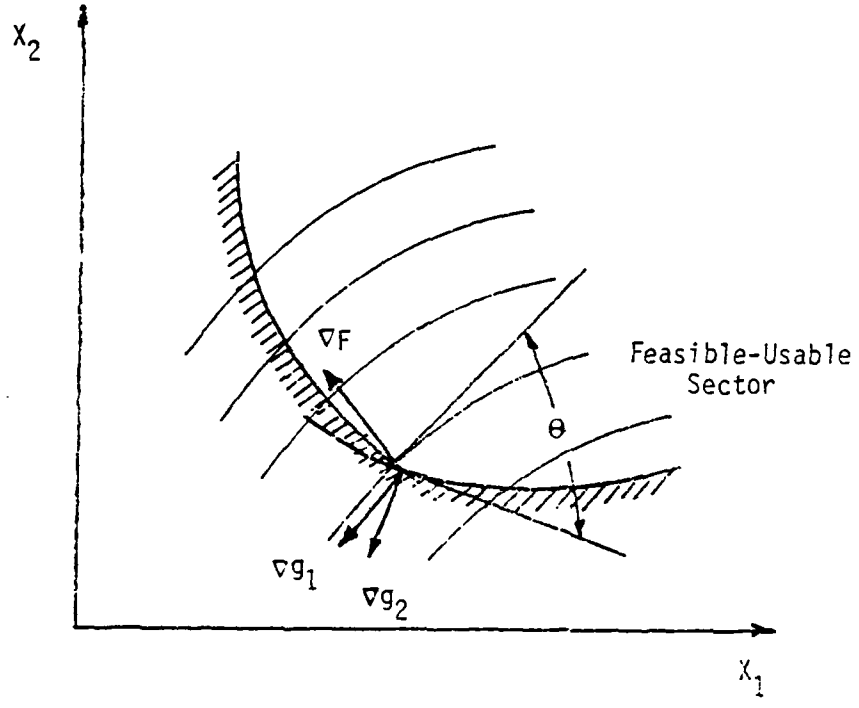

Figure 1. Geometric interpretation of the feasible usable search direction approach.

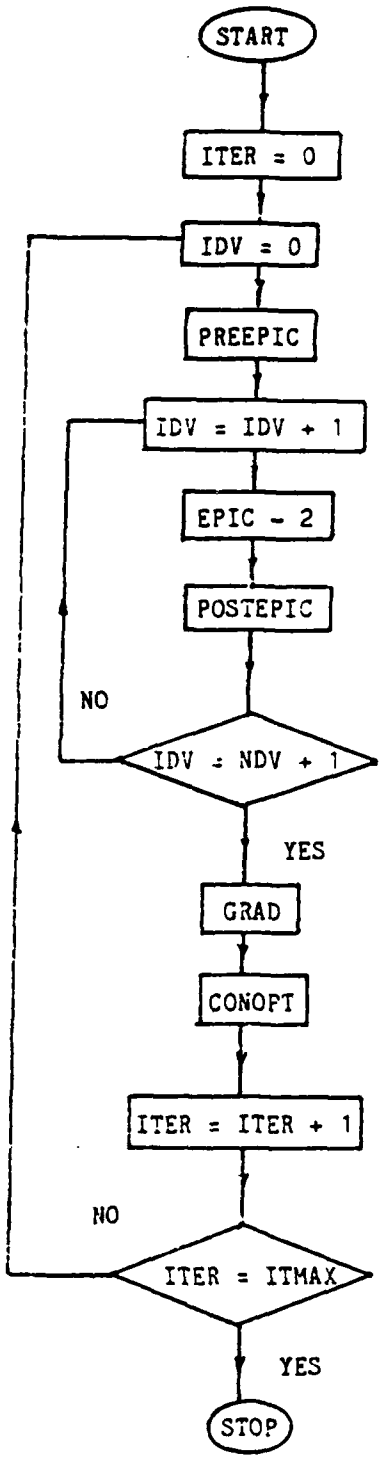

Figure 2. Flowchart for the optimization programming system.

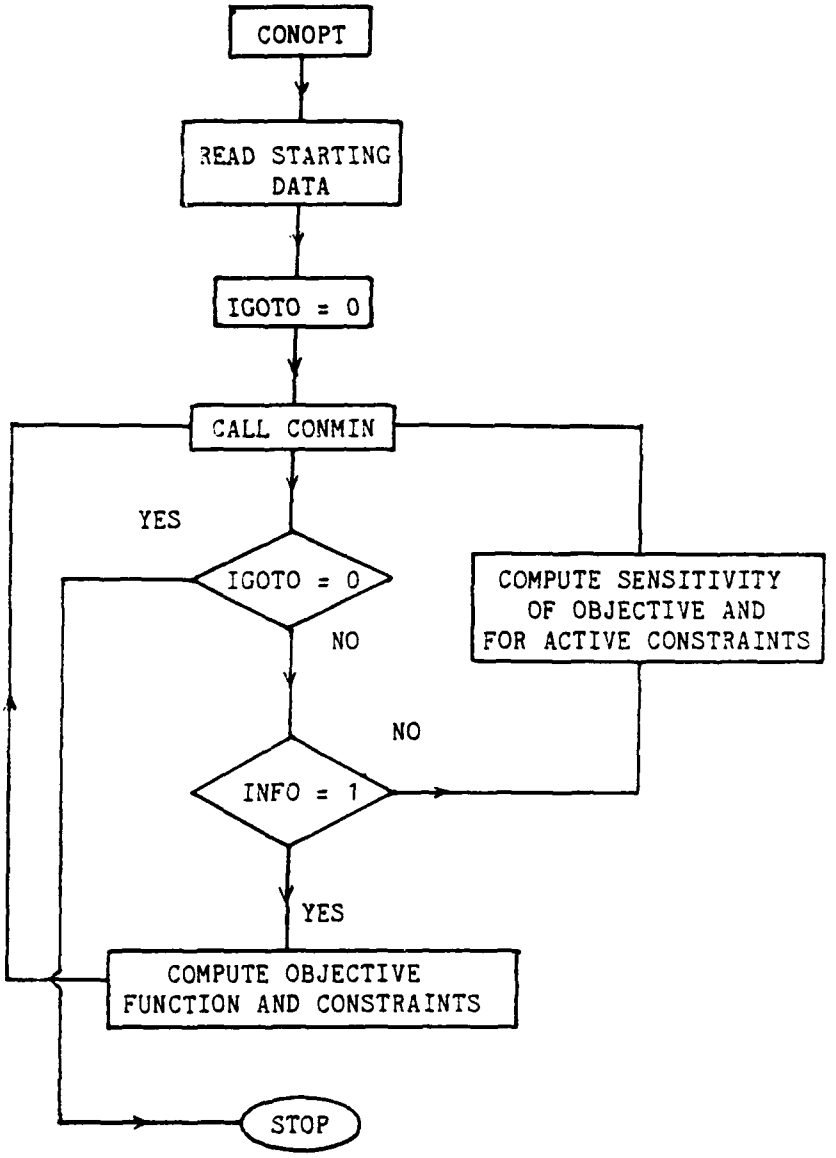

Figure 3. Flowchart for the CONMIN optimization algorithm.

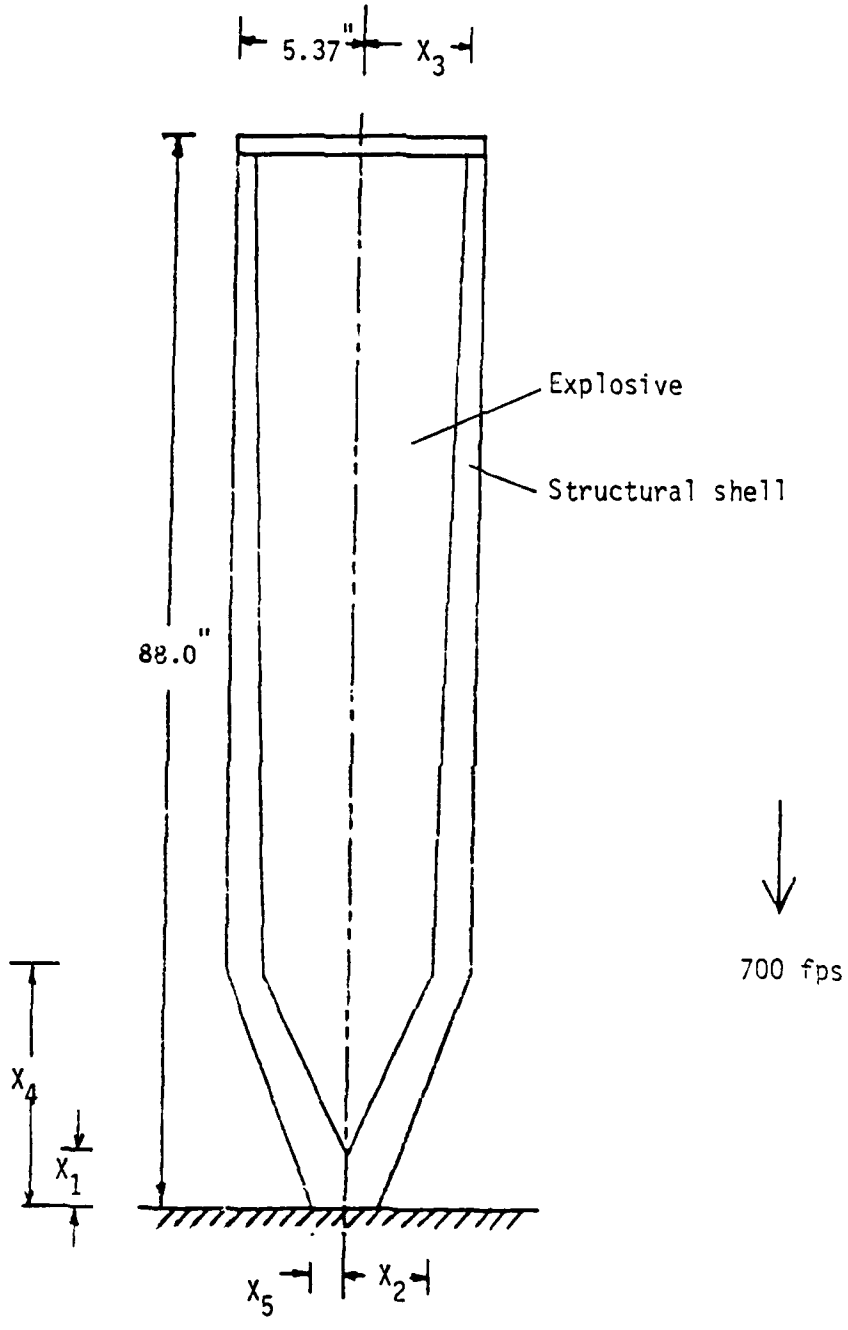

Figure 4. Projectile undergoing high speed impact against a rigid wall.

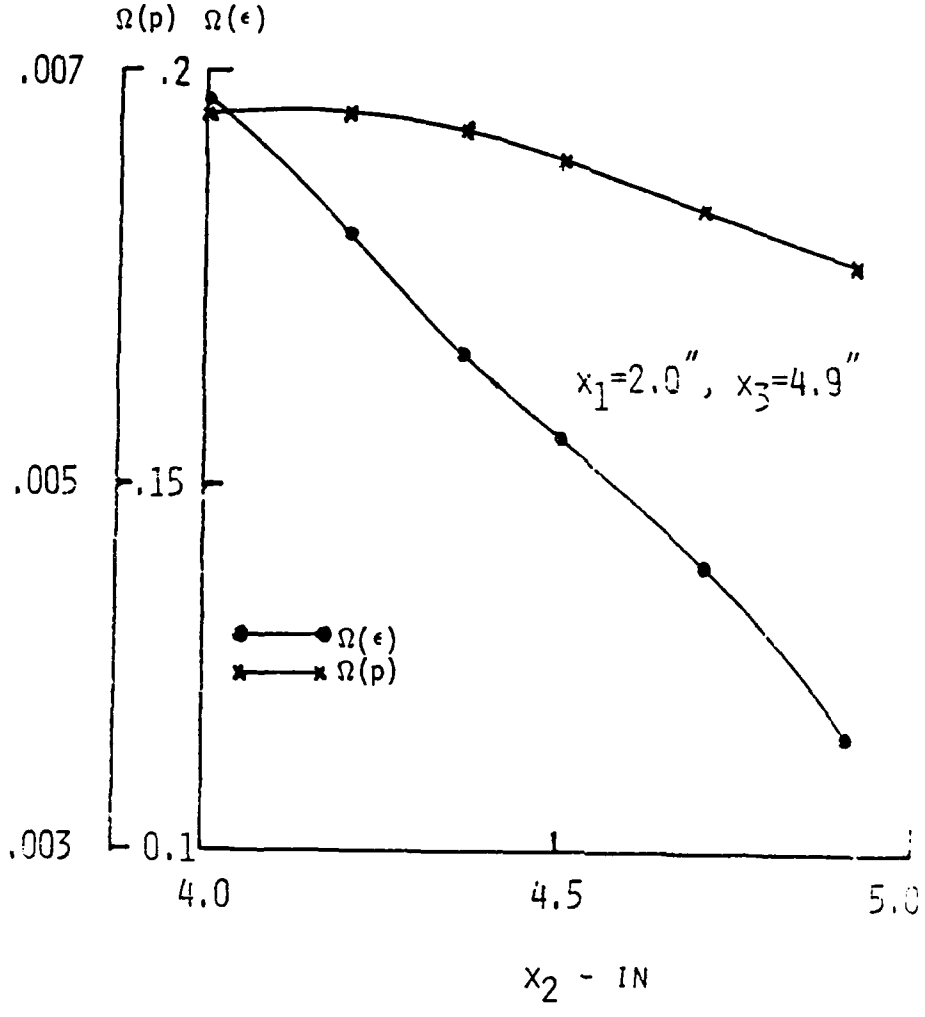

Figure 5. Effect of a parametric variation of design variables on the strain and pressure constraints.

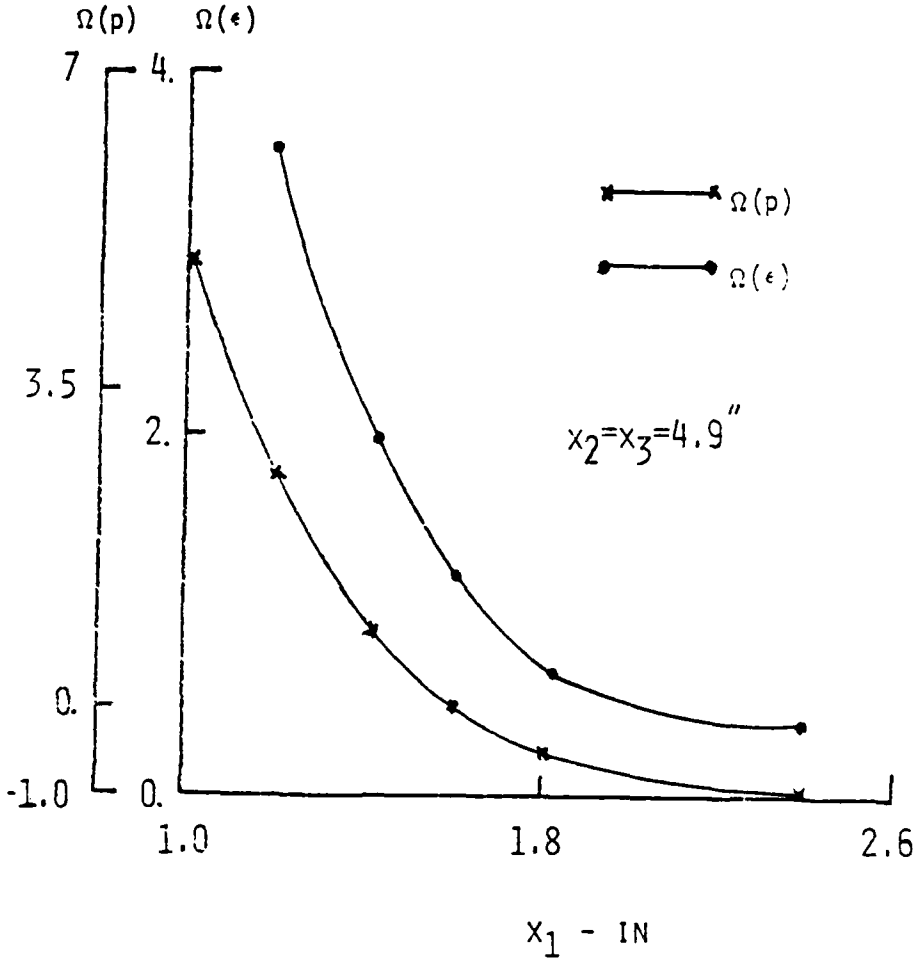

Figure 6. Effect of a parametric variation of design variables on the strain and pressure constraints.

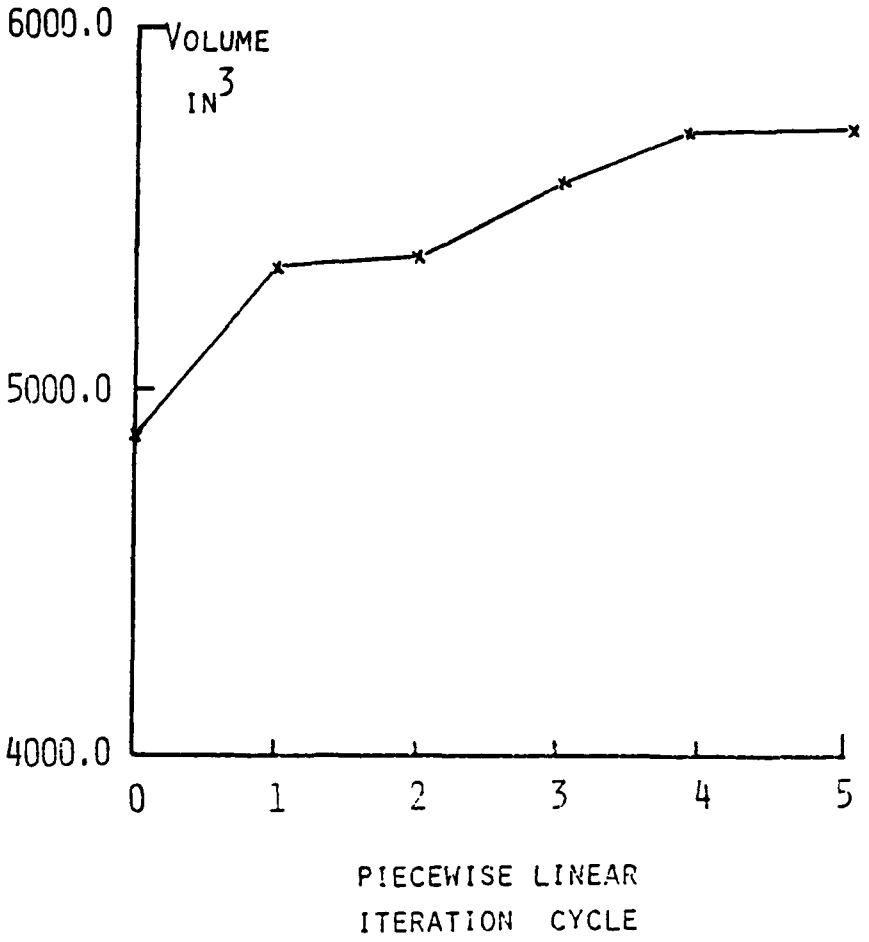

Figure 7. Iteration history for the objective function

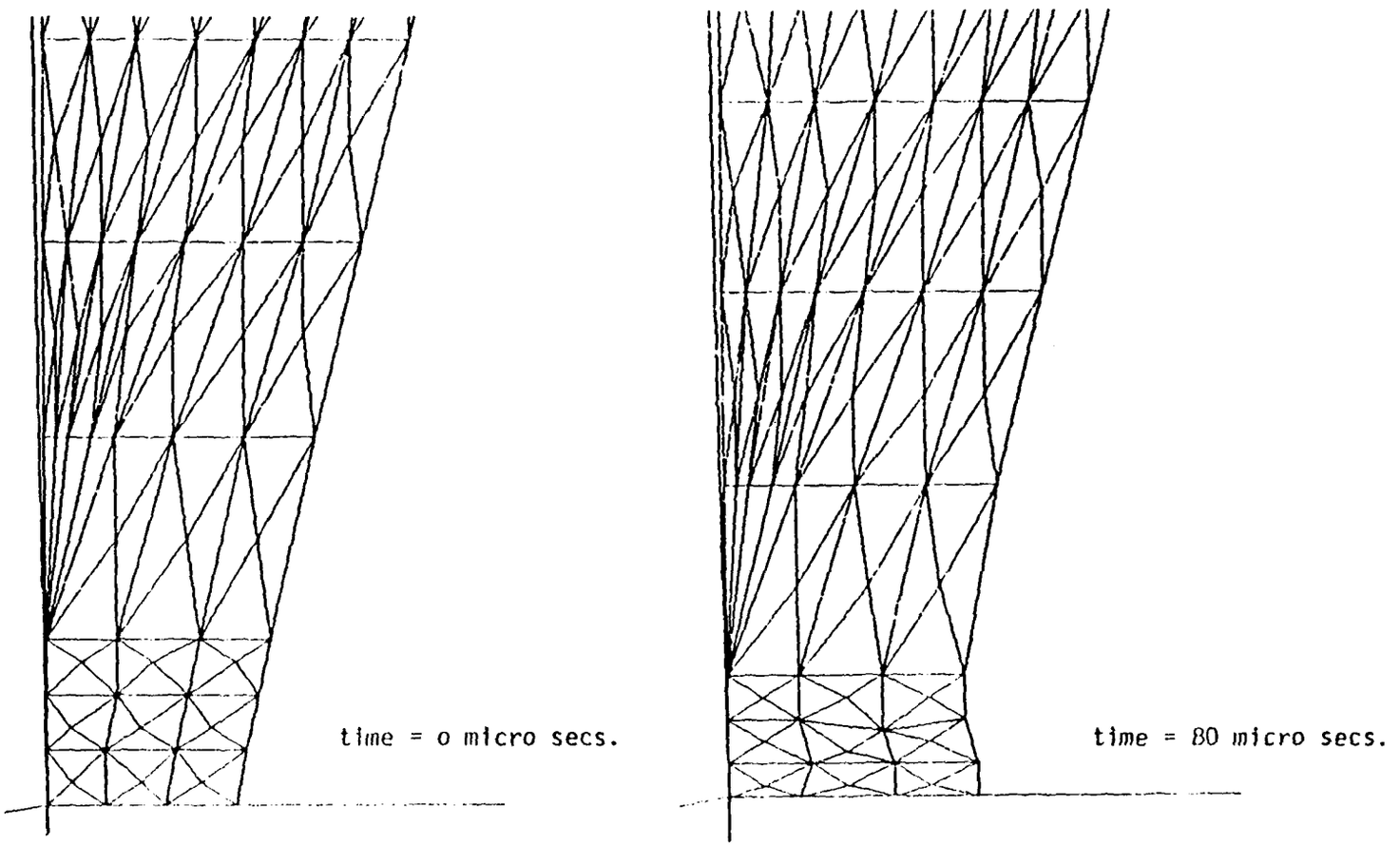

Figure 8. Initial and final geometry of the nose section of the projectile for the unoptimized design.

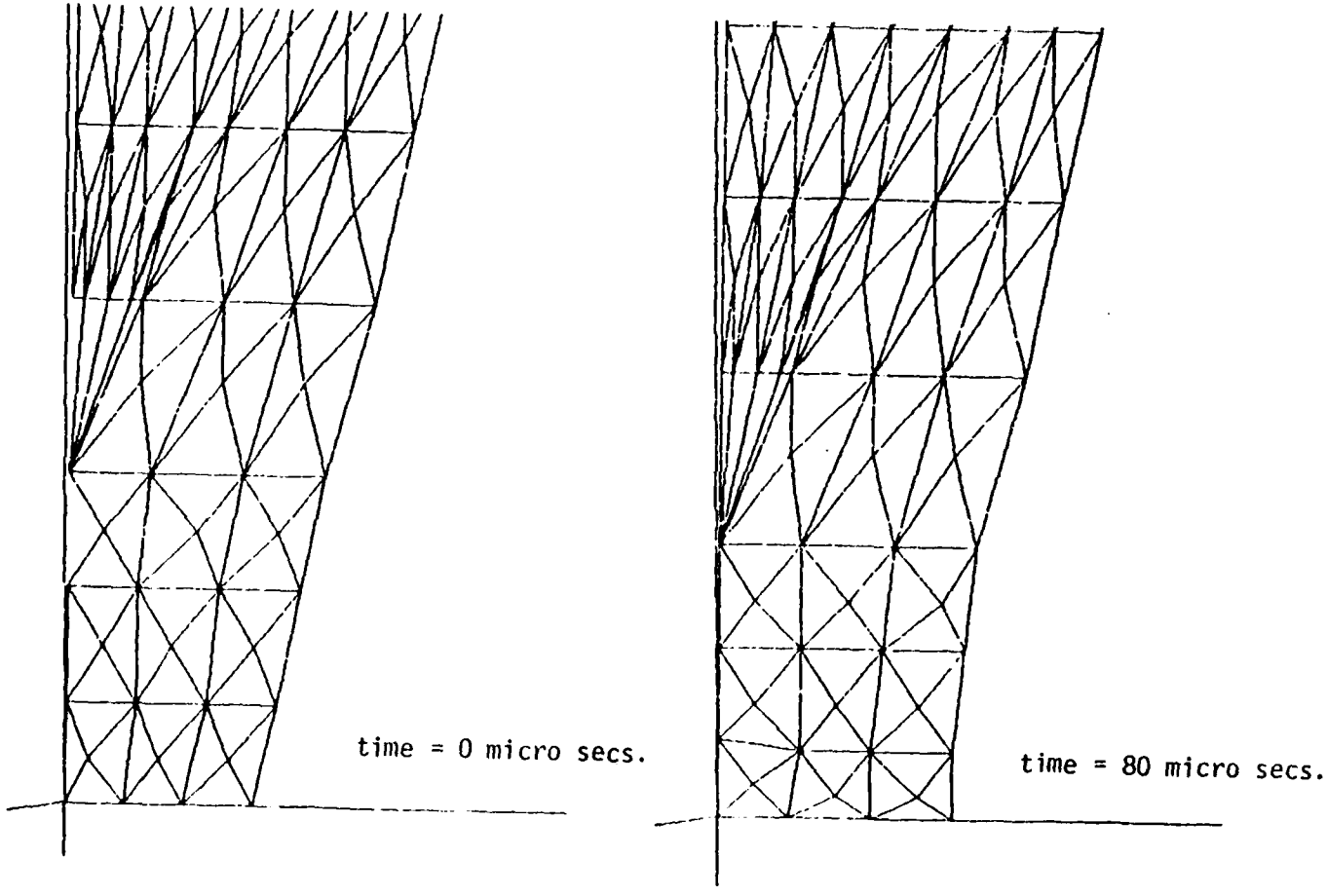

Figure 9. Initial and final geometry of the nose section of the projectile for the optimized design - 3 design variables.

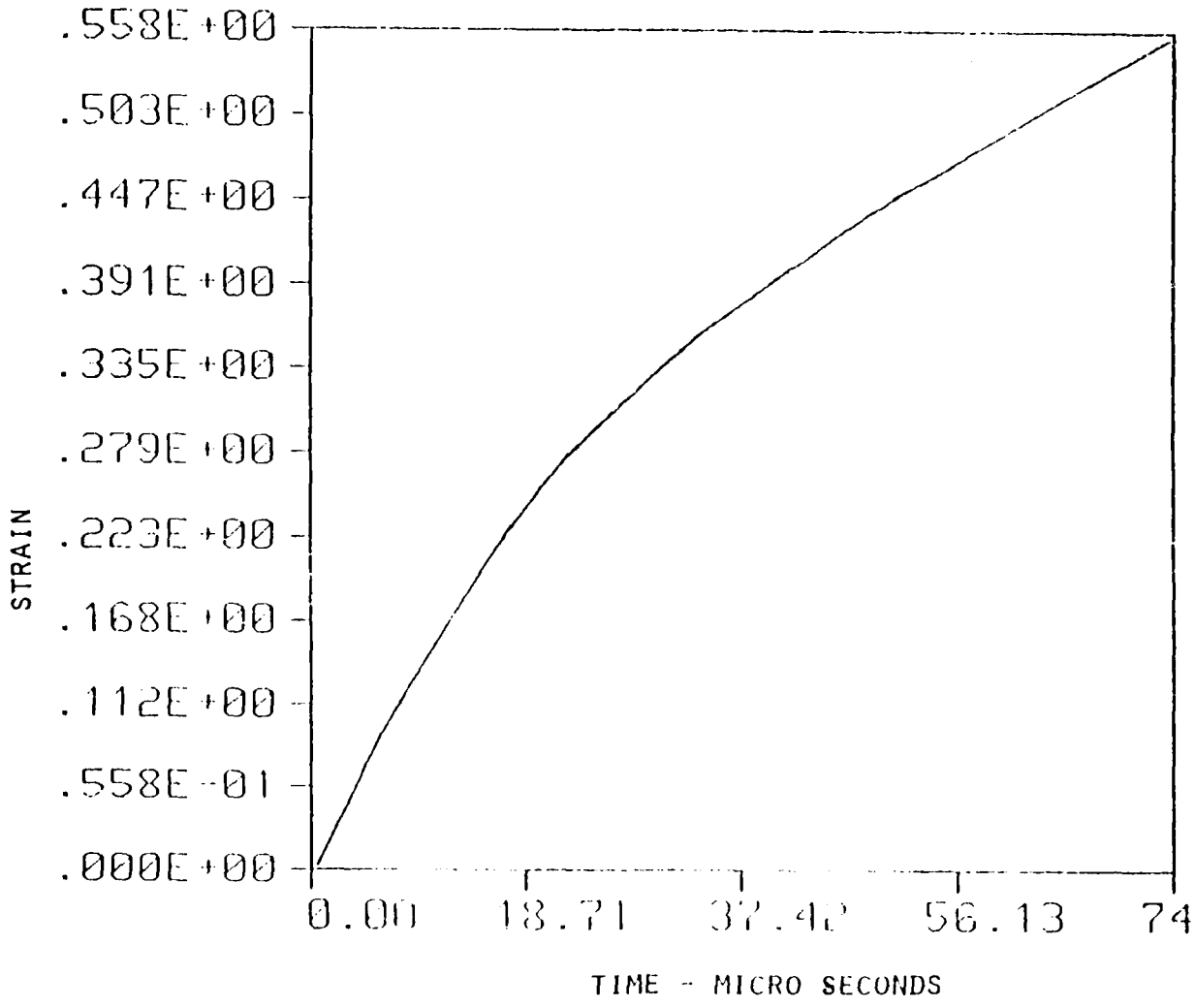

Figure 10a. Critical element strain history for the unoptimized design.

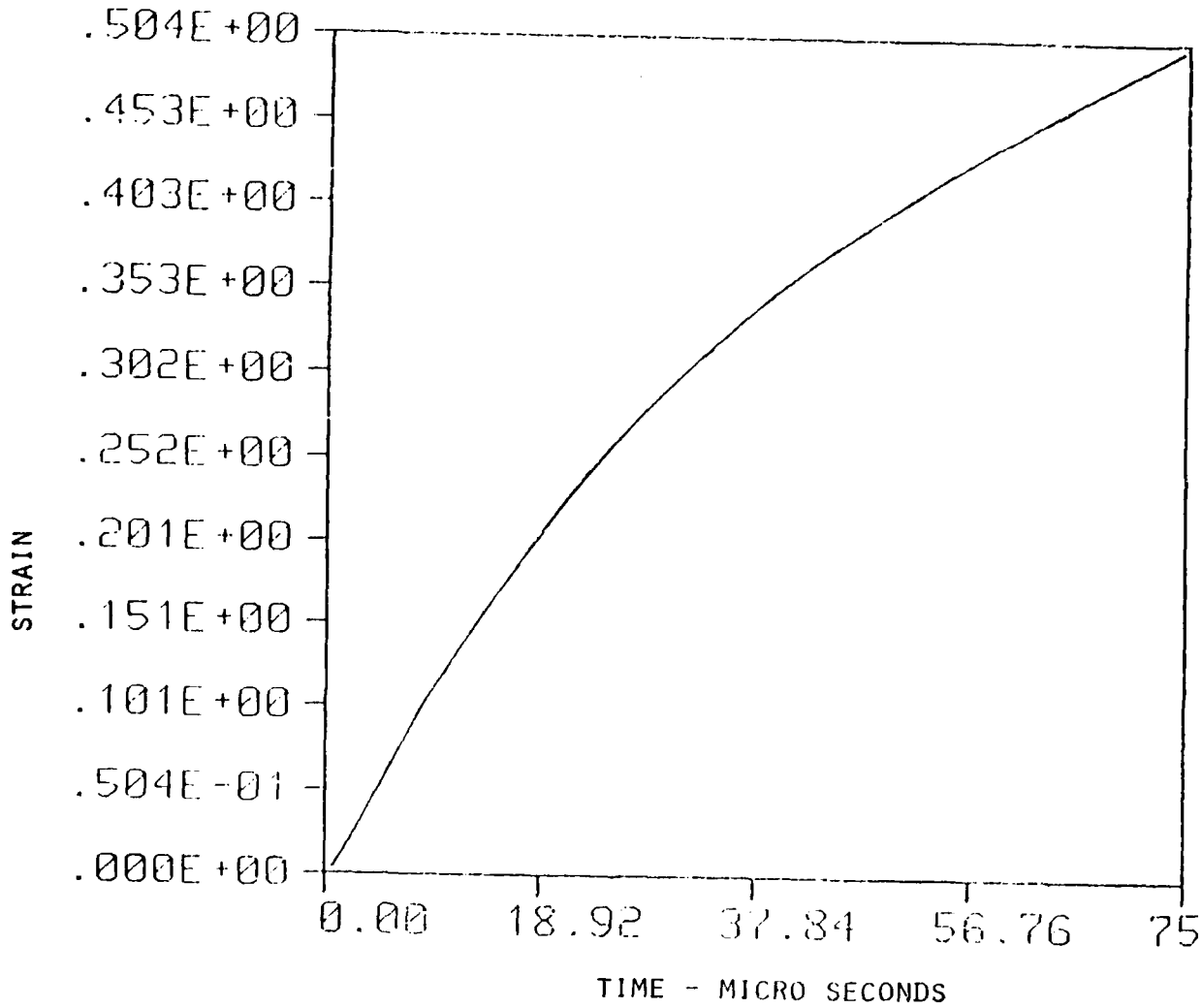

Figure 10b. Critical element strain history for the optimum design with five design variables.

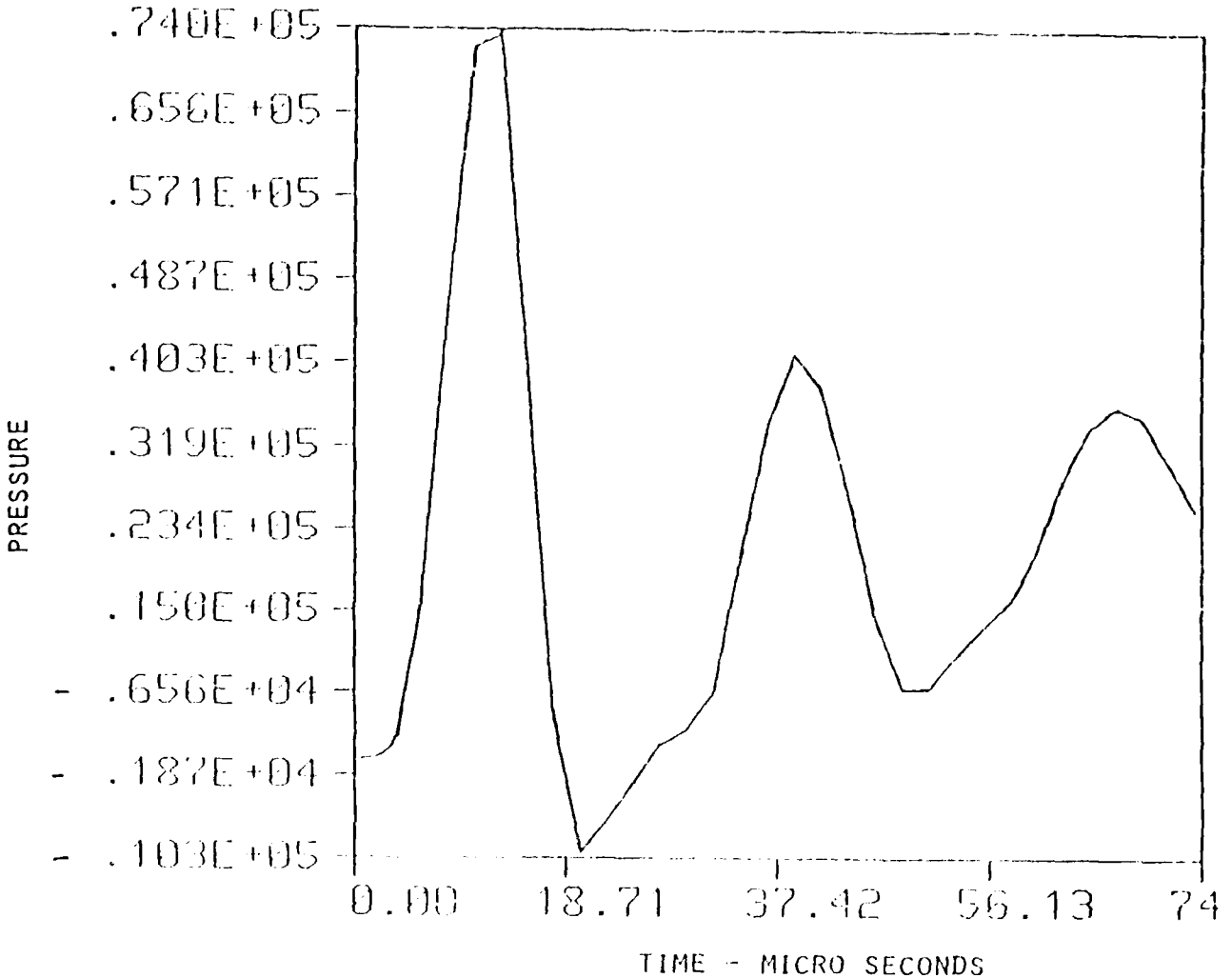

Figure 11a. Critical element pressure history for the unoptimized design.

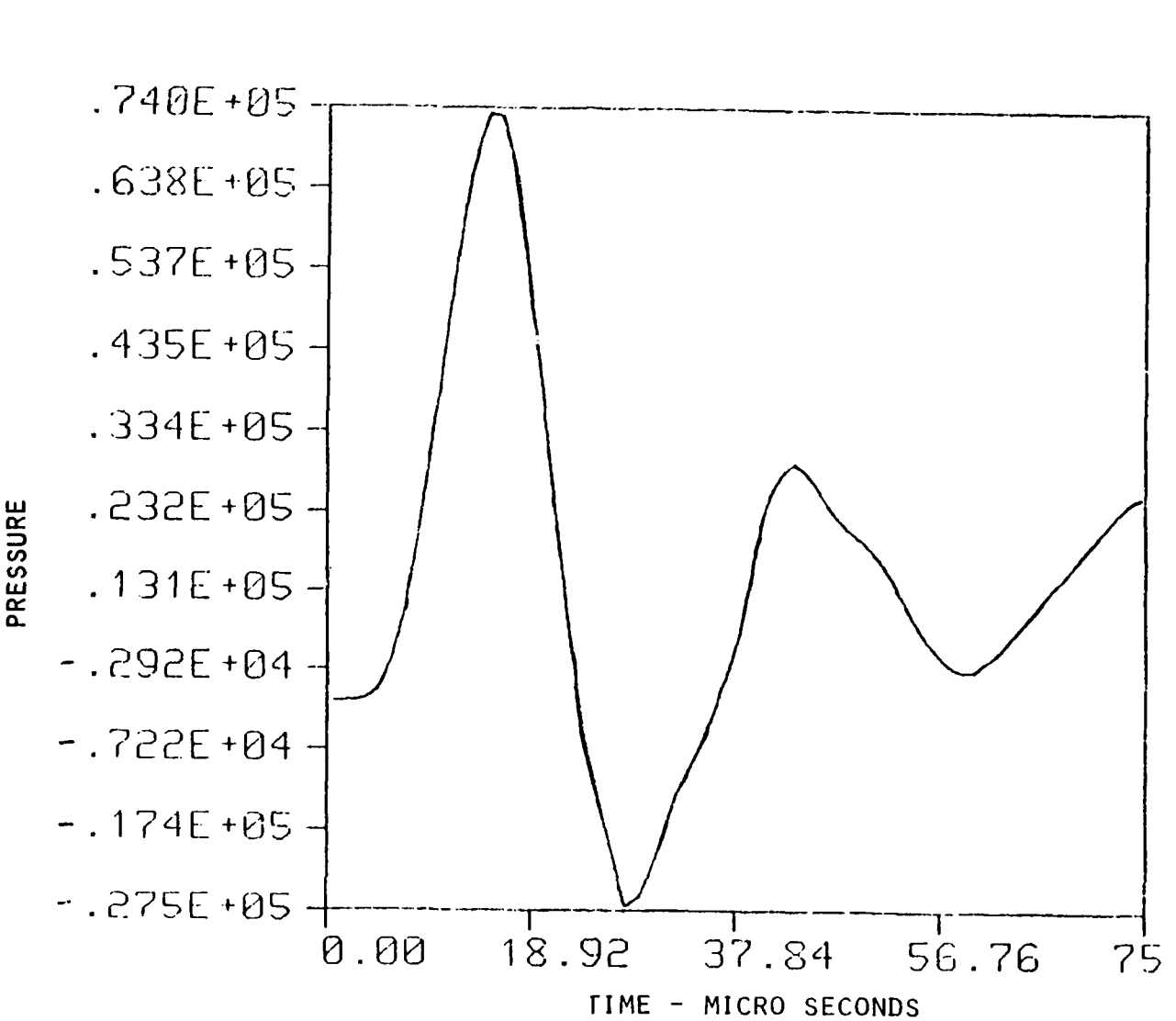

FFigure 11b. Critical element pressure history for the optimum design with five design variables.

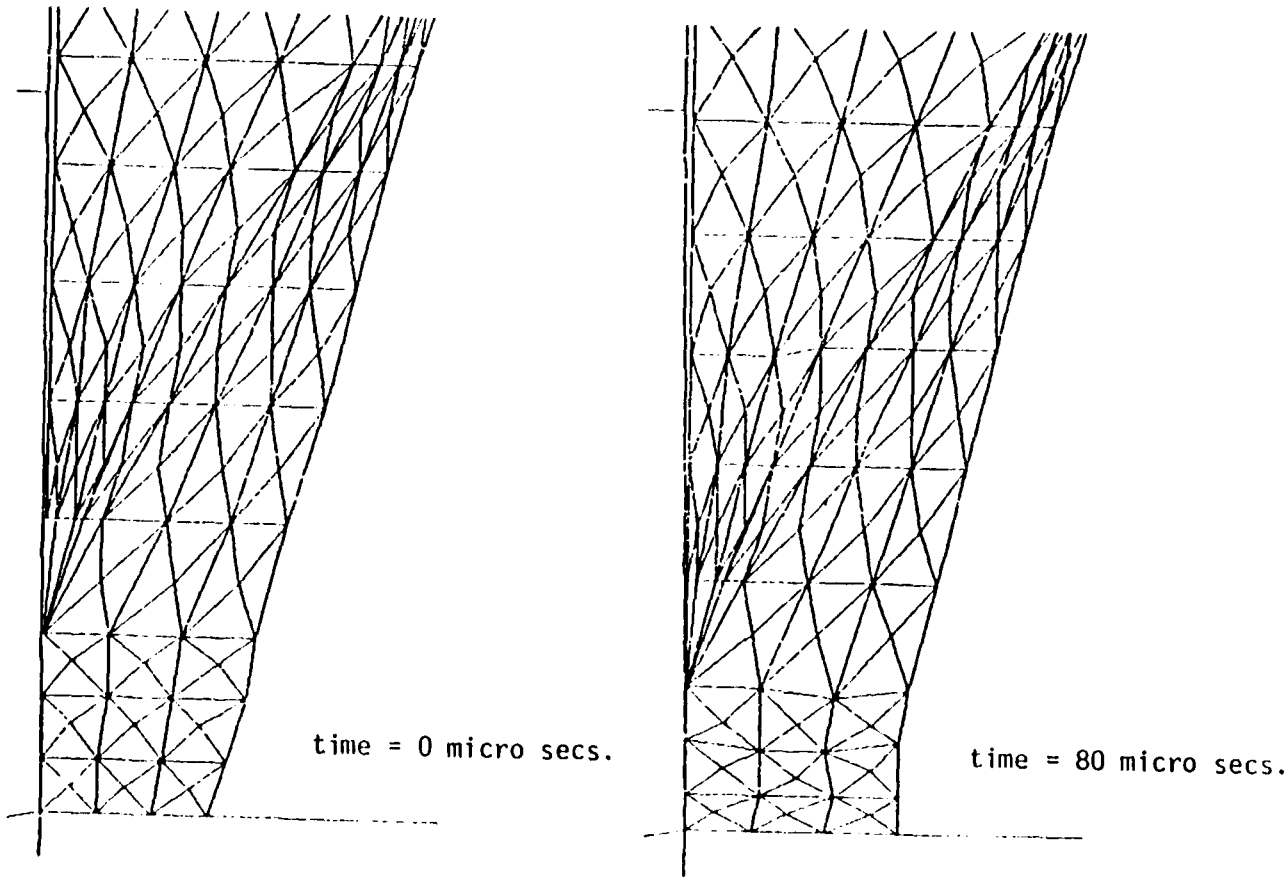

Figure 12. Initial and final geometry of the nose section of the projectile for the optimized design - 5 design variables.

1986 USAF-UES SUMMER FACULTY RESEARCH PROGRAM/

GRADUATE STUDENT SUMMER SUPPORT PROGRAM

Sponsored by the

AIR FORCE OFFICE OF SCIENTIFIC RESEARCH

Conducted by the

Universal Energy Systems, Inc.

FINAL REPORT

Modeling of Human Body Movement

Prepared by: Patrick R. Hannon

Academic Rank: Associate Professor

Department and University: Department of Health, Physical Education and Recreation, Northern Arizona University

David Jansen

Graduate Student

Department of Zoology

Washington State University

Research Location: The Harry G. Armstrong Aerospace Medical Research Laboratory, Biodynamics and Biomedical Engineering: Modeling and Analysis Wright-Patterson Air Force Base

USAF Researcher: Ints Kaleps-Chief, Modeling and Analysis

Date: September 3, 1986

Contract no: F49620-85-C-0013

Modeling of Human Body Movement

by

Patrick Hannon and David Jansen

ABSTRACT

The Articulated Total Body (ATB) model is used to simulate biodynamic responses due to forces on the human body such as localized contact forces, aerodynamic drag, or internal muscular forces. Validation and possible improvement of the model was investigated through two approaches. A skilled motor performance, the overhand baseball throw was selected as the basis for the validation study, and three-dimensional experimental data from human subjects were obtained. In the first approach, muscle forces derived from the literature were input to the model for the right upper limb. The time courses for the muscle forces were obtained from electromyography studies of overarm throwing. Good statistical correspondence between the experimental data and the output from the simulation resulted. The second approach involved prescribing the motion of a single joint (the right knuckle) and adjusting other parameters of the ATB model to obtain correspondence with the experimental data. No muscular forces were involved in this approach. Significant statistical correspondence resulted, though not as high as with the first approach. Recommendations for further validation and development of the ATB model were made.

ACKNOWLEDGEMENTS

We would like to thank the Air Force Systems Command and the Air Force Office of Scientific Research for sponsorship of our research. The Harry G. Armstrong Aerospace Medical Research Laboratory provided an intellectually stimulating environment. We would like to thank several people on the Biodynamics and Biomedical Engineering/Modeling and Analysis staff, Ms. Louise Obergefell, Dr. Bob Beecher, and Mr. Ric Rasmussen, for giving us the opportunity and the guidance necessary for our research. We would also like to thank Mr. Jim Ryerson of Systems Research Laboratories for his help in smoothing our raw data. A special thanks goes to Branch Chief Dr. Ints Kaleps for his guidance and interest in our project and also for his hospitality during this past summer.

I. Introduction

Patrick Hannon

I received my Ed. D. in Physical Education from the University of Northern Colorado with a major specialization in motor control and a minor specialization in biomechanics in 1980.

My research experience includes working in the Locomotion Laboratory of Northern Arizona University which is jointly operated by Biology and Physical Education. Much of the work done in this facility has been collaborative with Biology and Physical Therapy professors. My faculty exchange experience during the 1984-85 academic year at Montana State University allowed me to work with Dr. Ellen Kriegbaum in biomechanics and Dr. Jim McMillan in neurophysiology.

David Jansen

I am currently a Ph. D. candidate at Washington State University (WSU). My dissertation involves the evolution and biomechanics of the cephalic region of venomous snakes. During my research I employed static analysis to describe the actions of snake jaws. It was also necessary to mathematically model the results, using a microcomputer.

I was also trained in human anatomy while at WSU, having spent five years teaching anatomy of the head, neck and trunk to medical students.

The Armstrong Aerospace Medical Research Laboratory is involved in biomechanical analysis and computer modeling of human movement. The Articulated Total Body Model simulates human movement with a 15 segment model which allows 3-dimensional analysis, incorporating resistive joint

properties and musculature forces. Two current problems being investigated by the Modeling and Analysis Laboratory are human body motion during emergency aircraft ejection and abrupt horizontal deceleration. Although computer modeling of human motion was a new approach for us, our background in biomechanics and human and animal motor control were useful for our selected problem.

II. Objectives of the Research Effort:

The overall objective of our simulation study was to provide information about muscle activity across joints for a selected motor skill, and in turn make comparisons between the ATB model output and the measured 3-dimensional kinematics.

The overarm throwing pattern was chosen for analysis for a number of reasons. First, there exists good descriptive data for this motor skill (specifically x,y,z kinematic data). Secondly, the upper extremity in overarm throwing is a system of three kinetic links with internal muscle torques acting between the segments of the system. This segmental link system is classified as an open kinetic chain where the most distal segment (the hand) is not fixed, but is free to move in space. Therefore, the movement is reasonably but not overly complex. Thirdly, this movement presents similarities to the limb flailing which may occur as a response to aerodynamic drag and lift forces imposed upon a pilot during aircraft ejection.

Individual Objectives:

1. The major purpose of our research effort was to input estimated muscle force data for overarm throwing into the ATB model and compare the model's predicted kinematics with the actual reported three dimensional

kinematic data.

2. A second objective of our research effort was to prescribe limited kinematic data from an overarm throwing movement pattern for the ATB model and simulate the remaining kinematics.

The Articulated Total Body (ATB) model divides the human body into 15 segments linked by 14 diarthrodial joints. The hand and forearm are normally combined into one segment in the ATB model. Our investigation made it necessary to modify the model by resegmenting the forearms and creating right and left wrist joints and hand segments. Body segments of the ATB Model react to input in the form of imposed external forces and to internal "muscular" forces acting across segment articulations.

Recently, reasonably accurate x, y, z kinematic data, with estimated joint centers, has been collected by Feltner (1986). This data was collected on skilled college varsity baseball pitchers at Indiana State University. The reduced data from one right handed male pitcher, age 19, served as the criterion kinematics for the present computer simulations study.

III. Simulation 1

Our first approach involved inputing estimated muscle force data for overarm throwing into the ATB Model in order to compare the model's predicted kinematics with the experimentally collected 3-dimensional kinematic data. We were able to estimate muscle forces from electromyographic (EMG) records of the overarm throwing skill, since electromyographic measures provide a reasonably good within-subject approximation of force production (Bigland-Ritchie, 1981). Therefore, estimated forces from EMG data were used in the ATB model and refined in

an iterative fashion such that appropriate kinematics resulted. The approach that we used was to incorporate EMG on-off times for upper limb musculature during the overarm throwing motion into the modified 17 segment ATB model. The muscle activation patterns during overarm throwing were derived from several sources, including Anderson (1976), Fisk (1976), Jobe, et al. (1983), Jobe et al. (1984). Jobe et al. (1983) and Jobe et al. (1984) were able to estimate from rectified, integrated EMG data the percent of maximal voluntary isometric contraction of active muscles during the time history of the overarm throwing skill. These integrated EMG patterns permitted and led to our development of estimated force curves for agonist and antagonist musculature throughout the throwing sequence. These force curves were based in part on the work of Freivalds (1985). Freivalds (1985) incorporated a number of factors into his program modification of the ATB model (ATBMUS) including the relative percentage of fiber types within a muscle, the percentage of total motor unit recruitment, the parallel elastic component, the length-tension relationship of muscle, and the force-velocity relationship of muscle. Each muscle is assumed to act and react as a restraining belt applying tension to various body segments. Our use of Freivalds work included inputing twelve muscles (belts) in the upper torso, upper arm, and forearm and using his estimates of maximal muscle force production for each muscle as the basis for our force estimates at maximal and submaximal levels. Estimating force production at each interval during the time history was accomplished by calculating the product of the percentage of maximal voluntary isometric contraction and Freivald's estimated maximal force for each muscle. Thus, the musculature was made

active at specific times thoughout the motion and the intensity of the activity (magnitude of each belt function) was variable throughout the throwing motion (Table 1). Additionally, Frey/Alis work supplied the attachment points for each muscle within each affected segment. These points of force application for each muscle were also entered into the ATB Model.

Broer (1969) and Toyoshima et al.(1974) indicate that approximately 50% of the linear velocity of the ball is achieved prior to the upper limb segments coming into play. Cinematography indicates that much of this linear velocity is the result of trunk rotation about the longitudinal body axis. In order to model the overarm throw, we have prescribed the trunk orientation and rotations from the initial cine data. The input of trunk rotations along with muscle activated movement of the upper right limb segments allowed a computer simulation named Torque 1 that approximated the kinematic description of the throwing motion. The right shoulder coordinates along with the trunk rotations were prescribed and should have followed the experimental data for the shoulder. The ATB simulation did follow the trunk rotations, but drift was experienced for the linear position coordinates of the right shoulder throughout the motion. The ATB Model normally will follow prescribed data for a segment's orientation throughout the simulation. Nevertheless, high correlations for the elbow and wrist points are obtained when the simulated points are plotted against the experimental data. Correlations for the right wrist range from a low of .719 to a high of .944 on the z and x axis respectively (Table 2). In a similar fashion, correlations for the right elbow range from .972 for the z axis

to .988 for the x axis. However, the y coordinates for the wrist and elbow indicate virtually no correlation between the experimental and simulated data points. We feel that some of the error in the y coordinate may be due to the noncompliance of the prescribed right shoulder position imposed by the model. The graphics from this simulation were obtained using the VIEW plotting program and are presented in Figure 1.

IV. Simulation 2

A second objective of this work was to enter a limited amount of prescribed kinematic data from an overarm throwing movement pattern into the ATB model and simulate the remaining body kinematics. In order to accomplish this objective, the hand was forced through the known motion and the joint properties adjusted so that the arm segments matched the kinematic data. First, the right knuckle x,y,z data (Feltner, 1986) was prescribed for the ATB model. Preliminary simulations indicated a need to adjust joint stops and stiffness properties. Through a series of iterations a more accurate simulation and graphic representation labeled Throw 1 resulted (Figure 2). Linear correlations comparing Throw 1 simulation with the experimental data are presented in Table 2. In general this simulation yielded a reasonably good representation of the upper extremity motion performed by the experimental subject. Pearson r values for the wrist x, y, and z values were highest because of the wrist's close proximity to the right knuckle prescribed motion, but these values were also reasonably high for the right elbow and shoulder joints.

A second model (Throw 2) involved moving our simulation performer from the true starting position, with the left foot raised, to a more

stable position with both feet on the ground surface. This adjustment in the starting position was made in order to prevent the performer from falling over during the simulation sequence. Further, a contact force was added between the upper arm and upper torso segments to keep the upper arm and elbow from passing through the upper torso during the latter stages of the simulation. The x,y, and z data correlations for the right wrist, elbow and shoulder are presented in Table 3. In general this new starting position did not result in a closer approximation of the experimental data.

V. Recommendations

1. The use of active muscle elements to drive a motion is a valuable contribution to the Modeling and Analysis Branch effort. The important implication from the first approach is that the ATB program, which incorporates active elements acting at body segments, may be of significant value in the modeling of human motion. In our work, muscular forces were input for the trunk and right upper extremity to drive segments in an appropriate motion that approximated x,y, z experimentally gathered points in a complex motor skill. If this result can be shown to generalize to other types of human motion, then movements which incorporate active musculature would best be modeled using EMG pattern data and the ATB program. Our preliminary work indicates that reasonable estimation of maximal muscle forces and muscle attachment points may be reasonably accurate. Further, models of high acceleration situations such as high performance aircraft ejections probably involve the pretensing of musculature which can effect the resulting motion. Actions which involve pretensing musculature could be analyzed with

electromyography; then the data could be incorporated into human motion modeling efforts.

2. A second recommendation is that more work is needed to improve the ATB model. We are submitting a mini-grant proposal which will involve the collection of data in three areas: 1) 3-dimensional kinematics, 2) electromyography, and 3) force output measures. The major purpose of this work will be to integrate these measures during elbow flexion and extension motions. This will be accomplished by recording elbow force measures and electromyograms of selected upper arm and forearm muscles coincident with the measurement of 3-dimensional kinematics using a Watsmart analysis system.

3. A final recommendation is made for more work in the area of ATB model validation. This may be accomplished by comparing ATB and ATBMUS simulations with experimentally measured (3-dimensional) motion. In a similar fashion to our present work, a point on the body may be forced through a motion, and the other points can be made to follow this prescribed point during a simulation. What is needed are accurate 3-dimensional experimental data for complex human motions. Then joint stops, joint characteristics may be isolated and varied to successfully approximate the experimentally collected data set.

References

1. Anderson, M.B. (1976) Muscle patterning in the overarm throw and tennis serve: An electromyographic and film study of the skilled and less skilled performance. Ph. D.Thesis, U. of Wisconsin-Madison.

2. Andrews JG (1982) On the relationship between resultant joint torques and muscular activity. Med Sci Sports Exercise 14: 361-367.

3. Atwater, A.E. (1967) What film analysis tells us about movement. Paper presented at the annual meeting of the Midwest Association for Physical Education of College Women, French Lick, Indiana, October.

4. Bigland-Ritchie B (1981) EMG and fatigue of human voluntary and stimulated contractions. In: Human Muscle Fatigue: physiological mechanisms. Pitman Medical, London (Ciba Foundation symposium 82) p. 130-156

5. Chandler RF, Clauser CF, McConville JT, Reynolds HMN Young JW (1975) Investigation of inertial properties of the human body (AMRL-TR-74-137) Aerospace Medical Research Laboratory, Aerospace Medical Division, Wright-Patterson AFB, Ohio (NTIS No AD-A016 485)

6. Crowninshield RD, Brand RA (1981) The prediction of forces in joint structures: distribution of intersegmental resultants. In: Miller DI (ed) Exercise and sport sciences reviews, vol. 9. Franklin Press, Philadelphia pp 159-182.

7. Feltner,M (1986) Dynamics of the Shoulder and Elbow Joints of the Throwing Arm During a Baseball Pitch, accepted for publication, International Journal of Sports Biomechanics.

8. Fisk, C.S. (1976) The dynamic function of selected muscles of the forearm: an electromyographical and cinematographical analysis. Ph. D. Thesis Indiana University-Bloomington.

9. Freivalds, A.(1985) Incorporation of active elements into the articulated total body model. AAMRL-TR-85-061 Wright -Patterson AFB.

10. Jobe, F.W., Tibone, J.E.,Perry, J., and Moynes D. (1983) An EMG analysis of the shoulder in throwing and pitching: A preliminary report. The American Journal of Sports Medicine, Vol. 11, 1.

11. Jobe, F.W., Radovich Moynes, D., Tibone, J., and Perry, J.(1984) An EMG analysis of the shoulder in pitching: A second report. The American Journal of Sports Medicine, Vol 12, 3.

12. Lindner, E. (1971) The Phenomenon of the Freedom of Lateral Deviation in Throwing. Medicine and Sport, Vol.6, Biomechanics II, pp.240-245.

13. Tarbell, T. (1971) Some biomechanical aspects of the overhead throw. In J. M. Cooper (Ed.), Selected Topics on Biomechanics. Proceedings of the C.I.C. Symposium on Biomechanics. Chicago: The Athletic Institute, 1971, pp.71-81.

14. Toyoshima, S., Hoshikawa, T., Miyashita, M., Oguri, T. (1974) Contribution of the body parts to throwing performance. Biomechanics IV R. Nelson and C. Morehouse (Ed.) University Park Press: Baltimore, pp. 169-174.

Table 1

MUSCLE-HARNESS FORCES IN POUNDS ENTERED INTO THE VENUS UTRAM IMPROVING SIMULATION

	SECONDS							
	0	.1	.2	.3	.4	.5	.6	.7
MUSCLES								
Pect. Maj.#1	0	0	0	0	0	149.6	37.4	29.9
Ant. Delt.	20.2	20.2	40.4	0	24.2	80.7	40.4	60.6
Post. Delt.	0	0	0	20.2	0	80.7	60.6	16.1
Infraspinatus	0	0	0	13.2	131.6	98.7	131.6	65.8
Teres Minor	0	0	0	25.9	34.5	8.6	8.6	25.9
Supraspinatus	0	0	0	54.4	72.6	7.3	7.3	72.6
Subscapularis	0	0	0	32.7	217.8	21.8	21.8	217.8
Lat. Dorsi	0	0	0	0	227.7	22.7	227.7	0
Biceps	0	0	0	0	28.1	19.5	19.5	0
Triceps	0	0	0	0	350.5	381	381	0
Pron. Teres	0	0	0	0	0	0	35.4	0
Wrist Flex.	0	0	0	0	0	0	100.0	0

Table 2

Linear Correlation Coefficients for Criterion

Data and Simulations Throw 1, Throw 2, and Torque 1

Throw 1			Throw 2			Torque 1		
			Right Wrist					
X	Y	Z	X	Y	Z	X	Y	Z
.479	.963	.921	.516	.888	.858	.944	-.137	.719
			Right Elbow					
X	Y	Z	X	Y	Z	X	Y	Z
.437	.931	.840	.395	.662	.300	.988	-.151	.972
			Right Shoulder					
X	Y	Z	X	Y	Z	X	Y	Z
.372	.648	.667	.289	.421	.547	.990	.728	.997

Pearson r values for x,y,z coordinates -Critical value .497 $p < .05$ one-tailed test of significance

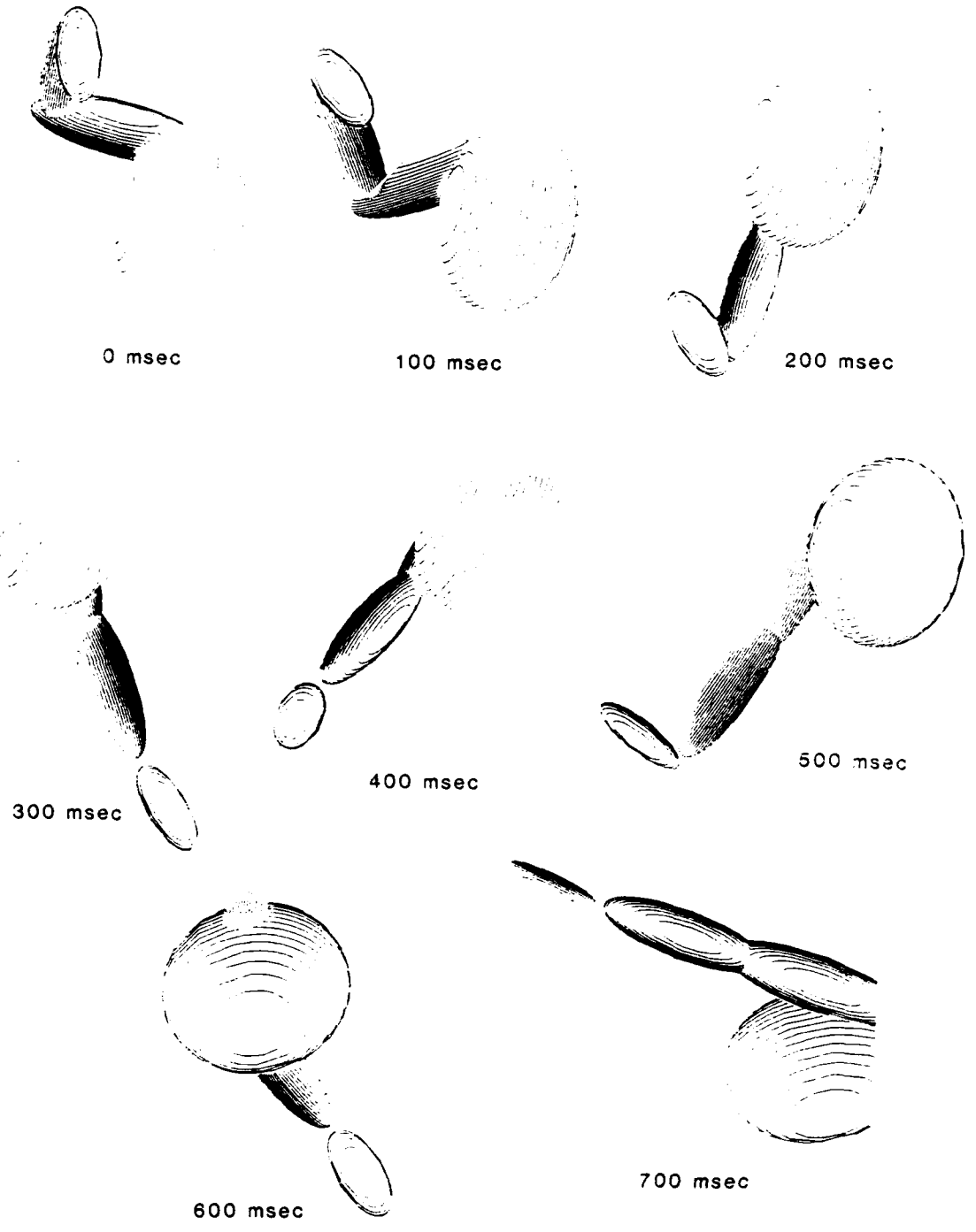

Figure 1. Tissue motion simulation of latex tissue and right side lower extremity. Movement is the result of imputed muscular forces.

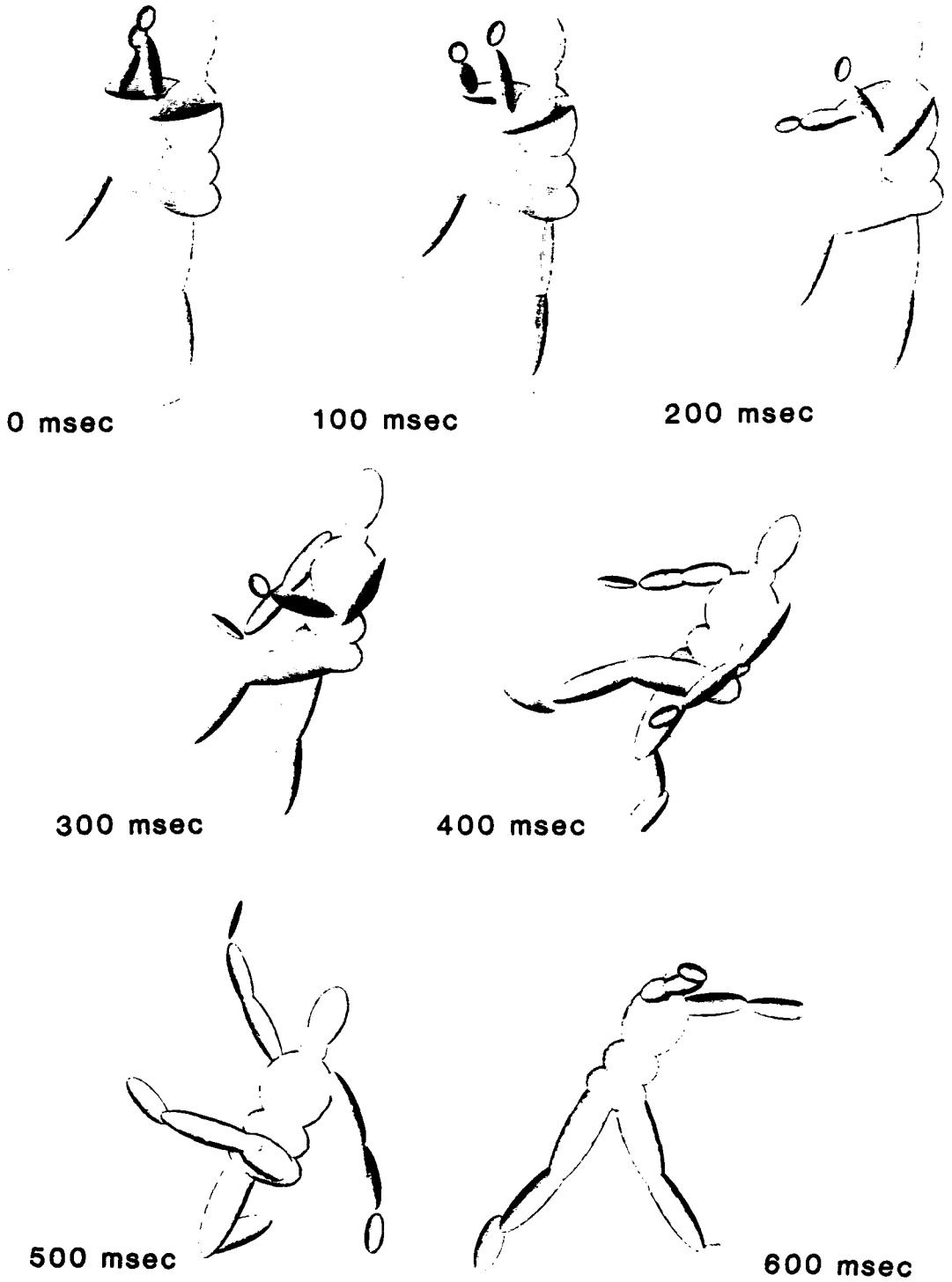

Figure 2. Throw 1 motion simulation based on the prescribed #3 metacarpalphalangeal joint motion of the right hand.

1986 USAF-UES SUMMER FACULTY RESEARCH PROGRAM

Sponsored by the

AIR FORCE OFFICE OF SCIENTIFIC RESEARCH

Conducted by the

UNIVERSAL ENERGY SYSTEMS, INC.

FINAL REPORT

FIELDS OF A SLOT ANTENNA ON A HALF-SPACE FED BY COPLANAR WAVEGUIDE USING THE METHOD OF MOMENTS

Prepared by:	Dr. Donald F. Hanson
Academic Rank:	Associate Professor
Department and University:	Department of Electrical Engineering University of Mississippi University, MS 38677
Research Location:	Rome Air Development Center EEA Hanscom AFB, MA 01731
USAF Research Contact:	Dr. Robert J. Mailloux
Date:	August 18, 1986
Contract No.:	F49620-85-C-0013

FIELDS OF A SLOT ANTENNA ON A HALF-SPACE FED BY COPLANAR WAVEGUIDE USING THE METHOD OF MOMENTS

by

Donald F. Hanson

ABSTRACT

This report describes the results of my summer's work at Hanscom AFB with Dr. Robert J. Mailloux's group, RADC/EEA. There is a need to determine the quality of a slot antenna system when the antenna is fed by coplanar waveguide. Therefore, the objective of the work is to model a coplanar waveguide-fed slot antenna. The method of moments is used to obtain numerical results for this problem.

First, an integral equation for the problem is derived. Next, the method of moments is applied to the integral equation, resulting in a 1643 line program SLTANT. Finally, the magnetic current, the input impedance, and antenna patterns are found. Data for one case are shown.

ACKNOWLEDGEMENTS

The author would like to thank the personnel of RADC for providing a stimulating environment within which to work. He would especially like to thank Dr. Robert J. Mailloux for providing him with this opportunity and for suggesting this problem. He would like to acknowledge the sponsorship of the Air Force Systems Command and the Air Force Office of Scientific Research.

I. INTRODUCTION

I received my Ph.D.E.E. degree from the University of Illinois in electromagnetics with a minor in mathematics. Since then, I have been employed by the University of Mississippi, where I am now Associate Professor. For my Ph.D. dissertation, I solved one problem using the method of moments and since then have lectured at two University of Mississippi short courses entitled, "Fundamentals of Numerical Solution Methods in Electromagnetics" which covered the method of moments.

The research problem at the Air Force Geophysics Laboratory (RADC/EEA) was to investigate the radiation properties of a slot antenna fed by coplanar waveguide. Such a problem is a perfect application for the method of moments. Therefore, a match existed between myself and the RADC/EEA Air Force Laboratory.

II. OBJECTIVES OF THE RESEARCH EFFORT

The overall objective of the project was to determine design data for slot antennas on a half-space fed by coplanar waveguide (CPW). This is needed in order to determine the feasibility of using CPW to feed slot antennas on integrated circuit phased array antenna systems. Several questions to be examined are the radiation from the CPW feed line. How much pattern distortion results from the feed line? Finally, the field in the slot needs to be found so input impedance and radiation patterns can be determined.

At the beginning of the summer, the following "Summer Research Goals and Objectives" were stated:

(1) Determination of radiation from CPW alone. This would involve investigating the dynamic behavior of CPW as a transmission line. In a report from last summer [1], this writer has already obtained quasi-TEM results for CPW. These results should be investigated to see if they provide sufficiently accurate results for radiation properties.

(2) Model CPW-fed slots both separately and in infinite phased arrays. First, design data (currents, fields, input impedance, radiation patterns) for modeling a single slot antenna fed by CPW over a dielectric half-space (GaAs) with $\varepsilon_r = 12.8$ will be obtained. Second, the same data will be obtained for modeling CPW-fed slots in infinite phased arrays. A dielectric half-space will again be used.

Objective (1) requires more data since only one test case was completed. For the one case studied so far, it can be said that the CPW itself radiates much less than the slot but that the lossless transmission line equations appear to be unsatisfactory. It also appears that the quasi-static TEM results for CPW are within 100% of the moment method results. More cases need to be studied to verify these ideas from objective (1) more conclusively.

A 1643 line computer program was completed which models part one of objective (2) and can be used for objective (1). The outputs of this program are magnetic current (or E field), input impedance, and radiation patterns. The second part of objective (2) was not started because learning the AFGL computer systems and writing the program took more time than anticipated.

III. FORMULATIONS

Two approaches, both using the method of moments, were examined. Figure 1 shows the situation to be solved. The slot antenna is in a conductor coating a dielectric half space of $\varepsilon_r = 12.8$ for $z<0$. The conductor with slot antenna is in the $z=0$ plane. Free space exists for $z>0$. The feed point is shown at $(x,y,z)=(0,0,0)$.

The first approach involved assuming the component of current transverse to the slot direction was small compared to the longitudinal component and taking the transverse variation of the longitudinal current to be that of the quasi-static case. The second approach, the general approach, assumed little and solved for both longitudinal and transverse components of current. No assumptions about the transverse behavior of the longitudinal component were made.

In another report[1], this writer determined the quasi-static magnetic current in the infinite case to be

$$\vec{M}_s = \frac{b\,\phi_0}{k'\,K'(a/b)} \frac{\mathrm{sgn}(x)}{\sqrt{[(x^2-a^2)(b^2-x^2)]}}\,\hat{z} \qquad (1)$$

The first approach would therefore use a $1/\sqrt{[(x^2 - a^2)(b^2 - x^2)]}$ behavior transverse to the slot direction and an unknown (to be found) longitudinal behavior. The kernel for such a case was found to be of the form

$$\frac{1}{\sqrt{2}\,b} \int_{2\sin^{-1}(a/b)}^{\pi} \frac{1}{\sqrt{\cos\psi - \cos\delta}} \frac{e^{-jk\sqrt{(y-y')^2+z^2+4(b/2)^2\sin^2(\delta/2)}}}{\sqrt{(y-y')^2+z^2+4(b/2)^2\sin^2(\delta/2)}}\,d\delta \qquad (2)$$

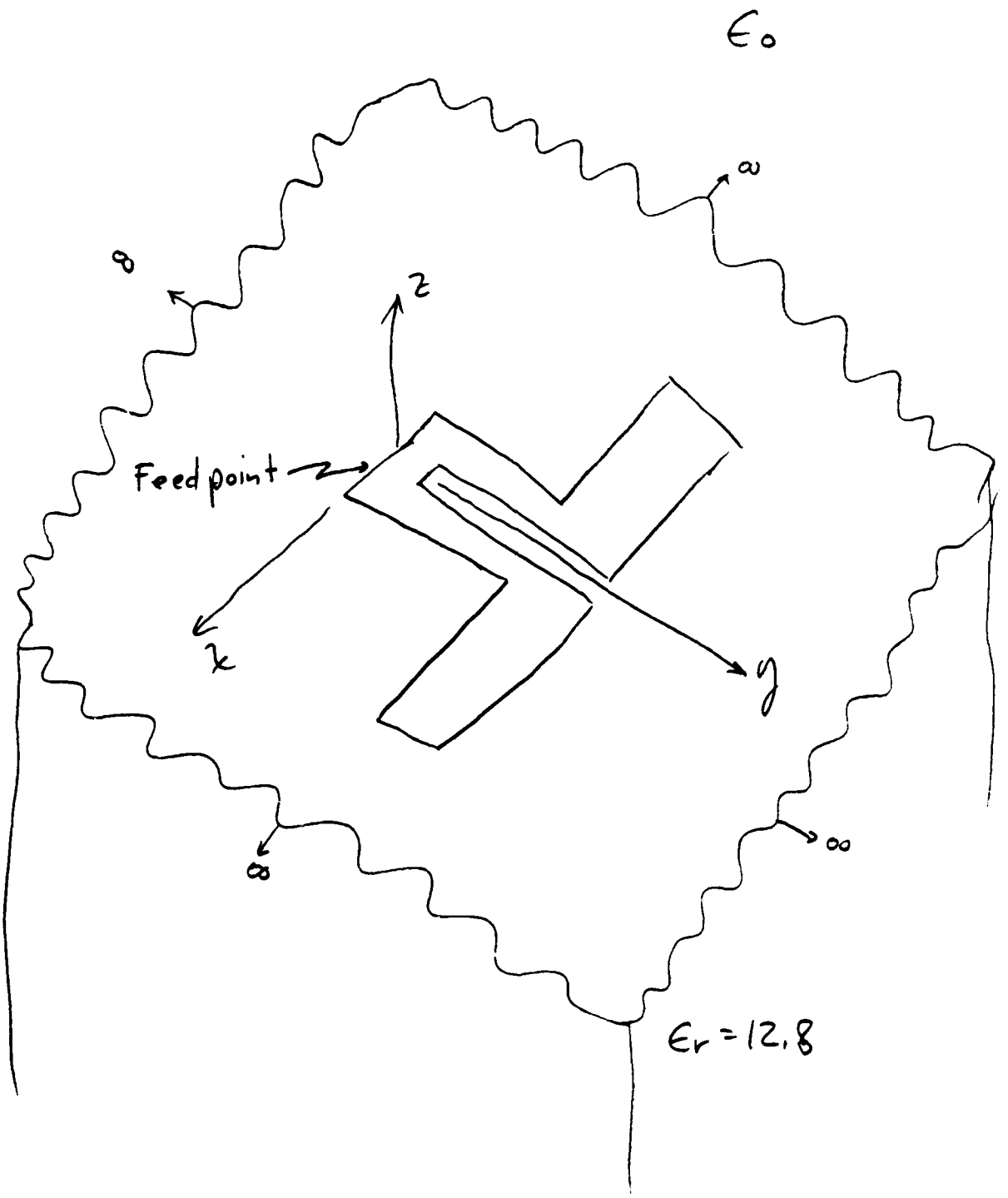

Figure 1. Slot Antenna Fed by CPW

where $\psi = 2 \sin^{-1}(a/b)$. This first approach was not chosen for use because too many assumptions about the form of the solution had to be made a priori. Therefore, the general approach was used here.

Instead of assuming longitudinal current flow, unknowns were taken in both the possible magnetic current directions, x and y. Both current components were solved for [2]. The dimensions for the program are shown in Figure 2. Three integers in y, N_1, N_2, and N_3 and four integers in x, M_1, M_2, M_3, and M_4, partially describe the expansion functions. The Δ's shown in Figure 2 are given by

$$\begin{aligned} \Delta w &= w/(N_1 + 1) \\ \Delta \ell &= \ell/(N_2 + 1) \\ \Delta c &= c/(N_3 + 1) \end{aligned} \qquad (3)$$

$$\begin{aligned} \Delta h_1 &= h_1/(M_1 + 1) \\ \Delta h_2 &= h_2/(M_2 + 1) \\ \Delta(b-a) &= (b-a)/(M_3 + 1) \\ \Delta 2b &= 2b/(M_4 + 1) \end{aligned}$$

Note that this allows for off-center feeds.

Different expansion domains are taken for the x and y cases. This is because the magnetic current $\vec{M}_s$ is zero for $\vec{M}_s$ normal to the edge. For $\vec{M}_s$ parallel to the edge, the magnetic current is singular as $s^{-1/2}$ away from the edge. The expansion domains are shown in Figure 3.

There are three ways of numbering the domains. First, there is continuous numbering. For the example shown, this is from 1 to 60 for the y case and from 61 to 117 for the x case. This numbering starts with the y case and proceeds from left to right. The five individual larger rectangular regions are also numbered together with the four regions present in the y case to insure continuity of the magnetic current. These are numbered in two ways. First, from 1 to 14 and second, from (1) to (8). The first numbers are shown and the second are given in parenthesis in Figure 3. For example, regions 2 and 3

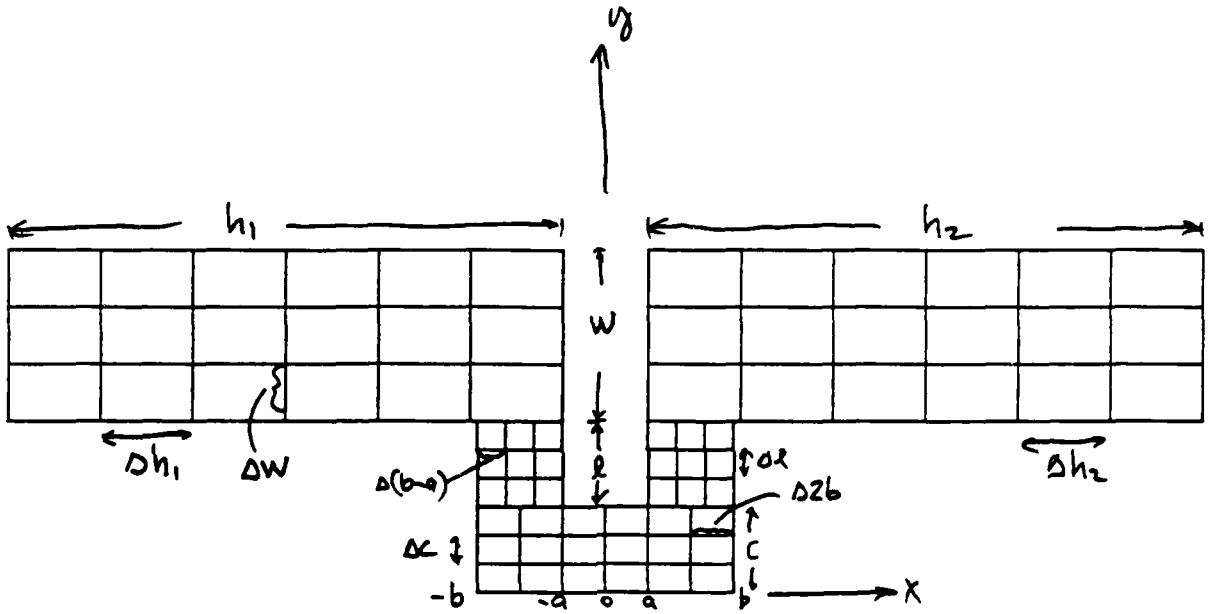

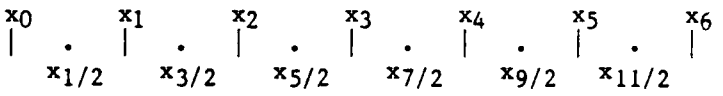

Figure 2. Dimensions of Slot Antenna

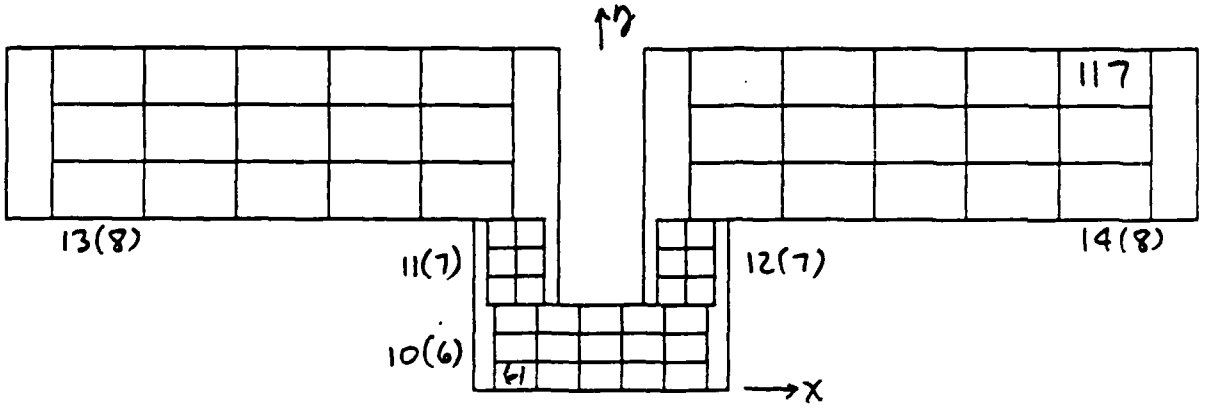

x-directed expansion domains

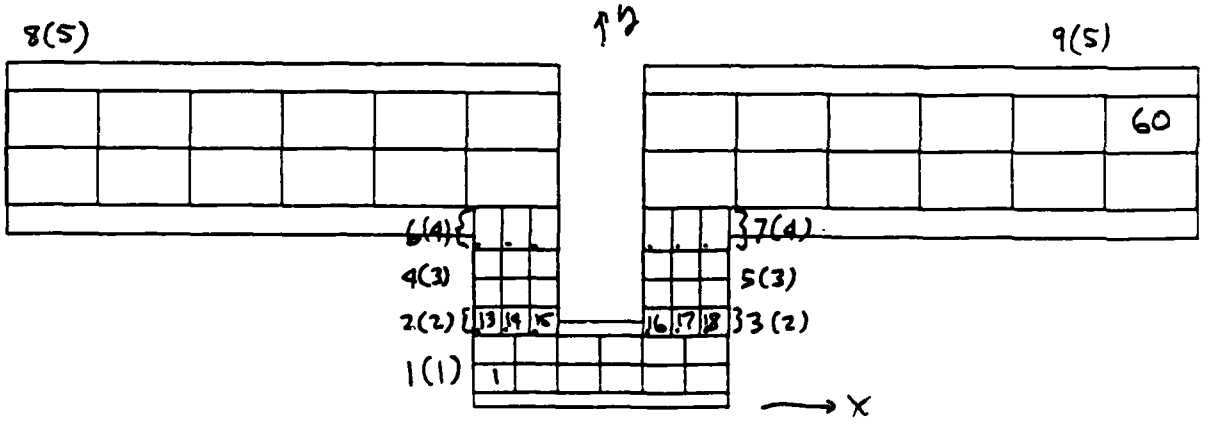

y-directed expansion domains

Figure 3. The magnetic current expansion domains for the general case.

are contained in (2). For regions 1, 4, 5, 8, and 9 in the y case,

$$\begin{aligned} n &= 1, 2, 3, \ldots, N && \text{in y} \\ m &= 1, 2, 3, \ldots, M+1 && \text{in x} \end{aligned} \qquad (4)$$

For regions 10, 11, 12, 13, and 14 in the x case,

$$\begin{aligned} n &= 1, 2, 3, \ldots, N+1 && \text{in y} \\ m &= 1, 2, 3, \ldots, M && \text{in x.} \end{aligned} \qquad (5)$$

This numbering allows for a half pulse of zero value on the edges where the magnetic current is normal to the edge. Therefore, any particular square can be identified by [region#, m, n]. Table I shows this in detail. Several mapping functions are used in the computer program. These are given in Figure 4. MAPBGN maps from parenthesized numbers to ordinary numbers and MUNSEG is the inverse mapping. MAP12 gives the number of rectangles (1 or 2) in each parenthesized number zone. MAPOFF is useful to convert a 10 through 14 series to an equivalent 1 through 9 number.

Regions 2, 3, 6, and 7 are special regions present for continuity of the magnetic current. For these four regions, the integer M_5 is input so that

$$\Delta_5 = (b-a)/(M_5 + 1) \qquad (6)$$

Therefore, m goes from 1 to M_5+1 while n is always 1 for regions 2,3,6, and 7.

IV. INTEGRAL EQUATION

The integral equation is derived by shorting the slot and covering the slot with an equivalent magnetic current $\vec{M}_s$ on both sides of the conducting sheet in the z=0 plane. Applying image theory to this effectively doubles the magnetic currents which now reside in homogeneous space. These currents are $\vec{M}_1 = -2\,\vec{M}_s$ and $\vec{M}_0 = 2\,\vec{M}_s$. Regions

TABLE I. Unknowns in Each Region

REGION	X	by	Y
1	M_4+1		N_3
2	M_5+1		1
3	M_5+1		1
4	M_3+1		N_2
5	M_3+1		N_2
6	M_5+1		1
7	M_5+1		1
8	M_1+1		N_1
9	M_2+1		N_1
10	M_4		N_3+1
11	M_3		N_2+1
12	M_3		N_2+1
13	M_1		N_1+1
14	M_2		N_1+1

```
MAPBGN(I) = I+I - (I+6)/8 -I/7 -1
MAP12(I) = (I+3)/5 - (I+3)/9 + 1
MUNSEG(I) = (I + 2 + (I/10))/2
MAPOFF(I) = I + 2*( (I)/2 )
```

(I)	MAPBGN((I))	MAP12((I))
(1)	1	1
(2)	2	2
(3)	4	2
(4)	6	2
(5)	8	2
(6)	10	1
(7)	11	2
(8)	13	2

I	MUNSEG(I)	MAPOFF(I-9)
1	(1)	
2	(2)	
3	(2)	
4	(3)	
5	(3)	
6	(4)	
7	(4)	
8	(5)	
9	(5)	
10	(6)	1
11	(7)	4
12	(7)	5
13	(8)	8
14	(8)	9

Figure 4. Useful Mappings

0 and 1 are identified as free space and dielectric, respectively.

One obtains

$$\vec{H}_0^s = -j\omega\vec{F}_0 - \nabla\psi_0 \tag{7}$$

and

$$\vec{H}_1^s = -j\omega\vec{F}_1 - \nabla\psi_1$$

where $\vec{F}$ and ψ are the vector and scalar potentials, respectively. For free space, one obtains

$$\vec{F}_0 = \varepsilon_0 \iint \vec{M}_0 \frac{e^{-jk_0R}}{4\pi R}\, dS'$$

$$\psi_0 = \frac{1}{\mu_0} \iint m_0 \frac{e^{-jk_0R}}{4\pi R} dS' \tag{8a}$$

where

$$m_0 = \frac{-1}{j\omega} \nabla\cdot\vec{M}_0$$

Similarly, for the dielectric case, one obtains

$$\vec{F}_1 = \varepsilon_1 \iint \vec{M}_1 \frac{e^{-jk_1R}}{4\pi R}\, dS'$$

$$\psi_1 = \frac{1}{\mu_1} \iint m_1 \frac{e^{-jk_1R}}{4\pi R}\, dS' \tag{8b}$$

where

$$m_1 = \frac{-1}{j\omega} \nabla\cdot\vec{M}_1$$

Assuming H_1^i(incident) = 0, one finds

$$H_0^t = H_0^s + H_0^i$$
$$H_1^t = H_1^s \tag{9}$$

The integral equation can be found by enforcing tangential $\vec{H}^t$ (total) to be continuous through the slot

$$\lim_{z\downarrow 0} \hat{z}\times H_0^t = \lim_{z\downarrow 0} \hat{z}\times H_1^t \qquad \text{through } S_a \text{ (aperture)} \tag{10}$$

This results in the coupled integral equation

$$2\left\{j\omega\varepsilon_1 F_{s1x} + j\omega\varepsilon_0 F_{s0x} - \frac{1}{j\omega\mu_1}\partial\psi_{s1}/\partial x - \frac{1}{j\omega\mu_0}\partial\psi_{s0}/\partial x\right\} = H_x^{sci} \quad \text{in slot} \tag{11a}$$

$$2\left\{j\omega\varepsilon_1 F_{s1y} + j\omega\varepsilon_0 F_{s0y} - \frac{1}{j\omega\mu_1}\partial\psi_{s1}/\partial y - \frac{1}{j\omega\mu_0}\partial\psi_{s0}/\partial y\right\} = H_y^{sci} \quad \text{in slot} \tag{11b}$$

where

$$\vec{F}_{s1} = \iint \vec{M}_s\, G(k_1R)dS'$$

$$\vec{F}_{s0} = \iint \vec{M}_s\, G(k_0R)dS' \tag{12}$$

$$\psi_{s1} = \iint \nabla\cdot\vec{M}_s\, G(k_1R)dS'$$

$$\psi_{s0} = \iint \nabla\cdot\vec{M}_s\, G(k_0R)dS'$$

and

$$G(kR) = \frac{e^{-jkR}}{4\pi R} \tag{13}$$

The Moment Method Approach

The current was expanded in the following manner:

$$M_y = \sum_{n=1}^{N_3} \sum_{m=1}^{M_4+1} M_{mn}^1 \Lambda_{mn}^1$$

$$+ \sum_{m=1}^{M_5+1} (M_{m1}^2 \Lambda_{m1}^2 + M_{m1}^3 \Lambda_{m1}^3)$$

$$+ \sum_{n=1}^{N_2} \sum_{m=1}^{M_3+1} (M_{mn}^4 \Lambda_{mn}^4(r) + M_{mn}^5 \Lambda_{mn}^5(r)) \qquad (14a)$$

$$+ \sum_{m=1}^{M_5+1} (M_{m1}^6 \Lambda_{m1}^6 + M_{m1}^7 \Lambda_{m1}^7)$$

$$+ \sum_{n=1}^{N_1} \left(\sum_{m=1}^{M_1+1} M_{mn}^8 \Lambda_{mn}^8(r) + \sum_{m=1}^{M_2+1} M_{mn}^9 \Lambda_{mn}^9(r) \right)$$

$$M_x = \sum_{n=1}^{N_3+1} \sum_{m=1}^{M_4} M_{mn}^{10} \Lambda_{mn}^{10}(r)$$

$$+ \sum_{n=1}^{N_2+1} \sum_{m=1}^{M_3} (M_{mn}^{11} \Lambda_{mn}^{11}(r) + M_{mn}^{12} \Lambda_{mn}^{12}(r)) \qquad (14b)$$

$$+ \sum_{n=1}^{N_1+1} \left(\sum_{m=1}^{M_1} M_{mn}^{13} \Lambda_{mn}^{13}(r) + \sum_{m=1}^{M_2} M_{mn}^{14} \Lambda_{mn}^{14}(r) \right)$$

where

$$\Lambda_{mn}^i = \Lambda_m^i(x) \, \Pi_{n-1/2}^i(y) \qquad i = 10, 11, \ldots, 14$$

$$\Lambda_{mn}^i = \Pi_{m-1/2}^i(x) \, \Lambda_n^j(y) \qquad i = 1, 2, \ldots, 9 \qquad (15)$$

Note that

$$\Pi_{i-1/2}^j(z) = \begin{cases} 1 & z_{i-1}^j < z < z_i^j \\ 0 & \text{otherwise} \end{cases} \qquad (16)$$

and

$$\Lambda_i^j(z) = \begin{cases} 1 - \dfrac{z_i^j - z}{z_i^j - z_{i-1}^j} & z_{i-1}^j < z < z_i^j \\ 1 - \dfrac{z - z_i^j}{z_{i+1}^j - z_i^j} & z_i^j < z < z_{i+1}^j \\ 0 & \text{otherwise} \end{cases} \tag{17}$$

The x_i and $x_{i-1/2}$ terms are shown in Figure 2. The superscript denotes the region number. This current expansion is convenient for determining

$$\nabla \cdot \vec{M}_s = \frac{\partial M_x}{\partial x} + \frac{\partial M_y}{\partial y} \tag{18}$$

The testing paths were chosen to be

$$\begin{aligned} t^i(x,y) &= \delta(x - x_{m-1/2}^i)\ \Pi_n^i(y) \qquad i = 1, 2, \ldots, 9 \\ t^i(x,y) &= \Pi_m^i(x)\ \delta(y - y_{n-1/2}^i) \qquad i = 10, 11, \ldots, 14 \end{aligned} \tag{19}$$

The tested integral equation can be shown to be

$$\begin{aligned} &\omega\varepsilon_1\ F_{s1y}(x_{m-1/2}^i, y_n^i)\Delta y^i + \omega\varepsilon_0\ F_{s0y}(x_{m-1/2}^i, y_n^i)\Delta y^i + \\ &+ \frac{1}{\omega\mu_1}\left\{\psi_{s1}(x_{m-1/2}^i, y_{n+1/2}^i) - \psi_{s1}(x_{m-1/2}^i, y_{n-1/2}^i)\right\} + \\ &+ \frac{1}{\omega\mu_0}\left\{\psi_{s0}(x_{m-1/2}^i, y_{n+1/2}^i) - \psi_{s0}(x_{m-1/2}^i, y_{n-1/2}^i)\right\} = \\ &= \frac{1}{2j} H_y^{sci}(x_{m-1/2}^i, y_n^i)\Delta y^i \end{aligned} \tag{20a}$$

$$\begin{aligned} i &= 1, 2, \ldots, 9 \\ m &= 1, 2, \ldots, M_i + 1 \\ n &= 1, 2, \ldots, N_i \end{aligned}$$

$$\omega\varepsilon_1 F_{s1x}(x^i_m, y^i_{n-1/2})\Delta x^i + \omega\varepsilon_0 F_{s0x}(x^i_m, y^i_{n-1/2})\Delta x^i +$$

$$+ \frac{1}{\omega\mu_1}\{\psi_{s1}(x^i_{m+1/2}, y^i_{n-1/2}) - \psi_{s1}(x^i_{m-1/2}, y^i_{n-1/2})\} +$$

$$+ \frac{1}{\omega\mu_0}\{\psi_{s0}(x^i_{m+1/2}, y^i_{n-1/2}) - \psi_{s0}(x^i_{m-1/2}, y^i_{n-1/2})\} =$$

$$= \frac{1}{2j} H_x^{sci}(x^i_m, y^i_{n-1/2})\ \Delta x^i \qquad (20b)$$

$$i = 10, 11, 12, 13, 14$$

$$m = 1, 2, \ldots, M_i$$

$$n = 1, 2, \ldots, N_i + 1$$

After applying the expansion functions to the tested equation, and approximating the triangle functions, where possible, by pulses, one obtains the result

$$\sum_{j=1}^{9} \sum_{q=1}^{N_j} \sum_{p=1}^{M_j+1} A^{ij}_{mn,pq} M^j_{pq} + \sum_{j=10}^{14} \sum_{q=1}^{N_j+1} \sum_{p=1}^{M_j} B^{ij}_{mn,pq} M^j_{pq} = H^i_{ymn} \qquad (21a)$$

for $i = 1, 2, \ldots, 9$, $m = 1, 2, \ldots, M_i+1$, $n = 1, 2, \ldots, N_i$;

and

$$\sum_{j=1}^{9} \sum_{q=1}^{N_j} \sum_{p=1}^{M_j+1} C^{ij}_{mn,pq} M^j_{pq} + \sum_{j=10}^{14} \sum_{q=1}^{N_j+1} \sum_{p=1}^{M_j} D^{ij}_{mn,pq} M^j_{pq} = H^i_{xmn} \qquad (21b)$$

for $i = 10, 11, 12, 13, 14$, $m=1, 2, \ldots, M_i$, $n = 1, 2, \ldots, N_i+1$.

The following expressions hold for A, B, C, and D:

For i = 1, 2, ..., 9 and j = 1, 2, ..., 9, one obtains

$$A^{ij}_{mn,pq} = \omega\varepsilon_1(y^i_{n+1/2} - y^i_{n-1/2})\ \Phi^j_{p,q+1/2}(k_1|x^i_{m-1/2}, y^i_n)$$

$$+ \omega\varepsilon_0(y^i_{n+1/2} - y^i_{n-1/2})\ \Phi^j_{p,q+1/2}(k_0|x^i_{m-1/2}, y^i_n)$$

$$+ \frac{1}{\omega\mu_1}\left\{\frac{\Phi^j_{pq}(k_1|x^i_{m-1/2}, y^i_{n+1/2}) - \Phi^j_{pq}(k_1|x^i_{m-1/2}, y^i_{n-1/2})}{y^j_q - y^j_{q-1}}\right.$$

$$\left. - \frac{\Phi^j_{p,q+1}(k_1|x^i_{m-1/2}, y^i_{n+1/2}) - \Phi^j_{p,q+1}(k_1|x^i_{m-1/2}, y^i_{n-1/2})}{y^j_{q+1} - y^j_q}\right\}$$

$$+ \frac{1}{\omega\mu_0}\left\{\frac{\Phi^j_{pq}(k_0|x^i_{m-1/2}, y^i_{n+1/2}) - \Phi^j_{pq}(k_0|x^i_{m-1/2}, y^i_{n-1/2})}{y^j_q - y^j_{q-1}}\right.$$

$$\left. - \frac{\Phi^j_{p,q+1}(k_0|x^i_{m-1/2}, y^i_{n+1/2}) - \Phi^j_{p,q+1}(k_0|x^i_{m-1/2}, y^i_{n-1/2})}{y^j_{q+1} - y^j_q}\right\} \qquad (22a)$$

Similarly, for i = 1, 2, ..., 9 and j = 10, 11, 12, 13, 14, one obtains

$$B^{ij}_{mn,pq} = \frac{1}{\omega\mu_1}\left\{\frac{\Phi^j_{pq}(k_1|x^i_{m-1/2}, y^i_{n+1/2}) - \Phi^j_{pq}(k_1|x^i_{m-1/2}, y^i_{n-1/2})}{x^j_p - x^j_{p-1}}\right.$$

$$\left. - \frac{\Phi^j_{p+1,q}(k_1|x^i_{m-1/2}, y^i_{n+1/2}) - \Phi^j_{p+1,q}(k_1|x^i_{m-1/2}, y^i_{n-1/2})}{x^j_{p+1} - x^j_p}\right\}$$

$$+ \frac{1}{\omega\mu_0}\left\{\frac{\Phi^j_{pq}(k_0|x^i_{m-1/2}, y^i_{n+1/2}) - \Phi^j_{pq}(k_0|x^i_{m-1/2}, y^i_{n-1/2})}{x^j_p - x^j_{p-1}}\right.$$

$$\left. - \frac{\Phi^j_{p+1,q}(k_0|x^i_{m-1/2}, y^i_{n+1/2}) - \Phi^j_{p+1,q}(k_0|x^i_{m-1/2}, y^i_{n-1/2})}{x^j_{p+1} - x^j_p}\right\} \qquad (22b)$$

For i = 10, 11, 12, 13, 14, and j = 1, 2, ..., 9, one obtains

$$C^{ij}_{mn,pq} =$$

$$= \frac{1}{\omega\mu_1}\left\{\frac{\phi^j_{pq}(k_1|x^i_{m+1/2},\, y^i_{n-1/2}) - \phi^j_{pq}(k_1|x^i_{m-1/2},\, y^i_{n-1/2})}{y^j_q - y^j_{q-1}}\right.$$

$$\left. - \frac{\phi^j_{p,q+1}(k_1|x^i_{m+1/2}, y^i_{n-1/2}) - \phi^j_{p,q+1}(k_1|x^i_{m-1/2}, y^i_{n-1/2})}{y^j_{q+1} - y^j_q}\right\} \qquad (22c)$$

$$+ \frac{1}{\omega\mu_0}\left\{\frac{\phi^j_{pq}(k_0|x^i_{m+1/2},\, y^i_{n-1/2}) - \phi^j_{pq}(k_0|x^i_{m-1/2},\, y^i_{n-1/2})}{y^j_q - y^j_{q-1}}\right.$$

$$\left. - \frac{\phi^j_{p,q+1}(k_0|x^i_{m+1/2}, y^i_{n-1/2}) - \phi^j_{p,q+1}(k_0|x^i_{m-1/2}, y^i_{n-1/2})}{y^j_{q+1} - y^j_q}\right\}$$

Finally, for i = 10, 11, 12, 13, 14, and j = 10, 11, 12, 13, 14, one obtains

$$D^{ij}_{mn,pq} = \omega\varepsilon_1(x^i_{m+1/2} - x^i_{m-1/2})\ \phi^j_{p+1/2,q}(k_1|x^i_m, y^i_{n-1/2}) +$$

$$+ \omega\varepsilon_0(x^i_{m+1/2} - x^i_{m-1/2})\ \phi^j_{p+1/2,q}(k_0|x^i_m, y^i_{n-1/2}) +$$

$$+ \frac{1}{\omega\mu_1}\left\{\frac{\phi^j_{pq}(k_1|x^i_{m+1/2},\, y^i_{n-1/2}) - \phi^j_{pq}(k_1|x^i_{m-1/2},\, y^i_{n-1/2})}{x^j_p - x^j_{p-1}}\right.$$

$$\left. - \frac{\phi^j_{p+1,q}(k_1|x^i_{m+1/2}, y^i_{n-1/2}) - \phi^j_{p+1,q}(k_1|x^i_{m-1/2}, y^i_{n-1/2})}{x^j_{p+1} - x^j_p}\right\} \qquad (22d)$$

$$+ \frac{1}{\omega\mu_0}\left\{\frac{\phi^j_{pq}(k_0|x^i_{m+1/2},\, y^i_{n-1/2}) - \phi^j_{pq}(k_0|x^i_{m-1/2},\, y^i_{n-1/2})}{x^j_p - x^j_{p-1}}\right.$$

$$\left. - \frac{\phi^j_{p+1,q}(k_0|x^i_{m+1/2}, y^i_{n-1/2}) - \phi^j_{p+1,q}(k_0|x^i_{m-1/2}, y^i_{n-1/2})}{x^j_{p+1} - x^j_p}\right\}$$

The potential function common to the A, B, C, and D terms is

$$\Phi^{j}_{pq}(k_a | x^{i}_{m-1/2},\ y^{i}_{n-1/2}) =$$

$$= \int_{x^{j}_{p-1}}^{x^{i}_{m-1/2} - x^{j}_{p}} \int_{y^{j}_{q-1}}^{y^{i}_{n-1/2} - y^{j}_{q}} \frac{e^{-jk_a\sqrt{(x^2 + y^2)}}}{4\pi\sqrt{(x^2 + y^2)}}\, dy\, dx \qquad (23)$$

This is related to an incomplete cylindrical function [3] and has been studied by Harvard University's Computation Laboratory [4]. Since the integral is singular, the singular part was evaluated analytically and the non-singular part was evaluated by numerical integration. Adding and subtracting identical terms, one obtains

$$\frac{e^{-jk_a\sqrt{(x^2 + y^2)}}}{4\pi\sqrt{(x^2 + y^2)}} = \frac{\cos k_a\sqrt{(x^2 + y^2)} - (1 - k_a^2(\sqrt{(x^2+y^2)})^2/2)}{4\pi\sqrt{(x^2+y^2)}} \qquad (24)$$

$$-j\,\frac{\sin k_a\sqrt{(x^2+y^2)}}{4\pi\sqrt{(x^2+y^2)}} + \frac{1 - k_a^2(\sqrt{(x^2+y^2)})^2/2}{4\pi\sqrt{(x^2+y^2)}}$$

The last term was integrated analytically. The other terms were integrated numerically using double integration with 4th order Gaussian Quadrature. The analytic integration becomes

$$\int_{x_a}^{x_b}\int_{y_a}^{y_b} \frac{1-\frac{(k_a\sqrt{(x^2+y^2)})^2}{2}}{4\pi\sqrt{(x^2+y^2)}}\,dy\,dx =$$

$$= \frac{1}{4\pi}\{x_b(1-\frac{k_a^2x_b^2}{12})[\ell n(y_b+\sqrt{(x_b^2+y_b^2)})-\ell n(y_a+\sqrt{(x_b^2+y_a^2)})]$$

$$+ x_a(1-\frac{k_a^2x_a^2}{12})[\ell n(y_a+\sqrt{(x_a^2+y_a^2)})-\ell n(y_b+\sqrt{(x_a^2+y_b^2)})]$$

$$+ y_b(1-\frac{k_a^2y_b^2}{12})[\ell n(x_b+\sqrt{(x_b^2+y_b^2)})-\ell n(x_a+\sqrt{(x_a^2+y_b^2)})]$$

$$+ y_a(1-\frac{k_a^2y_a^2}{12})[\ell n(x_a+\sqrt{(x_a^2+y_a^2)})-\ell n(x_b+\sqrt{(x_b^2+y_a^2)})] \qquad (25)$$

$$- \frac{k_a^2x_by_b}{6}\sqrt{(x_b^2+y_b^2)} + \frac{k_a^2x_ay_b}{6}\sqrt{(x_a^2+y_b^2)}$$

$$+ \frac{k_a^2x_by_a}{6}\sqrt{(x_b^2+y_a^2)} - \frac{k_a^2x_ay_a}{6}\sqrt{(x_a^2+y_a^2)}\}$$

The expressions for ϕ were evaluated for all i, j, p, q, m, and n and stored in two matrices, one for k_0 and the other for k_1. The matrix elements A, B, C, and D were obtained from them by proper manipulation of the matrices. This is estimated to cut the matrix element evaluation time by 6. The storage requirement more than doubled, however, to achieve the time savings.

The right-hand side is taken to be zero everywhere except in the feed region where it is taken to be 1/2j. Thus, $H_x^{sci}(x_m^i, y_{n-1/2}^i)\Delta x^i = 1$ over this region.

V. RESULTS

The results for the one special test case of Figure 3 are shown next. The input impedance for this case is found to be

$$Z_{in} = 83.2 - j\ 52.27\ \Omega \tag{26}$$

The real and imaginary parts of the magnetic currents are shown in Figure 5. The flow around the obstacle is as expected.

The pattern functions were determined to be

$$\begin{aligned}
|E_\theta^s| &= 2\,k_a\,|f_x^a(\theta,90°)| && \phi = 90,\ 270° \\
|E_\phi^s| &= 2\,k_a\,|\cos\theta|\,|f_y^a(\theta,90°)| && \phi = 90,\ 270° \\
|E_\theta^s| &= 2\,k_a\,|f_y^a(\theta,0°)| && \phi = 0, 180° \\
|E_\phi^s| &= 2\,k_a\,|\cos\theta|\,|f_x^a(\theta,0°)| && \phi = 0,\ 180°
\end{aligned} \tag{27}$$

where

$$\begin{aligned}
f_x^a(\theta,0°) &= \iint M_{sx}(x',y')\, e^{jk_a x'\sin\theta}\, dx'dy' \\
f_x^a(\theta,90°) &= \iint M_{sx}(x',y')\, e^{jk_a y'\sin\theta}\, dx'dy' \\
f_y^a(\theta,0°) &= \iint M_{sy}(x',y')\, e^{jk_a x'\sin\theta}\, dx'dy' \\
f_y^a(\theta,90°) &= \iint M_{sy}(x',y')\, e^{jk_a y'\sin\theta}\, dx'dy'
\end{aligned} \tag{28}$$

The pattern plots are shown in Figure 6.

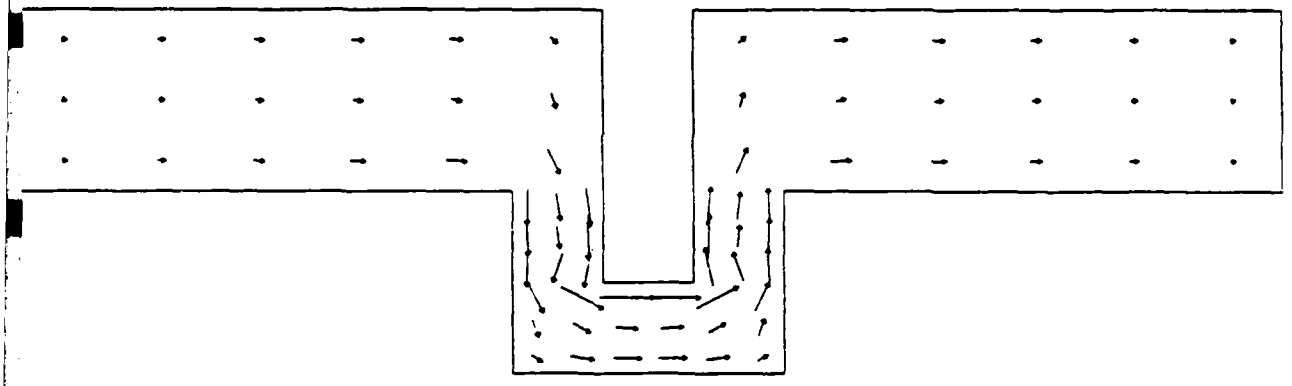

Real part of magnetic current

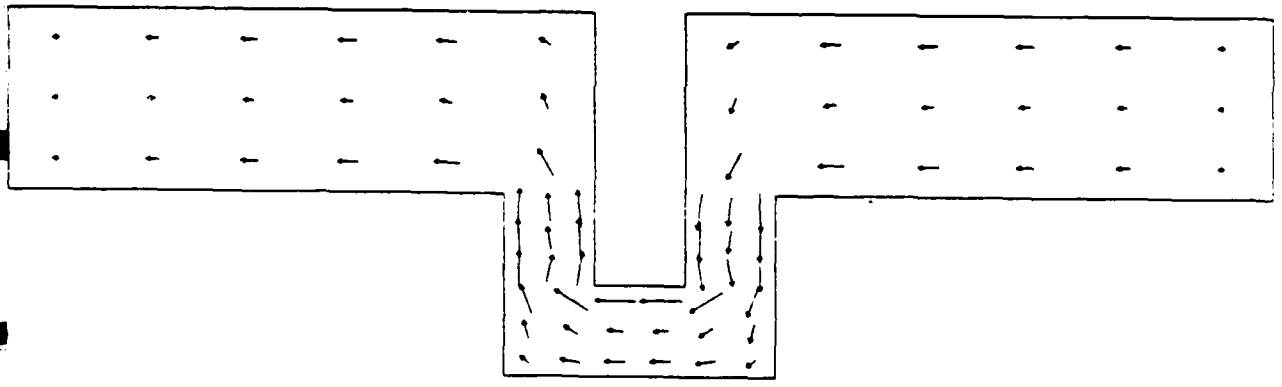

Imaginary part of magnetic current

Figure 5. Solution for Magnetic Current

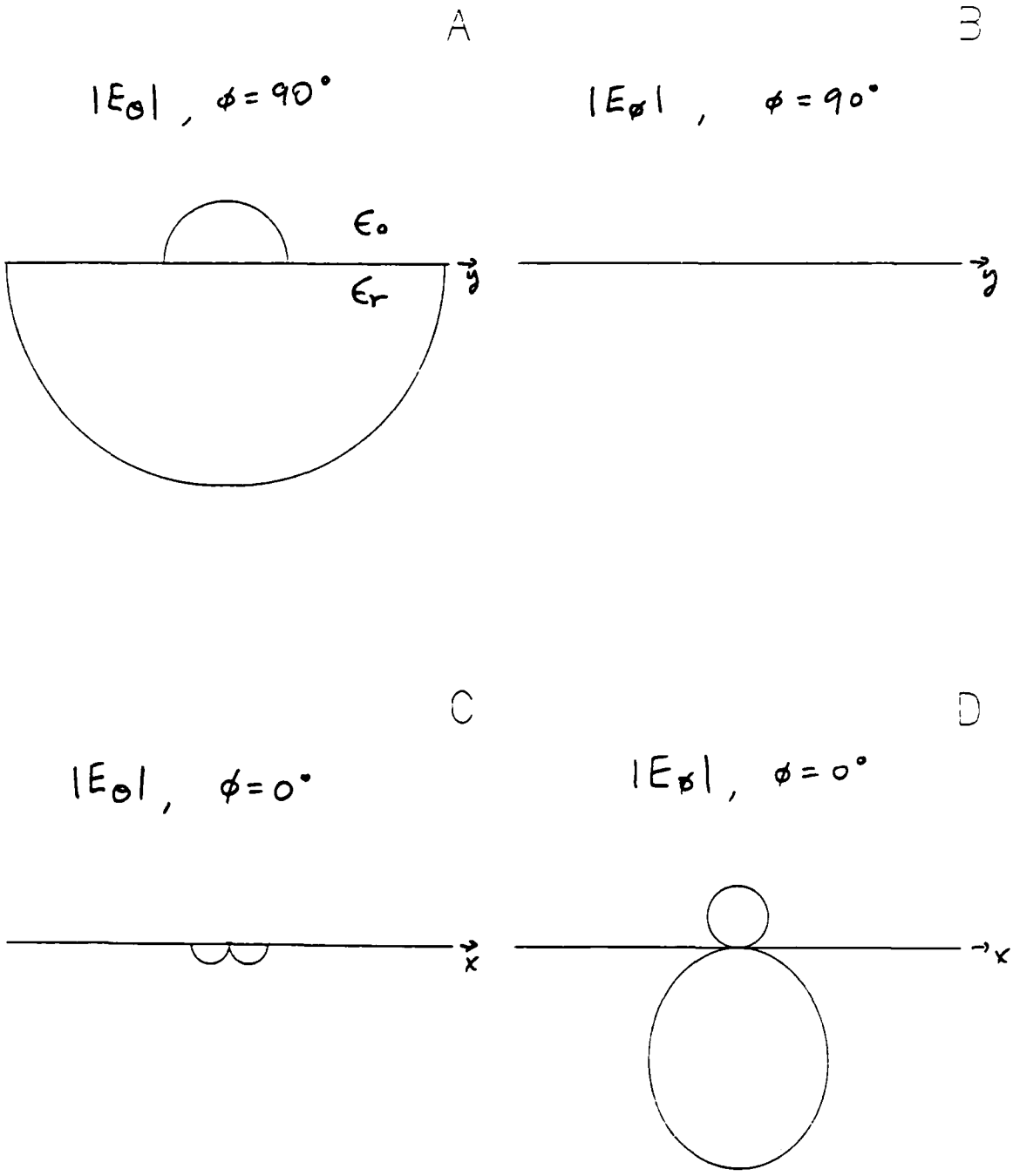

Figure 6. Patterns for Test Case

VI. RECOMMENDATIONS

The computer program was finished at the end of the research period. This left little time for analysis of run data. Therefore, runs using the computer program need to be made and the resulting data analyzed. Secondly, since time didn't permit starting the computer program for the phased array case, it is recommended that the computer program for this case be started next.

VII. REFERENCES

[1] Hanson, Donald F., "A Study of Coplanar Waveguide and its Application to Phased Arrays of Integrated Circuit Antennas," Final Report for 1985 USAF-UES Summer Faculty Research Program, Hanscom AFB, August 12, 1985.

[2] Butler, C. M., D. R. Wilton, and A. W. Glisson, Notes from a Short Course on "Fundamentals of Numerical Solution Methods in Electromagnetics," University of Mississippi, Oxford, MS, 1982.

[3] Agrest, M. M., and M. S. Maksimov, Theory of Incomplete Cylindrical Functions and their Applications, Springer-Verlag, New York, 1971.

[4] The Staff of the Computation Laboratory, Harvard University, Tables of Generalized Sine- and Cosine-Integral Functions, Cambridge, MA, Harvard University Press, 1949.

1986 USAF-UES SUMMER FACULTY RESEARCH PROGRAM/

GRADUATE STUDENT SUMMER SUPPORT PROGRAM

Sponsored by the

AIR FORCE OFFICE OF SCIENTIFIC RESEARCH

Conducted by the

Universal Energy Systems, Inc.

FINAL REPORT

Effect of Low Frequency Vibration on Bone Remodelling in the Rhesus Os Calcis

Prepared by: Gerald F. Harris

Academic Rank: Adjunct Assistant Professor

Department and University: Department of Mechanical Engineering, Marquette University

Research Location: Harry G. Armstrong Aerospace Medical Research Laboratory, Biodynamics Effects Branch, Wright-Patterson AFB, Dayton, Ohio

USAF Research: Dr. Leon Kazarian

Date: September 18, 1986

Contract No: F49620-85-C-0013

Effect of Low Frequency Vibration on Bone Remodelling in the Rhesus Os Calcis

by

Gerald F. Harris

ABSTRACT

The naturally occurring phenomena of bone growth, modelling and remodelling were first studied through a review of current literature. This was followed by a review of recent studies of hypogravic exposure and vibration. The anatomy of the Rhesus Os Calcis was then reviewed, and a series of dissections performed to better understand the structure and load transmission characteristics. The vibration protocol used in treating the study animals was then thoroughly reviewed. Control and vibrated Os Calces were then extracted from 6 vibrated and 2 control animals. The specimens were embedded in methyl methacrylate, cut, sanded, stained, and mounted on slides. Histomorphometric data including static and dynamic remodelling parameters was obtained. Further work needs to be done in computing the stereology parameters and in completing a statistical analysis of the results.

Acknowledgments

I would like to thank the Air Force Systems Command, Air Force Office of Scientific Research, Dr. Leon Kazarian (AAMRL/BBD), and the Shriners Hospitals for Crippled Children for sponsorship and support of my research effort. I would also like to thank Kristin Natvig, K.C. Smith, Suzanne Smith, Marvin Souder, and Pat Roberts for offering the environment and guidance needed to complete this work. Special thanks to Clarence Oloff and Edward Eveland for their tireless efforts and uplifting spirits. Thanks too to Nadia Greenidge for the anatomical discussions and help with dissections.

Lastly, I want to thank my wife, Marilyn, and my children Heather and Jeremy for their support and encouragement during my summer absence.

I. Introduction

I received my Ph.D. from Marquette University, Milwaukee, Wisconsin. My studies there concentrated on instrumented methods for the evaluation of children with Cerebral Palsy. Upon graduation I took a position as a Biomedical Engineer at Shriners Hospital for Crippled Children, Chicago Unit. At Shriners I have continued to develop instrumented methods for evaluating spasticity and hypertonicity. I have also done work in gait analysis, motor control, and orthopaedic biomechanics.

The opportunity provided at the Harry G. Armstrong Aerospace Medical Research Laboratories was one to study bone and the phenomenon of bone remodelling. My direct objectives were to gain a better understanding of bone for orthopaedic applications, and to investigate the potential for remodelling projects in Spinal Cord Injury patients.

The work performed addresses the fundamental issue of trying to define basic vibration parameters necessary for stimulation of bone remodelling in a primate. My effort focuses on an analysis of the Os Calcis and is part of a much larger and ongoing study sponsored by the Biodynamics Branch (AAMRL/BBD).

II. Objectives of the Research Effort

A. The overall objective of the bone remodelling research project is to investigate the effects of low frequency vibration and mechanical stress on lower appendage bone remodelling in a primate model. The amount and distribution of cross-sectional bone formation and resorption is being measured for each of 3 loading frequencies at various skeletal positions. The state of stress in the lower legs will then be correlated with observed bone changes. The experimental protocol is structured to investigate the existence of an effective frequency/stress "window" for producing significant bone remodelling.

My specific objectives were:

1. To review the existing literature on bone growth, modelling and remodelling including normal physiology, hypogravic exposure, and vibration.

2. To define the normal anatomy, architecture and geometry of the Rhesus os Calcis.
3. To extract and prepare for histomorphometric analysis Os Calces from the 8 animals used in the study.
4. To perform a histomorphometric analysis of the Os Calcis sections focused upon defining static and dynamic changes in trabecular architecture secondary to vibration.

B. A second major objective of my studies which was added after I began was to review work done in defining foot-to-floor contact forces during human gait.

My specific objectives were:

1. To review the existing literature on instrumentation and analysis of multiple point foot-to-floor contact forces during human gait.
2. To design an acceptable method for validating a force dosimeter ("bionic boot") currently under construction for the BBD Laboratory.

III. Bone Review

To gain a better understanding of bone (physiology, histomorphometry, growth, modelling, remodelling, hypogravic exposure, vibration, etc.) 2 literature investigations were performed. The first was initiated at Shriners prior to my arrival, and the second while at the BBD Laboratory. In total over 65 articles were identified and reviewed.

High points in these reviews included the theory of bone remodelling, minimum effective strain (MES), measurement of mechanical impedance, effects of hypogravic exposure, and studies of vibration (2-13).

The necessary foundation for preparing specimens and performing the histomorphometry was also established through the literature review and contact with BBD Laboratory personnel.

IV. Anatomy

The anatomical review concentrated on the Os Calcis and its articulations. Two dissections of Rhesus feet were also performed.

The Os Calcis, Calcaneus or heel bone is the largest of the

tarsals. It has 3 dorsal surface articulations with the talus and a distal (anterior) articulation with the cuboid. The sustentaculum tali projects from the junction of the dorsal and medial calcaneal surfaces, while the calcaneal tuberosity projects at the proximal end. The talus also articulates with the navicular which lies between the talus and cuneiforms.

The talocalcaneal joint structurally consists of three joints, one proximal and two distal. The proximal is between the bodies of the two bones while the two distal involve the neck and head of the talus, the body and sustentaculum of the calcaneus, and a fibrocartilage which fills the interspace between the sustentaculum tali and navicular. There are medial and dorsal ligaments as well (1).

Although the precise load transmission pathway between calcaneus, navicular and talus can't be established from anatomical observation alone, several assumptions can be made. Load acting vertically down through the tibia is transmitted to the talus and then to the 3 articulations of the Os Calcis and 1 articulation with the navicular. The Os Calcis articular structure would suggest that the greatest proportion of the vertical load is distributed to the Os Calcis.

Lateral sections of the talus-Os Calcis bones were utilized in this study. These lateral sections extended medially to a midsagittal plane. The 3 suspected load bearing areas of the Os Calcis are depicted in Figure 1, along with the name of the articulation with the talus which produces that load concentration. Loads are also borne by the distal or bottom portion of the Os

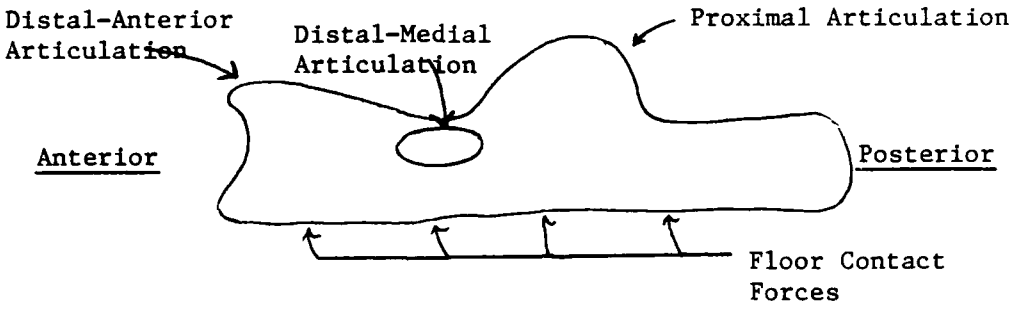

FIGURE 1. Os Calcis Forces.

Calcis.

The trabecular structure of the Os Calcis is depicted in Figure 2. A combination of load-transmission pathways and trabecular architecture was utilized in selecting the 4 areas noted for histomorphometric analysis.

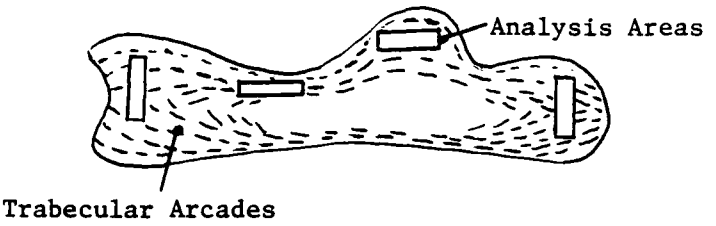

FIGURE 2. Os Calcis Analysis Areas.

V. Specimen Preparation

Specimens were extracted from frozen feet of the 8 vibrated and control animals used in the study. The talus-Os Calcis articulation was kept intact. A plastic embedding procedure was employed. Specimens were dehydrated in 70% and 100% ethyl alcohol for 3 days. They were then pre-stained for 7 days in Osteochrome Villanueva bone stain under vacuum. The embedding procedure was initiated with a 50:50 solution of ethyl alcohol and methyl methacrylate monomer. Specimens were then placed in a thin monomer solution for 3 days with changes each day. They were then placed in a thick monomer solution for 7 days under house vacuum. Polymerization was confirmed, and then the specimens were placed overnight in a 35 Deg. C oven followed by a 2 hour exposure in a 60 Deg. C oven. The embedded specimens were then refrigerated overnight and the containers broken to remove the blocks. [Thin monomer: 1 gm benzoyl peroxide to 100 ml inhibited methyl methacrylate monomer. Thick monomer: 2 gm benzoyl peroxide, 40 gm polymethyl methacrylate beads, to 100 ml inhibited monomer.]

The thin embedded specimens were then epoxied to small pieces of wood for mounting into the saw jig. All medial specimen faces were ground flat prior to cutting. Thirty-eight sections were cut. Typically the first cut was quite thick to insure the integrity of the mid-sagittal section (350-450 um). Subsequent sections

averaged 150 um in thickness. The best mid-sagittal sections from each specimen were then hand sanded (280 and 400 grit wet/dry paper) to a thickness of 6-9 um.

The sanded sections were then stained in Osteochrome Villanueva bone stain for 48 hours. After staining the sections were cleaned in tap water, lightly sanded (600 grit wet/dry paper), washed and rinsed with distilled water, differentiated in a 0.01% glacial acetic acid methanol (95%) solution for 15 minutes, and dehydrated in 95% and 100% ethyl alcohol. Sections were mounted on slides with cover slips using Euparal.

VI. Histomorphometry

A histomorphometric analysis was initiated for the 4 areas of interest shown in Fig. 2 for the following static parameters:

- Volumetric bone density (VV)
- Surface bone density (SV)
- Mean diameter (DQ)
- Mean Volume (VQ)
- Mean Surface (SQ)

These parameters were obtained for mineralized bone, osteoid, and resorption spaces. The number of resorption spaces per field was also tabulated. A total of 720 fields were analyzed in this portion of the study.

The dynamic analysis included an inspection of tetracycline double label over the entire surface of each section. Measurements included trabecular area, area of osteoid, distance between labels at multiple points, and length of double label.

Although time did not permit an analysis of the stereology parameters, they will be recomputed from the existing data. The selected parameters for future analysis are:

- Volumetric density of bone (VV)
- Surface density of bone (SV)
- Mean trabecular diameter (D-TRAB)
- Volumetric density of osteoid (V-VOS)
- % trabecular surface covered by osteoid (OS)

- Relative volumetric density of osteoid (VVO)
- % of trabecular surface exhibiting Howship's lacunae (OR)
- Mean distance between double labels (MD-D)
- Fraction of trabecular surface exhibiting double labels (LAB-TS)
- Appositional rate per year (AR/Y)

VII. Force Dosimeter

Current literature has been reviewed concerning the measurement of foot-to-floor contact forces during gait. Based upon this review and discussions with Dr. L. Kazarian (AAMRL/BBD) plans have been made to devise a mini-grant proposal for validating the force dosimeter ("bionic boot") output against that of a known standard (AMTI strain gage force plate). The protocol will include an assessment of the static and dynamic measurement characteristics of the isolated dosimeter as well as an analysis of force-time curves and frequency content of gait forces during heel strike, stance and toe-off. A correlation between force plate and dosimeter characteristics will be made. Power spectral analyses of gait forces from the dosimeter will be performed during a number of normal subject trials. The frequency characteristics of normal gait and their relationship to the production of the minimum effective strain needed for bone remodelling will be major long-term objectives of these studies.

VIII. Recommendations

1. In preparing sections for histomorphometry the pre-stain technique with Osteochrome bone stain under vacuum prior to embedding was ineffective. Sections should be stained after embedding and sectioning/sanding is complete.
2. Sections once embedded can be epoxied to pieces of wood in about 12 hours at room temperature. This will provide adequate material for using the Isomet cutting saw without the expense of a larger block of methacrylate.
3. A total of 38 sections were cut and sanded in this study, although only 18 have been examined histomorphometrically. The

remaining 20 sections should also be evaluated for static and dynamic parameters.

4. The technique of cutting frozen specimens to preserve the integrity of the joint articulation was successful and is recommended for future use.
5. The tetracycline label (5mg/Kg body weight administered on 2 successive days) was insufficient for marking the trabecular bone of the Os Calcis. There are several cases where only 1 label is seen on an entire specimen. There is also increased difficulty in confirming the presence of osteoid without label. An increased dose is recommended for future use.
6. This was the first study in which the Videoplan 2 computer system was used to study bone histomorphometry. There are a number of "bugs" in the system including difficulties in separating individual field information by sample number, stereological parameter definition/computation problems, and limitations in statistical data handling capabilities. Further study of the Videoplan capabilities is recommended with a strong suggestion for in-house programming to correct at least the field identification and stereology computation problems. Provisions for communication between the Videoplan and other on-site computers should also be considered. Because the Videoplan allows access to data files through Fortran programs, it should be possible to construct a tailored bone histomorphometry system capable of completing an entire analysis through statistical evaluation.
7. A final analysis of the data gathered in this study should be conducted. I will complete the transfer of Videoplan data to a PDP 11/34A minicomputer. Stereological parameters will then be computed from the raw data. A statistical analysis will be conducted using standard packages. At the completion of this work, the effects of low frequency vibration upon bone remodelling in the Os Calcis should be more clearly defined.

References

1. Bast, T. H., et al., The Anatomy of The Rhesus Monkey, New York, Hafner Publishing Company, 1971.
2. Broderson, A. B. and H.E. Von Gierke, "Mechanical Impedance and its Variation in the Restrained Primate During Prolonged Vibration," ASME Publ. No. 71-WA/BHF-8, 1971 (10 pp) (AMRL-TR-71-67).
3. Elson, R. A. and N. H. Watts, "Attempt to Stimulate Longitudinal Growth in the Dog by Mechanical Vibration," Med Biol. Eng. and Comp., 18:406-418, 1980.
4. France, E.P., "Effects of Acute Hypogravic Exposure and Recovery on the Vertebral Column of Juvenile Primates (Macaca Mulatta)," Doctoral Thesis, Wright State University, Dayton, OH, 1984.
5. Frost, H. M., The Laws of Bone Structure, Springfield, IL, Charles C. Thomas Publishing Company, 1964.
6. Frost, H. M., Bone Modeling and Skeletal Modeling Errors, Springfield, IL, Charles C. Thomas Publishing Company, 1973.
7. Frost, H. M., Bone Remodeling Dynamics, Springfield, IL, Charles C. Thomas Publishing Company, 1963.
8. Frost, H. M., "A Determinant of Bone Architecture," Clinical Orthop. Rel Res, 175:286-292, 1983.
9. Frost, H. M., "Tetracycline-based Histological Analysis of Bone Remodeling," Calc Tiss Res, 3:211-237, 1969.
10. Kazarian, L. E. and H. E. Von Gierke, "The Validation of Biodynamic Models," AMRL-TR-78-105, 1978.
11. Kazarian, L. E. and H. E. Von Gierke, "Bone Loss as a Result of Immobilization and Chelation," Clin Orth, 65:67-75, 1969.
12. Kazarian, L. E., C. Cann, M. Parfitt, D. Simmons, and E. Morey-Holten, "A 14-Day Ground Based Hypokinesia Study in the Non Human Primates - A Compilation of Results," NASA-TM-81268-NASA-ARC-Moffett Field, California, 1981.
13. O'Connor, J. A., L. E. Lanyon, and H. Macfie, "The Influence of Strain Rate on Adaptive Bone Remodeling," J Biomech, 15:767-781, 1982.

1986 USAF-UES SUMMER FACULTY RESEARCH PROGRAM/

GRADUATE STUDENT SUMMER SUPPORT PROGRAM

Sponsored by the

AIR FORCE OFFICE OF SCIENTIFIC RESEARCH

Conducted by the

Universal Energy Systems, Inc.

FINAL REPORT

Mental Rotation and Perspective-Taking Skills In Pilots and Non-Pilots

Prepared by: Edward J. Hass

Academic Rank: Assistant Professor

Department and University: Department of Psychology, Franklin & Marshall College

Research Location: Air Force Human Resources Laboratory, Operations Training Division, Williams Air Force Base, Arizona

USAF Researcher: Elizabeth L. Martin

Date: 8 August 1986

Contract No: F49620-85-C-0013

Mental Rotation and Perspective-Taking Skills In Pilots and Non-Pilots

by

Edward J. Haas

ABSTRACT

Spatial skills in pilots and non-pilots were compared using a traditional mental rotation task, and a new task combining mental rotation and perspective-taking. In the traditional task, subjects had to decide whether a rotated alphanumeric character appeared in its conventional version, or a mirror image of the conventional version. In the new task, subjects compared two views of a scene containing aircraft and terrain, and had to decide whether an objective, "God's eye view" (GEV) containing two aircraft depicted the same or mirror version of the scene as it would apear from the cockpit of the trailing aircraft. Different GEVs showed the same scene from various angles around and above the flight paths of the aircraft. In general, response times increased as both the alphanumeric stimuli and cockpit views were rotated away from upright. In the GEV task, response times were fastest when the perspective of the GEV was directly behind and above the cockpit view aircraft, and increased as the perspective of the GEV was increasingly to the side of and at the flight level of the cockpit view aircraft. Furthermore, the data suggested that non-pilots make mental movements in elevation and azimuth independently, whereas pilots may be able to combine both components of motion. This difference might be due to pilots' experience with three-dimensional movement and thought.

Acknowledgements

I would like to thank the Air Force Systems Command and the Air Force Office of Scientific Research for sponsorship of my research. The environment of the Air Force Human Resources Laboratory, Williams AFB, was the most supportive that I've been privileged to work in. I would like to thank Wally Ruth of the Singer Link Flight Simulation Division and Trish Russo of the AFHRL Media Lab for their help in generating and producing the stimuli employed in the project, and Dave Hubbard of the University of Dayton Research Institute for his help with the data analysis. I am especially grateful to Liz Martin of the AFHRL/Operations Training Division for stimulating discussion and guidance in focusing our mutual interests.

I. Introduction

I received my Ph.D. from Rutgers University studying the process of mental rotation in the cerebral hemispheres of the brain. In my current appointment at Franklin & Marshall College I am continuing this line of research, investigating the cooperation of the two hemispheres in carrying out mental rotation. Mental rotation is a cognitive skill that appears to involve continuous, analog transformations of visual stimulus representations.

The research problem I studied at the Air Force Human Resources Laboratory concerned mental rotation and perspective-taking skills in pilots and non-pilots. There were two general questions examined. First, mental rotation appears necessary for the discrimination of an alphanumeric character from its mirror version if the character is physically rotated through some angle. Would the spatial transformation skills applied to physically rotated scenes depicting terrain and aircraft employ the process of mental rotation as well? Second, are there differences in the spatial transformation skills of subjects who are pilots and those who have never flown an aircaft?

Although I had never before conducted research for the Air Force, I have a strong background in the study of basic cognitive skills, in particular mental rotation. Through private vendor positions with the University of Dayton Research Institute and MacAulay-Brown, Inc., I have also done extensive writing on the application of basic human factors research to problems concerning pilot performance. One area of interest to Dr. Elizabeth Martin at AFHRL was the rotational skills of pilots involved in air-to-air combat. It was the combination of these factors

that resulted in my study of mental rotation while appointed to the Human Resources Lab.

II. Objectives of the Research Effort

The overall objective of investigating this type of cognitive ability is to gain an understanding of the nature of the processes involved in mental spatial transformations. The research I conducted at AFHRL had three specific objectives:

1. A first investigation of the ability to mentally transform an objective, "God's eye view" of a scene depicting terrain and aircraft into a view of the same scene from the cockpit of one of the aircraft in the scene.

2. To compare the processes involved in such transformations to a basic laboratory task suggesting that subjects mentally rotate stimulus representations to upright orientation in order to discriminate physically rotated alphanumeric characters from their mirror images. Such mental rotation could involve a continuous transformation analogous to a physical rotation. If so, then the time to make the discrimination will increase as the angle of the rotation increases.

3. To compare the transformation abilities of pilots to non-pilots in both the basic laboratory and "God's eye view" tasks. It is plausible that the spatial abilities of pilots, particularly military pilots, will differ in some way from those of the "ordinary" subject. The third objective of the study was to determine whether the spatial abilities required by the mental rotation transformation tasks employed here would differ between the two populations.

III. Mental Rotation and Spatial Transformations

Cooper & Shepard (1973) required subjects to decide whether an alphanumeric character was either the normal version of the figure, or its mirror image. The subject's task was complicated by the fact that most of the time the stimulus was rotated through some angle, and so did not appear in its upright orientation. Cooper & Shepard found that the time required to make the normal-mirror decision depended upon the angle of rotation of the stimulus; the greater the disparity from upright, the longer the response time (RT). Furthermore, there was a strong linear component to the RT function, suggesting that subjects were mentally rotating the character back to upright at a constant rate in order to make their discrimination.

Mental rotation is an example of a mental spatial transformation; subjects mentally transform a representation of the stimulus to yield a representation of the same stimulus in a different orientation. Such "movement" through mental space has been studied with other tasks as well, with the result that RT is linearly related to the "distance" that must be travelled. For example, Kosslyn, et al. (1978) had subjects mentally move to various locations on the map of a desert island. He found that the greater the distance "travelled" between two points, the longer it took subjects to make the move. The robustness of this effect of mental distance on RT is well documented (Cooper & Shepard, 1978).

IV. God's Eye Views, Cockpit Views, and Perspective-Taking

The aircraft pilot has a particular view of the environment through which he is flying. His perspective is from the cockpit of his aircraft. However, this is only one of an infinite number of

perspectives. Assume, for example, a situation involving two aircraft, one pursuing the other, both flying over terrain. The view out the cockpit of the trailing aircraft would include the tail of the lead aircraft plus the terrain as it appears from this perspective. Consider now a view of the same scene from the rear of both aircraft, and from an angle above wing level of both aircraft. This is a more objective perspective, since the vantage point is from neither aircraft. Such a perspective is called a "God's eye view" (GEV).

Being asked to envision the scene through which he is flying as it would appear from a GEV involves perspective-taking on the part of the pilot. He must transform his perspective from inside his own aircraft to some "other" point outside. Since this transformation is a mental one, and involves "movement" through an environmental representation, it is possible that the perspective-taking involved in transforming a GEV into a cockpit view is mediated by the same process involved in mental rotation and other analog transformations. Moreover, it is possible that it may be easier to translate between certain GEVs and a cockpit view than other GEVs. For example, a view from directly behind the pilot's aircraft might be privileged relative to one off to the side, because the viewing angle of the former is very similar to that of the cockpit view. It would therefore require less of a transformation to bring it into alignment with the cockpit view.

V. The Experiment

1. Subjects were eight volunteers from various divisions at AFHRL, Williams AFB. There were four pilots and four non-pilots. The pilots had flown a variety of missions, including air-to-air, air-to-ground,

anti-submarine, and formation flight. Three of the pilots had 3000-plus flight hours; the remaining pilot had 600 flight hours.

2. Two types of stimuli were employed. The alphanumeric characters 4, 7, R, F, were presented in black on a white background. They were chosen because they are bilaterally asymmetric and therefore have mirror images that are discriminable from their normal versions. The second type of stimuli were color scenes generated using the IRIS graphics system. GEVs depicted two aircraft and terrain. An F-16 was shown pursuing an F-15, with the F-15 at approximately 45° angle off the nose of the F-16. Half of the GEVs included terrain cues (e.g., mountains), the other half showing simply green terrain and blue sky. GEVs were generated from a variety of perspectives. They showed the scene either from the same elevation as the two aircraft (0° elevation) or from above the level of the aircraft (15° elevation). Factorially combined with these two elevations were perspectives at various angles off the tail (AOT) of the F-16 (40° and 20° off each wing, and directly behind, or 0° AOT). These combinations produced a total of ten GEVs for each scene. Cockpit views of the same scene depicted in the GEV showed the scene as it would appear from the cockpit of the F-16. Both the GEVs and the cockpit views were bilaterally asymmetric, and therefore had discriminable mirror versions.

3. The stimuli were presented on a Gerbrands G1178 3-field projection tachistoscope. RT and responses were registered on a Gerbrands G1271 digital millisecond clock and Gerbrands G1360 response time apparatus.

4. Subjects were instructed that in both parts of the experiment

they would be seeing stimuli that could be either the same as a "standard", or its mirror version. The standard for alphanumeric characters was the normal appearance of the character, always presented on the left side of the test stimulus. The standard for the GEV task was the GEV (presented on the left), and the test stimulus was the cockpit view (presented on the right). In that case, subjects were instructed to decide if the scene depicted in the cockpit view was the same or mirror image of the scene depicted in the GEV. Subjects were instructed that most of the time the test stimulus would appear rotated through some angle. They were also told to stress accuracy of response over absolute speed.

The stimulus pairs on alphanumeric trials were presented for 3500 msec. Presentation time on GEV trials varied, adjusted for individual subjects to allow time for accurate decisions. However, presentation time was never less than 5 sec nor greater than 8 sec, and the proportion of trials requiring the limit for a given subject was less than 1%. There were a total of 48 alphanumeric trials and 240 GEV trials. Stimuli were presented in two sessions of approximately 45 mins each. Both sessions began with a block of 24 alphanumeric trials, followed by 120 GEV trials.

VI. Results

All analyses were conducted on mean correct RTs. Figure 1 presents an overall summary of the data. It shows that in both the alphanumeric task and the GEV task RTs increased with increasing angular disparity from upright up to 180°, then decreased again. This is consistent with earlier work, and suggests that subjects are mentally rotating the test

stimuli back to upright in whatever direction is necessary to achieve the rotation in the shortest amount of time. The reader will note that while the functions are formally similar for the two tasks, RTs in the GEV task are generally elevated approximately 1700 msec above RTs in the alphanumeric task.

Analysis of variance of the alphanumeric task data yielded a significant effect of angle of rotation of the test stimulus, $F(5, 30) = 22.45$, $MS_e = 196045$, $p < .001$. There was also a significant effect of stimulus version (same vs. mirror), $F(1, 6) = 6.10$, $MS_e = 119001$, $p < .05$. "Same" responses yielded a mean RT of 1345 msec, whereas responding "mirror" yielded a mean RT of 1423 msec. There were no significant differences between pilots and non-pilots in the alphanumeric task.

Analysis of variance of the GEV task was conducted separately for pilots and non-pilots. There was a significant effect of angle of orientation of the cockpit view in both groups. For the pilots, $F(5, 15) = 42.36$, $MS_e = 902795$, $p < .001$; for the non-pilots, $F(5, 15) = 9.60$, $MS_e = 2230957$, $p < .001$. As in the alphanumeric task, as angle of the test stimulus increased away from upright, RT increased. In both groups, there was a significant main effect of GEV elevation. For the pilots, $F(1, 3) = 18.43$, $MS_e = 2482388$, $p < .03$; for the non-pilots, $F(1, 3) = 233.26$, $MS_e = 388645$, $p < .001$. For both groups, a GEV elevation of 15° above flight level of the aircraft yielded faster RTs than a GEV at the same elevation as both aircraft. Finally, there was also a significant effect of AOT in both groups. For the pilots, $F(4, 12) = 3.98$, $MS_e = 3426662$, $p < .03$; for the non-pilots, $F(4, 12) = 5.14$,

MS_e = 3146174, $p < .02$. In general, for both groups, as the AOT of the F-16 increased either left or right of directly behind the aircraft, RTs increased.

There were also differences between the pilots and non-pilots. Some of the GEVs and cockpit views contained terrain cues (e.g., mountains) which in addition to aircraft position could have been used to indicate same vs. mirror, whereas others contained simply blue sky and uniform green terrain. For the pilots, this difference in scene had no significant effect on RT. However, for the non-pilots, the presence of terrain cues had a marginal effect on slowing RT, $F(1, 3) = 6.39$, MS_e = 1673068, $p < .10$. For the non-pilots, mean RT to a scene with terrain cues was over 200 msec slower than when no terrain cues were present.

The perspective of a particular GEV was a factorial combination of elevation above flight level and AOT of the F-16 (trailing aircraft). For the non-pilots, there was no interaction of these two factors, indicating that the factors had independent effects on RT. However, in the pilots, there was a significant interaction of elevation with AOT, $F(4, 12) = 4.46$, MS_e = 865533, $p < .02$. These facts suggest a possible difference in processing of the GEV information between the two populations. If it were true that subjects determined location of the F-15 relative to the F-16 by taking the perspective of a pilot in the F-16, then they transformed perspective between the GEV and the F-16 pilot's perspective. To do so, movement in both elevation and azimuth was necessary. The independence of the elevation and AOT factors in non-pilots suggests that they may perform these two movements independently, perhaps first changing elevation, then azimuth (or

vice-versa). Likewise, the interaction of elevation and AOT in pilots suggests that they may have combined both elevation and azimuth information to take the perspective of the F-16 pilot. This is plausible, given the pilot's greater experience with three-dimensional movement and thought.

VII. Recommendations

1. Mission briefing is done in terms of GEVs, not in terms of what the pilot will actually see from his cockpit. To minimize the time needed for the mental transformation between the GEV and the cockpit view, it is best to employ a GEV in briefing with a small AOT of the pilot's aircaft, and somewhat elevated above flight level of the pilot's aircraft.

2. Comparison of the basic laboratory and GEV tasks suggests that while both result in mental rotation, the GEV task adds a constant amount of processing time at all angles of disparity of the cockpit view from upright. It is possible that this added time is that required for the processing of the GEV and a scene more complex than an alphanumeric stimulus, but that the time required for the actual rotation of the cockpit view is very similar to that required in the basic lab task. Follow-up research will address this question in two experiments. First, GEVs and cockpit views will be presented sequentially, instead of simultaneously as in the present experiment. Subjects will be timed on how long it takes to "understand" the spatial relationship in the GEV, and only then presented with the cockpit view for comparison. If the hypothesis of a constant amount of time for GEV processing added to the basic rotational process is correct, then the time to understand the

spatial relationships in the GEV ought to approximate the difference between the GEV and basic laboratory tasks employed here (approximately 1700 msec). However, the stimuli employed in the GEV task are more complex than alphanumeric characters, possibly resulting in greater processing time. If stimuli could be designed so that the aircraft depicted were bilaterally asymmetric (e.g., F-16 with armament on one wing discharged), the same-mirror decision could be made on the more complex stimulus without the GEV component of the task. This would be a more direct comparison with the alphanumeric task. These two experiments would examine the nature of the time constant elevating RTs over those of the basic laboratory task in the current experiment.

3. The current experiment suggested that certain GEV perspectives (e.g., elevation above flight level and small AOT) are privileged, in that they yield faster RTs than other GEV perspectives. This question can be examined in a number of follow-up studies. For example, since we are forward-looking creatures, GEVs from small AOTs behind the pilot's aircraft are directed along a line of sight very similar to the pilot's forward-looking cockpit view. What would happen if GEVs were used depicting the scene from the <u>front</u> of both aircraft? If the GEV task is performed using a perspective-taking strategy, this would require a very great change in perspective and ought to increase RTs dramatically. It would also give further evidence on the question of privileged perspectives for certain GEVs. A variation of this would be to use GEV-cockpit view combinations in which the pilot's (subject's) aircraft is the leading aircraft, instead of the trailing aircaft as in the current experiment. Performance in such a situation would possibly

require additional perspective-taking transformations, as the cockpit point of view would now be rearward instead of forward. Such an experiment also has practical implications, because of air-to-air situations in which the pilot is being pursued.

References

Cooper, L. A., & Shepard, R. N. 1973. The time required to prepare for a rotated stimulus. Memory & Cognition, 1, 246-250.

Cooper, L. A., & Shepard, R. N. 1978. Transformations on representations of objects in space. In E. C. Carterette & M. P. Friedman (eds.), Handbook of Perception, Vol. 8. New York: Academic Press.

Kosslyn, S. M., Ball, T. M., & Reiser, B. J. 1978. Visual images preserve metric spatial information: Evidence from studies of image scanning. Journal of Experimental Psychology: Human Perception & Performance, 4, 47-60.

Figure 1 Caption

Mean correct response time as a function of angle of orientation of test stimulus in alphanumeric and God's eye view (GEV) tasks.

ANGLE OF ORIENTATION OF TEST STIMULUS (degrees)

1986 USAF-UES SUMMER FACULTY RESEARCH PROGRAM/

GRADUATE STUDENT SUMMER SUPPORT PROGRAM

Sponsored by the

AIR FORCE OFFICE OF SCIENTIFIC RESEARCH

Conducted by the

Universal Energy Systems, Inc.

FINAL REPORT

Revitalization of Operations and Controls for the Turbine Engine Test Cells at the Arnold Engineering Development Center

Prepared by:	Doyle E. Hasty
Academic Rank:	Associate Professor of Engineering and Physics
Department and University:	Engineering and Physics Department Motlow State College
Research Location:	Arnold Air Force Station, Engine Test Facility Systems and Software Group
USAF Researcher:	Mr Jack L. Welch
Date:	August 1, 1986
Contract NO:	F49620-85-C-0013

REVITALIZATION OF OPERATIONS AND CONTROLS FOR THE TURBINE ENGINE TEST CELLS AT THE ARNOLD ENGINEERING DEVELOPMENT CENTER

by

Doyle E. Hasty

ABSTRACT

The Arnold Engineering Development Center was contracted by the Air Force Systems Command to expedite and solve problems in the research, development, and testing of the nation's top priority aerospace systems. The AEDC operates the world's largest complex of aerospace flight simulation test facilities. As part of the facilities, the turbine engine test cells have received various modifications and adaptations over the last thirty years to accommodate the changing needs of technology.

The objectives of this research analysis were to specify, implement, and evaluate the new operational methods and new automated control systems to improve and modernize the turbine engine test cells. With this state-of-the-art updating that is being provided the turbine engine test cells, these test facilities will continue to be an active part of aerospace system's evaluators well into the next century.

ACKNOWLEDGEMENT

The author would like to thank the Air Force Systems Command, the Air Force Office of Scientific Research, and Universal Energy Systems, Inc., for providing him with the opportunity to spend a very educational summer at the Arnold Engineering Development Center, Tullahoma, Tennessee. He would like to thank Sverdrup Technology, Inc., for their hospitality, excellent working environment, and challenging assignment.

Additionally, he would like to thank Mr Jack Welch for his collaboration and assistance in this research area. He would like to acknowledge the assistance and cooperation of Mr Marshall Kingery, Mr Wayne Brock, Mr Carl Billingsley, and Mr Tom Cromer who gave of their time to make this such a meaningful appointment.

I. INTRODUCTION

The turbine engine test cells at the Arnold Engineering Development Center have provided simulation flight testing over the past three decades for many of the nation's top priority aerospace programs. As these test chambers begin their fourth decade of testing service, state-of-the-art operational methods, and automated control systems are being specified, implemented, and evaluated in two of these test facilities.[1] The author has had 15 years of experience in high-altitude aerospace testing and found this research area very challenging and well matched to his experience and abilities.

Since the Wright Brothers constructed their wind tunnel in 1901, the development and testing of aeronautical engines and systems have usually preceded the improved flight of aerospace vehicles.[2] The turbine engine test cells at AEDC will continue to play a role in the development and evaluation of aeronautical engines and systems for decades to come if state-of-the-art methods and automated control systems can be implemented into these facilities.

The beginning of the turbine engine test cells actually took place as one of many new technologies to grow out of World War II to shift the world's aeronautical effort away from the conventional aircraft of the time to high subsonic, transonic, supersonic, and space flight.

The Germans had recognized the need for special facilities for propulsion development, and in 1944 they placed in operation the Bavarian Motor Works (BMW) engine test plan to test turbojets and gas turbine engines. Following the end of the war, the BMW plant was dismantled and shipped to

the United States. Congress approved construction of the turbine engine test cells in 1949; and during construction in the early 1950's, the turbine engine test cells have been used to evaluate propulsion sytems for advanced aircraft missiles, satellites, and space vehicles. The advent of the computer age has provided many additional testing capabilities for new aeronautical systems. [3, 4, 5] Both quantity and quality of data must be greatly increased to meet the new testing demands and prepare these aging facilities for tests even into the next century.

The experience gained by this opportunity to work on the project of this complexity was very beneficial to the author. The specifying, implementation and evaluation of new operational methods and automated control system using state-of-the-art technology will be immeasurably beneficial to the author, as well as to his students, when he returns to the engineering classroom.

II. OBJECTIVES

The objective selected for the research effort included the study and evaluation of presently used test philosophies and techniques in these turbine engine test cells. The major objective was to assess state-of-the-art testing techniques using hardware and software technology that might be available presently or in the near future. Improved efficiency of operation through automation was established as the final goal of the effort. The accomplished of these goals would then allow the study of and implementation of state-of-the-art data acquisition and processing systems

which the author proposes to continue studying through a Mini Grant later this year.

III. PRESENT TESTING PHILOSOPHIES AND TECHNIQUES IN THESE TURBINE ENGINE TEST CELLS.

Turbine engine testing requires that the turbine engine and associated test cell systems be controlled precisely and safely to given test requirements. When the required test conditions are met, the data acquisition system is activated. The control room personnel control the turbine engine and associated test cell equipment to the desired test requirements. Presently, the environmental conditions, however, are maintained at another location by personnel responsible for that assignment. Interaction and coordination between these two areas are primarily audio and alphanumeric display communications, indicating the environmental set points and conditions. Primarily manual interaction with the turbine engine and its on-board controls are performed. The total control of the turbine engine and the test environment are maintained by observing visual indications and performing manual responses. [6]

IV. SELECTION AND IMPLEMENTATION OF HARDWARE AND SOFTWARE FOR AUTOMATION OF OPERATION

The proposed Turbine Test Area Controller (TTAC) is a distributed processor network. This controller will increase test productivity and efficiency by reducing the energy and manpower resources required to maintain control of the test article and facility systems through state-of-the-

art methods that are safe and reliable. The first two of the control systems are being checked out in two test units. This activity is continuing in other test cells presently.

Based on the design specifications and criteria, the Westinghouse Distributed Processing Family (WDPF) was selected as the principal system to be integrated into the TTAC program.[7, 8] Some of the special features required of the WDPF are as follows:

- Standard hardware building blocks
- Distributed global data base
- Update of 16,000 analog values or 256,000 packed digital values, or any combination, every second.
- No traffic director
- Expandable to 254 drops
- Passive coaxial highways
- Completely redundant
- No host computer required
- CRT displays in 1 second
- Customer graphics
- Problem - oriental languages

The WDPF system consists of a selection of various drops linked by the Data Highway. The Gateway drop interfaces to other computers or other non-Westinghouse controllers and computers. The Historical Storage and Retricial drop provides mass memory and intelligence to store and retrieve the total plant historical data for later analysis. The Logger drop collects data for logging and prints data on demand or periodically in a standard format.

The engineer's console drop provides all the tools needed to program the WDPF System. The Calculator drop provides a general purpose processor for special calculations and logs which are used to optimize modeling and plant performance evaluation.

The Batch Processing Unit drop provides the WDPF with the ability to sequence groups of equipment for production and to select and modify programs that control a particular test. The Operator's/Alarm Console drop provides a CRT-based control display and alarm console for operator use. The Distributed Processing Unit drop performs data acquisition and control functions and interfaces to the different processors.

The WDPF system consists of three sets of hardware: the Data Highway, the functional processor, and the Input/Output (I/O) interface. These sets of hardware were used as building blocks for this system. Communications to and from the Data Highway are provided by a subsystem controller which consists of a modem, shared memory, and a data base manager. The functional processor performs the specific functions associated with the drop and obtains or stores data from the memory shared between it and the Data Highway Controller (DHC). The I/O communicates to the processors, CRT's, printers, and various drops.

Every 100 milliseconds each drop has access to the highway. Data variables are broadcast at least every second. The two megabaud speed of the highway guarantees that these update rates are possible.

Extensive online diagnostics exist in each DHC to ensure its integrity, as well as that of the whole system. Failed drops are automatically bypassed. Alarms indicating such failure are displayed on the Operator's/Alarm Console.

The Data Highway acts as a distributed global data base available to any drop on the system. The speed and architecture of this system ensures that this global data base is always current and never more than one second old.

Transparent access to the distributed global data base means that control loops can run in one Data Processing Unit (DPU) using data values physically residing in other drops. The ability of any drop on the system to access the total global base transparently allows fuctions that would previously have required a host computer to be distributed among many drops.

V. RECOMMENDATIONS

The author proposes to continue this effort through a Mini Grant so that he can see the final implementation, checkout, and performance of a modernized test cell during the next several months. This year-long activity would complete the implementation and checkout of the completely updated test cell. The performance of this design could be evaluated and then the other major test units could follow this plan. This would give the Engine Test Facility a state-of-the-art testing technique with modernized computer-controlled facilities and equipment.

The author feels that this summer research effort has been very beneficial to him as well as to the future of high altitude turbojet engine and rocket testing at the Arnold Engineering Development Center. He looks forward to being able to see the research effort totally completed and implemented to prepare the Engine Test Facility for testing into the twenty-first century.

REFERENCES

1. Test Facilities Handbook, Arnold Engineering Development Center, Air Force Systems Command, United States Air Force, March 1984.

2. Goethert, B. H. Transonic Wind Tunnel Testing. Pragmon Press, London, England, 1961.

3. Binion, T. W., Jr. "Special Wind Tunnel Test Techniques used at the AEDC." AGARD Conference on Flight/Ground Testing Facilities Correlation, AGARD-CO-187, Ref. 3, April 1976.

4. El-Ramly, Z. M. and W. J. Rainbird. "Computer-Controlled System for the Investigation of the Flow Behind Wings." Journal of Aircraft, Vol 14, pp. 668-674, 1977.

5. Gunn, J. A. and J. R. Christopher, Jr. "Automatic Control of a Transonic Wind Tunnel with a Real-Time Computer System." AGARD Conference on Numerical Methods and Wind Tunnel Testing. AGARD-CP-210, Ref. 8, October 1976.

6. Welch, Jack L. and Jerry L. Brinkley. "Automating the Test Area Controls Systems of the Turbojet Test Units of the Engine Test Facility," AEDC No. EA44, CECROS No. 820072-1, September 1983.

7. Rosinger, George. "Preliminary Human Factors Standards, Specification, and Guidelines for Engine Testing Control Room," Battelle Laboratories, Columbus, Ohio, September 1983.

8. Hasty, D. E. and S. C. Williams. "Steady-State Measurement Uncertainties," Engine Test Facility, Arnold Engineering Development Center, July 1984.

1986 USAF-UES SUMMER FACULTY RESEARCH PROGRAM/
GRADUATE STUDENT SUMMER SUPPORT PROGRAM

Sponsored by the
AIR FORCE OFFICE OF SCIENTIFIC RESEARCH
Conducted by the
Universal Energy Systems, Inc.

FINAL REPORT

Operation of the Electron Ion Momentum Transfer Instability Mechanism in Moderately Dense Plasmas

Prepared by:	Michael A. Hayes
Academic Rank:	Asstant Professor
Department and	Physics and Astronomy
University:	Dartmouth
Research Location:	AFGL/LIS
USAF Researcher:	John R. Jasperse
Date:	86:8/22
Contract No:	F49620-85-C-0013

Operation of the Electron Ion Momentum Transfer Instability Mechanism in Moderately Dense Plasmas

by

Michael A. Hayes

ABSTRACT

The physical mechanism leading to the fast growth rate collisional instability for ion acoustic waves in highly ionized plasmas was investigated. This mechanism was describable as the growth of the spatially periodic electron density perturbation which results from a spatially periodic electron velocity perturbation. The peridocity of the velocity is in turn a result of the relationship between the electron-ion collisional momentum transfer and the spatially periodic ion density perturbation associated with the ion acoustic wave. Direct calculation of the moment equations and the instability growth rate from the physics describing this mechanism gives, to within the precision of this approach, quantitative agreement with the more formal treatment of Jasperse and Basu. This work will be submitted for publication.

Experiments designed to search for the theoretically predicted were proposed, and the proposed experiments are here described. A review of electromagnetic wave-plasma scattering diagnostic literature was performed, and the relation of this literature to the experimentlal problem at hand was assessed. Experimental work on lower hybrid wave propagation was also performed, in conjunction with the Research Laboratory of Electronics at MIT, and an abstract of the results of this work is soon to be published.

ACKNOWLEDGEMENTS

Sponsorship of the Summer Faculty Research Program by the Air Force Systems Command and the Air Force Office of Scientific Research is gratefully acknowledged. I wish to thank all with whom I have dealt at Air Force Geophysics Lab for helping to make my summer pleasant and productive, and I wish to thank Bob Skrivanek, director of the Ionospheric Physics Division, and Herb Carlson, chief of the Ionospheric Effects Branch, for being very gracious hosts.

Particular thanks are due to Jack Jasperse and Bamandas Basu for involving me in their research, and to John Retterer, Dwight Decker, Henry Wadzinski, Charles Dubs, and Milt Klein for numerous valuable discussions.

I. INTRODUCTION

In 1981 I received my doctorate, for work in plasma physics, from the University of Califormia at Davis. Since then I have been on the faculty of the department of Physics at Dartmouth, and I have built, and continue to improve, a plasma physics laboratory there. At Dartmouth I have worked on both theoretical and experimental aspects of wave particle interaction kinetics, and so was drawn to the problem of the collisional instability which Jasperse and Basu had analytically discovered in a two temperature plasma. As it happened, this problem was at a stage where I felt particularly well suited to make a contribution, since what were lacking were an understanding of the physical mechnism by which the instability operated, and ideas for how to test the theoretical prediction experimentally. I have attacked both of these problems, and have been very pleased with the results. In addition to these two main areas of endeavor, I have also accomplished some tasks of secondary importance; these tasks are also described below.

II. OBJECTIVES

1) Review literature on experimental measurements of fluctuation spectra and correlation functions for ion acoustic fluctuations in dense plasmas, and assess the relevance of these experimental data to recent developments in the theory of dense non-equilibrium plasmas which have been made at AFGL.

2) Study in detail the feasability of performing a conclusive experimental test of the theory referred to above.

3) Further explore (theoretically) the physical nature of the mechanisms by which instability may occur in a two temperature plasma.

4) Use facilities at the Research Laboratory of Electronics at MIT to perform measurements of lower hybrid wave propagation in magnetized plasma, and compare these measurements with theoretical predictions.

III. Productivity Overview

The literature was reviewed, with particular emphasis on two papers which my hosts wished assesed for relevance to their theoretical development. This review is presented in section IV. The conclusion of my review was that while there is much of general interest in the literature, and in these two papers in particular, but no presently existing experimental literature may be used as a basis upon which to assess the validity recent theoretical developments. The feasability of performing a conclusive experimental test of the theory referred to above was explored, with the conclusion that such a test is indeed feasable, and should be given a very high priority. The suggested design for such an experiment is dealt with in the Recomendations section. Further theoretical exploration of the mechanism by which the predicted instability operates was investigated very successfully, and the results of this investigation will be published. A qualitative description of these results is presented in section V. Measurements of lower hybrid wave propagation using the experimental facilities of the Research Laboratory of Electronics at MIT are progressing, and comparison of these measurements with theory will be presented at the November meeting of the American Physical Society, Division of Plasma Physics.

IV. A Brief Review of Fluctuation Literature

This section incorporates detailed evaluations of two experiments particularly valuable in understanding fluctuation measurement, as well as a compilation, under appropriate headings, of valuable papers in four relevant areas. The two papers evaluated were chosen in part because of their chronology in relation to the rest of the work in this field: they represent the early seminal work in this field (Ramsden & Davies), and the current state of the art (Mostovych & De Silva). The other reason why these were chosen is because, in spite of any deficiencies which may be pointed out, they are very valuable papers.

1966 Feb. Ramsden & Davies, PRL **16** 303

Laboratory research from the National Research Council of Canada. Plasma formation is by θ - pinch discharge (0.55μF, 35 kV discharge through a single turn coil)

in Hydrogen gas at 1.5×10^{-4} torr. Measurements are made using a high power (10 MW), short pulse (30ns) ruby laser (6943Å) in the afterglow of the discharge, 18 μs after the beginning of the discharge, when the plasma is assumed to be thermalized. Scattered light is measured at 13.5°, and at 90°. Spectrum analysis of the 13.5° scattered light indicates a central peak with two "satellite" peaks shifted 8Å to either side of the main peak. Theoretical analysis of the satellite sideband shift yields a value for ω_p which indicates that the plasma density was 2.4×10^{15}. Analysis also relates the power in the sidebands divided by the power in the central peak to the ratio of the laser wavelength to λ_D. The value of λ_D obtained indicates that T_e = 1.1 eV.

This experiment provides some positive information on the internal consistency of theory, but only looks at two scattering angles, and hence at fluctuations centered on only two different wavelengths. The analysis assumes thermalization without proof, and makes no attempt to independently measure density and temperature as another check on theory. In addition, though the laser power used is large, no attempt is made to consider what effect, if any, laser heating will have on the results.

1984 Oct. Mostovych & De Silva, PRL **53** 1563

Laboratory research from University of Maryland. Plasma formation is by linear discharge in a 1 to 7 torr He or Ar atmosphere. Pinching effects are claimed to be ignorable because the discharges last on the order of 120 μs while the magnetic diffusion time is on the order of 2 μs due to the low temperature (T_e= 2eV) of the discharge. The plasma density is very high ($n_e=10^{17}$ cm^{-3}), and the plasma appears to be about 50% ionized. To form plasma, a 1200 μF capacitor bank is charged to 1-2 kV, and then discharged across electrodes spaced about 30 cm apart. Peak discharge currents are from 10-25 kA, and the radius of the discharge is about 2 cm. The inverse plasma parameter $g^{-1} \equiv n(\lambda_D)^3$ is about 3.5. It is not mentioned in the PRL, but is clear from Mostovych's thesis, that the experimental set-up was operated very near to

the MHD kink instability threshold. Indeed, while results are reported in the PRL for He and Ar, the thesis indicates that the original intent was to report results for H as well, but that stabilization of the kink mode in H discharges was not consistently achieved. In this light, uncertainty about the possible presence of an enhanced MHD fluctuation spectrum, in addition to an enhanced ion acoustic fluctuation spectrum, is not unreasonable.

It is worthy of note that intuition gained in the treatment of other plasmas may fail in the case of so dense a plasma as this. One example of such a failure, which also illustrates a further cause for concern over the possible contribution of an enhanced MHD fluctuation spectrum, is the relative ordering of various energy densities within the plasma. In a sparse laboratory plasma ($n_e \leq 10^{10}$ cm^{-3}), or in a geophysical plasma, the densities are much lower; as a result, for an electron drift $v_{dr} < C_s$, where C_s is the ion acoustic speed, the ordering: $\eta_{mg} << \eta_{dr} << \eta_{th}$ is usually valid, where η_{mg} is the magnetic energy density, η_{dr} is the drift kinetic energy density, and η_{th} is the thermal energy density. However, since $\eta_{mg} \propto B^2 \propto j^2 \propto (n_e v_{dr})^2$, while $\eta_{dr} \propto n_e (v_{dr})^2$, the net result is that the ratio $(\eta_{mg}) \div (\eta_{dr}) \propto n_e$. Consequently, for the plasma in this paper, $\eta_{dr} << \eta_{mg} \approx \eta_{th}$, which reverses the previous ordering of drift kinetic and magnetic energies; thus the free energy source available for MHD fluctuations greatly exceeds that available for ion acoustic fluctuations, contrary to the usual case for more typical plasmas. Despite the fact that $\eta_{mg} \approx \eta_{th}$, it is yet correct to describe this plasma as unmagnetized since, because of the extraordinarily high density, $\omega_{pe}/\omega_{ce} \approx 10^3$.

Possible doubts as to the physical nature of the observed fluctuations aside, the experiment described measures scattered laser power, as a function of time, at 4.7 °, and at 8.75 °. The frequency spectrum of the scattered power at each angle is compared against the predictions arrived at by taking different models for $S(k,\omega)$. Of the theoretical models compared, the best agreement is found with the BGK theory. It should be noted that in the plots of calculated and observed ratios of scattered to

incident power, the calculated ratio has been scaled so that its peak will be at the height of the highest measured value on a particular graph. A 200W CO_2 laser with wavelength 10.6 μ is used. The laser power is very low in comparison to the discharge power (up to 50 MW), so temperature perturbation as a result of the use of the laser is very unlikely.

Theory of Fluctuations and Wave Scattering

'60 Can. J. Phys. **38** 1114; J. A. Fejer

'60 Proc. Roy. Soc. **A259** 79; J. P. Dougherty & D. T. Farley

'60 Phys. Rev. **120** 1528; E. E. Salpeter

'61 Nuclear Fusion **1** 101; N. Rostoker

'62 Phys. Fluids **5** 776; M. N. Rosenbluth & N. Rostoker

Wave Scatter Experiments

'58 PRL **1** 454; K. L. Bowles

'66 PRL **16** 303; S. A. Ramsden & W. Davies

'71 PRL **26** 67; B. Kronast & Z. Pietrzyk

'71 PRL **26** 694; M. Keilhacker & K.-H. Stuer

'72 PRL **29** 81; C. M. Surko, *et al*

'84 PRL **53** 1563; A. N. Mostovych & A. W. DeSilva

Double Dipole Probe Theory

'75 J. Plasma Phys. 14 209; R. Pottelette, B. Rooy, & V. Fiala

'77 J. Plasma Phys. 17 201; R. Pottelette, C. Chauliaguet, & L. R. O. Storey

Double Dipole Probe Experiments

'79 Phys. Fluids **22** 534; R. Pottelette

'81 Phys. Fluids **24** 1517; R. Pottelette, M. Hamelin, J. M. Illiano, & B. Lembege

Some Relevant Books

Radiation Processes in Plasmas, George Bekefi, Wily, N. Y. 1966

Stat. Mech. of Charged Particles, Vol. 4, series on Stat. Phys., I. Prigogine, ed. 1963

V. Developmet of Physical Understanding for the Fast Electron Ion Momentum Transfer Ion-Acoustic Instability

Recent calculations of the dielectric function for the Balescu-Lenard-Poisson kinetic equations by Jasperse and Basu have resulted in a number of interesting predictions, including the prediction of collisional growth of long wavelength ion acoustic waves on the electron-ion slowing down time scale, given a sufficiently large ratio of electron temperature to ion temperature. I have developed a technique for directly incorporating the effects of collisions into the electron continuity equation, and then using this equation in conjunction with other fluid-like equations to corroborate the predictions of wave behavior resulting from the more involved kinetic calculation of the dielectric function. While, compared to a complete solution of the kinetic equations, my provides a mathematically simpler approximate method for incorporating the effects of collisions into plasma wave equations, the principle advantage of my method is that it illustrates the physical mechanism governing the effect of collisions on wave propagation, including the above mentioned collisional instability.

The essence is that a spatially periodic ion density will result in a spatially periodic electron-ion drag, which when integrated over electron velocity space, will result in a spatially periodic divergence of the average electron velocity. The electron continuity equation which results gives a collisional increase of the electron density which is proportional to the collisional slowing rate multiplied by the perturbed part of the ion density. The remainder of the moment equations may, in the limit of a sufficiently large ratio of electron temperature to ion temperature, be obtained in a manner similar to that by which the standard collisionless fluid results are obtained, and the entire set of equations may be solved to obtain the same long wavelength predictions as the full kinetic theory in the same limit. This technique has value for its relative simplicity of application, but its principle merit is that it starts with a well understood feature of collisional systems, collisional drag, and reproduces the most startling results of the full kinetic theory from there. By demonstrating the physical relationship between collisional drag and unstable wave growth, this development facilitates a more basic understanding of the latter phenomenon.

In the derivations of fluid-like equations which include the effects of momentum

transfer collisions between electrons and ions, the minimum kinetic treatment which will enable a physically reasonable and self-consistent inclusion of collisional momentum transfer is employed. Specifically, no attempt is made to include the effects of resonant particles, so of course Landau damping does not come out of these equations. As a result, the growth rate thus derived will be valid only in the limit of a sufficiently large electron to ion temperature ratio that resonant particle effects are indeed negligable, and Landau damping may legitimately be ignored. For other temperature ratios, the effects of Landau damping must be independently calculated and added in to obtain the correct total growth or damping rate.

The work outlined above has been competed, but awaits final preparation for publication. In any case, details of this work could not be included in this report because of space constraints.

VI. Recommendations

As a result of my recent findings, I put a very high priority on the experimental search for the collisional electron slowing ion acoustic instability. I have arrived at a good basic design for experiments to detect and measure this instability, but more work must be done on the detailed planning and optimization of these experiments. It may be possible to perform some crude tests using modifications of facilities present in typical plasma laboratories, such as my laboratory at Dartmouth, but conclusive tests can not be performed without access to more elaborate facilities. Construction of facilities sufficient for the performance of conclusive tests would be very expensive. Fortunately, it is likely that the tests can be performed at a great reduction in total cost by using facilities already in existence.

An optimal test of theory would require the use of a Q-machine, since such a machine has much higher ionization fraction, and much smaller drifts than do other types of plasma machine. Most importantly, use of a Q-machine would allow variation of the electron temperature as a free parameter, independent of the electron density, over a wide range. Since the instability under consideration would only exist for a plasma in which the electron temperature exceeded the ion temperature, the suggested experiment will require electron cyclotron resonant heating (ECRH), which

is not a feature commonly found on Q-machines. Fortunately, there exists a Q-machine which may prove more easily adapted to the performance of a heated electron experiment. This is the new Super-Q at Lausanne, Switzerland.

With access to a Q-machine which is adaptable for ECRH, experiments to test theoretical predictions will be possible in principle; what needs to be determined is how best to pursue these delicate but important experiments in practice. The basic idea may be easily stated: one must first form a high density, highly ionized plasma which is very quiet, in the ion-acoustic range of frequencies, and drift free, and then proceed to heat the electrons in this plasma. Care should be taken to monitor the uniformity of the plasma as the electrons are heated, and also to monitor both the electron and ion temperatures as a function of applied ECRH power. The relative values of the perpendicular and parallel electron temperature should also be measured, although it is unlikely that any difference would be observable. For 2 eV electrons at a density of 10^{12} cm^{-3}, the classical collisional electron temperature anisotropy relaxation rate would be about 4×10^{-6} sec^{-1}, while the electron thermal velocity would be about 6×10^{5} m/s. Using the length of the Lausanne Super-Q (which is 4 m) gives a thermal residence time of about 6.7×10^{6} sec, or about 27 temperature anisotropy relaxation times: far more than required for an essentially Maxwellian distribution. Even at much lower densities where the classical electron collisionality would be insufficient to Maxwellianize the electrons, the rapidly growing high frequency kinetic instabilities which feed off of the free energy available in an anisotropic electron distribution make it extremely unlikely that the experimenter would observe a significant temperature anisotropy. Neither these very high frequency unstable waves, if present, nor the ECRH itself should affect the quiescence of the plasma in the ion-acoustic range of frequencies; ion-acoustic waves have much lower frequencies than the above-mentioned phenomena, hence these phenomena would not be picked up by our ion acoustic wave diagnostics.

Concurrent with the monitoring of the thermal characteristics of the plasma, the experimenter should launch ion acoustic waves into the plasma, and measure their growth or damping. By measuring both the real and imaginary parts of the wave vector

k as a function of the real angular frequency ω of the launched wave, the experimenter would be able to test the most important predictions of theory, including the prediction of a fast growth rate (ie. growth rate comparable to the electron slowing rate) ion acoustic instability for dense plasmas in which the electron temperature exceeds the ion temperature. Also, the monitoring of the electron and ion temperatures as a function of ECRH power may be used to obtain additional indications of the presence of this instability.

The calculated rate for the classical collisional transfer of thermal energy between electrons and ions is much less than the thermal ion residence time for the parameter regions of interest, so classical heat transfer would have a negligible effect on the measured ion temperature. Consequently, the rate of energy transfer from electrons to ions via the process of unstable wave growth (due to the fast growth rate instability predicted by theory) and the subsequent transfer (via Landau damping) of wave energy to the ions would be obtainable from measurements of the electron and ion temperatures as functions of ECRH power. This experimental thermal transfer rate would thus provide the experimenter with an independent characterization of the instability which could be quantitatively checked against the measured instability growth rate.

The above experimental plan is based on sound physical principles and tried experimental techniques, but a substantial amount of work must be completed, much of it at the site of the Q-machine chosen and in collaboration with the local experimenters, before the plan of execution for this experiment is complete. I am very interested in taking this work further, and it is for this purpose that I have applied for an AFOSR Mini-Grant.

REFERENCES

1. Jasperse, J.R., and B. Basu, "The Dielectric Function for the Balescu-Lenard-Poisson Kinetic Equations," Phys. Fluids , **29** (1986) 110.

2. Trubnikov, B. A. , "Particle Interactions in a Fully Ionized Plasma," in Reviews of Plasma Physics , New York, N.Y., Consultants Bureau, 1965

3. Chen, F.F., Plasma Physics and Controlled Fusion , New York, N.Y., Plenum Press, 1984

4. Schmidt, G. , Physics of High Temperature Plasamas , New York, N.Y., Academic Press, 1979

5. Nicholson, D. R. , Introduction to Plasma Theory , New York, N.Y., Wiley Publishing Co., 1983

6. Ramsden, S.A. and W.E.R. Davies, "Observation of Cooperative Effects in the Scattering of a Laser Beam from a Plasma," Phys. Rev. Lett. ,**16** (1966) 303

7. Mostovych, A.N., and A.W. DeSilva, "Laser Scattering Measurements of Thermal Ion-Acoustic Fluctuations in Collisional Plasmas," Phys. Rev. Lett. ,**53** (1984) 1563

8. Rosenbluth, M.N., and N. Rostoker, "Scattering of Electromagnetic Waves by a Nonequilibrium Plasma," Phys. Fluids , **5** (1962) 776

1986 USAF-UES Summer Faculty Research Program

Sponsored by the

Air Force Office of Scientific Research

Conducted by the

Universal Energy Systems, Inc.

Final Report

Evaluation of Several High Strength Composite Conductors

Prepared by:	James C. Ho
Academic Rank:	Professor
Department and	Physics and Chemistry
University:	Wichita State University
Research Location:	Aero Propulsion Laboratory, AFWAL
USAF Research:	Dr. Charles E. Oberly
Date:	July 27, 1986
Contract No.:	F49620-85-C-0013

Evaluation of Several High Strength Composite Conductors

by

James C. Ho

ABSTRACT

Micrographic examination was made on a recently produced composite conductor. This conductor consists of 2,989 (61x7x7) high purity aluminum filaments in an aluminum-iron-cerium alloy matrix. Deformation of the filaments, having a total of 4,096 (16x16x16) : 1 area reduction through three consecutive extrusions, appears to be well acceptable.

Another aspect of the program aims at assessing high temperature electrical resistivity of several dispersion strengthened conductors with potential applications in high current opening switches. Measurements were made on copper-niobium, copper-alumina, aluminum-silicon carbide, and aluminum-iron-cerium.

Acknowledgments

I would like to thank the Air Force Systems Command and the Air Force Office of Scientific Research for sponsorship of my research. I would like to thank Dr. Charles E. Oberly of the Air Force Aero Propulsion Laboratory and Dr. Harold L. Gegel of the Air Force Materials Laboratory, for stimulating discussions.

I. Introduction

Our research was very much interdisciplinary in nature. It is part of a materials development program, with the final goals aiming at applications in advanced power systems. Toward this end, my education background (B.S. in engineering; M.S. and Ph.D. in chemistry), teaching experience (Professor of Physics between 1971 and 1986 and Professor of Physics and Chemistry since 1986), and extensive research interest (cryogenics, physical and microstructural properties, alloys and compounds, with some 130 articles in publications or conference presentations) allow me to interact with and draw expertise input from many individuals at the Air Force Wright Aeronautical Laboratories, thus forming an integral approach to our studies. I consider this to be of particular importance for my successful participation in the Summer Faculty Research Program.

Specifically, our effort centered around the characterization of high strength conductors intended for advanced power systems.

II. Objectives of the Research Effort

The overall objective of the materials research program at AFAPL is (1) to develop a cryoconductor for pulse power applications and (2) to evaluate various high strength conductors as high current opening switch materials.

My individual objectives were:

1. Assessment of a newly produced high-purity aluminum/aluminum-iron-cerium composite conductor through micrographic examinations.

2. High temeprature electrical resistivity measurements on dispersion strengthened materials including copper-niobium, copper-alumina, aluminum-silicon carbide, and aluminum-iron-cerium.

III. Composite Aluminum Conductors

To meet the ever increasing need for devices generating high power pulses, particularly when weight factor is of great importance, multifilamentary superconductors have been considered as the most promising materials[1]. Their advantages are based on the practically zero electrical resistance and consequently very large current densities. Nevertheless, producing and maintaining the extremely low temperatures required demand liquid helium. Peripheral equipment for helium storage and liquifaction adds extra complication and weight to the overall operation of a given power system. Moreover, for pulsed power applications, transient heat transfer problems are yet to be solved. Consequently, a different type of cryogenic conductors have been considered as a reliable alternative as winding materials[2]. These conductors are not superconducting, but have sufficiently low electrical resistivities at service temperatures near 20K, which are easily attainable whenever liquid hydrogen is available. Indeed, the feasibility of fabricating one such conductor has been demonstrated at AFAPL[3]. Specifically, it is a composite conductor consisting of high purity aluminum filaments embedded in an Al-Fe-Ce alloy matrix.

The matrix material satisfies the following criteria: (1) lightweight, (2) high strength, (3) good thermal conductivity, (4) reasonably high electrical resistivity to minimize eddy current loss and to enhance electromagnetic diffusion rate, (5) workability compatible with that of high purity aluminum, and (6) diffusionless alloying elements (Fe and Ce) in Al. This alloy was initially developed at ALCOA with AFML sponsorship for high temperature structural applications[4].

Earlier work on Al/Al-Fe-Ce composites has been limited to small number of filaments. Most recently a triply extruded product, which contains 2,989 (61x7x7) high purity aluminum filaments, became available. Our effort was to evaluate this product through micrographic examinations. Fig. 1 and Fig. 2 show the original billet and the final product, respectively. It appears that the filaments, after having a 4,096 (16x16x16) to 1 area reduction, maintain roughly the same cross section areas (i.e., no necking as precusor to breaking). There is also no contact between any of the filaments. These results confirm the feasibility of manufacturing this type of advanced composite conductors for the stated purposes.

IV. High Temperature Electrical Resistivities of Dispersion Strengthened Conductors

The requirements for conductor materials of high current repetitive opening switches include, among others, high strength and reasonably good electrical and thermal conductivity. The strength requirement arises from the fact that the primary switch loss is associated with the contact electrical resistance[5]. Even the thermal diffusivity of pure copper does not warrant adequate cooling of the contact surface which will quickly reach its softening temperature. When this happens, the contact pressure decreases and the contact loss rises even further.

One thermal management approach being considered is to fabricate the major part of the switch contact with conductor materials which retain high strength at elevated temperatures (300-600°C or higher). They will then be coated with a thin layer of soft materials as the actual contact tips.

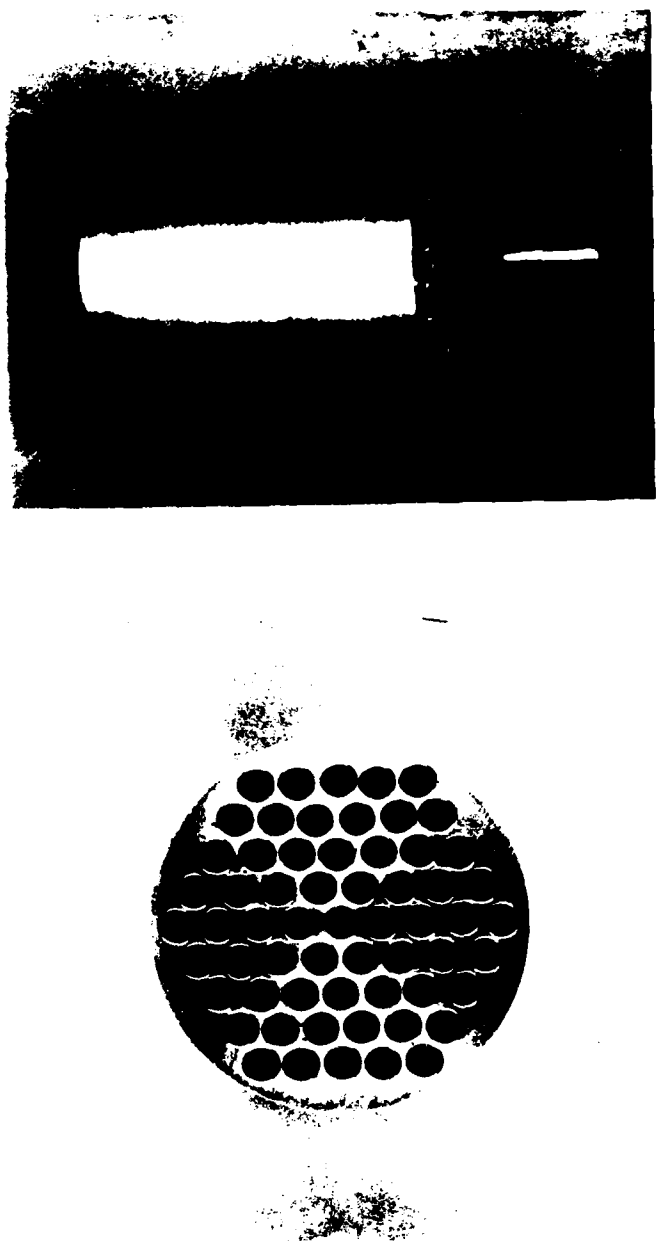

Fig. 1. The original 3-inch-diameter Al-Fe-Ce billet with 61 1/4-inch holes for inserting high purity aluminum rods (only one shown here).

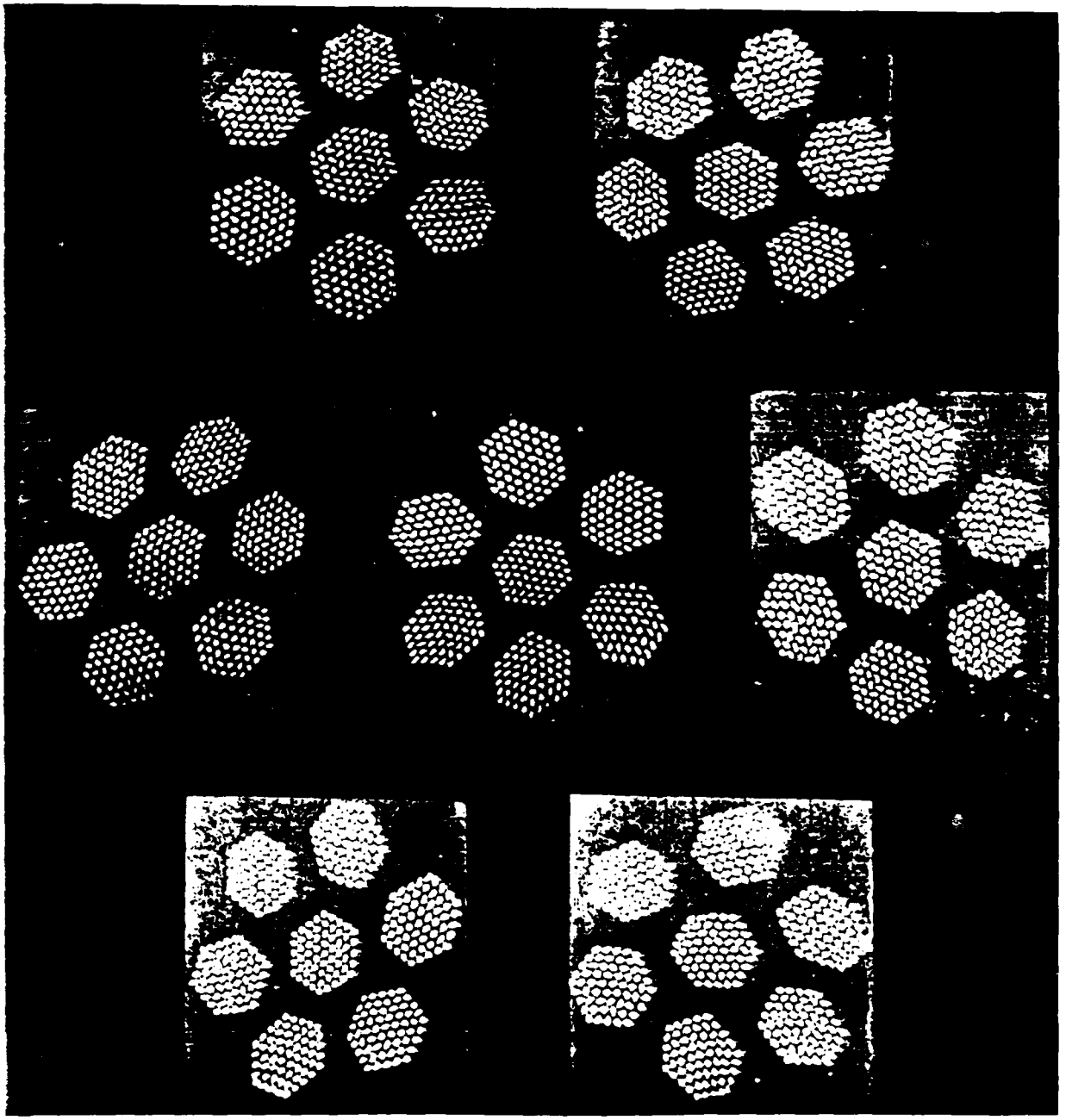

Fig. 2. Micrograph of the seven sections of the final composite conductor following three consecutive extrusions with required restackings. It is 3/4-inch in diameter, and consists of 2,989 high purity aluminum filaments.

In this work, we selected several high strength materials and measured their electrical resistivities as a function of temperature. The materials are basically dispersion strengthened copper and aluminum (copper-niobium from Supercon, Copper-alumina from SCM Metal Products, aluminum-silicon carbide from ARCO Chemical and from DWA Composite Specialties, and aluminum-iron-cerium from ALCOA).

The measurements were made with the standard four-terminal method. The results, in terms of electrical resistivity, $\rho(T)$, and resistivity ratio, $\rho(T)/\rho(295\ K)$, are shown in Figures 3 to 9. Correlations between these values and the microstructural properties of the materials are being analyzed. The results can be useful in future switch design.

V. Recommendations

1. Electrical resistivity at cryogenic temperatures of the new composite conductor (Al/Al-Fe-Ce) needs to be evaluated. Particular attention should be placed on the annealing effect of this property. Annealing at elevated temperatures could alleviate processing-induced residual resistivity, provided that alloying elements in the matrix do not diffuse into the high purity filaments.

It is also recommended to examine presently available high strength aluminum alloys with diffusionless alloying elements, other than the Al-Fe-Ce used here, as alternative matrix materials. Comparisons are to be made in terms of workability, alloying element diffusion rate, and the final residual electrical resistivities.

2. With the recent advancement in processing technology, many new materials are being developed. A majority of them are designed for high temperature structural applications. However, for those with suitable

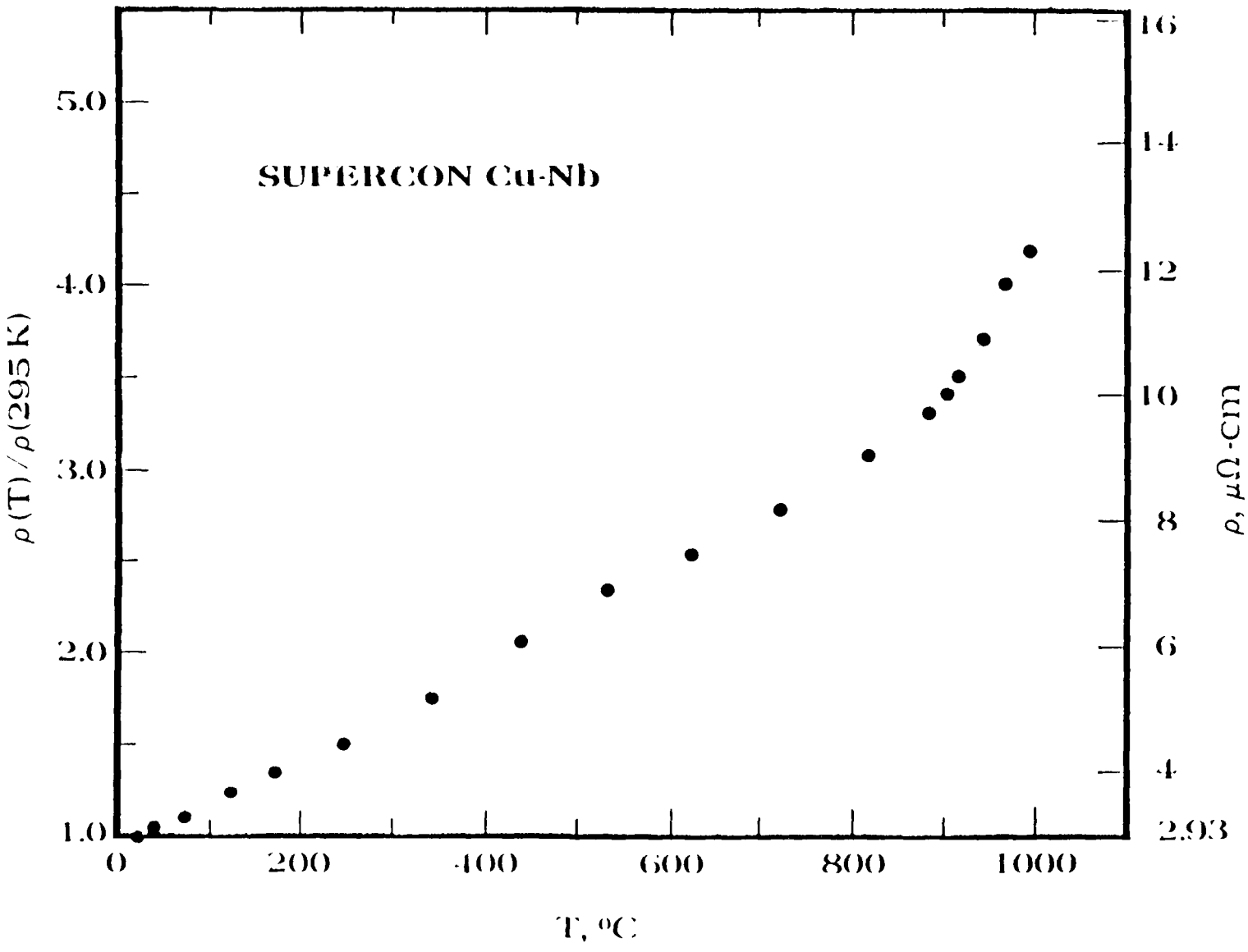

Fig. 3. Temperature dependence of electrical resistivity of copper-niobium from Supercon.

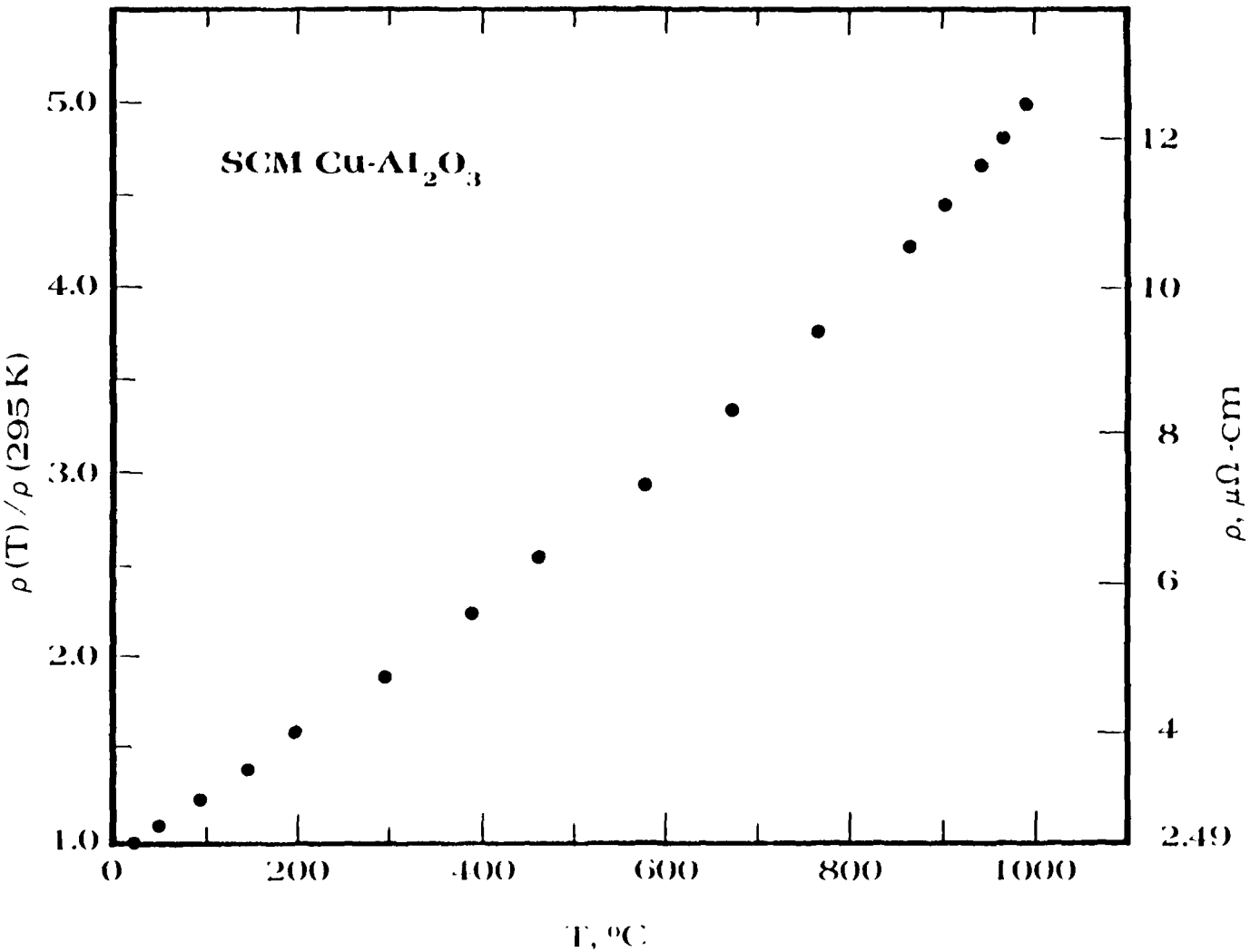

Fig. 4. Temperature dependence of electrical resistivity of copper-alumina from SCM metal products.

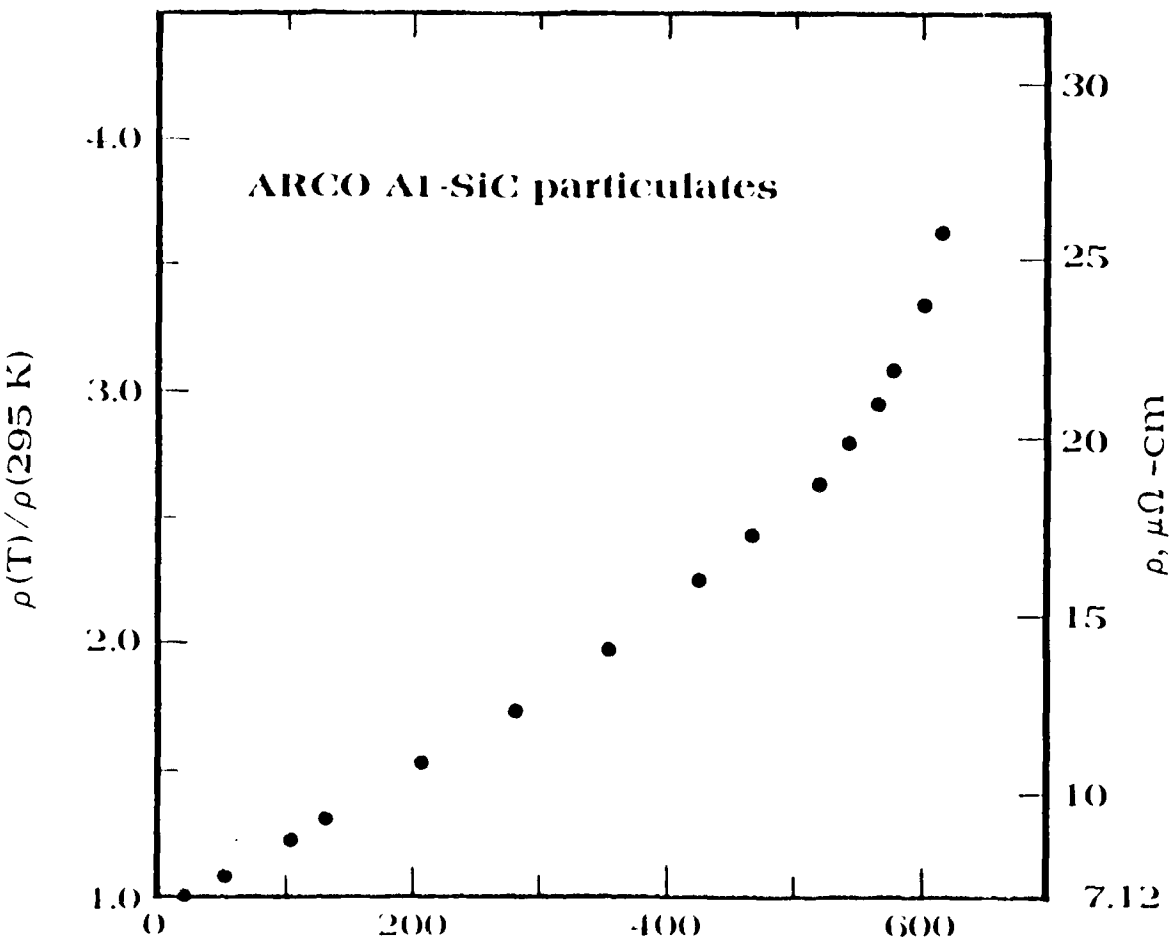

Fig. 5. Temperature dependence of electrical resistivity of aluminum-silicon carbide particulates from ARCO chemical.

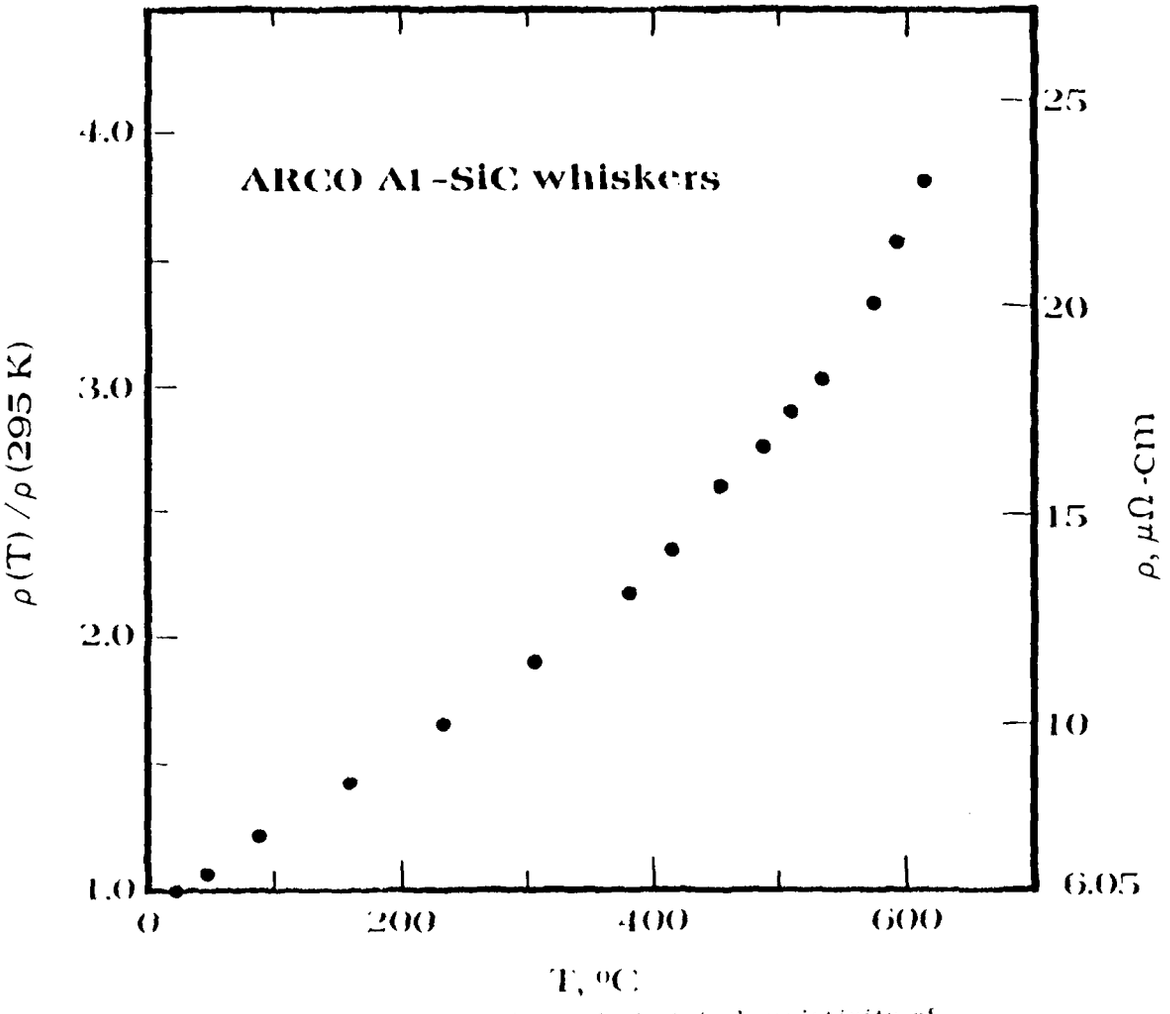

Fig. 6. Temperature dependence of electrical resistivity of aluminum-silicon carbide whiskers from ARCO chemical.

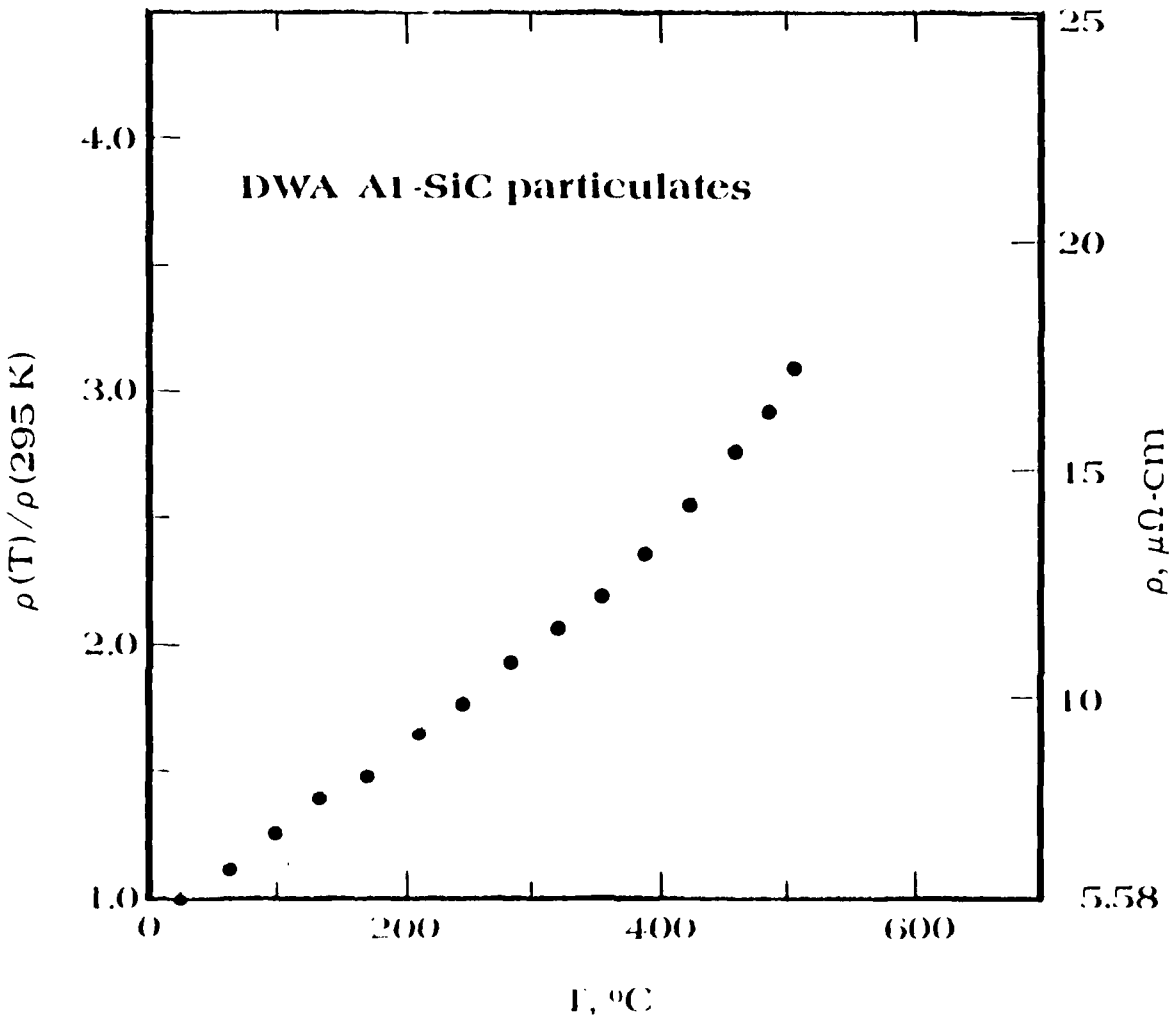

Fig. 7. Temperature dependence of electrical resistivity of aluminum-silicon carbide particulates from DWA composite specialties.

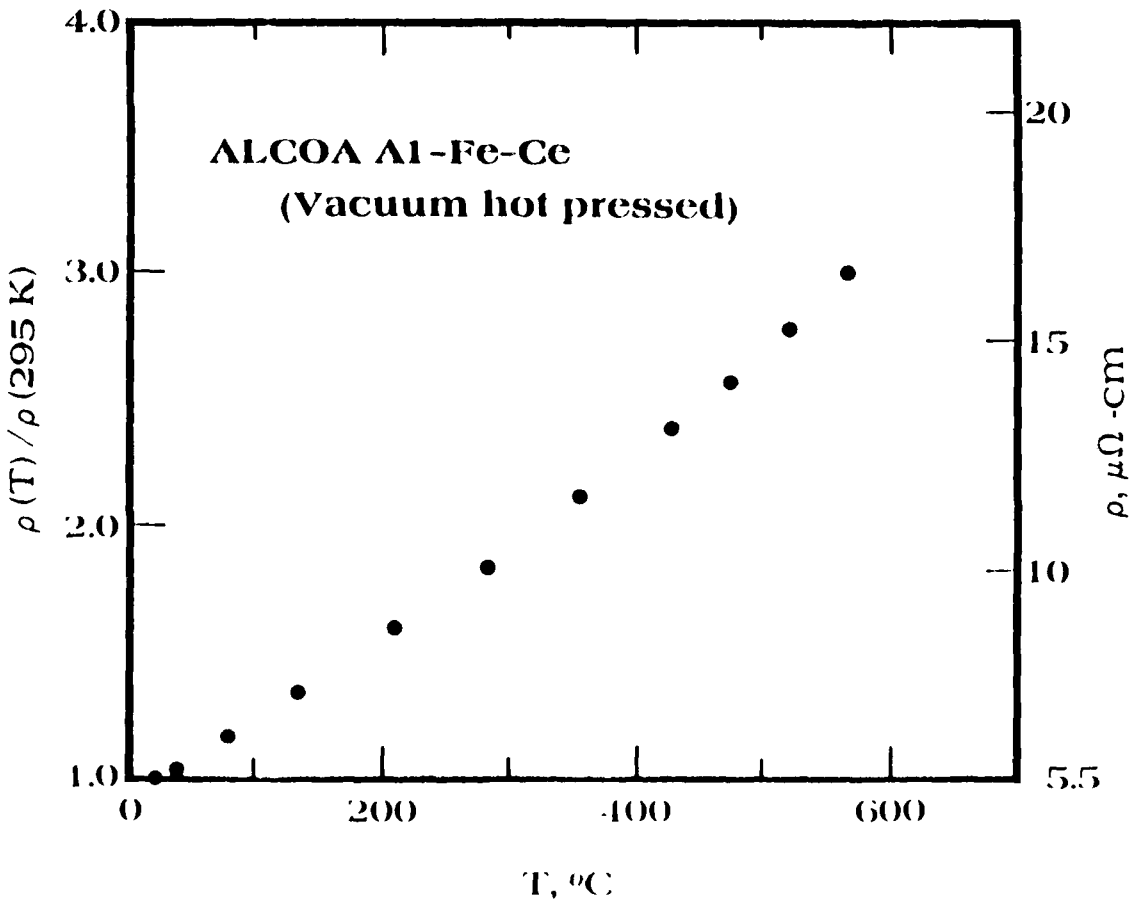

Fig. 8. Temperature dependence of electrical resistivity of vacuum hot pressed aluminum-iron-cerium from ALCOA.

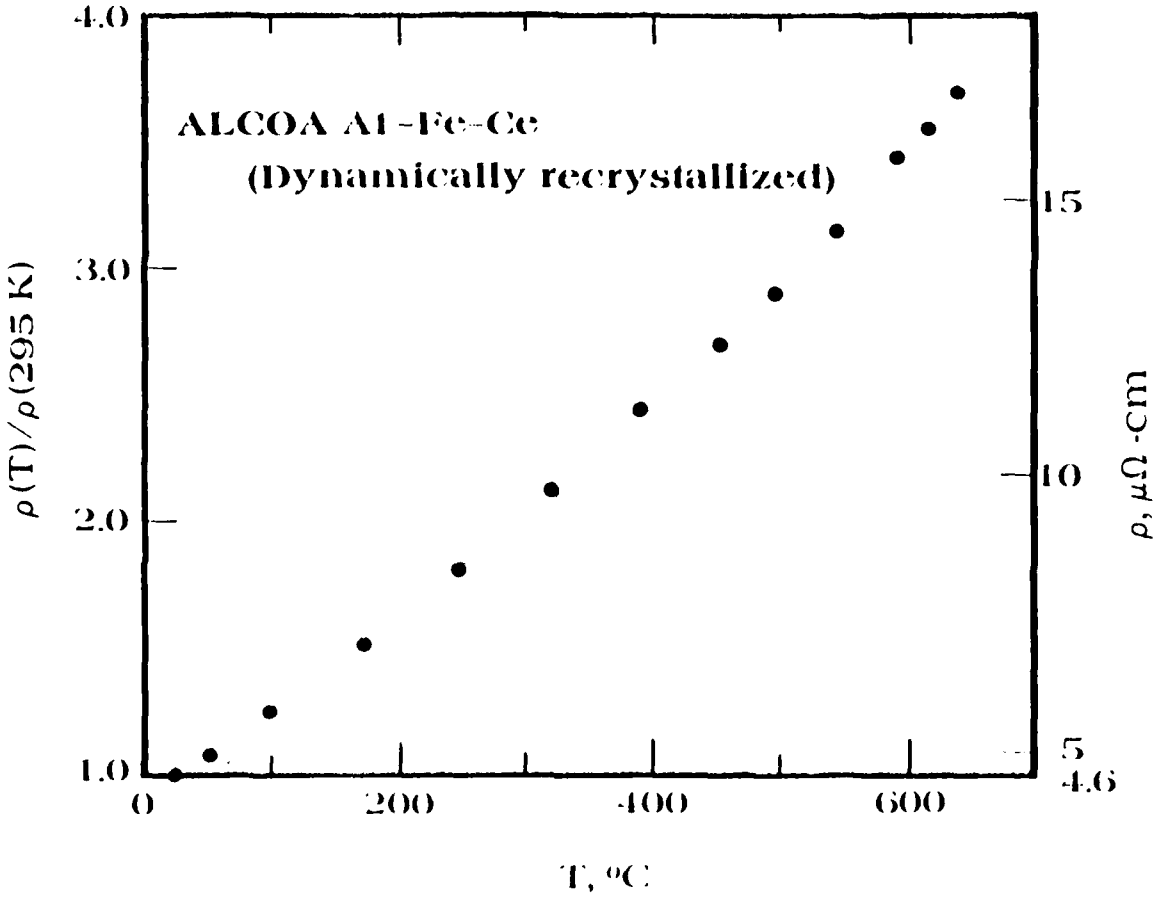

Fig. 9. Temperature dependence of electrical resistivity of dynamically recrystallized aluminum-iron-cerium from ALCOA.

electrical and thermal properties. Applications in high current devices should also be of great interest. A systematic assessment beyond this is strongly recommended.

Correlations between the various physical properties and the microstructures of these materials should be carefully analyzed, towards the final goal of tailor-making low loss switches.

References

1. Many reports are included in the series of Proceedings of Applied Superconductivity Conferences (1966-).

2. R. L. Schlicher and C. E. Oberly, "Cryogenic Aluminum-Wound Generator Rotor Concept", Proc. 5th IEEE Pulsed Power Conference, Arlington VA, June 1985, 752-755.

3. J. C. Ho, C. E. Oberly, H. L. Gegel, W. T. O'Hara, J. T. Morgan, Y. V. R. K. Prasad, and W. M. Griffith, "Composite aluminum Conductors for Pulsed Power Applications at Hydrogen Temperatures", Proc. 5th IEEE Pulsed Power Conference, Arlington VA, June 1985, 627-629.

4. W. M. Griffith, R. E. Sanders, Jr., and G. J. Hildeman, "Elevated Temperature Aluminum Alloys for Aerospace Applications", in High-Strength Powder Metallurgy Aluminum Alloys, edited by M. J. Koczak and G. J. Hildeman, the Metallurgical Society of AIME, 1985, 209-224.

5. Several related articles can be found in Advances in Electrical Current Collection, edited by I. R. McNab, Elsevier Sequoia, NY, 1982.

1986 USAF-UES Summer Faculty Research Program/

Graduate Student Summer Support Program

Sponsored by the

Air Force Office of Scientific Research

Conducted by the

Universal Energy Systems, Inc.

Final Report

The Locally Implicit Method for Computational Aerodynamics

Prepared by:	Peter Hoffman
Academic Rank:	Assistant Professor
Department and University:	Department of Mathematics, University of Colorado at Denver
Research Location:	Arnold Engineering Development Center, Arnold Air Force Station
USAF Research:	Dr. Jim Jacocks
Date:	August 8, 1986
Contract No.:	F49620-85-C-0013

The Locally Implicit Method for Computational Aerodynamics

by

Peter Hoffman

ABSTRACT

Investigation of the locally implicit method is part of the search for a less expensive method to compute viscous flows in aerodynamics. Viscous flow calculations are subject to severe Courant Number restrictions unless implicit methods are used. However, implicit methods require structured grids, which are expensive to compute, and are impeded by the use of approximate factorization. The locally implicit method requires neither. This research investigates the Courant Number restriction on the stability of the locally implicit method and provides variations of the method which have no restriction. In 2D and 3D, this algorithm is an ideal candidate for parallel computation.

ACKNOWLEDGMENTS

I would like to thank the Air Force Office of Scientific Research and the Air Force Systems Command for this research opportunity. In particular, I thank Marshall Kingery, who served as my point of contact with the Air Force.

Furthermore, I appreciate my research relationship with Jim Jacocks, Head, Computational Fluid Dynamics, Propulsion Wind Tunnel Facility, Arnold Engineering Development Center, and with K.C. Reddy, Professor, and Mark Ratcliff, graduate student, University of Tennessee Space Institute.

Finally, I am happy to have had the opportunity to spend this time in Tennessee with the folks of the Computational Fluid Dynamics Section and Calspan/AEDC.

1. Introduction. The locally implicit method was developed by K.C. Reddy and Jim Jacocks of the Computational Fluid Dynamics Section in the Propulsion Wind Tunnel Facility at the Arnold Engineering Development Center. The goal is to reduce the cost presently required to obtain solutions to viscous aerodynamics problems.

If cost were no object, the central difference spatial approximation with implicit Euler time stepping would be good. It is certainly better than explicit time stepping when very fine spatial discretizations impose Courant Number restrictions. Locally implicit methods avoid the cost of implicit solutions by time-lagging either the right point and marching to the right or the left point and marching to the left. This is the basic one-point locally implicit method.

An N-point locally implicit method uses N-1 central difference stencils with implicit Euler time stepping. Depending upon the direction of march, either a left or right one-point locally implicit stencil is added to the group so that the resulting system is solvable. It has N equations to solve simultaneously and, hence, is implicit locally.

Because the N-1 fully implicit stencils impose no stability restriction, the stability restriction on the group is imposed by the one-point locally implicit stencil.

2. Objective. The object of this research was to analyze the one-point locally implicit method. In particular,

1. A thorough understanding of the stability of the basic locally implicit method had to be achieved.

2. If the basic method were found deficient, seek a method or methods which remedied these deficiencies.

3. Examine the practical aspects of a real implementation of the method for a system of equations in several dimensions on modern computing machinery.

This paper discusses the basic method which is found to have an unusual reason for a Courant Number restriction. Then, three methods for removing this restriction are outlined. Next, tabulated data for all four methods is presented and interpreted. Finally, conclusions and recommendations are given.æ

3. Basic Method. Consider the one point method for one dimensional linear convection.

$$u_t + cu_x = 0.$$

Marching to the right uses the numerical discretization

$$\frac{u_j^{n+1} - u^r}{\Delta t} + c\frac{u_{j+1}^n - u_{j-1}^{n+1}}{2\Delta x} = 0$$

or

$$(I - \frac{c\Delta t}{2\Delta x}E^{-1})u_j^{n+1} = (I - \frac{c\Delta t}{2\Delta x}E)u_j^n, \quad \text{where } u_{j+1} = Eu_j.$$

Fourier transformation gives

$$(1 - \frac{c\Delta t}{2\Delta x}e^{-i\omega h})\hat{u}_j^{n+1} = (1 - \frac{c\Delta t}{2\Delta x}e^{i\omega h})\hat{u}_n. \tag{1}$$

so that the amplification factor $|z| = \left|\frac{\hat{u}^{n+1}}{\hat{u}^n}\right|$ is

$$|z| = \left|\frac{1 - \frac{c\Delta t}{2\Delta x}e^{i\omega h}}{1 - \frac{c\Delta t}{2\Delta x}e^{-i\omega h}}\right| = 1. \tag{2}$$

The method appears to be unconditionally stable according to this modal or von Neumann analysis.

In Eulerian formulations, the convection equation is nonlinear.

$$u_t + uu_x = 0.$$

This equation needs entropy information so viscosity is added

$$u_t + uu_x = \epsilon u_{xx},$$

to eliminate expansion shocks. Numerically, viscosity gives thickness to shocks and permits stable algorithms. Jameson[1] advocates the use of an artificial viscosity which gives a shock thickness proportional to meshwidth: this implies that $\epsilon u_{xx} = \nu_2 \Delta x\, u_{xx}$. Away from the shock, he switches to a

fourth derivative artificial viscosity, $\nu_4 \Delta x^3 u_{xxxx}$, to remove high frequency error components from the numerical solution. Being of third order in Δx, this term cannot contaminate our second order spatial discretization. Both artificial viscosity terms vanish as the mesh is refined.

$$u_t + uu_x - \nu_2 \Delta x u_{xx} + \nu_4 \Delta x^3 u_{xxxx} = 0,$$

and the equation describing the original physics is recovered.

The necessary inclusion of viscosity, real or artificial, couples with convection to destabilize the locally implicit method.

The basic one point locally implicit method has a von Neumann stability criterion of the form

$$C \geq -2 + \alpha V$$

where the signed Courant Number, $C = c\frac{\Delta t}{\Delta x}$, and $V = (\nu_2 + \nu_4)\frac{\Delta t}{\Delta x}$. In aerodynamics, stability problems will occur in this basic method because of the negative characteristic velocities arising in subsonic and transonic calculations.

To see the reasoning in the special case,

$$u_t + cu_x - \nu \Delta x u_{xx} = 0,$$

consider

$$u_j^{n+1} = u_j^n - \frac{C}{2}(u_{j+1}^n - u_{j-1}^{n+1}) + V(u_{j+1}^n + u_{j-1}^{n+1} - 2u_j^{n+1}).$$

Fourier transformation gives, when $h = \Delta x$,

$$z = \frac{1 - \frac{C}{2}e^{i\omega h} + Ve^{i\omega h}}{1 - \frac{C}{2}e^{-i\omega h} + V(2 - e^{-i\omega h})}$$
$$= \frac{(1 - \frac{C}{2}\cos\omega h + V\cos\omega h) + i(-\frac{C}{2}\sin\omega h + V\sin\omega h)}{1 - \frac{C}{2}\cos\omega h + V(2 - \cos\omega h)) + i(\frac{C}{2}\sin\omega h + V\sin\omega h)}.$$

The amplification factor, $|z|$, is not greater than one if and only if

$$(1 - \frac{C}{2}\cos\omega h + V(2 - \cos\omega h))^2 + (\frac{C}{2}\sin\omega h + V\sin\omega h)^2 \geq$$

$$(1 - \frac{C}{2}\cos\omega h + V\cos\omega h)^2 + (-\frac{C}{2}\sin\omega h + V\sin\omega h)^2,$$

which, for $V > 0$, simplifies to

$$C \geq -2 + \alpha V \tag{3}$$

where $\alpha = -2$. Notice that for the highest frequency, $\omega h = \pi$, the denominator of z is

$$1 - \frac{C}{2}e^{-i\pi} + V(2 - e^{-i\pi}) = 0,$$

which vanishes when $\alpha = -6$, and unbounded amplification occurs.

A variety of approximations for the viscous term are possible. For $0 \leq \theta \leq 1$,

$$u_j^{n+1} = u_j^n - \frac{C}{2}(u_{j+1}^n + u_{j-1}^{n+1} - 2(\theta u_j^n + (1 - \theta)u_j^{n+1}))$$

has the same stability criterion but with

$$\alpha = \begin{cases} \text{positive.} & \text{for } \theta < \frac{1}{2} \\ \text{zero.} & \text{for } \theta = \frac{1}{2} \\ \text{negative.} & \text{for } \theta > \frac{1}{2} \end{cases}.$$

Unfortunately, simple computations with the basic method for, say, $C = +2$, fail miserably. Another explanation is necessary; the notion of group velocity must be introduced. A complete explanation can be found in Vichnevetsky and Bowles[3] or Trefethen[2].

Briefly, the group velocity, $v*$, is function of frequency and is the velocity with which the Fourier component of that frequency is observed to travel. This is not to be confused with the phase velocity, $c*$, which is not observable. Components of differing frequencies and phase velocities interact in the phenomenon called beating to give the observed group velocity.

The group velocity is computed from z as follows.

$$z = Re\, z + i\, Im\, z$$

$$\text{Arg}\, z = \tan^{-1}\left(\frac{Im\, z}{Re\, z}\right)$$

$$\text{phase velocity, } c* = -\frac{\text{Arg}\, z}{\omega \Delta t}$$

$$= -\frac{c\, \text{Arg}\, z}{C\, \omega h}.$$

where the Courant Number, $C = \frac{c\Delta t}{h}$, and c is the true characteristic velocity for the partial differential equation. Then,

$$\text{group velocity, } v* = \frac{d}{d\omega}(\omega c*).$$

Using $z = \frac{\hat{u}^{n+1}}{\hat{u}^n}$ from equation [1] gives

$$\text{Arg}\, z = \tan^{-1}\left(\frac{-C\sin\omega h + \frac{C^2}{4}\sin 2\omega h}{1 - C\cos\omega h + \frac{C^2}{4}\cos 2\omega h}\right).$$

In the special case, $C = 2$,

$$\text{Arg}\, z = \tan^{-1}\left(\frac{-2\sin\omega h(1-\cos\omega h)}{-2\cos\omega h(1-\cos\omega h)}\right) = \omega h.$$

$$c* = \frac{-c\text{Arg}\, z}{C\omega h} = -\frac{c}{2},$$

$$c* = \frac{d}{d\omega}(\omega c*) = -\frac{c}{2}.$$

This indicates that at a Courant Number of 2, components of all frequencies travel in the wrong direction at half their proper speed. This is confirmed numerically. The pulse which should have moved four units to the right, moves instead 2 units to the left.

This is not unusual. Many popular, common schemes exhibit this property at high frequencies. It causes unwanted reflections at boundaries and GKS instability. Artificial viscosity is commonly used to control it.

What is unusual in this case is that all components, both low and high frequencies, travel in the wrong direction for $C = 2$. Artificial viscosity is effective only for controlling high frequencies.

In summary, if viscosity is small, the amplification factor can be unbounded for $C < -2$. The group velocity of the important low frequency

components is reversed if $C \geq 2$. Thus, the locally implicit method in its basic form is stable only if $|C| < 2$.

The modified equation is another way of providing the preceding analysis. When the basic locally implicit method is applied to

$$u_t + cu_x - \nu_2 \Delta x\, u_{xx} + \nu_4 \Delta x^3\, u_{xxxx} = 0. \tag{4}$$

the equation actually solved is the modified equation,

$$(1+\frac{\Delta t}{\Delta x}(-\frac{c}{2}+\nu_2+3\nu_4))u_t+cu_x-\nu_2 \Delta x\, u_{xx}+\nu_4 \Delta x_3\, u_{xxxx} = O(\Delta x+\Delta t).$$

where the right hand side vanishes as the mesh is refined for a given Courant Number. The modified equation is derived by replacing each of the finite difference approximations by its Taylor expansion and collecting terms.

If viscosity is negligible, the equation resembles

$$u_t + \frac{c}{1-\frac{c\Delta t}{2\Delta x}} u_x = 0.$$

Observe that it represents a flow which reverses direction when $\frac{c\Delta t}{2\Delta x} = 1$, that is, when $C = 2$. This agrees with the group velocity analysis.

The viscous portion,

$$u_t - \nu_2 \Delta x\, u_{xx} = 0.$$

is unstable if the time coordinate is reversed. For $\Delta t < 0$, the coefficient $1 + \frac{\Delta t}{\Delta x}(-\frac{c}{2})$ changes sign when $\frac{c|\Delta t|}{2\Delta x} = -1$, or $C = -2$, which coincides with the unbounded amplification predicted by the modal analysis.

4. Artificial Viscosity Method. The traditional quick and dirty remedy for unstable methods is artificial viscosity. Examination of the modified equation shows how the additional viscosity stabilizes the basic ($\theta = 1$) locally implicit method, at least in the low frequencies. The leading coefficient,

$$1 + \frac{\Delta t}{\Delta x}(-\frac{c}{2} + \nu_2 + 3\nu_4).$$

should be positive in order that the group velocities remain positive for low frequencies. This gives the restriction.

$$C \leq 2(1 + \frac{\Delta t}{\Delta x}(\nu_2 + 3\nu_4)).$$

Reversing the sign on the viscosity term gives an indicator for behavior of the amplification factor for the critical low frequencies.

$$C \leq -2(1 + \frac{\Delta t}{\Delta x}(\nu_2 + 3\nu_4)).$$

which agrees with formula [3] derived by modal analysis. Therefore, the addition of artificial viscosity stabilizes the locally implicit method, if $\theta = 1$, for

$$|C| \leq 2(1 + \frac{\Delta t}{\Delta x}(\nu_2 + 3\nu_4)).$$

For general values of θ, one obtains

$$|C| \leq 2(1 + \frac{\Delta t}{\Delta x}(2\theta - 1)(\nu_2 + 3\nu_4)).$$

so that, for $\theta = \frac{1}{2}$, artificial viscosity has no stabilizing effect, and for $\theta < \frac{1}{2}$, it has a destabilizing effect.

5. Modified Equation Method. If, using the basic locally implicit method, we attempt to solve

$$p u_t + c u_x - \nu_2 \Delta x\, u_{xx} + \nu_4 \Delta x^3\, u_{xxxx} = 0, \tag{5}$$

for some p, we get instead the solution of

$$(p + \frac{\Delta t}{\Delta x}(-\frac{c}{2} + \nu_2 + 3\nu_4))u_t + c u_x - \nu_2 \Delta x\, u_{xx} + \nu_4 \Delta x^3\, u_{xxxx} = O(\Delta x - \Delta t).$$

Wanting the leading coefficient to be one, we solve for p,

$$p = 1 - \frac{\Delta t}{\Delta x}(-\frac{c}{2} + \nu_2 + 3\nu_4),$$

or with general θ,

$$p = 1 - \frac{\Delta t}{\Delta x}(-\frac{c}{2} + (2\theta - 1)(\nu_2 + 3\nu_4)).$$

Discretization of equation [5] with this particular p leads to the solution of the original equation [4] by a method which is automatically stable if only the lower frequencies are considered. Problems at higher frequencies can be handled by a combination of multigrid and artificial viscosity.

6. Modified Equation Method with Alternate Marching. The modified equation method has desirable amplification factors for positive

Courant Numbers and desirable group velocities for negative Courant Numbers. Therefore, following a forward sweep by a backward sweep

$$u_j^{n+1} = u_j^n - \frac{C}{2}(u_{j+1}^{n+1} - u_{j-1}^n) + V(u_{j+1}^{n+1} + u_{j-1}^n - 2u_j^{n+1})$$

has the effect of providing a superior overall method. Use of $\theta = \frac{1}{2}$ rather than 1 appears to give identical results.

Incidentally, referring back to the basic method, alternate marching failed to be effective at large Courant Numbers because of the unbounded amplification factor for $C \leq -2$. These instabilities are too large to be damped during the alternate sweep.

7. Interpretation of Tables. Appended are tables containing amplification factors and group velocities for each of the four methods. Throughout, $\theta = 1$ was used. In each table, the left column is the signed Courant Number, $C = \frac{c\Delta t}{\Delta x}$, and the other columns contain values tabulated for $\omega h = j\pi/3$, $j = 0, 1, \ldots, 3$. In each case, the equation

$$u_t + cu_x - \nu_2 \Delta x\, u_{xx} = 0$$

is discretized. If $\nu_2 = 0$, equation [2] shows that the amplification factor is always one. So $\nu_2 = 0.01|c|$ is used to show which components are amplified and which are attenuated. In the artificial viscosity method, however, ν_2 must be quite large, and a value of $\nu_2 = 0.5|c|$ is used for that case only.

Likewise, it would be desirable for group velocities to be one, or as large as possible, for all components. This is impossible except for high order methods such as spectral methods. Negative group velocities denote components which move in the wrong direction; these are present in all non-dissipative schemes. They cause spurious reflections at boundaries, shocks, and grid interfaces and thereby foster GKS instability. If the group velocity is negative for the critical low frequencies, the algorithm will certainly fail. Group velocities which are small in magnitude cause convergence to be slow; these error components move slowly. If the component lies in the upper half of the frequency range, it can easily be removed by artificial viscosity. If it lies in the lower half of the frequency range, multigrid is about the only method for removing it quickly. Multigrid converts the low frequency on a fine grid to a high frequency on a coarse grid.

BASIC METHOD: Observe that the amplification factor is no greater than one for $-2 \leq C$. The group velocity of the lowest frequency is non-negative for $C < 2$. Hence, the Courant Number restriction $|C| < 2$ is appropriate.

ARTIFICIAL VISCOSITY METHOD: The leading coefficient in the modified equation is made one for $|c| > 0$ by choosing $\nu_2 = |\frac{c}{2}|$. In the lowest frequencies, this makes the group velocity one for $C > 0$, and positive

for all Courant Numbers. No amplification factors are greater than one. Furthermore, sufficient dissipation exists at those frequencies and Courant Numbers where the group velocity is zero, to make the method converge reasonably. In practice, this method performed well in conjunction with the basic method. The artificial viscosity method was used with a large Courant Number to obtain coarse convergence; then, the Courant Number was reduced to one, and the viscosity was reduced to that of the original problem to achieve convergence.

MODIFIED EQUATION METHOD: This method was implemented to give the leading coefficient in the modified equation the value one. So, the group velocity for the lowest frequency is always one. The profile of group velocities resembles that of the artificial viscosity method. Unfortunately, the profile of the amplification factor does not; there is no dissipation to remove the stagnant group velocities. Convergence is expected to be slow and probably should be accelerated by a multigrid scheme. In fact, this was the experience of Jacocks and Reddy in their 2D locally implicit Euler solver.

MODIFIED EQUATION METHOD WITH ALTERNATE MARCHING: This substantially reduces the variation in amplification factors over all the preceding methods and creates an essentially non-dissipative algo-

rithm. Furthermore, there are no zero group velocities in the lower frequencies or at large Courant Numbers. Therefore, its convergence is rapid; this was tested in a 1D nonlinear scheme.

The presence of negative group velocities, which exist only at small Courant Numbers in the upper half of the frequency range, properly reflect the fact that this scheme must resemble a central difference scheme as $\Delta t \to 0$.

8. Conclusions and Recommendations. The locally implicit method in its basic form is only stable for those Courant Numbers whose absolute value is less than two. A number of variations exist which remove the Courant Number limitation.

The best of these variations alternates the direction of marching. In most circumstances, it will have no negative group velocities.

In higher dimensions, the absence of negative group velocities eliminates stability problems. This follows because a velocity vector is resolved and propagated by its directional components, none of which can have a negative group velocity.

For systems of equations, linear stability is guaranteed if the modified equation is adjusted for the largest characteristic velocity in the system.

Time accuracy may be lost, but when steady-state solutions are sought,

everything is gained. This method permits large Courant Numbers, but it is not implicit. It no longer requires the generation of structured grids or the use of approximate factorization. It is a perfect algorithm for the inexpensive, new parallel computers.

It has tremendous potential for aerodynamics applications. It should be capable of matching the speed of existing Euler solvers. More importantly, it should provide a speed increase for Navier-Stokes solvers.

References

1. Jameson, Antony. "Solution of the Euler Equations for Two Dimensional Transonic Flow by a Multigrid Method," Applied Mathematics and Computation, 13 (1983) 327-355.

2. Trefethen, Lloyd. "Group Velocity in Finite Difference Schemes," SIAM Review, 24 (1982) 113-136.

3. Vichnevetsky,R. and Bowles,J. "Fourier Analysis of Numerical Approximations of Hyperbolic Equations," SIAM 1982.

1986 USAF-UES SUMMER FACULTY RESEARCH PROGRAM/
GRADUATE STUDENT SUMMER SUPPORT PROGRAM

Sponsored by the

AIR FORCE OFFICE OF SCIENTIFIC RESEARCH

Conducted by

UNIVERSAL ENERGY SYSTEMS, INC.

FINAL REPORT

PROCEDURES FOR EFFICIENTLY EXTRACTING THE KNOWLEDGE OF EXPERTS

Prepared by: Robert R. Hoffman, Ph.D.

Academic Rank: Associate Professor of Experimental Psychology

Department and

University: Department of Psychology

Adelphi University

Garden City, NY 11530 (516) 663-1055

Research Location: Electronic Systems Division

Strategic Planning Directorate

Deputy for Development Plans

Hanscom AFB, MA 01731

USAF Researcher: Gary M. Grann, ESD/XR

Date: August 11, 1986

Contract No.: F49620-85-C-0013

PROCEDURES FOR EFFICIENTLY EXTRACTING THE KNOWLEDGE OF EXPERTS

Robert R. Hoffman

ABSTRACT

The first step in the development of an artificial intelligence "expert system" is the extraction and characterization of the knowledge and skills of experts. This step is widely regarded as the major bottleneck in the system development process. In previous work (Hoffman, 1984) I analyzed a number of methods for extracting experts' knowledge. The present report summarizes an analysis of another method, the "unstructured interview" method. I also compare the various methods in terms of their overall efficiency at generating propositional information for a data base. I conclude with a recommmended series of steps for extracting experts' knowledge, steps that should apply to any expert system development project.

ACKNOWLEDGMENTS

I would like to acknowledge the support of the U.S. Air Force Systems Command, the U.S. Air Force Office of Scientific Research, the Summer Faculty Research Program, and the Deputy for Development Plans of the Electronic Systems Division of the U.S. Air Force. I would like to thank Gary M. Grann, Lt Col John Whitcomb, 2Lt Joseph Besselman, 2Lt Ray Harris, Capt Thomas Moran, and Capt Jeffrey Valiton, all of the Strategic Planning Directorate of the ESD, and Murray Daniels of the Strategic PLanning Division of the MITRE Corporation, for their help and support. Thanks are also due to Rodney Darrah and the people at Universal Energy Systems, Inc. for their expertise at managing the Summer Faculty Research Program. I would especially like to thank 2Lt Joseph Besselman for his support as I conducted this research project, and for his helpful comments on earlier versions of this Final Report.

I. INTRODUCTION

Modern artificial intelligence (AI) systems are often called "expert systems" since they rely on characterizations of the knowledge and skills of experts. What the experts in a given domain know is codified in a knowledge base, and the knowledge base is used in the inference-making component of an AI system. Examples of such systems are DENDRAL (Duda and Shortliffe, 1983), which generates descriptions of chemical compounds on the basis of spectrographic data, and the "Pilot's Associate" system being developed by the Air Force (Stefik, 1985) (for a good general survey of expert systems work, see Bramer [1982], Buchanan [1986], Coombs [1984], or Weiss and Kulikowski [1984]).

It is widely recognized in expert systems research that the process of extracting the knowledge of experts is the primary bottleneck in the system development process (cf. Duda and Shortliffe, 1983, p.265). It can take many months of the expert's and the system builder's time to extract and characterize the knowledge that goes into an expert system, and yet, experts' knowledge must be extracted before one can complete the programs. There has apparently been no systematic or programmatic research on the question of how to extract the knowledge of experts (Duda and Shortliffe, 1983; Hartley, 1981; Gilmore, personal communication).

My work falls at this nuts-and-bolts level of the development of expert systems. As a cognitive psychologist, I am interested in applying the research methods of experimental psychology to the domain of expert systems engineering. The overall goal of my research is to develop general methods for extracting and characterizing the knowledge of experts, with an eye toward making the system development process as efficient as possible.

II. OBJECTIVES OF THE RESEARCH EFFORT

The work I report on here is an extension of my earlier work (Hoffman, 1984) in which I analyzed certain methods for extracting experts' knowledge. In this report I analyze another method, what I call "unstructured interviews." The various methods for extracting experts' knowledge are briefly described in Table 1. For full details on the various methods, see Hoffman (1986).

TABLE 1

Various methods for extracting the knowledge of experts.

METHOD	DESCRIPTION AND PURPOSE
ANALYSIS OF "FAMILIAR" TASKS	Analysis of the tasks that the expert usually performs. Includes analysis of available texts and technical manuals. Facts and rules are written out in the form of propositions. A categorized list of the propositions constitutes a "first-pass" data base.
UNSTRUCTURED INTERVIEWS	The expert is queried with regard to his knowledge of facts, rules, etc., and with regard to user needs and system design (e.g., the kinds of screen faces that would be helpful).
STRUCTURED INTERVIEWS	The expert goes over the first-pass data base, making comments on each entry. The result is a "second-pass" data base, in a format ready for inputting into the computer.
LIMITED INFORMATION TASKS	A familiar task is performed, but the expert is not given certain information that is usually available. Lack of information encourages strategic thinking (e.g., "What if . . . . ").
CONSTRAINED PROCESSING TASKS	A familiar task is performed, but the expert must do so under constraints. For example, the task may have to be performed within a limited amount of time. Another example involves running the expert at a simulation of the familiar task using archived data. At any point during the task, the expert can be stopped and queried with regard to knowledge or reasoning strategy.
THE METHOD OF "TOUGH CASES"	A familiar task is performed for a set of data that presents a "tough case." The expert's ruminations over a tough case can generate evidence about refined reasoning strategies.

In my previous work I analyzed the efficiency of all the methods with the exception of unstructured interviews. As I will show in this report, having now analyzed the unstructured interview method I can answer a key question:

What steps should be taken to extract and characterize the knowledge of experts for any expert system project?

My answer to this question should be of interest to anyone who is working on an expert system or who is planning such a system. This includes the the burgeoning AI research efforts of the U.S. Air Force and other branches of the Department of Defense.

III. APPROACH TAKEN

The work to be reported here was conducted in the context of a project that was aimed at developing an expert system to assist Military Airlift Command (MAC) planners as they design plans for airlift operations. The Knowledge-based Systems Office of the Strategic Planning Directorate (XR) of the Electronic Systems Division (ESD) was in the beginning stages of developing an expert system to augment MAC planners' abilities in the use of FLOGEN, an Automatic Data Processing System that is one part of the Integrated Military Airlift Planning System (MAC, 1985). It was at that point that I joined the project.

With FLOGEN, expert MAC planners develop plans for airlift operations in both crisis and deliberate planning. Available to FLOGEN is a great deal of stored information (e.g., information about the range,

speed, and cargo preferences of different types of aircraft; information about the ramp space and cargo handling capabilities of various airfields). FLOGEN accepts as input information about the logistical considerations involved in a particular operation (e.g., cargo priorities, available-for-loading dates, origins and destinations, need for refueling stops, etc.). Plans that are developed using FLOGEN need to meet a number of criteria: To maximize the tonnage shipped, to maximize the tonnage arriving on time, to maximize the flying time per aircraft, to minimize scheduling conflicts, etc.

AI techniques should apply well to the FLOGEN-based planning process. Some reasons for this applicability are:

(1) The use of FLOGEN requires considerable expertise.

(2) The use of FLOGEN involves a large number of variables and facts---hundreds of different bases, scores of different types of aircraft, etc. The plan reports that stem from FLOGEN fill volumes.

(3) After their many years of experience, the MAC planners have developed many personalized heuristics ("rules of thumb") for dealing with the details and problems that are encountered during FLOGEN-based planning.

(4) The procedures that are followed during FLOGEN-based planning are only partially described in the available documentation. The FLOGEN User's Manual (MAC, 1985) has chapters that define the fields that appear in various screens, chapters that define the various files and acronyms, and chapters that define the various command codes. Nowhere in its 400 pages does their appear a significant explanation of what the planners do.

It would seem prudent to attempt to extract and characterize the knowledge of the experts, in order to form the basis for an expert system for assisting MAC planners in the FLOGEN-based planning process.

METHOD

The method used was quite straight-forward. Individuals from the MITRE Strategic Decision Aids Group spent a week engaged in unstructured interviews of the expert MAC planners. The interviews resulted in over ten hours of audio taped interviews. The interviewers and the experts were all naive with regard to my ruminations about research methodology, making the tapes an ideal source of data for my analysis of the efficiency of the unstructured interview method.

Basically, what I did was to transcribe the interviews and then analyze the transcriptions for their propositional content. The transcription process involved listening to the interviews (over headphones) on a small tape recorder and typing the dialog into a word processor. (for details on the preparation of a verbal protocol, see Ericcson and Simon, 1984; and Hoffman, 1986). An example exerpt from the transcripts appears in Table 2. This exerpt is prototypical in that it includes queries from the interviewer, speech hesitations and errors, unintelligible segments, and monologs by the expert. The monologs in this exerpt are all brief; occasionally they can be a page or more in length.

TABLE 2

Example exerpt from the unstructured interviews.

I: What information are you given about airports?

E: Now just some rudimentary information comes with it. Common name, latitude and longitude, ah . . . no information comes with it about the ah . . . maximum number of airplanes on the ground or the port capability that is at the field. None of that comes along with it.

I: What's the difference between MOG and airport capability?

E: Ah . . . MOG maximum on the ground is parking spots . . . on the ramp. Airport capability is how many passengers and tons of cargo per day it can handle at the facilities.

I: Throughput . . . ah . . . throughput as a function of . . .

E: It all sorta goes together as throughput. If you've only got . . . if you can only have ah . . . if you've only got one parking ramp with with the ability to handle 10,000 tons a day, then your . . . your throughput is gonna be limited by your parking ramp. Or, the problem could be vice versa.

I: Yeah . . .

E: So it's a [unintelligible phrase].

I: What if you only had one loader, so that you could only unload one wide-body airplane at a time? You wouldn't want to schedule five airplanes on the ground simultaneously. How would you restrict that?

E: We know we're not gonna get all the error out of it. We're gonna try and minimize the error. And then we'll say that . . . ah . . . we'll say an arrival-departure interval of one hour, so that means that the probability of having two wide-bodies on the ground tryin' to get support from the loader is cut . . .

The process of recoding the transcripts into propositions was also straight-forward (for details, see Hoffman, 1984 or 1986). An example proposition contained in the Table 2 exerpt is:

"MOG STANDS FOR MAXIMUM NUMBER OF AIRCRAFT ALLOWED ON THE GROUND."

This would be an example of a potential fact to be incorporated into the data base. The transcripts also included potential rules. An example of a rule, one that appears in the Table 2 exerpt, would be:

"IF YOU NEED TO RESTRICT THE NUMBER OF AIRPLANES ON THE GROUND AT A STATION, THEN MANIUPLATE THE ARRIVAL-DEPARTURE INTERVAL."

Other example propositions gleaned from the transcripts are:

"OVERSIZED CARGO IS LARGER THAN A PALLET BUT WILL FIT ON A C-130 OR A C-141."

"IF CARGO IS SHORTFALLED, THEN FLOGEN FLAGS IT WITH AN EXPLANATION OF WHY THE CARGO DID NOT MOVE."

"INFORMATION ABOUT STATIONS IS AUTOMATICALLY ACCESSED BY FLOGEN FROM A PARAMETRIC FILE."

"IF CARGO CANNOT BE MOVED, THEN THE USER MUST MAKE ADJUSTMENTS IN THE TIME-PHASED FORCE DEPLOYMENT DATA FILE."

"AIRCRAFT CANNOT REFUEL FOLLOWING OFFLOAD IN GERMANY AND MUST RECOVER TO ENGLAND."

IV. RESULTS

The ten hours of unstructured interviews resulted in 510 pages of transcript. The coded transcripts contained a total of 529 proposition facts and 224 proposition rules. They contained a total of 957 questions questions asked by the Interviewers.

In order to compute the efficiency with which the unstructured interview generated propositional data, one must first compute the total time it took to derive the propositions. This includes the total interview time (10 hours), plus the time to prepare the transcripts (77 hours), plus the time to code for propositional content (13 hours). Thus, the total task time for these unstructured interviews was 100 hours. This figure could then be divided into the total number of propositions obtained (753), yielding an overall efficiency rate of 0.13 propositions per total task minute. Another metric of efficiency is to see how many propositions were generated, on the average, for each question asked by the interviewer. For the present results, this figure is 0.79.

The question to be asked now is, How do these data compare with those from other tasks that can be used to extract experts' knowledge? Detailed figures for the other tasks can be found in Hoffman (1984, 1986), Basically, structured interviews, constrained processing and limited information tasks have been found to yield between one and three propositions per task minute. Thus, the results of the present research indicate that unstructured interviews are an inefficient method for extracting experts' knowledge.

V. RECOMMENDATIONS

I have a few recommendations to make, some having to do with interviews, some having to do with methods and methodology in general.

Unstructured interviews are a good way for the knowledge engineer to familiarize himself with the domain, but should not be conducted prior

to an analysis of familiar tasks (analysis of available texts and technical manuals and preparation of a first-pass data base). Unstructured interviews are a good way to learn about user needs and to generate ideas about system design (such as screen faces that would be helpful). Unstructured interviews are not an efficient way of generating propositional data for a data base---the transcription process is simply too time-consuming. Indeed, unstructured intervews need not be tape recorded at all---shorthand notes should suffice.

The first step in conducting a structured interview is to prepare a preliminary data base by analyzing available texts and technical manuals. The data base would consist of propositions of the kind exemplified earlier in this Report, organized into meaningful or functional categories. In the actual structured interview, the expert goes over the data base, one proposition at a time, commenting on each one. In essence, the structured interview forces the expert to go systematically over their knowledge. The structured interview method is a good way of generating propositional data data for a knowledge base, especially since it does not require tape recordings and transcriptions.

Detailed information and advice on how to conduct both structured and unstructured interviews is presented in Hoffman (1986).

Given the results of the present work, I can now answer the key question:

What steps should be taken to extract and characterize the knowledge of experts for any expert system project?

My answer can be found in Table 3 in the form of a general procedure for the development of an expert system.

TABLE 3

Steps to be followed in extracting and characterizing the knowledge of experts prior to the construction of an expert system. The activity designated "Special tasks" includes limited information tasks, constrained processing tasks and analyses of "tough cases."

STEP	ACTIVITY	PURPOSE	EFFORT REQUIRED
1.	Analysis of Familiar Tasks	Familiarizes the knowledge engineer with the domain. Yields information for the first-pass data base.	One man-month.
2.	(Optional) Unstructured Interviews	Familiarizes the knowledge engineer with the domain. Yields information for the first-pass data base. Helps in determining user needs and system design.	One to two man-weeks.
3.	Preparation of First-pass data base.		One man-month or more.
4.	(Optional) Unstructured Interviews	Familiarizes the knowledge engineer with the domain. Yields information for the second-pass data base. Helps in determining user needs and system design.	One to two man-weeks.
5.	Structured Interviews	Yields information for the second-pass data base.	One to two man-weeks.
6.	Preparation of second-pass data-base		Two man-weeks or more.
7.	Special tasks	Yields refinements of the data base.	Variable.

All domains of expertise differ, so too do all expert systems projects. Different methods will be best suited to different domains. There are probably situations for which the recommended series of steps is not quite fitting. However, some variation on this theme should fit. A good example is the airlift planning project itself. The system developers began with an unstructured interview. That was the only way to get the project off the ground since the available technical manuals provided little information about what the experts actually do. Hence, an attempt to generate a data base at the outset would not have been very fruitful.

The figures in Table 3 for "effort required" are, of course, only approximations based on my experiences. According to my estimates, one can expect it to take at least three months to get to the point of having a refined or second-pass data base. How does this compare with the experiences of other AI researchers? It is impossible to tell from a reading of the expert systems literature exactly how much effort went into building the data base in any expert system project. (It is for that reason that I feel compelled to present my own estimates.) Typically, authors do not even state precisely how the knowledge was gotten---sometimes from texts and manuals, sometimes from archived data, and usually from unstructured interviews. Typically, research reportsjump right into a discussion of system architecture.

Some discussions of expert system projects state how long it took to develop a prototype, but one can only guess how long it took to build the knowledge base. The development of MYCIN (Davis, Buchanan &

Shortliffe, 1977), a system for diagnosing infectious diseases, took many years. The development of INTERNIST, also a medical diagnosis system, took ten years with the help of a full-time specialist in internal medicine (Buchanan, 1982). R1, which configures the VAX computer (McDermott, 1980), took two man-years to develop by a team of about a dozen researchers, and is still being refined today. In general, it takes one to two man-years to develop a prototype, and about five man-years to develop a full system (Duda and Shortliffe, 1983; Gevarter, 1985).

In contrast, the PUFF system for the diagnosis of pulmonary disorders was reported to have been developed in less than ten weeks (Bramer, 1982). One reason for this is that most of the rules were easily gleaned from archived data (Feigenbaum, 1977), and only one week was spent interviewing the experts (Bramer, 1982).

Apparently, if one is relying on unstructured interviews, or if one is interviewing a large number of experts (as in the MYCIN project), or if the system requires hundreds or thousands of rules and facts in its data base (as in the INTERNIST system), then many years of effort are required to develop a system to the prototype stage. In this light, a minimum of three months just to get to the stage of having a refined data base does not seem unreasonable. If anything, it is an underestimate, but it is probably not a gross underestimate. The knowledge base of the aerial photo interpretation project (Hoffman, 1984) consisted of over a thousand entries, and it took just a few months to develop by means of structured interviews.

I recommend that expert system researchers routinely report data on the methods used to extract experts' knowledge, the efficiency of the methods, and the amount of effort taken to construct the knowledge base.

One final recommendation is in order. I feel that the research reported here (see also Hoffman, 1986) "wraps up" this aspect of expert systems research. No further methodological research is needed. Enough is now known about methods for extracting the knowledge of experts to permit anyone who is interested in developing an expert system to generate reasonably efficient methods for extracting the experts' knowledge. For any given expert systems project, methods will have to be devised, and that will take some research and development effort. However, at the level of methodology (the comparative analysis of various methods), the picture seems fairly clear.

REFERENCES

Bramer, M.A. (1982) A survey and critical review of expert systems research. In D. Michie (Ed.) Introductory readings in expert systems. London, England: Gordon and Breach Science Publishers.

Buchanan, B.G. (1982) New research on expert systems. In J. Hayes, D. Michie & Y-H. Pao (Eds.) Machine intelligence 10, New York, NY: John Wiley and Sons, Inc.

Buchanan, B.G. (1986) Expert systems: Working systems and the research literature. Expert Systems, 3, 32-51.

Coombs, M.J. (Ed.) (1984) Developments in expert systems. New York, NY: Academic Press.

Davis, R., Buchanan, B.G. & Shortliffe, E.H. (1977) Production systems as a representation for a knowledge-based consultation program. Artificial Intelligence, 8, 15-45.

Duda, R.O. & Shortliffe, E.H. (1983) Expert systems research. Science, 220, 261-276.

Ericcson, K.A. & Simon, H.A. (1984) Protocol analysis: Verbal reports as data. Cambridge, MA: The MIT Press.

Feigenbaum, E.A. (1977) The art of AI. Procedings of the fifth international joint conference on AI. Cambridge, MA: International Joint Conferences on AI.

Gevarter, W.B. (1984) Artificial intelligence computer vision and natural language processing. Park Ridge, NJ: Noyes Publications.

Gilmore, J. (1986) Personal communication. Georgia Technical Research Institute, Atlanta, GA.

Hartley, R. (1981) How expert should expert systems be? Procedings of the seventh international joint conference on AI. Vancouver, BC: International Joint Conferences on AI.

Hoffman, R.R. (1984) Methodological preliminaries to the development of an expert system for aerial photo interpretation. Report No. ETL-0342, Engineer Topographic Laboratories, Ft. Belvior, VA.

Hoffman, R.R. (1986) The problem of extracting the knowledge of experts from the perspective of experimental psychology. The AI Magazine, in press.

McDermott, J. (1980) R1: A rule-based configurer of computer systems. Technical Report, Computer Science Department, Carnegie-Mellon University, Pittsburgh, PA.

Military Airlift Command (1985) User's Manual for FLOGEN. MACR 171-189.1, Volume II (H). Scott AFB, IL: Headquarters Military Airlift Command.

Stefik, M. (1985) Strategic computing at DARPA. Communications of the ACM, 28, 690-704.

Weiss, S. & Kulikowski, C. (1984) A practical guide to designing expert systems. Totowa, NJ: Rowman and Allanheld Publishers.

1986 USAF-UES SUMMER FACULTY RESEARCH PROGRAM/

GRADUATE STUDENT SUMMER SUPPORT PROGRAM

Sponsored by the

AIR FORCE OFFICE OF SCIENTIFIC RESEARCH

Conducted by the

Universal Energy Systems, Inc.

FINAL REPORT

FLUORESCENT DYE BINDING ANALYSIS

FOR THE

IDENTIFICATION OF ASBESTOS

Prepared by:	Cliff Houk, Ph.D.
Academic Rank:	Professor
Department and University:	Department of Health Sciences (Industrial Hygiene) Ohio University Athens, Ohio
Research Location:	USAF Occupational and Environmental Health Laboratory (USAFOEHL) Analytical Services Division Environmental Chemistry Branch
USAF Researcher:	Ken Roberson, Chief Asbestos and Particle Analysis
Date:	29 August 1986
Contract No.:	F49620-85-C-0013

FLUORESCENT DYE BINDING ANALYSIS

FOR THE

IDENTIFICATION OF ASBESTOS

by

CLIFF HOUK

ABSTRACT

The fluorescent dye binding properties of several organic dyes for the identification of asbestos in bulk samples and on membrane filters were studied and compared to previously reported results. Five dyes, Morin, chromotropic acid, Clayton-Yellow, 8-hydroxyquinoline and Bathocuproine exhibited easily detected fluorescence on bulk samples containing chrysotile asbestos. Fluorescence microscopy data suggests that Morin and Clayton-Yellow bind to other forms of asbestos that may be found on membrane filters from personal or area sampling at work sites. These dyes do not bind to other substances commonly found in building materials.

Preliminary methods using these dyes for the analysis of bulk samples and membrane filters from personal or area air samples are presented. Extended research is necessary in both areas.

ACKNOWLEDGMENTS

I thank the Air Force Systems Command and the Air Force Office of Scientific Research for sponsorship of my research. In order for research to be meaningful it must be done in an intellectually stimulating environment. The USAFOEHL, Brooks AFB, provided such an environment. I would like to thank several members of the USAFOEHL staff for their assistance and guidance:

Col James Rock

Col Jerry Thomas

Mr Tom Thomas

Capt Ray Nakasone

Ms Doris Tessmer

Mr Joe Hillsberry

Extra special thanks are extended to the members of the USAFOEHL/SA asbestos section and particle analysis section.

Ken Roberson

Jo Jean Mullen

Russell Lundy

for their patience and willingness to answer my questions and teach me the skills necessary to move the research forward. Their teaching was most effective and the frequent open discussions provided valuable insights into the problems associated with asbestos identification.

Finally, I would like to thank my wife, Evelyn, for her willingness to relocate, to be separated from her children and grandson, and for her encouragement and support throughout the summer.

The USAFOEHL at Brooks AFB must have efficient methods to perform the analysis of bulk materials for asbestos content and the identification of fibers on membrane filters submitted to the laboratory (10,000 in 1985 and 15,000 projected for 1986). The need for such methods is evidenced by the increased concern for the health and safety of Air Force personnel, their families and its contractors who may be exposed to asbestos in the performance of their duties. Asbestos is a known carcinogen and considerable effort has been made to develop rapid, accurate methods of detection and identification. Commercial field test kits for bulk sample analysis have been developed but are inaccurate and unreliable.

Field personnel often ask, "Are the fibers present on the air filter asbestos?". The current method of analysis for air samples allows the analyst to only count the fibers per unit area on the filter which is converted to fibers per cubic centimeter of air sampled.

I. INTRODUCTION:

I earned my Ph.D. in inorganic chemistry emphasizing synthesis and characterization of transition metal complex compounds. X-ray diffraction and UV-VIS spectrophotometric methods of analysis were used to characterize the compounds produced. In 1980, I earned a MS in Environmental Health with an industrial hygiene emphasis. Part of my training involved the sizing and counting of particulates and fibers on personal and area membrane filters using light microscopy (LM), polarized light microscopy (PLM) and phase contrast microscopy (PCM). Since that time my research interests have been directed towards environmental-occupational health problems. I have been involved in the formation of a private environmental analytical services laboratory and am familiar

with the problems associated with field sample analysis and data control.

The research problem at the USAFOEHL involved the identification of asbestos fibers on membrane filters using a fluorescent dye-binding method suggested in the literature (1). What dyes fluoresce in the UV-VIS region of the electromagnetic spectrum when bound to asbestos? Can a method be developed that would be feasible for the identification and counting of fibers on membrane filters?

This problem, therefore involved methods I was familiar with and had interest in pursuing at a professional research level. Because of this interest I was assigned to investigate the problem at the USAFOEHL.

II. STATEMENT OF OBJECTIVES:

1. To determine the feasibility of using a procedure described by F. A. Albright, et al, (1) for the identification of asbestos on membrane filters and in bulk materials.

2. To develop specific fluorescent dye binding analytical methods for amosite, anthophyllyte, crocidolite, and other forms of asbestos.

The overall goal of the research was to develop compound specific analytical methods for the rapid identification of all forms of asbestos on membrane filters and in bulk materials.

III. REVIEW OF THE LITERATURE:

Prior to arrival at Brooks AFB Toxline, Medline and NIOSH data base systems were searched for appropriate references. Upon arrival, ACS Chemical Abstracts, Wiley Catalog On-Line and Enviroline systems were searched by the USAFOEHL library staff. Only two articles pertinent to the research were found (1,2). The original article by F. R. Albright, et al that prompted the research proposal dealt primarily with bulk

sample analysis (1). An earlier article by Italian researchers B. Sperduto, F. Burragato and A. Altieri discussed the use of fluorescent dyes as a means to identify asbestos fibers on membrane filters and to differentiate between different forms of asbestos (2). Several dyes were investigated but both groups settled on Morin as the best to use. It was specific for chrysotile and produced a visible orange-yellow fluorescence when exposed to long wave-length ultraviolet radiation. As my research progressed it became evident that the dye was probably forming a chelate with the magnesium in the chrysotile and the binding was pH dependent. Additionally, the structure and functionality of the dye appeared to be critical. With the structure of Morin in mind and the need for a conjugated system within the chelate to produce fluorescence, standard reference materials and additional journal references were examined to determine what indicators have been used for the qualitative analysis of Mg^{+2} and Fe^{+2} and other forms of asbestos (3-7).

IV. RESULTS - BULK SAMPLE FLUORESCENCE ANALYSIS:

Several dyes were tested at three different pH levels with five different forms of asbestos to determine the binding and fluorescent properties of each dye. The results for Canadian Chrysotile and Rhodesian Chrysotile are given in Table I. Based upon these data bulk samples submitted to the USAFOEHL for analysis were split for simultaneous analysis by PLM and fluorescent dye binding with Morin and Clayton-Yellow at pH 11. Results of these analyses are given in Table II. The data indicates 97/113 correct identifications with Morin as the dye and 68/70 correct identifications with Clayton-Yellow. Chromotropic acid fluorescence is difficult to discern with long wave length UV

Table I

Dyes Tested For Binding Affinity

to Chrysotile Asbestos

Dye Tested	Description of Fluorescence		
	pH2	pH7	pH11
A. Functionally Acidic			
Alizarin	N	N	N
Alizarin Red-S	N	N	N
1-amino-2-naphthol-4-sulfonic acid	N	N	N
Aluminon	N	N	N
Carmine	N	N	N
Chromotropic Acid	N	N	S (Blue)
Clayton-Yellow	N	W (Org.-Yellow)	S (Red)
Cresol-Red	N	N	N
Eosin Y	N	N	W (Org.-Yellow)
Eriochrome Black T	N	N	N
Fuschin A	N	N	N
Fuschin B	N	N	N
8-hydroxyquinoline	N	W (Mint Green)	S (Mint Green)
Morin	W	W	S (Org.-Yellow)
B. Functionally Neutral			
Bathocuproine	S (Blue)	N	N
1,5 Diphenylcarbohydrazide	N	N	N
Eriochrome Cyanin R	N	N	N
1,10 Phenanthroline	N	N	N
Quinalidine Red	N	N	N

N = No fluorescence W = Weak S = Strong

TABLE II

Split Sample Analysis

SAMPLE CONTENTS

	Chrysotile	Amphiboles	No Asbestos	False +	False -
PLM	29	17	67	NA	NA
Morin	21+	17-	59-	8	8
PLM	30	4	36	NA	NA
C-Y	28+	4-	36-	0	2

+ = Positive fluorescence

- = No fluorescence

NA = Not applicable

light. It was dropped from further study. Bathocuproine and 8-hydroxyquinoline exhibit very distinctive light blue and mint green fluorescence respectively with chrysotile. However, they were introduced late in the study and warrant continued investigation because preliminary tests indicated they both appear to bind to other forms of asbestos used during this study.

Other substances commonly found in building materials and environmental samples were present in the bulk samples completed during the split analyses. Table III lists those materials and others that do not interfere with Morin and Clayton-Yellow fluorescence.

V. RESULTS - MICROSCOPIC MEMBRANE FILTER FLUORESCENCE ANALYSIS:

Early work on this part of the problem was stymied by two major problems: a calibrated incandescent lamp was not available for the microscope and the computer operating the monochromator on the microscope was malfunctioning. The temperature of the lamp at specific voltages must be known so a black body correction may be made to subtract the fluorescence characteristics of the microscope's optics, slide, cover slip, mounting media and dye from the observed fluorescence of the specimen. A check of the literature suggested 3300 K would be a likely temperature for the lamp in question and the monochromator was operated manually. Initial spectra were obtained from slides with 1%, 0.1%, 0.01%, 0.001% and 0.0001% weight/weight (w/w) dispersions of the five forms of asbestos with Morin as the dye. The results were encouraging in that clearly identifiable fluorescence peaks were recorded in the orange-yellow region as expected for chrysotile. However, other forms of asbestos also produced spectra with contrasting identifiable bands. These data, however, are unacceptable as the monochromator

TABLE III

Noninterfering Materials

	Morin	Clayton-Yellow
Cement	N	N
Polyethylene	N	N
Muscavito mica	N	N
Mineral wool	N	N
Cellulose	N	N
Gypsum	N	N
Fiber glass	N	N
Cotton	N	N
Clay	N	N
Plaster	N	N
Kevlar	N	N
Rust Corrosion Preventative (Na_2SiO_4)	N	N
Vermiculite	N	N
Quartz	N	N
Diatomaceous Earth	N	N
Kaolin	N	N
Talk	N	N
Wood	N	Y
Potassium Titanate	Y (Bright)	N
Cotton	N	Y

and computer became totally inoperable. The monochromator and computer were repaired (twice) and the calibrated bulbs arrived so 1 drop of the 0.1%, 0.01%, 0.001% and 0.0001% w/w dispersions were mounted with Morin and Clayton-Yellow dyes as separate sets. The spectra from the Clayton-Yellow set were much easier to interpret and more reproducible than those with Morin so Clayton-Yellow became the dye of choice for further study. Table IV lists the characteristic absorption bands for the dispersions under investigation. It appears that chrysotile and amosite bind Clayton-Yellow and fluoresce in the red region. Anthophyllyte and crocidolite do not fluoresce strongly in the red region but do in the violet region.

Air samples arrive at USAFOHEL on cellulose membrane filters so 1 mL of the 0.01% w/w dispersions were diluted to 100 mL with distilled water and filtered through standard cellulose acetate, 37 mm, 0.8 u filters and dried over silica gel overnight. A wedge was cut from each filter, mounted with 1 drop of Clayton-Yellow in the media, allowed to clear and spectra obtained. Table V lists the characteristic absorption bands obtained from these filtered dispersions. These data suggest that all forms studied fluoresce in the red region and the filter does not interfere with the identification. The ethanol washed filters tended to curl and wrinkle making them more difficult to mount. The washing apparently had no effect upon the nature of the fluorescence so that step was eliminated from use. Filters containing substances found in environmental samples were prepared in the same manner and spectra of mounted wedges were obtained. The spectra contain multiple fluorescence bands and shoulders that require extended interpretation but it is obvious that considerable research is required for the development of the method.

TABLE IV

Fluorescence Bands of Various

Forms of Asbestos with Clayton-Yellow

Type	% w/w	Bands (nm)
CC	0.1	610-620 sh, 660 s
	0.01	610-620 sh, 640 s
	0.001	640 s, 670 s
	0.0001	610-620 sh, 660 s
RC	0.1	610-620 sh, 670 s
	0.01	610-620 sh, 650 s
	0.001	610-620 sh, 660 s
	0.0001	660 s
AMO	0.1	430 s, 640 w, 670 m
	0.01	410 s, 630-640 sh, 670 w
	0.001	430 w, 600 m, 630 m, 670 s
	0.0001	430 w, 630 m, 670 s
ANTHO	0.1	410 s, 650 m, 680 w
	0.01	470 s, 650 m
CROC	0.1	480 s, 670 w
	0.01	470 s

CC = Canadian chrysotile

RC = Rhodesian chrysotile

AMO = Amosite

ANTHO = Anthophyllyte

CROC = Crocidolite

s = strong

m = moderate

w = weak

sh = shoulder

TABLE V

Fluorescence Bands of Asbestos

on Membrane Filters with Clayton-Yellow

Type	Bands
CC	670 vs
CC-ET	610-620 sh, 660-670 sh, 680 vs
CC_2	680 vs
CC_2-ET	610-620 sh, 670 s
RC	610-620 sh, 660 s, 680 vs
RC-ET	610-620 sh, 660-670 sh, 690 s
AMO	610-620 sh, 670 s
AMO-ET	590-600 sh, 620-630 sh, 670 s
CROC	550-560 sh, 610-620 sh, 670 vs
CROC-ET	610-620 sh, 660 s
ANTHO	590-600 sh, 630-640 sh, 670 s
ANTHO-ET	700 s

ET = Filter washed with 10 mL ethyl alcohol

^{2} = 100 mL dispersion brought to pH 11 before filtering

vs = Very strong

Selected spectra are included as examples of the graphics display and data presentation of the instrument package. Copies of all pertinent spectra are on file at the USAFOEHL along with copies of my laboratory notebook pages.

VI. CONCLUSIONS:

These preliminary data indicate that Clayton-Yellow is a suitable dye for the fluorescence identification of chrysotile in bulk samples and on cellulose acetate filters. Bulk samples containing as little as 1-5% chrysotile within several different matrices were identified correctly by visual observation. Clayton-Yellow appears to bind to other forms of asbestos not evident through visual examination but readily observed microscopically. Other dyes, Morin, chromotropic acid, 8-hydroxyquinoline and Bathocuproine, may be suitable but additional research is required.

Both techniques show promise for use by the USAFOEHL personnel as the procedures are refined. The bulk sample analysis by USAF field personnel could reduce the number of samples submitted to the USAFOEHL by 20-25%, therefore, reducing the number of samples that must be sent to contract laboratories.

VII. RECOMMENDATIONS:

1. Additional research be completed to refine, improve and simplify the bulk analysis procedure leading to the development of a field test kit suitable for accurate, rapid identification of asbestos.

2. Continued refinement and development of the microscopic technique under normal phase contrast counting conditions.

3. Additional research with Morin, 8-hydroxyquinoline, Bathocuproine and other dyes to determine their usefulness as fluorescent indicators.

4. Include other forms of asbestos, actinolite and tremolite, in these studies.

5. Investigate the kinetics of the binding between asbestos and various dyes. Does the binding increase with time? Does the level or intensity of the fluorescence increase as binding increases? Is the fluorescence quantitative? Can it be used to determine % asbestos in a sample?

6. Institute a program of research for the development of easier, less costly methods of identification of actinolite and tremolite, commonly found in ceramic and talc materials.

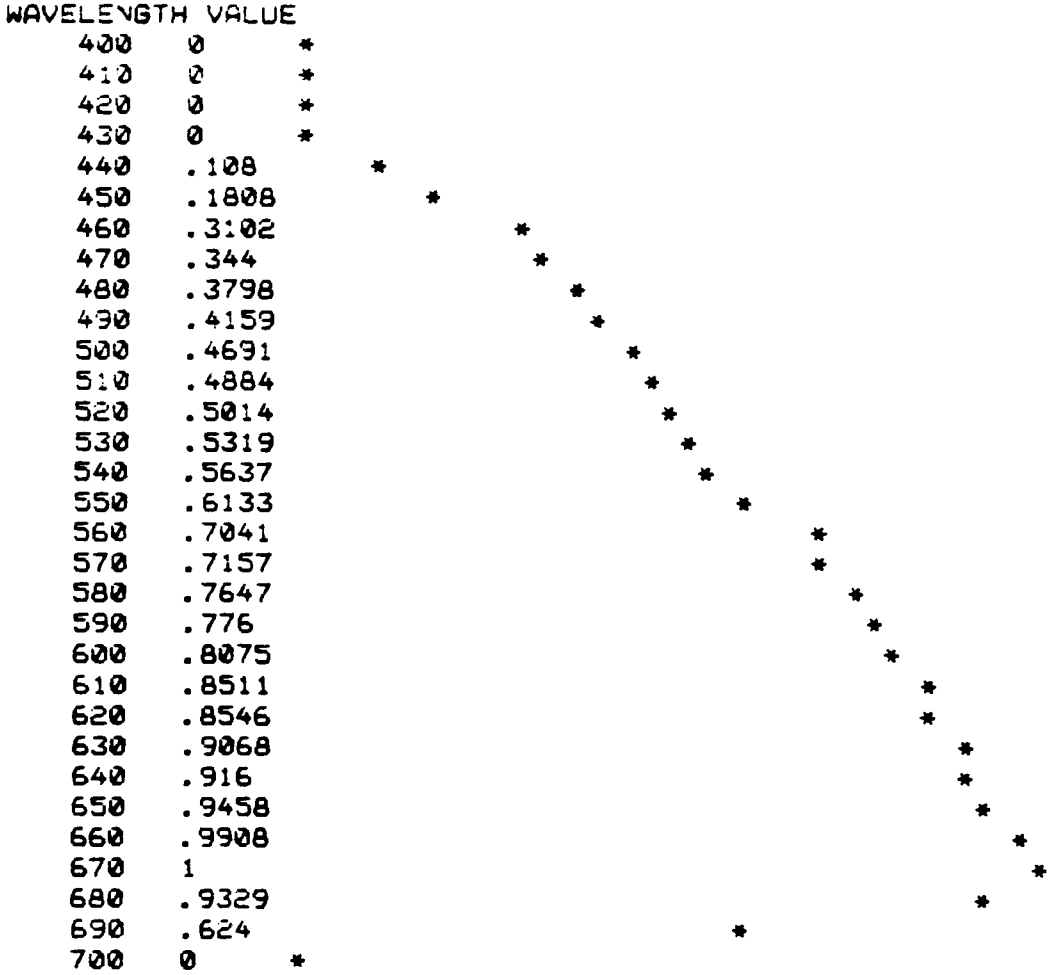

Fig. 1 Canadian Chrysotile Clayton-Yellow Dye Fluorescence (Emission)

WAVELENGTH	VALUE
400	1
410	1
420	1
430	1
440	.8205
450	.8219
460	.7204
470	.674
480	.6273
490	.6033
500	.5748
510	.5415
520	.4961
530	.4791
540	.4585
550	.4507
560	.4151
570	.4254
580	.3463
590	.3295
600	.308
610	.2257
620	.211
630	.1758
640	.1566
650	.0837
660	0
670	.0427
680	2.7E-03
690	.1776
700	.5597

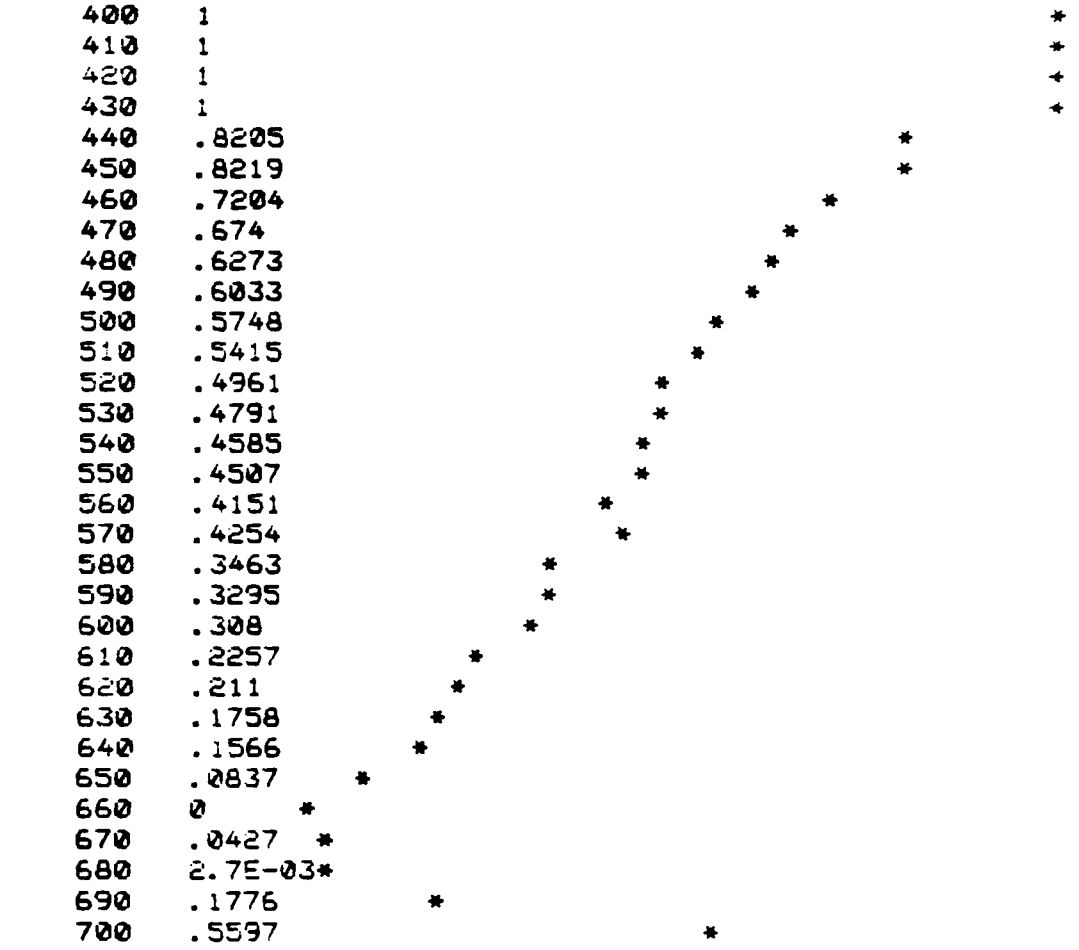

Fig. 2 Rhodesian Chrysotile Clayton-Yellow Dye Fluorescence (Absorbance)

EXPERIMENTAL

Bulk Analysis

1. 10 mg or less of sample
2. Grind to maximize surface area
3. Place in 4 inch disposable plastic test tube
4. Add 1 mL of pH 11 buffer
5. Shake, mix, allow to stand 10 minutes
6. Centrifuge, decant buffer
7. Add 1 mL, 95% ethanol to residue
8. Shake, mix, centrifuge
9. Decant ethanol, leave no liquid behind
10. Expose residue to long wavelength UV light against a black background
11. Observe fluorescence

Microscopic Analysis

1. Cut two wedges from membrane filter
2. Mount one wedge (a) per normal USAFOEHL procedure for phase contrast counting (background slide)
3. Mount second wedge (b) with 1 drop dye added to mounting media before placing wedge in media on the slide (Specimen Slide).
4. Mount a blank filter wedge (c) with one drop of dye (Channel A background)
5. Place slide c on stage, focus, hit key A, follow directions on screen. When "scan complete" appears:
6. Hit key U, uncorrected spectrum appears on screen.
7. Hit key B, read instructions, enter lamp temperature as directed, blackbody calculations will be made, blackbody curve will appear on

screen and corrected curve will appear on the screen. This data will be entered automatically and "subtracted" as background from specimen spectrum.

8. Place slide b on stage, locate and focus on specimen fiber, select channel 1, hit A key, follow screen instructions, remove slide when "scan complete" appears.
9. Place slide a on stage, hit key C, hit key B, Channel 1B should appear beside Channel, locate and focus on specimen fiber, hit key A, follow instructions, remove slide from stage.
10. Hit key G, hit key A or T (your choice), hit key Y, hit key P, hit key 4, hit return key, correct specimen fluorescence spectrum will be printed.
11. Hit SEL tab on printer, hit form advance, remove spectra, hit SEL on printer.
12. Repeat steps 8-11 for additional samples to a maximum of 5. Once all 5 channels available are used and spectra printed channels 1-5 and 1B-5B must be cleared or saved to allow for further analyses.

REFERENCES

1. Albright, F.R., D.V. Schumacher, B.J. Feltz and J.A. O'Donnell, "A Fluorescent Dye Binding Technique For Detection of Chrysotile Asbestos," Microscope, 30 (1982) 267-280.
2. Sperduto, B., F. Burragato, A. Altieri and M. Gasperetti, "I minerali dell asbestos: loro riconoscimento e determinazione," Ann. Ist. Super. Sanita 13 (1977) 127-136 (In Italian). Translated through the Technical Services Division, School of Aerospace Medicine, Brooks AFB, TX.
3. Welcher, F.J. (Ed.), Standard Methods of Chemical Analysis, 6th Ed., Van Nostrand, Princeton N.J., 1963.
4. White, C.E., Y. Argauer, Fluorescence Analysis, Dekker, New York, 1970.
5. Sandell, E.B., Colorimetric Determination of Trace Metals, 2nd ed., Interscience Publ. Ltd., London, 1950.
6. Windholz, M., (Ed.), The Merck Index, 10th ed., Merck and Co., Rahway, N.J., 1983.
7. Vaughn, N.P., S.J. Rooker and J.M.M. LeGuen, "In situ Identification of Asbestos Fibers Collected on Membrane Filters for Counting," Ann. Occup. Hyg., 24 No. 3 (1981) 281-290.

1986 USAF-UES SUMMER FACULTY RESEARCH PROGRAM/

GRADUATE STUDENT SUMMER SUPPORT PROGRAM

Sponsored by the

AIR FORCE OFFICE OF SCIENTIFIC RESEARCH

conducted by the

Universal Energy Systems, Inc.

FINAL REPORT

Thrust Computing System

Prepared by:	Ming-Shing Hung
Academic Rank:	Associate Professor
Department and University:	Department of Administrative Sciences Kent State University
Research Location:	Directorate of Management Sciences, HQ Air Force Logistics Command
USAF Researcher:	Mr. Victor Presutti, Jr.
Date:	August 20, 1986
Contract No:	F49620-85-C-0013

Thrust Computing System

by

Ming-Shing Hung

ABSTRACT

A new model for analyzing the TCS data set was formulated and executed. The results indicate that engines behave differently from one trim to another. They also show that the data set is unstable, highly sensitive to small changes in some data items and deletions of some items. These observations cast doubt on the ability to use the results to help set the trim, both installed, using TCS, and uninstalled, under the current procedure. Therefore, it is recommended that explanation for such engine behavior be pursued first, before the issue of whether to use TCS can be settled.

ACKNOWLEDGMENTS

I would like to thank the Air Force Systems Command and the Air Force Office of Scientific Research for sponsorship of this research. The Directorate of Management Sciences at the Headquarters of the Air Force Logistics Command has provided friendly and continuous support. In particular, I would like to thank Mr. Victor Presutti, Jr. and Lt. Col. Michael Lacey for involving me in the TCS project. Fred Rexroad has been very helpful with showing me how to use the various computer systems. Major Ronald Stokes has stimulated my interest in the Aircraft Availability Model.

I. INTRODUCTION

I have been teaching and conducting research in Operations Research for the past 13 years. The courses I have taught include statistics, applied probability theory, mathematical programming and computer simulation. Most of my research has been in the computer implementation of mathematical programming methods. I have been interested in logistics management. A few of my publications are related to that. That is why I applied for a research appointment in the Directorate of Management Sciences of the Air Force Logistics Command.

This project involves data analysis, which is a part of statistics. My experience in using computer software helps in the execution of this research.

II. OBJECTIVES OF THE RESEARCH EFFORT

Aircraft engines are "trimmed" after maintenance has been done to insure they can produce sufficient thrust. Dynamic thrust, that is, thrust during takeoff, is the quantity of interest. Since it is unavailable, surrogate measures have been used to help trim the engine. The current procedure trims an engine in a test cell, off the aircraft, and sets the "uninstalled" thrust to a "nomograph" level. That level is a function of compressor inlet temperature (CIT). The nomograph thrust level for the J85-5 engine (for T-38A aircraft), which is the engine used in this study, is 2680 lb at 59° F of CIT. A

significant amount of thrust is lost when the engine is installed on the aircraft (13 to 24 percent for J85-5), due primarily to the air inlet. The engine is then operated for up to 600 hours before it is removed and retrimmed.

Computing Devices Company (COMDEV) has developed a Thrust Computing System (TCS) which measures the thrust of an engine after it is installed. TCS will allow engines to be trimmed when they are installed and, COMDEV claims, at a lower EGT than the current method. An engine running at lower EGT will last longer and thus save money for the USAF. In order to evaluate the claim, it is necessary to determine the thrust level to which an engine should be trimmed, both installed and uninstalled.

A study was conducted in 1982 to measure static thrust levels of J85-5 engines. Uninstalled static thrust readings were taken in the test cell. After an engine was installed, more readings were taken using TCS. Henceforth at roughly every 50 flying hours, thrust levels were measured again by TCS. 19 engines were involved in the study which resulted in 51 streams of observations, each stream corresponding to a sequence of readings between engine trims (after maintenance had been accomplished on the engine).

The main question to be evaluated from data analysis was: How is the loss of thrust related to changes in CIT and flying hours? The loss of thrust according to raising CIT is called the "lapse rate" and that according to flying hours is the "degradation rate". Engineering data support the existence of

these rates. The remaining questions are: What is the functional form relating the variables and what are the values of the degradation and lapse rates?

III. PAST STUDIES

COMDEV performed linear regression analyses on the data set. Each of the 51 streams of observations was fitted to the following equation:

$$(1) \qquad y = b_0 + b_1 h + b_2 t + e$$

where

y : thrust = current thrust;
h : flying hours;
t : difference in CIT = current reading - reading at trim;
b_0 : Intercept, loss of thrust due to installation;
b_1 : Degradation rate;
b_2 : Lapse rate;
e : Error of regression estimate.

The major reason that 51 streams were separated for regression analysis was the claim by COMDEV that each engine behaves differently and, in fact, each engine behaves differently from on trim to another. Their results [Ref. 1] seem to support the claim. The degradation rates range from 1.46 lb/hr (positive value indicates that the engine gains thrust per hour of flying) to -1.33 and the lapse rates from -1.44 to -7.66 lb/$^{\circ}$ F.

The dilemma with the position that engines behave differently from one trim to another is: How does one use the results to set the trim for an arbitrary engine, or, for that matter, an engine that was recently trimmed?

COMDEV resorted to fitting another regression line through the different degradation rates. First, "short streams", those whose maximum time since overhaul (TSO) was less than 150 hours, were removed from the data set since their degradation rates were at both the high and the low ends of the range. The remaining 33 degradation rates were fitted against each stream's maximum TSO on a simple regression function. This resulted in a "mean" degradation rate of -.21 lb/hr with a standard error of .23 lb/hr. (2 x standard error has been used as the "95%" confidence band and is called the "spread".)

ARINC, a consultant to the USAF, criticized the "regression on regression" approach of COMDEV. It instead recommended taking a weighted sum of the degradation rates. The weight used was the number of observations of each stream times the R^2, the coefficient of determination [Ref. 2].

The above two reports performed analysis on segregated data and thus they can not test, statistically, whether the differences in the regression coefficients b_1 and b_2 are systematic or merely due to random variations of a sampling process.

The Directorate of Management Sciences at the headquarters of the Air Force Logistics Command (AFLC/XRS) "pooled" the data into one set and performed multiple linear regressions similar to equation (1). The main difference is that there were two equations, one for y = current thrust - uninstalled thrust (denoted as $M_f - C_i$) and the other for y = current thrust - first installed thrust at 0 flying hours ($M_f - M_i$). The first one measures thrust

from the time of uninstalled trim and thus can be used to help set the uninstalled trim level. The second one begins with the first installed reading and thus can be used to help set the installed trim. In order for the models to be comparable, data streams without M_i readings available were deleted, which resulted in 34 streams remaining. The results from the regression analyses were quite different from those of COMDEV's, with degradation rates equal to -.114 for M_f-C_i and -.104 for M_f-M_i, and lapse rates at -5.42 and -5.02, respectively. The coefficients of determination R^2 were .763 and .735, and the standard errors of estimate were 63.6 and 63.5, respectively for M_f-C_i and M_f-M_i [Ref. 3].

Dr. Barr of the Air Force Institute of Technology was asked to evaluate the modeling differences. He suggested a more comprehensive model that uses the pooled data but is capable of taking different streams into consideration. The model uses indicator variables to designate different streams. When the interaction terms are also included, each stream can have different degradation and lapse rates [Ref. 4]. Details will be given below.

IV. THE APPROACH

The model I use is the same as Dr. Barr's and can be written,

$$y = b_0 + b_1 h + b_2 t + b_3 s + b_4 sh + b_5 st + e \qquad (2)$$

where

s : a categorical variable designating individual streams;
sh : interaction between streams and flying hours;
st : interaction between streams and changing CIT.

The categorical variable has no intrinsic numeric meaning. It can be set to 1 for stream 1 and 2 for stream 2, etc. or A for

stream 1 and B for stream 2. The first three terms in (2) are the regression coefficients for a base stream (say, the last one). For each other stream, the coefficient b_3 will have to be added to b_0 to get the actual intercept for the stream. Similarly, the coefficient b_4 of a stream will have to be added to b_2 to get the actual degradation rate, and b_5 added to b_3 for the actual lapse rate.

The regression coefficients one gets from (2) for each stream are the same as those one would get by fitting regression function (1) on the stream by itself. The choice of the base stream is immaterial. There are two major advantages of Model (2), however. The first one is that (2) provides one standard error of estimate which is more precise than the individual errors from (1). Therefore, statistical inferences based on (2) are more reliable. The second advantage is that general results, pertaining to the overall contribution of individual variables (h,t,s,sh,st) to the explanation of loss of thrust, are only available from (2). This is also called an "Analysis of Covariance" model [Ref. 5]. The only possible difficulty with this model is computational. Some statistical software may not be able to handle the categorical variable and the interaction variables. However, large packages like SAS do have this capability. Examples for how to interpret the model are given in the following results section.

V. RESULTS

1. All Streams

The XRS data set was used in the analysis. The computer program used was Procedure GLM (General Linear Model) of SAS [Ref. 6]. Both $M_f - C_i$ and $M_f - M_i$ sets, each with 34 streams, were run using Model (2). The details are shown in Appendix 1 and 2. A summary is given in Table 1. The overall fit of Model (2) is the best among all models that have been tried so far. R^2 for $M_f - C_i$ is .952 and for $M_f - M_i$ is .922. That means that the model can explain 95.2% of the variation in the loss of uninstalled thrust and 92.2% of the installed thrust.

TABLE 1

	$M_f - C_i$	$M_f - M_i$
R^2, Coeff of Determination	.952	.922
Standard Error of Estimate	29.397	29.203
Prob (Model insignificant)	.0001	.0001
Prob (h insignificant)	.0001	.0001
Prob (t insignificant)	.0001	.0001
Prob (s insignificant)	.0001	.0001
Prob (sh insignificant)	.0001	.0001
Prob (st insignificant)	.0001	.0001

The probabilities in the table denote the probability that a variable contributes an insignificant amount of explanatory power to the variation of loss of thrust. As can be seen, every

variable definitely is important. (By the way, the value .0001 is the smallest that can be shown. So the actual probability can be a lot smaller.) So, not only does loss of thrust vary according to flying hours and change in CIT, but it also varies from one stream to another. COMDEV's position on this issue is justified.

The categorical variable s being significant means that the regression intercept does vary from one stream to another. For $M_f - C_i$, the intercept represents thrust loss due to installing the engine on the aircraft. For $M_f - M_i$, the intercept should be 0 since there is no installation loss but the statistics clearly show there is still some loss. From Appendix 1, where $M_f - C_i$ results are shown, column "ESTIMATE" contains the regression coefficients. The value -529.96 in row "INTERCEPT" is the intercept for the base stream, which is Stream 34. Then for Stream 1, the value -75.63 represents the difference between the intercept of Stream 1 and the intercept of Stream 34. Therefore, the intercept for Stream 1 is actually -529.96-75.63=-605.59. Similarly, the intercept for Stream 2 is -529.96+2.46=-527.50.

When we said the intercept varies from one stream to another, it does not mean that the intercept of Stream A is statistically different from that of Stream B. (A and B merely denote two different streams.) For comparisons between two intercepts, we can use the column "PR > |T|" which indicates the probability that the value on the same row is = 0. Since the value is the difference between the intercept of a stream and that of the base stream, the probability of its being 0 is the same probability for

the corresponding two intercepts being equal. Thus for Stream 1 the probability of .0001 indicates that there is little chance the intercept of Stream 1 is equal to that of Stream 34. Similarly, there is an 87.78% chance that the intercept of Stream 2 is equal to that of Stream 34.

Back to Table 1. The probability that interaction variable sh is insignificant being .0001 indicates that the degradation rates indeed vary from one stream to another. The way to interpret the degradation rates from Appendix 1 is similar to the intercepts. The value of -.314 in column "ESTIMATE" and row "HOURS" is the degradation rate for the base stream, Stream 34. The values in rows headed by "HOURS*STREAM" are the differences between the degradation rates of specific streams and that of Stream 34. For example, the degradation rate for Stream 1 is -.314+.117=-.197. A complete set of compiled values from the computer output is given on page 2 of Attachment A.

The degradation rates and lapse rates are different from those obtained by COMDEV (shown on page 1 of Attachment A). The major source for this discrepancy is the differences in data sets. There are some observations in the COMDEV data set that are not in the XRS data set and vice versa. A few data points that are common to both have different values, due to corrections in either set. Another source for the discrepancy is that COMDEV took the average of three successive observations whose readings were taken at about the same time. Therefore, COMDEV has only about a third of the data points available in the XRS set.

The details of $M_f - M_i$ are shown in Appendix 2. From the summary in Attachment A, one can see that except for intercept, the regression coefficients are quite close to those in $M_f - C_i$. This is to be expected.

For a summary view of the results, the means of the regression coefficients are compiled in Table 2 in the following. A word of caution is in order here. Since we have concluded that all regression coefficients are different from one stream to another and they were computed from streams of varying sample sizes and varying goodness of fit (as measured by R^2), the means should not be used as the sole representative values and can not be used in statistical inferences.

TABLE 2 : Average Statistics

	All Streams		Long Streams Only	
	$M_f - C_i$	$M_f - M_i$	$M_f - C_i$	$M_f - M_i$
Intercept	-563.27	-2.01	-563.47	-7.22
Degradation Rate	-.2413	-.2508	-.2767	-.2855
Lapse Rate	-4.2157	-4.1557	-3.8348	-3.8199

2. Long Streams Only

If one looks closely into the degradation rates on page 1 of Attachment A, it is possible to discern the same phenomenon observed by COMDEV; namely, the short streams tend to have degradation rates at both the high and the low ends of the range. It indicates that short streams, by having fewer observations, are more likely to have their regression coefficients influenced by

one or two extreme observations, called outliers. So I also removed the short streams, those whose maximum TSO is less than 146 hours. 146 hours is an arbitrary choice, but it is close to 150 hours and the two streams with 146 hours have enough observations to make them stable. The data set is accordingly reduced to 25 streams.

Model (2) was applied to the new data set and the results are given in Appendix 3. Individual regression coefficients are not shown there since they are identical to those in Appendix 1 and 2 for the same streams. (They are, however, shown on page 3 of Attachment 3 for easy reference.) The only difference is in the overall statistics. The coefficient of determination, R^2, for $M_f - C_i$ is now .950 and for $M_f - M_i$ is .915; indicating a small drop in the overall fit but the explanatory power of the model is still remarkably high. Again, all variables are significant. The streams are still as individualistic as ever. One interesting statistic deserves comment. As one compares the F value of variable "HOURS" for "TYPE III SS", it goes from 32.23 in Appendix 1 to 219.30 in Appendix 3 for $M_f - C_i$ and from 32.09 in Appendix 2 to 74.80 for $M_f - M_i$ in Appendix 3. Flying hours becomes more important as a predictor when the short streams are removed and i is more important for $M_f - C_i$. It means that if one uses the degradation rate to help set the trim, the estimate for uninstalled trim would be better than for the installed trim. But the degradation rates for the long streams average out higher than for all streams, as shown on Table 2.

3. Observations with Hours >= 146

XRS observed that there might not be any degradation in thrust after 150 hours of engine operation. In order to verify that, observations with flying hours less than 146 were removed from the data set and the remaining ones were fitted on Model (2). The results are given in Appendix 4 and 5 whereas the compiled regression coefficients are shown in Attachment A. A summary of Appendix 4 and 5 is given below.

The numbers paint a different picture than Table 1. They show that variable h (flying hours) is statistically insignificant as predictor for loss of thrust. The streams have become even more individualistic.

Table 3

	$M_f - C_i$	$M_f - M_i$
R^2	.967	.951
Standard Error of Estimate	29.22	29.22
Prob (Model insignificant)	.0001	.0001
Prob (h insignificant)	.7104	.7104
Prob (t insignificant)	.0001	.0001
Prob (s insignificant)	.0001	.0001
Prob (sh insignificant)	.0001	.0001
Prob (st insignificant)	.0001	.0001

The degradation rates and lapse rates of $M_f - C_i$ are identical to those of $M_f - M_i$, as seen on page 4 of Attachment A. The reason is that the two sets now contain exactly the same observations

after those below 146 hours have been deleted. (In the previous two subsections, the only difference between an $M_f - C_i$ stream and its corresponding $M_f - M_i$ stream was in the first zero-time installation reading, which the latter did not contain since it was designated as M_i.)

Comparing the regression coefficients in Attachment A, one sees large differences from the previous models for the same data streams. There are a few possible reasons. One is that engines behave differently after 150 hours. Another is that some streams have small number of observations and are thus sensitive to outliers. There is some justification for the former, if only from the point of view of numerical results. If one ignores the streams with few observations, say those whose flying hours did not go beyond 300 hours--which are #11,13,15,18,26,31 and 34--, there are still large differences in the regression coefficients in the remaining streams. Regardless of whether that makes sense from physical and engineering points of view, the differences reveal the instability of the data set.

VI. RECOMMENDATIONS

The TCS data set was analyzed using the Analysis of Covariance method. The results on the entire data set supported COMDEV's position that engines behave differently from on trim to another. Not only is the categorical variable s statistically significant, but the interaction variables sh and st are also significant. Thus each stream has a different intercept (which represents

installation loss for $M_f - C_i$ and zero-time variation for $M_f - M_i$) and different degradation and lapse rates.

The high R^2's indicate that linear functions are reasonable forms for relating loss of thrust to flying hours and changing CIT. Recently, COMDEV suggested degradation rates may be an exponential function of M_i, the first zero-time reading of installed thrust. Since M_i remains constant for one trim sequence, its effect would have already been included in the degradation rate for that stream, under Model (2).

The overall objective for the TCS project was to use the data to help set the trim. Since the intercept, degradation rate and lapse rate are all different from one trim to another, the objective does not seem possible, at this time. COMDEV's approach of fitting a regression line on the degradation rates lacks methodological justification. Their reason was that degradation rate varies with the maximum flying hour. Since degradation rate was obtained from regressing thrust loss on flying hours, regressing degradation rates on flying hours again is tantamount to saying that thrust loss is a quadratic function of flying hours. There is nothing wrong, mathematically speaking, about quadratic relationships, but the implication was apparently unexpected to COMDEV. Another problem with their approach is that it ignores the fact the degradation rates and lapse rates are mildly correlated ($r=-.4$ for long streams, using COMDEV results on page 1 of Attachment A). By overlooking this interaction between the two rates, the estimates based on degradation rates alone may be

biased.

There is little understanding on why engines behave the way as it was observed in the data. Only some general, qualitative explanations have been given so far. Repair and replacement of parts affect the engine performance. Removal and reinstallation of an engine, even without any other adjustments, seem to change the engine also. (In fact, some long data streams appear to have more removals and reinstallations than short streams, according to the latest COMDEV analysis of removal records. This may help explain why long streams have smaller variation in degradation rates, as shown in Figure 7 of Reference 1.)

It is important to find out the factors which contribute toward the thrust loss of an engine. Unless we can explain the loss in quantitative terms, we can not predict it and thus can not set the trim at optimal levels. By optimality, we mean the best operational efficiency of the aircraft for the required safety considerations. Therefore, this problem should be resolved first, ahead of the current issue of whether or not to implement TCS.

(Due to page limitation, Attachment A and Appendices 1-5 are not included in this report. A complete copy of the report is available in HQ AFLC/XRS, Wright-Patterson AFB, Ohio 45433.)

REFERENCES

1. "Engine Degradation Rate--Fleet Implementation of Thrust Computing System on J85-5 Engines Installed in T-38 Aircraft," Computing Devices Company Report PHOO/FR, August 1985.

2. "Evaluation of Report Entitled 'Engine Degradation Rate--Fleet Implementation of Thrust Computing System on J85-5 Engines Installed in T-38 Aircraft'," ARINC Research Corp Publication 2981-Ø1-TR-3665, June 1985.

3. "The TCS and Installed Static Thrust on the J85-5 Engine," AFLC/XRS, March 1986.

4. "Evaluation of Thrust Computing System Analysis," Dr. Barr, AFIT/ENC, Jan 1986.

5. J. Neter, W. Wasserman & M. Kutner, Applied Linear Statistical Models, 2nd ed., 1985, Irwin, Inc., Homewood, IL.

6. SAS User's Guide: Statistics, Version 5 Edition, SAS Institute Inc., Cary, NC, 1985.

1986 USAF-UES SUMMER FACULTY RESEARCH PROGRAM/GRADUATE STUDENT SUMMER SUPPORT PROGRAM

Sponsored by the

AIR FORCE OFFICE OF SCIENTIFIC RESEARCH

Conducted by the

UNIVERSAL ENERGY SYSTEMS, INC.

FINAL REPORT

Estimation and Discrimination Procedures for a New Measure of Maintainability/Reliability

Prepared by: J. Marcus Jobe

Academic Rank: Assistant Professor

Department and University: Department of Decision Sciences
Miami University
Oxford OH 45056

Research Location: Rome Air Development Center
Systems Reliability & Engineering Branch
Reliability & Maintainability Technologies Section
Griffiss AFB NY 13441-5700

USAF Research: Jerome Klion

Date: August 1, 1986

Contract No: F49620-85-C-0013

Estimation and Discrimination Procedures for a New Measure of Maintainability/Reliability

by

J. Marcus Jobe

ABSTRACT

The maintainability/reliability measure discussed in this report is referred to as MTUT. It corresponds to the average number of maintenance hours required per operating hour. This measure integrates maintenance and repair time expenditures of all types from three levels of maintenance. Other measures discussed in the literature commonly reflect just one of the following: operational readiness (availability), logistics and support burden, or system maintainability. MTUT logically incorporates the information from these three sources into a single coherent figure of merit. This report presents estimation and discrimination procedures for MTUT under various assumptions. It is assumed that all failure rates are constant throughout this report. This corresponds to interarrival times which have an exponential distribution. Large sample theory is used to construct both interval estimates and discrimination procedures for the MTUT parameter . A minor theorem stating a simple sufficient condition for the existence of a steady state availability is stated and proved. Recommendations concerning further work concludes the report.

ACKNOWLEDGEMENTS

I am grateful to the Air Force Systems Command, the Air Force Office of Scientific Research, and the Rome Air Development Center for the opportunity to participate in the 1986 Summer Faculty Research Program. I would especially like to express my appreciation to my RADC effort focal point Jerry Klion for his assistance in making the summer program a rewarding experience. Finally, I would like to thank my new friends at RADC/RBET for making the summer so pleasant.

I. Introduction

This report describes research that was conducted as a part of the 1986 AFOSR/UES Summer Faculty Research Program at Rome Air Development Center, Griffiss AFB, NY. The author is currently an assistant professor in the Department of Decision Sciences at Miami University in Oxford, Ohio. He received the Ph.D. degree in Statistics from Iowa State University in 1984. His main research areas are in applied reliability and Poisson process applications and theory. He has worked with Poisson process applications and theory since 1982. His Ph.D. thesis involved mathematical theory associated with Poisson process discrimination procedures. During the summer of 1985, he worked at General Motors Institute on applied reliability problems associated with the automobile industry. Specifically, the prediction of warranty times and miles for specific parts were studied.

The purpose of this research is the investigation of maintainability/reliability specification. Equipment which supports the operations of military and civilian interests must have the capability to consistently perform its intended tasks under various extreme conditions. Upon breakdown, the design of a piece of equipment partially determines the time necessary to restore the item to functional status. Since a short maintenance time for a given operating time is optimum, a measure of this quantity would be beneficial for both military and industrial concerns. How to encompass the rate of failure and repair time into a single measure is studied in this paper.

Common measures of maintainability/reliability consider only the first level of maintenance and the rate at which failures occur. The most common of these measures are availability (A), Mean Time To Repair (MTTR), and Mean Time Between Failure (MTBF). See references (2), (4), (5) for a detailed discussion. However, in the military or some large industrial plants, the maintenance on a failed part affects several levels of operation. Attempts to salvage the broken piece are made at each of several preassigned steps in a maintenance system. A measure of maintainability/reliability which takes into account the "ripple effect" on a maintenance system is considered in this paper. This measure is

referred to as the Mean Equipment Corrective Maintenance Time required to support a unit hour of operating time (MTUT). Reference (3) presents the rationale behind this measure.

II. Objectives

Generally, the goal of the research was to determine the form of appropriate estimators of the measure MTUT under various conditions. Similarly, the construction of appropriate discrimination procedures for MTUT under these same conditions was desired. The accomplishment of these goals would allow the military or large civilian industries to assess operating equipment in a more informative manner than is now being done. Also, added insight into the demonstration phase of a piece of equipment would be provided. Some specific goals of the research were as follows:

(a) Estimating and testing procedures for MTUT when the failure rates are assumed constant and known. It was hoped that an unbiased estimate of MTUT could be given as well as an unbiased estimate of variance for the MTUT estimator. Using these, an interval estimate of MTUT could be constructed with a degree of certainty associated with it. A simple testing procedure would follow. The failure rates would be determined from an engineering prediction model already in use.

(b) Estimating and testing procedures for MTUT when the failure rates are unknown. Another goal was to derive an interval estimate for MTUT when the failure rates were assumed unknown. This estimate would use only information from the data itself. It was hoped that an estimation and testing procedure could be derived for finite samples and large samples. The large sample conclusions would have to be used only in the assessment stage because of time constraints.

(c) Sufficient condition for steady state availability when failure rates and maintenance rates are not necessarily constant. Many situations arise where the assumption of a constant failure rate and a constant repair rate is not correct. A simple sufficient condition for steady state availability is derived.

III. MTUT and MTTR as Measures of Maintainability

MTTR is usually thought of by managers and engineers as a measure of maintainability design quality. Equipment or system MTTR for highly modularized equipment is represented as:

$$MTTR = \sum_{i=1}^{k} (\lambda_i/\lambda_T) M_{cti} \quad (1)$$

where

λ_i = the failure rate associated with the i^{th} removable or repairable item (module) of the equipment.

λ_T = total failure rate of the equipment.

Mct_i = the mean time required to repair/replace the i^{th} item (module) of the equipment which takes into account test system/troubleshooting protocol and execution times, access, spare retrieval, remove/replace alignment, checkout etc. times associated with i).

k = the number of failure modes.

Similarly, a simple expression for MTUT is

$$MTUT = \sum_{i=1}^{k} \lambda_i \; Mct_i \quad (2)$$

(the maintenance time required to support a unit hour of operating time).

It can be seen that MTTR is a weighted average of the mean times to repair/replace the failures from the k failure modes. It should be understood that Mct_i, not MTTR, is the average repair time for the i^{th} module. The measure MTUT is the mean equipment time spent in repair per hour of operation of the system. Both measures are dependent upon average time to repair for each of the k failure modes and the frequency with which

each part fails. If all Mct_i are held constant and all but a few of the λ_i's are kept at certain values, the remaining λ_i's may be adjusted so that the corresponding MTTR decreases but MTUT increases. Or the λ_i's may be adjusted in such a way that MTTR increases and MTUT decreases. This is mentioned to shed light on the interpretation of MTTR in comparison to MTUT. As previously pointed out, it is possible to have the MTTR decrease when the average maintenance burden (reflected by MTUT) increases. Hence, item A with a lower MTTR than item B is not necessarily a preferred selection. It very well could be that item B has the smaller maintenance burden. As can be seen, the application of MTTR as a general measure of maintainability can be misleading. This measure is a linear combination of average maintenance times. Each broken module should not be thought of as having the same average maintenance time. The equipment or system made up of the different modules has a specific mean time to repair (MTTR).

As pointed out in reference (3), MTUT is perhaps easier to understand by the engineer or manager. When only the first level of maintenance is considered, it is related to MTTR in the following manner:

$$\lambda_T \bullet MTTR = MTUT$$

or

$$MTTR = MTBF \bullet MTUT, \qquad (3)$$

where λ_T is the failure rate of the system or whole equipment piece. Thus, if any of the individual failure rates are increased with the average repair times fixed, MTUT will increase. Likewise, if any of the failure rates decrease and all average maintenance times remain fixed, MTUT will decrease. Another aspect of this measure is the fact that the maintenance support burden can be incorporated into it. Thus, MTUT can reflect the effect on the whole maintenance system, not just the initial level of restoration.

IV. Estimation and Testing for MTUT when λ_{ijl} known.

The measure MTUT incorporates information from organizational, intermediate, depot, and scheduled sources of maintenance. In this paper, scheduled maintenance times will not be considered. Therefore, the expression for MTUT will take on the following form:

$$MTUT = \sum_{i=1}^{k} \lambda_i Mct_i + \sum_{i=1}^{k} \lambda_i Mct_i^* + \sum_{i=1}^{k} \sum_{j=1}^{k_i} \lambda_{ij} Mct_{ij}$$

$$+ \sum_{i=1}^{k} \sum_{j=1}^{k_i} \sum_{l=1}^{k_{ij}} \lambda_{ijl} Mct_{ijl} \qquad (4)$$

where,

λ_i = failure rate of i^{th} line replaceable unit (LRU)

λ_{ij} = failure rate of the j^{th} shop replaceable SRU unit in the i^{th} LRU.

λ_{ijl} = failure rate of the l^{th} circuit in the j^{th} SRU in the i^{th} LRU.

Mct_i = average time to locate a failed LRU and remove and replace it.

Mct_i^* = average time to disassemble the i^{th} LRU, identify, remove, and replace the failed SRU in the i^{th} LRU and reassemble the i^{th} LRU.

Mct_{ij} = average time to disassemble the failed SRU, identify, remove, and replace the faulty circuit in the j^{th} SRU and reassemble the j^{th} SRU.

Mct_{ijl} = average time to disassemble the faulty circuit and correct or fix the l^{th} circuit.

Because we are assuming constant failure rates and independence of the failure processes, we see that

$$\lambda_T = \sum_{i=1}^{k} \lambda_i = \sum_{i=1}^{k} \sum_{j=1}^{k_i} \lambda_{ij} = \sum_{i=1}^{k} \sum_{j=1}^{k_i} \sum_{l=1}^{k_{ij}} \lambda_{ijl}$$

where k = total number of LRU's, k_i = total number SRU's in the i^{th} LRU, and k_{ij} = total number of circuits in the j^{th} SRU in the i^{th} LRU.

Rewriting, (4) becomes:

$$MTUT = \sum_{i=1}^{k} \sum_{j=1}^{k_i} \sum_{l=1}^{k_{ij}} \lambda_{ijl} \left(Mct_i + Mct_i^* + Mct_{ij} + Mct_{ijl} \right) \qquad (5)$$

Throughout this paper we assume that the repair times at each level of maintenance are independent.

The term:

$$\sum_{i=1}^{k} \sum_{j=1}^{k_i} \sum_{l=1}^{k_{ij}} \lambda_{ijl} \, (Mct_i)$$

may be written as

$$\lambda_T \sum_{i=1}^{k} (\lambda_i/\lambda_T) \, Mct_i. \qquad (6)$$

In the demonstration phase of the development of a system, time constraints usually prohibit the observation of at least one failure from all modes. Since a simple random sample distributes itself approximately proportionally over all failure modes, a sample mean time ($\bar{X}$) can be used to unbiasedly estimate $\sum_{i=1}^{k} (\lambda_i/\lambda_T) \, Mct_i$. Thus, $\lambda_T \bar{X}$ is used to estimated equation (6). An appeal to the central limit theorem gives

$$\lambda_T \bar{X} \sim N\left(\sum_{i=1}^{k} \lambda_i \, Mct_i, \; \sigma^2_{\lambda_T \bar{X}} \right) \qquad (7)$$

for n large.

When the number of observations for any one failure mode is small (< 50), according to (1),

$$\hat{\sigma}^2_{\lambda_T \bar{X}} = \lambda_T^2 \left(1/n\right)\left[\sum_{i=1}^{k} w_i s_i^2 - \sum_{i=1}^{k} \left(w_i s_i^2 / \lambda_i T\right) + \sum_{i=1}^{k} \left(w_i^2 s_i^2 / \lambda_i T\right) + \sum_{i=1}^{k} w_i \bar{X}_i^2 - \left(\sum_{i=1}^{k} w_i \bar{X}_i\right)^2\right] \quad (8)$$

where,

n = total number of observed equipment failures in time T.

$w_i = \lambda_i / \lambda_T$

$$s_i^2 = \sum_{j=1}^{n_i} \left(X_j - \bar{X}_i\right)^2 / n_i - 1$$

When the number of observations for all failure modes is large (> 30), according to [1],

$$\hat{\sigma}^2_{\lambda_T \bar{X}} = \lambda_T^2 \left(1/n\right) \sum_{i=1}^{n} \left(X_i - \bar{X}\right)^2 / n-1 \quad (9)$$

has a negligible bias for $\sigma^2_{\lambda_T \bar{X}}$.

In the demonstration phase it is possible to observe at least 30 repair times for each LRU, SRU, and each circuit. Thus, an unbiased estimate for MTUT is,

$$\text{MTUT} = \lambda_T \bar{X} + \sum_{i=1}^{k} \sum_{j=1}^{k_i} \sum_{l=1}^{k_{ij}} \lambda_{ijl} \left(\bar{X}_i^* + \bar{X}_{ij} + \bar{X}_{ijl}\right) \quad (10)$$

where

$\bar{X}_i$ = mean time to repair the i^{th} LRU from at least 30 observations.

$\bar{X}_{ij}$ = mean time to repair j^{th} SRU from the i^{th} LRU for at least 30 observations.

$\bar{X}_{ijl}$ = mean time to repair l^{th} circuit from j^{th} SRU for the i^{th} LRU for at least 30 observations.

Thus, $\hat{MTUT} \sim N\left(MTUT, \ Var\ (\hat{MTUT})\right)$

where $\hat{Var}\ \hat{MTUT} = \underset{\lambda_T \bar{Y}}{\hat{\sigma}^2} + \sum_{i=1}^{k} \sum_{j=1}^{k_i} \sum_{l=1}^{k_{ij}} (\lambda_{ijl})^2 \left(\frac{s_i^2}{n_i} + \frac{s_{ij}^2}{n_{ij}} + \frac{s_{ijl}^2}{n_{ijl}} \right)$. (11)

Therefore, a $(1 - \alpha)100\%$ interval estimate of MTUT (when all λ_{ijl} are known and large samples from each maintenance level are taken) is

$$\hat{MTUT} \pm Z_{\alpha/2} \sqrt{Var\ \hat{MTUT}}. \qquad (12)$$

Using these concepts, a test statistic for a hypothesized value of MTUT, say C_o, would be $\hat{MTUT} - C_o \Big/ \sqrt{\hat{Var}\ \hat{MTUT}}$. This statistic would be compared to an appropriate standard normal value for a given test. A typical test might be of the following form:

$$H_o: \quad MTUT = C_o \qquad (13)$$

$$H_A \quad MTUT > C_o \ .$$

The decision procedure for this type of testing problem is:

$$\text{If } (\hat{MTUT} - C_o) \Big/ \sqrt{\hat{Var}\ \hat{MTUT}} > Z_{\alpha} \qquad (14)$$

conclude MTUT > C_0, otherwise fail to reject the hypothesis that MTUT = C_0. The value Z_{α} is the $(1-\alpha)$ percentile of the standard normal distribution.

Expressions (10), (11), (12), (13), and (14) change slightly when data is recorded during the assessment stage of a piece of equipment. For a large enough sample of failures, all failure modes will occur. Some modes will occur more than others, but under the assumption that the number of failures of each mode is large, the term $\lambda_T \bar{X}$ can be written as:

$$\sum_{i=1}^{k} \lambda_i \bar{X}_i \quad \text{and}$$

$$\hat{\sigma}^2_{\lambda_T X} = \sum_{i=1}^{k} \lambda_i^2 \, s_i^2 \Big/ n_i \quad \text{where}$$

$\bar{X}_i$ = mean time to locate, remove, and replace the i^{th} failed LRU types, and

$$s_i^2 = \sum_{j=1}^{n_i} (X_j - \bar{X}_i)^2 \Big/ n_i - 1.$$

Substituting these expressions into (10), (11), (12), (13), and (14) gives the form of an interval estimate and discrimination procedure for MTUT when data is taken during the assessment stage and all assumptions are met.

V. Estimation and Testing for MTUT when λ_{ijl} Unknown.

Two scenarios to be considered in this section are (1) finite sample sizes at all levels of maintenance and for all parts and (2) large sample size (> 30) at every level of maintenance for each part type.

The following notation will be used in this section:

t_m = the m^{th} time between failure of the i^{th} LRU.

t_m^* = the m^{th} time between failures of the j^{th} SRU in the i^{th} LRU.

t_m^{**} = the m^{th} time between failures of the l^{th} circuit in the j^{th} SRU in the i^{th} LRU.

n = number of equipment or system failures.

n_i = number of failures for the i^{th} LRU (> 0).

n_{ij} = number of failures for the j^{th} SRU in the i^{th} LRU (> 0).

n_{ijl} = number of failures for the l^{th} circuit in the j^{th} SRU in the i^{th} LRU (> 0).

Case (1) is to be considered first. A conservative $(1-\alpha)100\%$ confidence interval for finite sample size is stated with an outline of its derivation.

We assume for the first condition that the repair times are exponential and independent. Likewise, the assumption of exponential interarrival times is necessary. It should be noted that $n_i \Big/ \sum_{m=1}^{n_i} t_m$ is the maximum likelihood estimate of λ_i and $\bar{X}_i$ is the maximum likelihood estimate of Mct_i. The expression

$$Mct_i \left(2\lambda_i \sum_{m=1}^{n_i} t_m / 2n_i\right) / \bar{X}_i \sim F_{2n_i, 2n_i}$$ proves useful in the

construction of a $(1-\alpha)100\%$ confidence interval for MTTR. The interval

$$\left[F_{2n_i, 2n_i, \alpha/\lambda} \cdot \bar{X}_i \Big/ \sum_{m=1}^{n_i} t_m/n_i \;,\quad F_{2n_i, 2n_i, 1-\alpha/\lambda} \cdot \bar{X}_i \Big/ \sum_{m=1}^{n_i} t_m/n_i \right]$$

is a $(1-\alpha)100\%$ confidence interval for $\lambda_i Mct_i$. Hence, a conservative $(1-\alpha)100\%$ confidence interval for

$$\sum_{i=1}^{k} \lambda_i Mct_i \qquad \text{is}$$

$$\left(\sum_{i=1}^{k} F_{2n_i, 2n_i, \alpha/\lambda} \cdot \bar{X}_i \Big/ \sum_{m=1}^{n_i} t_m/n_i \;,\; \sum_{i=1}^{k} F_{2n_i, 2n_i, 1-\alpha/\lambda} \cdot \bar{X}_i \Big/ \sum_{m=1}^{n_i} t_m/n_i \right).$$

Using this approach for all terms in MTUT gives the following interval which includes the true MTUT at a level of certainty at least $(1-\alpha)100\%$:

$$L_{\alpha/2} = \sum_{i=1}^{k} F_{2n_i,\,2n_i,\,\alpha/2}\left(\left(\bar{X}_i + \bar{X}_i^{*}\right)\Big/\sum_{m=1}^{n_i} t_m \Big/ n_i\right)$$

$$+ \sum_{i=1}^{k}\sum_{j=1}^{k_i} F_{2n_{ij},\,2n_{ij},\,\alpha/2}\left(\bar{X}_{ij}\Big/\sum_{m=1}^{n_{ij}}\left(t_m \Big/ n_{ij}\right)\right)$$

$$+ \sum_{i=1}^{k}\sum_{j=1}^{k_i}\sum_{l=1}^{k_{ij}} F_{2n_{ijl},\,2n_{ijl},\,\alpha/2}\left(\bar{X}_{ijl}\Big/\sum_{m=1}^{n_{ijl}}\left(t_m \Big/ n_{ijl}\right)\right)$$

$$U_{1-\alpha/2} = \sum_{i=1}^{k} F_{2n_i,\,2n_i,\,1-\alpha/2}\left(\left(\bar{X}_i + \bar{X}_i^{*}\right)\Big/\sum_{m=1}^{n_i} t_m \Big/ n_i\right)$$

$$+ \sum_{i=1}^{k}\sum_{j=1}^{k_i} F_{2n_{ij},\,2n_{ij},\,1-\alpha/2}\left(\bar{X}_{ij}\Big/\sum_{m=1}^{n_{ij}}\left(t_m \Big/ n_{ij}\right)\right)$$

$$+ \sum_{i=1}^{k}\sum_{j=1}^{k_i}\sum_{l=1}^{k_{ij}} F_{2n_{ijl},\,2n_{ijl},\,1-\alpha/2}\left(\bar{X}_{ijl}\Big/\sum_{m=1}^{n_{ijl}}\left(t_m \Big/ n_{ijl}\right)\right).$$

For testing purposes, if L_{α} is larger than the assumed value of MTUT, say $MTUT_0$, then conclude H_A: $MTUT > MTUT_0$. This conclusion has a type I error associated with it less than α. If L_{α} is less than $MTUT_0$ fail to reject H_0: $MTUT = MTUT_0$. If $U_{1-\alpha}$ is less than $MTUT_0$, conclude $MTUT < MTUT_0$. This conclusion has a type I error of at most α. When $U_{1-\alpha}$ is larger than $MTUT_0$, fail to reject H_0: $MTUT = MTUT_0$. For a two-sided test, if the interval $(L_{\alpha/2},\ U_{1-\alpha/2})$ does not include $MTUT_0$ conclude $MTUT \neq MTUT_0$ with a type I error probability of at most α. Otherwise fail to reject H_0: $MTUT = MTUT_0$.

The estimation and testing procedures outlined above are for scenario (1). They are reasonably straightforward but the levels of certainty and error probabilities are very conservative. Scenario (2) is considered next.

A brief derivation of an estimate for the contribution to MTUT at the organizational level is given. Its estimated variance is also derived. An approximate distributional property of this estimator is concluded according to reference (4). An extenstion of these ideas results in an approximate $(1-\alpha)100\%$ interval estimate of MTUT. Repair times are assumed exponential and independent for each failure type (k LRUs, $\sum_{i=1}^{k} k_i$ SRUs, $\sum_{i}^{k}\sum_{j}^{k_i} k_{ij}$ circuits). The interarrival times of failures are assumed independent for each failure type as well as among different failure types. (i.e. The failure time of the j^{th} SRU in the i^{th} LRU is independent of a failure time in the i^{th} LRU etc.)

Let $\theta_i = \lambda_i \, Mct_i$. It has been shown that $\hat{\theta}_i = n_i \bar{X}_i \Big/ \sum_{m=1}^{n_i} t_m$ is a maximum likelihood estimator of θ_i. According to reference (4), the vector of estimates $\hat{\underset{\sim}{\theta}}$ has a multivariate normal distribution with mean vector $\underset{\sim}{\theta}$. The large sample variance of θ_i is

$$\frac{2}{n_i} \left(\frac{n_i \bar{X}_i}{\sum_{m=1}^{n_i} t_m} \right)^2 . \tag{15}$$

Because of our assumptions, an approximate $(1-\alpha)100\%$ level confidence interval for $\sum_{i=1}^{k} \lambda_i \, Mct_i$ is

$$\sum_{i=1}^{k} (n_i \bar{X}_i) \Big/ \sum_{m=1}^{n_i} t_m \pm Z_{\alpha/2} \sqrt{\sum_{i=1}^{k} \left(\frac{2}{n_i} \right) \left(\frac{n_i \bar{X}_i}{\sum_{m=1}^{n_i} t_m} \right)^2} \; . \tag{16}$$

Extending this idea to $\hat{MTUT}$, it is straightforward that

$$\begin{aligned} MTUT \;=\; & \sum_{i=1}^{k} (n_i \bar{X}_i) \Big/ \sum_{m=1}^{n_i} t_m + \sum_{i=1}^{k} (n_i \bar{X}_i^{*}) \Big/ \sum_{m=1}^{n_i} t_m \\ & + \sum_{i=1}^{k}\sum_{j=1}^{k_i} (n_{ij} \bar{X}_{ij} \Big/ \sum_{m=1}^{n_{ij}} t_m^{*} \\ & + \sum_{i=1}^{k}\sum_{j=1}^{k_i}\sum_{l=1}^{k_{ij}} (n_{ijl} \bar{X}_{ijl}) \Big/ \sum_{m=1}^{n_{ijl}} t_m^{**} \; . \end{aligned} \tag{17}$$

Equation (18) can be derived with similar reasoning used to derive (15). Reference (4) helps in this derivation. Thus,

$$\widehat{\text{Var}}\ \widehat{\text{MTUT}} = \sum_{i=1}^{k} (2/n_i)\,(n_i\bar{X}_i)^2 \Big/ \left(\sum_{m=1}^{n_i} t_m\right)^2$$

$$+ \sum_{i=1}^{k} (2/n_i)\,(n_i\bar{X}_i^*)^2 \Big/ \left(\sum_{m=1}^{n_i} t_m\right)^2 \qquad (18)$$

$$+ \sum_{i=1}^{k}\sum_{j=1}^{k_i} (2/n_{ij})\,(n_{ij}\bar{X}_{ij})^2 \Big/ \left(\sum_{m=1}^{n_{ij}} t_m^*\right)^2$$

$$+ \sum_{i=1}^{k}\sum_{j=1}^{k_i}\sum_{l=1}^{k_{ij}} (2/n_{ijl})\,(n_{ijl}\bar{X}_{ijl})^2 \Big/ \left(\sum_{m=1}^{n_{ij}} t_m^{**}\right)^2.$$

Hence, an approximate $(1-\alpha)100\%$ confidence interval for MTUT is

$$\widehat{\text{MTUT}} \pm Z_{\alpha/2} \sqrt{\widehat{\text{Var}}\ \widehat{\text{MTUT}}} \qquad (19)$$

where $\widehat{\text{MTUT}}$ and $\widehat{\text{Var}}\ \widehat{\text{MTUT}}$ are from equations (17) and (18).

VI. Steady state availability when failure rate and repair rate are not necessarily constant.

Generally speaking, the term availability is defined as the probability that a system or piece of equipment is operating satisfactorily at any point in time and considers only operating time and downtime. Availability may be thought of as a ratio of the operating time of a system to the operating time plus the downtime. Hence, this measure includes both reliability and maintainability. When a system for which the time to failure is exponential with failure rate λ and the downtime is assumed to have an exponential distribution with a repair rate of μ, it is straightforward to determine the steady state availability (i.e. availability for large time). This measure becomes

$$A = \lim_{t \to \infty} A(t) = u/(u + \lambda). \tag{20}$$

Reference (2) gives a complete derivation of this expression.

Now, what about the situation where the rates are not constant? The following theorem gives a simple sufficient condition for the existence of a steady state availability.

Theorem

The function $A(t)$ is defined to be the availability of the system. It is assumed the repair times are interarrival times from a Poisson process with cumulative intensity function $H_2(t)$. The failure times are also assumed to follow a Poisson process with cumulative intensity function $H_1(t)$. Both $H_1(t)$ and $H_2(t)$ are assumed to be differentiable and $\lim_{t \to \infty} H_i(t) = \infty$, $i = 1,2$. If $H_1(t)$ is proportional to $H_2(t)$ then $\lim_{t \to \infty} A(t)$ exists.

Proof: For a small interval of time Δt

P (system failure during Δt) $= h_1(t)\Delta t$

P (repair during $\Delta t \mid$ system failure) $= h_2(t)\,\Delta t$.

Thus,

$$A(t + \Delta t) = A(t)(1 - h_1(t)\,\Delta t) + (1 - A(t))h_2(t)\,\Delta t$$

or

$$\frac{A(t + \Delta t) - A(t)}{\Delta t} = -(h_1(t) + h_2(t))A(t) + h_2(t).$$

Taking the limit as $\Delta t \longrightarrow 0$,

$$\frac{d\,A(t)}{d(t)} = -(h_1(t) + h_2(t))A(t) + h_2(t).$$

Which is recognizable as a differential equation whose solution is

$$A(t) = e^{-\left[H_1(t) + H_2(t)\right]} \int_0^t h_2(x)\, e^{\left[H_1(x) + H_2(x)\right]}\, dx + c_1 e^{-\left[H_1(t) + H_2(t)\right]}$$

where c_1 is some constant.

Taking the limit as $t \longrightarrow \infty$ when $H_1(t) = C_0 H_2(t)$ gives

$$\lim_{t \longrightarrow \infty} A(t) = 1/C_0 + 1.$$

The measure MTUT and Availability are similar. MTUT is such that

$$MTUT = (1 - A)/A$$

when only the organizational maintenance level is considered. MTUT does not give any more information than availability in this case. Since the organizational level of maintenance is not the only level of maintenance which occurs, the use of MTUT gives more information about the total impact on the maintenance system than does availability.

VII. Recommendations

This report decribes a measure of reliability/maintainability which was introduced and discussed in reference (3). The main thrust of this investigation is to present estimators and discrimination procedures for this measure of reliability/maintainability that includes information about the maintainability support burden. A principle problem is to derive an interval estimate of this measure which is narrow and has associated with it an accurate degree of certainty.

A similar problem occurs in the discrimination approach involved with this reliability/maintainability measure. What is the form of a procedure for a test which has an accurate error probability?

An interval estimate for MTUT with an accurate degree of certainty has been derived when all failure rates are assumed known. A testing procedure with an exact error probability under the same scenario has also been presented in this report. The values of the failure rates can be assigned according to prediction models already developed by the Air Force.

Because of the strong subjective nature of many of the assumed failure rates from the prediction models, treating them as a known value is technically incorrect. In spite of this, their values can provide insightful information. It would be beneficial under these circumstances to combine the information from the observed data and the information from the predicted failure rates without treating the rates as known. This can be done using a Bayes approach.

This report has presented a form of an interval estimate of MTUT when the failure rates are unknown. Information from the predicted failure rates was ignored. An important assumption was made in the scenario of a large sample. The assumption that the estimates of the λ_i's, λ_{ij}'s, and λ_{ijl}'s have negligible covariances should be investigated. When these covariances are not negligible, a new interval estimate needs to be derived.

A characterization of a learning curve for MTUT would be useful for comparing several systems or pieces of equipment. Examining the system or piece of equipment which has the "best" learning curve might provide insight as to design changes for future products as well as information valuable for the modification of equipment under current use.

The test procedures developed for MTUT in this report do not specify standards for the particular failure rates or average repair times. The problem of allocating particular specifications for each of these parameters given an MTUT requirement needs to be developed. Choosing the values of these parameters such that the cost of development is minimized while simultaneously minimizing the value of the parameter would be beneficial to both the contractor and the Air Force. Determining error probabilities under this scheme would need to be solved.

REFERENCES

1. Cochran, W.G., Sampling Techniques, New York, New York, John Wiley & Sons, 1963.

2. Kapur, K.C., L.R. Lamberson, Reliability in Engineering Design, New York, New York, John Wiley & Sons, 1977.

3. Klion, J., "Specifying Maintainability - A New Approach", Proc. Annual Reliability and Maintainability Symposium, Las Vegas, Nevada, January 1986, pp 338-343.

4. Lawless, J.F., Statistical Models and Methods For Lifetime Data, New York, New York, John Wiley & Sons, 1982.

5. Mann, N.R., R.E. Schafer, and N.D. Singpurwalla, Methods of Statistical Analysis of Reliability and Life Data, New York, New York, John Wiley & Sons, 1974.

1986 USAF-UES SUMMER FACULTY RESEARCH PROGRAM/

GRADUATE STUDENT SUMMER SUPPORT PROGRAM

Sponsored by the

AIR FORCE OFFICE OF SCIENTIFIC RESEARCH

Conducted by the

Universal Energy Systems, Inc.

FINAL REPORT

DESIGN SYNTHESIS OF NONLINEAR SYSTEMS

Prepared by:	Glen E. Johnson
Academic Rank:	Associate Professor
Department and	Mechanical and Materials Engineering
University:	Vanderbilt University
Research Location:	Arnold Engineering Development Center
USAF Researcher:	H. LeRoy Henderson
Date:	July 9, 1986
Contract No:	F49620-85-C-0013

DESIGN SYNTHESIS OF NONLINEAR SYSTEMS

by

Glen E. Johnson

ABSTRACT

The automated optimal design of reinforced concrete footings is considered. Software is described and presented for use in the design of cylindrical footings when the only significant loading is due to wind. Software is described and presented for the design of rectangular footings subjected to both bearing and wind loads. Program features are discussed and suggestions for future work are outlined. A companion report by Mr. C. R. Hammond presents the work on the development of an expert system to set up and solve problems in nonlinear optimal design.

ACKNOWLEDGMENTS

The sponsorship of the Air Force Systems Command and the Air Force Office of Scientific Research is gratefully acknowledged. We appreciate the space provided for us in the Design Engineering group of Schneider Systems International at the Arnold Engineering Development Center. Special thanks are due to Mr. Marshall K. Kingery, USAF, for his help and encouragement throughout this summer project.

I. Introduction

For the past 12 years Dr. Johnson has been involved in the development of strategies for the design of mechanical systems. Since receiving a Ph.D. from Vanderbilt University in 1978, he has written numerous articles on design and optimization. He has published software for general purpose nonlinear programming and software has been developed under his direction for the optimal design of specific mechanical components (such as gears, bearings, springs, electric motors,etc.). He is currently interested in the development of an expert system that will automatically set up and solve general nonlinear programming problems in mechanical design using the principles of the Method of Optimum Design [1] and Monotonicity Analysis [2].

This summer, Dr. Johnson has been joined by Charles R. Hammond. Mr. Hammond has been involved in the development of nonlinear programming software since 1980 as an undergraduate at the University of Virginia. He has written software for automated signature analysis of mechanical vibrations in paper manufacturing machines and he completed an extensive optimization study of journal bearings as part of his master of science program at the University of Virginia. He is presently working toward a Ph.D. degree at Vanderbilt and his dissertation research project is the development of an automated procedure (based on symbolic manipulation software) to set up and solve nonlinear optimization problems in mechanical design.

We have been assigned to the Design Engineering group (part of Schneider Services International) in the Model Shop at AEDC. This group is production oriented and their mission appears to be to provide support for the physical plant. We are aware of their involvement

in the design of foundations, structures, electrical, and HVAC systems. They are currently using some computer based design methods for HVAC work, and they have a computer aided drafting group. They may provide design services in other areas as well. We were assigned to this group because of our mutual interest in design and design methodology.

II. Objectives of the Research Effort

Our goal was to identify some specific design problems at AEDC and to develop computer based design strategies for those problems. The development of an expert system for design was also to be considered.

III. Design of Cylindrical Concrete Footings

A project referred to as "the steam line" is currently in the construction phase at AEDC. The steam line is supported by steel T's that are set in cylindrical, reinforced concrete footings. We have reviewed the design procedure for these footings with the engineers in Design Engineering. The method used was first given by Ivey and Hawkins [3].

In 1966 Ivey and Hawkins formulated a set of equations and a procedure for the design of drilled, reinforced concrete footings to resist wind loads. The problem can be stated as: Design a cylindrical concrete footing to resist wind loads. The footing must be deep enough to resist frost heaving, but not so deep as to be impractical to drill. The diameter should correspond to a standard auger size. The stress in the soil should not exceed the expected soil strength. We have added the additional goal of identifying the footing that meets the requirements while using the least amount of concrete.

In this prose format, the problem makes sense and the development of a suitable mathematical model can proceed in a logical fashion. The goal (or objective) is readily determined to be a function of footing

diameter and footing depth. The constraints pose trivial inequality relations that must be satisfied by the footing depth and the footing diameter. The last constraint requires that the designer assume a failure mode (or modes) and develop functional inequalities that will define success or failure.

Ivey and Hawkins used the well-known Rankine formula for soil strength as a function of soil properties and depth and they estimated soil stress as a function of wind load, height to centroid of wind load, footing diameter, and footing depth using standard equations of static equilibrium. Wind load could be estimated from information contained in the Southern Building Code, and soil properties could be determined by experiment.

At this point, the designer has an equation system to work with (see Figure 1). The equation system will define the design variables and the parameters that are necessary for successful design. The variables are clearly footing depth, footing diameter, and soil stresses. The depth and diameter are decision variables (they are the variables that would traditionally be selected by the designer). The stresses are state variables (they would be directly calculable once the decision variables were specified).

We have taken this design model, and written a computer program to select and evaluate candidate footing designs (see Figure 2). The program is interactive and has some protection against user error in entering data. For example, negative input data will cause the program to inform the user that the input data is bad. The user is asked to try again. After data has been entered, the user has the opportunity to review the data before proceeding.

The program includes soil data that is believed by AEDC engineers to be reasonable for this area.

However, the program gives the user the option of changing the data if it isn't correct. The user also has the option of specifying the maximum wind speed that the installation will be subjected to. The program takes the user specified speed, and computes the expected wind pressure at the height of the centroid of the wind load using the equations and tabulated data given in the Southern Building Code [4].

The algorithm takes advantage of the monotonic behavior of the objective function with respect to the design variables. For each candidate auger diameter, the depth is set at its lower limit, and the soil constraints are tested. If the constraints are satisfied, then the design is printed and the auger size is incremented by one half foot. If the constraints are not satisfied, then the depth is incremented by one foot and the new candidate design is tested. The program prints the smallest depth that will work with each auger diameter. After the last auger diameter has been considered, the program prints the feasible design that used the smallest volume of concrete. By taking advantage of the mathematical structure in this problem, it was possible to develop a very efficient code that considers a fairly small number of candidate designs in identifying the optimal design. The program runs off floppy disk virtually instantaneously on an IBM PC XT, even without a math coprocessor.

IV. Design of Rectangular Concrete Footings

In the design of rectangular concrete footings, the soil stress under the toe of the footing is considered critical and so the soil failure equations are different from those used by Ivey and Hawkins. Once again, the objective was to identify the footing that would use the least concrete while resisting overturn by the wind. The design variables were

length, width, thickness, and depth below grade of the footing.

The FORTRAN 77 source code is presented in Figure 3. The algorithm used in this program is not very efficient, however running times are not excessive. Even running off of floppy disk on an IBM PC, execution times are less than a minute for most practical cases.

The program is interactive, and user input error protection is incorporated. The design space is divided up into a set of discrete points, essentially representing a grid of candidate designs. Each point is tested for feasibility and the feasible point that would use the least amount of concrete is saved and printed out at the end of the run. There was insufficient time to refine this program to make it more efficient during the ten week period. Nevertheless, run times are reasonably short and there are no tuning parameters or other obstacles that could make the program difficult to use.

V. Expert System for Design

Considerable effort has been devoted to the development of an automated strategy for the implementation of the Method of Optimum Design [1]. Mr. Hammond has outlined the steps that will be necessary to complete this project, and he has made considerable progress in writing software to identify all of the possible optimization design spaces if one is already known. His report (which has been prepared separately under his authorship) will describe this part of our summer research project.

VI. Recommendations

The two FORTRAN 77 programs for footing design work well and can be used for design work at AEDC. At the present time, the programs reflect current design practice in the Design Engineering group. The

cylindrical footing design program could be improved by adding a constraint on bearing pressure under the footing.

The rectangular footing design program could be improved by adding a constraint on the stress that occurs in the concrete slab. Additional study could also lead to a more efficient algorithm for the design calculations. This may not be warranted, since computation times are already quite short.

In the long term, the development of an automated method to set up and solve nonlinear optimization problems in engineering design is a worthwhile goal. The existence of such software would greatly reduce the effort required to develop optimum design programs for specific mechanical devices and systems. We expect to submit a proposal to continue our work on the expert design system through the mini grant program.

REFERENCES

1. Johnson, Ray C., Optimum Design of Mechanical Elements. New York, NY, Wiley-Interscience, 1980.
2. Wilde, Douglass J., Globally Optimal Design, New York, NY, Wiley-Interscience, 1978.
3. Ivey, D. L. and Leon Hawkins, "Signboard Footings to Resist Wind Loads," Civil Engineering, December 1966, pp.34-35.
4. Southern Building Code Congress International Inc., Standard Building Code, Section 1205, Birmingham, AL, 1979.

objective:	minimize $V = (Pi)(b^2)(D)/4$	(1)
constraints:	$S_1 = (P)(H+.9D)/(.38bD^2)$	(2)
	$S_2 = S_1/[(.28D/(H+.34D))+.5]$	(3)
	$S_L = 2S_2$	(4)
	$S_1 < 2(.34DK_1+K_2)/3SF$	(5)
	$S_2 < (.68DK_1+K_2)/SF$	(6)
	$S_L < DK_1+K_2$	(7)
	$D_{min} < D < D_{max}$	(8)
	$\{ b \mid b_1, b_2, b_3, \ldots, b_n \}$	(9)
given:	$N_{phi} = [Tan(45+phi/2)]^2$	(10)
	$K_1 = (Gamma)N_{phi}$	(11)
	$K_2 = 2C(N_{phi})^{.5}$	(12)
	$p = max\{ 20.9.7H^{.29} \}$ or other suitable relation from the building code	(13)
	$P = pAK_3$	(14)
input:	H, Gamma, C, SF, A, K_3, phi	

FIGURE 1A. CYLINDRICAL FOOTING DESIGN MODEL

H	height to centroid of wind load
Gamma	soil density
C	soil cohesion
phi	soil angle of internal friction
SF	safety factor against overturn
A	cross sectional area subjected to wind
K_3	shape factor for area defined by A
N_{phi}, K_1, K_2	constants in Rankine's equation
p	wind pressure (from building code)
P	wind load
S_1	stress in upper region of soil
S_2	stress in lower region of soil
S_L	soil stress at bottom of footing
b	diameter of footing
D	depth of footing
Pi	3.14159265

FIGURE 1B. NOMENCLATURE FOR CYLINDRICAL FOOTING DESIGN MODEL

```
      DATA GAMMA,C,PHI /120.,1500.,20./
      WRITE(*,38)
   38   FORMAT(3X,'THIS PROGRAM WILL ASSIST YOU IN THE DESIGN',/,
     $  3X,'OF CYLINDRICAL CONCRETE FOOTINGS WHEN THE PRIMARY',/,
     $  3X,'LOADING IS DUE TO WIND.',/)
   39   WRITE(*,11)
   11   FORMAT(3X,'IF YOU WANT INFORMATION ABOUT THIS PROGRAM',/,3X,
     $  'ENTER 5.',/,3X,'OTHERWISE, ENTER ANY OTHER INTEGER.',/)
        BSAVE=0.0
      KOUNT=1
      READ(*,*)L
      IF(L.EQ.5)GO TO 14
      GO TO 15
   14     WRITE(*,16)
   16      FORMAT(3X,
     $  'THIS PROGRAM WILL IDENTIFY THE FEASIBLE FOOTING',/,3X,
     $  'DESIGNS FOR CYLINDRICAL CONCRETE FOOTINGS',.3X,
     $  'WHEN THE PRIMARY LOADING IS DUE TO WIND.  THE PROGRAM',/,3X,
     $  'CONSIDERS AUGER DIAMETERS IN HALF FOOT INCREMENTS AND',/,3X,
     $  'FOOTING DEPTHS IN ONE FOOT INCREMENTS.  AUGER DIAMETER,B,',/,3X
     $  ,'CAN RANGE FROM 1 TO 3 FEET.  FOOTING DEPTH, D, CAN RANGE ',/,
     $  3X,'FROM 4 TO 10 FEET.  THE PROGRAM CHECKS TO SEE THAT THE ',/,
     $  3X,'SOIL STRESS CONSTRAINTS ARE SATISFIED USING THE EQUATIONS',/
     $  ,3X,'GIVEN BY IVEY AND HAWKINS IN 1966.  THE EQUATIONS ARE NOT',
     $  /,3X,'USED IN THE SAME WAY AS THEY WERE BY IVEY AND HAWKINS,',/,
     $  3X,'ALTHOUGH DESIGN CONCLUSIONS WILL BE THE SAME BY EITHER',/,
     $  3X,'METHOD.  WIND VELOCITY CAN BE CHOSEN BETWEEN 90 AND 130',/,
     $  3X,'MPH IN 10 MPH INCREMENTS.  COMPUTATIONS ARE BASED ON THE ',/
     $  ,3X,'REQUIREMENTS OF THE SOUTHERN BUILDING CODE.',//)
      WRITE(*,80)
   80     FORMAT(3X,'DEPRESS ENTER KEY TO CONTINUE.',/)
      READ(*,*)
      WRITE(*,81)
   81   FORMAT(3X,'YOU MUST ENTER THE HEIGHT ABOVE THE GROUND OF',/,
     $  3X,'THE CENTROID OF THE WIND LOAD (H IN FEET), THE SAFETY',/,3X,
     $  'AGAINST OVERTURN (SF), THE AREA SUBJECTED TO THE WIND LOAD',/,
     $  3X,'(A IN SQUARE FEET), AND THE SHAPE FACTOR FOR THE AREA',/,3X,
     $  'SUBJECT TO THE WIND LOAD (RK3).  SOIL PARAMETERS ARE ASSUMED',/
     $  ,3? 'TO BE AS FOLLOWS:  DENSITY=120#/CU.FT., COHESION=1500PSF.',
     $  /,3X,'ANGLE OF INTERNAL FRICTION=20DEGRES.  THESE PARAMETERS',/,
     $  3X,'SHOULD BE CHANGED IF THEY DO NOT REPRESENT THE CONDITIONS',/
     $  ,3X,'AS THEY WILL EXIST IN THE PROPOSED INSTALLATION.',//)
   15   WRITE(*,59)
   59     FORMAT(3X,'ALL VARIABLES SHOULD BE ENTERED AS POSITIVE REALS',/)
      WRITE(*,61)
   61   FORMAT(3X,'ENTER THE HEIGHT ABOVE THE GROUND FOR THE CENTROID',/
     $  ,3X,'OF THE WIND LOAD IN FEET.',//)
      GO TO 53
   45   WRITE(*,46)
   46   FORMAT(/,3X,'BAD DATA.  TRY AGAIN.',/)
   53   READ(*,*) H
      IF(H.LT.0.0) GO TO 45
      WRITE(*,62)
   62     FORMAT(3X,'ENTER THE SAFETY FACTOR AGAINST OVERTURN',/,3X,
     $  'THIS SHOULD BE A REAL NUMBER GREATER THAN 1.',/)
      GO TO 54
   48   WRITE(*,49)

   49   FORMAT(/,3X,'BAD DATA.  TRY AGAIN.',/)
   54   READ(*,*) SF
      IF(SF.LT.1.0)GO TO 48
      WRITE(*,63)
   63     FORMAT(3X,'ENTER THE AREA SUBJECTED TO THE WIND LOAD',/,3X,
     $  'IN SQUARE FEET.',//)
        GO TO 43
   57   WRITE(*,55)
   55   FORMAT(/,3X,'BAD DATA.  TRY AGAIN.',/)
   43   READ(*,*) A
      IF(A.LE.0.0) GO TO 57
      WRITE(*,64)
   64     FORMAT(3X,'ENTER THE SHAPE FACTOR FOR THE AREA SUBJECTED',/,3X,
     $    'TO THE WIND LOAD.',//)
      GO TO 56
   37   WRITE(*,58)
   58   FORMAT(/,3X,'BAD DATA.  TRY AGAIN.',/)
   56   READ(*,*) RK3
      IF(RK3.LE.0.0) GO TO 37
      WRITE(*,52)H,SF,A,RK3
   52   FORMAT(/,3X,'ROUNDED TO ONE DECIMAL PLACE YOU HAVE CHOSEN ',/,3X
     $  ,'HEIGHT TO CENTROID OF WIND LOAD = ',F5.1,' FT.',/,3X,
     $  'SAFETY FACTOR AGAINST OVER TURN = ',F4.1,/,3X,
     $  'AREA SUBJECTED TO WIND LOAD = ',F7.1,' SQ.FT.',/,3X,
     $  'SHAPE FACTOR FOR THE AREA = ',F3.1,//,3X,
     $  'IF YOU WANT TO CHANGE THIS DATA, ENTER 5.',/,3X,
     $  'OTHERWISE, ENTER ANY OTHER INTEGER.',/)
        READ(*,*)JKL
      IF(JKL.EQ.5) GO TO 15
C     THE NEXT LINE GIVES THE SOIL PROPERTIES.  GAMMA IS THE
C     SOIL DENSITY, C IS THE SOIL COHESION, AND PHI IS THE
C     ANGLE OF INTERNAL FRICTION.
      WRITE(*,72)
   72     FORMAT(3X,'THE FOLLOWING DATA IS ASSUMED BY THE PROGRAM',/)
      WRITE(*,65) GAMMA, C, PHI
   65     FORMAT(3X,'THE SOIL DENSITY IN #/CU.FT. IS'.2X,F5.1,/,3X,
     $  'THE SOIL COHESION IN PSF IS',2X,F6.1,/,3X,
     $  'THE SOIL ANGLE OF INTERNAL FRICTION IN DEGREES IS',2X,F4.1,/,
     $  3X,'THESE VALUES SHOULD BE CHANGED IN THE PROGRAM IF THEY DO',
     $  /,3X,'NOT CORRESPOND TO THE EXPECTED VALUES IN THE FIELD.',//,
     $  3X,'IF YOU WANT TO CHANGE THESE VALUES, ENTER 5.',/,3X,
     $  'IF THESE VALUES ARE OK, THEN ENTER ANY INTEGER BUT 5.',/)
      READ(*,*) LL
        IF(LL.EQ.5) GO TO 30
      GO TO 31
   30     WRITE(*,32)
   32   FORMAT(/,3X,'ENTER SOIL DENSITY IN #/CU FT.',/)
        READ(*,*) GAMMA
      IF(GAMMA.LE.0.)THEN
           WRITE(*,108)
           GO TO 30
      ELSE
      END IF
  215   WRITE(*,216)
  216   FORMAT(/,3X,'ENTER SOIL COHESION IN PSF.',/)
      READ(*,*)C
      IF(C.LE.0.0)THEN
```

FIGURE 2A. SOURCE CODE FOR CYLINDRICAL FOOTING DESIGN

```
            WRITE(*,108)
            GO TO 215
         ELSE
         END IF
  217    WRITE(*,218)
  218    FORMAT(/,3X,'ENTER SOIL ANGLE OF FRICTION IN DEGREES.',/)
         READ(*,*)PHI
         IF(PHI.LE.0.0) THEN
            WRITE(*,108)
            GO TO 217
         ELSE
         END IF
         WRITE(*,12)GAMMA, C, PHI
   12    FORMAT(//,3X,'YOU HAVE CHOSEN ',/,3X,
     $   'SOIL DENSITY = ',F5.1,' #/CU.FT.',/,3X,'COHESION = ',F6.1,
     $   ' PSF',/,3X,
     $   'ANGLE OF INTERNAL FRICTION = ',F4.1,' DEGREES',/,
     $   3X,'CHECK TO SEE THAT THESE ARE OK BEFORE CONTINUING.',/,3X,
     $   'IF YOU WANT TO CHANGE THESE DATA ENTER 5.',/,3X,
     $   'OTHERWISE, ENTER ANY OTHER INTEGER.'/)
         READ(*,*)MM
         IF(MM.EQ.5) GO TO 30
   31    ENPHI=(TAN(.0175*(45.+PHI/2.)))**2
         RK1=GAMMA*ENPHI
         RK2=2.*C*SQRT(ENPHI)
  302    WRITE(*,300)
  300    FORMAT(/,3X,'ENTER THE MAXIMUM WIND SPEED IN MPH.',/,3X,
     $   'CHOICES ARE 90,100,110,120, OR 130.',//)
         READ(*,*)KVEL
         IF((KVEL.LT.90.).OR.(KVEL.GT.130.).OR.(MOD(KVEL,10).NE.0))THEN
            WRITE(*,301)
  301       FORMAT(/,3X,'BAD DATA.  TRY AGAIN.',/)
            GO TO 302
         ELSE
            IF(KVEL.EQ.90)THEN
               WIND=7.85*(H**.29)
               IF(WIND.LT.16.7) WIND=16.7
            ELSE
            END IF
            IF(KVEL.EQ.100)THEN
               WIND=9.69*(H**.29)
               IF(WIND.LT.20.) WIND=20.
            ELSE
            END IF
            IF(KVEL.EQ.110)THEN
               WIND=11.72*(H**.29)
               IF(WIND.LT.24.) WIND=24.
            ELSE
            END IF
            IF(KVEL.EQ.120) THEN
               WIND=13.95*(H**.29)
               IF(WIND.LT.29.) WIND=29.
            ELSE
            END IF
            IF(KVEL.EQ.130) THEN
               WIND=16.38*(H**.29)
               IF(WIND.LT.34.) WIND=34.

               ELSE
               END IF
            END IF
            WRITE(*,303)KVEL
  303       FORMAT(/,3X,'YOU HAVE SELECTED WIND SPEED = ',I3,' MPH',/,3X,
     $      'IF YOU WANT TO CHANGE THIS, ENTER 5.  IF THIS IS OK,',/,3X,
     $         'ENTER ANY OTHER INTEGER.',//)
            READ(*,*)IQK
            IF(IQK.EQ.5) THEN
               GO TO 302
            ELSE
            END IF
C           THE NEXT LINE COMPUTES THE WIND LOAD IN POUNDS BASED ON THE
C           AREA SUBJECTED TO THE WIND IN SQUARE FEET, AND THE SHAPE FACTOR.
            P=WIND**A*RK3
C           THE VALUE FOR B THAT APPEARS IN THE NEXT LINE IS THE MINIMUM
C           AUGER DIAMETER THAT WILL BE CONSIDERED BY THE PROGRAM IN FEET.
            B=1.0
            DO 10 I=1,5
C           THE VALUE OF D THAT APPEARS IN THE NEXT LINE IS THE MINIMUM
C           FOOTING DEPTH THAT WILL BE CONSIDERED BY THE PROGRAM IN FEET.
            D=4.5
            JOUNT=0
            DO 20 J=1,7
C           S1 IS THE AVERAGE STRESS IN THE UPPER TWO THIRDS OF THE SOIL
C           IN PSF.
            S1=P*(H+.9*D)/(.38*B*D*D)
C           S2 IS THE AVERAGE STRESS IN THE LOWER THIRD OF THE SOIL IN PSF.
            S2=S1/(.5+.28*D/(H+.34*D))
C           SL IS THE MAXIMUM STRESS IN THE SOIL AT THE BOTTOM OF THE
C           FOOTING IN PSF.  ACCORDING TO IVEY AND HAWKINS, LOCAL
C           YIELDING OCCURS IN THE SOIL, AND SO IT IS NOT NECESSARY
C           TO STRICTLY LIMIT SL.  IT IS INCLUDED IN THE CALCULATIONS
C           ONLY FOR INFORMATION PURPOSES.
            SL=2.*S2
C           TEST1 IS THE ALLOWABLE STRESS IN THE SOIL FOR THE UPPER
C           TWO THIRDS OF THE FOOTING IN PSF.
            TEST1=.67*(RK1*.34*D+RK2)/SF
C           TEST2 IS THE ALLOWABLE STRESS IN THE SOIL FOR THE LOWER
C           THIRD OF THE FOOTING IN PSF.
            TEST2=(.68*D*RK1+RK2)/SF
C           TESTL IS THE ALLOWABLE STRESS IN THE SOIL AT THE BOTTOM OF
C           THE FOOTING.  ACCORDING TO IVEY AND HAWKINS, LOCAL YIELDING
C           OCCURS AT THIS POINT TO RELIEVE ANY EXCESSIVE STRESS.  IT IS
C           INCLUDED IN THE CALCULATIONS ONLY FOR INFORMATION PURPOSES.
            TESTL=RK1*D+RK2
C           THE NEXT LINE CHECKS TO SEE IF THE SOIL STRESS IS OK IN THE
C           UPPER TWO THIRDS OF THE FOOTING.  IF IT IS, THEN THE STRESS
C           IS CHECKED IN THE LOWER THIRD.  IF IT IS NOT, THEN THIS
C           CANDIDATE DESIGN IS INFEASIBLE AND THE PROGRAM SKIPS TO THE
C           NEXT CANDIDATE DESIGN.
            IF(S1.LE.TEST1) GO TO 41
            JOUNT=JOUNT+1
            GO TO 21
C           THE NEXT LINE CHECKS TO SEE IF THE SOIL STRESS IS OK IN THE
C           LOWER THIRD OF THE FOOTING.  IF IT IS, THEN THIS CANDIDATE
C           DESIGN IS FEASIBLE.  THE PROGRAM WILL COMPUTE THE VOLUME OF
```

FIGURE 2B. SOURCE CODE FOR CYLINDRICAL FOOTING DESIGN (CONTINUED)

```
C    CONCRETE IN THE FOOTING AND PRINT OUT THE AUGER DIAMETER,
C    THE FOOTING DEPTH, AND THE VOLUME OF CONCRETE.  IF THIS
C    CHECK INDICATES THAT THE SOIL STRESS IN THE LOWER THIRD OF THE
C    FOOTING IS NOT OK, THEN THE PROGRAM WILL SKIP TO THE NEXT
C    CANDIDATE DESIGN.
   41     IF(S2.LE.TEST2) GO TO 42
          JOUNT=JOUNT+1
          GO TO 21
   42     V=.785*B*B*D/27.
          KOUNT=KOUNT+1
          IF(KOUNT.EQ.2) GO TO 17
          GO TO 18
   17     BSAVE=B
          DSAVE=D
          VSAVE=V
   18     WRITE(*,60) B,D,V
   60     FORMAT(3X,'AUGER DIA. = ',F3.1,2X,'FT.',/,3X,'FOOTING DEPTH = ',
         $  F4.1,2X,'FT.',/,3X,'FOOTING VOLUME = ',F7.2,2X,'CU.YDS.',
         $  3X,'DEEPER FOOTINGS WILL ALSO WORK, BUT WILL USE MORE CONCRETE.'
         $  ,//)
          GO TO 25
C    THE NEXT LINE INDICATES THE AMMOUNT THE DEPTH SHOULD BE
C    INCREMENTED BY WHEN IDENTIFYING THE NEXT CANDIDATE DESIGN (FEET).
   21     D=D+1.0
          IF(JOUNT.GT.6) GO TO 26
          GO TO 20
   26     WRITE(*,27) B
   27     FORMAT(/,3X,'NO FEASIBLE DESIGNS FOR AUGER DIA. = ',F3.1,
         $  ' FT.',/,3X,'AND DEPTHS UP TO 10.0 FT.',//)
   20     CONTINUE
C    THE NEXT LINE INDICATES THE AMMOUNT THE AUGER DIAMETER
C    SHOULD BE INCREMENTED BY WHEN IDENTIFYING THE NEXT
C    CANDIDATE DESIGN (FEET).
   25     B=B+.5
          IF(I.EQ.5)GO TO 10
          WRITE(*,70)
   70     FORMAT(/,3X,'DEPRESS ENTER KEY FOR NEXT AUGER SIZE')
          READ(*,*)
   10     CONTINUE
          IF(BSAVE.EQ.0.0) GO TO 99
          WRITE(*,19) BSAVE, DSAVE, VSAVE
   19     FORMAT(//,3X,'THE SMALLEST FOOTING THAT WILL WORK',/,3X,
         $  'UNDER THESE CONDITIONS WILL HAVE',/,3X,'DIAMETER = ',F3.1,
         $  ' FT.',/,3X,'DEPTH = ',F4.1,' FT.',/,3X,'VOLUME = ',F5.2,
         $  ' CU.YDS.',/)
   99     WRITE(*,35)
   35     FORMAT(/,3X,'DO YOU WANT TO RUN AGAIN WITH DIFFERENT',/,
         $  3X,'CONDITIONS ?',/,3X,'IF YES, ENTER 5.',/,3X,
         $  'IF NOT, ENTER ANY OTHER INTEGER.',/)
          READ(*,*)LK
          IF(LK.EQ.5)GO TO 39
  108     FORMAT(/,3X,'BAD DATA.  TRY AGAIN.',/)
      END
```

FIGURE 2C. SOURCE CODE FOR CYLINDRICAL FOOTING DESIGN (CONTINUED)

```
      INTEGER LPEN(9)
      DATA GAMMA,C,PHI /120.,1500.,20./
      DATA YMIN,YMAX,DC /0.,.5,150./
   39   WRITE(*,212)
        KTEST=1
          VSAVE=9999999999999999.
  212     FORMAT(/,3X,'IF YOU WANT INFORMATION ABOUT THIS PROGRAM,',/,3X,
     $    'ENTER 5.  OTHERWISE, ENTER ANY OTHER INTEGER.',/)
        READ(*,*)IX
        IF(IX.EQ.5) THEN
            WRITE(*,213)
  213     FORMAT(/,3X,'THIS PROGRAM WILL IDENTIFY THE RECTANGULAR FOOTING'
     $    ,/,3X,'DESIGN THAT USES THE LEAST AMMOUNT OF CONCRETE FROM A',
     $    /,3X,'POPULATION OF CANDIDATE DESIGNS CHOSEN BY THE USER.',/,3X,
     $    'THE USER RESPONDS TO PROMPTS FROM THE PROGRAM TO ENTER THE',/,
     $    3X,'DATA. THE DIMENSIONS OF THE FOOTING ARE INCREMENTED AS'
     $  ,/,3X,'SPECIFIED BY THE USER.  THE FOOTING THAT USES THE LEAST'
     $  ,/,3X,'CONCRETE IS SAVED AND PRINTED OUT AT THE END OF THE RUN.'
     $  ,/,3X,'THE PROGRAM USES THE WIND LOAD EQUATIONS GIVEN IN THE',/,
     $  3X,'SOUTHERN BUILDING CODE FOR 100MPH WINDS.  SOIL STRENGTH IS'
     $  ,/,3X,'COMPUTED USING STANDARD EQUATIONS.  THE PROGRAM CHECKS',/
     $  ,3X,'STABILITY AND LOAD BEARING CAPABILITY OF THE FOOTING TO '/
     $  ,3X,'DETERMINE FEASIBILITY.  THE DENSITY OF CONCRETE ASSUMED',/,
     $  3X,'BY THE PROGRAM IS 150#/CU FT.  IF THE USER WANTS TO JUST',/,
     $  3X,'CHECK A SINGLE DESIGN, THEN MIN AND MAX VALUES SHOULD BE',/,
     $  3X,'CHOSEN EQUAL TO THE DIMENSION BEING CONSIDERED.',/,3X,
     $  'THE INCREMENTS FOR STEPPING THROUGH THE VARIABLES',/,3X,
     $  'WILL HAVE NO EFFECT IN THIS CASE.  ANY NONZERO POSITIVE',/,3X,
     $  'VALUE WILL WORK EQUALLY WELL.',/,3X,
     $  'IF THE DESIGN IS INFEASIBLE, THE PROGRAM WILL STATE THIS.',/)
        WRITE(*,214)
  214   FORMAT(/,3X,'PRESS ENTER KEY TO CONTINUE',/)
        READ(*,*)
        WRITE(*,221)
  221   FORMAT(//,3X,'IN CASES WHERE MORE THAN ONE DESIGN IS TO',/,3X,
     $  'BE CONSIDERED, THE INCREMENT SHOULD BE CHOSEN SO THAT ',/,3X,
     $  'IT DIVIDES WITHOUT REMAINDER INTO THE DIFFERENCE BETWEEN',/,3X,
     $  'THE MAXIMUM AND MINIMUM VALUES.',//)
        WRITE(*,214)
        READ(*,*)
        ELSE
        END IF
        WRITE(*,81)
   81   FORMAT(3X,'YOU MUST ENTER THE HEIGHT ABOVE THE GROUND OF',/,
     $  3X,'THE CENTROID OF THE WIND LOAD (H IN FEET), THE SAFETY',/,3X,
     $  'AGAINST OVERTURN (SF), THE AREA SUBJECTED TO THE WIND LOAD',/,
     $  3X,'(A IN SQUARE FEET), AND THE SHAPE FACTOR FOR THE AREA',/,3X,
     $  'SUBJECT TO THE WIND LOAD (RK3).',//)
   15   WRITE(*,59)
   59     FORMAT(3X,'ALL VARIABLES SHOULD BE ENTERED AS POSITIVE REALS',
        WRITE(*,61)
   61   FORMAT(3X,'ENTER THE HEIGHT ABOVE THE GROUND FOR THE CENTROID',
     $  ,3X,'OF THE WIND LOAD IN FEET',//)
        GO TO 53
   45   WRITE(*,46)
   46   FORMAT(/,3X,'BAD DATA.  TRY AGAIN.',/)
   53   READ(*,*) H

        IF(H.LT.0.0) GO TO 45
        WRITE(*,62)
   62     FORMAT(3X,'ENTER THE SAFETY FACTOR AGAINST OVERTURN',,3X,
     $  'THIS SHOULD BE A REAL NUMBER GREATER THAN 1.',//)
        GO TO 54
   48   WRITE(*,49)
   49   FORMAT(/,3X,'BAD DATA.  TRY AGAIN.',/)
   54   READ(*,*) SF
        IF(SF.LT.1.0)GO TO 48
        WRITE(*,63)
   63     FORMAT(3X,'ENTER THE AREA SUBJECTED TO THE WIND LOAD',/,3X,
     $  'IN SQUARE FEET',//)
        GO TO 43
   57   WRITE(*,55)
   55   FORMAT(/,3X,'BAD DATA.  TRY AGAIN.',/)
   43   READ(*,*) A
        IF(A.LE.0.0) GO TO 57
        WRITE(*,64)
   64     FORMAT(3X,'ENTER THE SHAPE FACTOR FOR THE AREA SUBJECTED',,3X,
     $    'TO THE WIND LOAD',//)
        GO TO 56
   37   WRITE(*,58)
   58   FORMAT(/,3X,'BAD DATA.  TRY AGAIN.',/)
   56   READ(*,*) RK3
        IF(RK3.LE.0.0) GO TO 37
C       THE NEXT LINE GIVES THE SOIL PROPERTIES.  GAMMA IS THE
C       SOIL DENSITY, C IS THE SOIL COHESION, AND PHI IS THE
C       ANGLE OF INTERNAL FRICTION.
        WRITE(*,72)
   72     FORMAT(3X,'THE FOLLOWING DATA IS ASSUMED BY THE PROGRAM',/)
        WRITE(*,65) GAMMA, C, PHI
   65     FORMAT(3X,'THE SOIL DENSITY IN #/CU.FT. IS',2X,F5.1,/,3X,
     $  'THE SOIL COHESION IN PSF IS',2X,F6.1,/,3X,
     $  'THE SOIL ANGLE OF INTERNAL FRICTION IN DEGREES IS',2X,F4.1,/,
     $  3X,'THESE VALUES SHOULD BE CHANGED IN THE PROGRAM IF THEY DO',
     $  /,3X,'NOT CORRESPOND TO THE EXPECTED VALUES IN THE FIELD.',//,
     $  3X,'IF YOU WANT TO CHANGE THESE VALUES, ENTER 5.',/,3X,
     $  'IF THESE VALUES ARE OK, THEN ENTER ANY INTEGER BUT 5.',/)
        READ(*,*) LL
          IF(LL.EQ.5) GO TO 30
        GO TO 31
   30     WRITE(*,32)
   32   FORMAT(/,3X,'ENTER SOIL DENSITY IN #/CU FT.',/)
          READ(*,*) GAMMA
        IF(GAMMA.LE.0.)THEN
            WRITE(*,108)
            GO TO 30
        ELSE
        END IF
  215   WRITE(*,216)
  216   FORMAT(/,3X,'ENTER SOIL COHESION IN PSF.',/)
        READ(*,*)C
        IF(C.LE.0.0)THEN
            WRITE(*,108)
            GO TO 215
        ELSE
        END IF
```

FIGURE 3A. SOURCE CODE FOR RECTANGULAR FOOTING DESIGN

```
  217   WRITE(*,218)
  218   FORMAT(/,3X,'ENTER SOIL ANGLE OF FRICTION IN DEGREES.',/)
        READ(*,*)PHI
        IF(PHI.LE.0.0) THEN
             WRITE(*,108)
             GO TO 217
        ELSE
        END IF
        WRITE(*,12)GAMMA, C, PHI
   12   FORMAT(//,3X,'YOU HAVE CHOSEN ',/,3X,
        $  'SOIL DENSITY = ',F5.1,/,3X,'COHESION = ',F6.1,/,3X,
        $  'ANGLE OF INTERNAL FRICTION = ',F4.1,/
        $  3X,'CHECK TO SEE THAT THESE ARE OK BEFORE CONTINUING.',/,3X,
        $  'IF NOT OK, ENTER 5.  IF OK, ENTER ANY OTHER INTEGER.',/)
        READ(*,*)MM
        IF(MM.EQ.5) GO TO 30
   31   RNPHI=(TAN(.0175*(45.+PHI/2.)))**2
        RK1=GAMMA*RNPHI
        RK2=2.*C*SQRT(RNPHI)
  302   WRITE(*,300)
  300   FORMAT(/,3X,'ENTER THE MAXIMUM WIND SPEED IN MPH.',/,3X,
        $  'CHOICES ARE 90,100,110,120, OR 130.',//)
        READ(*,*)KVEL
        IF((KVEL.LT.90.).OR.(KVEL.GT.130.).OR.(MOD(KVEL,10).NE.0))THEN
             WRITE(*,301)
  301        FORMAT(/,3X,'BAD DATA.  TRY AGAIN.',/)
             GO TO 302
        ELSE
             IF(KVEL.EQ.90)THEN
                  WIND=7.85*(H**.29)
                  IF(WIND.LT.16.7) WIND=16.7
             ELSE
             END IF
             IF(KVEL.EQ.100)THEN
                  WIND=9.69*(H**.29)
                  IF(WIND.LT.20.) WIND=20.
             ELSE
             END IF
             IF(KVEL.EQ.110)THEN
                  WIND=11.72*(H**.29)
                  IF(WIND.LT.24.) WIND=24.
             ELSE
             END IF
             IF(KVEL.EQ.120) THEN
                  WIND=13.95*(H**.29)
                  IF(WIND.LT.29.) WIND=29.
             ELSE
             END IF
             IF(KVEL.EQ.130) THEN
                  WIND=16.38*(H**.29)
                  IF(WIND.LT.34.) WIND=34.
             ELSE
             END IF
        END IF
        WRITE(*,303)KVEL
  303   FORMAT(/,3X,'YOU HAVE SELECTED WIND SPEED = ',I3,' MPH',/,3X,
        $  'IF YOU WANT TO CHANGE THIS, ENTER 5.  IF THIS IS OK,',/,3X,

        $     'ENTER ANY OTHER INTEGER.',//)
        READ(*,*)IQK
        IF(IQK.EQ.5) THEN
             GO TO 302
        ELSE
        END IF
C       THE NEXT LINE COMPUTES THE WIND LOAD IN POUNDS BASED ON THE
C       AREA SUBJECTED TO THE WIND IN SQUARE FEET, AND THE SHAPE FACTOR.
        P=WIND*A*RK3
C       QMAX IS THE ALLOWABLE STRESS IN THE SOIL AT THE BASE OF
C       THE FOOTING.
        QMAX=RK1*DBIG+RK2
  105   WRITE(*,103)
  103   FORMAT(/,3X,'ENTER THE WEIGHT THAT THE FOOTING WILL BEAR.',/,
        $     3X,'UNITS SHOULD BE POUNDS.',/)
        READ(*,*)WEIGHT
        IF(WEIGHT.LT.0.0) THEN
             WRITE(*,104)
  104        FORMAT(/,3X,'BAD DATA.  TRY AGAIN.',/)
             GO TO 105
        ELSE
        END IF
  106   WRITE(*,107)
        WRITE(*,220)
  107   FORMAT(/,3X,'ENTER THE MINIMUM AND MAXIMUM LENGTHS',/,3X,
        $     'FOR THE FOOTING IN THE HORIZONTAL PLANE IN THE DIRECTION',/,3X,
        $  'OF THE MAXIMUM WIND LOAD.  THESE SHOULD BE IN FEET.',/3X,
        $  'ALSO ENTER THE INCREMENT BY WHICH THE PROGRAM SHOULD STEP'
        $     ,/,3X,'BETWEEN THESE VALUES.',/)
  220   FORMAT(/,3X,'THE INCREMENT SHOULD DIVIDE, WITHOUT ',/,3X,
        $  'REMAINDER, INTO THE DIFFERENCE BETWEEN THE MIN AND',/,3X,
        $  'MAX VALUES.  DO NOT CHOOSE ZERO, EVEN IF ONLY ONE',/,3X,
        $  'DESIGN IS TO BE CONSIDERED.  WHEN ONLY ONE DESIGN IS',/,3X,
        $  'TO BE CONSIDERED, MIN AND MAX VALUES ARE THE SAME AND',/,3X,
        $  'ANY NONZERO POSITIVE INCREMENT WILL GIVE THE SAME RESULT.',/)
        READ(*,*)ELMIN,ELMAX,XINCL
        IF((ELMIN.GT.ELMAX).OR.(ELMIN.LT.0.0).OR.(XINCL.LE.0.0)) THEN
             WRITE(*,108)
  108        FORMAT(/,3X,'BAD DATA.  TRY AGAIN.',/)
             GO TO 106
        ELSE
        END IF
  109   WRITE(*,110)
        WRITE(*,220)
  110   FORMAT(/,3X,'ENTER THE MINIMUM AND MAXIMUM WIDTHS',/,3X,
        $     'FOR THE FOOTING IN THE HORIZONTAL PLANE IN THE DIRECTION',/,3X,
        $  'PERPENDICULAR TO THE MAXIMIMUM WIND LOAD.',/,3X,
        $  'THESE SHOULD BE IN FEET.  ALSO ENTER THE INCREMENT BY',/,3X,
        $     'WHICH THE PROGRAM SHOULD STEP BETWEEN THESE VALUES.',/)
        READ(*,*)BMIN, BMAX,XINCB
        IF((BMIN.GT.BMAX).OR.(BMIN.LT.0.0).OR.(XINCB.LE.0.0)) THEN
             WRITE(*,108)
             GO TO 109
        ELSE
        END IF
  111   WRITE(*,112)
        WRITE(*,220)
```

FIGURE 3B. SOURCE CODE FOR RECTANGULAR FOOTING DESIGN (CONTINUED)

```
112     FORMAT(/,3X,'ENTER THE MINIMUM AND MAXIMUM DEPTHS FOR THE',/,
     $    3X,'BOTTOM OF THE FOOTING.  THESE SHOULD BE IN FEET.',/,3X,
     $  'ALSO ENTER THE INCREMENT BY WHICH THE PROGRAM SHOULD STEP',/,
     $    3X,'BETWEEN THESE TWO VALUES.',/)
     READ(*,*)DBMIN,DBMAX,XINCDB
     IF((DBMIN.GT.DBMAX).OR.(DBMIN.LT.0.0).OR.(XINCDB.LE.0.0)) THEN
          WRITE(*,108)
          GO TO 111
     ELSE
     END IF
113  WRITE(*,114)
     WRITE(*,220)
114     FORMAT(/,3X,'ENTER THE MINIMUM AND MAXIMUM DEPTHS FOR THE',/,
     $    3X,'TOP OF THE FOOTING.  THESE SHOULD BE IN FEET.',/,3X,
     $  'ALSO ENTER THE INCREMENT BY WHICH THE PROGRAM SHOULD STEP',/,
     $    3X,'BETWEEN THESE TWO VALUES.',/)
     READ(*,*)DSMIN,DSMMAX,XINCDS
     IF((DSMIN.GT.DSMMAX).OR.(DSMIN.LT.0.0).OR.(XINCDS.LE.0.0)) THEN
          WRITE(*,108)
          GO TO 113
     ELSE
     END IF
115     WRITE(*,116)
116     FORMAT(/,3X,'ENTER THE MINIMUM THICKNESS FOR THE FOOTING',/,3X,
     $  'IN THE VERTICAL PLANE.',/,3X,
     $    'THIS SHOULD BE IN FEET.',/)
     READ(*,*)CPHMIN
     IF(CPHMIN.LT.0.0) THEN
          WRITE(*,108)
          GO TO 115
     ELSE
     END IF
     TEST2=1./(2.*SF)
     EL=ELMIN
206  B=BMIN
204  DSMALL=DSMIN
201  DBIG=DBMIN
202  X=EL/B
     W=P*(H+DSMALL)
     CAPH=(DBIG-DSMALL)
     U=DC*(CAPH)+DSMALL*GAMMA
     Z=(EL*B*(U)+WEIGHT)
     V=W/EL
     Y=V/Z
     IF(Y.GE..1666667) THEN
          Q=2.*Z/(3.*B*((EL/2.)-W/Z))
     ELSE
          Q=U+WEIGHT/(EL*B)+6.*W/(EL*EL*B)
     END IF
     ITEST=0
     IF(Q.GT.QMAX) THEN
          LPEN(1)=1
     ELSE
          LPEN(1)=0
     END IF
     IF(Y.GT.TEST2) THEN
          LPEN(2)=1

     ELSE
          LPEN(2)=0
     END IF
     IF((Y.LT.YMIN) .OR. (Y.GT.YMAX)) THEN
          LPEN(3)=1
     ELSE
          LPEN(3)=0
     END IF
     IF(X.LT.1.0) THEN
          LPEN(4)=1
     ELSE
          LPEN(4)=0
     END IF
     IF((EL.LT.ELMIN) .OR. (EL.GT.ELMAX)) THEN
          LPEN(5)=1
     ELSE
          LPEN(5)=0
     END IF
     IF((B.LT.BMIN) .OR. (B.GT.BMAX)) THEN
          LPEN(6)=1
     ELSE
          LPEN(6)=0
     END IF
     IF((DBIG.LT.DBMIN) .OR. (DBIG.GT.DBMAX)) THEN
          LPEN(7)=1
     ELSE
          LPEN(7)=0
     END IF
     IF((DSMALL.LT.DSMIN) .OR. (DSMALL.GT.DSMMAX)) THEN
          LPEN(8)=1
     ELSE
          LPEN(8)=0
     END IF
     IF(CAPH.LT.CPHMIN) THEN
          LPEN(9)=1
     ELSE
          LPEN(9)=0
     END IF
     DO 100 II=1,9
     IF(LPEN(II).EQ.1) THEN
          ITEST=1
     ELSE
     END IF
100  CONTINUE
     IF(ITEST.EQ.0) THEN
          VOLUME=EL*B*CAPH/27.
               IF(VOLUME.LT.VSAVE) THEN
                    VSAVE=VOLUME
                    BSAVE=B
                    DSSAVE=DSMALL
                    DBSAVE=DBIG
                    ELSAVE=EL
                    HSAVE=CAPH
                    KTEST=0
               ELSE
               END IF
     ELSE
```

FIGURE 3C. SOURCE CODE FOR RECTANGULAR FOOTING DESIGN (CONTINUED)

```
      END IF
      DBIG=DBIG+XINCDB
      IF(DBIG.GT.DBMAX) THEN
            GO TO 203
      ELSE
            GO TO 202
      END IF
  203   DSMALL=DSMALL+XINCDS
      IF(DSMALL.GT.DSMMAX) THEN
            GO TO 205
      ELSE
            GO TO 201
      END IF
  205     B=B+XINCB
      IF(B.GT.BMAX) THEN
            GO TO 207
      ELSE
            GO TO 204
      END IF
  207   EL=EL+XINCL
      IF(EL.GT.ELMAX) THEN
            GO TO 208
      ELSE
            GO TO 206
      END IF
  208   IF(XTEST.NE.0) THEN
            WRITE(*,211)
  211       FORMAT(/,3X,'NONE OF THE CANDIDATE DESIGNS WILL WORK.',/
     $      ,3X,'TRY A RUN WITH LARGER MAXIMUM VALUES IF POSSIBLE.',/)
      ELSE
  210       WRITE(*,209)DBSAVE,ELSAVE,BSAVE,HSAVE,DSSAVE,VSAVE
  209       FORMAT(/,3X,'OF THE CANDIDATE FOOTINGS, THE ONE THAT WOULD USE',
     $      /,3X,'THE LEAST CONCRETE WOULD HAVE THE FOLLOWING DIMENSIONS.',
     $      //,3X,'DEPTH FROM GRADE TO BOTTOM OF FOOTING = ',F4.1,1X,'FT',/
     $  ,3X,
     $      'LENGTH OF FOOTING IN HORIZONTAL PLANE IN DIRECTION OF MAXIMUM',
     $  /,3X,'WIND LOAD = ',F4.1,1X,'FT',/,3X,
     $      'WIDTH OF FOOTING IN HORIZONTAL PLANE IN DIRECTION',/,3X,
     $      'PERPENDICULAR TO MAXIMUM WIND LOAD = ',F4.1,1X,'FT',/,3X,
     $      'THICKNESS OF FOOTING IN VERTICAL PLANE = ',F4.1,
     $  1X,'FT',/,3X,
     $      'DEPTH FROM GRADE TO TOP OF FOOTING = ',F4.1,1X,'FT',/,3X,
     $  'VOLUME OF CONCRETE IN FOOTING = ',F5.1,1X,'CU YDS',/)
      END IF
   99   WRITE(*,35)
   35   FORMAT(/,3X,'DO YOU WANT TO RUN AGAIN WITH DIFFERENT',/,
     $  3X,'CONDITIONS ?',/,3X,'IF YES, ENTER 5.',/,3X,
     $  'IF NOT, ENTER ANY OTHER INTEGER.',/)
        READ(*,*)LX
        IF(LX.EQ.5)GO TO 39
      END
```

FIGURE 3D. SOURCE CODE FOR RECTANGULAR FOOTING DESIGN (CONTINUED)

1986 USAF-UES SUMMER FACULTY RESEARCH PROGRAM

Sponsored by the

AIR FORCE OFFICE OF SCIENTIFIC RESEARCH

Conducted by the

Universal Energy Systems, Inc.

FINAL REPORT

Analysis of Tracking Radar for Error Reduction/and Seminar Series

Prepared by:	Jeremy Jones
University:	University of South Florida
Department:	Computer Science and Engineering
Research Location:	Directorate of Computer Sciences,
	Applied Mathematics Laboratory (AD/KR)
	Eglin Air Force Base
USAF Research:	Mr. Ken Cranford
Appointment Dates:	May 19 through July 29, 1986

Analysis of FPS Tracking Radar for Error Reduction and Modeling

by

Jeremy C. Jones

ABSTRACT

This report deals with the problems of understanding and reducing errors in range, azimuth and elevation of the FPS-16 precision tracking radar systems, in use at Eglin Air Force Base for detailed mission analysis. Low elevation angles involve more difficult error reduction due to a large, complex error involving multipath interference, and refraction. High refraction gradients of warm humid Gulf air mass edges, give a larger random component of refractive errors than at many of our (often desert) Air Force bases. A method is conjectured to reduce these refraction errors. Correlations between measured parameters and calibrated errors were found which permit preprocessing or real-time direct error reduction. For instance a strong correlation between range and the low frequency component of elevation error was found. Another form of correlation which was less directly useful for error reduction, but tended to give insight into FPS-16 functional parameters and performance limits, was a causal link between two or more types of error, e.g. between range error and azimuth error. Because of velocity/acceleration influence on radar errors, the first and second derivatives were considered in the analysis. Twelve technical seminars were also given on those areas thought to be most directly usable to Eglin AFB math and computer science personnel.

Table of Contents

10. Local Area Networks: Ethernet, Wangnet and Token Ring nets

11. Back of the Envelope Computer Performance Estimates

12. More detailed modeling of System Throughput and Turnaround

6. References

1. The Need for Analysis

It seems essential for our survival in an increasingly sophisticated hostile environment that we continue to make our weapons smarter. A distinct limit and potential bottleneck in this evolution toward artificial intelligence is radar precision and measurement accuracy. This is so because of the need for feedback information in the control system itself, and also in the testing and refinement of devices and algorithms as we seek to correct and improve them.

The high frequency tracking radars provide much of this detailed feedback needed to improve our control systems. A reduction of these tracking radar errors is the principle effort of this report.

2. Computer Software Tools Developed for This Analysis

To make it clearer to see low frequency correlations, a variable window, smoothing filter was used on all data. Because of the coarse nature of range measurements, this became important for removing the large range quantization error found during analysis. For example, the computed correlation coefficient between range error and azimuth error was roughly doubled when range data was smoothed in the correlation.

a. Smoothed Auto-Scaled Multi-Graph with Derivatives

A number of analytical computer program tools were developed for dealing with these questions. The most heavily used tool was a program to automatically scale and graph simultaneously all of the basic seven radar track parameters and their first and second derivatives, with a variable smoothing window. These seven mission parameters were range, azimuth, elevation, range-error, azimuth-error, elevation-error and spherical error.

This sliding window, used in performing the noise smoothing, was effectively used as a frequency filter. It was stepped through a range of values in the output, so that a sampling of frequency ranges could be examined in the data. This program was applied at least once to all of the (representative) data from several Pad-21 and Pad-23 tracking missions.

b. Data Scattergram with Smoothed Correlation Coefficient

Of special interest were error correlations with measured variables which could be directly used to reduce radar error. As a preliminary tool to identify likely relationships, a computer program was written. This program automatically scales and sorts the point pairs of any two selected radar parameters in descending vertical order for display on a non-reversing printer. The output from this program is a scatter diagram relating any two chosen parameters. The input to the program was several missions from Pad-21 and Pad-23 FPS-16 tracking radar.

This autoscaled scattergram program also permitted selection of first or second derivative of any radar variable, as well as adjustable amounts of data smoothing. This turned out to be essential in seeing several important relationships, since in some cases a correlation would be with a derivative (e.g. high frequency component of elevation error vs derivative of elevation), and in some cases smoothing was vital to see through quantization (i.e. coarse measurement) error (e.g. range-error vs azimuth-error correlation).

c. Autoscaled Correlation Coefficient vs. Phase Shift

Another tool was developed for two reasons: to confirm tentative hypothesis regarding relationships between parameters, and also to check for the possibility of a delay or phase shift in the effect of one variable on another. This program automatically scaled and graphed the correlation coefficient between any two radar parameters as a function of phase shift between the two variables. This program provided reassuring output in the form of a strong peak in correlation coefficient at zero phase, for strongly correlated variables, confirming the immediacy of their functional dependence.

A number of linearizing transformations were provided to test for a limited number of forms of non-linear correlations. These seemed unnecessary after eyeballing the data and so were used only initially, and then dropped.

This program provides a facility similar to the autocorrelation

function used for pattern matching (e.g. target recognition). But in this program the feature being matched is either an increasing or decreasing monotonic relation, covered by noise.

d. Fourier Transform of All Radar Track Variables

Because certain correlations seemed to be cyclic, a program was written to display the Fourier transform of any radar track parameter. The peaks in this output, taken over all seven variables over several missions, did not seem prominent enough to warrent further analysis in this regard.

3. The Results and Their Applications

a. Directly Usable Correlations

Directly usable correlations would most simply involve using a linear adjustment to radar data, whose slope and y-intercept came from the linear fit of the error to a correlated observed variable.

i. Range vs. Low Frequency Component of Elevation Error

The strong low frequency correlation between elevation error and range, could have indicated a more fundamental relation between elevation and elevation-error. This is because the missions were flown at constant altitude wherein elevation and range are related by the sine function: sine(elevation) = altitude/range. In any event, this correlation provides a direct reduction in the slowly varying part of elevation error. In its simplest form this correction could involve the addition to elevation of a

correction computed from each range value. This correction would just be a linear function of range data whose range and bias are from the linear regression between range and elevation-error.

ii. Elevation-Error vs Derivative of Elevation Correlation

The scatterdiagram showed a strong correlation between elevation-error and the first derivative of elevation data. This relation is immediately usable since differences of the elevation data may then be used for self-correction of the elevation data. The slope and y-intercept of this strong correlation were: m=-8.8E-4 and b=-0.17 where the time derivative was approximated in units of degrees of arc per second of time. Thus to apply the above correction, one would have to multiply the change in elevation per second by -8.8E-4, add this value to -0.17, and then add the result into elevation as a correction.

Note that the elevation-error/elevation-derivative correlation involved high frequency components of elevation error, while the elevation-error/range(elevation) correlation provided a tool to remove much of the very low frequency component of elevation error. So these should be regarded as two separately applied corrections to elevation error.

It would clearly be safer to use best fit coefficients for each individual radar installation periodically to calibrate, which would then automatically include systematic error calibration corrections. Then the standard installation dependent systematic errors, such as droop error, zero-set, and mis-level error could be included along with this dynamic term, by curve fitting.

b. Results Whose Application is Less Direct

i. Strong Correlation Between Range Error vs Azimuth Error

The very strong correlation between range-error and azimuth-error seemed accounted for by the main radar pulse beam width and shape in the following way: If we assume a return pulse trigger threshhold intensity of I0, then as the antenna moves beam center off the target, the small but non-zero rise time of the beam edge will be noticed as a delay in intensity reaching this trigger threshhold. Of course this delay will appear as an increase in target range, since range is measured by the time between transmitted pulse and triggering on the return beacon pulse.

We should note that this effect may appear doubled as a beacon trigger delay plus a delay in the misaligned receiving antenna. This predicted error in range for slightly off target radar pulse was observed in my analysis as a very strong correlation between range-error and azimuth-error. These errors were provided as differences of the radar data from reference cinetheodolite readings, and was regarded as reliable, particularly given the redundant overdetermination in the camera data.

ii. Weaker and Less Consistent Relationships in the Data

The above relations were distinct and unmistakable. Other seeming relations were more tenuous, and so did not seem very usable.

4. Methods for Improving Track Radar Accuracy

In addition to the above simple dynamic and calibration corrections, the following more sophisticated (and expensive) corrections might prove useful:

a. Real-time Elevation and Azimuth Refraction Correction

Given our location on the Gulf of Mexico, relatively discontinuous interfaces between moist and dry air masses are common. This large ambiant humidity gradient is associated with a gradient of radar index of refraction. This gradient can give rise to large angle errors, even to the extent of "evaporation ducts" in which the refractive radius of curvature equals or exceeds the radius of curvature of the Earth (see [Meeks] pages 4-13).

"Evaporation ducts" and other vertical refraction effects are usually described as a modified Earth radius in the radar range equation (e.g. the familiar 4/3 Earth radius "standard" correction). This is convenient in two respects: It directly relates to (possibly over the horizon) increased range. And the general physica expression for refraction is usually expressed as a change of direction (radians) per unit distance (called rate of curvature), whose reciprocal is radius of curvature. In applying this to an Earth radius correction, we must subtract the rate of radar beam direction change, from the rate of earth surface change per unit distance. This is because we can add or subtract rates, but not radii.

We currently use a weather balloon to sample the atmospheric pressure, P, temperature, T and (indirectly) partial pressure of

water vapor, C, needed to calculate the refractive error of our radar beams ([Meeks] page 4: n=1+77.6(P/T)+3.73xE5(C/T^2)xE-6). But this is static data taken well before or after each mission. Particularly in our humid climate the refractive error can vary substantially over a time of seconds at the edge of a humid air mass. Thus since refraction tends to be a substantial error correction, continuous correction for refraction would often provide a large improvement in tracking accuracy (see [Meeks] page 11, radius of curvature refractive variation frequency for Canada).

Since refraction varies with frequency (this variation is called dispersion), refraction will cause a high frequency radar beam to be bent through a different angle than a low frequency beam. And the (smaller) difference between the bending at different frequencies is functionally dependent on the (much larger) total bending (azimuth or elevation errors). Thus if we had access to a wide enough range of frequencies, the observed dispersion would give us a measure of refraction which could then be corrected.

The articulation of the quarter-microsecond, half-microsecond or full microsecond FPS-16 main pulse contains a range of frequencies given by the Fourier transform of the pulse shape (the rise time and pulse duration roughly give the approximate highest and lowest frequency components). These highest and lowest frequency components will be refracted by different angles (dispersion), this angular difference depending on total refraction.

For skin tracking the difference is cancelled on return except for different frequencies striking different parts of the target, and seeing different target scattering cross-sections. Hence a statistically characteristic pulse deformation might be identified with a given target. But this would be a subtle and difficult way to attempt refraction correction.

But we generally use beacon tracking in our testing missions. In this case beacon pulse articulation would be reshaped through dispersion, a function of refraction. Thus in principle refraction could be measured, and hence corrected, in real time by return beacon pulse distortion. In principle the beacon return pulse would have a horizontal and a vertical distortion, from which an azimuth and elevation correction could be made, respectively. Of course, the available frequency range is limited to those frequencies high enough for tracking, and low enough to penetrate weather, and have other desirable characteristics. We should note that the FPS-16 one microsecond pulse has more low frequency content than the half or quarter-microsecond pulse. And given the same pulse rise time, their highest frequency components are similar.

In any event it is exciting to conjecture that at least in principle, these large and varying refractive corrections are correctable in real time. Of course the electronic filtering required to see this level of pulse distortion may be beyond our present equipment bandwidth/noise characteristics.

b. Beam Shape Improvements through Range/Azimuth Correlation

Because of the extremely strong and reliable correlation between observed range-error and observed azimuth-error, a synthetic beam tightening might be achieved. Thus range information could be improved by observing variations in azimuth, or vice versa.

Alternatively, if the effect is due to power reduction as a target moves off beam center (azimuth error), then this correlation provides an indirect measure of pulse beam width.

5. Summary of the Twelve Summer Seminar Series at Eglin AFB

An effort was made to select these seminar topics for their direct relevance and usefulness as much as possible, given the type of work being done at Eglin Air Force Base. Each seminar was a very accelerated exposure to the given subject, as necessary in the short summer period of the SFRP. The seminar started with motivating why the particular subject was important to Eglin AFB and useful in a person's career, and where it might be used. Then a theoretical framework was given to help people relate to and remember the material. After this the detailed subject matter was covered, followed by examples, and finally a summary and scenario of impact where appropriate. Separate seminars on the following topics were given:

1. Reduced Instruction Set Computer Systems

   The Berkeley RISC-1 reexamination of instruction set tradeoffs given limited VLSI area was examined. Particularly the elegant use of sliding register windows for local context swapping (e.g. subroutine call/return) was given as a chip

area tradeoff compromise, given subroutine use (abstraction) in typical programming. The IBM 801 and Stanford MIPS RISC projects were described, and RISC advantages/disadvantages were given to help identify application niches.

2. Inexpensive Parallelism through Multimicro Computers

   Gene Amdahl's serial bottleneck law was the context for discussing parallel computer processing in general, and the new multimicro computers in particular. The Cray series of supercomputers was described as more general purpose than other supercomputers, primarily for their unmatched scalar mode speed, minimizing the damage of Amdahl's law, especially faced with non-vectorizable computation. The various Crayettes were discussed as less-expensive options.

3. Information Theory and Shannon's Magical Theorem

   Shannon's theorem was motivated as suggesting a way to penetrate jamming, or pass information through other noise. Shannon's theorem states that given sufficiently clever encoding, the chance of a transmission error may be made arbitrarily small, so long as the required data rate is less than the channel capacity. It was attempted to relate this to radar pulse bandwidth, and possible ECM applications.

4. Linear Block Codes for Error Detection and Correction

5. Designing Linear Cyclic Codes to See Through Given Noise

   Methods for designing error-correcting codes for a wide variety of noise levels were given. Here the noise must be random (i.e. additive white Gaussian noise). Burst errors were mentioned, but not treated in any sufficient depth.

6. Convolutional Error Control Codes

7. The Philosophy and Syntax of ADA: Software Engineering

   Evidence was given of a severe software crisis, and features of ADA were introduced as attempts to deal with this crisis. For instance, the ADA feature of enforced abstraction by separating the specification and body of a package was treated more as a management tool and a design tool than a programmer tool. Use of the various predefined data types was illustrated, and an example of indexing aircraft speeds over a programmer-defined aircraft enumerator type was given to suggest to the predominantly FORTRAN programmers in attendance how natural and readable an ADA program can appear.

8. Real Time Task and Exception management in ADA

   Exception handling was illustrated as a tool for enhancing reliability, and the task rendezvous as a parallelism tool to increase real-time performance.

9. Wide Area Networks: HDLC in ARPANET/DDN protocols,SNA & DNA

10. Local Area Networks: Ethernet, Wangnet and Token Ring nets

11. Back of the Envelope Computer Performance Estimates

12. More detailed modeling of System Throughput and Turnaround

6. References

1. Brunt, Leroy B. 1984. The Glossary of Electronic Warfare. Dunn Loring, VA: EW Engineering.

2. Meeks, M.L. 1982. Radar Propagation at Low Altitudes. Dedham, MA: Artech House.

3. Tagliaferro, Wm. 1986. Trajectory Estimate and Engineering

Parameter Computation. Sunnyvale, CA: Computer Sciences Corporation.

4. Toomay, J.C. 1982. Radar Principles for the Non-Specialist. Belmont, CA: Lifetime Learning Publications

1986 USAF-UES SUMMER FACULTY RESEARCH PROGRAM

GRADUATE STUDENT SUMMER SUPPORT PROGRAM

Sponsored By

AIR FORCE OFFICE OF SCIENTIFIC RESEARCH

Conducted By

UNIVERSAL ENERGY SYSTEMS, INC.

FINAL REPORT

ORGANOPHOSPHATE INHIBITORS: REPEATED LOW DOSE EFFECTS OF DIISOPROPYFLUROPHOSPHATE ON SEROTONIN RECEPTORS IN RAT CORTEX

Prepared By: Betty Ruth Jones, Ph.D.

Academic Rank: Associate Professor of Biology
Director of the Institute of Electron Microscopy
Director of the Scanning Electron Microscopy Research Laboratory

Department and University: Department of Biology
Morehouse College

Research Location: Brooks Air Force Base School of
School of Aerospace Medicine
Crew Technology Division
San Antonio, Texas 78235-5301

USAF Research Collaborator: Major Judith Greenamyer, DVM

Date: November 20, 1986

Contract Number: F49620-85-C-0013

ORGANOPHOSPHATE INHIBITORS: REPEATED LOW DOSE EFFECTS OF DIISOPROPYLFLUROPHOSPHATE ON SEROTONIN RECEPTORS IN RAT CORTEX

BY

Betty Ruth Jones, Ph.D.

ABSTRACT

The proposed study will apply biochemical and morphological procedures to investigate repeated low dose effects of diisopropyl-fluorophosphate (DFP) on serotonin receptors in the cortical areas of rat brain. We propose to determine whether there is a reduction in the number, alteration in concentration and binding of serotonin$_1$ (S_1) or (5-HT_1) and serotonin$_2$ (S_2) or (5-HT_2) receptors following repeated low doses of DFP. The proposed study will further determine if there are morphological alterations in presynaptic and postsynaptic membranes; and innervating serotonergic fibers of the cortex of rats following DFP administration.

The methods of approach will inlcude the following: Biochemical Receptor Binding Assays, Scanning Electron Microscopy, Transmission Electron Microscopy and Fluorescent Immunohistochemistry using Light Microscopic methods. Such studies are significant in better understanding structural-functional and neurobiochemical mechanisms of serotonin receptors and drug interactions (i.e., effects of DFP on serotonin receptors).

ACKNOWLEDGEMENTS

I am indebted to the Air Force Systems Command, the Air Force Office of Scientific Research and Brooks Air Force Base, Veterinary Sciences Division, Veterinary Pathology Branch in San Antonio, Texas (Summer, 1985) and the Crew Technology Division (Summer, 1986) for providing me with the opportunity of further advancing and expanding my research interest. The summer faculty research program sponsored by the Air Force Office of Scientific Research and conducted by Universal Energy Systems has not only enhanced my research capabilities but has provided me an opportunity for follow-on-research at my home institution. In my opinion this is one of the most exciting and attractive components of the program.

Please refer to the final report from last summer for acknowledgements for the summer of 1985. For the current summer (1986), I would like to express sincere appreciation to the Crew Technology Division at Brooks Air Force Base for a productive summer that allowed me to learn biochemical procedures and do an extensive library search for the preparation of a research proposal to be submitted to the USAF. I am grateful to Dr. Judith Greenamyer for going beyond the call of duty to make my research visit a good and productive one. I wish to thank Don, research associate with Dr. Greenamyer for his novel and well organized biochemical procedures and good sense of humor during the course of the project. Many thanks are extended to Dr. Brice Hartman for his motivating, stimulating and encouraging remarks throughout the summer and other researchers and staff members at Brooks that made my stay a pleasant one.

I also wish to acknowledge the support and assistance of Dr. William Carter Alexander, Chief and Research Director of the Crew Technology Division, and Dr. West Baumgardener, Chief of the Chemical Defense Brance.

With sincere gratitude I am pleased to acknowledge Mr. Rodney Darrah and Ms. Sue Espy of Universal Energy Systems for their patience and support during my two summers at Brooks AFB. A special thanks is extended to Ms. Debbie Withers whose sincere dedication, enthusiasm and concern for the faculty and student fellows goes beyond the call of duty. I commend her for the good job she is implementing at Universal Energy Systems. Finally, I wish to thank Major Amos Otis, Program Manager at the Air Force Office of Scientific Research for his assistance throughout the program and for his motivation and positive interactions with faculty members at Morehouse College.

I. INTRODUCTION

The following is a brief account of background information on the summer faculty fellow.

A. EDUCATION:

Institute and Location	Degree	Year Conferred	Field of Study
1. Rust College, Holly Springs, MS	B.S.	1973	Biology
2. Atlanta University Atlanta, GA	M.S.	1975	Cell Biology and EM
3. Atlanta University Atlanta, GA	Ph.D.	1978	Parasitology and EM
4. Morehouse College Atlanta, GA	Post-Doc.	1978-1979	Cell Biology, Parasitology and EM
5. Harvard School of Public Health Boston, MA	Post-Doc.	1981-1983	Med. Parasit., Trop. Med. & EM
6. Mary Ingrahm Bunting Inst. (Radcliffe) Cambridge, MA	Post-Doc.	1981-1983	Med. Parasit., Trop. Med. & EM
7. Brooks Air Force Base San Antonio, TX	Post-Doc.	1985 Summer	Neurobiology (Brain Tumor Pathology)
8. Brooks Air Force Base San Antonio, TX	Post-Doc.	1986 Summer	Nerve Gas Inhibitors

Because of the page stipulations of this report, complete publication citations can be found in the submitted research proposal to the USAF. The faculty fellow has published 2 books in Electron Microscopy; published 20 research publications in reputable scientific journals; made 36 oral presentations at local, state, national and international conferences (overseas and in the United States) and implemented 5 Electron Microscopy workshops.

B. NATURE OF USAF RESEARCH AREA WHICH RESULTED IN A LABORATORY ASSIGNMENT

This is the second productive research assignment for the faculty fellow at Brooks Air Force Base. The first assignment (Summer 1985) took place in the Veterinary Sciences Division and Veterinary Pathology Branch of the Electron Microscopy Unit at Brooks AFB. The final report from this research consisted of a comprehensive and detailed 116 page final report with numerous electron micrographs of Brain Tumors developed in Macaca mulatta following exposure to proton radiation. This research collaboration was with Dr. Harold Davis, Chief of the Veterinary Sciences Pathology Branch.

The current research collaboration (Summer 1986) with Dr. Judith Greenamyer in the Crew Technology Division at Brooks AFB proved to be just as productive. Since the current faculty fellow has had more than 15 years of training and experiences in electron microscopy techniques, it was the primary goal of the faculty fellow and USAF collaborators (i.e., Dr. Judith Greenamyer, Dr. Brice Hartman, and Dr. William Carter Alexander) that the current research experience would consist of part laboratory training on techniques other than electron microscopy and extensive library work for the preparation of a research proposal to be submitted to the USAF. Thus, the faculty fellow spent half of the summer learning biochemical procedures and techniques from Dr. Greenamyer and half of the summer doing extensive library work for the preparation of a research proposal to be submitted to the USAF.

The ongoing research and training that I have received at Brooks AFB the last two summers is very much in accord with my research interests and goals. My area of research specialization in Biology

is concerned with problems in Cell Biology and Parasitology using Electron Microscopy and Biochemical techniques as a tool for investigating structural-functional mechanisms. The research problems I have investigated as a faculty fellow at Brooks AFB fall into the discipline of Cell Biology.

II. OBJECTIVES OF THE RESEARCH EFFORT

NOTE TO THE REVIEW COMMITTEE: This progress report is a continuation research training and library work implemented by the faculty fellow this current summer. It is in part a brief account of a research proposal o be submitted to the mini-grant program of USAF. The ideals for the report were developed by the faculty fellow and the effort focal point collaborator, Dr. Judith Greenamyer.

A. SPECIFIC OBJECTIVES:

The proposed study will apply biochemical and morphological procedures to investigate repeated low dose effects of diisopropyl-fluorophosphate (DFP) on serotonin receptors in the cortical areas of rat brain. We propose to determine whether there is a reduction in the number, alteration in concentration and binding of serotonin$_1$ (S_1) OR ($5\text{-}HT_1$) and serotonin$_2$ (S_2) or ($5\text{-}HT_2$) receptors following repeated low doses of DFP. The proposed study will further determine if there are morphological alterations in presynaptic and postsynaptic membranes; and innervating serotonergic fibers of the cortex following DFP administration. Thus, the specific aims of this project are as follows:

1) To determine whether there is a reduction in the number, concentration and binding of S_1 and S_2 receptors following low doses of DFP.

2) To determine whether there are morphological alterations in presynaptic and postsynaptic membranes; and innervating serotonergic fibers of the cortex.

3) To determine which neurons and innervating fibers of the cortex are serotonergic and what is their central, peripheral and terminal field of aborization(s) in control (untreated) and experimental (drug-treated) tissues using light microscopy fluorescent immunohistochemistry.

4) To continue the research at Morehouse College by submitting a research proposal to the mini-grant program of Universal Energy Systems, Inc. under the auspices of the USAF.

III. INTRODUCTION

Most organophosphates are irreversible inhibitors of acetylcholinesterase. They hinder the degradation of acetylcholine released at central or peripheral cholinergic synapses. In sufficient concentrations, they may give rise to a cholinergic crisis, leading to very severe acute intoxications, manifested in man by diverse muscarinic and nicotinic symptoms and central nervous system effects: drowsiness, coma, convulsions (Koller and Klawans 1979).

Acute organophosphate poisoning may also cause intellectual and psychiatric sequelae, which may be transient or last several months (Namba et al. 1971; Sidell 1974). Only certain organophosphates are known to produce a delayed neuropathy (Abou-Donia, 1981).

Sustained exposure to low levels of organophosphates may lead to electroencephalographic alterations, insomnia, neurobehavioral abnormalities, disorders of memory and concentrations, and to

psychiatric sequelae (Gershon and Shaw, 1961; Dille and Smith, 1964; Korsak and Sato, 1977; Duffy et al., 1979).

Serotonin receptors have been extensively studied using both radioligand binding techniques and physiological preparations. Serotonin elicits both synaptic inhibition and excitation in the brain (Roberts and Straughan, 1967; Boakes et al., 1970; Bramwell and Gonye, 1973; Haigler and Aghajanian, 1974). Increased concentrations of serotonin in the brain result in a behavioral hyperactivity syndrome with head twitching, resting tremor and hypertonicity (Grahame-Smith, 1971; Corne et al., 1963).

After an extensive review of the literature, no pertinent published papers could be found showing the effects of the organophosphate inhibitor, DFP on serotonin receptor number, concentration and binding in rat brain cortex. Moreover, no morphological data could be found showing the effects of DFP on pre- and post-synaptic membranes and innervating serotonergic fibers and cortical tissue. An abstract by Barnes et al. 1975 indicated that AFP affects rabbit brain serotonin. These investigators reported that DFP increased the levels of serotonin. These studies did not shed any light on serotonin receptors. Thus, it is the aim of our proposal to investigate the affects of DFP on serotonin receptors.

IV. EXPERIMENTAL DESIGN AND METHODS

NOTE: The experimental design for the research proposal to be submitted is carefully being developed by the following:

ROLES OF PARTICIPANTS IN THE PROJECT:

DR. BETTY JONES, Summer Faculty Fellow will serve as Principal Investigator (PI) for the project. Dr. Jones will carry out the electron microscopy component of the research.

DR. EVAN WILLIAMS, Assistant Professor of Pharmacology, Department of Pharmacology, Morehouse School of Medicine, Atlanta, Georgia, will be responsible for carrying out the biochemical assays (i.e., receptor binding assays for serotonin). Dr. Williams will serve as co-investigator for the project.

DR. JEANNE STAHL, Professor of Psychology, Department of Biology, Morris Brown College, Atlanta, Georgia, will serve as co-investigator on the project. She will be responsible for surgery of the animals and anatomical identification of cortical regions.

DR. CYRIL MOORE, Professor of Biochemistry, Morehouse School of Medicine, Atlanta, Georgia, will serve as a consultant for the project.

A Curriculum Vita of each investigator will be placed in the Appendix of the proposal.

The methodology presented in the progress report is subject to modification by the given participants of this project. Thus, the methodology utilized is standard and according to McDonald, Stancel and Enna 1984, (i.e., biochemical procedures) and the methods of Jones (1985) are used for the electron microscopy component of the project. The methods and procedures described below are a brief summation of procedures.

A. Drug Treatment of Animals

Female Sprague-Dawley rats weighing 150-200g will be used in this study. A total of 100 rats will be utilized and during the entire course of the study (50 control and 50 experimental animals). Five rats will be housed in each cage with food and water. The rats will be exposed to a 12 hour light and dark cycle. The drug DFP will be administered in low doses for five consecutive days. Note: The LD_{50} level has already been determined in other studies for this compound (See Review of Literature).

B. Behavioral Tests

Serotonin activity will be measured 24 or 48 hours after the last injection of DFP. This will be according to the wet-dog behavior induced by the administration of 1,5-hydroyxtryptophan (5-HTP; Bedard and Pycock, 1977; Yap and Taylor, 1983). Dr. Stahl will implement these studies.

C. Receptor Binding Assays

Following the behavioral tests, animals will be decapitated and the brains rapidly removed, dissected on ice and stored at $-20^{o}C$ until assayed. The binding of both 5-HT_2 and 5-HT_1 receptors will be analyzed using established procedures (Peroutka and Synder, 1979; Bennett and Synder, 1976) with modifications according to Williams (1985).

Briefly, 5-HT_2 receptor binding will be assayed by incubating the brain membranes with 0.3 nM [3H]spiroperidol (29 Ci/mmol). Specific 5-HT_2 binding will be defined as the amount of labelled spiroperidol displaced in the presence of 100 uM cinanserine. For saturation studies, specific binding will be assayed over a range (0.2-10 nM) of concentrations of [^{3}H]spiroperidol in the presence and

absence of a fixed (100 uM) concentration of cinanserine. For the 5-HT_1 assay, the brain membranes will be incubated in the presence of 7 nM [^{3}H]5-HT (13 Ci/mmol) with and without 10 uM unlabelled serotonin. Specific binding will be defined as the amount of labelled serotonin displaced by the unlabelled ligand. For both assays the reactions will be terminated by filtering the samples under reduced pressure through glass-fiber filters. The filters will be washed twice with 5 ml of ice-cold buffer, placed into scintillation vials with 10 ml of Aquasol (New England Nuclear) and shaken for 2 hr at room temperature. Radioactivity will be analysed by liquid scintillation spectrometry. The results will be expressed as pmoles of specifically bound radioligand per mg protein. Protein will be analyzed by the method of Lowry, Rosebrough, Farr and Randall (1951).

Materials

Diisopropylfluorophosphate will be purchased from Sigma Chemical Co. (St. Louis, Missouri). Radioisotopes will be purcnased from New England Nuclear (Boston, Massachussets). All other chemicals and reagents were obtained from commercial sources.

Statistics

The significance of the differences between means will be calculated by an analysis of variance. Differences will be considered significant when $P < 0.05$. The Morehouse College statistician will be responsible for this aspect of the study.

D. Electron Microscopy

1. Scanning Electron Microscopy

Membranes will be fixed in 3% Karhovsky's fixature for 1 hour, rinsed in 3 changes of 0.25 M of sodium cacadylate, pH 7.4,

post-fixed for two hours in 1% osmium tetroxide buffered with sodium cacodylate at 4°C, rinsed again in cacodylate buffer, dehydrated in a graded series of ethanol (50-100%/15 minutes each, and then 2 changes of 100%). Specimens will be placed in a graded series of amyl acetate for 24 hrs, critical-point dried in liquid carbon dioxide, sputter coated with carbon and gold-palladium and observed in a Etec Omni Scan Scanning Electron Microscope. Photographs will be taken at desirable magnifications.

2. Transmission Electron Microscopy

The same procedure will be followed as above except following dehydration in ethanol, membranes will be infiltrated and embedded in Epon 812 or LX-12 epoxy resin and polymerized for 24-48 hrs at 60°C. One micron think sections were cut from resin blocks using glass and diamond knives. Thick sections were then stained with toluidine blue. Ultrathin sections were cut with diamond knives at 500-800 A° on a LKB Number V Ultramicrotome and picked up on 400 mesh copper grids. Sections were stained in uranyl acetate and lead citrate in a LKB ultrastainer and viewed in a Zeiss 95-2 transmission electron microscope. Photographs were taken at desirable magnifications on electron image film.

3. Preparation of Membranes and Brain Cortex for Light Microscopy, Immunofluorescent Histochemistry

Membranes and brain cortex will be fixed for 2-4 hours in 4% paraformaldehyde in 0.1 M phosphate buffer (pH 7.4). In some experiments 1.3% lysine monohydrochloride and 0.2% sodium metaperiodate will be added to the fixative (McLean and Nakane 1974). After fixation, organisms will be rinsed in several

changes of 0.1 M of phosphate buffer (ph &.4) containing 0.3% triton X-100 and 0.1% sodium azide for 1 hour, and then incubated at 4°C in a 1:200 dilution of antiserotonin antibody (the primary antibody). Antiserotonin antibodies will be obtained from Immunonuclear Corporation where they will be generated in rabbits against a formaldehyde crosslinked serotonin-bovine serum albumin (BSA) conjugate (Steinbush et. al., 1978). Following primary antibody treatment, the organisms will be rinsed in phosphate/triton x100/azide for 1 hour, then incubated with the secondary antibody which will be goat antirabbit IgG labeled with fluorescein isothiocyanate (FITC). This antibody preparation will be an affinity-isolated IgG produced by Boehgringer Mannheim Biochemicals.

Tissues will be incubated in IgG-conjugated FITC at 40°C for 6 hrs. or overnight. Excess secondary antibody will be removed by multiple rinses in 0.1 M of phosphate buffer (1 to 2 hours total). Organisms will then be rinsed once in 4mm of sodium carbonate buffer (pH 9.5), mounted in 80% glycerol in 20 mm of Carbonate buffer, and viewed with the proposed Zeiss standard 16 light microscope set up for epifluorescent excitation. Exciter barrier filters and reflector combination cubes will be used containing a blue excitation at 440 to 490 mm and a selective barrier filter at 520 to 560 mm.

Sectioned Material: Specimens will be fixed in 4% paraformaldehyde or paraformalhyde/periodate (PLP) fixative used for whole mount preparations. After 1-2 hours of fixation, organisms will be infiltrated with 20% sucrose in 0.1 M phosphate

buffer for 1-2 hours. Tissues will then be mounted and frozen with dry ice in preparation for cryostat sectioning. Sections (6 to 10 microns) will be cut, mounted on gelatin-coated slides and processed by the same procedure used for whole mounts, except incubations will be at room temperature.

Specific Controls: Absorption controls will be conducted by preincubating the antiserotonin antibody, at working dilutions, with the following antigens: (1) sertonin creatinine sulfate (1 mg/ml); (2) formaldehyde crosslinked serotonin-BSA serotonin ratio of approximately 10:1 (w/w); (3) BSA (500 mg/ml); (4) octopamine (1 mg/ml). The serotonin-BSA conjugate will be supplied by Immunonuclear Corporation and the concentration will be determined from analysis of the compound. The antigen/antiserotonin antibody mixture will be incubated at 4°C for 16 to 24 hours with occasional gentle agitation, centrifuged at 100,000 x g for 20 minutes, and the supernatant fluid (preabsorbed serum) will be collected. In some experiments tissues will be fixed with PP for 1-2 hours, and rinsed with phosphate/triton x-100/azide. One group of miracidia will be incubated with a 1:200 dilution of antiserotonin antibody, and another group will be incubated in preabsorbed serum. The method of Hokfelt et. al., (1975) modified by Beltz and Kravitz (1983) has been found to be superior for the localization of serotonin in the nervous system of immature lobsters using the indirect immunofluorescent technique. Other older fluorescent methods by Falk and Owman (1965), Rude (1966) and Marsden and Kerkut (1969) have also been found to produce satisfactory results.

V. RECOMMENDATIONS

The summer faculty fellow has spent two productive summers at Brooks AFB carrying out biomedical research. One of the primary objectives of the current summer research participation developed by the faculty fellow and effort focal point collaborator was to submit a research proposal to the mini-grant program of the USAF. This project report reflects a brief summation of the research proposal to be submitted. Thus, the recommendations are as follows:

1. Submit a research proposal to the mini-grant program of USAF so that the research can be continued at the faculty member's home institution.
2. Involve three other faculty members to serve as co-investigators and/or consultants for the proposed project. See text for role of each faculty involved.
3. If a favorable review is received for the research proposal, ask the review committee to grant permission for the proposal to be placed in the pool of proposals for 1987 with a start date of September 1, 1987; or if the proposal is reviewed favorably for this year, inquire about the possibility of funding from supplemental or excess funds.

REFERENCES

1. Barnes, L., Karczmar, A. G. and Ingerson, A. (1975). Abstract in Federation Proceedings.
2. Bedard, P. and Pycock, C. J. (1977). Neuropharmacol. 16:663-670.
3. Beltz, B. and T. Kravitz (1983). J. Neurosci., 3:585-602.
4. Bennett, J. and S. Snyder (1976). Mol. Pharmacol., 12:373-389.
5. Bramwell, G. J., Bramwell and T. Gonye (1973). Ibid, 48:3578.
6. Boakes, R. J., Bradley, P. B., Briggs, I., Dray, A. (1970). Br. J. Pharmacol., 40:202.
7. Corne, S. J., R. W. Pickering, B. T. Warner (1963). Br. F. Pharmacol., 20:106.
8. Abou-Donia, M. B. (1981). Ann. Rev. Pharmacol. Toxicol. 21:511-548.
9. Dille, J. R. and P. W. Smith (1964). Aerospace Med. 35:475-478.
10. Duffy, F. H., J. L. Burchfiel, P. H. Bartels, M. Gaon, And M. V. Sim (1979).
11. Falk, B.and Owman, C. 1965. Acta. Univ. Lund., Section II. No. 7, 1023.
12. Gershon, S. and F. H. Shaw (1961). Lancet 1:1371-1374.
13. Grahame-Smith, D. G. (1971). J. Neurochem., 18:1053.
14. Haigler, H. J. and G. K. Aghajanian (1974). J. Neural. Transm., 35:357.
15. Hokfelt, T. and M. Goldstein 1958. Ann. N.Y. Acad. Su., 25:407-437.

16. Jones, F. R. Betty (1985). Electron Micrescopy by 17 Scientist. Second Edition, Library Research Associates, Monroe, New York.

17. Koiller, W. C. and H. L. Klawans (1979). Organophosphosphorous Intoxication. Part II. Handbook of Clinical Neurology, vol. 37. Elseuier, pp. 5541-5562.

18. Korsak, R. J. and M. M. Sato (1977). Clin. Toxicol., 11:83-96.

19. Marden, C. and G. Kerdut (1969). Exp. Physiol. Biochem., 2:237-360.

20. McDonald, D., G. M. Stancel and S. J. Enna (1984). Neuropharmol., 23:12655-1269.

21. Pheroutka, S. and S. Snyder (1979). Mol. Pharmac., 12:373-389.

22. Roberts, M. H. T. and D. W. Straughan (1967). Physiol., 193:269.

23. Rude, F. (1966). J. Comp. Neurol., 128:397-412.

24. Sidell, F. R. (1974). Clin. Toxicol., 7:1-17.

25. Williams, Evan (1985). Personnal Communications.

1986 USAF-UES Summer Faculty Research Program/

Graduate Student Summer Support Program

Sponsored by the

Air Force Office of Scientific Research

Conducted by the

Universal Energy Systems, Inc.

Final Report

Optimal Filtering

Prepared by:	Marvin S. Keener
Academic Rank:	Professor
Department and	Mathematics Department
University:	Oklahoma State University
Research Location:	Air Force Armament Laboratory
	Guidance and Control Branch
	Advanced Guidance Concepts Section
USAF Researcher:	Dr Norman Speakman
Date:	1 August 1986
Contract No:	F04962-85-C-0013

Optimal Filtering

by

Marvin S. Keener

ABSTRACT

Two problems are studied which arise in tracking problems. The first involves the modification of a tracking filter which incorporates the missile dynamics in order to account for the delay in the commanded missile acceleration and the achieved missile acceleration. The original signal model is reformulated through state augmentation so that the standard Kalman filter applies. The second problem concerns filter stability. In particular, comparison type results are sought in order that stability of a time-varying filter may be established.

Acknowledgements

I would like to thank the Air Force Systems Command and the Air Force Office of Scientific Research for sponsorship of my research. The research environment provided by the Armament Laboratory and Eglin Air Force Base was excellent. In this regard, Dr Donald Daniel and Major Tony Clavin deserve special thanks. I also wish to thank Mr Johnny Evers, Mr Michael Vanden-Heuvel, Lt Roger Smith, and Dr James Cloutier for many stimulating conversations. In particular, Dr Norman Speakman provided much encouragement and guidance for this research effort. I also appreciate the patience and understanding of Mrs Mary Triska during the typing of this manuscript.

I. Introduction

I received my Ph.D. from the University of Missouri-Columbia studying the qualitative behavior of solutions of ordinary differential equations. More specifically, my research has been along the lines of oscillation theory and questions surrounding the notions of disconjugate operators and conjugate points. These ideas are closely related to control theory, and, therefore, over the years I have obtained a passing knowledge of the theory and techniques used in control problems.

One of the primary research efforts under consideration at the Armament Laboratory involves the development and analysis of guidance laws for air-to-air missiles. This includes developing algorithms for locating a target and determining optimal trajectories for interception of the target. Various time-varying filters have been applied to the target tracking problem. However, due to their time varying nature, the behavior of such algorithms is not well understood, particularly in terms of stability and robustness.

II. Objectives of the Research Effort

The overall objective of my research project was to study two particular questions of concern.

1. Derive a filter for a particular time varying signal model which arises naturally in target tracking problems.
2. Perform a preliminary identification of general, robust techniques for establishing filter stability with particular attention given to results of a comparison nature.

Since my expertise in the theory and techniques of filtering was minimal, the first several weeks were spent improving my background in these areas.

III. A Filter Derivation

Modern estimation techniques are used to process tracking data obtained from terminal seekers. There are three basic types of seekers: Infrared (passive), radar (active and semi-active), and laser (active). The most familiar tracking algorithm is the Kalman filter which processes sensor information recursively in order to provide a minimum variance estimate of the states in a dynamical system.

The particular signal model of interest is a linear time-varying model of the form

$$\dot{x}=F(t)x+B(t)u+G(t)w,\ y=H(t)x+v, \qquad (1.1)$$

where x represents the vector of state variables, u a vector of control variables, and w and v are vectors of zero mean, Gaussian white noise. Since the coefficient matrices F, B, G and H are time-varying, the usual eigenvalue (or frequency-domain) analysis is meaningless.

Derivation of a Particular Signal Model

For a particular example of such a system, the following model is derived. The seeker actually has two-channels, one for the pitch plane and one for the yaw plane. Therefore, we shall concentrate on a planar model for which the geometry is indicated in Figure 1.

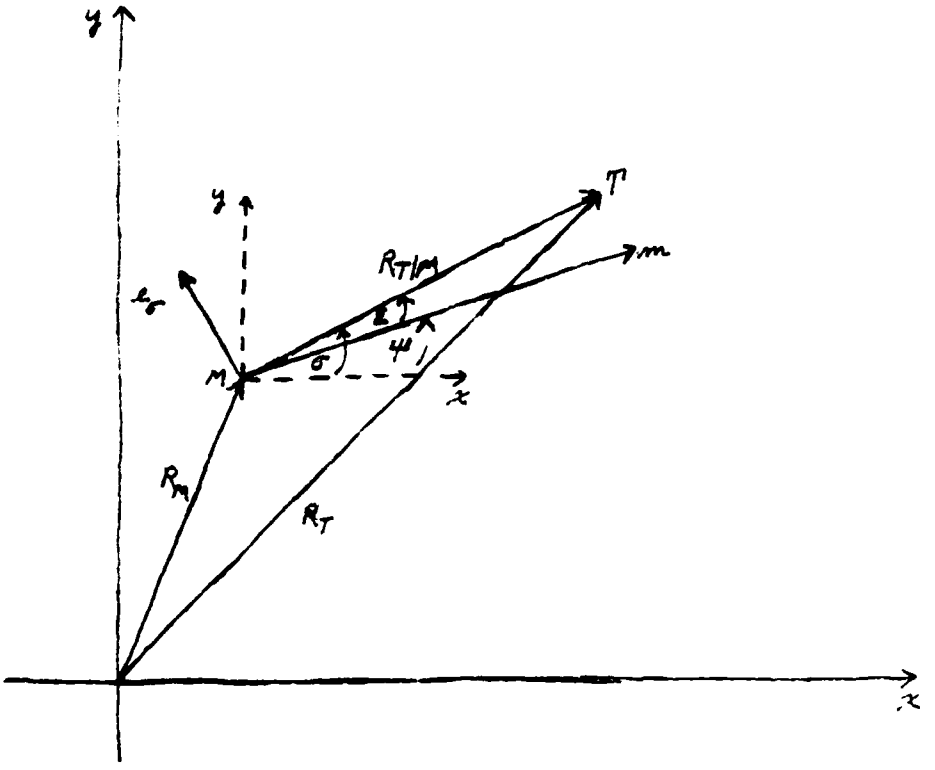

Figure 1

Geometry of the Planar Model

It is assumed that the missile and target can be considered as point masses located at points M and T, with position vectors R_M and R_T, respectively, in the inertial coordinate system. The relative position vector is

$R_{T/M} = R_T - R_M$.

The line-of-sight angle σ is the angle between the positive x-axis and the vector $R_{T/M}$.

At time t the seeker is actually looking along the vector m as indicated in Figure 1. The boresight angle ψ is the angle between the x-axis and the vector m. The error angle ε is the

difference between the line-of-sight angle and the boresight angle, i.e.,

$$\varepsilon(t) = \sigma(t) - \psi(t). \tag{1.2}$$

In order to develop the dynamics of the model, define

$$e_r(t) = \frac{1}{\| R_{T/M}(t) \|} R_{T/M}(t).$$

If $R(t) = \| R_{T/M}(t) \|$ (the Euclidean norm), then from elementary geometry

$$e_r(t) = (\cos\sigma(t), \sin\sigma(t))$$

and $R_{T/M}(t) = R(t)e_r(t)$. A vector $e_\sigma(t)$ which is orthogonal to $e_r(t)$ at time t is given by

$$e_\sigma(t) = (-\sin\sigma(t), \cos\sigma(t)).$$

By a straight forward calculation

$$\frac{d}{dt} e_r(t) = \dot{\sigma}(t) e_\sigma(t)$$

and

$$\frac{d}{dt} e_\sigma(t) = -\dot{\sigma}(t) e_r(t).$$

Since the relative position vector $R_{T/M}(t) = R(t)e_r(t)$, it follows that the relative velocity $V_{T/M}(t)$ is given by

$$V_{T/M}(t) = \frac{d}{dt} R_{T/M}(t) = \dot{R}(t)e_r(t) + R(t)\dot{\sigma}(t)e_\sigma(t).$$

Furthermore, the relative acceleration $A_{T/M}(t)$ is given by

$$A_{T/M}(t) = [\ddot{R}(t) - R(t)\dot{\sigma}^2(t)]e_r(t) + [R(t)\ddot{\sigma}(t) + 2\dot{R}(t)\dot{\sigma}(t)]e_\sigma(t).$$

Thus, if $a_T(t)$ and $a_M(t)$ denote the accelerations normal to the line of sight of the target and missile, respectively, then $R(t)\ddot{\sigma}(t) + 2\dot{R}(t)\dot{\sigma}(t) = a_T(t) - a_M(t)$, or

$$\ddot{\sigma}(t) = -2\frac{\dot{R}(t)}{R(t)}\dot{\sigma}(t) + \frac{1}{R(t)}\left[a_T(t) - a_M(t)\right]. \tag{1.3}$$

Finally, the target dynamics are modeled as a first order Gauss-Markov process, i.e.,

$$\dot{a}_T = -\frac{1}{\tau_T}a_T + W_T, \tag{1.4}$$

where W_T is Gaussian white noise with zero mean.

Equations (1.2-1.4) form the basic dynamic model with the state variable $x = (\varepsilon, \dot{\sigma}, a_T)^T$. Thus

$$\begin{bmatrix} \dot{\varepsilon} \\ \ddot{\sigma} \\ \dot{a}_T \end{bmatrix} = \begin{bmatrix} 0 & 1 & 0 \\ 0 & -2\frac{\dot{R}(t)}{R(t)} & \frac{1}{R(t)} \\ 0 & 0 & -\frac{1}{\tau_T} \end{bmatrix} \begin{bmatrix} \varepsilon \\ \dot{\sigma} \\ a_T \end{bmatrix} + \begin{bmatrix} -\dot{\psi} \\ -\frac{1}{R(t)}a_M \\ 0 \end{bmatrix} + \begin{bmatrix} 0 \\ 0 \\ W_T \end{bmatrix}. \tag{1.5}$$

System (1.5) is of the form (1.1).

Now a_M is modeled as pro-nav, i.e., $a_M = -\lambda \dot{R}(t)\dot{\sigma}(t)$, where $\lambda = 3$. Thus a_M is a commanded acceleration used as a control. The measurement y made by the seeker is on the variable ε, and hence,

$$y = Hx + v, \tag{1.6}$$

where $H = [1, 0, 0]$ and v is Gaussian white noise with zero mean due to measurement errors.

Incorporation of Missile Dynamics

When the standard Kalman filter was used to estimate the states for the signal model (1.5)-(1.6), some usual behavior was observed in the error covariance matrices. Furthermore, the filter had trouble tracking the target in certain simulations. This led to speculation that perhaps the model and corresponding filter might be improved.

The above signal model (1.5)-(1.6) assumes that the commanded acceleration a_M at time t is achieved at time t. In reality, there is a small delay between the time the acceleration is commanded and the time it is achieved. This phenomenon is due to the missile response mechanisms.

In view of the above statements, it might be desirable to account for these dynamics by modeling missile acceleration as

$$\dot{a}_M = -\frac{1}{\tau_M} a_M + W_m. \tag{1.7}$$

where τ_M is the time constant associated with the missile and W_m is a white noise process which accounts for inaccuracies in this model.

The Discretization of the Signal Model

For implementation, (1.5) and (1.7) are discretized and incorporated into a single model. There are several ways in which this can be done, but the method chosen here highlights the delay in missile response.

The variables $\dot{\varepsilon}$, $\ddot{\sigma}$, and $\dot{a}_T$, are approximated by first order forward difference on a Δt time interval.

For a_M, it follows from (1.7) that

$$a_M(t) = a_M(t-\Delta t)\exp\left(-\frac{\Delta t}{\tau_M}\right) + \int_{t-\Delta t}^{t} \exp\left(\frac{s-\tau}{\tau_M}\right) W_m(s)ds$$

According to Singer [9] the above integral may be considered as a discrete white noise process, which shall be denoted by W_M. Since the commanded acceleration is pro-nav, it follows that

$$a_M(t) = -\lambda \dot{R}(t-\Delta t)\dot{\sigma}(t-\Delta t)\exp\left(-\frac{\Delta t}{\tau_M}\right) + W_M$$

$$\approx -\lambda \dot{R}(t-\Delta t)\dot{\sigma}(t-\Delta t) + W_M + O(\Delta t).$$

Substituting these approximations for $\dot{\varepsilon}$, $\ddot{\sigma}$, $\dot{a}_T$ and a_M into (1.5) yields (to first order in Δt)

$$\begin{bmatrix} \varepsilon(t+\Delta t) \\ \dot{\sigma}(t+\Delta t) \\ a_T(t+\Delta t) \end{bmatrix} = \begin{bmatrix} 0 & 0 & 0 \\ 0 & 1-2\Delta t\,\frac{\dot{R}(t)}{R(t)} & \frac{\Delta t}{R(t)} \\ 0 & 0 & 1-\frac{\Delta t}{\tau_T} \end{bmatrix} \begin{bmatrix} \varepsilon(t) \\ \dot{\sigma}(t) \\ a_T(t) \end{bmatrix}$$

$$+ \begin{bmatrix} 0 & 0 & 0 \\ 0 & \lambda\Delta t\,\frac{\dot{R}(t-\Delta t)}{R(t)} & 0 \\ 0 & 0 & 0 \end{bmatrix} \begin{bmatrix} \varepsilon(t-\Delta t) \\ \dot{\sigma}(t-\Delta t) \\ a_T(t-\Delta t) \end{bmatrix} \qquad (1.8)$$

$$+ \begin{bmatrix} -\Delta t \\ 0 \\ 0 \end{bmatrix} \dot{\psi}(t) + \begin{bmatrix} \Delta t & 0 & 0 \\ 0 & \Delta t & 0 \\ 0 & 0 & \Delta t \end{bmatrix} \begin{bmatrix} 0 \\ 0 \\ w_T \end{bmatrix} + \begin{bmatrix} 0 \\ w_M \\ 0 \end{bmatrix}.$$

The term involving $\dot{\sigma}(t-\Delta t)$ can be measured. Thus the measurement equation (1.6) must also be changed. Accordingly,

$$\begin{bmatrix} \varepsilon(t) \\ a_M(t) \end{bmatrix} = \begin{bmatrix} 1 & 0 & 0 \\ 0 & 0 & 0 \end{bmatrix} \begin{bmatrix} \varepsilon(t) \\ \dot{\sigma}(t) \\ a_T(t) \end{bmatrix} + \begin{bmatrix} 0 & 0 & 0 \\ 0 & -\lambda\dot{R}(t-\Delta t) & 0 \end{bmatrix} \begin{bmatrix} \varepsilon(t-\Delta t) \\ \dot{\sigma}(t-\Delta t) \\ a_T(t-\Delta t) \end{bmatrix}. \qquad (1.9)$$

The signal model (1.8) and (1.9) is of the form

$$x_{K+1} = F_K x_K + B_K u_K + A_K u_K^* + G_K w_K,$$

$$u_K = C_{1K} x_{K-1} + z_K,$$

$$y_K = H_{0K} x_K + H_{1K} x_{K-1} + v_K \qquad (1.10)$$

where

$$x_K = \begin{bmatrix} \varepsilon(K\Delta t) \\ \dot{\sigma}(K\Delta t) \\ a_T(K\Delta t) \end{bmatrix}, \quad u_K^* = \dot{\psi}(K\Delta t), \quad w_K = \begin{bmatrix} 0 \\ 0 \\ w_T(K\Delta t) \end{bmatrix},$$

$$z_K = -\frac{\Delta t}{R(K\Delta t)} w_M, \quad y_k = \begin{bmatrix} \varepsilon(K\Delta t) \\ a_M(K\Delta t) \end{bmatrix}, \quad G_K = \Delta t\, I,$$

$$F_K = \begin{bmatrix} 1 & 0 & 0 \\ 0 & 1-2\Delta t \frac{\dot{R}(K\Delta t)}{R(K\Delta t)} & \frac{\Delta t}{R(K\Delta t)} \\ 0 & 0 & 1-\frac{\Delta t}{\tau_T} \end{bmatrix}, \quad B_K = \begin{bmatrix} -\Delta t \\ 0 \\ 0 \end{bmatrix}, \quad B_K = \begin{bmatrix} 0 \\ -\frac{\Delta t}{R(K\Delta t)} \\ 0 \end{bmatrix}$$

$$H_{0K} = \begin{bmatrix} 1 & 0 & 0 \\ 0 & 0 & 0 \end{bmatrix}, \quad H_{1K} = \begin{bmatrix} 0 & 0 & 0 \\ 0 & +\lambda \dot{R}((K-1)\Delta t) & 0 \end{bmatrix}.$$

A General Filter Problem

The filter developed in this report is a Kalman filter for signal models for which (1.10) is an example. It is applicable to signal models of the form given below where any deterministic input u * has been neglected:

$$\begin{aligned} x_{K+1} &= F_K x_K + B_K u_K + G_K w_K \\ u_K &= \sum_{i=1}^{N} C_{iK} x_{K-i} + z_K \\ y_K &= \sum_{i=0}^{M} H_{iK} x_{K-i} + v_K \end{aligned} \tag{1.11}$$

It is assumed that

i) x_0 is $N(\bar{x}_0, P_0)$;

ii) x_0, $\{w_K\}$, $\{z_K\}$, $\{v_K\}$ are jointly Gaussian and mutually independent;

iii) $\{w_K\}$, $\{z_K\}$, $\{v_K\}$, are each of zero mean and white with covariances $Q_K \delta_{KL}$, $S_K \delta_{KL}$, and $R_K \delta_{KL}$, respectively, and $\delta_{KL} = 1$ for K=L and zero otherwise.

In the signal model (1.11), the sizes of the given vectors and matrices are provided in Table 1 for reference.

SYMBOL	SIZE	SYMBOL	SIZE
x_K	nxl	F_K	nxn
u_K	pxl	B_K	nxp
y_K	mxl	H_{iK}	mxn
w_K	qxl	Q_K	qxq
z_R	pxl	S_K	pxp
v_K	mxl	R_K	mxm
C_{iK}	pxn	G_K	nxq

TABLE 1

Table of Symbols for Signal Model

It is important to note that the process noise is represented by the term $G_K w_K$. The uncertainty in the control model is represented by z_K. In this manner, the errors due to different modeling factors can be isolated.

In this setting the filtering problem can be stated as follows: Determine the estimates

$$\hat{x}_{j/K} = E[x_j / y_0, \ldots, y_K], \quad j = K-N, \ldots, K,$$

and the associated covariance matrices.

Rather than develop a filter for this problem from a first-principles approach, the signal model (1.11) and the corresponding filter problem can be reformulated so that the standard Kalman filter is applicable. To this end, define

$X_K = [x_{K-N}, \ldots, x_K]^T$ size: (N+1)mxl

$c_K = [C_{NK}, \ldots, C_{1K}]$ size: pxNn

$h_K = [H_{NK}, \ldots, H_{0K}]$ size: mX(N+1)n

$$f_K = \begin{bmatrix} O_{Nnxn} & I_{NnxNn} \\ B_K C_K & F_K \end{bmatrix} \quad \text{size: } (N+1)n \times (N+1)n$$

$$g_K = \begin{bmatrix} O_{Nmxq} \\ G_K \end{bmatrix} \quad \text{size: } (N+1)nxq$$

$$b_K = \begin{bmatrix} O_{Nmxp} \\ B_K \end{bmatrix} \quad \text{size: } (N+1)nxp$$

Under these definitions, (1.11) may be reformulated as

$$X_{K+1} = f_K X_K + b_K z_K + g_K w_K, \; Y_K = h_K X_K + v_K.$$

The corresponding reformulated filter problem is to determine the estimates

$$\hat{X}_{K/K} = E[X_K \mid Y_0, \ldots, Y_K]$$

$$\hat{X}_{K/K-1} = E[X_K \mid Y_0, \ldots, Y_{K-1}]$$

and the associated covariance matrices

$$P_{K/K} = E[X_K - \hat{X}_{K/K})\,(X_K - \hat{X}_{K/K})^T \mid Y_0, \ldots, Y_K]$$

$$P_{K/K-1} = E[X_K - \hat{X}_{K/K-1})\,(X_K - \hat{X}_{K/K-1})^T \mid Y_0, \ldots, Y_K]$$

The size of these covariance matrices are $(N+1)n \times (N+1)n$.

The solution of this filter problem is given by the standard Kalman filter. The estimates sought for the problem corresponding to (1.11) appear as the components in $\hat{X}_{K/K}$, while the desired associated covariance matrices appear as block matrices along the diagonal for $P_{K/K}$. In order to apply these ideas to the signal model stated in (1.10), the deterministic input u^* is taken as zero. To test the effectiveness of the Kalman filter applied to this model, it should be incorporated into a tracking filter. Time did not permit such an analysis.

IV. Stability.

There are a host of papers dealing with the question of stability for differential systems. For example, one may peruse any issue of the IEEE Transactions on Automatic Control to obtain a feel for the overwhelming number of articles. Often these papers deal with a relatively small class of filters in which a particular characteristic is exploited to establish stability. Robust techniques applicable to very general systems are difficult to find in the literature.

Linear Systems

The Kalman filter for linear problems is fairly well understood. It may be stated as follows for the continuous time case. Let the signal model be given as

$$\dot{x} = F(t)x+G(t)u,\ y=H(t)x+v(t), \tag{2.1}$$

where F, G, and H are continuous matrices on (t_0,∞) of size nxn, nxq and mxm respectively, and w and v are Gaussian white noise processes with zero means and covariances Q(t) and R(t) of size qxq and mxm, respectively. The estimate $\hat{x}(t)$ provided by the continuous Kalman filter satisfies the differential equation

$$\dot{\hat{x}} = F(t)\hat{x}+K(t)(y-H(t)\hat{x}),$$

where $K(t) = P(t)H^T(t)R^{-1}(t)$ is the Kalman gain and P is the unique solution of the Riccati equation

$$\dot{P} = F(t)P+PF^T(t)+G(t)Q(t)G^T(t)-PH^T(t)R^{-1}(t)H^T(t)P \tag{2.2}$$

for which $P(t_0) = P_0$ and P_0 is the initial error covariance matrix. Setting $\tilde{x}(t) = x(t)-\hat{x}(t)$, it follows that

$$\dot{\tilde{x}}(t) = [F(t)-K(t)H(t)]\tilde{x}(t) + G(t)w(t)-K(t)H(t)v(t)$$

Thus the behavior of the error x between the state and its estimate is governed by the coefficient $F-KH = F-PH^TR^{-1}H$. Ideally, uniform asymptotic stability is desired so that $\tilde{x}(t)$ will converge to zero uniformly.

In the time invariant case, the problem is well understood in the literature. Since the matrices F, G, H, R, and Q are constant, the stability of the system is governed solely by the eigenvalues of $F-PH^TRH$. Furthermore, solutions of (2.2) converge to the steady state solution and P may be found as the solution of a so-called algebraic Riccati equation

$$PF^T+FP+GQG^T-PH^TR^{-1}H = 0.$$

With the aid of high speed computers such problems are easily solved for the size matrices considered in this study.

Time-varying linear systems are somewhat more complicated. One must establish the existence of a solution of (2.2) which remains positive definite on the half-line (t_0, ∞). Given this, one then must analyze the equation

$$\dot{x} = [F(t)-P(t)H^T(t)R^{-1}(t)H(t)]x \qquad (2.3)$$

for its stability character. In general, the eigenvalue technique, so successful for time-invariant systems, is worthless in this setting. On the other hand there is a rich literature concerning the stability of (2.3); see for example [8].

The best known result is due to Kalman [5] and [6]. It provides a sufficient condition for the stability of the Kalman filter in terms of the so-called observability and controllability Grammians, namely,

$$M(t-\sigma,t) = \int_{t-\sigma}^{t} \Phi^T(s,t)H^T(s)R^{-1}(s)H(s)\Phi(s,t)ds$$

and

$$N(t-\sigma,t) = \int_{t-\sigma}^{t} \Phi(t,s)G(s)Q(s)G^T(s)\Phi^T(t,s)ds,$$

respectively, where Φ denotes the state transition matrix corresponding to the equation $\dot{x} = F(t)x$. The theorem is now stated.

Theorem 1. The Kalman filter is uniformly asymptotically stable if there exists positive constants α, β, σ such that for all $t \in (t_0, \infty)$,

$$0 \leq \alpha I \leq M(t-\sigma,t) \leq \beta I$$

and

$$0 \leq \alpha I \leq N(t-\sigma,t) \leq \beta I.$$

Much of the general theory of filter stability revolves around the construction of Lyapunov functions for the system. Indeed, the proof of Theorem 1 (see [3] or [5]) involves such a construction by exploiting the bounds on the functions M and N. While the Lyapunov theory is powerful, it usually requires a good deal of ingenuity in the selection of a suitable Lyapunov function.

A Comparison Question

While Theorem 1 provides a sufficient condition for filter stability, it can be cumbersome to apply in that the selection of σ, α, and β must be done a priori to the evaluation of the integrals. The following question then arises. Suppose there are two signal models of the form (2.1), say $(F_i, G_i, H_i, Q_i, R_i)$, $i = 1,2$, and suppose f_1 and f_2 represent the Kalman filter for the respective model. What conditions on the matrices need exist so

that the stability (or instability) of filter f_1 will imply the same characteristic of filter f_2?

Such questions seem to have been ignored in the literature. Answers to similar questions in differential equations typically require techniques different from those in the Lyapunov theory. Such an approach is now presented. Although it has not yielded any results at this time, the ideas seem to be absent from the engineering literature. For this reason alone, it seems worth presenting.

The idea is to represent the matrix P of the variance equation (2.2) as the product of "nice" functions. Recalling the notation previously used for $(t,s) \in (t_0, \infty) \times (t_0, \infty)$

$$\frac{d}{dt} \Phi(t,s) = F(t)\Phi(t,s), \quad \Phi(s,s) = I, \text{ the identity.}$$

It is well-known that for $s, t, u \in [t_0, \infty)$,

$$\Phi(t, u)\Phi(u, s) = \Phi(t, s) \text{ and } \Phi^{-1}(t, s) = \Phi(s, t).$$

Now define

$$h(t, s) = [\Phi^{-T}(t,s)\, H^T(t)R^{-1}(t)H(t)\Phi^{-1}(t,s)]^{-1}$$

and

$$g(t,s) = \Phi(s,t)\, G(t)Q(t)\, G^T(t)\Phi^T(s,t)$$

Recalling the observability and controllability Grammians, note that

$$M(s-\sigma,s) = \int_{s-\sigma}^{s} h^{-1}(t,s)dt \text{ and } N(s-\sigma,s) = \int_{s-\sigma}^{s} g(t,s)dt. \qquad (2.4)$$

For $s = t_0$, let $Y(t,t_0)$ denote the unique solution of the initial value problem

$$[h(t,t_0)\dot{Y}]^{\cdot} = g(t,t_0)Y, \; Y(t_0) = I, \; h(t_0,t_0)\dot{Y}(t_0) = P_0. \qquad (2.5)$$

Define $P(t) = \Phi(t,t_0)h(t,t_0)Y(t,t_0)Y^{-1}(t,t_0)\Phi^T(t,t_0)$.

A straight forward calculation yields that P satisfies (2.2).

V. Recommendations

1. To test the effectiveness of the particular filter developed in Section III, it should be incorporated into a tracking simulation. Time did not permit such analysis during my stay at Eglin. However, by choosing constant values for the time-varying parameters, it was possible to obtain some comparisons. The error covariances for the system (1.10), which include the missile dynamics, had smaller entries than the corresponding covariance matrices of the usual Kalman filter for the model (1.5) - (1.6). Though such results do not confirm the effectiveness of the filter, at least they encourage further consideration.

2. While my approach to determining comparison type results for filters has not yielded any positive results as yet, the relationship (2.4) is too tempting to be ignored. Comparison type results for equations of the form (2.5) are often found in the mathematics literature under the general heading of oscillation theory. Much of this literature was not available here. Whether or not the questions can be resolved, or have already been resolved, can only be determined by further study.

References

1. Anderson, B.D.O., "Stability Properties of the Kalman-Bucy Filter," J. Franklin Inst., Vol. 291, No. 2, February 1971, pp. 137-144.
2. Anderson, B.D.O., and J.B. Moore, Optimal Filtering, Englewood Cliffs, New Jersey, Prentice-Hall, 1979.
3. Jazwinski, A.H., Stochastic Processes and Filtering Theory, New York, Academic Press, Inc., 1970.
4. Kailath, T., "A View of Three Decades of Linear Filtering Theory," IEEE Trans. Inform. Theory, Vol. IT-20, No. 2, March 1974, pp. 141-181.
5. Kalman, R.E., "New Methods in Wiener Filtering," Chapter 9, Proc. of the First Symposium on Engineering Applications of Random Function Theory and Probability, New York, John Wiley and Sons, Inc., 1963.
6. Kalman, R.E., and J.E. Berton, "Control System Analysis and Design Via the Second Method of Lyapunov," Trans. ASME J. Basic Eng., Vol 82, pp. 371-392, 1960.
7. Kalman, R.E., and R. Bucy, "New Results in Linear Filtering and Prediction," Journal of Basic Engineering (ASME), Vol. 83D, pp. 95-108, 1961.
8. Lehnizk, S., Stability Theorems for Linear Motion, Englewood Cliffs, New Jersey, Prentice-Hall, 1966.
9. Singer, R.A., "Estimating Optimal Tracking Filter Performance for Manned Maneuvering Targets," IEEE Trans. on Aerospace and Electronic Systems, Vol. AES-6, No. 4, July 1970, pp. 473-483.

1986 USAF-UES SUMMER FACULTY RESEARCH PROGRAM/

GRADUATE STUDENT SUMMER SUPPORT PROGRAM

Sponsored by the

AIR FORCE OFFICE OF SCIENTIFIC RESEARCH

Conducted by the

UNIVERSAL ENERGY SYSTEMS, INC.

FINAL REPORT

A PRELIMINARY STUDY FOR CENTRIFUGE MODEL TESTING OF SEMIHARDENED CONCRETE ARCHES

Prepared by:	Dr. Yong S. Kim
Academic Rank:	Assistant Professor
Department and University:	Department of Civil Engineering The Catholic University of America
Research Location:	Air Force Engineering and Services Center, Engineering Research Division, Facility System and Analysis Branch
USAF Research:	Mr. Paul L. Rosengreen
Date:	July 20, 1986
Contract No.:	F49620-85-C-0013

A PRELIMINARY STUDY FOR CENTRIFUGE MODEL TESTING OF SEMIHARDENED CONCRETE ARCHES

by

Yong S. Kim

ABSTRACT

The centrifuge model technique is reviewed in order to investigate the behavior of semihardened concrete arches. The centrifuge facility at the Air Force Engineering and Services Center is evaluated, and the required equipment and instrumentation for the centrifuge model study are recommended accordingly. In addition, the parameters influencing the stability of concrete arches are elaborated with a discussion for classifying them as to the design criteria.

ACKNOWLEDGEMENT

The author would like to thank the Air Force Systems Command, the Air Force Office of Scientific Research and the Universal Energy Systems, Inc. for providing him with the opportunity to spend a very worthwhile and interesting summer at the Air Force Engineering and Services Center, Tyndall AFB, Florida. He would like to acknowledge the Center, in particular the Facility Systems and Analysis Branch for its hospitality and excellent working conditions.

Also, he would like to thank Dr. Paul Y. Thompson and Mr. Jack Hayes for suggesting this area of research and for their collaborations. Finally, he would like to acknowledge many helpful discussions with Mr. Paul L. Rosengren.

A PRELIMINARY STUDY FOR CENTRIFUGE MODEL TESTING OF SEMIHARDENED CONCRETE ARCHES

I. INTRODUCTION

I.1. General

The author is an Assistant Professor of Civil Engineering at the Catholic University of America. He received his B.S., M.S. and Ph.D. degrees in Civil Engineering from the University of California at Davis. During his graduate study, the author worked as a research civil engineer at the California State Department of Transportation. His research interest has primarily focused on static and dynamic soil-structure interactions of buried structures and foundations. His published articles include centrifuge model study and numerical analysis of reinforced earth support systems, oil storage tank foundations on soft ground, rigid box culverts under shallow embankments, and rigid and flexible circular culverts under deep embankments with different bedding and backpacking compactions.

With this background, the author was invited for research at the Facility Systems and Analysis Branch, Engineering Research Division in the Air Force Engineering and Services Center at Tyndall Air Force Base. During his stay at the Center, the author learned that one of the Center's major missions is to develop new innovative and advanced high technologies for military facilities to withstand various conventional weapons attacks. Specifically, one of the Branch's upcoming research projects is a model study to investigate the structural behavior of reinforced concrete arches (e.g., aircraft shelters) under antipenetration systems. The study is to be done in an economical way

and without losing structural integrity. The preliminary study described herein fulfills the above requirement by providing new model technology to the Air Force that demonstrates potential savings and enhances insight into soil-structure interactions.

I.2. Statement of Problem

During recent years, several research programs were undertaken by the United States Air Force (References 1,2,3,16) to develop a protective antipenetration system for military facilities (e.g., arch-, circular-, and box-type structures) constructed on the ground surface. Protective concepts consisting of rock rubble/boulder and burster slab over soils were introduced, and full-scale models were tested to determine the levels of protection against conventional weapons (Figure 1). A parametric study on the thickness of rock rubble/boulder layer, ratio of size of rock rubble/boulder to size of the weapons, thickness of burster slab, and density and thickness of sand layer was performed and qualitative results have been obtained from the field model tests. Based on information observed, the system has proven effective to resist the penetration of conventional weapons. It is now being considered for application over military facilities as a hardening protective structure. However, the designers are facing one critical question before application of the system (Reference 14): Will these military structures be safe under static loadings due to the weight of embankment soil, rock rubble/boulder layers and/or burster slab?

There are numerous arch-type protective structures (e.g., 1st, 2nd and 3rd generation aircraft shelters) which have been constructed on the ground surface in the United States and NATO countries. At the present

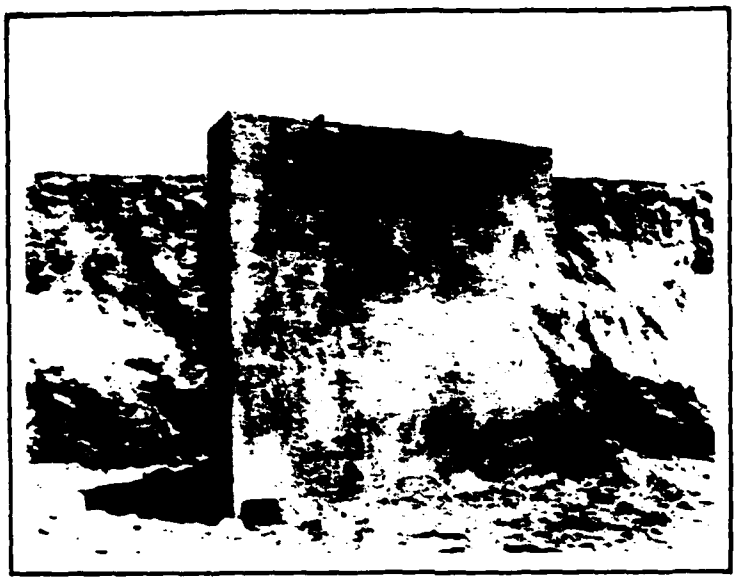

(a)

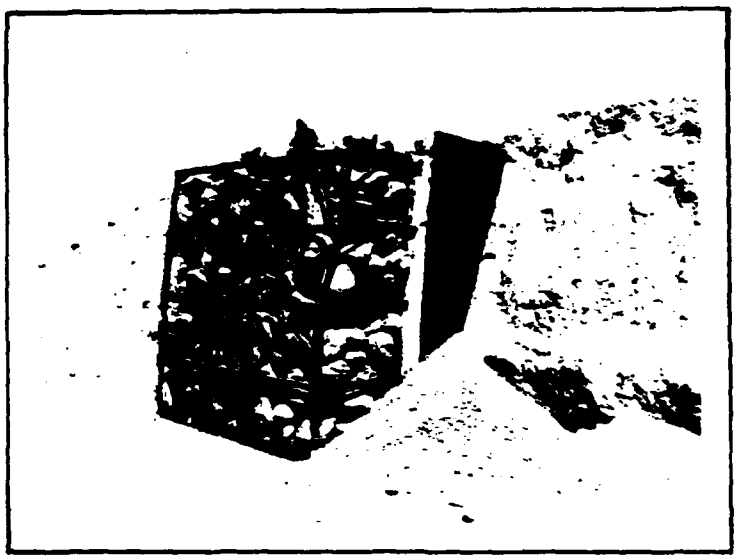

(b)

Figure 1. A View of Antipenetration System: (a) Concrete Burster Slab; (b) Concrete Burster Slab with Layers of Boulder Overlay (Reference 2).

time all of these structures maintain a certain factor of safety. However, the factor of safety for those structures under static loadings of an antipenetration system is unknown since the design method used for the structures did not take into account this particular additional static loading. No field tests have been performed on this study and no data is available. The structural behavior of the concrete arches therefore must be understood and the factor of safety of the structures must first be predicted under static loadings before installation of the protective antipenetration system over prototype military structures.

I.3. Objective

There are three model testings applicable for study of buried structural behavior: full-scale model testing, small-scale laboratory model testing and small-scale centrifuge model testing. Among those model testings, full-scale would be the most ideal approach for obtaining information for buried structures in soils. A full-scale model with the necessary instrumentation could give the best results for estimating prototype behavior of buried structures. Unfortunately, full-scale model testing has serious major drawbacks: mainly, cost and time of construction, and operation. Because of these reasons, small-scale model testing in the laboratory is becoming a favorite testing method in geotechnical engineering.

However, use of small-scale model tests in the laboratory is severely limited when the gravity body force of the structure itself is the principal load on the system, such as in dams and embankments. It is impossible to duplicate the prototype stress in a corresponding small-scale model. Because of this deficiency of small-scale laboratory

testing, the centrifuge model testing has recently become a favorite method in geotechnical engineering. This technique offers a comparatively inexpensive and easy way of obtaining the data which could be obtained from field tests. It also provides opportunities for studying the effect of individual parameters including long-term effects. The objective of this study therefore is to develop a research plan for soil-structure interaction with various types of antipenetration systems in a centrifuge in order to obtain a better understanding of antipenetration-structure interactions of hardening military structures.

I.4. Scope

With this objective in mind, the study as carried out is reported in the following sections. They contain a review of the centrifuge technique; a review of the Air Force Engineering and Services Center's geotechnical centrifuge facility; a discussion of the required testing equipment and instrumentation; and investigation of the factors influencing the stability of the hardened reinforced concrete arches. Finally, a summary of the study is presented.

II. CENTRIFUGE MODELING OF GEOTECHNICAL STRUCTURES

II.1. The Principle of Centrifuge Modeling

Small-scale laboratory models are severely limited in their applicability to geotechnical structures, particularly when gravity (or body) force is the principal load of the system. The stresses in a small-scale model due to its own weight are much smaller in magnitude than those in the corresponding prototype. Since soil is non-linear and

stress-dependent, the difference in stress states between the two renders model behavior dissimilar to that of the prototype. However, if a small model is appropriately scaled and placed inside a centrifuge, a simulated higher gravity field can be generated so that the state of stress at every point in the model is equal to that at the corresponding point in the prototype. Thereby, a major deficiency in model testing of geotechnical structures can be eliminated.

II.2. General Scaling Relationships

In general, scaling relationships can be obtained in two ways: (1) by evaluation of the differential equations governing associated physical phenomena; and (2) by dimensional analysis using a range of scales in testing. The researchers in geotechnical centrifuge modeling have commonly used scaling relations that are based on the the analysis of governing differential equations for the behavior. For example, the governing equation for consolidation phenomena in soils can be written in the form (Reference 4):

$$du/dt = k(1+e) \,/\, (((d^2u/dx^2) + (d^2u/dy^2) + (d^2u/dz^2)) \cdot a \cdot r) \quad - - - - (1)$$

where

u = excess pore water pressure,

t = time,

k = coefficient of permeability,

e = void ratio,

a = coefficient of compressibility, and

r = unit weight of water.

Then one can find the scaling relation of time, $(time)_m = 1/n^2 * (time)_p$ using 1/n dimensional factor, where n is the gravity increase and subscripts m and p designate the model and prototype, respectively. A list of scaling relations determined by this approach can be seen in Reference 4.

The main problem, however, with the differential equation approach is that the method presupposes the physical relations. If the physics of the problem is not throughly known, then the method of dimensional analysis must be used in order to establish a complete set of scaling relationships. Schmidt and Holsapple (Reference 17) demonstrated the capability of dimensional analysis with their centrifuge cratering experience.

II.3. Areas of Application

In principle, the centrifuge modeling technique can be applied in the following areas of geotechnical engineering: (1) determination of mechanisms; (2) parametric studies; (3) validation of numerical analyses; (4) prototype response predictions; and (5) verification of theories.

II.4. Advantages

There are numerous advantages which follow from the use of a centrifuge modeling technique. Some of them are: (1) accurate soil-structure responses, since the stress levels in the model are identical to those in the corresponding prototype; (2) a comparatively inexpensive and simple way of obtaining essentially the same data which could be obtained from the field tests; (3) opportunities for studying

the effects of individual parameters including long-term effects, and collecting more data than field tests usually yield; (4) observation of progressive failure mechanisms and physical process of deformation of the model during the test using video cameras and high speed still cameras; and (5) feasible simulation of dynamic events such as earthquakes and explosive loadings.

III. THE AIR FORCE ENGINEERING AND SERVICES CENTER'S GEOTECHNICAL CENTRIFUGE, AND DESIGN AND CONSTRUCTION OF EXPERIMENTAL APPARATUS

There are about nine centrifuge facilities available in the United States for geotechnical modeling purposes (Reference 4). One of them was located at NMERI (New Mexico Engineering Research Institute). Recently the machine has been transfered to the AFESC (Air Force Engineering and Services Center) and is being assembled at the Center. The author is presently involved in the centrifuge construction project with other research engineers in the Center. It is planned that the centrifuge facility at the Center should be operational by the end of 1986 and will be used for Air Force research projects. The Center's centrifge facility and required instrumentation to carry out the proposed study are discussed in this section.

III.1. The Centrifuge

The Air Force Engineering and Services Center's geotechnical centrifuge is a Genisco Model 185 (Serial Number 11) rotary accelerator. The machine is designed to apply controlled centrifugal accelerations up to 100 g's and a limit of 30,000 g-lbs at a nominal radius of 72 inches. The payload of the testing package can be as heavy as 500 pounds.

The centrifuge facility is under construction in Operation Branch of AFESC. The machine is housed in the 7-feet high, 16-feet diameter and 9-inch thickness reinforced concrete retaining structure. Sub-assembles including the drive motor, the timing belt derive, the RPM pick-up, the rotating arm assembly, the termmal box for control and test connections are supported within this retaining wall.

The boom consists of two symmetrical cantilever arms and adjustable 30-inch square cradle-type mounting platforms. The platform is held by two arms attached to the spokes by two pivots. It can be locked into either the horizontal, 45, 90, 135 or 180 degree positions. This permits the soil surface to remain perpendicular to the vector sum of centrifuge acceleration and the acceleration due to gravity.

Hydraulic and electrical services are available to the model in flight. The hydraulic lines may be used to conduct compressed air or fluids from the outside control area to the model. Hydraulic services are transmitted through rotary journals. Electrical signals are transmitted to the centrifuge rotor and then to the model in flight through a stack of slip rings. A total of 40 slip rings (electrical channels) are provided on the machine, of which 28 are available for sending power to and receive signals from transducers which monitor behavior of the model. These 28 slip rings include 12 instrumentation slip rings (shielded-conductor) designed for 1-amp, low resistance and low noise, and 16 power slip rings (shielded-conductor) of 5-amp current rating. The twelve slip rings (Nos 29 through 40) not used for test purposes are part of the static and dynamic balancing motor and control circuitry and televsion.

For safety reasons, strict operating procedures including both

static and dynamic balancing of the rotating parts must be enforced.

III.2. Photographic and Video Recording Systems

A still photographic system is required to permanently record selected moments of the centrifuge model tests. A camera could be mounted near the hub of the centrifuge. Thus still photographs can be taken with an on-board camera-flash unit by remote control during the tests. The photographs may be used later for analyses.

Video camera and recording device are also required as the monitoring system. This video camera could be mounted near the hub of the centrifuge. This system provided not only a continuous and instantaneous monitor of the test while in progress but also a permanent, replayable record of the model tests.

III.3. Computer Based Data Acquisition Systems

One of the most important considerations in conducting model testing is the accurate monitoring of model behavior. Indeed, model studies will have little value if no quantitative information is accurately recorded. This section discusses the various computer based data acquisition systems suitable for centrifuge model studies. The description given below is a brief one; readers interested in more detailed information should refer elsewhere (References 5-6,8-13,15,18).

Transmission of Signals: Direct transmission of signals is used the most in model studies mainly because of its simplicity and relatively low cost. Also there is no distortion of signals. When used in centrifuge modeling, direct transmission consists of the physical linkage of system

components by wire cables. Brush-and-slip ring riggings are a commonly used method of providing a signal path from the centrifuge shaft to the outside. Brush noise is caused by dynamic vibration in the area in which the brush is in contact with the slip ring. This vibration in contact area gives a variation in circuit resistance. An increase in signal level before reaching slip rings, through amplication, can give a desirable increase in the signal-to-noise ratio. Another beneficial technique is to decrease the total brush resistance by providing multiple parallel current paths; noise would be reduced because variations in brush contact for individual brushes would not be as significant when other brushes are in the path. If a large number of slip rings dedicated to signal transmission are available, the direct transmission system should be considered. It has the advantage of simplicity and uninterrupted transmission of signals.

However, for most of the smaller size centrifuges, there are only a limited number of slip rings for data transmission. A multiplexer-demultiplexer unit (indirect method) is therefore used to facilitate the transmission of signals from a relatively large number of sensors. The two most commonly used multiplexer-demultiplexer units are the time division unit and the frequency modulation (FM) frequency division unit. The time division unit works as a synchronized channel selector as shown in Figure 2 where the frequency division unit works as a dedicated frequency carrier along with FM detectors as shown in Figure 3. Of the two indirect methods of signal transmission, the time division technique is relatively simple and less costly to install; however, additional control signals are needed to synchronize the functions of the multiplexer and demultiplexer. This additional control and operation

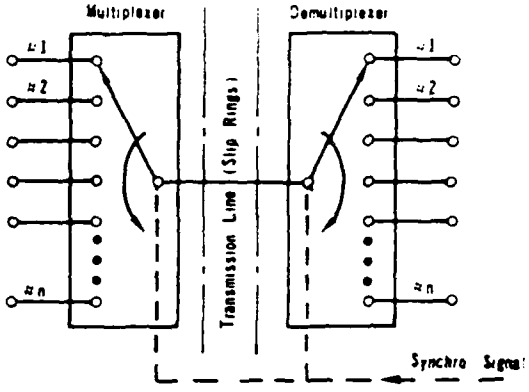

Figure 2. A Time Division Multiplexer-Demultiplexer Unit (Reference 18).

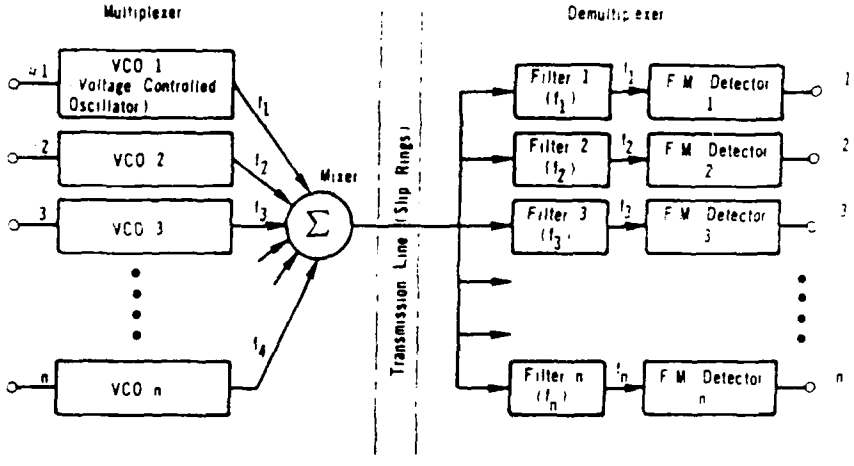

Figure 3. A Frequency Division Multiplexer-Demultiplexer Unit (Reference 18).

time impedes the sampling rate of the system. The frequency division technique, on the other hand, is costly but capable of transmitting signals at much higher rates. Since the FM system is sensitive only to frequency variations and not amplitudes, it is immune to most noises induced along the transmission line.

It should also be mentioned that wireless sensors can be adopted to transmit radio frequency signals thus bypassing the use of connecting wires between sensors and the signal conditioning unit. However, these sensors are very expensive and usually too big in size and too heavy, not readily suitable for geotechnical use. The author does not foresee the need to use wireless sensors in centrifuge modeling in the future.

III.4. Insrumentation

Displacment Gage: In general, linear variable differential transducers (LVDT) are used for measurement of deformations. However, LVDTs are not suitable for measuring soil deformation in the centrifuge because their moveable cores become so heavy during flight that they may punch into the soft soil. A light-weight, low-cost transducer incorporating a light-sensitive element and thin rod can be developed for use in centrifuge as explained in Reference 7. This optical-electrical displacement (OED) transducer has a linear range of 1.5 inches, and the weight and the cost are 1/5 and 1/100, respectively, of the corresponding commercial LVDT currently available in the market.

Strain and Stress Gages: A commercial strain gage (i.e., Measurement Group, Inc. gages) can be used to measure the strains on the surface of the structures. These gages have been widely used by industries and academia and user responses have been very favorable. No

difficulties are anticipated in use of the strain gages for the centrifuge model study. However, unlike to strain gages, stress gages to measure the soil pressure around the structure are still in infancy. Further development is necessiciated to measure the reliable soil pressures.

III.5. Model Box

A centrifuge model box to contain the soil model is needed to be designed for model tests. All the components must be safe operational under at least centrifugal loading of 100 g.

The model box could be made of aluminum alloy plates. The plates would be rolled, and welded together to form a cylindrically-shaped tub or rectangular-type box. The maximum outside diameter or width of the model box could be 28 inches and the height of the model box would be 15 inches.

IV. FACTORS INFLUENCING THE STABILITY OF BURIED CONCRETE ARCHES

The safety factors considered as the traditional criteria for the design of the reinforced concrete arches are: (1) safety factor against reinforcement yielding; (2) safety factor against concrete crushing; (3) safety factor against diagonal cracking; (4) safety factor against bowstringing; and (5) safety factor against diametrical displacement. These criteria state that if the calculated safety factor of the structure is at all greater than the allowable safety factor, the structure will remain stable. On the other hand, if the calculated safety factor becomes less than the allowable safety factor, the structure will be unstable. Accordingly, an investigation of the

stability of the hardended concrete arches is to determine the factors causing a reduction in strength of the structure.

A number of factors have been identified that cause a reduction in strength. They are: (1) material types in an embankment (backfill) and foundation (bedding); (2) thickness and slope of an embankment; (3) accumulation of water within an embankment; (4) freezing and thawing action and weathering of the soil; and (5) applying shock loads. These factors will cause a wall yielding, crushing, seam failure, excessive deflection and/or buckling of the hardended reinforced concrete arches. During the course of the model study (Figure 4), the effects of the aforementioned factors will be critically investigated through the centrifuge model study.

V. SUMMARY

During the last a few years, several research programs were undertaken by the United States Air Force to develop the protective antipenetration system for military facilities constructed on the ground surface. Protective concepts consisting of rock rubble/boulder and burster slab over soils were introduced, and full-scale models were tested to determine the levels of protection againt conventional weapons. Based on information obtained from the field tests, the system has proven effective to resist the penetration of conventional weapons. It is now being considered for application over military facilities. However, structural designers are facing one critical question before application of the system: Will these military structures be safe under static loadings due to the weight of soil, rock rubble/boulder layers and/or burster slabs?

● : Soil Stress Meter
— : Strain Gage
—[L]— : LVDT (displacement gage)

Variables : t (thickness), r (radius), d (diameter), T (thickness), W (width), S (slope), and H (height)

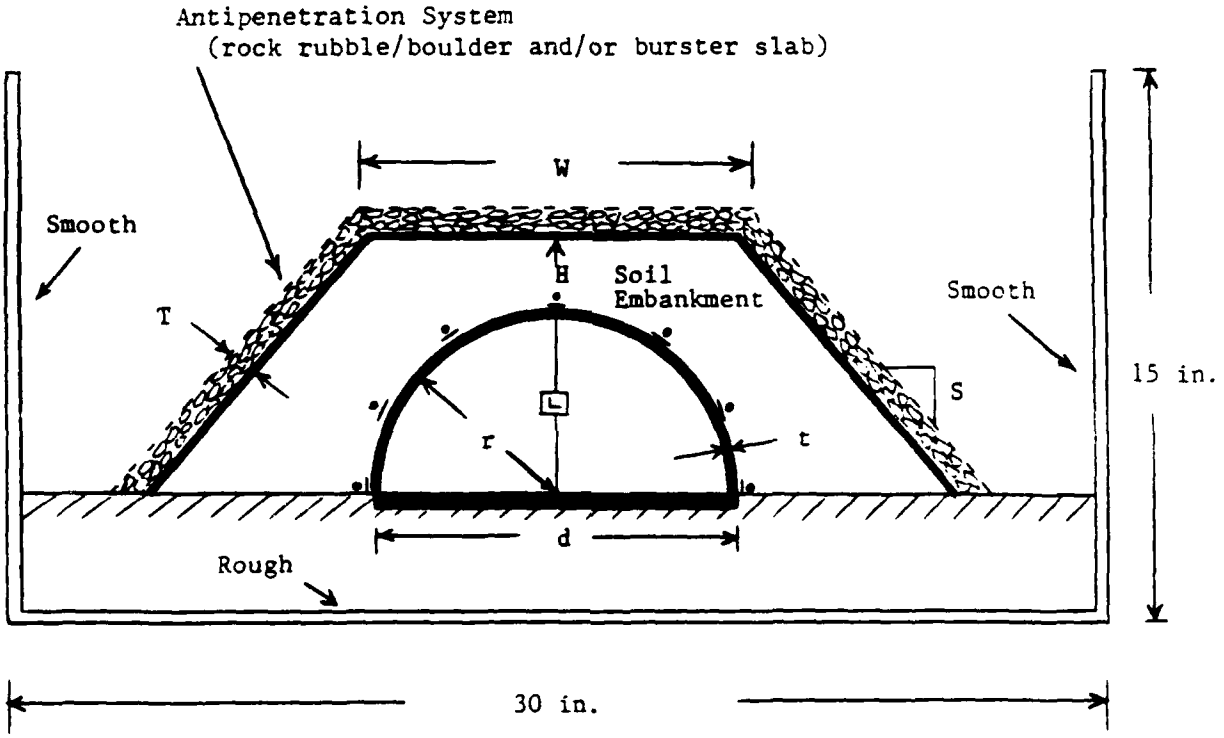

Figure 4. Reinforced Concrete Arch Model with Instrumentation and Boundary Condition.

There are numerous arch-type protective structures (e.g., 1st, 2nd and 3rd generation aircraft shelters) which have been constructed on the ground surface in the United States and NATO countries. The factor of safety for those structures under static loadings of an antipenetration system is unknown since the design method used for the structures did not take into account this particular additional static loading. No field tests have been performed on this study and no data is available. The structural behavior of the concrete arches therefore must be understood and the factor of safety of the structures must first be predicted under static loadings before installation of the protective antipenetration system over prototype structures.

The author therefore proposes to study the stability and behavior of the concrete arches under static loadings by means of model studies in the centrifuge. Accordingly, the centrifuge model technique is first reviewed, and the centrifuge facility at Air Force Engineering and Services Center is evaluated. The required equipment and instrumentation for the centrifuge model study at the Center are recommended based on the findings of the evaluation. In addition, the parameters influencing the stability of concrete arches are elaborated with a discussion for classifying them as to the design criteria.

REFERENCES

1. Austin, C.F., Halsey, C.C., Clodt, R.L., and Berry, S.L., "Full-Scale Penetration into Semiconfined Diorite Boulders by a Semiarmor-Piercing (SAB) Bomb," Report No. ESL-TR-81-47, Air Force Engineering Services Center, Tyndall AFB, Florida, January, 1982, UNCLASSIFIED.

2. Austin, C.F., Halsey, C.C., Clodt, R.L., and Berry, S.L., "Protective Antipenetration Systems Development," Report No. ESL-TR-83-39, Air Force Engineering Services Center, Tyndall AFB, Florida, September, 1983, UNCLASSIFIED.

3. Austin, C.F., Halsey, C.C., Berry, S.L., and Anderson, C.R., "Burster Slab Penetration Test," Report No. ESL-TR-84-49, Air Force Engineering Services Center, Tyndall AFB, Florida, July, 1985, UNCLASSIFIED.

4. Cheney, J.A, and Fragaszy, R.J.,"The Centrifuge as a Research Tool," Proceedings of the ASTM, Geotechnical Testing Journal, Volume 7, Number 4, December, 1984.

5. Finkel,J., Computer-Aided Experimentation, John Wiley, New York, 1975.

6. Freeman, R.L., Telecommunication Transmission Handbook, Wiley, New York, 1975.

7. Kim, Y.S., Shen, C.K. and Bang, S., "Centrifuge Model Study of an Oil Storage Tank Foundation on Soft Clay," Proceedings of the 8th 8th European Conference on Soil Mechanics and Foundation Engineering, Helsinki, Finland, May 23-26, 1983.

8. Moore, C.A., "Modern Electronics for Geotechnical Engineers, 1. Introduction to Integrated Circuits," Proceedings of the ASTM, Geotechnical Testing Journal, Volume 3, Number 1, March, 1980.

9. Moore, C.A., "Modern Electronics for Geotechnical Engineers, 4. Waveform Generators," Proceedings of the ASTM, Geotechnical Testing Journal, Volume 3, Number 2, June, 1980.

10. Moore, C.A., "Modern Electronics for Geotechnical Engineers, 5. Digital Logic Circuits," Proceedings of the ASTM, Geotechnical Testing Journal, Volume 3, Number 3, September, 1980.

11. Moore, C.A., "Modern Electronics for Geotechnical Engineers, 6. Process Control Applications," Proceedings of the ASTM, Geotechnical Testing Journal, Volume 3, Number 4, December, 1980.

12. Moore, C.A., "Modern Electronics for Geotechnical Engineers, 7. Introduction to Microprocessors," Proceedings of the ASTM, Geotechnical Testing Journal, Volume 4, Number 1, March, 1981.

13. Moore, C.A., "Modern Electronics for Geotechnical Engineers, 8. Microprocessor Applications," Proceedings of the ASTM, Geotechnical Testing Journal, Volume 4, Number 2, June, 1981.

14. Research Engineers, Personnal Communication, Facility Systems and Analysis Branch, and Operations Support Branch, Air Force Engineering Services Center, Tyndall AFB, Florida, May-August, 1986.

15. Roden, M.S., Analog and Digital Communication, Prentice-Hall, Englewood Cliffs, NJ, 1979.

16. Rohani, B., "Effectiveness of Rock-Rubble/Boulder Screens for Degrading the Penetration Capability of Kinetic Energy (KE) Projectiles," Report to Office, Chief of Engineers, U.S. Army, Waterways Experiment Station, Vicksburg, Mississippi, December, 1982, UNCLASSIFIED.

17. Schmidt, R.M., and Holsapple, K.A., Journal of Geophysical Research, Vol. 85, No. B1, January, 1980.

18. Shen, C.K., Li, X.S. and Kim, Y.S., "Microcomputer Based Data Acquisition Systems for Centrifuge Modeling," Proceedings of the ASTM, Geotechnical Testing Journal, Volume 7, Number 4, December, 1984.

1986 USAF-UES SUMMER FACULTY RESEARCH PROGRAM/

GRADUATE STUDENT SUMMER SUPPORT PROGRAM

Sponsored by the

AIR FORCE OFFICE OF SCIENTIFIC RESEARCH

Conducted by the

Universal Energy Systems, Inc.

FINAL REPORT

The Synthesis of Fluorodinitroethylnitraminoalkyl Nitrates and Compatibility Studies of GAP-Nitrate and TAET

Prepared by: Joel R. Klink

Academic Rank: Professor

Department: Department of Chemistry

University: University of Wisconsin-Eau Claire

Research Location: The Air Force Rocket Propulsion Laboratory

MKPL, Edwards Air Force Base

USAF Researcher: Dr. Claude Merrill

Date: August 19, 1986

Contract No.: F49620-85-C-0013

The Synthesis of Fluorodinitroethylnitraminoalkyl Nitrates and Compatibility Studies of GAP-Nitrate and TAET

by

Joel R. Klink

ABSTRACT

A series of hydroxyalkylamines were condensed with 2-fluoro-2,2-dinitroethanol. Nitration of the resulting products with a mixture of fuming nitric and sulfuric acids yielded the nitraminoalkyl nitrates. Notably tris(hydroxymethyl)methylamine was found to undergo this reaction sequence to yield 5-fluoro-2,2-bis(hydroxymethyl)-3,5,5-trinitro-3-aza-1-pentanol trinitrate. The compatibility of glycidyl azide polymer containing nitrate end-groups (GAP-nitrate) and 2,2,2-tris(azidomethyl)ethyl 4,4,4-trinitro-n-butyrate (TAET) with typical solid propellant components was also studied. After 62 days at 63°C (145°F) no extensive degradation was observed as evidenced by the lack of gas evolution. Some color changes did occur, however.

Acknowledgements

I would to thank the Air Force Systems Command and the Air Force Office of Scientific Research for sponsoring this research. Dr. Claude Merrill, to whom I owe special thanks, directed this research and provided the needed guidance in the preparation and handling of these explosive materials. I would also like to thank Mr. Louis Dee and members of his staff for obtaining the spectral data and elemental analyses. Finally, I would like to thank my wife, Joann, and daughter, Cara, for their willingness to temporarily relocate and for their support and encouragement throughout the summer.

I. Introduction

I received my Ph.D. in organic chemistry from Ohio State University in 1964. My doctoral research, under the direction of Dr. William N. White, involved a study of the acid-catalyzed rearrangement of N-nitroanilines, the so-called "nitramine rearrangement." Ring substituted N-nitroanilines were synthesized and kinetic studies conducted under pseudo first-order conditions in acid solution.

Although the synthesis of aromatic nitramines and their thermal properties differ quite markedly from the aliphatic analogs, my research experience provided at least a working knowledge of the properties of nitramines. Furthermore, my research at the University of Wisconsin-Eau Claire has involved the synthesis and chemistry of the toxic and thermally unstable compound, 3-diazapropene. Given this background plus my knowledge of organic synthetic techniques and characterization methods, I felt sufficiently prepared to pursue the synthesis project and the compatibility studies.

II. Objectives of the Research Effort

A. Synthesis

The Air Force desires materials for use in solid propellants that are capable of being advantageously substituted for nitroglycerin (a plasticizer) or HMX, cyclotetramethylenetetranitramine (a solid oxidizer). New plasticizers would hopefully have an energy content equal to or better than nitroglycerin and/or other improvements in properties such as lower volatility, greater density, lower melting point, and greater thermal stability. New oxidizers

should have greater energy content and/or density than HMX with good thermal stability.

As a plasticizer nitroglycerin has favorable energetics but has thermal stability and vapor pressure shortcomings. Its vapor pressure is sufficiently high so that a thin film of nitroglycerin often condenses on cooler equipment surfaces during a propellant mixing process. Since nitroglycerin can easily undergo thin film friction and impact initiation to detonation, a potential hazard to personnel and the mix facility is provided.

Synthesis of a plasticizer is challenging because of the required emphasis on liquid range. This synthesis effort was aimed at gaining some insight into how chemical structure and melting point are related for compounds containing the energetic primary alkyl nitrate ($-CH_2ONO_2$), fluorodinitroethyl [$-CH_2C(NO_2)_2F$] and ($-\overset{|}{N}-NO_2$) groups. Therefore, we decided to condense a series of closely related hydroxyalkylamines with 2-fluoro-2,2-dinitroethanol, 1, and nitrate the resulting 2-fluoro-2,2-dinitroethylhydroxyalkylamines with a mixture of nitric acid and sulfuric acid, equations 1 and 2. The modified Mannich reaction of 1 and the related reactions of trinitromethane

$$HO\text{-}R\text{-}NH_2 + (O_2N)_2CFCH_2OH \longrightarrow (O_2N)_2CFCH_2N(NO_2)\text{-}R\text{-}ONO_2 \qquad (1)$$

$$(O_2N)_2CFNH\text{-}R\text{-}OH + HNO_3 \xrightarrow{H_2SO_4} (O_2N)_2CFCH_2N(NO_2\text{-}R\text{-}ONO_2 \qquad (2)$$

or fluorodinitromethane and formaldehyde occur with a variety of primary alkylamines and hydroxyalkylamines.[1-4] It has been reported that tris(hydroxymethyl)methylamine, 2, will not condense

with fluorodinitromethane and formaldehyde under a variety of conditions.[5] On the other hand, 2-amino-2-methyl-1,3-propanediol reacts readily with nitroform and formaldehyde to give the Mannich product.[3] The reaction of hydroxyalkylamines with nitric acid-sulfuric acid mixtures to simultaneously form nitramino nitrates has been studied.[4,6]

We were particularly interested in the synthesis of 5-fluoro-3,5,5-trinitro-2,2-bis(hydroxymethyl)-3-aza-1-pentanol trinitrate, 3, as shown in equations 3 and 4. It was

$$(O_2N)_2CFCH_2OH + NH_2C(CH_2OH)_3 \longrightarrow (O_2N)_2CFCH_2NH(CH_2OH)_3 \quad (3)$$

$$(O_2N)_2CFCH_2NHC(CH_2OH)_3 + HNO_3 \xrightarrow{H_2SO_4} (O_2N)_2CFCH_2N(NO_2)C(CH_2ONO_2)_3 \quad (4)$$

anticipated that 3 might have energetics similar to nitroglycerin but have a lower vapor pressure as indicated by the greatly increased molecular weight. This could eliminate the condensation hazard mentioned above. Other properties such as density and sensitivity to impact, shock, and friction as well as improved thermal stability could be predicted to be favorable for this substance.

Although 3 has been prepared by a five-step procedure,[5] given the apparent inconsistency of published reports on the Mannich condensations of hydroxyalkylamines with fluorodinitroethanol or fluorodinitromethane-formaldehyde reagents, we felt that the proposed two-step sequence might be realized. Furthermore, doubt arose that the multistep synthesis of 3 and its melting point, 98.5°C were correct.

B. Compatibility Studies

In addition to the synthesis effort, a 62-day, 145°F compatibility study was conducted between typical solid propellant ingredients and two candidate azidoplasticizers, one of which was an oligomeric glycidyl azide terminated by nitrate groups, called GAP-nitrate, and the other 3-azido-2,2-bis(azidomethyl)propyl 4,4,4-trinitro-n-butyrate or tris(2,2,2-azidomethyl)ethyl 4,4,4-trinitro-n-butyrate, identified as TAET. Specifically, serious degradation, as evidenced by gassing, was to be examined.

III. Synthesis of Fluorodinitroethylnitraminoalkyl Nitrates

The series of hydroxyalkylamines, varying in the number of hydroxymethyl groups, and some related compounds were reacted with 1 using the published procedure for 2-aminoethanol.[1] Table I lists the amines treated with 2-fluoro-2,2-dinitroethanol and the yields of unpurified products.

Unlike the other amines, tris (hydroxymethyl)methylamine failed to yield an insoluble oil and a continuous methylene chloride extraction of the reaction mixture resulted in the isolation of only a small amount of unreacted 2. Evaporation of the water from the aqueous phase of the reaction mixture in a stream of nitrogen left a yellow semicrystalline mass which upon work-up, as detailed in the experimental section, yielded the expected condensation product.

Proton (^{1}HNMR) magnetic resonance and infrared (IR) spectra support the structural assignments. The expected IR absorption bands and NMR signals are apparent. Until analytically pure samples of each compound have been prepared, a listing of peak assignments would not be meaningful.

Table I. Reaction of 2-Fluoro-2,2-dinitroethanol with Hydroxyalkylamines. R = $CH_2CF(NO_2)_2$

Amine	Product	Yield (in percent)
$HOCH_2CH_2NH_2$	$HOCH_2CH_2NHR$	74
$HOCH_2C(CH_3)_2NH_2$	$HOCH_2C(CH_3)_2NHR$	76
$(HOCH_2)_2C(CH_3)NH_2$	$(HOCH_2)_2C(CH_3NHR$	48
$(HOCH_2)_3CNH_2$	$(HOCH_2)_3CNHR$	84
$HOCH(CH_3)CH_2NH_2$	$HOCH(CH_3)CH_2NHR$	76
$(HOCH_2CH_2)_2NH$	$(HOCH_2CH)_2NR$	54

Table II. Nitration of 2-Fluoro-2,2-dinitroethyl Hydroxyalkyl Amines. R = $CH_2CF(NO_2)_2$

Amine	Product	Yield (in percent)
$HOCH_2CH_2NHR$	$O_2NOCH_2CH_2N(NO_2)R$	70
$HOCH_2C(CH_3)_2NHR$	$O_2NOCH_2C(CH_3)_2N(NO_2)R$	65
$(HOCH_2)_2C(CH_3)NHR$	$(O_2NOCH_2)_2C(CH_3)N(NO_2)R$	86
$(HOCH_2)_3CHNR$	$(O_2NOCH_2)_3CN(NO_2)R$	60
$CH_3CH(OH)CH_2NHR$	$CH_3CH(ONO_2)CH_2N(NO_2)R$	90
$(HOCH_2CH_2)_2NR$	$(O_2NOCH_2CH_2)_2NR$	43

Nitration of the 2-fluoro-2,2-dinitroethylhydroxyalkylamines with a mixture of fuming nitric and fuming sulfuric aicds in methylene chloride gave the N-nitraminoalkyl nitrates. The results are given in Table II. The assigned structures were confirmed by proton NMR and infrared spectroscopy.

All of these nitrates detonate upon hammer impact on steel but appear to be resistant to detonation by friction between steel surfaces.

IV. Experimental

CAUTION!! Most of the products described in this report are explosives of moderate to high sensitivity to initiation by impact, shock or other means and must be handled with appropriate care. 2-Fluoro-2,2-dinitroethanol, 1, is a vessicant and skin irritant and must be handled in an adequate exhaust hood with skin contact avoided.

A. Mannich condensations (general). To an aqueous solution of 1 consisting of 4-6 ml of water per 0.010 mol of 1 was added an aqueous solution of the amine (4-6 ml of water per 0.010 mol of amine). The reaction mixture was stirred at room temperature for two hours and then was extracted 2 or 3 times with 15 ml portions of methylene chloride. The combined extracts were washed 2 x 10 ml of water, dried over anhy magnesium sulfate and the solvent evaporated at reduced pressure to yield the crude oil or solid.[1] The reaction with tris(hydroxymethyl)-methylamine required a different work-up as described below.

5-Fluoro-5,5-dinitro-3-aza-1-pentanol. From 1.54g (0.0100 mol) of 1 and 0.61 g (0.010 mol) of ethanolamine was obtained 1.45 g (74%) of pale yellow oil.

5-Fluoro-2,2-dimethyl-5,5-dinitro-3-aza-1-pentanol. From 1.54 g (0.0100 mol) of 1 and 0.90 g (0.010 mol) of 2-amino-2-methyl-1-propanol was obtained 1.70 g(76%) of yellow oil.

5-Fluoro-2-hydroxymethyl-2-methyl-5,5-dinitro-3-aza-1-pentanol. From 1.44 g (0.0094 mol) of 1 and 0.987 g (0.0094 mol) of 2-amino-2-methyl-1, 2-propanediol was obtained 1.09 g (48%) of a pale yellow solid, m.p. 61-68°C.

5-Fluoro-5,5-dinitro-4-aza-2-hexanol. From 1.55 g (0.0101 mol) of 1 and 0.77 g (0.0103 mol) of 1-amino-2-propanol was obtained 1.62 (76%) of yellow oil.

5-Fluoro-3-(2-hydroxyethyl)-5,5-dinitro-3-aza-1-pentanol. From 1.54 g (0.010 mol) of 1 and 1.05 g (0.010 mol) of diethanolamine was obtained 1.31 g (54%) of yellow oil.

5-Fluoro-2,2-bis(hydroxymethyl)-5,5-dinitro-3-aza-1-pentanol. To a stirred solution of 5.08 g (0.0330 mol) of 1 in 10 ml of water was added all at once a solution of 3.63 g (0.300 mol) of tris(hydroxymethyl)methylamine in 12 ml of water. The mixture was stirred 2 hours at room temperature and then was washed twice with 15 ml of methylene chloride. Evaporation of water from the aqueous phase followed by air drying for 24 hr. yielded 6.47 g (84%) of a semicrystalline solid, m.p. 69-80°C. Recrystallation of 3.20 g of the crude solid from 125 ml of ethylene dichloride yielded 2.30 g (72% recovery) of faintly yellow crystals, m.p 79-83°C.

B. Nitrations

To a magnetically stirred mixture of 0.010 mol of the fluorodinitroethylhydroxyalkylamine and 20 ml of methylene chloride was added dropwise 90% fuming nitric acid (1 ml of acid/0.0010 mol of amine) maintaining the temperature at 0-5°C. To the resulting solution was added dropwise 20% fuming sulfuric acid, 1 ml/0.0010 mol of amine, keeping the temperature at 0-5°C. The reaction mixture was stirred 30 min, the ice-bath removed and stirring continued for 2 hours. The reaction mixture was poured slowly with vigorous stirring over a mixture of 40-50 ml of methylene chloride and ice and the layers separated. The aqueous layer was extracted twice with 15 ml methylene chloride and the combined organic extracts were wasned 2 or 3 times with 15 ml of 10% aq. sodium bicarbonate and once with 15 ml water. After drying over magnesium sulfate, roto evaporation of the solvent yielded the product. The procedure was modified in one instance, as detailed below, since the staring amine was tertiary.

5-Fluoro-3,5,5-trinitro-3-aza-1-pentanol nitrate. From 0.986 g (0.0050 mol) of crude amine was obtained 0.997 g (70%) of pale yellow oil.

5-Fluoro-2,2-dimethyl-3,5,5-trinitro-3-aza-1-pentanol nitrate. From 1.132 g of crude amine was obtained 1.036 g (65%) of pale yellow oil.

5-Fluoro-2-hydroxymethyl-2-methyl-3,5,5-trinitro-3-aza-1-pentanol-dinitrate. From 0.602 g (0.00250 mol) of crude amine was obtained 0.812 g (86%) of yellow oil.

5-Fluoro-2,2-bis(hydroxymethyl)-3,5,5-trinitro-3-aza-1-pentanol trinitrate. From 2.06 g (0.00800 mol) of the purified amine was obtained 2.10 g (60%) of faintly yellow crystals, M.p 93-97°C, lit[5] 98.5°C.

5-Fluoro-3,5,5-trinitro-4-aza-2-hexanol nitrate. From 1.06 of crude amine was obtained 1.36 g (90%) of pale yellow oil which solidified after two weeks, m.p. 51-54°C.

5-Fluoro-3-(2-hydroxyethyl)-5,5-dinitro-3-aza-1-pentanol dinitrate. After the nitration mixture was poured over ice, solid sodium bicarbonate was added in portions to neutralize the acid. The resulting mixture was extracted with methylene chloride, the combined extracts washed with water and then dried. From 0.718 g (0.00298 mol) of crude amine was obtained 0.427 g (43%) of pale yellow oil.

V. Compatibility Studies

Weighed mixtures of glycidyl azide polymer containing nitrate end groups (GAP-nitrate) and 2,2,2-tris(azidomethyl)ethyl 4,4,4-trinitro-n-butyrate (TAET) in capped plastic vials were placed in a 145°F oven. The mixtures were examined periodically to determine whether chemical degradation had occurred. Tables III and IV list the mixture compositions which were similar in proportion to solid propellant formulations. Listed below are definitions of the abbreviations used: NC, nitrocellulose; MNA, N-methyl-4-nitroaniline; PEG-4000, poly(ethylene glycol); N-100, an isocyanate curing agent product by Mobay formed from reaction of hexamethylene diisocyanate and water; HMX, cyclotetramethylenetetranitramine; TMETN, trimethylolethane trinitrate; TPB, triphenylbismuth; AP, ammonium perchlorate; Al, aluminum powder. Mixtures 1-10 were examined visually after 1, 4,

Table III. GAP-Nitrate Mixtures.

Mixture No.	Components	Percent by Weight
1	GAP-nitrate	22.8
	NC	3.0
	MNA	3.0
	PEG-4000	9.7
	N-100	3.4
	HMX	58.0
2	GAP-nitrate	47.5
	TMETN	52.4
3	GAP-nitrate	89.3
	TPB	10.7
4	GAP-nitrate	49.0
	Al	51.0
5	GAP-nitrate	67.9
	AP	32.1

Table IV. TAET Mixtures.

Mixture No.	Components	Percent (by weight)
6	TAET	17.6
	NC	4.6
	MNA	4.3
	PEG-4000	9.7
	N-100	6.8
	HMX	57.0
7	TAET	55.0
	TMETN	45.0
8	TAET	90.4
	TPB	9.6
9	TAET	50.0
	Al	50.0
10	TAET	68.3
	AP	31.7
11	TAET	66.9
	PEG-4000	33.1
12	TAET	95.6
	NC	4.4
13	TAET	97.0
	MNA	3.0
14	TAET	87.1
	N-100	12.9
15	TAET	33.3
	HMX	66.7

8, 15, 21, and 62 days at 145°F. Mixtures 11-15, which were prepared later, were examined after 1, 2, 5, 8, 16, and 32 days.

GAP-Nitrate Mixtures. None of the mixtures gave any evidence of extensive chemical degradation. No gas evolution occurred, only some color changes were noted. Mixture 1 developed a small orange spot after 8 days and several small brown-orange spots by 32 days. Mixture 3 (GAP-NO_3, TPB) was cloudy at 4 days. Mixtures 2, 4, and 5 did not appear to change. The change in mixture 1 could be due to reaction with MNA or perhaps degradation of MNA itself since the vials were not flushed with nitrogen and therefore oxygen was present. In mixture 3 perhaps the TPB was oxidized slightly.

TAET Mixtures. Again none of the mixtures appeared to degrade extensively since no gas evolution occurred. Mixture 6 turned orange within 4 days and developed brown spots by 15 days. Mixture 8 (TAET, TPB) was orange after 1 day and had solidified. Mixtures 7, 9, 10 did not change visibly. An attempt was made to identify which components in mixture 6 were causing the color change with TAET. The binary mixtures 11-15 were prepared and stored at 145°F. Mixture 11 (TAET, PEG-4000) became yellow after 1 day but did not change thereafter. Mixture 13 (TAET, MNA) was amber after 2 days and had become homogenous. Mixture 14 (TAET, N-100) had gelled and was amber at 16 days. Mixtures 12 and 15 did not change in appearance.

FTIR spectra were obtained on the "aged" mixtures 13 and 14 and compared with spectra of freshly prepared mixtures. In both cases the spectra were nearly identical. The N-H stretch at ca.

3400cm^{-1} in mixture 13 is broader which may reflect increased hydrogen bonding in the homogenous matrix compared to the heterogeneous freshly prepared mixture. The TAET/N-100 mixture, mixture 14, shows an N-H or O-H stretch at about 3350 cm^{-1}, which is absent in the freshly prepared mixture. Since mixture 14 gelled, this bond may be due to a small amount of water resulting from cross-linking of the N-100.

In summary, both GAP-nitrate and TAET are compatible with the propellant components examined. Although some minor color changes were observed no significant chemical degradation occurred.

VI. Recommendations

1. Since most of the compounds synthesized in this research are new, samples should be carefully purified to permit complete characterization, particularly their relative thermal stabilities, densities, and melting points. To complete the series, 2-amino-1, 3-propanediol, and 2-amino-1-propanol should be subjected to the reaction sequence. With this additional work, publication of the results would be warranted.

2. Although the target compound has an undesirable melting point to permit use as a plasticizer in solid propellant formulations, it may have desirable energetics. A study should be undertaken to see if a blend with another energetic plasticizer can be found which will lower the melting point sufficiently.

3. An attempt should be made to synthesize 2,2-difluoro-2-nitroethanol and its condensation with tris(hydroxymethyl)-methylamine investigated. In effect, this would result in the replacement of one nitro group by fluorine in the final product which should lower the melting point since the molecular weight, symmetry, and, presumably, the polarity of the final molecule will be lowered. This could be a good blending agent to be used with 1.

4. Since we have shown that tris(hydroxymethyl)methylamine will condense with 2-fluoro-2,2-dinitroethanol, its condensation with 2,2-dinitro-1,3-propanediol should be studied. Nitration of the condensation product should yield a very dense energetic material with possibly a high melting point given its symmetry and high molecular weight. Such a material might find use as an energetic oxidizer.

5. Similarly, 2,2-dinitropropanol should condense with tris(hydroxymethyl)methylamine and nitration of the product should yield another energetic plasticizer that should be lower melting than 3. Blending of this material with 3 should be considered.

6. TMETN, trimethylolethane trinitrate, has been used as part of an alkyl nitrate plasticizer blend in solid propellant formulations. Its density, 1.47 g/cc, is somewhat lower than desired and the presence of a methyl group gives it a low oxygen balance. The synthesis of the fluoro analog, i.e.,

fluorine in place of methyl, may yield a plasticizer of greater density than TMETN and probably of greater energetics. This material could be used directly as a single plasticizer or be blended with 3 to make a low melting mixed plasticizer.

Literature References

1. Graukauskas, V. and K. Baum, "Mannich Reactions of 2-Fluoro-2, 2-dinitroethanol," Journal of Organic Chemistry, 36(1971), 2599-2602.

2. Witucki, E.F., G.L. Rowley, N.N.Ogimachi, and M.B. Frankel, "Dinitrofluoroethyl Derivatives," Journal of Chemical and Engineering Data, 16(1971), 373-375.

3. Feuer, H. and W.A. Swarts, "Chemistry of Trinitromethane. IV. Preparation of N-Nitro-N-trinitroethylamino Alcohols," Journal of Organic Chemistry, 27(1962), 1455-6.

4. Eremenko, L.T., D.A. Nesterenko, and N.S. Natsibullina, "N-(2-Fluoro-2, 2-dinitroethyl)-N-nitroamino Alcohols and Some of Their Derivatives," Bulletin of the Academy of Sciences of the USSR. Division of Chemical Science, English Translation, 1970, 1261-1264.

5. Nesterenko, D.A., O.M. Savchenko, and L.T. Eremenko, "Trimethylalaminomethane in the Mannich Reaction," Bulletin of the Academy of Sciences of the USSR. Division of Chemical Science, English Translation, 1970, 1039-1042.

6. Baum, K. and W. T. Maurice, "The Mannich Condensation of 3-Amino-1, 2-propanediol with 2, 2-Dinitropropanol and Nitration of the Product." Journal of Organic Chemistry, 27(1962), 2231-33.

1986 USAF-UES SUMMER FACULTY RESEARCH PROGRAM/

GRADUATE STUDENT SUMMER SUPPORT PROGRAM

Sponsored by the

AIR FORCE OFFICE OF SCIENTIFIC RESEARCH

Conducted by the

UNIVERSAL ENERGY SYSTEMS, INC.

FINAL REPORT

RELIABILITY IN SATELLITE COMMUNICATION NETWORKS

Prepared by:	Stephan E. Kolitz
Academic Rank:	Assistant Professor
Department and	Management Sciences Dept.
University:	University of Massachusetts/Boston
Research Location:	ESD/MD
USAF Research:	George Richardson
Date:	September 24, 1986
Contract No:	F49620-85-C-0013

RELIABILITY IN SATELLITE COMMUNICATION NETWORKS

Stephan E. Kolitz

ABSTRACT

A very important requirement of a communication network is to deliver data from a source node to a destination node. The physical layout of a communication network and the method of routing data in it are very closely related. This report looks at a class of network layouts called loop topologies and identifies reasonable measures and some algorithms that appear useful in calculating these measures. In addition, an algorithm which finds the most reliable path between nodes is presented.

I. INTRODUCTION

A very important requirement of a communication network is to deliver data from a source node to a destination node. In practice, communication networks can be categorized based on the architecture and techniques used to deliver the data. For the purpose of this report, the communication networks can be regarded as packet switching networks, but the issues that are addressed here are applicable for other types of networks. Some excellent references in this field are Rosner [1982], Tanenbaum [1981] and especially Stallings [1985].

The physical layout of a communication network and the method of routing data in it are clearly very closely related. Tanenbaum suggests a number of desirable attributes in the routing function of a communication network: correctness, simplicity, robustness, stability, fairness and optimality. Stallings adds efficiency to this list. There is no way to optimize routing over all these objectives; there is always a trade-off involved. However, the design of the network should allow for routing which is "good", however the "goodness" may be measured. This report looks at a class of network layouts called loop topologies and identifies reasonable reliability measures and some algorithms that appear useful in calculating these measures. A loop topology is a natural topology to consider for linking satellites in space.

II. OBJECTIVES OF THE RESEARCH EFFORT

The goal of this report is to begin to develop tools which will allow

descriptive quantitative analyses of various reliability measures of interest in a communication network. Given the existence of a proposed design for a communication network, this design could then be analyzed in terms of appropriate reliability measures and the design iteratively changed if desired.

III. MATHEMATICAL PRELIMINARIES

Complexity Theory

A problem which requires n bits to be fully specified is said to be of size n. If such a problem can be solved by an algorithm whose running time is a polynomial function of n, then the algorithm is said to be solvable in polynomial time. If an algorithm's running time cannot be bounded by a polynomial function of n, then the algorithm is called an exponential time algorithm. If no polynomial time algorithm exists to solve a particular problem, the problem is said to be intractable. NP-complete problems form an equivalence class in the following sense: if a polynomial time algorithm exists for one of the NP-complete problems, then every NP-complete problem has a polynomial time algorithm. As of now, no polynomial time algorithm has been found for any of the known NP-complete problems. While many people believe the conjecture that NP-complete problems are intractable, it has not been proved and it is the most important open question in current complexity theory.

Graphs

A graph G = (V,E) consists of a vertex set

$$V = \{ v(1), v(2), \ldots, v(N) \}$$

and an edge set

$$E = \{ e(1), e(2), \ldots, e(M) \}.$$

Each element in E is a two-element subset of V. A directed graph (called a digraph) is a graph where E consists of ordered pairs of v(i)'s. A path in a graph is an alternating sequence of vertices and edges, where the vertices and edges can be labelled so that if the path is written

$$v(1)\ e(1)\ v(2)\ \ldots\ e(k-1)\ v(k) \quad \text{then}$$

$$e(j) = \begin{cases} \{ v(j), v(j+1) \} & \text{for a graph} \\ (v(j), v(j+1)) & \text{for a digraph.} \end{cases}$$

Vertex 1 and vertex k are said to be connected if there is a path as above. A graph is connected if all possible vertex pairs are connected. If two vertices are connected, they are said to be able to communicate with each other.

At any time of interest, the event "v(i) is operative" has probability denoted p(v(i)) or p(i); this probability is the reliability of vertex i. Similarly, p(e(j)) or p(j), the probability that edge e(j) is operative, is the reliability of edge j.

This paper is concerned with reliability problems in communication networks, hence the more suggestive terminology nodes and links will be used for the generic terms vertices and edges. In addition, the notation v(i) and e(j) will be simplified by suppressing the "v" and "e" unless necessary for clarity. Network will be used instead of graph, with the understanding that the network could be a digraph. The particular layout of the network will be called the network topology. A network is represented through the use of a picture in the usual way; an example is Figure 1. Note that the links from node 1 are directed while all other links are not directed; therefore a message can be sent from any node except 4,5 and 6 to any other node if all nodes and links are operative. N, the number of nodes in the network, equals 12 in this example.

FIGURE 1. An example of a network.

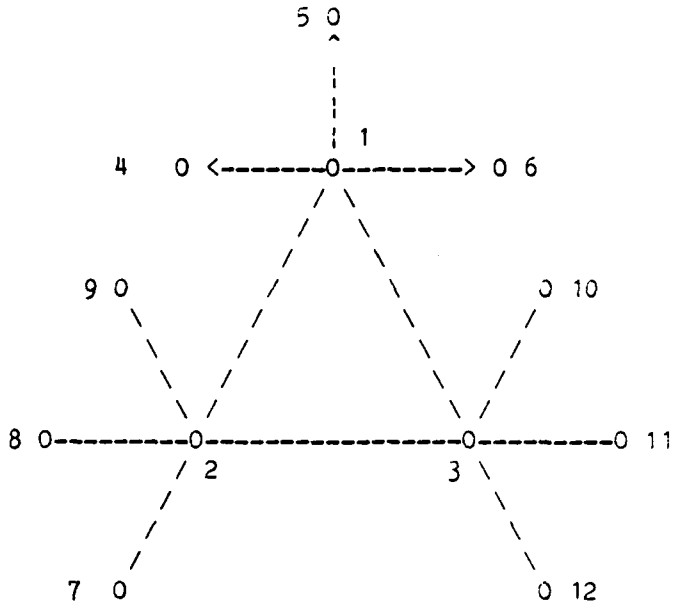

One example of a network reliability problem is as follows.

Let G be a network and let s and t be nodes (source and terminal nodes respectively). Given the reliabilities for all nodes and links in the network, what is the probability that s and t are connected, for all s and t in the network?

This problem and most other network reliability problems are at least as hard as the NP-complete problems. Hence the existance of an algorithm which solves this problem in polynomial time would imply the existence of polynomial time algorithms for all NP-complete problems.

This is the fundamental problem with virtually all network reliability problems; no one has found polynomial time algorithms which solve them, and furthermore most researchers feel that these problems are intractable. All is not lost however; there are recent algorithms which appear to be quite useful for certain network topologies.

IV. A TRACTABLE NETWORK RELIABILITY PROBLEM

The following is given:

1) the network topology

2) the reliability of all nodes and links.

The objective is to route messages by the most reliable path.

Any network with node and link failures are can be transformed into a network with only link failures. Replace every node i in the original network with two nodes i_1 and i_2 ; the reliability of the original node is assigned to the link connecting the nodes in the new network. Thus, if $p(v(i)) = p$ in the original network then in the new network the probability of the link between i_1 and i_2 being operative is is $p((v(i_1),v(i_2)) = p$. An illustration follows.

FIGURE 2. Replacement of node reliability by link reliability

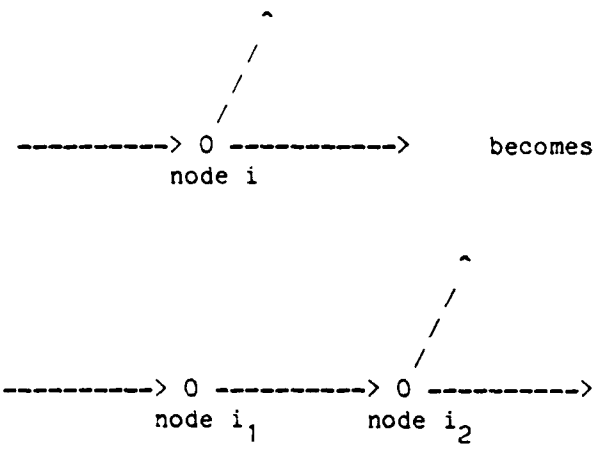

Thus, without loss of generality, we can make the very useful assumption that any network has only link failures. Suppose there exists such a network. Then

let $W(s,t) = \{ w(s,t) \mid w(s,t)$ is a path from node s to node t $\}$.

Let $R(s,t) = \max \{ \prod_{\substack{\text{all} \\ w(s,t)}} \prod_{\substack{e(j) \text{ in} \\ \text{in } W(s,t)}} p(e(j)) \}$.

R(s,t) is the reliability of the most reliable path from node s to node t; i.e. the path with the largest product link probabilities (a subset of which were node probabilities in the original network). The most reliable path is denoted w*(s,t).

Let $d(e(j)) = -\ln (p(e(j)))$ and $D(s,t) = -\ln (R(s,t))$.

Then

$$D(s,t) = \min \{ \sum_{\substack{\text{all} \\ w(s,t)}} \sum_{\substack{e(j) \text{ in} \\ \text{in } W(s,t)}} d(e(j)) \}$$

is the "shortest" route from s to t in the network with distances given by the function d above.

This is the well known shortest route problem and can be solved very efficiently with existing algorithms.

The algorithm presented below is a modification of Dijkstra's label setting algorithm for finding the shortest route between nodes in a network. For large sparse matrices, the Bellman-Moore label correcting algorithm as improved by d'Esopo and coded by Pape [1980] appears to be faster. Recent work by Glover [1984] indicates that THRESH, a hybrid of label setting and label correcting algorithms, is the currently fastest available algorithm in general. An excellent reference for this area is Syslo [1983]; it includes all but the latest work by Glover.

Assume now that there exists a directed network with only node failures. While this assumption is made primarly for ease of exposition, it is not necessarily a bad assumption for a model of a communications network based in space. The probability of node i being operative is denoted p(i). The nodes are labelled 1,2,...,N. The algorithm as stated will find the most reliable path from node s to every other node. By following the algorithm for s = 1,2,...,N the most reliable path from any node to any other node is found. When the network is not directed, i.e. all links go both ways, the computational load is cut somewhat.

ALGORITHM

Let $u(i,j) = \begin{cases} 0 & \text{if there is no link from } i \text{ to } j \\ p(j) & \text{if there is a link from } i \text{ to } j \end{cases}$

and $T = N$ (the set of nodes).

1) For node s, set $r(s) = 1$ and $r(j) = u(s,j)$ for $j > 1$ where j is an element of $T = N - \{s\}$. The set T is labelled the set of temporary nodes.

2) Find i in T such that

$$r(i) = \max \{ r(j) \mid j \text{ is in } T \}.$$

3) Set $T \leftarrow T - \{i\}$. If T is the empty set, then stop; else go to step 4. Node i is labelled permanent.

4) For each j in T, set

$$r(j) \leftarrow \max \{ r(j) , r(i)u(i,j) \}$$

5) Go to Step 2.

The final value of r(j) is equal to the probability that node j is operative and connected to node s along the the most reliable route. Optimal routes are generated by recording the nodes which solve the maximization problem in Step 4) above. The time complexity of this algorithm is $O(N^3)$, which includes finding the most reliable path from every node to every other node.

An example using the algorithm follows. Let s = 1.

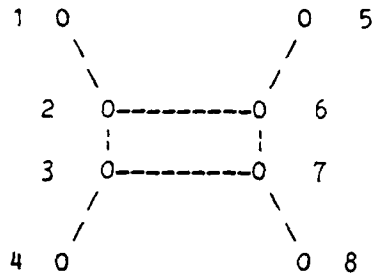

Node reliabilities:

node	reliability
1	0.2
2	0.3
3	0.4
4	0.5
5	0.6
6	0.7
7	0.8
8	0.9

node	r(j)						
1	1.000						
2	0.300						
3	0.000	0.120	0.120	0.120	0.120	0.120	
4	0.000	0.000	0.000	0.000	0.060	0.060	0.060
5	0.000	0.000	0.126	0.126	0.126		
6	0.000	0.210					
7	0.000	0.000	0.168				
8	0.000	0.000	0.000	0.1532			
i=	2	6	7	8	5	3	4

Thus the most reliable routes from 1 to j are:

j	route
2	1-2
3	1-2-3
4	1-2-3-4
5	1-2-6-5
6	1-2-6
7	1-2-6-7
8	1-2-6-7-8

This very simple example only shows how the algorithm works, not the full utility of the routing scheme.

V. RELIABILITY MEASURES AND ALGORITHMS

Network reliability analysis is very difficult for a number of reasons. First of all, it is not easy to even define what the problem is. Secondly, all of the measures presented below result in problems that are at least as hard as the NP-complete problems. In addition, solution algorithms do not lend themselves to optimization of network design, but rather to a description of proposed topologies. In practice, a combination of analysis and simulation is used to try to produce one network design.

There is a large growing literature in network reliability. One or more of the following reliability measures have appeared in many recent papers. (See Bibliography section on reliability.)

1) the probability that all nodes are communicating
2) the probability that all operative nodes are communicating
3) the probability that all operative nodes are communicating with a given node
4) the expected number of nodes communicating
5) the expected number of nodes communicating with a given node
6) the expected number of node pairs communicating with a given node
7) the probability that the system operates

Two of the best papers are Ball [1979] and Ball and Nemhauser [1979]. Ball [1979] specialized algorithms which calculate the first six measures for networks in which only nodes can fail. The foundation of these and virtually all other reliability algorithms is clever partitioning of the sample space and appropriate conditioning of events. The details of these algorithms require too much space for inclusion in this report, but early indications are that they hold promise for use in analyzing communication networks with loop topologies.

At the current time, there is at least one study under way attempting to compare as many network reliability algorithms as possible.

VI. LOOP TOPOLOGIES

Loop topologies have received a fair amount of attention in recent years. There are a series of papers which deal with loop topologies set up without a central control node. The advantage of doing it this way is to allow for routing schemes which are adaptive to changes (additions or deletions) in the network. Loop topologies can be used in networks ranging from local area networks to world-wide satellite communication networks.

Saltzer [1981] found some good reasons for using a ring (or loop) network in local area networks. Raghavendra [1981] proved that the optimal loop topology should have forward short links to the next node

and backward long links to the node ⌊ SQRT (N) ⌋ nodes away. Optimal here means that this topology minimizes the maximum distance between nodes. See Figure 3. Claims are made for optimality in terms of reliability, but the reliability measure used is very primitive.

Brayer [1984] took this result and a routing algorithm from Chyung [1975] to develop an algorithm which automatically updates routing when there are either additions to or deletions from the network. Raghavendra [1985] studied the performance of the double loop network topology using a variety of adaptive routing algorithms. He compared utilization and delay figures derived from a simple queueing model to estimated values based on a series of simulations.

Figure 3. A 12-node optimal double loop

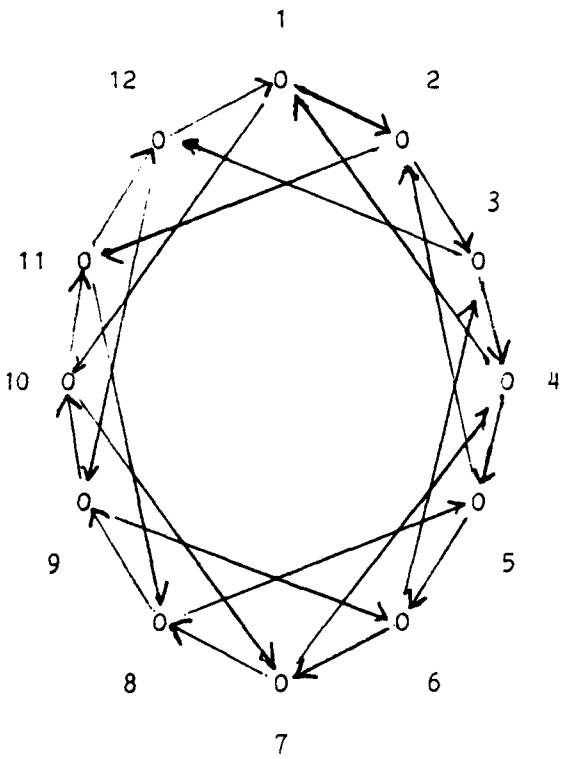

There is nothing in the literature which analyzes a loop network in the terms of the reliability measures discussed in this report. The loop topology and associated routing algorithms have obvious advantages in a dynamic communication network of satellites. The reliability algorithms could be used to analytically determine the reliability of this topology and related topolgies.

VII. RECOMMENDATIONS

It is very clear that this research is at an early stage. The complex nature of the problem makes descriptive analysis very difficult, without even trying to get into optimization issues. However, I feel that there is enough evidence to indicate further research in this area. The potential payoff would be that network designers would have a number of useful tools which could aid them in their analysis.

In addition, since the available research in the literature is steadily increasing, it would be very important to keep track of what others in the field are doing.

A few examples of the types of questions which could be answered using the tools suggested in this paper.

1) How much change would there be in the reliability of the entire network if there were additional links set up?

2) What is the minimum reliability of getting a message through in the existing network? How would this change if additional links were set up?

ACKNOWLEDGEMENTS

I would like to acknowledge the support and assistance of the Air Force Systems Command, Air Force Office of Scientific Research, ESD/XR and ESD/MD. Without their support, this research would not have been possible.

In particular, there were a number of individuals who were extremely helpful to me and to whom I owe great thanks.

In ESD/MD, Mr. George Richardson provided excellent logistical assistance and willingly shared his considerable expertise in the engineering problems found in the design and operation of communication networks. Lt. Col. Ted Mervosh made it possible for me to enrich my own professional background and Col. Richard Paul showed a great willingness to listen to my comments and concerns, in the midst of his extremely busy schedule, providing strong support and encouragement to me.

In the MITRE Corporation, I would like to thank Mr. Burt Noyes and Dr. Bill Collins who willingly shared their vast experience and knowledge.

Finally, I would like to thank Mr. Gary Grann of ESD/XR, my Effort Focal Point, whose overall guidance and assistance was critical to the project's success, and who helped make this summer's project a genuine learning experience for me.

BIBLIOGRAPHY

DATA COMMUNICATIONS

Rosner, Roy D., Packet Switching, Lifetime Learning Publications, Belmont, California, 1982

Stallings, William, Data and Computer Communications, Macmillan Publishing Company, New York, New York, 1985

Tanenbaum, Andrew S., Computer Networks, Prentice-Hall, Inc., Englewood Cliffs, New Jersey, 1981

LOOP TOPOLOGIES

Brayer, Kenneth, "Packet Switching for Mobile Earth Stations Via Low-Orbit Satellite Network", Proceedings of the IEEE, Vol. 72, No. 11, pp. 1627-1636 (1984)

Brayer, Kenneth, "Autonomous Adaptive Local Area Networking: Ring Communications Via Point-To-Point Implementation," Proc. INFOCOM, pp. 49-58, (April 1984)

Chyung, Dong H. and Sudhakar M. Reddy, " A Routing Algorithm for Computer Communication Networks," IEEE Transactions on Communications, Vol COM-23, pp. 1371-1373 (1975)

Raghavendra, C.S. and M. Gerla, "Optimal Loop Topologies for Distributed Systems," ACM SIGCOMM, Vol. 11, No. 4, pp. 218-223 (1981)

Raghavendra, C.S. and J.A. Silvester, "Double Loop Network Architectures-- A Performance Study," IEEE Transactions on Communications, Vol COM-33, pp. 185-187 (1985)

Silvester, J.A. and C.S. Raghavendra, "Analysis and Simulation of a Class of Double Loop Network Architectures", Proc. INFOCOM, pp. 30-35, (April 1984)

Saltzer, Jerome H. and David D. Clark, "Why a Ring?", ACM SIGCOMM, Vol. 11, pp. 211-217, (1981)

COMPLEXITY THEORY

Garey, Michael R. and David S. Johnson, Computers and Intractability, W.H. Freeman and Company, 1979

Even, S., O. Goldreich, S. Moran and P. Tong, "On the NP-Completeness of Certain Network Testing Problems," Networks, Vol. 14, PP. 1-24 (1984)

RELIABILITY

Aggarwal, K.K. and K.B. Misra, and J.S. Gupta, "A Fast Algorithm for Reliability Evaluation," IEEE Transactions on Reliability, Vol. R-24, pp. 83-85 (1975)

Agrawal, Avinash and Richard E. Barlow, "A Survey of Network Reliability and Domination Theory", Operations Research, Vol. 32, pp. 478-492, (1984)

Agrawal, Avinash and A. Satyanarayana, "An O(|E|) Time Algorithm for Computing the Reliability of a Class of Directed Networks,", Operations Research, Vol 32, pp. 493-515, (1984)

Ball, Michael O., "Computing Network Reliability," Operations Research, Vol. 27, pp. 823-838, (1979)

Ball, Michael O. and George L. Nemhauser, "Matroids and a Reliability Analysis Problem," Mathematics of Operations Research, Vol 4, pp. 132-143 (1979)

Ball, Michael O., "Complexity of Network Reliability Computations," Networks, Vol. 10, pp. 153-165, (1980)

Boesch, Frank T., Frank Harary and Jerald A. Kabell, "Graphs as Models of Communication Network Vulnerability: Connectivity and Persistance," Networks, Vol. 11, pp. 57-63, (1981)

Buzacott, J.A., "A Recursive Algorithm for Finding Reliability Measures Related to the Connection of Nodes in a Graph," Networks, Vol. 10, pp. 311-327 (1980)

Buzacott, J.A., "A Recursive Algorithm for Directed-Graph Reliability," Networks, Vol. 13, pp. 241-246, (1983)

Johnson, R., "Network Reliability and Acyclic Orientations," Networks, Vol. 1984, pp. 489-505, (1984)

Evans, T. and Derek Smith, "Optimally Reliable Graphs for Both Edge and Vertex Failures," Networks, Vol 16, pp. 199-204, (1986)

Ma, Y.W. and C.M. Chen, "The Application of the Random Graph Model for the Reliability Analysis of Dynamic Computer Networks," Proceedings INFOCOM, pp. 43-48, April (1984)

Provan, J. Scott, and Michael O. Ball, "Computing Network Reliability in Time Polynomial in the Number of Cuts," Operations Research, Vol. 32, pp. 516-526, (1984)

Rai, Suresh, "A Cutset Approach to Reliability Evaluation in Communication Networks," IEEE Transactions on Reliability, Vol. R-31, pp. 428-431 (1982)

Satyanarayana, A., "A Unified Formula for Analysis of Some Network Reliability Problems," IEEE Transactions on Reliability, Vol R-31, pp. 23-32, (1982)

Satyanarayana, A., and Mark K. Chang, "Network Reliability and the Factoring Theorem," Networks, Vol. 13, pp. 107-120, (1983)

Satyanarayana, A. and Jane N. Hagstrom, "Combinatorial Properties of Directed Graphs Useful in Computing Network Reliability," Networks, Vol. 11, pp. 357-366 (1981)

Satyanarayana, A. and A. Prabhakar, "New Topological Formula and Rapid Algorithm for Reliability Analysis of Complex Networks," IEEE Transactions on Reliability, Vol R-27, pp. 82-100 (1978)

Shier, D.R. and D.E. Whited, "Iterative Algorithms for Generating Minimal Cutsets in Directed Graphs," Networks, Vol. 16, pp. 133-147, (1986)

Wilkov, Robert S., "Analysis and Design of Reliable Computer Networks," IEEE Transactions on Communications, Vol. COM-20, pp. 660-678, (1972)

Willie, Randall R., "A Theorem Concerning Cyclic Directed Graphs with Applications to Network Reliability," Networks, Vol. 10, pp. 71-78 (1980)

SHORTEST PATH

Denardo, Eric V., and Bennett L. Fox, "Shortest-Route Methods: 1. Reaching, Pruning, and Buckets," Operations Research, Vol. 27, pp. 161-187 (1979)

Dial, R., F. Glover, D. Karney, and D. Klingman, "A Computational Analysis of Alternative Algorithms and Labelling Techniques for Finding Shortest Path Trees," Networks, Vol. 9, pp. 215-248, (1979)

Glover, Fred , Randy Glover and Darwin Klingman, "Computational Study of an Improved Shortest Path Algorithm," Networks, Vol. 14, pp. 25-36, (1984)

Pape, U., Algorithm 562: Shortest Path Lengths, ACM Trans. Math. Software, Vol. 5, pp. 450-455, (1980)

Shier, D. R., "On Algorithms for Finding the k Shortest Paths in a Network," Networks, Vol. 9, pp. 195-214 (1979)

Syslo, Maciej M., Narsingh Deo and Janusz S. Kowalik, Discrete Optimization Algorithms, Prentice-Hall, Inc., Englewood Cliffs, New Jersey, 1983

1986 USAF-UES SUMMER FACULTY RESEARCH PROGRAM

Sponsored by the

AIR FORCE OFFICE OF SCIENTIFIC RESEARCH

Conducted by the

Universal Energy System, Inc.

FINAL REPORT

INVESTIGATION OF VAPOR DEPOSITED ALUMINUM ALLOY FILMS

Prepared by:	Philipp Kornreich
Academic Rank:	Professor (EE)
Department Location:	Department of Electrical and Computer Engineering, Syracuse University, Syracuse, N. Y., 13244
Research Location:	RADC/RBRE, Griffiss AFB, Rome, N.Y.
USAF Research:	Joseph Reesock
Date	October 16 1986
Contract No.	F49620-85-C-0013

INVESTIGATION OF VAPOR DEPOSITED ALUMINUM ALLOY FILMS

by

Philipp Kornreich

ABSTRACT

I originally planed to investigate electromigration in Al-Cu alloy films. I planed to fabricate these films in our Micro-Electronics facility at Syracuse University. However, when I started the project at RADC we decided to convert an old Auger apparatus to an MBE machine and use it to grow the Al-Cu alloy films. The construction of the MBE machine in the RADC machine shop left mi some spare time. I decided to deign a Spectroscopic Epitaxy (SE) machine for the Syracuse University Micro-Electronics Laboratory. I also heped out the EDRE group at RADC by investigating various metalizations on Leadless Chip Carriers (LCC). This information is used for military specifications of LCC's.

ACKNOWLEDGMENTS

I would like to thank the Rome Air Development Center RBRE Group and the Air Force Office of Scientific Research for sponsorship of my research. I would like to thank several members of the staff, Robert Thomas, Chef, Joseph Beesock, Jean Blackburn and Lt. Bela Vastoc, for giving me the opportunity and the guidance necessary for my research.

Finally, I would like to thank my wife, Sandra and son Paul for putting up with my commuting.

Thus only one of the machinists could be employed at a time.

In the mean time. The work at Syracuse University work on the growth of epitaxial CdTe films, that are later to be used in ultra high speed field effect transistors and multi-circuit layer structures, progressed to the point point where a Spectroscopic Epitaxy (SE) would be useful for the fabrication of these films. I will describe the SE machine later. There is also some interest in this project at RADC. Thus I decided to design such a machine out of spare scrap ultrahigh vacuum components available at RADC. The reason for using scrap parts for this machine is that ordering new parts in a government installation takes of the order of one year. We wanted to complete the SE machine this summer (1986). For the same reason we, also, fabricated pneumatic cylinders and the pneumatic controls for the MBE machine in the machine shop rather then purchase them. The SE machine is, also, nearing completion at this time. The components for the SE machine are, also, manufactured one <u>after the other</u> in order to assure that they would all fit. This again left me some free time.

During my free time I decided to assist with testing Leadless Chip Carrieres (LCC). There was a need for testing these devices at that time and the RBRE group did not have sufficient people power (formally man power) to do the job.

I INTRODUCTION

I originally planed to study electromigration in Al-Cu alloy films. I planed to fabricate these films in our Syracuse University Micro-Electronics Laboratory and study the response of these films to large electrical current densities at RADC. At Syracuse we fabricate the Al-Cu alloy films with a diffusion pumped vacuum system. The films can be either deposited by thermal evaporation or by electron beam evaporation. The films are than patterned by photolithography. We use both the "Lift Off Method" or etching to pattern the films.

However, when I started the summer project at RADC we decided to convert an old Auger apparatus to an MBE machine in which we would fabricate the Al-Cu alloy films for the electromigration study. Indeed, it is possible to fabricate much purer and better controlled films with an MBE machine. The conversion of the Auger apparatus to an MBE machine involved the design of various components, which I will describe later. These components where than fabricated in the RADC machine shop. The two people in the RADC machine shop are excellent machinists. Nevertheless, there were long periods of time when my consultations in the shop were not required. The components had to be manufactured one after the other in order to assure that they would all fit.

I decided to help out.

Thus, I worked this summer (1986) on three tasks. I converted an old Auger apparatus to an Molecular Beam Epitaxy (MBE) machine for RADC/RBRE. I designed and supervised the construction of a Spectroscopic Epitaxy (SE) machine for the Syracuse University Micro-Electronics Laboratory. I, also, performed various tests on Leadless Chip Carriers (LCC) for the RBRE group of RADC where I worked.

I shall describe each task below:

II CONSTRUCTION OF MBE MACHINE

In order to convert the old Auger apparatus to an MBE machine it was necessary to design and construct a cylindrical liquid nitrogen cooled vapor shield and a liquid nitrogen cooled source holder with pneumatically actuated shutters. I designed these parts and supervised thier construction in the RADC machine shop.

The old Auger apparatus consists of the following components: The main vacuum chamber consists of a 12 inch inside diameter 30 high stainless steel chamber with various ultra high vacuum feed-throughs. A large gate valve at the bottom of the main chamber separates it from the pumping unit. The pumping units consist of four ion pumps which are supplemented by integral titanium sublimation pumps. The chamber is initially evacuated from atmospheric pressure with a mechanical pump and a turbo pump through the load lock. The load lock uses a horizontal rod which passes through a viton "O" ring seal. There is a metal to metal seal valve where the loading rod passes into the main chamber. Thus, when the loading rod is withdrawn the main vacuum chamber is sealed completely by metal to metal seals. All feed-throughs in the main chamber, have copper "C" rings.

Ther is, of course, an Auger probe, a sputtering gun, and a mass spectrometer in the main chamber. The sputtering gun is used for either Auger or SIMS profiling. The mass spectrometer is used for SIMS analysis. The electron beam gun from the Auger apparatus can also be used to obtain SEM pictures of the substrate surface. There is a CRT in this equipment for this purpose. In the middle of the main chamber is a substrate stage. The substrate is loaded onto this stage with the loading rod described previously. The substrate stage has to be rotated ninety degrees to face the Auger probe or 180 degrees to face the deposition sources. We will be able to heat the substrate. However, the substrate heater is yet to be constructed.

The main modification of the equipment is the addition of an evaporation source holder. The source holder consists of a central two inch diameter liquid nitrogen tank. Six 3.5 inch long vanes radiate from the front of this tank. The vanes are inclosed by a 3.5 inch inside diameter, 3.5 inch long stainless steel cylinder. In fact, the whole source holder is fabricated out of stainless steel. The liquid nitrogen tank, the vanes, and the outer cylinder form six pie shaped chambers. The effusion sources and source heaters are located in these chambers. Each chamber can be closed, in the front, by a shutter door. A rod leads from each shutter through a vacuum tight bellows to a pneumatic

cylinder. The rods are attached near the hinge of the shutter doors. They are used for opening and closing of the shutters. The source holder is mounted on a six inch diameter stainless steel flange. An extension of the liquid nitrogen tank is welded to the flange and forms a liquid nitrogen feed-through. Two 1/4 inch diameter stainless steel tubes protrude from the feed-through for liquid nitrogen input and exhaust. The 1/4 inch diameter tubes are not directly welded to the flange. They pass inside a, normally evacuated, two inch diameter tube through the flange. The two inch diameter tube is sealed at some distance past the flange. It is there that the two 1/4 diameter tubes protrude. This construction is used to minimize thermal conduction. Six bellows, through which the shutter actuating rods pass, surround the liquid nitrogen feed-through. The bellows are welded to the flange. An aluminum ring holding the six pneumatic cylinders, that are used for opening and closing of the shutters, is mounted, by means of spacer rods, on the outside of the flange. I designed the pneumatic cylinders and they were build in the RADC machine shop since it would take nearly one year to obtain the cylinders if we had ordered them. I also designed pneumatic control valves for these cylinders. The six control valves were build in the machine shop for the same reason. Each control valve either provides air pressure

to the "top" and vents the "bottom" of a cylinder, or vents the "top" and provides air pressure to the "bottom" of a cylinder. The pneumatic control valves are located in the MBE machine control panel.

The Source holder is located in a six way cross. The six way cross is bolted to the main chamber of the MBE machine opposed the load lock. The flange holding the source holder is bolted to the end opposed the main chamber of the six way cross. The other four openings of the six way cross are used for electrical power and thermocouple feed-throughs.

The liquid nitrogen cooled vapor shield is located between the source port in the main chamber and the substrate stage. It consists of a six inch outside diameter, 3.5 inch inside diameter, five inch long cylindrical nitrogen tank. The vapor stream passes through the middle of this tank. Liquid nitrogen and venting are provided to the vapor shield through stainless steel flexable tubes connected to two liquid nitrogen feed-throughs located at the top of the main chamber.

The parts for the MBE machine, except, for the substrate holder, welding of the actuating rods to the bellows, and some air line fittings, which will be locally purchased, are complete. It remains to install and test these parts.

III SPECTROSCOPIC EPITAXY MACHINE

We have a research program, currently, at Syracuse University that involves fabricating high quality CdTe-InSb-CdTe layers. The InSb layers, in this sandwich structure, is only 80 A thick. Since very thin InSb layers are semiconductors at room temperature one can construct field effect transistors with these layers. Since InSb has both a very high mobility and high saturation velocity it is possible to construct exceedingly high speed and high power transistors. We use CdTe, which has a very good lattice match to InSb, as an insulator. Thick, bulk, InSb layers have essentially metalic conduction they can be used as Ohmic contacts to the InSb films, Schottky barrier contacts to the CdTe layers, and as leads.

By using single crystal CdTe as insulator, thick crystalline InSb layers as contacts and leads, and very thin InSb layers as semiconductors it is possible to construct multi-circuit layer structures. In fact, we could build true three-dimensional circuits. This is not possible in Si or GaAs since these materials require high temperature processing, use non-crystalline metal leads and Si circuits use non-crystalline oxide insulating layers. It is very difficult to grow single crystal material on these non-crystalline layers.

Currently we fabricate these layers with our Hot Wall Epitaxy (HWE) apparatus. The HWE apparatus that we use is quite different from the conventional HWE system currently in use. Our system, like the conventional HWE systems is located in an diffusion pumped vacuum system. However, our HWE system is closed except for an adjustable leak. It operates at a true 10^{-3} torr. pressure inside the HWE system. It uses a capacitance bridge micro-balance to measure deposition thickness. The micro-balance has a sensitivity of one Angstrom. There is a modified ion gauge connected to the HWE system. We plan to replace the ion gauge with a gas cyclotron resonance detector, which like a mass spectrometer, can detect Isotope concentrations. Our HWE system uses two sources. One source contains Cd and the other source contains Te. A similar arrangement is used for InSb.

However, our HWE system depends on the purity of the source materials. An MBE machine would also not produce purer material since it, too, depends on the purity of the source material. We, therefore, decided to design a Spectroscopic Epitaxy (SE) apparatus that uses quadrupoles in the vapor streams to select a single isotope of a material for deposition.

The protctype SE system, which is nearing completion, in

the RAIC machine shop is designed for the deposition of CdTe only. It is based on our current HWE system with quadrupoles located in the vapor streams above each source. The atoms emanating from each source are ionized by a Tesla coil. They are accelerated by a small d. c. voltage before entering the quadrupole. Above the two quadrupoles is an ion collector and substrate. The substrate is electrically connected so that the ion current can be monitored. The ion current is proportional to the film growth rate.

The substrate is suspended from a fused quartz substrate holder with tungsten wire clips. The substrate holder has a ring that makes contact with a metal ring on the ion collector. A conductor, passing through an electrical feed-through, allows the measuring of the substrate ion current.

Above the ion collector is a substrate preheater. Above the substrate preheater is a metal to metal seal valve. The vertical substrate loading, vacuum interlock is located above the above described metal seal valve. The substrate holder with substrate is transported through the load lock by a clam shell bucket. The clam shell bucket is suspended from two chains. One chain supports the clam shell bucket and the other chain is used to open and close the clam shell bucket. The chains are wound on a drum at the top of the apparatus. The drum is turned by a rotary feed-through.

There is no long insertion rod. Long insertion rods are used in conventional load locks. The clam shell bucket can also be used to retrieve substrates, and other parts, that might come loose. This is not possible with the insertion rod of a conventional load lock. The load lock is evacuated with the same turbo pump that is used to evacuate the main deposition system. The turbo pump is connected to various parts of the SE system by means of a system of valves. The turbo pump is backed up by a mechanical fore pump. There is an ion holding pump, always, connected to the deposition chamber.

The SE system functions as follows: A dummy substrate holder is positioned on the ion collector. The sources, quadrupoles, and ion collector are heated. The substrate holder and substrate are lowered into the preheater after the rest of the SE system has reached an equilibrium temperature. While the substrate holder with substrate remains in the preheater the dummy substrate holder is removed with the clam shell bucket from the ion collector. The dummy substrate holder is removed through the load lock. The substrate is heated in the preheater to the correct deposition temperature. The substrate holder with substrate is, next, lowered onto the ion collector from the preheater with the clam shell bucket, and deposition starts. After a sufficiently thick film has been deposited the substrate holder with substrate is removed from the ion collector and

the SE system through the load lock with the clam shell bucket. The dummy substrate holder is replaced with the clam shell bucket and the SE system is ready for recycling.

Our HWE system functions similarly, except it does not have a load lock. It also uses dummy and "real" substrate holders.

IV LEADLESS CHIP CARRIERS

I investigated the effect of temperature cycling, moisture, and salt spray on the solderability of ceramic Leadless Chip Carriers (LCC). I used two types of LCC's. One type had metalizations consisting of a tungsten bonding layer, a thick nickel layer, and a thin gold overlay. The other type of LCC's, also, had a tungsten bonding layer. However, this layer was followed by a thick cobalt layer. There, also, was a gold overlay on this type of LCC's. I first tested the Ni type LCC's. I performed temperature and steam cycling. Auger analysis was performed after the temperature and steam cycling. The Auger analysis revealed that the nickel had migrated through the gold layer after temperature and steam cycling. I next tested the solderability of the Ni type LCC's with the "Meniscograph". I found that, indeed, there were bare spots where the solder did not wet the LCC's contacts. This was caused by the nickel migrating through the gold cover layer. This, was actually known before I performed my tests. I just repeated these tests for comparison with the cobalt type LCC's.

In order to correct this situation cobalt was used as the thick metal layer in a second set of LCC's. I, next, put the cobalt type LCC's through the same temperature and steam cycles. Auger analysis showed that no cobalt had migrated

through the gold layer to the surface. Indeed, much better wetting of solder was observed on the cobalt type LCC's.

We, next, exposed the cobalt LCC's to salt spray. The salt spray badly decomposed the surface of the cobalt type LCC's. SIMS analysis of these LCC's showed that the cobalt, under the thin gold overlay, had been oxidized. Since the cobalt oxide has a larger volume then the cobalt film it destroyed the gold overlay. Which in turn exposed more cobalt to oxidation. No cobalt salts where found in the SIMS analysis. Evidently, the nickel type LCC's had never been exposed to salt spray. We exposed some nickel type LCC's to salt spray this week. A coating formed on some spots on the gold film of the nickel type LCC's. However, the metalization, including the castlations, remained in tact.

The results of the tests performed on the LCC's will be used to establish military specifications for LCC's.

1986 USAF-UES SUMMER FACULTY RESEARCH PROGRAM/

GRADUATE STUDENT SUMMER SUPPORT PROGRAM

SPONSORED BY THE

AIR FORCE OFFICE OF SCIENTIFIC RESEARCH

CONDUCTED BY THE

Universal Energy Systems, Inc.

FINAL REPORT

MODIFICATION OF PRIORITY HANDLING ALGORITHM IN THE INTEGRATED NODE NETWORK

Prepared by:	Mou-Liang Kung
Academic Rank:	Associate Professor
Department and University:	Mathematics and Computer Science, Norfolk State University
Research Location:	Rome Air Development Center, Griffiss Air Force Base, NY
USAF Researcher:	John J. Salerno
Date:	July 25, 1986
Cotract No:	F49620-85-C-0013

MODIFICATION OF PRIORITY HANDLING ALGORITHM IN THE INTEGRATED NODE NETWORK

BY

Mou-Liang Kung

ABSTRACT

The integrated Node Network Simulator is a software package simulating a fully connected integrated digital network implementing both circuit switching for voice and packet switching for data. A maximal bandwidth is reserved for voice and the remaining bandwidth is for data packets. However unused voice bandwidth can be taken by data packets. When voice traffic becomes excessive over a period of time, the data packet queuing also becomes excessive. Two solutions are investigated to increase the data transmission throughput at the expense of the voice. The first solution is to adjust the maximal voice bandwidth dynamically and the other is to use variable frame scheme rather than the fixed frame. The solutions further lead to the question of what constitutes the "best" priority handling algorithm to satisfy the demand under heavy voice and data traffic.

ACKNOWLEDGMENTS

I would like to thank the Air Force System Command and the Air Force Office of Scientific Research for sponsoring my research at the Rome Air Development Center, Griffiss Air Force Base, New York. Special thanks go to Mr. John J. Salerno, my USAF research colleague for numerous comments and suggestions and to Mr. John Ritz for making my stay on the Base most pleasant.

Words of gratitude can not express my appreciation for the understanding and support from my loving wife Pat, and our three children Steven, Debbie and Phyllis to make the trip for this research possible.

I. INTRODUCTION.

I received my Ph.D. in Mathematics from the University of Virginia and my M.S. degree in Computer Science from the Old Dominion University. My research interest is in the performance and evaluation of the networks and protocols.

According to [7] , one of the research areas at the Rome Air Development Center (RADC) is the Integrated Node "Performance" Experiments. A particular challenge is aimed at increasing data throughput by avoiding excessive queuing of data packets when both voice and data traffic peak. Therefore this particular research experiment is well suited to my training and interest.

II. OBJECTIVES OF THE RESEARCH EFFORT.

The Time Division Multiplexed frames of digitized voice and data are sent through all internodal trunks in an integrated network ([1]). A frame is divided into a circuit-switching region and a packet-switching region. The circuit-switching technique is used to handle voice traffic and packet-switching for the bursty data transmission. In order to simplify our argument, we shall use the terms voice region and data region for the sake of convenience. A maximal bandwidth is set aside for the voice region. Any unused voice region can be occupied by data packets. My goal is to modify the priority handling algorithm to allow higher data transmission throughtput when voice traffic is heavy.

The specific objective is

1. to analyze the performance of the dynamic adjustment of the maximal voice bandwidth using the Working Set Model and to determine the

optimal working set window size.

In addition, the following objective was added during the course of my research effort:

2. to analyze the implementation of variable length frames instead of fixed length frames.

III. DYNAMICALLY ADJUSTED MAXIMAL VOICE BANDWIDTH.

The concept of dynamically adjusting the maximal voice bandwidth in a frame is intuitively sound since the decision for adjustment should be made according to the current needs rather than initial projection or posterior statistical mean.

A. The Algorithm.

The working set ([2]) in the current context is simply the set of immediate past history of the traffic pattern . The past history can be used in many different ways to allocate bandwidth in a frame ranging from the simplest proportional allocation to the more sophisticated curve fitting techniques. To meet the objective of analyzing the effect of dynamic adjustment of bandwidth allocation, we only considered the proportional allocation due to its simplicity. If the outcome of the proportional allocation is encouraging, then further investigation on other techniques will be justified.

There is an extra consideration to make in this algorithm. The voice is assumed to be not buffered for more than one frame duration. (The discussion on buffered voice can be found in [4].) The voice termination is assumed to be erratic and its arrival time can not be estimated. We have to make sure that the non-terminated calls will all

have their "slots" in the next frame.

Let V = total number of voice calls came through or blocked during the last frame duration,

D = total number of data packets came through, queued or dropped during the last frame duration,

F = frame size,

T = the number of terminated calls during the last frame duration

Then

m = the estimated maximal voice bandwidth by proportion

= (V /(V+D)) * F,

M = the actual maximal voice bandwidth allocated

= maximum $\{ V - T, \lceil m \rceil \}$.

In terms of using the working set, the variables V, D, F, T are replaced by their arithmetic means from the working set rather then those from the single frame duration from the past.

B. The Implementation.

The testbed for the algorithm installed at RADC is called the Integrated Node (IN) developed by RCA ([7]). One of the testing components is the Network Simulator. The Network Simulator is a software package written in Perkin-Elmer Common Assembly Language (CAL), running on the Perkin-Elmer 8/32 minicomputer.

The input is taken from a prerecorded tape generated off-line by a discrete-event simulation program written in Fortran. Individual voice traffic and data traffic tapes were prepared and then merged into a single tape in chronological order. The output written to a tape consists

of 4 types of data blocks: label, completed transaction, packet delay, and major trunk utilization record to be used for compiling statistical data.

Our main interest in the Network Simulator is the part that implements the channel bandwidth allocation. The existing channel allocation algorithm is scattered in two modules of the Network Simulator. The flow chart (figure 1.) gives the execution sequence of various modules in the main program called SIMPRG. When voice arrival is detected in TGUPRG, the available bandwidth is checked and allocated until either no more voice is available for the time being or no more available bandwidth is found. the On the other hand, the arriving data are only queued in TGUPRG. Next, the data is packetized in DEDS. The data packets are not multiplexed into the frame until the execution reaches ISUPRG. Thus the modification to implement our algorithm is made in SIMPRG, ISUPRG, and the data initialization module, SCONPL, along with the data definition module in ADPTLIB macro-library. We do not have the result for analysis since the modified software is still in the debugging stage. The step-by-step procedure in carrying out the implementation is included in Appendix A for resuming the test in the future.

IV. VARIABLE FRAMES.

The variable frames are frames with lengths being adjustable within the tolerable range of the voice gaps created by the extra delay. When the length of a frame is extended, the circuit-switching will no longer preserve the synchronization requirement for the voice. However, according to [6], the problem is manageable if the frame is not extended too long. The delay in voice transmission provides the opportunity to

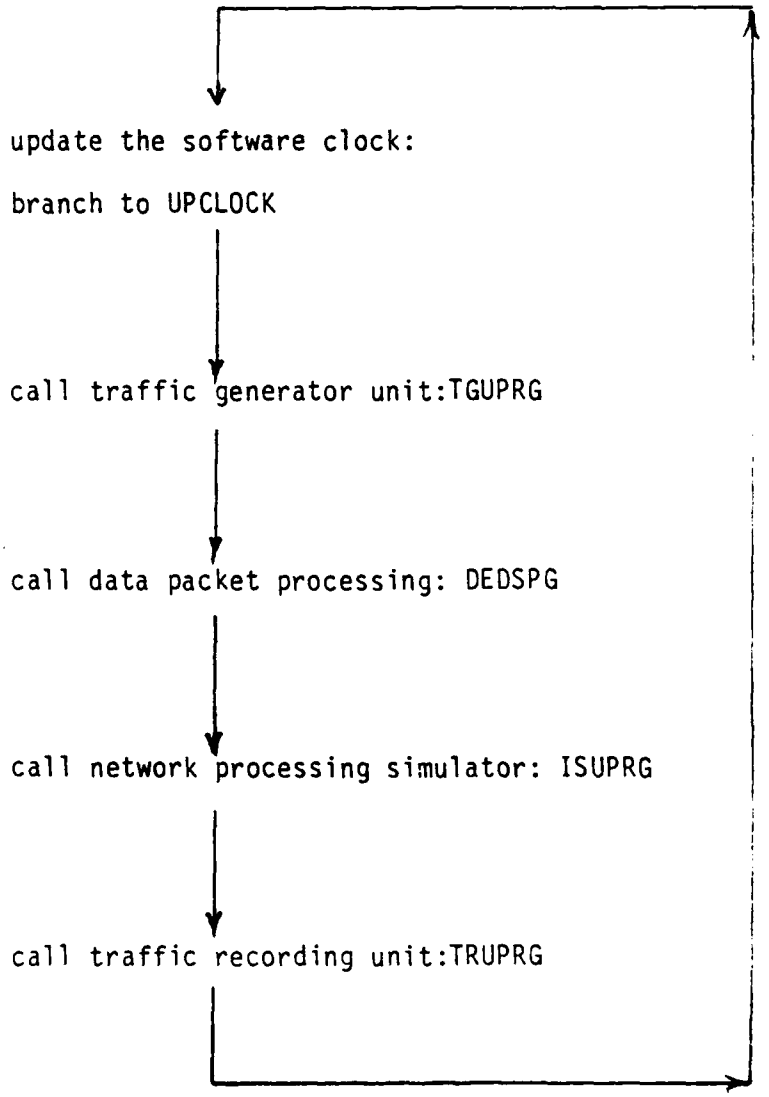

figure 1. Main Loop in SIMPRG

insert extra data bits. It is clear that the savings can be achieved in overhead cost when a whole data packet can be sent in one piece instead of being cut off into two smaller packets with individual headers. More data packets can be sent by delaying the voice slightly thus avoiding or postponing long data queuing or data queue overflow.

A. The Algorithm

The idea behind the algorithm is quite simple, we pretend that the frame can now be lengthened. Since we are only dealing with the effect of variable frames in simulation, the actual intricacy in the implementation will be totally ignored. We shall use the original movable boundary with static maximal voice allocation scheme as described in [7] so that results can be easily understood. However, if the dynamically adjusted maximal bandwidth for voice is found to be effective in improving the data throughput, then there is no reason why it can not be used for variable frames as well.

The variable frame with movable boundary was shown to have better performance in channel utilization, blocking and delays in the single server queuing model ([3] , [5]). The minimal length of the variable frame divided by the trunk speed must be greater than or equal to the time in processing a frame of maximal length. The maximal length is dictated by the time transparency for the voice transmission.

However, if the node in the network does not buffer the voice over a frame duration then a curious phenomenom can occur: when a node sends out a short frame with a voice call destined for a certain node, all intermediate nodes must also conform and forward the short frame. The

reason is that the voice arriving at a fast pace can not be switched out slowly if there is no buffer to hold it. The variable frame scheme is reduced back to the fixed frame scheme on this connected path. The resulting interaction of the network is not at all clear and further investigation is warranted.

B. The Implementation.

The existing Network Simulator software implements fixed frames by using a software clock in which each frame is timed 1 msec of the software clock. The transmission of a longer frame will result in a delay of more than 1 msec of the software clock. Hence the trick of lengthening the frame is to have another counter keeping track of any extra time consumption due to a longer frame. A caution must be exerted to make sure that the software clock is properly incremented. The implementation involves two new variables

```
SLOTCNT  :  INTEGER;
FLAG     :  BOOLEAN; (* to indicate whether the software clock has *)
                     (* already been updated for the next frame.  *)
```

and the modification of the segment labeled UPCLOCK in SIMPRG into

```
IF (FLAG = TRUE)  THEN  FLAG := FALSE
ELSE BEGIN          (*the short frame was not completely filled*)
        SLOTCNT := 0;
        SWCLOCK := SWCLOCK + 1
     END;
```

and SWCLOCK needs to be incremented whenever a data packet is extended beyond the short frame boundary in the current frame allocation. Thus we

make the following changes in ISUPRG:

```
IF (SLOTCNT   = short_frame_length)  THEN
BEGIN
    SLOTCNT := SLOTCNT - short_frame_length;
    FLAG    := TRUE;
    SWCLOCK := SWCLOCK + 1
END;
```

(These changes in Pascal laguage were translated into Perkin-Elmer Common Assembly language for testing.)

No result has been obtained yet since the modified software is still in the debugging stage. However, the step-by-step procedure in conducting the test is included in Appendix B for the continuation of the test.

C. Remarks.

In addition to the uncertainty in the interaction of frames of variable lengths in the network, this implementation on the Network Simulator is not quite satisfactory since the prerecorded traffic tape contains voice calls of predetermined lengths. If the delay due to lengthened frames is introduced, then the arrival time of the call termination should also be delayed. Since the source code of the Network Simulator is difficult to modify, no attempt was made to take the call termination delay into our consideration.

V. RECOMMENDATIONS.

A. The two modifications of the software to implement the dynamic adjustment of the maximal voice bandwidth and the variable frames need to

be further debugged for proper execution to obtain statistical results for comparison. However, this Network Simulator was not written with flexibility in mind. Rather than attempting to make this Network Simulator written in assembly language, flexible enough for the testing of various algorithms, it would be a lot easier if a new simulation model is constructed using a high level portable language such as C along with standard graphics implementation such as GKS. The icon based user input to configure the network with user selected algorithm can be most convenient. Next, the software development environment should be properly selected. The Perkin-Elmer OS32 is not as convenient to use as UNIX* or other operating systems. An easy to use operating system environment such as UNIX should be chosen. Finally, the standard software engineering techniques should be practiced in developing an easily maintainable and well documented simulation software.

B. The study of bandwidth allocation for two types of traffic such as voice and data in which the voice has the higher priority can be further generalized to the study of more than two types of traffic with several priority levels. This leads us into the so called Priority Handling Algorithm problem.

I strongly recommend the construction of a simulation software package modelling the priority handling algorithm for the bandwidth allocation with the following specifications:

1. allowing the user to input the number and the types of traffic with

---

*UNIX is a trademark of AT&T Bell Laboratories.

various priority levels such that a queue is constructed for each type of traffic that can be buffered,

2. allowing the user to specify the length for each queue if the default setting is not to be used,

3. allowing the user to input the "strategy" for priority promotions of the queue entires among the queues,

4. allowing the user to input a new bandwidth allocation function if it is not any function such as proportional allocation, polynomial curve fitting allocations built in the model,

5. the model should record a snapshot of the queues at certain regular interval in time on some secondary storage for later analysis.

A separate traffic generator should also be constructed to generate different types of traffic of various priority levels with the user's input of a mean data length and the type of distribution assumed. This recommendation shall be further explained in details and submitted as a separate research proposal under the same Summer Faculty Research Program for a Mini-Grant.

REFERENCES

1. G. Coviello and P. Vena, "Integration of Circuit/Packet Switching by a SENET (Slotted Envelop Network) Concept," Proc Nat Telecom Conf, , 1975 pp.42.12-42.17

2. P. Denning, "The Working Set Model for Program Behavior," Communications of the ACM, Vol.11, No.5, May 1968, pp. 323-333

3. N. A. Janakiraman, B. Pagurek, and J. E. Nelson,"Performance Analysis of an Integrated Switch with Fixed or Variable Frame Rate and Movable Voice/Data Boundary," IEEE Trans. Commun., Vol.COM-32, No.1, January 1984, pp.34-39

4. A. Konheim and R. L. Pickholtz, "Analysis of Integrated Voice/Data Multiplexing," IEEE Trans Commun, Vol.COM-32, No.2, February, 1984, pp.140-147

5. B. Maglaris and M. Schwartz, "Performance Evaluation of a Variable Frame Multiplexer for Integrated Switched Networks," IEEE Trans Commun, Vol.COM-29, No.6, June 1981, pp.800-807

6. H. Miyahara and T. Hasegawa, "Integrated Switching with Variable Frame and Packet," Proc Int Commun Conf, 1978,pp.20.3.1-20.3.5

7. J. J. Salerno, "An Integrated Packet, Message, and Voice Switch Utilizing the Slotted Envelop (SENET) Concept," In-House Report, RADC-TM-85-9, April, 1985

APPENDIX A

We shall outline the software modification and testing procedure for the DYNAMICALLY ADJUSTED MAXIMAL VOICE BANDWIDTH experiment. This procedure is only to be repeated at RADC/DCLD LAB:

1. Source code for the modification is on VOL8 (removable disk) for the Perkin-Elmer 8/32. Only 4 CAL modules were modified, they are

    SIMPRGØ6.CAL

    ISUPRGØ6.CAL

    SCONPLØ3.CAL

    ADPTLIB.MAC

Changes are noted in the comments.

2. If the source code is ready to be assembled, call

    VOL8:MC8NU SIMPRG,Ø6 (MC8LP, for a hardcopy of the listing)

to expand the macro and assemble the source code (in this case:SIMPRGØ6) and produce the object code SIMPRG.OBJ. Repeat the same for ISUPRGØ6.CAL and SCONPLØ3.CAL. Please note that ADPTLIB.MAC should be modified via Macro utility called MLU on VOL2:.

3. If all modified modules were assembled with no error, then they can be linked by calling:

    VOL8:BLD8

The load image is now created under the name OS32SIMU.ØØA.

4. To execute the simulation:

Load input traffic tape in MAG2: and blank output tape in MAG1:. Key in C633 at address 7A through the control panel and press INIT key. Next, you must initialize the lines by typing:

C D E Ø

C D E 1

C D E 2

C D E 3

C D E 4

C D E 5

C D F 6

C D E 7

C D E 8

C D E 9

C D E A

C D E B

C D E F

P 1115Ø, Ø32ØØ2EØ (to poke the address with frame length 8ØØ or channel bw 8ØØ Kbps, and max voice bw 736 Kbps)

0

5. When the simulation run is stopped, load the volume (removable disk) called TM14, rewind MAG1:, and type TM14:RUN STAT to execute the statistics program.

Note: An RS232 interface from PE 8/32 to the Tektronix 4025 graphics terminal should be connected with the proper termainal setting.

6. Several simulation runs with different input traffic tapes and different initial max voice bandwidth should be conducted. The THROUGHTPUT EDIT data are to be compared to those from the original simulation runs.

APPENDIX B

The software modification of the VARIABLE FRAMES experiment differs from those in APPENDIX A in the following CAL modules:

SIMPRGØ5.CAL

ISUPRGØ5.CAL

The operating procedure is identical to those described in APPENDIX A except when poking address 1115Ø, you may poke the address with various frame lengths as long as they are believed to be tolerable rather than 8ØØ.

1986 USAF-UES SUMMER FACULTY RESEARCH PROGRAM/

GRADUATE STUDENT SUMMER SUPPORT PROGRAM

Sponsored by the

AIR FORCE OFFICE OF SCIENTIFIC RESEARCH

Conducted by the

Universal Energy Systems, Inc.

FINAL REPORT

Ability, Experience and Task Characteristic Predictors of Performance

Prepared by:	Charles E. Lance Ph.D.
Academic Rank:	Assistant Professor
Department and	Department of Psychology
University:	University of Georgia
Research Location:	Air Force Human Resources Laboratory
	Brooks Air Force Base
USAF Researcher:	LtCol Rodger Ballentine
Date:	3 September 1986
Contract No:	F49620-85-C-0013

Ability, Experience and Task Characteristic Predictors of Performance

by

Charles E. Lance Ph.D.

ABSTRACT

This study investigated main effects and interactions among aptitude, job and task experience and task characteristics in predicting Jet Engine Mechanic (JEM) (AFS 426x2) task performance. Aptitude (ASVAB MEC-AI), job and task experience composites and task learning difficulty indices (LDIs) all were significant predictors of task performance. Contrary to hypotheses, task differences did not moderate relations between task performance and either aptitude or experience. However, small but statistically significant aptitude x experience interactions indicated that task performance becomes less predictable from aptitude scores over a JEM's first term of enlistment. Finally, one approach to determining aptitude requirements from indices of situational demands (LDIs) was illustrated. Future research should (a) be extended to levels of aggregation appropriate to the desired level of inference; (b) sharpen the definition and measurement of the job experience construct, (c) investigate temporal changes in performance determinants, (d) identify determinants of latent performance variables, and (e) seek to corroborate statistical models for correcting for rater biases.

Acknowledgements

I thank the Air Force Office of Scientific Research, the Air Force Human Resources Laboratory/IDE for sponsorship of my research and LtCol Rodger Ballentine for serving as my research effort focal point. Thanks also go to SRA Jim Hawks, Dr. Jerry Hedge, Dale Bracken, Doris Black, A1C Roger Ballance, Calvin Fresne, Jerry Moran, Dr. Malcolm Ree, Mark Teachout and especially to Drs. Bill Alley and Hank Ruck for their individual support and guidance.

Finally, I thank my wife, Vicki, her dog J.P., and my dog, Bob for understanding why I was away from home for ten weeks.

I. Introduction.

Three metatheoretical approaches guide contemporary research in industrial/organizational psychology (Terborg, 1981). A situational approach (Bowers, 1973; Epstein & O'Brien, 1985) seeks to explain human behavior (performance) in terms of differences in situational characteristics (e.g., Komaki, Zlotnick & Jensen, 1986; Oldham, Hackman & Pearce, 1976); intrasituational variability in behavior is regarded as experimental error.

A trait approach seeks to explain behavior in terms of stable, latent individual difference variables (Schmidt, Hunter & Pearlman, 1981; Stagner, 1977) and attributes cross-situational variability in behavior to statistical artifacts, measurement inadequacies and random fluctuations in behavior. An interactional approach (Ekehammer, 1974; Endler & Magnusson, 1976; Epstein & O'Brien, 1985) assumes that both situational characteristics and stable individual differences determine behavior (e.g., James & White, 1983; Kozlowski & Hults, 1986). Both intrasituational and cross-situational variability in behavior represent "to-be-explained" sources of variance.

The general lack of research on person-situation interactional determinants of job performance (O'Connor, Eulberg, Peters & Watson, 1984; Schneider, 1978; Terborg, Richardson & Pritchard, 1980), and practical concerns of the U.S. Air Force motivated this study of predictors of Jet Engine Mechanic (AFS 426x2) task performance.

Within the ongoing Joint-Service Job Performance Measurement/Enlistment Standards Project, the Air Force is the lead service for demonstrating the Walk Through Performance Testing (WTPT) methodology (a work sample approach to performance testing) and for determining the suitability of other less ex, ensive and time consuming surrogate

job performance measures. These include measures of job and task experience (Maier & Hiatt, 1985; Maier & Mayberry, 1986) job/task learning difficulty (Burtch, Lipscomb & Wissman, 1982; Weeks, 1984), interview testing and performance ratings. This research sought to define relations among task-relevant aptitudes, job and task experience, task learning difficulty, and task performance.

II. Research Objectives.

Three issues guided the research efforts described below: (a) To what extent do situational (task learning difficulty, Weeks, 1984) and person variables (job/task experience and task-relevant aptitudes) predict jet engine mechanic task performance? (b) Does task learning difficulty and/or job or task experience interact with task-relevant aptitudes in predicting performance? and; (c) Is the establishment of differential aptitude requirements based on analysis of situational demands feasible?

III. Predictors of Task Performance.

III.1. Task-Relevant Aptitudes.

Meta-analyses of validity studies suggest that cognitive ability tests are consistent predictors of job performance (e.g., Hunter & Hunter, 1984; Pearlman, Schmidt & Hunter, 1980; Schmidt, Hunter & Caplan, 1981). The Armed Services Vocational Aptitude Battery (ASVAB) is used by the U.S. military for selection and classification decisions (Vineberg & Joyner, 1983), and its validity in predicting training success criteria is well documented (e.g., Mullins, Earles & Ree, 1981). One goal of the Joint-Service Job Performance Measurement/Enlistment Standards Project is to assess the validity of ASVAB composites in predicting measures of on-the-job performance, and

although ASVAB composites should be more highly related to measures of overall job performance, we also hypothesized:

H1: A significant and positive relation between ASVAB Mechanical Aptitude Indices and Jet Engine Mechanic task performance.

III.2 Task Difficulty.

The notion of task difficulty is found in literature relating to goal setting (e.g., Locke, Shaw, Saari & Latham, 1981); perceived job characteristics (e.g., Stone & Gueutal, 1985) task taxonomies (e.g., Fleishman, 1978) and human factors research on workload (e.g., Moray, 1982). Task difficulty has been defined and measured in terms of characteristics intrinsic to the task (e.g., production standards, Locke et al., 1981) and the task performer (e.g., physiological measures such as pulse rate variability; Casali & Wierwille, 1983; Wierwille, Rahimi & Casali, 1985). Measures of difficulty also range from relatively objective (e.g., normative task difficulty, Terborg, 1977) to quite subjective indices (e.g., self ratings of subjective workload, Moray, 1982).

Burtch et al. (1982), Fugill (1973) and Weeks (1984) defined task difficulty in terms of time required for a typical employee to learn to perform a task satisfactorily. Task Learning Difficulty Indices (LDIs) are derived from Subject Matter Expert (SME) ratings that are linked to ASVAB aptitude area Benchmark scales (Burtch et al., 1982). Thus, this approach operationalizes task difficulty in terms of subjective ratings of a characteristic of the task performer and focuses on tasks' cognitive demands.

Some approaches to defining "task difficulty" predict a positive relation between difficulty and performance. Goal setting literature

supports the notion that higher production goals lead to increased productivity (Locke et al., 1981) and literature relating to perceived job characteristics suggests that employees' perceptions of challenging and autonomous work environments are associated with higher levels of job performance and satisfaction (Loher, Noe, Moeller & Fitzgerald, 1985; Stone & Gueutal, 1985). However, an inverse relation is generally proposed (Fleishman, 1978; McGrath, 1976; Moray, 1982; Weeks, 1984). We also hypothesized:

H2: An inverse relation between task learning difficulty and task performance.

There are also rationale for an interactive relationship between task difficulty and task-relevant aptitudes in predicting task performance. Terborg (1977), for instance, suggested that restricted variance in performance on extremely easy and extremely difficult tasks would limit the predictability of performance from aptitudes to tasks of intermediate difficulty. None of the tasks in the present study were considered extremely difficult, so we hypothesized:

H3: Increasingly stronger positive relationships between task-relevant aptitudes and task performance on tasks of increasingly higher learning difficulty.

III.3. Job and Task Experience.

It is a common assumption that a greater amount of job-related experience leads to more effective job performance. This assumption may partly underlie the larger salaries afforded more experienced workers (Medoff & Abraham, 1980; 1981) and prior experience requirements for entry into many jobs. Work experience is correlated with and generally confounded with age (Mathews & Cobb, 1974; Rhodes, 1983; Schwab & Heneman, 1977; Waldman & Avolio, 1986). Experience has been indexed by aggregate measures (e.g., Horowitz & Sherman, 1980) and

individual measures of career stage (e.g., Katz, 1978), organizational tenure (e.g., Maier & Hiatt, 1985), position tenure (e.g., Gininger, Dispenzieri & Eisenberg, 1983; Kozlowski & Hults, 1986) and the number of times a task has been performed (e.g. Spiker, Harper & Hayes, 1985).

There is evidence for an inverse (e.g., Rothe, 1949), zero (e.g., Cobb, 1968), positive (e.g., Gininger et al., 1983; Maier & Hiatt, 1985) and curvilinear relationship (Mathews & Cobb, 1974; Spiker et al., 1985) between experience and job performance. Cobb (1968) suggested that negative associations between experience and performance at extremely long lengths of tenure may be attributable to aging effects, whereas Brown (1982) has argued that beneficial effects of additional experience may only be observed in samples of relatively short mean lengths of tenure. Since the participants in this research were all first-term airmen, we hypothesized that:

H4a: Job experience, indexed by organizational tenure and,

H4b: Task experience would both relate positively to task performance.

Literature also suggests that experience and aptitudes may interact in predicting task performance (Maier & Hiatt, 1985). We hypothesized:

H5: Weaker positive relations between task-relevant aptitudes and task performance with greater levels of experience.

Support for this hypothesis would have implications for setting differential aptitude cutoff scores as a function of time allowed for airmen to attain task proficiency through on-the-job training.

III.4. Other Interactions.

Fugill's (1973) definition of task learning difficulty implies:

H6: Increasingly stronger positive relations between experience

and performance on tasks of increasing learning difficulty.

Maier and Hiatt (1985) also alluded to the possibility of a three-way interaction between task difficulty, experience and aptitudes in predicting task performance. We hypothesized:

H7: (a) for low difficulty tasks, a positive relation between task experience and task performance for lower aptitude but not for higher-aptitude airmen,
(b) for moderately difficult tasks, experience and aptitude would combine in a linear and additive fashion in predicting task performance, and
(c) for high difficulty tasks, a positive relation between aptitude and performance for higher aptitude, but not for lower-aptitude airmen.

IV. Method.

The Walk-Through Performance Testing (WTPT) methodology and the collection of job performance and related measures on 255 Jet Engine Mechanics (AFS 426x2) are described in detail elsewhere (Hedge, 1984; Hedge & Teachout, 1986).

IV.1 Measures.

The following measures were adapted from the Jet Engine Mechanic Job Performance Measurement Data Base for the present research:

IV.1.1 Performance Measures.

IV.1.1.1 WTPT scores.

Each task in each AFS 426x2 Walk-Through Test is composed of a varying number of performance steps. Steps within tasks vary in their criticality. The WTPT scores used in this research were 10-point weighted step scores that (a) reflect the relative criticality of task steps and (b) express task scores on a comparable 10-point metric.

IV.1.1.2 Overall Performance (OAP) Ratings.

These ratings were completed by WTPT administrators immediately after an airman completed a WTPT task. The 5-point rating scale ranged from 1 = Far below the acceptable level of proficiency, to 5 =

Far exceeded the acceptable level of proficiency.

IV.1.1.4 Task Proficiency Ratings.

Prior to the WTPT, airmen used a 5-point scale ("1 = Never meets acceptable level of proficiency" to "5 = Always exceeds acceptable level of proficiency") to rate their own proficiency on tasks performed by AFS 426x2 incumbents, including those they would perform during the Walk-Through test. Comparable Supervisory ratings were also obtained prior to WTPT administration.

IV.1.2 Experience Measures.

IV.1.2.1 Job Experience.

Several measures of job experience were collected: (a) Total Active Federal Military Service (TAFMS), (b) Months in Present Unit; (c) Months assigned to an engine type; (d) Months of shop experience, and; (e) Months of flightline experience. Since these measures were highly correlated (median r = .635) they were averaged to create a job experience (JOBEXP) composite.

IV.1.2.2 Task Experience.

Two measures of task experience were collected. Task Experience Ratings (TERs) were 7-point self-ratings of relative experience on tasks performed by AFS 426x2 incumbents, including the WTPT tasks ("1 = No Experience" to "7 = A Very Great Amount"). Number of times performed (NTP) was a self-report estimate of the number of times each WTPT task had been performed previously (coded 0 to 999). NTP's distribution was markedly bimodal and its correlation with TER (r = .32) was lower than expected. NTP scores were transformed to alleviate the severe bimodality. Transformed and original NTP scale values were: 1 = 0 times performed; 2 = 1-9 times performed; 3 = 10-19; 4 = 20-50; 5 = 51-100; 6 = 101-800; and 7 = 801-999. This trans-

formation left the relationship between the transformed NTP and the original NTP reasonably intact (r = .80) and increased the correlation with TER (r = .55). TER and the transformed NTP were then averaged to form a task experience (TASKEXP) composite.

IV.1.3 Task Difficulty.

The 25-point Benchmark Task Learning Difficulty Indices (LDIs) described by Burtch et al. (1982) were used to index WTPT tasks' difficulties.

IV.1.4 Aptitude.

Each airman's pre-enlistment specialty area (Mechanical) aptitude index (MEC-AI) was used to indicate task-relevant aptitude.

IV.2 Research Data Base.

Task performance and task experience measures were recorded for each ith airman (i-->N = 255) on the jth task (j --> J_i = 15 for each airman) attempted in the WTPT. This yielded 3825 (255 participants times 15 WTPT tasks) unique measures of individuals' task performance and task experience. LDIs varied appropriately with tasks and were constant for all n_j performers of the jth task. MEC-AIs and JOBEXP measures varied appropriately with the N airmen and were constant for the ith participant across all WTPT tasks attempted.

IV.3 Data Editing.

Since inferences from this research were to be drawn to the population of first-term airmen who meet or exceed minimal Air Force-wide enlistment standards, data records were excluded from analysis if: (a) An airman's ASVAB General-AI score was less than 30; (b) An airman's reported TAFMS was longer than 60 months, (c) An airman's reported Months on Engine was over 50 months (M. Ree, personal commu-

nication, July, 1986), or; (a) There were missing data on variables being analyzed;

IV.4 Analyses.

Hierarchical moderated regression (e.g., Arnold, 1982, 1984; Ward & Jennings, 1973) was the primary analytic tool used to test hypotheses H1 through H7. Main effect hypotheses were evaluated by conventional significance tests of parameter estimates in multiple linear regression models that contained appropriate aptitude, task difficulty and experience predictors. Two-way interactions were tested by comparing (a) the R^2 obtained from a regression model that included linear terms plus a cross-product term between variables involved in the interaction hypothesis to (b) the R^2 obtained from a regression model that included only linear terms (Arnold, 1982; Cohen & Cohen, 1975). The three-way interaction hypothesis (H7) was similarly evaluated by comparing (a) the R^2 obtained from a regression model that included linear terms, all two-way cross-product terms and the three-way cross-product to (b) the R^2 obtained from a regression model that included only linear and two-way cross-product terms. Significant increments in R^2 due to inclusion of cross-product terms was interpreted as support for a statistical interaction whose form was explored in subgroup regression analysis (Arnold, 1982).

Dummy-coded task (situational) variables were also created and used with MEC-AIs, experience and performance measures to test for homogeneity of regression across WTPT tasks. Dummy-coded task and person main effects also provided backdrops to assess the relative proportions of variance in task performance measures attributable to task learning difficulty, aptitude and job experience.

V. Results

Table 1 shows study variables' descriptive statistics. All were within anticipated ranges. Table 2 shows intercorrelations among study variables.

V.1 Main Effects.

Hypotheses H1, H3a, H3b and H5 all concerned main effects and all received support (see Table 2). Task learning difficulty was the strongest predictor of the WTPT scores and, as expected, TASKEXP was a better predictor of WTPT scores than JOBEXP.

Table 1

Descriptive Statistics - Study Variables

	Scale Range	Mean	S.D.	N of Cases[a] (possible)
Performance Measures:				
1. WTPT Scores	0 -10	7.34	2.37	3255(3825)
2. OAP Ratings	1 - 5	2.85	1.58	3211(3825)
3. Self Task Ratings	1 - 5	3.87	0.94	3222(3825)
4. Supervisor Task Ratings	1 - 5	3.86	1.23	3248(3825)
Experience Measures:				
5. Job Experience Composite	0 -48	19.36	8.80	217(255)
6. Task Experience Composite	1 - 7	3.55	1.47	3255(3825)
Task Difficulty Measure:				
7. Task Learning Difficulty Index	1 -25	13.91	2.18	23(23)
Aptitude Measure:				
8. ASVAB MEC-AI	4 -396	225.74	25.98	217(255)

[a] Number of valid cases (of total possible). N of cases vary due to level of analysis and missing data.

Table 2

Intercorrelations Among Study Variables

	1	2	3	4	5	6	7	8
1. WTPT Scores	1.00							
2. OAP Ratings	.64	1.00						
3. Self Task Ratings	.17	.07	1.00					
4. Supervisor Task Ratings	.18	.10	.26	1.00				
5. Job Experience Composite	.07	.02	.22	.18	1.00			
6. Task Experience Composite	.20	.08	.54	.23	.26	1.00		
7. Task LDIs	-.26	-.02	-.22	-.15	.01	-.24	1.00	
8. ASVAB MEC-AI	.05	.05	.06	.06	-.26	.01	-.01	1.00

Table 3

Hierarchical Regression Results - Main Effects[a]

Dependent Variable:	WTPT Scores	OAP Ratings	Self Task Ratings	Supervisor Task Ratings
Predictors:[b]				
1. ASVAB MEC-AI	.081**	.057**	.115**	.120**
2. Task LDIs	-.239**	-.016	-.231**	-.153**
3. Job Experience Composite	.088**	.030	.217**	.213**
1. ASVAB MEC-AI	.056**	.049**	.055**	.061**
2. Task LDIs	-.203**	.004	-.096**	-.102**
3. Task Experience Composite	.140**	.090**	.513**	.193**

[a] Main effects including Job (Task) Experience composite are shown in the upper (lower) half of the Table.

[b] Ordinary least squares standardized partial regression parameter estimates.

*p<.05; **p<.01

MEC-AI was a significant predictor of all dependent variables, but effects were small. This may be partly due to the relative non-correspondence in specificity/globality between the predictor and criteria (e.g., Fishbein & Ajzen, 1974).

Only MEC-AI was a consistent predictor of the OAP rating. This suggests either that WTPT administrators (a) may have been "leveling" their proficiency ratings for perceived differences in task difficulty and airman experience, (b) differed from one another in their implicitly assumed proficiency standards, or (c) may have considered subtleties in perfoprmance not assessed by the dichotomous WTPT step scoring procedure.

Patterns of main effects predicting Self and Supervisory ratings were more similar to those relating to the WTPT scores than the OAP ratings. This might suggest that supervisory and self task ratings are more convergent with WTPT scores as indicators of task performance than OAP ratings (Cook & Campbell, 1979). However, the low correlations between task ratings and other criteria suggest otherwise (see Table 2). WTPT scores, Self and Supervisor task ratings may instead represent assessments of distinct aspects of overall proficiency.

LDI, tended to be less predictive, while experience composites tended to be more predictive of the rating criteria than the WTPT scores. These prediction differences may in part be attributable to method variance effects. In particular, the large regression weight linking self proficiency ratings to the TASKEXP composite may be inflated.

By some standards, the proportion of variance in task performance scores accounted for by the main effects was small. Golding (1975) and Abelson (1985), however, have argued against an unquestioning "variance-accounted-for" standard for judging the importance of research findings. Still, we asked: What proportion of predictable task performance score variance was accounted for by the study's variables?

To attempt a preliminary answer, the total variance in WTPT performance scores attributable to (unspecified) differences in situations (tasks) was estimated by creating a dummy-coded variable for all but one of the WTPT tasks (to keep the implied design matrix nonsingular). WTPT scores were regressed on the dummy coded task variables with R^2 = .2462 (F (22,3232) = 47.99, p < .01). A ratio of the squared correlation between LDI and WTPT scores, and the squared multiple correlation from the regression of the WTPT scores on the dummy coded task variables (.0567/.2462 = .23) suggested that 23% of the variance in WTPT scores that was attributable to (unspecified) differences in tasks was attributable to differences in the tasks' learning difficulties (see James, Demaree & Hater, 1980 for a similar approach). Tasks were deliberately sampled over a range of difficulties, so this percentage might be attributed to a successful experimental manipulation. However, similarly calculated ratios for Self (.0229/.0528 = .43) and Supervisory Task Proficiency Ratings (.0522/.1246 = .42) corroborate the conclusion that task difficulty has a significant impact upon task performance.

We also asked: what proportion of the variance in WTPT scores predictable by (unspecified) interindividual differences is attributable to individual differences in aptitude and job experience? WTPT

scores were regressed on dummy-coded person variables with R^2 = .2244 (F (214,3010) = 4.07, p < .01). The squared correlations between WTPT scores and MEC-AI (.00363) and JOBEXP (.00393), and the squared multiple correlation from the linear regression of WTPT on MEC-AI and JOBEXP (.01043) were used to index the proportions of interindividual difference variance attributable to study variables. Ratios similar to those computed in analysis of between-task variance suggested that only 1.6% (.00363/.2244) of the total variance accounted for by interindividual differences was attributable to aptitude (MEC-AI), 1.8% (.00393/.2244) to job experience and 4.6% (.01043/.2244) to the combined influence of aptitude and job experience.

Similar ratios were computed for Self and Supervisory Task ratings. Of the total variance in the Self ratings accounted for by (unspecified) interindividual differences, only 1% (.0036/.3763) was attributable to aptitude (MEC-AI) and 8.9% (.0336/.3763) to job experience. For the Supervisory ratings, these percentages were .8% (.0042/.5209) for MEC-AI and 6.2% (.0323/.5209) for job experience.

In summary, main effects analyses implied that aptitude, experience and task learning difficulty were significant predictors of task performance. Patterns of WTPT prediction parameter estimates were more similar to those associated with Self and Supervisory ratings than the WTPT administrator OAP ratings. Task learning difficulty appeared to account for a sizeable proportion of predictable inter-task variance in task performance measures. On the other hand, aptitude and job experience measures accounted for relatively little of the predictable interindividual variance in task performance measures.

V.2 Interactions.

Hypothesis H7 predicted a three-way interaction between experience, aptitude and task difficulty in predicting task performance. The three-way cross-product term was highly collinear with linear and two-way cross-product regression terms and accounted for essentially no additional variance in any dependent variable beyond that accounted for by the lower order effects. H7 was regarded as disconfirmed.

Tables 4 and 5 show hierarchical moderated regression tests of two-way interaction hypotheses (H3, H5 and H6). Hypothesis H3 predicted an interaction between aptitude and task difficulty in predicting task performance, and received no support. The MEC-AI x LDI cross-product did not account for a significant proportion of additional variance in any dependent variable beyond that portion accounted for by the main effects.

Hypothesis H6 predicted that experience and task learning difficulty would interact to predict task performance. This hypothesis also received no support. Apparent significant interaction effects between LDI and TASKEXP in predicting Self and Supervisory Task Ratings (Table 5) were instead the result of spurious suppressor effects (Lord & Novick, 1968; McFatter, 1979). Cross-product terms were nearly collinear with at least one of the constituent main effects. Partial correlations between the cross-product term and the dependent variables were essentially zero, while correlations with constituent variables were high. Thus the partial regression parameter estimates functioned as "classical suppressors" (McFatter, 1979) in the multiple regression equations.

Table 4

Hierarchical Moderated Regression Results - Work Sample Measures

	Dependent Variable					
	WTPT Scores			OAP Rating		
	R^2	F	S.E.	R^2	F	S.E.
Linear Terms:						
(M) ASVAB MEC-AI +						
(L) Team LDIs +						
(J) Job Experience Composite	.06726	78.14**	3.3251	.00357	9.50**	3.32[illegible]
(M) ASVAB MEC-AI +						
(L) Team LDIs +						
(T) Team Experience Composite	.07845	92.25**	3.3251	.00870	23.18**	3.3207
	ΔR^2	F	S.E.	ΔR^2	F	S.E.
Cross-Product Terms:						
M x L	.00056	1.95	1,3250	.00000	.00	1,3206
M x J	.00212	7.40**	1,3250	.00300	9.68**	1,3206
L x J	.00080	2.79	1,3250	.00002	0.06	1,3206
M x L	.00059	2.08	1,3250	.00000	.00	1,3206
M x T	.00128	4.52*	1,3250	.00184	5.96*	1,3206
L x T	.00071	2.51	1,3250	.00002	0.06	1,3206

*p<.05; **p<.01

Table 5

Hierarchical Moderated Regression Results - Task Performance Ratings

	Dependent Variable					
	Self Ratings			Supervisory Ratings		
	R^2	F	S.E.	R^2	F	S.E.
Linear Terms:						
(M) ASVAB MEC-AI +						
(L) Team LDIs +						
(J) Job Experience Composite	.09044	118.04**	3.3218	.06920	80.39**	3.32[illegible]
(M) ASVAB MEC-AI +						
(L) Team LDIs +						
(T) Team Experience Composite	.30187	463.82**	3.3218	.06194	71.94**	3.3244
	ΔR^2	F	S.E.	ΔR^2	F	S.E.
Interaction Terms:						
M x L	.00003	0.11	1,3217	.00000	.00	1,3243
M x J	.00122	4.36**	1,3217	.00570	19.99**	1,3243
L x J	.00037	1.32	1,3217	.00016	0.56	1,3243
M x L	.00001	0.05	1,3217	.00000	.00	1,3243
M x T	.00393	18.22**	1,3217	.00011	0.38	1,3243
L x T	.02009	95.31**	1,3217	.00702	24.46**	1,3243

*p<.05; **p<.01

Hypothesis H5 predicted an interaction between aptitude and experience in predicting task performance. This hypothesis was consistently supported by small, but significant increments in variance explained in task performance measures by the aptitude x experience cross-product terms, above and beyond linear effects (see Tables 4 and 5). The subgroup regression analysis results in Table 6 illustrate the typical interaction pattern.

Table 6

Subgroup Analysis of Aptitude-Performance Relations by Job Experience Level

	Low Experience (n = 1254)			Medium Experience (n = 1029)			High Experience (n = 917)		
Var.	Mean	S.D.	r's[a]	Mean	S.D.	r's	Mean	S.D.	r's
WTPT	7.2	2.5		7.3	2.3		7.6	2.3	
OAP	2.8	1.6	.65**	2.8	1.6	.60**	2.9	1.5	.68**
MEC-AI	229.6	25.1	.11** .12**	228.6	22.0	.07* .01	216.7	29.2	.02 .02

[a] Intercorrelations. *p<.05; **p<.01

Low, Medium and High Experience subgroups were formed by selecting individuals whose JOBEXP scores were below, within or above .5 standard deviation of the JOBEXP mean. Subgroup ns are unequal due to the skewness of JOBEXP. The predictability of task performance from aptitude scores decreased among more experienced airmen (correlations, rather than unstandardized regression parameter estimates are shown for interpretive ease, Kerlinger & Pedhazur, 1973). Note that this interaction is not attributable to (a) a ceiling effect, since mean performance scores did not tend toward the maximum score of 10, (b) differential range restriction, since standard deviations were quite similar across subgroups, or (c) performance becoming less predictable over time, since the non-significant Experience x Task Difficulty interactions implied that prediction of task performance from LDI is constant over various levels of task and job experience. Rather, the interaction suggests that (a) proficiency increases with experience, and (b) aptitude is a significant predictor of performance relatively early in an airman's first term of enlistment, but that later, other (unmeasured) factors may serve as better predictors.

V.3 Predicted Aptitude Requirements.

A final research question concerned the feasibility of establishing differential aptitude requirements as a function of situational (task) demands. This work was considered preliminary, since analyses were conducted at the disaggregated task level, while selection and classification decisions are made at the specialty level.

Results in Tables 4 and 5 show that task learning difficulty did not moderate the relationship between task performance and either experience or aptitude. Results in Table 7 reinforce this conclusion.

Model I in Table 7 is the regression of WTPT task performance on dummy-coded variables representing the WTPT tasks. Comparisons between Models II and I, and between Models V and II, corroborate results in Tables 4 and 5, and imply that significant predictors of WTPT task performance are task differences, aptitude, job experience and an aptitude x experience interaction. Nonsignificant interaction effects between task variables and other regression terms indicated homogeneous Model V regressions across tasks.

Table 7

Hierarchical Moderated Regression of WTPT Scores on Job Experience, MEC-AI and Dummy-Coded Task Variables

Model	Predictor(s)	R^2	d.f.	F
I.	Task Variables(T)	.24625	22,3232	47.99**
II.	Task Variables(T) + MEC-AI(M) + JOBEXP(J)	.25636	24,3230	46.40**
III.	T + M + J + TxM	.25939	46,3208	24.42**
IV.	T + M + J + TxJ	.26331	46,3208	24.93**
V.	T + M + J + MxJ	.25872	25,3229	45.08**
VI.	T + M + J + TxM + TxJ + MxJ	.26906	69,3185	16.99**
VII.	T + M + J + TxM + TxJ + MxJ + TxJxM	.27423	91,3163	13.13**

Model Comparisons	ΔR^2	d.f.	F
II vs. I	.01011	2,3230	21.96**
III vs. II	.00302	22,3208	0.59
IV vs. II	.00695	22,3208	1.38
V vs. II	.00236	1,3229	10.28**
VI vs. V	.01034	44,3185	1.02
VII vs. VI	.00517	22,3163	1.02

**p<.01

Overall, the results in Tables 3 through 7 imply that Jet Engine Mechanic task performance is predicted by task differences, aptitude, job and task experience, and an interaction between aptitude and experience. In order to illustrate one approach to linking aptitude requirements to task (situational) demands, unstandardized parameter estimates from the regression of WTPT scores on MEC-AI, task LDIs and JOBEXP were selected:

$$WTPT = 8.81 + .007*MEC\text{-}AI + .024*JOBEXP - .259*LDI \quad (1)$$

WTPT was fixed arbitrarily at the mean (7.34). MEC-AI cutoff scores implied by various task LDIs were then examined at three levels of JOBEXP (the mean and plus/minus one standard deviation). Figure 1 summarizes these relationships. Implied MEC-AIs were converted to percentile equivalents and those that were beyond the upper or lower ranges were set to the boundary values (i.e., the 1st and 99th percentiles). Figure 1 illustrates that for an airman to achieve a level of performance at or above the sample mean, predicted MEC-AI requirements are a function of: (a) difficulty level of the task to be performed, and (b) amount of experience allowed to attain the desired level of proficiency.

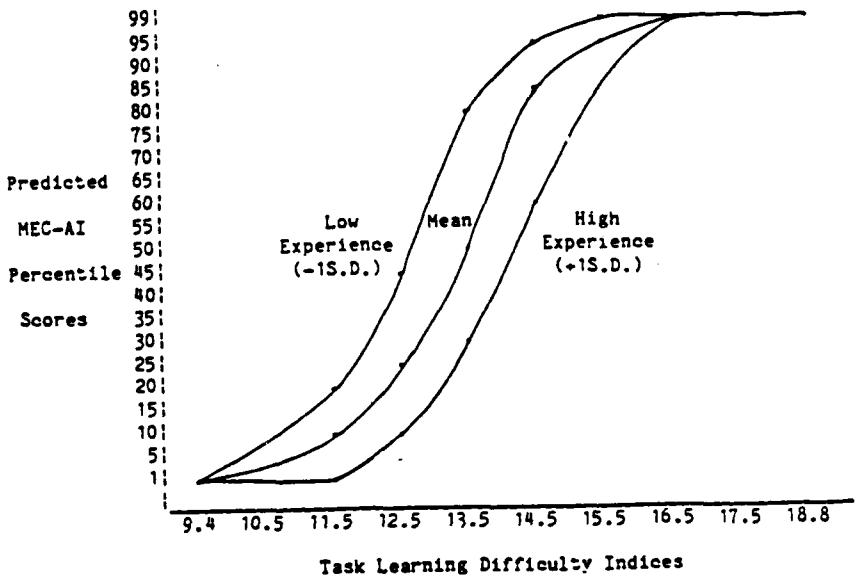

Figure 1. Aptitude cutoff scores implied for tasks of varying learning difficulty at three levels of experience and constant target performance level.

VI. Conclusions.

Overall, findings from main effect and interaction analyses suggest that (a) ASVAB MEC-AI is a valid predictor of Jet Engine Mechanic (JEM) (AFS 426x2) task performance, and (b) JEM task performance is optimally predicted as a linear function of aptitude, experience, task difficulty and an interaction between aptitude and experience. Thus, prediction of performance from aptitude may be enhanced by including additional person and situational predictors and interactions among predictors.

Prediction results for WTPT scores and Self and Supervisory Task Proficiency Ratings were quite similar. One piece of evidence for convergent validity between measures is that they do share similar predictors (Cook & Campbell, 1979). In this sense, Self and Supervisory task ratings appeared to converge much better with the WTPT scores than the OAP ratings. However, lack of convergence was implied by low correlations between WTPT scores and task ratings. One stated purpose of the Air Force Job Performance Measurement Project is to determine whether there are appropriate surrogates for the labor-intensive hands-on and interview WTPT proficiency measures. Results presented here suggest that while WTPT scores and task ratings may be similarly predicted from aptitude scores, these proficiency measures may assess distinct aspects of the total criterion space.

Finally, a prototype methodology for linking aptitude requirements to situational (task) demands (LDIs) was demonstrated. The methodology requires that measures of: (a) airman performance, (b) airman aptitude, and (c) salient differences between situations (tasks, occupations) be obtained. Successful application of the

prototype methodology also requires that performance be significantly related to (a) aptitude, and (b) the salient situational variable. Additional variables related to performance (e.g., experience) may further define the link between situational characteristics and implied aptitude requirements. This procedure may prove useful, for example, in addressing the following question: Given a desired level of performance (proficiency) and a constant amount of time allowed to attain proficiency, what required aptitude minima are implied for tasks (specialties) of various difficulty levels?

VII. Recommendations.

VII.1 Extend research to cross-specialty comparisons. Within-specialty analyses of relations among aptitude, experience, task difficulty and task performance reported here suggest that linking enlistment standards to situational demands may ultimately be feasible. However, this suggestion is preliminary and can not be extrapolated to cross-specialty inferences. To do so would be to commit the ecological fallacy (James, 1982). Attempts to link enlistment standards to situational demands (e.g., Occupational Learning Difficulty) must relate performance and aptitude predictors at the individual level to macro, specialty-level difficulty indices. Realization of this goal will require: (a) development of appropriate statistical rationale for relating measures taken at different conceptual levels of aggregation, (b) collection of aptitude, performance, and job/task difficulty scores on incumbents and tasks across several specialties, (c) common proficiency standards for airmen in different specialties, and (d) a demonstrated cross-specialty relationship between proficiency and specialty-level difficulty indices.

VII.2 Refine the definition and measurement of job and task experience. A stated objective of the Air Force Job Performance Measurement Project is to study effects of variables other than aptitudes upon job/task proficiency. The Air Force research effort has considered job/task experience important in this regard. "Experience" connotes acquisition of job-related skills and abilities that, over time, affect proficiency. But just as chronological age is a deficient indicator of aging effects (Minton & Schneider, 1985), so is tenure a deficient indicator of experience. Future work should attempt to sharpen the definition of the experience construct to reflect meanings accorded it and develop measures that more fully tap the meaning of the construct.

VII.3 Conduct longitudinal research on aptitude and experience effects on performance. For many research questions, longitudinal studies merely afford a comparison between a static correlation and prediction over some time interval. In general, longitudinal designs do <u>not</u> bolster confidence in causal inferences from nonexperimental data (Cook & Campbell, 1979; Rogosa, 1980). However, experience effects on performance imply changes over time, which, in cross-sectional studies can be misattributed from maturation, nonrandom selection, or attrition effects. Cross-sectional time series (lagged endogenous variable) designs permit statistical (e.g., pseudo-generalized least squares) estimates for (a) bias in parameter estimates due to unmeasured relevant causes of performance which, when corrected, would permit (b) unbiased estimates of causal effects leading to job performance.

Similarly, the problem of diminishing predictability of perfor-

mance from aptitudes should be studied in the contexts of: (a) indirect aptitude effects upon later task performance; (b) temporally proximal aptitude and skill determinants of performance, and (c) non-ability determinants of performance beyond the first few years of enlistment (e.g., motivation, situational constraints, leader facilitation and support, commitment to performance).

VII.4 Identify determinants of latent, true proficiency scores. Table 3 shows that different conclusions about the prediction of proficiency may be reached depending on the performance measure chosen. However, patterns of results for WTPT scores, Self and Supervisory task ratings were similar. Research should be expanded to include latent proficiency variables as dependent variables. Existing models of latent true performance scores (e.g., Hulin, Drasgow & Parsons, 1983; Kenny & Berman, 1980; Lance, Tsacoumis & Bayless, 1986; Lance & Woehr, in press; Lord & Novick, 1968) should provide the conceptual springboard.

VI.5 Research procedures for statistical control of rater bias. Ultimately, the services will likely opt for one or more performance rating systems as a suitable surrogate for the high fidelity but expensive and time-consuming WTPT methodology. The present research suggested that Self and/or Supervisory task ratings may be viable candidates. But ratings are notoriously susceptible to unconscious and deliberate biases, and earlier attempts to control biases statistically (e.g., Landy, Vance, Barnes-Farrell & Steele, 1980) have failed (Harvey, 1982; Lance & Woehr, in press). However, some (e.g., Lance & Lautenschlager, 1986; Lance & Woehr, in press) maintain that

tatistical control of rater bias may be feasible within the context f a tenable structural theory of ratee true score and rater bias ffects. Relatively simple multitrait multimethod models (e.g., Widaan, 1985) and more complex models derived from performance rating and lassical test theory (e.g., Kenny & Berman, 1980; Wherry & Bartlett, 982) should be starting points for this research.

References

Abelson, R.P. (1985). A variance explanation paradox: When a little is a lot. Psychological Bulletin, 97, 129-133.

Arnold, H.J. (1982). Moderator variables: A clarification of conceptual, analytic, and psychometric issues. Organizational Behavior and Human Performance, 29, 143-174.

Arnold, H.J. (1984). Testing moderator variable hypotheses: A reply to Stone and Hollenbeck. Organizational Behavior and Human Performance, 34, 214-224.

Bowers, K.S. (1973). Situationism in psychology: An analysis and a critique. Psychological Review, 80, 307-333.

Brown, C. (1982). Estimating the determinants of employee performance. Journal of Human Resources, 17, 178-194.

Burtch, L.D., Lipscomb, M.S. & Wissman, D.J. (1982). Aptitude requirements based on task difficulty: Methodology for evaluation. (AFHRL-TR-81-34). Manpower and Personnel Division, Air Force Human Resources Laboratory, Brooks AFB, TX.

Casali, J.G., & Wierwille, W.W. (1983). A comparison of rating scale, secondary-task, physiological, and primary-task workload estimation techniques in a simulated flight task emphasizing communications load. Human Factors, 25, 623-641.

Cobb, B.B. (1968). Relations among chronological age, length of experience, and job performance ratings of air traffic control specialists. Aerospace Medicine, 39, 119-124.

Cohen, J., & Cohen, P. (1975). Applied multiple regression/ correlation analysis for the behavioral sciences. New York: Wiley.

Cook, T.D. & Campbell, D.T. (1979). Quasi-experimentation: Design & analysis issues for field settings. Boston, MA: Houghton Mifflin.

Endler, N.S. & Magnusson, D. (1976). Toward an interactional psychology of personality. Psychological Bulletin, 83, 956-974.

Ekehammer, B. (1974). Interactionism in personality from a historical perspective. Psychological Bulletin, 81, 1026-1048.

Epstein, S. & O'Brien, E.J. (1985). The person-situation debate in historical and current perspective. Psychological Bulletin, 98, 513-537.

Fishbein, M. & Ajzen, I. (1974). Attitudes towards objects as predictors of single and multiple behavioral criteria. Psychological Review, 81, 59-74.

leishman, E.A. (1978). Relating individual differences to the dimensions of human tasks. Ergonomics, 21, 1007-1019.

ugill, J.W.K. (1973). Task difficulty and task aptitude benchmark scales for the administrative and general career fields. (AFHRL-TR-73-13) Air Force Human Resources Laboratory, Personnel Research Division, Brooks AFB, TX.

ininger, S., Disperzieri, A. & Eisenberg, J. (1983). Age, experience and performance on speed and skill jobs in an applied setting. Journal of Applied Psychology, 68, 469-475.

olding, S.L. (1975). Flies in the ointment: Methodological problems in the analysis of the percentage of variance due to persons and situations. Psychological Bulletin, 82, 278-288.

arvey, R.J. (1982). The future of partial correlation as a means to reduce halo in performance ratings. Journal of Applied Psychology , 67, 171-176.

edge, J.W. (1984, August). The methodology of walk-through performance testing. Paper presented at the meeting of the American Psychological Association, Toronto, Ontario, Canada.

edge, J.W. & Teachout, M.S. (1986, April). Job performance measurement: A systematic program of research and development. Paper presented at the Conference of the Society for Industrial and Organizational Psychology, Chicago, IL.

orowitz, S.A. & Sherman, A. (1980). A direct measure of the relationships between human capital and productivity. Journal of Human Resources, 15, 67-76.

ulin, C.L., Drasgow, F. & Parsons, C.K. (1983). Item response theory. Homewood, IL: Dow Jones-Irwin.

unter, J.E. & Hunter, R.F. (1984). Validity and utility of alternative predictors of job performance. Psychological Bulletin, 96, 72-98.

ames, L.R. (1982). Aggregation bias in estimates of perceptual agreement. Journal of Applied Psychology, 67, 219-229.

ames, L.R., Demaree, R.G. & Hater, J.J. (1980). A statistical rationale for relating situational variables and individual differences. Organizational Behavior and Human Performance, 25, 354-364.

ames, L.R. & White, J.F. III (1983). Cross-situational specificity in managers' perceptions of subordinate performance, attributions, and leader behavior. Personnel Psychology, 36, 809-855.

atz, R. (1978). The influence of job longevity on employee reactions to task characteristics. Human Relations, 31, 703-725.

Kenny, D.A. & Berman, J.S. (1980). Statistical approaches to the correction of correlational bias. Psychological Bulletin, 88, 288-295.

Kerlinger, F.N. & Pedhazur, E.J. (1973). Multiple regression in behavioral research. New York: Holt, Rinehart and Winston.

Komaki, J.L., Zlotnick, S. & Jensen, M. (1986). Development of an operant-based taxonomy and observational index of supervisory behavior. Journal of Applied Psychology, 71, 260-269.

Kozlowski, S.W.J. & Hults, B.M. (1986). Joint moderation of the relation between task complexity and job performance for engineers. Journal of Applied Psychology, 71, 196-202.

Lance, C.E. & Lautenschlager, G. (1986). Cautionary notes on the use of item analysis procedures in performance rating scale construction and a proposed alternative. (Manuscript submitted for publication).

Lance, C.E., Tsacoumis, S. & Bayless, J.A. (1986, August). Valid and invalid halo in ratings: Comparisons among alternative models. Paper presented at the annual meeting of the American Psychological Association, Washington, DC.

Lance, C.E. & Woehr, D.J. (in press). Statistical control of halo: A clarification from two cognitive models of the performance appraisal process. Journal of Applied Psychology.

Landy, F.J., Vance, R.J., Barnes-Farrell, J.L. & Steele, J.W. (1980). Statistical control of halo error in performance ratings. Journal of Applied Psychology, 65, 501-506.

Locke, E.A., Shaw, K.N., Saari, L.M. & Latham, G.P. (1981). Goal setting and task performance: 1969-1980. Psychological Bulletin, 90, 125-152.

Loher, B.T., Noe, R.A., Moeller, N.L. & Fitzgerald, M.P. (1985). A meta-analysis of the reelation of job characteristics to job satisfaction. Journal of Applied Psychology, 70, 280-289.

Lord, F.M. & Novick, M.R. (1968). Statistical theories of mental test scores. Reading, MA: Addison-Wesley.

Maier, M.H. & Hiatt, C.M. (1985). On the content and measurement of validity of hands-on job performance tests. (CRM 85-79) Alexandria, VA: Marine Corps Operations Analysis Group, Center for Naval Analyses.

Maier, M.H. & Mayberry, P.W. (1986). Improving the design of the Marine Corps job performance measurement project. Paper presented at the 10th Annual Psychology in the DoD Symposium, April.

Mathews, J.J. & Cobb, B.B. (1974). Relationships between age, ATC

experience, and job ratings of terminal air traffic controllers. Aerospace Medicine, 15, 186-216.

McFatter, R.M. (1979). The use of structural equation models in interpreting regression equations including suppressor and enhancer variables. Applied Psychological Measurement, 3, 123-135.

McGrath, J.E. (1976). Stress and behavior in organizations. In M.D. Dunnette (Ed.) Handbook of Industrial/Organizational Psychology. Chicago, IL: Rand-McNalley.

Medoff, J.L. & Abraham, K.G. (1980). Experience, performance, and earnings. The Quarterly Journal of Economics, 95, 703-736.

Medoff, J.L. & Abraham, K.G. (1981). Are those paid more really more productive? The case of experience. The Journal of Human Resources, 16, 186-216.

Minton, H.L. & Schneider, F.W. (1985). Differential Psychology. Prospect Heights, IL: Waveland.

Moray, N. (1982). Subjective mental workload. Human Factors, 24, 25-40.

Mullins, C.J., Earles, J.A. & Ree, M. (1981). Weighting of aptitude components based on differences in technical school difficulty. (AFHRL-TR-81-19) Brooks AFB, TX: Manpower and Personnel Division, Air Force Human Resources Laboratory.

O'Connor, E.J., Eulberg, J.R., Peters, L.H. & Watson, T.W. (1984). Situational constraints in the Air Force: Identification, measurement, and impact on work. (AFHRL-TP-84-10) Brooks AFB, TX, Manpower & Personnel Division, Air Force Human Resources Laboratory.

Oldham, G.R., Hackman, J.R. & Pearce, J.L. (1976). Conditions under which employees respond positively to enriched work. Journal of Applied Psychology, 61, 395-403.

Pearlman, K., Schmidt, F.L. & Hunter, J.E. (1980). Validity generalization results for tests used to predict job proficiency and training success in clerical occupations. Journal of Applied Psychology, 65, 373-406.

Rhodes, S.R. (1983). Age-related differences in work attitudes and behavior: A review and conceptual analysis. Psychological Bulletin, 93, 328-367.

Rogosa, D. (1980). A critique of cross-lagged correlation. Psychological Bulletin, 88, 245-254.

Rothe, H.F. (1949). The relation of merit ratings to length of service. Personnel Psychology, 2, 237-242.

Schmidt, F.L., Hunter, J.E. & Caplan, J.R. (1981). Validity generalization results for two groups in the petroleum industry. Journal of Applied Psychology, 66, 261-273.

Schmidt, F.L., Hunter, J.E., & Pearlman, K. (1981). Task differences as moderators of aptitude test validity in selection: A red herring. Journal of Applied Psychology, 66, 166-185.

Schneider, B. (1978). Person-situation selection: A review of some ability-situation interaction research. Personnel Psychology, 31, 281-297.

Schwab, D.P. & Heneman, H.G. III (1977). Effects of age and experience on productivity. Industrial Gerontology, 4, 113-118.

Spiker, V.A., Harper, W.R. & Hayes, J.F. (1985). The effect of job experience on the maintenance proficiency of Army automotive mechanics. Human Factors, 27, 301-311.

Stagner, R. (1977). On the reality and relevance of traits. Journal of General Psychology, 96, 185-207.

Stone, E.F. & Gueutal, H.G. (1985). An empirical derivation of the dimensions along which characteristics of jobs are perceived. Academy of Management Journal, 28, 376-396.

Terborg, J.R. (1977). Validation and extension of an individual differences model of work performance. Organizational Behavior and Human Performance, 18, 188-216.

Terborg, J.R. (1981). Interactional psychology and research on human behavior in organizations. Academy of Management Review, 6, 569-576.

Terborg, J.R., Richardson, P. & Pritchard, R. D. (1980). Person-situation effects in the prediction of performance: An investigation of ability, self-esteem and reward contingencies. Journal of Applied Psychology, 65, 574-583.

Vineberg, R. & Joyner, J.N. (1983). Performance measurement in the military. In F.J. Landy, S. Zedeck & J. Cleveland (Eds.) Performance measurement and theory. Hillsdale, NJ: Erlbaum.

Waldman, D.A & Avolio, B.J. (1986). A meta-analysis of age differences in job performance. Journal of Applied Psychology, 71, 33-38.

Ward, C.J. & Jennings, E. (1973). Introduction to linear models. Englewood Cliffs, NJ: Prentice Hall.

Weeks, J. (1984). Occupationl learning difficulty: A standard for determining the order of aptidude requirement minimums. (AFHRL-SR-84-26). Manpower and Personnel Division, Air Force Human Resources Laboratory, Brooks AFB, TX.

Wherry, R.J. Sr. & Bartlett, C.J. (1982). The control of bias in ratings: A theory of rating. Personnel Psychology, 35, 521-551.

Widaman, K.F. (1985). Hierarchically nested covariance structure models for multitrait-multimethod data. Applied Psychological Measurement, 9, 1-26.

Wierwille, W.W., Rahimi, M. & Casali, J.G. (1985). Evaluation of 16 measures of mental workload using a simulated flight task emphasizing mediational activity. Human Factors, 27, 489-502.

1986 USAF-UES Summer Faculty Research Program/

Graduate Student Summer Support Program

Sponsored by the

Air Force Office of Scientific Research

Conducted by the

Universal Energy Systems, Inc.

Final Report

Multiaperture Optical Systems and Neural Networks Capable of the Detection of Motion, Speed, Direction and Distance

Prepared by:	David Lawson
Academic Rank:	Assistant Professor
Department and University:	Department of Mathematics and Computer Science Stetson University DeLand, Fl. 32724
Research Location:	The Air Force Armament Laboratory Advanced Seeker Division Electro Optical Terminal Guidance Branch Eglin Air Force Base, Fl. 32542
USAF Research:	Martin Wehling
Date:	August 6, 1986
Contract No.:	F49620-85-C-0013

Multiaperture Optical Systems and Neural Networks Capable of the Detection of Motion, Speed, Direction and Distance

by

David Lawson

Abstract

An artificial multiaperture optical system is an array of sensors. The insect eye is a natural example of the same thing. We use insect behavior as a guide to the development of neural networks capable of organizing and responding to data collected by multiaperture systems. We present networks capable of detecting motion, speed, and direction. We demonstrate that the Aperture Problem (the problem of determining the direction of large objects by local direction mechanisms alone) can be solved for a restricted class of objects. Distance presents a special problem which can be resolved by binocular vision, peering, and/or ranging. In addition, we present a neural derivative capable of detecting the motion of light edges, and an off-center version capable of detecting dark edges. Recent experiments have shown that motion detection mechanisms in the Rhesus monkey react in this manner. Neural tracking and attention mechanisms are also presented.

Acknowledgements

I would like to thank the Air Force Systems Command, the Air Force Office of Scientific Research, and the Air Force Armament Laboratory for sponsoring this research. I must also thank the Air Force Armament Laboratory, the Advanced Seeker Division, and the Electro Optical Terminal Guidance Branch for the space, the time, the support, the interest and the help that each of them provided.

This report is the direct result of a collaboration with David Zeigler during the summer of 1986. Conversations with and contributions from Dennis Goldstein and David Crane were of tremendous value. Many other people also made contributions and suggestions during the period of our tenure at Eglin Air Force Base. Special thanks must go to Rick Wehling and Dennis Goldstein for having the foresight and the initiative to invite a neural modeler and a biologist to work at the laboratory for the summer. This collaboration is due to them.

Many people have made a special effort to make this period successful and enjoyable. In particular, I would like to thank Sam Lambert, and Jerry Hudson for their time and the attention that they have provided. Mary Murphy of the Technical Library has also been a considerable help.

I must also thank my wife, Karen, and my children Paul, Jessica, Melissa, and Angela, for their understanding and support during the time I have been gone.

I. INTRODUCTION:

The research problem at the Air Force Armament Laboratory involves the investigation and development of neural networks which are capable of the organization of and proper response to data collected by multiaperture optical systems.

I am a professor of mathematics and computer science at Stetson University in DeLand, Florida. During the past year I have presented two papers, each of which was an introduction to a facet of Stephen Grossberg's work. The first, Logic Gates of the Mind, was presented to the Florida Section of the Mathematical Society of America. The second, Mathematics of the Mind, Stephen Grossberg's Dynamic Geometry of the Mind, was presented at the Fiftieth Annual Meeting of the Florida Academy of Sciences. In addition, I have working with me an enthusiastic group of students who are developing a software package capable of producing neural models.

II. OBJECTIVES OF THE RESEARCH EFFORT:

The overall objective of the research is to develop a series of neural models which are capable of organizing and responding to multi aperture data. Insects are obvious and ubiquitous examples of functional multiaperture systems. An investigation and explanation of the neural principles involved in the collection of data and control of insect behavior could prove directly applicable to artificially created multiaperture systems. For this reason we wish to explain and emulate insect visual and motor phenomena.

Particular emphasis is placed upon: motion detection mechanisms, target tracking mechanisms, distance determination, and attention mechanisms.

III. NEURAL MODELING

The theoretical component of neuroscience is developing in

the fledgling field of neural modeling. This field has yet to become a recognized academic discipline, so the academic respectibility of anyone who works in it is at risk.

David Hestenes, "HOW THE BRAIN WORKS: the next great scientific revolution"

IV. MODELS OF THE NEURON

We have used two models of the neuron. The first model was developed by McCulloch and Pitts in the 1940's. The second model is a more sophisticated model, characterized via a set of differential equations developed by Stephen Grossberg in the 1970's.

A. Logic Gates of the Mind - The McCulloch-Pitts Neuron.

The McCulloch-Pitts neuron can have a large number of inputs, each of which is a 0 or a 1. Each neuron can connect to many other neurons. Each neuron had a threshold T. If the threshold is exceeded at time t, because more than T inputs are 1 at time t-1, then the neuron will fire. eg. Its output will be 1 at time t.

B. Differential Equations of the Mind - The Grossberg Neuron.

> "It has proven difficult ... to model the observed psychophysical data using the McCulloch-Pitts (neuron). The reason is that the psychophysical data reflect interactions ... over a span of time. Such a view converts potential into firing frequency, and Boolean logic into differential equations." [Levine, 1982]

Single spikes are spontaneously generated, but single spikes are not believed to carry information. Rather, information in an axonal signal resides in the pulse frequency of the burst. The neuron described below is a frequency generating and frequency modulating neuron. We will only present one of the differential equations Grossberg has developed to

characterize neural behavior. For others, and several examples see Hestenes, 1983.

A neural net will consist of K neurons, N_1, N_2, ... , N_K. Each neuron will be connected to every other neuron.

Grossberg's equation governing neural activity within the net:

$$dx_i/dt = -A_i(t)x_i(t) + \sum_{j=1}^{K} S_{ij}(t)z_{ij}(t) - \sum_{j=1}^{K} C_{ij}(t) + I_i(t)$$

with: $S_{ij}(t)$ = the average rate (frequency) of pulses traveling down the axon from neuron i to neuron j.

$X_i(t)$ = the average potential difference on neuron i (at the axon hillock).

$Z_{ij}(t)$ = the synaptic strength of the knob lying at the end of the axon running from neuron i to neuron j.

$A_i(t)$ = the rate of decay of neuron i.

$C_{ij}(t)$ = an inhibitory signal similar to S_{ij}.

$I_i(t)$ = the total input to the ith neuron which comes from sources other than the cells N_1, ... ,N_K

V. MOTION DETECTION

We have created neural implementations of several methods of motion detection. We have also discovered a neural solution to a resticted form of the Aperture Problem.

Section 1. Detection Mechanisms.

A. The delayed-comparison motion detection scheme.

This scheme, proposed originally by Reichardt and Hassenstein, uses two detectors A and B each of which responds transiently to a spot of light.

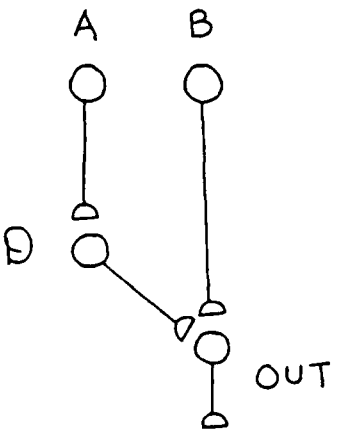

DELAYED
COMPARISON

FIG 1

The intent: A(t) = 1 B(t+1) = 1 Out(t+2) = 1
D(t+1) = 1

B. Direction Sensitive Apparent Speed Detection.

This simple model is easily extended to one capable of speed detection. This is could be an example of what is called an emergent property. An emergent property is a property which emerges unexpectedly when an organism is confronted with new environmental constraints. As an example, a redundant net capable of motion detection could have evolved. This same net is capable of speed detection (the emergent property), and could be used for speed detection if the correct environmental pressure were to appear.

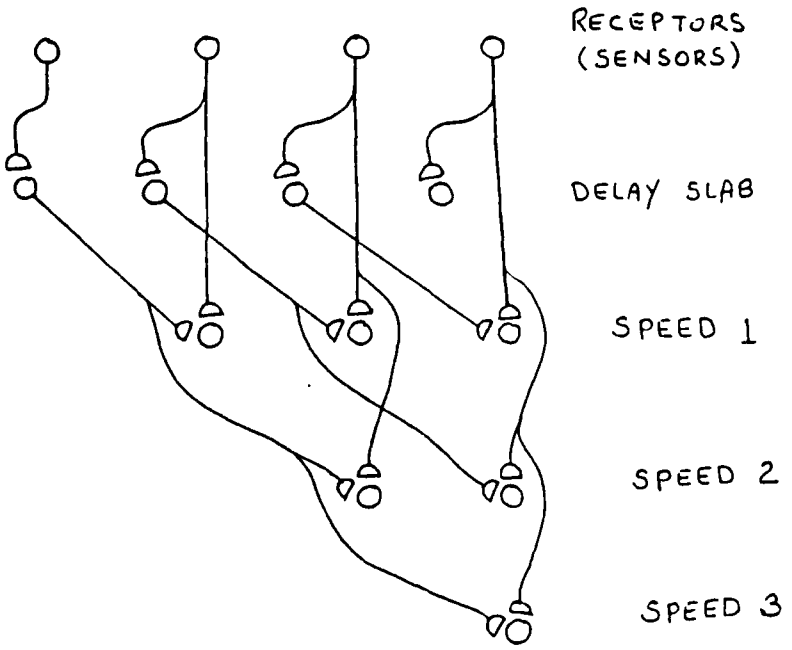

DIRECTION SENSITIVE APPARENT
SPEED DETECTION

FIG 2

The intent: A(t) = 1 B(t+1) = 1 Out(t+2) = 1
X(t+1) = 1

C. Non-Direction Sensitive Apparent Speed Determination.

The same model can be constructed using Grossberg's equations. In this case, a neuron will not physically embody the delay. Instead, a change in the result of the rate of change of the neural potential will be governed by the parameter D, the decay rate. The network will no longer be direction sensitive!

The equation for the rate of change of neural activity:

$$dx/dt = -Dx + A + B$$

The neural implementation:

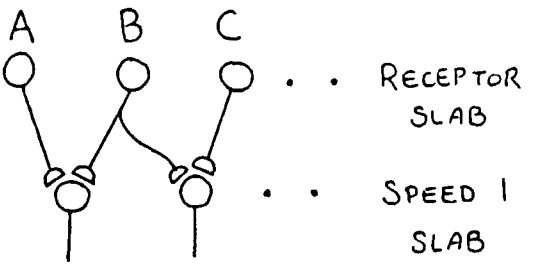

NON-DIRECTION SENSITIVE MOTION AND APPARENT SPEED DETECTION

FIG 3

D. Speed determination with a smaller network: Varying Thresholds and Graded Responses.

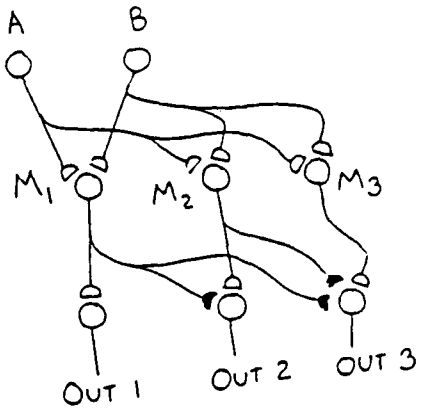

DARKENED SYNAPTIC KNOBS ARE INHIBITORY

FIG 4

The decay rate of each cell M_i is identical, but the thresholds differ. Let T_i be the threshold of the cell M_i. Suppose that $T_1 > T_2 > \ldots > T_K$.

The faster that an object moves from A to B the less the cell X_i has decayed. If M_i fires then M_j will also fire for all $i > j$, but M_i will inhibit the output of the cells M_j, for $i > j$.

Note: Care must be taken to insure that Out_i does not just momentarily inhibit Out_j.

E. A veto mechanism.

Barlow and Levick have suggested a model of motion detection called the veto mechanism. Implemented as a neural model this appears as:

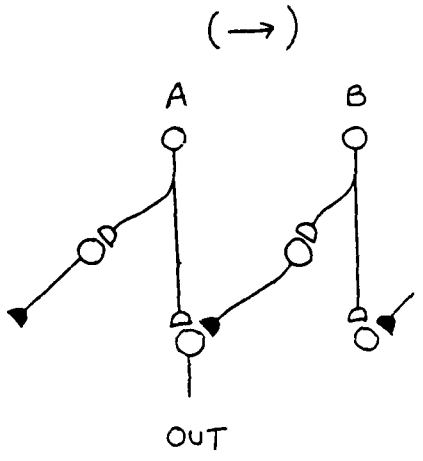

LATERAL INHIBITION
AS A VETO
FIG 5

The intent: Out = 1 if motion is from A to B
= 0 otherwise.

This is termed an AND-NOT operation because the output could be written as A(t+1) - B(t) or equivalently as A(t+1) AND (NOT B(t)).

This is linear inhibition because the activity or internal potential of the cell can be written as

$$X(t) = A(t) - B(t-1)$$

Since lateral inhibition is one of the major architectural features of vision this is an appealing natural model.

We can of course remove the delay cell and replace it with an appropriate decay factor D for X. Using Grossberg's generic equations the cell activity changes at the rate:

$$dx/dt = -Dx + A - B$$

F. A non-linear veto mechanism.

Shunting is the multiplicative effect that characterizes the interaction of an excitatory and an inhibitory neuron which are in close proximity to one another. [Poggio,1983]

A network with a non-linear, or shunting, veto mechanism can be connected in exactly the same manner as the linear veto mechanism. The differential equation governing the rate of change of cell potential will contain, however, the shunting, or multiplicative term, $-B(t)X(t)$. [Grossberg,1982]

$$dx/dt = -Dx + A - xB$$

Section 2. The Aperture Problem.

The Aperture Problem : Can an array of local detectors be integrated in a manner that will allow them to accurately determine speed and direction?

It is suspected that a separate mechanism must determine the direction of large objects, a mechanism that uses something other than local detectors alone. The following example will illustrate why.

An example. A short line, at a 45 degree angle to the vertical, moving

horizontally.

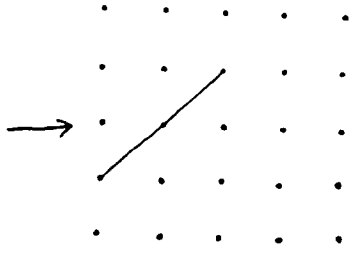

A SHORT LINE
MOVING HORIZONTALLY

FIG 6

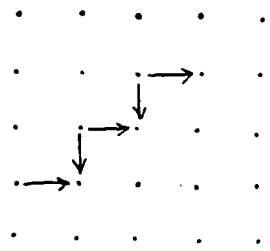

DIRECTION SENSORS
FIRED

FIG 7

Move this line over a cartesian array of detectors and you will find that the direction sensors indicated above via arrows have been fired.

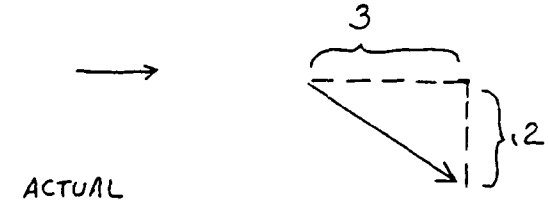

ACTUAL DIRECTION

DIRECTION INDICATED BY VECTOR SUM

FIG 8

This is very disconcerting because a simple vector sum of the directions does not yield the correct direction.

Insect Vision, Symmetry, and Local Detectors.

Insects, and many other animals find that prey are symmetric, or approximately symmetric, at an appropriate time. An airplane, for instance, is symmetric when viewed while in flight from below. In such a case, we have been able to demonstrate that local detectors can be used to correctly predict the direction of motion.

The demonstration assumes:

1. the object is symmetric about the line of motion.

2. that if point A is tripped (sensor A) then the same object will not trip it again. We wish to avoid reporting motion in direct opposition to the line of flight in this manner.

3. that the object is stationary with respect to the line of flight (we do not want to allow rotary movement of the object). In order to give an analytical meaning to this notion, we say that an object is stationary with respect to the line of flight if given points (sensors) A and B both on a line parallel to the line of flight and if B directly follows A, then is the object is sensed by A it will also be sensed by B. This is just to say that the direction sensor AB will be tripped.

Under these assumptions we can show that the bigger the object, the closer the vector sum of the local detectors will be to the correct direction.

Section 3. The Neural Derivative

David Marr and Shimon Ullman have proposed a gradient scheme for the detection of motion. An implementation of that notion is a neural derivative. The neural derivatives displayed are of interest because they react in accordance with recent experiments.

The idea behind the gradient method :

At point P the intensity profile has a positive slope. If the stimulus moves to the left the intensity I at p will increase. If the stimulus moves to the right the intensity I at p will decrease.

In order to implement this idea consider the following sketch.

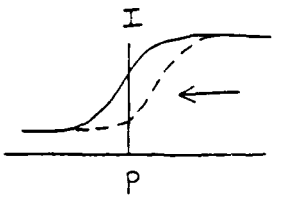

LIGHT EDGE MOVING TO THE LEFT

FIG 9

A light edge is the leading edge of a light figure moving across a dark background. The same intensity profile moving to the right is called a dark edge, the leading edge of a dark figure moving across a light background. (or the trailing edge of a light figure)

A neural net that can implement the gradient scheme of movement detection:

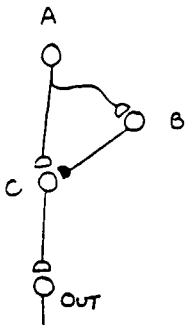

A NEURAL DERIVATIVE

FIG 10

If neuron A and neuron B are both firing at the same rate then neuron C

does not fire. If the stimulation to A increases, then A and B are no longer firing at the same rate, and C will fire. The rate at which A exceeds B will determine the rate at which C will fire. Thus, C will not fire for a flat intensity profile. If the slope increases then the rate of firing of C will increase as well. In other words C reacts exactly as a derivative would (for positive slopes).

Fact 1. The neural derivative as presented above will respond to a moving light edge only.

A light edge moving across a dark background will cause the stimulation at A to increase. A dark edge moving across the sensor A will reduce the stimulation to C. Signals from B will continue to inhibit C. Thus, the neural derivative presented above will not respond to a dark edge.

Fact 2. An off-center model of the neural derivative will respond to moving dark edges alone.

An off-center cell is a cell which will increase its rate of firing as stimulation to it decreases. If neuron A is an off-center cell we will call the neural derivative an off-center model of the derivative.

It had been conjectured that a combination of on-center and off-center cells worked in conjunction to detect edges. Schiller's (1982) APB experiments have shown that in the Rhesus monkey at least this is not the case. The neural derivatives displayed above do, on the other hand, react in accordance with Schiller's experiments (Schiller's experiments were with moving edges).

VI. ATTENTION MECHANISMS.

A multitude of data bombards an organism. To what must it shift its attention? Attention mechanisms are those mechanisms which play a part

in this determination.

A. Central priority.

Ommatidia in the center of an insects visual field are very sensitive. This sensitivity decreases as the distance from the central field increases. This property can play a role in determining attention. An insect which is responding to level of stimulation to choose between two objects of the same actual level of stimulation.

B. A neural centering and tracking mechanism.

We have discovered a mechanism which finds the center of whatever is presented to it. The insect will align its body to the object. This mechanism is thus also a tracking mechanism. It will continue to center a moving target and thus track it.

VII. DISTANCE DETERMINATION.

Apparent speed, the speed that on object moves across an array of sensors, is not the true speed. On object at a great distance might appear to be moving slowly, even though is is actually traveling very fast. To determine the true speed the distance to the object must be discovered.

Two essentially distinct methods of determining distance are attributed to insects, binocular or stereoscopic vision and peering.

A. Binocular vision.

Binocular vision refers to the use of both eyes in conjunction. The essential fact is that in a small central area of the insect fovea there are ommatidia from the left eye that are angled to the right, and ommatidia in the right eye that look to the left. The field of view of the ommatidia on the left crosses the field of view of those on the right. This will provides the insect with the information needed to do a

sort of neural triangulation. Subtle problems are hidden here if the shading of the object is complex. A simple mechanism will work well if the insect first filters the object and presents a specific edge to the triangulation network.

VIII. RECOMMENDATIONS.

1. What kind of constraint, behaviorally and neurally, is the restriction we have created in order to obtain a solution to the Aperture Problem?
2. Neural triangulation is not possible on a complex image unless one os able to match the image from one eye with the image from the other. If, however, one can triangulate then one can also match the images. Is this then a natural, perhaps behavioral way (an emergent property?) to explain the use of focus(matching) and the multiaperture eye?
3. Can feedback from motor mechanisms be used in conjunction with imaging in a self-organizing fashion to create neural triangulation and focus.
4. The reticular formation: We have not yet constructed a complete description of the control mechanism. In other words, what kind of neural mechanism decides that the object in the center of the field of view is no longer of interest?
5. What neural mechanisms are capable of target tracking, matching, prediction and correction, and predator/prey selection?
6. Parallel processing: How can the insect brain be organized to keep track of and react to a multitude of stimuli?

REFERENCES

Conference and journal publications:

1. Grossberg, Stephen, "Why do cell compete? Some examples from visual perception," The UMAP Journal, Vol. III, No. 1, Birkhaeuser Boston Inc., 380 Green Street, Cambridge, Ma., 1982, pp. 105-121.
2. Hestenes, David, "HOW THE BRAIN WORKS: The next Great Scientific Revolution", presented at the third workshop on Maximum Entropy and Bayesian Methods in Applied Statistics, The University of Wyoming, 1983.
3. Levine, Daniel S., "Neural Population Modeling and Psychology: A Review", Mathematical Biosciences, 66, 1983, pp. 1-86.
4. Poggio, T., "Visual Algorithms", Physical and Biological Processing of Images, Eds.: O.J. Braddick and A.C. Sleigh, Springer-Verlag, 1983, pp. 128-153.
5. Schiller, Peter H., "Central Connections of the Retinal On and Off Pathways", Nature, Vol. 297, June, 1982, pp. 580-583.
6. Ullman, S., "The measurement of visual motion," Trends in Neurosciences, 1983, vol. 6, no. 5, 177-179.
7. Ullman, S., "ARTIFICIAL INTELLIGENCE AND THE BRAIN: Computational Studies of the Visual System", Annual Review of Neuroscience, Vol. 9, 1986, pp1-26.

Textbooks:

1. Marr, David, Vision, W. H. Freeman and Company, 1982.

1986 USAF-UES FACULTY RESEARCH PROGRAM

Sponsored by the

AIR FORCE OFFICE OF SCIENTIFIC RESEARCH

Conducted by the

Universal Energy Systems, Inc.

FINAL REPORT

EXPERIMENTAL DESIGN AND TRANSPARENCY DURABILITY PREDICTION

Prepared by:	Paul S. T. Lee, Ph.D.
Academic Rank:	Associate Professor
Department and	Business Administration
University:	North Carolina A&T State University
Research Location:	Flight Dynamic Laboratory, AFWAL
USAF Researcher:	Mr Robert McCarty
Date:	28 July 1986
Contract No.	F49620-85-C-0013

ABSTRACT

This paper developed and discussed two experimental designs: Completely Randomized Design and Factorial Experimental Designs. They were designed mainly for the purpose of achieving three objectives: (1) To have high power in testing the effects of major factors affecting aircraft transparency failure modes, (2) To be cost-effective in testing materials, and (3) To be able to make predictions using data obtained from laboratory tests.

Multiple regression, both of linear and non-linear, have been discussed along with analysis of variance for the purpose of making predictions. It has been demonstrated that little effort was needed to conduct regression analysis once the analysis of variance is completed. Empirical data were used to the extent it is possible. Recommendations were made in four areas, namely: Applications, sample size, the ability to make predictions and a planned experiments. In short, it is highly recommended that experienced statisticians be consulted in the planning stage of an experiment for his advice to gain power of testing, efficiency in testing materials and to be able to make predictions.

ACKNOWLEDGEMENTS

Many thanks to my friends at the Vehicle Equipment Division, Flight Dynamic Laboratory,(AFWAL/FIER) at Wright-Patterson Air Force Base for their valuable suggestions and assistance in conducting this study. This includes Dr Arnold H. Mayer, Mr Edward R. Schultz, Mr Robert McCarty, Mr Mal Kelley and Mr R.J. Speelman. For assistance in computer, word processing, editing and report preparation, I am indebted to Mr Bob Pinnell, Lt Kristen Alexander, Lt D. Davis, Mrs E. Schutte and Ms C. Shalan.

I. INTRODUCTION

In striving for acquiring the best available quality of aircraft transparencies in the market, the Subsystems Development Group of the Air Force Flight Dynamic Laboratory at the Wright-Patterson Air Force Base (AFWAL/FIER) has been seeking better laboratory testing methods to effectively identify factors affecting the durability of aircraft transparencies, the relationship between these factors and various transparency failure modes and to be able to make predictions on transparency durability.

Responding to this call, two experimental designs were developed and discussed as part of my summer research project. These are Completely Randomized Design and Factorial Experimental Design. Both analysis of variance and multiple regression were used as relevant procedures to conduct hypothesis testing and to making predictions.

II. OBJECTIVES:

The major objectives of the experimental design discussed in this paper are: (1) To develop and recommend effective laboratory testing methods that would yield the highest result in detecting the factors affecting the various failure modes (i.e., reducing the probability of committing a Type II error); and (2) To develop testing designs that would increase the efficiency of a test within a given amount of resources; and (3) To develop statistical analysis procedures capable of making predictions on the durability of aircraft transparencies.

III. COMPLETELY RANDOMIZED DESIGN AND ANALYSIS OF VARIANCE.

1. COMPLETELY RANDOMIZED DESIGN: Completely randomized design is one of the simplest designs available. It is easy to understand and it can be used at ease even by many new and inexperienced scientists.

The design can best be described with an example. For instance, experiences indicate that the percentage of coating removal caused by rain impingement varies with the length of time exposure to the rain. Based upon this contention, a null hypothesis that the amount of time exposure to the rain has no effect on the coating removal on certain design of canopies can then be formulated. To test such a hypothesis, 15 pieces of specimen or full-scale canopies were randomly selected from a transparency production line. If all the 15 specimens were assigned randomly to three different amount of time exposure in the rain. Then, one is said to have a completely randomized experiment design.

2. ANALYSIS OF VARIANCE: The mechanism used to test a hypothesis such as "the amount of time exposure to the rainfall has no effect on the coating removal" is called "Analysis of Variances". In plain language, the analysis of variance is a process of partitioning the sum of squares of the deviation between each individual observation or value and its mean into two main components: The among-sample sum of squares (ASS) and within-sample sum of squares (WSS). Statistical procedure is then applied to compare the observed variance ratio (F-value) with the theoretical one and a conclusion relative the acceptance and rejection of the hypothesis can then be reached.

As an emperical example, data on rain erosion tests were obtained from an University of Dayton Research Institute (UDRI) testing report (Ref. 1) as shown in Table 1. The one-way analysis of variance was conducted as shown in Table 2. Since the calculated F-value is much greater than the theoretical F-value with 2 and 27 degrees of freedom, the null hypothesis is rejected at 1% significant level. The conclusion is that the percentage of coating removal is significantly affected by the amount of time exposure at a rate of 1 inch/hour of simulated rainfall.

3. REGRESSION ANALYSIS AND DURABILITY PREDICTION: Regression deals with the relation between X, the values of one or more independent variables and the population means of Y, the dependent variable. In the context of experiments,the values of X may be the different levels of

TABLE 1

COATING ADHESION (RAIN EROSION) TEST DATA

Speed: 500 mph

Rainfall: 1 in/hr

Exposure: 3 equiv. yrs. of accelerated weathering plus stress

Specimen Number	Coating Removal, Percent		
	Test Time, Minutes		
	1	2	5
CS-1	5	30	64
CS-2	1	5	33
CS-3	5	25	85
CS-5	3	20	91
CS-6	2	10	69
CS-7	10	30	84
CS-8	2	25	68
CS-9	2	20	76
CS-10	1	10	30
CS-11	1	10	70

Sources: K.I. Claton, et. al, AIRCRAFT TRANSPARENCY TEST METHODOLOGY, AFWAL TR-85-3125, University of Dayton Research Institute, P.74, March 1986

time exposure in the rainfall; and the means of Y may be the average percentages of coating removal. The relation can be expressed in the following mathematical form:

$$\mu y.x = \alpha + \beta X \qquad \ldots \quad (1)$$

where $\mu y.x$ is the population mean corresponding to each value of X; α, the intercept and β, the regression coefficient or the slope the regression line. The advantage of having a regression equation lies in its predicting power, i.e. the population means corresponding to each value of X can be calculated once the values of α and β are estimated. Many computer software packages have the capability of solving regression, linear or non-linear, problems. This includes the estimation of α and β and the predicted means of Y. Using the rain erosion test data discussed in the previous section, the regression equation is estimated as follows:

$$\hat{y}.x = -13.1 + 16X \qquad \ldots \quad (2)$$

The calculated "coefficient of determination", R-square, is 82.7%. This indicates, regardless the validity of laboratory testing procedure, that the simulated rainfall alone explains 82.7% of the variations in the coating removal.

As stated in previous sections, the major advantage of having a regression is to make predictions. For instance, if the amount of time exposure in the simulated rainfall is 4 minutes, the predicted coating removal is 50.9%. In another words, the durability of a particular type of windshield coating can be predicted if the amount of rainfall can be converted into months or years in a particular region where several Air Force bases are located.

TABLE 2

ANALYSIS OF VARIANCE ON RAIN EROSION TEST

SOURCES OF VARIATION	SUM OF SQUARES	DEGREE OF FREEDOM	MEAN SQUARE	F-VALUE
Among Sample	22,189.267	2	11,094.633	64.5300**
Within Sample	4,642.1	27	171.9296	
Total	26,831.367			

$F_{.01}$ = 5.4881 at 1% significant level

**Very Significant

Conclusion: Since the calculated F-value is much greater than the theoretical F-value at 1% significant level, the null-hypothesis is rejected, i.e., the length of rainfall exposure at high speed (500 mph) is a major contributor to the differences of coating removal of F-16A coated monolithic polycarbonate canopy.

4. INTERVAL ESTIMATE: Once the prediction is made, the information obtained from regression analysis can also be used to make interval estimate. For example, the 95% confidence interval of the predicted value can be estimated through the following equation:

$$\hat{y}.x \pm t_{.025} s_{y.x} \qquad \ldots (3)$$

where $\hat{y}.x$ is the predicted mean value of the dependent variable, the percent of coating removal, $t_{.025}$ is the 5% point of t-value and $s_{y.x}$ is the estimated standard error of the regression equation. In this particular case,

$$\hat{y}.x = 50.9 \qquad t_{.025} = 2.048 \quad \text{and} \quad s_{y.x} = 2.98.$$

Hence, the estimated 95% confidence interval of the predicted coating removal at 4 minutes of rainfall is from 44.8% to 57.0%.

5. TEST OF LINEARITY: Regression analysis and analysis of variance are two different versions of the same general topic. The hypothesis underlying the regression analysis is the same as that of the analysis of variance. The advantage of conducting a regression analysis lies in the fact that the regression has a higher testing power if it is proved to be linear. The "test of linearity" can be conducted along with the calculation of analysis of variance with very little extra effort involved. Again, using the rain erosion test data, the test of linearity is conducted as shown in Table 3. The small F-value relative to the "deviation from linearity" indicated the existence of linear relationship between the amount of rain exposure and coating removal. Since the nature of the regression model is established to be linear, the F-value corresponding to the linear regression can then be used to test the hypothesis that $\beta = 0$, which is equivalent to the null hypothesis in the analysis of variance that all populations means are equal. The larger F-value relative to the "linear regression" indicates the power of testing has been increased by the use of linear regression. If, on the other hand, the non-linear relationship were established, the F-value in the analysis of variance may still be used to test the same hypothesis. The non-linear regression analysis will be discussed in the following section.

TABLE 3

TEST OF LINEARITY ON RAIN EROSION

SOURCES OF VARIATION	SUM OF SQUARES	DEGREE OF FREEDOM	MEAN SQUARE	F-VALUE
Among Sample	22,189.267	2	11,094.633	64.530**
Linear Regression	22,186.67	1	22,186.67	129.040**
Deviation from Linearity	2.60	1	2.60	0.015
Error	4,642.100	27	171.930	
Total	26,831.367	29		

$F_{.01}$ = 5.4881 with 2 and 27 degrees of freedom

$F_{.01}$ = 7.6767 with 1 and 27 degrees of freedom

**Very Significant

IV. FACTORIAL DESIGN:

1. ADVANTAGES: One of the most popular experimental designs is called "Factorial Design". As the name implies, this design was developed to study the effects of several factors simultaneously in one testing design using the same testing articles. For example, one may test the effects of temperature as well as moisture (rainfall) on transparency coating removal in one testing design. The result is economy in effort and savings in testing materials. The second advantage of the factorial design is that the effects of two or three factors combined can be studied in one testing design. In statistical terminology, the test of interaction of two or more factors on certain material can be carried out in a factorial experimental design. For example, one may test the combined effects of both the temperature and the rainfall simultaneously. While a series of simple experiments throws no light on the interaction of two or three factors. The third advantage is that the conclusion reached through a factorial experiment is more general. A well designed factorial experiment in which the effects of several factors can be studied simultaneously is probably the only simulation next to the in-service field experience.

2. AN ARTIFICIAL EXAMPLE: The factorial experiment can best be illustrated through the use of an example. Table 4 presents an artificial data set on transparency coating removal. Factor A stands four levels of temperature, and Factor B stands for three levels of moisture (rainfall). The methods of analysis in the factorial experiment are identical to those given in the preceding sections. What is new in the factorial experiment is the breakdown of the Treatment (Among-sample) Sum of Squares into three components: A Effect, B Effect and AB Effect or Interaction. Table 5 shows details of analysis of variance using a "random variable model" assumption. The random variable model assumes that values of various levels of temperature and rainfall were randomly selected. The conclusions were that both A and B effects were significant but AB effect or interaction was not. In other words, both temperature and rainfall were proved to be significant factors contributing to coating removal. And no significant combined effects between temperature and rainfall were detected.

TABLE 4

4 x 3 FACTORIAL EXPERIMENT ON
TEST OF TRANSPARENCY COATING REMOVAL
(ARTIFICIAL DATA, % COATING REMOVAL)

FACTOR A		TEMPERATURE				
FACTOR B		-65°F	10°F	85°F	160°F	TOTAL
Rainfall in minutes (1 inch/hr)		5	4	1	2	
	1	9	4	3	4	32
		10	2	2	2	
	2	12	6	2	4	36
		12	9	3	8	
	3	12	11	7	10	72
	TOTAL	60	36	18	30	144

TABLE 5

ANALYSIS OF VARIANCE OF FACTORIAL EXPERIMENT

SOURCES OF VARIATION	SUM OF SQUARES	DEGREE OF FREEDOM	MEAN SQUARE	F-VALUE
Treatment	292.00	11		
A Effect	156.00	3	52	13.00**
B Effect	112.00	2	56	14.00**
AB Interaction	24.00	6	4	1.33
Error	36.00	12	3	
Total	328.00	23		

$F_{.01}$ = 9.7795 with 3 and 6 degrees of freedom

$F_{.01}$ = 10.925 with 2 and 6 degrees of freedom

$F_{.01}$ = 4.8206 with 6 and 12 degrees of freedom

**Very Significant

3. DETERMINATION OF DEGREE OF MULTIPLE REGRESSION EQUATION: For purpose of making predictions, multiple regression analysis may also be used along with analysis of variance in factorial experiment as it is with completely randomized design. Again, the nature of the multiple regression equation or the degree of each of the independent variables has to be determined before it is applied to the factorial experiment data. One way to determine the degrees of independent variables is through the use of an individual degree of freedom technique and an orthogonal set of multipliers. The sum of squares due to factor A (temperature or x_1), which has 4 levels, is partitioned into linear, quadratic and cubic components by the following multipliers:

	M_1	M_2	M_3	M_4
Linear --	-3	-1	1	3
quadratic --	1	-1	-1	1
Cubic --	-1	3	-3	1

and the individual degree of freedom equation:

$$Q^2x_i = (\Sigma M_i T_i)^2/n(\Sigma M_i^2) \qquad \ldots (4)$$

where Q^2x_i is the sum of squares for a particular component; M_i^2 is the multiplier and T_i, the treatment (sample) total.

For example, the sum of squares of the linear component is calculated as follows:

$$Q^2x_1 = ((-3)60+(-1)36+(1)18+(3)30)^2/6((-3)^2+(-1)^2+(1)^2+(3)^2) = 97.2$$

Likewise, the sum of squares due to factor B (rainfall), which has three levels, is partitioned into linear and quadratic components through the use of an individual degree of freedom (equation 4) and the following multipliers:

	M_1	M_2	M_3
Linear --	-1	0	1
quadratic --	1	-2	1.

TABLE 6

TEST OF LINEARITY AND FACTORIAL EXPERIMENT

SOURCES OF VARIATION	SUM OF SQUARES	DEGREE OF FREEDOM	MEAN SQUARE	F-VALUE
Factor A	156.00	3		
Linear Regression	97.20	1	97.20	24.3**
Deviation from Linearity	58.80	2	29.40	7.35**
Factor B	112.00	2		
Linear Regression	100.00	1	100.00	25.00**
Deviation from Linearity	12.00	1	12.00	3.00
AB Interaction	24.00	6	4.00	1.33
Error	36.00	12	3.00	
Total	328.00	13		

$F_{.01}$ = 10.925 with 2 and 6 degrees of freedom

$F_{.05}$ = 5.1433 with 2 and 6 degrees of freedom

**Very significant at 1% level

* Significant at 5% level

And finally, the sum of squares due to AB effect is partitioned into various components using the products of multipliers for factor A and those for factor B. The detail analysis is shown in Table 7.

As shown by the F-values in Table 7, the analysis indicates that both the linear and quadratic components for factor A are statistically significant and the linear component for factor B is significant. All the rests of the components are not.

4. PREDICTION AND INTERVAL ESTIMATE: Once the degree of the regression equation is determined, the multiple regression equation can then be constructed as follows :

$$\mu_{y.x} = \alpha + \beta_1 X_1 + \beta_2 X_2 + \beta_3 X_1^2 \qquad \ldots (5)$$

Through the use of SAS softwares, parameters in the above equation were estimated as follows:

$$\hat{y}.x = 0.866667 - 0.049333 X_1 + 2.5 X_2 + 0.000267 X_1^2 \quad \ldots (6)$$

The estimated coefficient of determination, R-square, is 76.6% and the estimated population variance (the within-sample mean square) is $\hat{s}^2 = 3$.

This equation can be used for making prediction on the durability of transparency coating involving temperature and rainfall. For example, the average coating loss in an environment equivalent to 85°F and 2 minutes of rainfall can be estimated through the use of the above equation with $X_1 = 85$, $X_2 = 2$ and $X_1^2 = 7225$ as :

$$\hat{y}.x = 3.6 \ .$$

Of course, the predicted value does not have to be found at an experimental point. It can be determined at any point within the given ranges of X_1 and X_2.

TABLE 7

DETERMINATION OF DEGREE OF EQUATION FOR
A 4 x 3 FACTORIAL EXPERIMENT

SOURCE OF VARIATION	SS	DF	MS	F
Treatment	292.0	11		
Factor A (X_1)	156.0	3		
X_1 Linear	97.2	1	97.2	32.40**
X_1^2 Quadratic	54.0	1	54.0	18.00**
X_1^3 Cubic	4.8	1	4.8	1.60
Factor B (X_2)	112.0	2		
X_2 Linear	100.0	1	100.0	33.33*
X_1^2 Quadratic	12.0	1	12.0	4.00
Interaction AB	24.0	6		
X_1X_2	0.0	1	0.0	0.00
$X_1^2X_2$	1.0	1	1.0	0.33
$X_1^3X_2$	5.0	1	5.0	1.67
$X_1X_2^2$	9.6	1	9.6	3.20
$X_1^2X_2^2$	3.0	1	3.0	1.00
$X_1^3X_2^2$	5.4	1	5.4	1.80
Within Treatment	36.0	12	3.0	
TOTAL	328.0	23		

$F_{.05}$ = 4.7472 With 1 and 2 Degrees of Freedom

$F_{.01}$ = 9.3302 with 1 and 12 degrees of Freedom

**Very Significant

Again, the 95% confidence interval at this point may also be estimated through the use of equation 3. In this particular case,

$$\hat{y}.x = 3.6, \qquad t_{.025} = 2.1790 \quad \text{and} \quad s_{y.x} = 0.5244 .$$

Using equation 3, the 95% confidence interval of the estimated coating loss is from 2.46% to 4.74%.

V. SUMMARY AND RECOMMENDATIONS

1. APPLICATIONS: This paper discussed two frequently used experimental designs, the completely randomized experiment and the factorial experiment design. Each of these designs has particular applications. The former is recommended in conducting coupon tests for its simplicity both in concept and in calculation. The latter is strongly recommended in conducting sub-scale or full-scale article tests where testing materials are relatively expensive. In addition to savings from economy in testing materials, the factorial experiment design is often the choice for testing interaction effects of two or more factors combined.

2. SAMPLE SIZE: Sample size or the number of replications at a particular testing point is directly related to the costs of testing materials and to the power of testing as well. As a rule of thumb, the minimum sample size for the completely randomized design is 5 at each testing point and that for the factorial design is 2. One should consider to increase sample size whenever the decision requires high level of precision or a huge amount of costs is at stake.

3. REGRESSION ANALYSIS AND MAKING PREDICTIONS: Whenever possible, regression analysis should be conducted along with the analysis of variance in testing of hypotheses. In general, regression would result higher power of testing if the regression is proved to be linear. The test of linearity requires little effort once the analysis of variance is done.

The major advantage of conducting regression analysis is its prediction power. Once the regression equation is constructed and parameters estimated, the mean values of the dependent variable can be estimated corresponding to a specific value of explanatory factors (independent variables). The potential in using regression analysis for predicting the durability of aircraft transparencies is high.

4. A PLANNED EXPERIMENT: It is highly recommended that all laboratory tests have to be planned in advance. A planned test or experiment requires the knowledge and expertise of an experienced statistician. Many laboratories have statisticians on their staff for helping to plan the tests, to validate the testing methods, to increase in power of testing, and to conduct the statistical analysis. At any rate, the testing engineer should consult a statistician for his advice before the test starts but not after the test is completed. This is much the same as one should consult a architect for his advice in building design before the construction starts but not for his blessing after the construction is completed.

REFERENCES

1. K. I. Clayton, B. S. West and D. R. Bowman: Aircraft Transparency Test Methodology. AFWAL-TR-85-3125, University of Dayton Research Institute, March 1986.

2. K. I. Clayton and B. S. West: Aircraft Transparency Testing Methodology and Evaluation Criteria. AFWAL-TR-3045, Part I and Part II, University of Dayton Research Institute, April 1985.

3. S. A. Morolo: Report for the Conference on Aerospace Transparent Materials and Enclosures. AFWAL-TR-83-4154, Material Laboratory, Air Force System Command, Wright-Patterson AFB, December 1983.

4. Sir Ronald A. Fisher: The Designs of Experiment. Hafner Publishing Company, New York, 1971.

5. Jerome C. R. Li: Statistical Inference. Edward Brothers, Inc., Ann Arbor, Michigan, 1968.

6. Henry Scheffe: The Analysis of Variance. John Wiley and Sons, New York, 1959.

7. W. G. Cochran, and G. M. Cox: Experimental Designs. John Wiley and Sons, New York, 1957.

8. C. R. Ursell, et. al.: Investigation/Analysis of Acrylic Panel Failure on F-5E Aircraft Canopy. Volume I, Southwest Research Institute, June 26, 1978.

1986 USAF-UES SUMMER FACULTY RESEARCH PROGRAM/

GRADUATE STUDENT SUMMER SUPPORT PROGRAM

Sponsored by the

AIR FORCE OFFICE OF SCIENTIFIC RESEARCH

Conducted by the

Universal Energy Systems, Inc.

FINAL REPORT

ION-MOLECULE REACTIONS OF H_2O^+/H_2O, N_2^+/CO_2, and N^+/CO_2

Prepared by:	C. Randal Lishawa
Academic Rank:	Instructor
Department and	Department of Chemistry and Physics
University:	Jefferson State Junior College
Research Location:	Air Force Geophysics Laboratory
	Space Physics Division
	Spacecraft Interactions Branch (PH/K)
USAF Researcher:	Dr. Edmond Murad
	Mr. R. Salter
Date:	August 30, 1986
Contract No:	F49620-85-C-0013

ION-MOLECULE REACTIONS OF H_2O^+/H_2O, N_2^+/CO_2, and N^+/CO_2

by

C. Randal Lishawa

ABSTRACT

We have measured the reactive cross section as a function of translational energy for the reaction $H_2O^+ + H_2O \longrightarrow H_3O^+ + OH$. By using isotopically labelled compounds, we have been able to distinquish between the proton transfer and hydrogen transfer reaction channels, as well as the the symmetric charge exchange cross section. Using the same techniques, we have measured the cross section as a function of translational energy of collisions of N^+ and N_2^+ with CO_2. We have observed the product channels CO_2^+, NO^+, and CO^+ (for N^+ only).

Acknowledgments

I would like to thank the the Air Force Systems Command, Air Force Office of Scientific Research, and the Air Force Geophysics Laboratory for sponsorship of my research. I must thank several persons at the Air Force Geophysics Laboratory, Dr. A. Jursa and Dr. Agnes Bain for their help in acclimating to the base, Mr. Dick Salter for his many hours spent with me at the experimental equipment and Dr. Edmond Murad who has been an invaluable resource for this project.

Most of all I must thank my wife, Chris, and my son, Adam, for their willingness to support me in this project in a new and temporary location.

I. Introduction

I received a Ph.D. from the University of Florida studying molecular electronic energy transfer processes using molecular beam techniques.

The research at the Air Force Geophysics Laboratory (AFGL) involved investigations of ion-molecule reactions relating to the physical processes observed during spacecraft reentry. The method of molecular beams is also used in these studies.

II. Objectives of the Research Effort

The overall objective of the Spacecraft Interactions Branch is the analysis of the impact of spacecraft on their operating environment. Perhaps the most publicized example of this is the so-called "Shuttle Glow". The objective of this summer research was to obtain cross section data required to explain some of these reactions.

III. Experimental

The experimental apparatus is shown schematically in Figure 1 and has been described in a previous paper.[1] In general, it is a tandem mass spectrometer employing an electron bombardment source (from 30 - 3000 primary ions

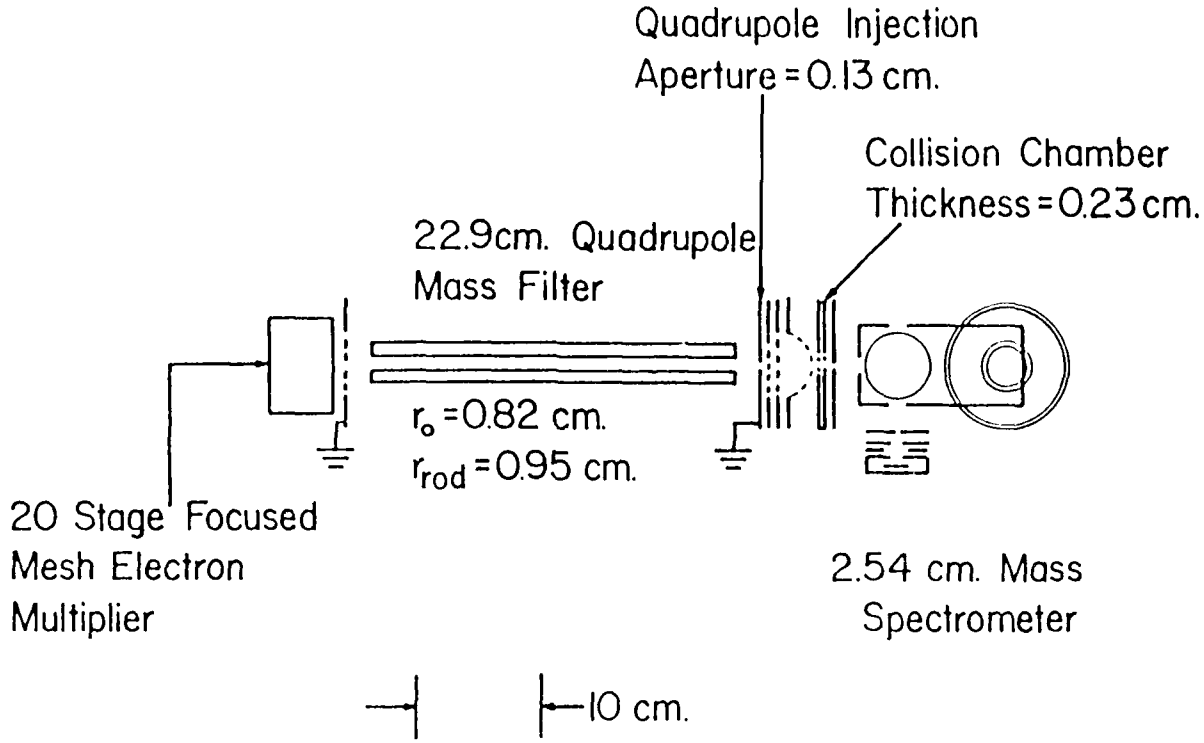

Figure 1. Experimental Apparatus.

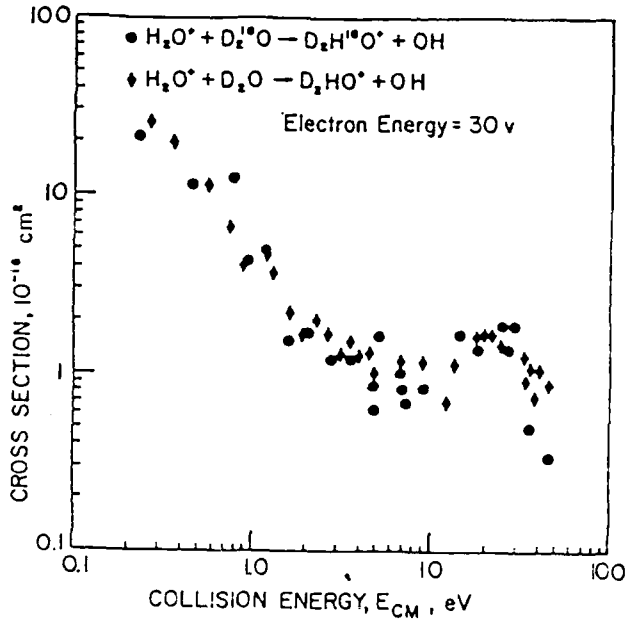

Figure 2. Cross Section for Proton Tranfer.

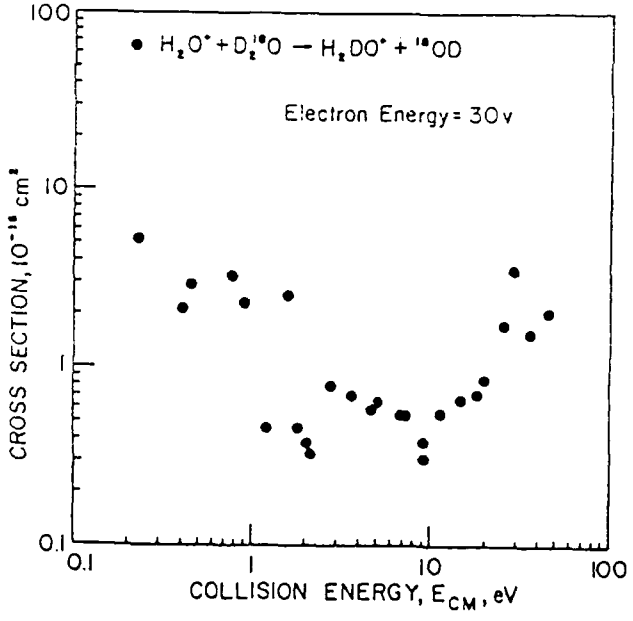

Figure 3. Cross Section for Deuteron Transfer.

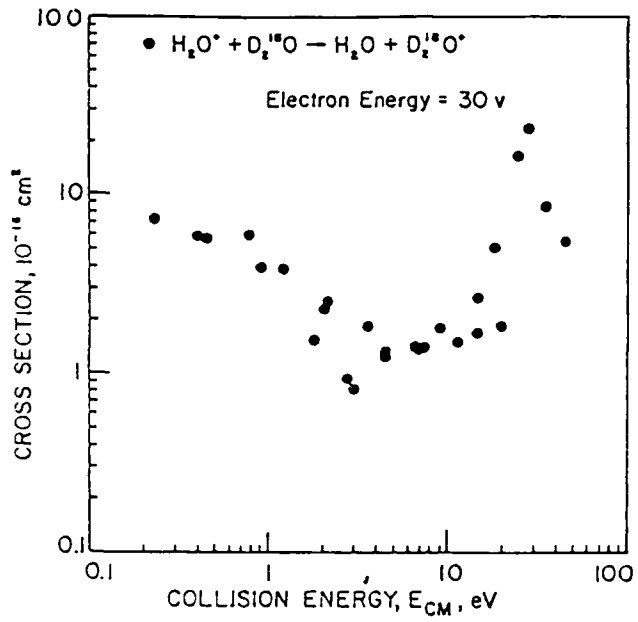

Figure 4. Cross Section for Charge Exchange ($H_2O^+ + D_2{}^{18}O$).

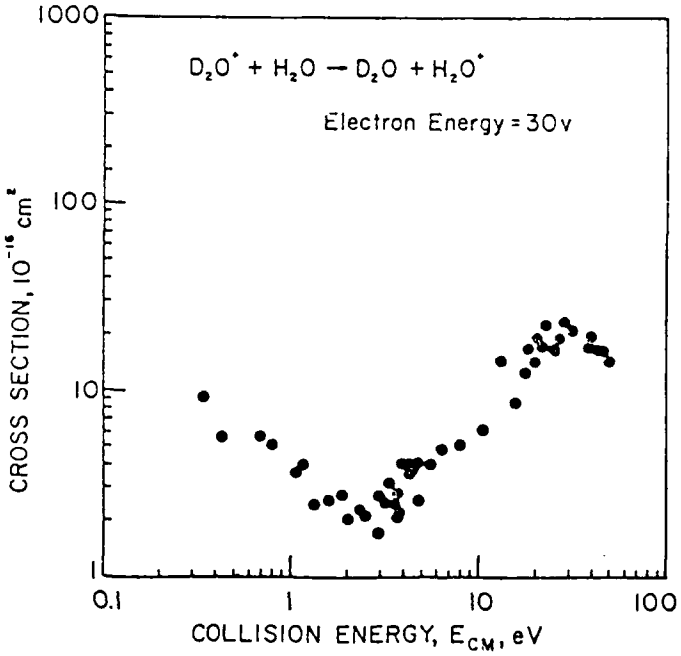

Figure 5. Cross Section for Charge Exchange ($D_2O^+ + H_2O$).

per second) and a thin collision chamber (pressure about 5×10^{-5} torr). The apparatus was calibrated using the $N_2^+ + D_2 \rightarrow N_2D^+ + D$ system.[2]

IV. Discussion

We have looked at the following reactions

$$H_2O^+ + H_2O \longrightarrow \text{products} \quad (1)$$

$$^{15}N_2^+ + CO_2 \longrightarrow \text{products} \quad (2)$$

$$^{15}N^+ + CO_2 \longrightarrow \text{products} \quad (3)$$

as a funciton of translational energy (approximately 0.5 to 50 eV in the center of mass system). Reaction (1) is of interest because of the recent observation of H_3O^+ on the space shuttle[3]. Most of the previous work on these systems has been carried out at thermal energies.[4-6] A few beam experiments have also been reported.[7-11]

The cross sections measured for Reaction (1) are shown in Figures 2 - 5. The trends of our results are consistent with the results obtained in previous experiments. However, those experiments measured the total production of H_3O^+ regardless of the process. The data reported here are for proton exchange (Figure 2), hydrogen exchange (Figure 3), and the symmetric charge exchange (Figures 4 and 5). Even if our results on the

proton exchange and hydrogen exchange are summed, our results are significantly lower than previously reported (about a factor of 4 less). Although the reason for this discrepency is unclear, one possible source could be the presence of excited states in the H_2O^+ beam. Previous studies of discharge sources producing H_2O^+ have indicated a large fraction of the beam to be composed of excited states.[12] However, based on the reported lifetimes of the excited states of H_2O^+ (0.8, 3.0, and 10 microseconds)[13-15] and the known path length of our experimental apparatus, we believe our beam will probably be mostly ground state (1×10^{-5}%, 2%, or 30% of the original excited state population for 0.8, 3, or 10 microsecond lifetimes respectively) at the entrance to the collision chamber. We find no variation in cross section with the electron energy of the discharge (see Figure 6) which would be expected if the population ratio of the excited states within the beam were to vary. We recognize that this experiment does not adequately address the possibility of excited states in the ion beam. This would require a series of attentuation measurements which are not readily accomplished in the current experimental apparatus.

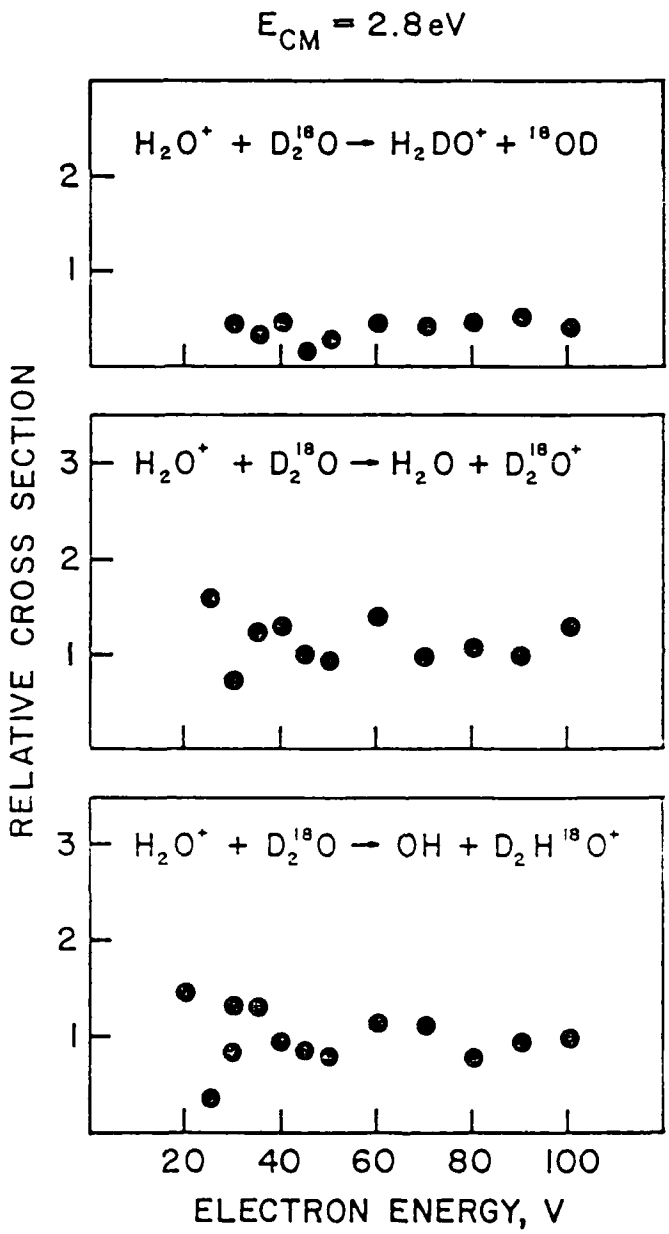

Figure 6. Variation of Cross Section with Electron Energy.

Reactions (2) and (3) are of interest because of the mass spectrometric observation of N_2^+, N^+, and CO_2^+ on the space shuttle. The charge exchange reactions of N^+ and N_2^+ in reactions with CO_2 have been measured at thermal energies.[16,17] The cross sections for these reactions are shown in Figures 7 - 11.

A previous study using the apparatus described in this report found that excited states did not play a role in the nitrogen beams[1].

VII. Recommendations

An effort should be made to determine the theoretical mechanisms that would lead to the experimental cross sections reported in this paper. One approach will involve ab initio calculations of the potential energy surfaces relevant to the system followed by trajectory calculations of the cross sections. However, most of the efforts to calculate the reaction cross sections from first principles has centered around atom/diatom systems.[18]

Other efforts to perform these calculations will be made using model potentials and various theoretical constructs to characterize the systems. The most promising of the model systems is one developed several

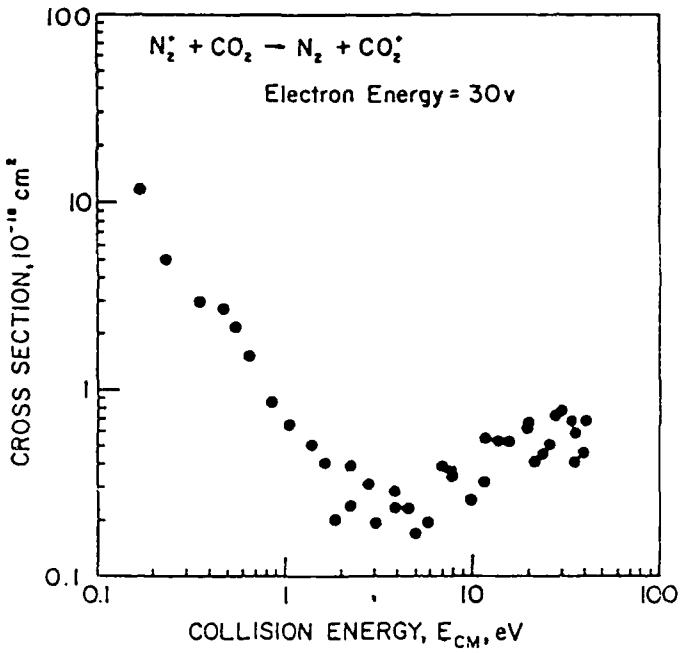

Figure 7. Cross Section for Charge Exchange ($N_2^+ + CO_2$).

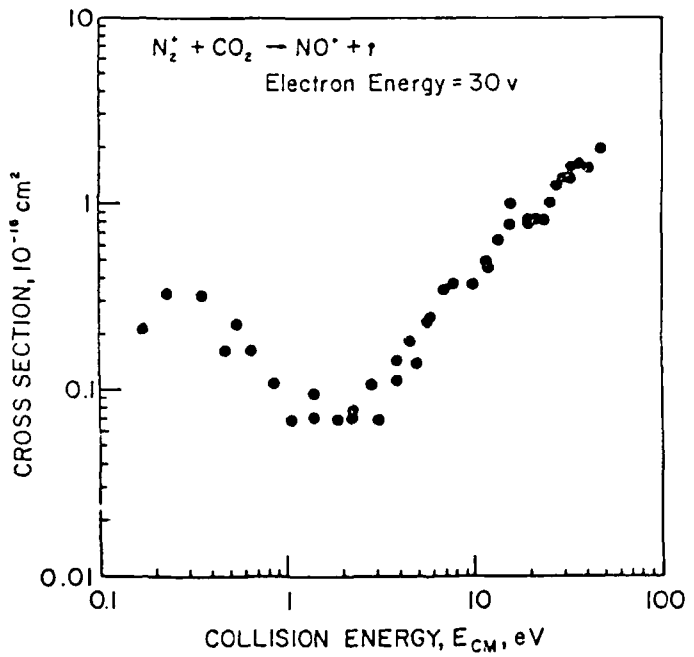

Figure 8. Reactive Cross Section ($N_2^+ + CO_2 \rightarrow NO^+ + ?$).

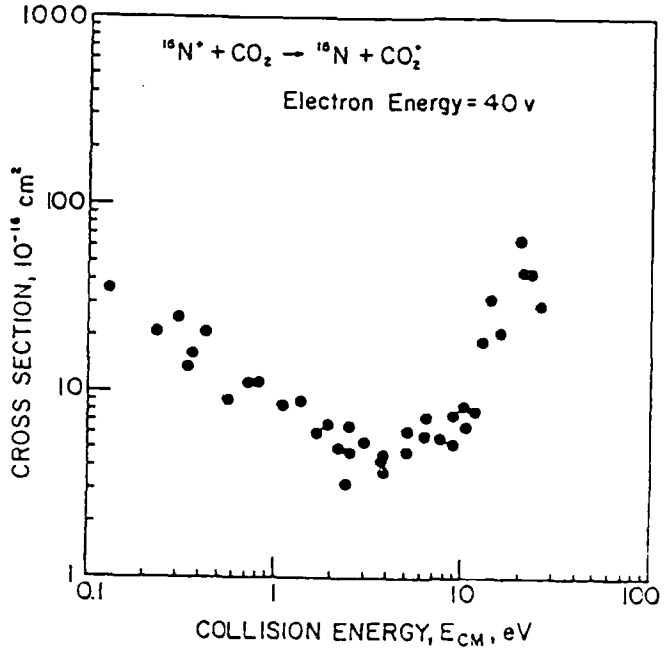

Figure 9. Cross Section for Charge Exchange ($^{15}N^+ + CO_2$).

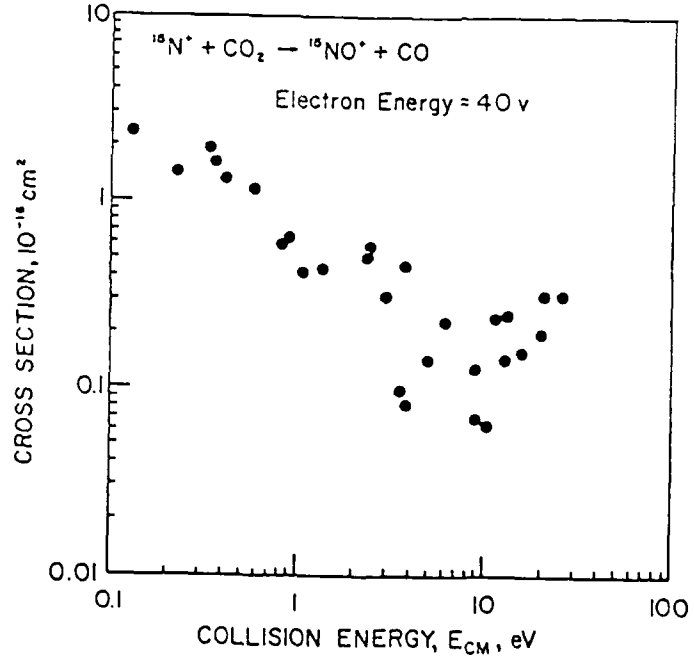

Figure 10. Reactive Cross Section ($^{15}N^+ + CO_2 \rightarrow {}^{15}NO^+ + CO$).

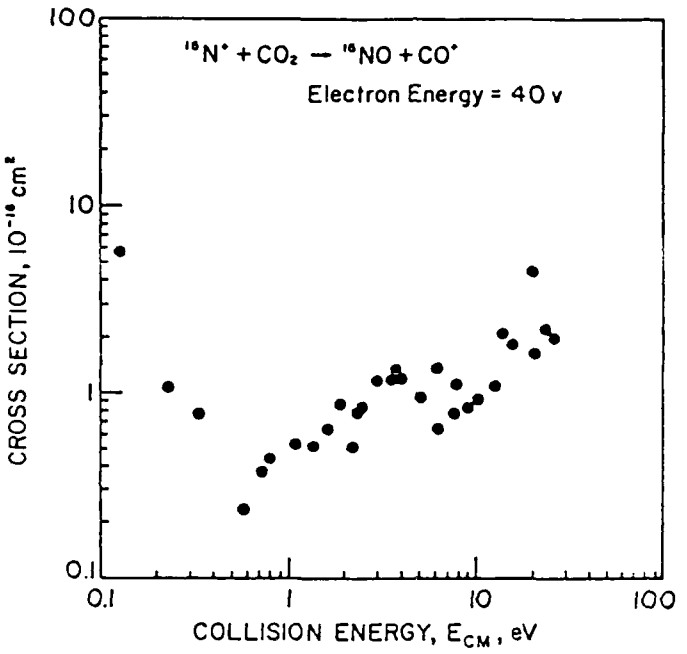

Figure 11. Reactive Cross Section ($^{15}N^+ + CO_2 \rightarrow {}^{15}NO + CO^+$).

years ago.[19] This model involves treating the ionic species as a point charge and the neutral molecule as a point dipole (either fixed or induced). The motion of the ion is treated classically and a trajectory calculated for its motion. If the ion reaches a critical position relative to the dipole, capture is assumed. A capture cross section may be calculated from multiple trials. This cross section provides an upper bound to the observed cross section, assuming a unit probablity of reaction once the critical position has been reached. This technique has been extended with a transition state formulation[20] that looks at the capture cross section statistically.

References

1. Maier II, W.B., and E. Murad, "Study of Collisions between Low-Energy N^+ and N_2: Reaction Cross Sections, Isotopic Compositions, and Kinetic Energies of the Products", J. Chem Phys., 55(5), 1 September 1971, pp. 2307-2316.
2. Turner, B.R., M.A. Fineman, and R.F. Stebbings, "Crossed-Beam Investigation of N_2D^+ Production in N_2^+-D_2 Collisions", J. Chem. Phys., 42(12), 15 June, 1965, pp. 4088-4096.
3. Narcissi, R., E. Trzcinski, G. Federica, L. Wlodyka, and D. Delorey, in AIAA Shuttle Environment and Operations II Conference, 1983, p. 183.
4. Fluegge, R.A., "Ion-Molecule Reactions in Alpha-Particle-Irradiated Methane and Water Vapor.", J. Chem. Phys., 50(10), 15 May 1969, pp. 4373-4380.
5. Boulden, R.C., and N.D. Twiddy, "A Flowing Afterglow Study of Water Vapour.", Faraday Discussions, 53, 1972, pp. 192-200.
6. Huntress, Jr., W.T., and R.F. Pinizzotto, Jr., "Product distribution and rate constants for ion-molecule reactions in water, hydrogen sulfide, ammonia, and methane.", J. Chem. Phys., 59(9), 1 November 1973, pp. 4742-4756.

7. Turner, B.R., and J.A. Rutherford, "Charge Transfer and Ion-Atom Interchange Reactions of Water Vapor Ions.", J. Geophys. Res., Space Phys., 73(21), 1 November 1968, pp. 6751-6758.

8. Ryan, K.R., and J. H. Futrell, "Effect of Translational Energy on Ion-Molecule Reaction Rates. I", J. Chem. Phys., 42(3), 1 February 1965, pp. 824-829.

9. Ryan, K.R., and J. H. Futrell, "Effect of Translational Energy on Ion-Molecule Reaction Rates. II", J. Chem. Phys., 43(9), 1 November, 1965, pp. 3009-3014.

10. Ryan, K.R, "Ionic Collision Processes in Water Vapor", J. Chem. Phys., 52(12), 15 June 1970, pp. 6009-6016.

11. Sunner, J., and I. Szabo, "Ion-Molecule Reactions In H_2O after Charge Transfer Ionization.", Int. J. of Mass Spectrom. and Ion Phys., 31, 1979, pp. 213-226.

12. Lindemann, E., R.W. Rozett, and W.S. Koski, "Electonic States of H_2O^+ Produced by Electron Bombardment of H_2O.", J. Chem. Phys., 56(11), 1 June 1972, pp. 5490-5492.

13. Erman, P., and J. Brzozowski, "Direct Measurements of Lifetimes of Excited Levels in H_2O^+.", Phys. Lett., 46A(2), 3 December 1973, pp.79-80.

14. Brzozowski, J., P. Erman, and H. Lew, "Lifetimes of Excited States in D_2O^+ and OD^+ and Relative Lifetimes between the Normal and Deuterated Species.", Chem. Phys. Lett., 34(2), 15 July 1975, pp. 267-270.

15. Mohlmann, G.R., K.K. Bhutani, F.J. De Heer, and S. Tsurubuchi, "Lifetimes of the Vibronica $\tilde{A}^2A_1$ States of H_2O^+ and of the $^3\Pi_i(\gamma'=0)$ State of OH^+.", Chem. Phys., 31, 1978, pp 273-380.

16. Fehsenfeld, F.C., Schmeltekopf, and E.E. Ferguson, "Thermal Energy Ion-Neutral Reaction Rates. IV. Nitrogen Ion Charge-Transfer Reactions with CO and CO_2.", J. Chem. Phys., 44(12), 15 June 1966, pp. 4537-4538.

17. Savage, H.F., and F.C. Witteborn, "Charge-Exchange Cross Sections of N_2^{2+} in N_2, CO_2, and Ar and Contamination of N^+ Beams of N_2^{2+}.", J. Chem. Phys., 48(4), 1968, pp. 1872-1873.

18. Light, J.C.,"Reactive Scattering Cross Sections I: General Quantal Theory", Atom-Molecule Collision Theory, A Guide for Experimentalists, R.B. Bernstein (ed.), New York, Plenum Press, 1979.

USAF-UES SUMMER FACULTY RESEARCH PROGRAM

Sponsored by the

Air Force Office of Scientific Research

Conducted by

Universal Energy Systems, Inc.

Final Report

Study of Rutting of Asphalt Pavement Under High Tire Pressure and Temperature

Prepared by: Cheng Liu

Academic Rank: Associate Professor

Department: Department of Engineering Technology

University: The University of North Carolina at Charlotte

Research Location: Enginering and Services Center
Tyndall AFB, Florida

USAF Research: Jim Murfee

Date: August 8, 1986

Contract No.: F49620-85-C-0013

Study of Rutting of Asphalt Pavement under High Tire Pressure and Temperature

by

Cheng Liu

ABSTRACT

Since a new generation of heavier Model F-15 C/D aircraft has come into use, rutting of asphalt pavement under high tire pressure and temperature has become a matter of concern. A variety of factors contribute to rutting of asphalt pavements. Parameters affecting rutting of asphalt pavement were identified and their contribution to rutting were explored in this study. The Shell method of predicting the amount of rutting that would occur in an asphalt pavement was briefly discussed. A field traffic test plan designed to compare the rutting effects of the main gear of the F-4 (265 psi, 27,000 lbs) and the F-15 C/D (355 psi, 30,500 lbs) on 4-inch asphalt concrete overlaying 12-inch jointed portland cement concrete is currently underway at Tyndall AFB. Rut depth and other pertinent design properties are to be measured every 300 to 600 passes of the F-4 and F-15 C/D loadcarts.

Acknowledgments

I would like to thank the Air Force System Command and the Air Force Office of Scientific Research for sponsorship of this research. I would also like to thank members of the Air Force Engineering and Services Center at Tyndall Air Force Base, Major Robert Costigan and Mr. Jim Murfee, for giving me the opportunity and the guidance necessary for the research.

I. Introduction

My fields of specialty are paving materials and geotechnical engineering. I had been in charge of the pavement laboratory and conducted flexible pavement research in the West Virginia State Road Commission for six years.

The research problem at the Air Force Engineering and Services Center involved rutting of asphalt pavement under high tire pressure and temperature.

The problem under investigation at the Engineering and Services Center has some similarity to the problems I had studied at the West Virginia State Roads Commission. Because of this similarity I was assigned to work on the rutting study at the Engineering and Services Center.

II. Objectives of the Research Effort

The overall objective of this research was to investigate the parameters affecting rutting of high quality asphalt pavements under high tire pressure and temperature. Once the parameters affecting rutting of asphalt pavement are identified and their effects on pavements are explored, appropriate measures can be taken to reduce or prevent rutting problems.

This study did not deal with the influence or contributions to rutting of the subgrade soils and base materials.

III. Mechanism of Rutting in Asphalt Concrete

With increasing wheel load passes on a single wheel path, rutting in asphalt concrete develops gradually. It generally appears as a longitudinal depression in the wheel path.

Rutting in asphalt pavement is caused by:

(1) Differential traffic densification

(2) Plastic deformation or lateral displacement of asphalt material from beneath the wheel paths due to insufficient mix stability, and

(3) Wear or erosion of surface material under traffic.

The test track studies reported by Hofstra and Klomp[1] and trenching studies conducted at the AASHO Road Test[2] both indicate that plastic deformation (lateral displacement) of the asphalt concrete is the primary rutting mechanism rather than differential traffic densification and wear or erosion of surface material under traffic.[3]

In general, the rutting problem anticipated due to the fully-loaded F-15 C/D is not associated with subgrade deformation or failure. Instead, it is thought to be primarily due to the instability of the asphalt paving mix.

IV. Parameters Affecting Rutting of Asphalt Pavements

The following parameters are known to affect rutting of asphalt pavements:

- Temperature
- Traffic density
- Magnitude of wheel load and tire pressure
- Aggregate gradation
- Aggregate particle sizes
- Aggregate angularity and texture
- Asphalt cement hardness
- Asphalt cement content
- Asphalt additives
- Density of asphalt paving mix
- Thickness of asphalt pavement

Effects of each parameter on rutting of asphalt pavement are discussed as follows:

Influence of Temperature

Consistency of asphaltic materials, particularly paving grade asphalt, is susceptible to temperature. In temperate and tropical regions, pavement temperature often reaches the range of 110 to 140 Degrees F in the summer. When rutting occurs, pavement temperatures are generally in this range.

Figure 1 illustrates the relationship between rutting and pavement temperature established by Hofstra and Klomp[1] and Lister and Addis[4] from model asphalt pavement studies.

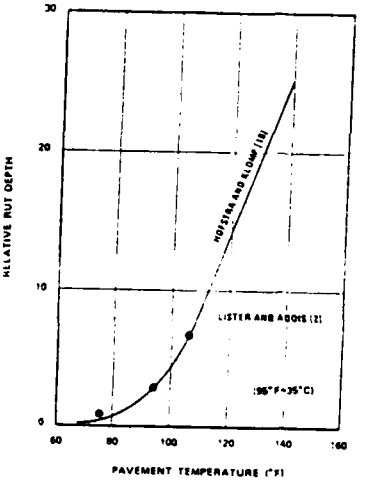

Fig. 1 Rut depth vs. pavement temperature[1,4,5]

The figure shows that rutting of asphalt pavement is quite sensitive to temperature.[5]

Influence of Traffic Density, Magnitude of Wheel Load and Tire Pressure

The effects of traffic density (i.e. no. of passes of wheel load on a single wheel path), magnitude of wheel load and tire pressure (i.e. type of aircraft) on rutting of asphalt pavement at different thicknesses are depicted in Figure 2.

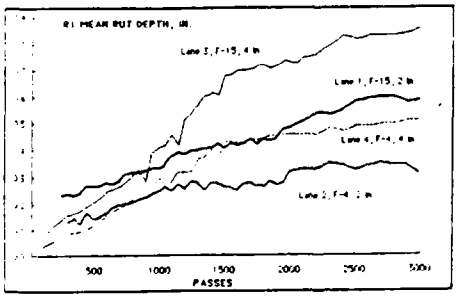

Figure 2 [6]

The F-4 Phantom fighter has a maximum main gear load of 27,000 pounds per tire at 265 psi tire pressure. The F-15 C/D carries a maximum main gear load of 30,500 pounds per tire at 355 psi tire pressure. As is illustrated in Figure 2, the heavier the wheel load and tire pressure, the deeper the rut, and up to a point the higher the number of passes, the deeper the rut.

Influence of Aggregate Gradation

The grain-size distribution or gradation of an aggregate is a primary consideration for a stable mix. The grain-size distribution can be represented by the following equation:[7]

$$p = 100\ (d/D)^n \qquad (1)$$

Where:

d = the sieve in question

p = the percent by weight finer than the sieve

D = the maximum size of aggregate

n = exponent *

*The maximum density of aggregate generally occurs when n equals 0.5.

The 0.45 power gradation (i.e. n = 0.45) is extremely useful in reducing tender mixes. The use of 0.45 power gradation is recommended by Western Association of State Highways and Transportation Officials to lessen rutting problems.[8]

Influence of Aggregate Particle Sizes

Aggregate particle sizes would affect the rutting depth of an asphalt pavement. An asphalt paving mix with a top size of one inch aggregate would most likely produce a lower rut depth as compared with a mix containing a top size of 3/4 inch aggregate.

Influence of Aggregate Angularity and Texture

Angularity and texture of aggregate in an asphalt paving mix affect rutting of an asphalt pavement. Angularity and texture of aggregate can be evaluated quantitatively by "particle index". The higher the particle index the more angular the aggregate. A particle index of six would be considered low, indicating a fairly well-rounded material, while a particle index of 15 would be high, indicating a very angular material.[9,10]

Particle index (I_a) can be determined by ASTM D-3398. The procedure determines densities of material which has been rodded 10 times and 50 times each layer for a total of three layers respectively in a six inch diameter steel mold with seven inch height by a 3/8 inch diameter steel rod weighing 2.05 pounds. The percent of voids at 10 drops and 50 drops respectively can then be calculated by the following equations:[11]

$$V_{10} = [1 - W_{10}/S\ v] \times 100 \qquad (2)$$

$$V_{50} = [1 - W_{50}/S\ v] \times 100 \qquad (3)$$

Where: V_{10} = Voids in aggregate compacted at 10 drops per layer for a total of 3 layers (%).

V_{50} = Voids in aggregate compacted at 50 drops per layer for a total of 3 layers (%).

W_{10} = Weight of the aggregate in the mold compacted at 10 drops per layer for a total of 3 layers (g).

W_{50} = Weight of the aggregate in the mold compacted at 50 drops per layer for a total of 3 layers (g).

S = Bulk-dry specific gravity of the aggregate.

v = Volume of the cylindrical mold (ml).

Particle index (I_a) can now be computed by the following equation:[11]

$$I_a = 1.25V_{10} - 0.25V_{50} - 32 \qquad (4)$$

The North Dakota Highway Department studied three aggregates from three different quarries. With all conditions (such as gradation, a/c content, etc) being equal except the aggregate sources, the Lawrence pit was predicted by the Shell Pavement Design Manual to have the highest rutting and the Lefor, the lowest, with the Degel pit falling in between. When the particle index (I_a) of the minus No. 10 material for each three pits was determined and plotted against the rut depth prediction for each of the three aggregates (see Fig 3), correlation between the predicted rut

depth and particle index of the aggregates became apparent. With an increase in the particle index, there is a decrease in the predicted rut depth (see Fig 3). The particle index (I_a) seems to provide a quantitative over all measure of particle shape, angularity and surface texture characteristics of an aggregate.[9]

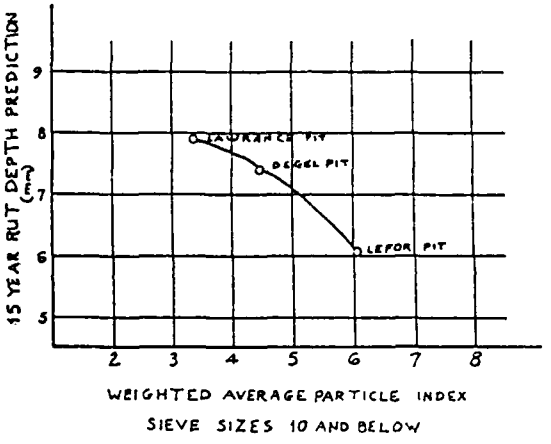

Figure 3 [9]

Influence of Asphalt Cement Hardness

Consistency (or hardness) of asphalt cement was found to be related to rut depth of an asphalt pavement. Barksdale[3] reported that the mix prepared using AC-40 asphalt cement at asphalt content in the vicinity of 5% should experience approximately 20% less rutting than a similar mix prepared utilizing AC-20.

The use of the harder asphalt cement as a binder would, while improving rutting problems, produce an asphalt paving mix that is more susceptible to cracking.

Therefore, only as a last resort would a harder grade of asphalt cement be used to improve rutting problems.[9]

Influence of Asphalt Cement Content

Increase of asphalt cement content would generally result in an increase of rut depth. However, an increase in asphalt cement content has the potential to reduce asphalt paving cracking. Hills et al. [12] reported that the most severe rutting was found in a mix which had round sand and a high asphalt cement content. The least rutting was shown by a mix which contained crushed sand (i.e. aggregate passing No.10 sieve and retaining No.200 sieve) and had an optimum asphalt cement content according to the Marshall method.

Influence of Asphalt Additives

Two problems affecting the performance of asphalt concrete pavements are rutting in conjunction with high temperature and cracking associated with low temperature. Many studies have been done utilizing different types of asphalt additives to alleviate these problems. One of the modifiers, an oil-based soluble manganese manufactured by Chemkrete Technologies Inc., appears to be capable of improving the high temperature stiffness[13], therefore, reducing the rutting problem. However, the degree of modification of asphalt cements by soluble manganese has to be carefully selected to prevent low temperature cracking.[14]

Influence of Density of Asphalt Paving Mix

Density of asphalt paving mix has a direct effect on rutting of asphalt pavement. With all conditions being equal, the higher the density of the asphalt pavement, the less the rut depth can be expected.

Influence of Thickness of Asphalt Pavement

Based on a rutting study made on the cores obtained from highways in North Dakota, Brauer[9] reported that there is a direct correlation between the rut depth prediction and the depth of the asphalt paving mix. A plot of the thickness of asphalt pavement on actual projects vs. the 15-year rut depth predictions is illustrated in Fig. 4. It is evident that the thicker the pavement, the higher the rut depth predicted. The report of Tyndall AFB Rutting Study (see Figure 1) is an example of this behavior.

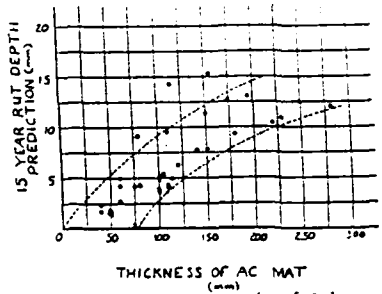

Figure 4 [9]

V. Method to Predict Rut Depth of Asphalt Pavement

There are several methods presently available to predict rut depth of an asphalt pavement. One of the better known methods, the Shell method, is briefly discussed here. The Shell method was developed by the

Shell International Petroleum Co., Amsterdam, in 1977. It estimates the rut depth by the following equation:[15]

$$\text{Rut depth} = C_m \, H \, Z \, \sigma_o / S_{mix} \qquad (5)$$

Note:

Where: C_m = Correction factors for dynamic effects (see Table 1)

H = Thickness of asphalt pavement

Z = Proportionality factor (see Fig 5)

σ_o = Contact pressure

S_{mix} = Value of Stiffness modulus of asphalt paving mix at $S_{bit} = S_{bit,visc}$

$S_{bit,visc}$ is the viscous or nonelastic component of the bitumen stiffness and can be obtained by the following equation:[15]

$$S_{bit,visc} = \frac{3}{N t_o} \frac{}{\eta_{visc}} \qquad (6)$$

Where: N = total number of wheel passes

t_o = loading time of one wheel pass

VISC = bitumen viscosity. (see Fig 6)

The results of the Shell creep test can be used to establish the relationship between S_{mix} and S_{bit}. (The log-log plot of S_{mix} vs. S_{bit} is known as creep curve.)

The stiffness modulus of mix (S_{mix}) is defined as follows:

$$S_{mix} = \frac{\sigma_{mix}}{\epsilon_{mix}} \qquad (7)$$

Where: σ_{mix} = stress applied during the creep test (N/m^2)

ε_{mix} = axial strain measured = $\Delta h/h_o$

Δh = change in height of the test specimen

h_o = original height of the test specimen

The stiffness modulus of the bitumen (S_{bit}) can be secured from Van der Poel's nomograph (see Fig 7) under the same conditions of temperature and loading time for the asphalt paving mix.

Mix type		C_m
Open ↑	Sand sheet and lean sand mixes Lean open asphaltic concrete	1.6-2.0
	Lean bitumen macadam	1.5-1.8
	Asphaltic concrete Gravel sand asphalt Dense bitumen macadam	1.2-1.6
↓ Dense	Mastic types Gußasphalt Hot rolled asphalt	1.0-1.3

Table 1. Correction Factors for Dynamic Effects [15]

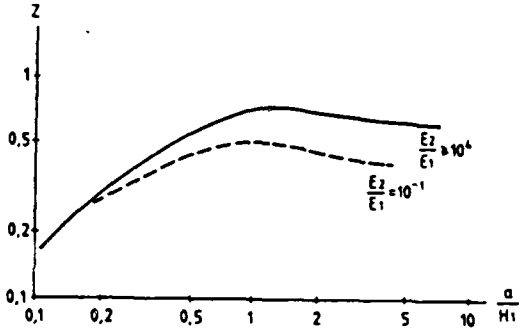

a = loaded area

H_1 = Asphalt concrete layer thickness

E_1 = Modulus of elasticity of asphalt concrete layer

E_2 = Modulus of elasticity of second layer

Figure 5 Proportionality factor Z for an elastic two-layer system with $\mu_1 = \mu_2 = 0.35$ (μ = Poisson ratio)[16]

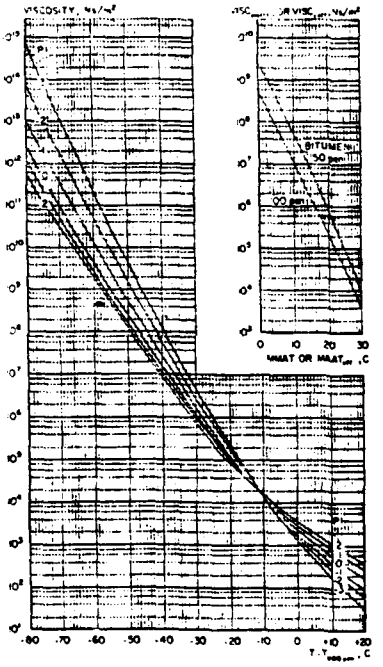

Fig. 6 Viscosity as a Function of the Temperature Difference $T-T_{800\ pen}$ [15]

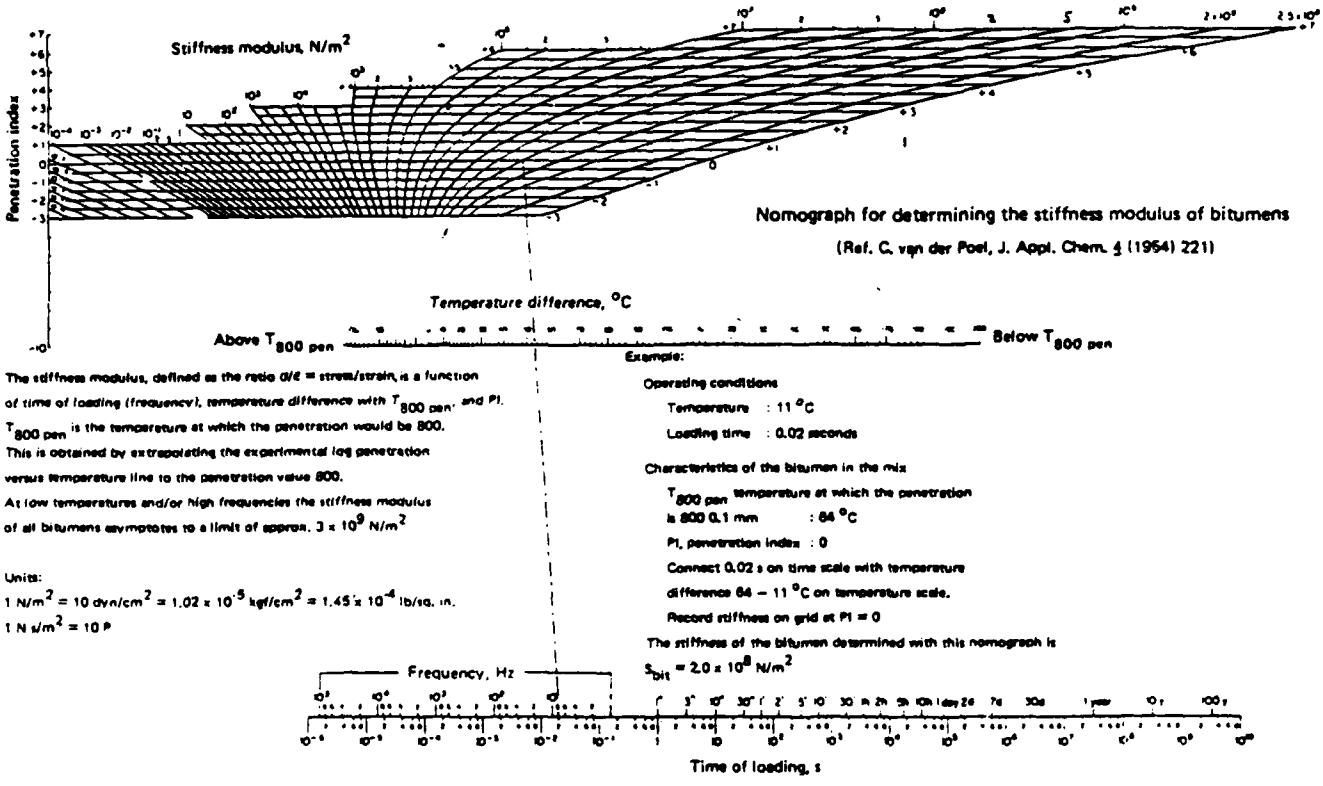

Figure 7 Van der Poel nomograph for bitumen stiffness [17]

The standard test parameters normally adopted for the Shell creep test are as follows:[16]

Temperature(T) = 40° C (or 104° F)

Stress(σ) = 0.1 MN/m^2 (i.e. 14.5 psi)

Loading time(t) = 60 minutes

Dimension of cylindrical specimen:

Diameter: 100mm or 150mm

Height: 60mm or 100mm

Max particle size of aggregate:

-for 100mm (or 4 in) diameter specimen: 16mm

-for 150mm (or 6 in) diameter specimen: 16-40mm

Duration of test: 60 minutes

VI. Test Plan to Study Rutting of Asphalt Pavements

Field traffic tests designed to compare the rutting effects of the main gear of the F-4 (265 psi, 27,000 pounds) and F-15 C/D (355 psi, 30,500 pounds) on 4-inch asphalt concrete overlaying 12-inch jointed portland cement concrete are currently underway at Tyndall AFB.

Five test sections of asphalt concrete pavement with the dimension of each section being 12' x 300' were built. The mixes of the first three sections are designed in accordance with MIL-STD-620A using aggregate blends conforming to AFM 88-6, Chapter 2, Table 7-4 for high pressure tire wearing course, 3/4 inch maximum aggregate size and AC 20 asphalt cement. The mixes of the last two lanes are the same mix except using manganese-modified asphalt cement, commonly known as Chemkrete. According to the Chemkrete Technologies, Inc., the manufacturer of manganese modification of asphalt cements with soluble manganese can change the rheology of the asphalt cements so that the stability of the resulting asphalt concrete mixtures at high temperature is significantly increased.[14]

Asphalt concrete cores are taken after every 300 to 600 passes of F-4/F-15 loadcarts. Material characteristics measured from the core samples include density, percent air voids, percent V.M.A., % of void filled with asphalt cement. Resilient modulus and Shell

creep tests are also to be conducted on the cores. Pavement and air temperatures as well as rut depth are recorded for every 300 to 600 passes of loadcarts.

VII. Recommendations

1. The parameters affecting rutting problems are varied and complex. It is believed that chances of reducing or preventing rutting of asphalt pavement can be achieved if most or all of the following recommendations are adopted:

a. A dense graded aggregate should be used for asphalt paving mix. The 0.45 power gradation is recommended to help reduce rut depth.

b. A larger particle size of aggregate should be employed. Using a top size of 1-inch instead of the current 3/4-inch would lessen rutting problems.

c. Only aggregate with high angularity and texture should be utilized for asphalt paving mix. Aggregate angularity and texture might be quantitatively evaluated by particle index(I_a), which can be determined by ASTM Designation D-3398.

d. Using a harder grade of asphalt cement would improve rutting problems. However, employing harder asphalt cement would likely produce a mix that is more susceptible to cracking.

e. In the field, the paving contractor should be required to achieve a specified percent of the 75-blow Marshall density or the voidless density as determined

in the laboratory by the Rice method.

5. In the field, the paving contractor should achieve the required density before the mix temperature drops below 225° F.

2. It is strongly recommended that the results of the field measurements of rut depth from the test plan conducted at Tyndall AFB this summer be correlated with the predicted rut depth estimated by the Shell method. Therefore, I am submitting, under separate cover, a mini grant proposal to follow the work of this rutting study. If correlation is found to be promising (i.e. the field measurements of rut depth have good correlation with the predicted ones), the Air Force should initiate a full scale study to develop a model for predicting rut depth, a procedure for using the model and set a limit on the maximum acceptable rut depth as predicted by the model. If the predicted rut depth exceeds the maximum acceptable value, the mix composition should be changed and the procedure repeated. If the predicted rut depth is within the acceptable limit, the other pertinent properties, such as fatigue life, durability etc. should then be investigated.

References

1. Hofstra, A. and A. Klomp, "Permanent Deformation of Flexible Pavements Under Simulated Road Traffic Conditions," Proceeding, Third International Conference on Structural Design of Asphalt Pavements, Vol. 1, London, 1972, 13-62.
2. The AASHO Road Test, Highway Research Board Special Report 73, Publication No. 1012, Washington, D.C. (1962).
3. Barksdale, Richard and John Miller III, "Development of Equations and Techniques for Evaluating Fatigue and Rutting Characteristics of Asphalt Concrete Mixes," Georgia Institute of Technology, Atlanta, Georgia, Prepared for Federal Highway Administration, Washington, D.C., June (1977).
4. Lister, N.W. and R.R. Addis, "Field Observation of Rutting in Practical Implication," Paper prepared for symposium on Rutting in Asphalt Concrete Pavements, Annual Meeting of the Transportation Research Board, Washington, D.C., January (1976).
5. Barksdale, Richard D., "Practical Application of Fatigue and Rutting Tests on Bituminous Base Mixes," Proceeding Association of Asphalt Paving Technologists, (1978).
6. Mckeen, R.G., et al, "Letter Report--Tyndall AFB Rutting Study," Air Force Engineering and Services Center, Tyndall AFB, Florida, May (1986).

7. Yoder, E.J. and M.W. Witczak, Principles of Pavement Design, Second Edition, John-Wiley & Sons, New York (1975).

8. Warburton, R.G., et al, "Asphalt Pavement Rutting--Western States," Western Association of State Highways and Transportation Officials, May (1984).

9. Brauer, Michael G., "An Evaluation of the Shell Creep Test Procedure to Predict Rutting in Asphalt Pavements," North Dakota State Highway Department, January (1982).

10. McLeod, Norman W. and Keith J. Davidson, "Particle Index Evaluation of Aggregates for Asphalt Paving Mixtures," Proceeding Association of Asphalt Paving Technologies, February (1981).

11. ASTM Designation: D-3398-81, Annual Books of ASTM Standards.

12. Hills, J.F., D. Brien and P.J. Van de Loo, "The Correlation of Rutting and Creep Tests on Asphalt Mixes," Institute of Petroleum, London, England, January (1974).

13. Epps, Jon, et al, "Chemistry, Rheology, and Engineering Properties of Manganese Treated Asphalts and Asphalt Mixtures," Prepared for presentation at the 65th Annual Meeting of Transportation Research Board, January (1986).

14. Moulthrop, James S., et al, "Manganese Modified Asphalt Pavements," Prepared for presentation at the 64th Annual Meeting of the Transportation Research Board, January, (1985)

15. Van de Loo, P.J., "The Creep Test: A key Tool in Asphalt Mix Design and in the Prediction of Pavement Rutting," Proceedings Asphalt Paving Technology, February (1978).

16. Bolk, Ir.H.J.N.A., "The Creep Test," Study Centre for Road Construction, SCW Publication, The Netherlands, February (1981).

17. Bonnuare, F., et al, "A New Method of Predicting the Stiffness of Asphalt Paving Mixtures," Proceeding on the Association of Asphalt Paving Technologists, (1977).

August 15, 1986

1986 USAF-UES SUMMER FACULTY RESEARCH PROGRAM/ GRADUATE STUDENT SUMMER SUPPORT PROGRAM

Sponsored by the

AIR FORCE OFFICE OF SCIENTIFIC RESEARCH

Conducted by the

Universal Energy Systems, Inc.

FINAL REPORT

SELECTED SPECTRAL STUDIES OF THE SUN

Prepared by:	Dr. James Charles LoPresto
Academic Rank:	Full Professor of Astronomy and Physics
Department and University:	Department of Chemistry and Physics, Edinboro University of Pennsylvania
Research Location:	U.S. Air Force AFGL/PHS SOLAR RESEARCH BRANCH SACRAMENTO PEAK OBSERVATORY NATIONAL SOLAR OBSERVATORY SUNSPOT, NEW MEXICO 88349
USAF Researcher	Dr. Steven Keil
Date:	August 15, 1986
Contract No:	F49620-85-C-0013

August 15, 1986

SELECTED SPECTRAL STUDIES OF THE SUN

by

James Charles LoPresto

ABSTRACT

Selected spectral data of Fe I 3969Å, Mg I 5184Å and K I 7699Å at many spatial positions on the Sun have been obtained with a CCD camera at the Vacuum Tower Telescope at the National Solar Observatory at Sacramento Peak. This data will be combined with additonal K I 7699Å data obtained by Dr. Steven Keil in a similar fashion and with still additional data obtained by Dr. James LoPresto and Dr. Keith Pierce with a rapid scanning photoelectric detector at the McMath Telescope at the National Solar Observatory, Kitt Peak. The Fe I and Mg I data are used to measure systematic errors between the two telescopes. The combined K I 7699Å data set will be analyzed to obtain the solar rotation parameters and the gravitational red shift. This is relevant to detecting any short and long term changes in solar rotation and increasing the accuracy in measuring the solar gravitational red shift. The results of a computer analysis of this data at Edinboro University will be published in SOLAR PHYSICS .

I. INTRODUCTION: I received my Ph. D. from the University of Michigan studying the atmospheres (via the spectrum) of red giant stars. One facet of this research was to observe bright stellar spectra at the McMath telescope. These were the first successful night time observations of stars using the McMath telescope. A summary of some of this work is published in P.A.S.P (1971). I did additional research, while a graduate research assistant, on solar spectral studies of velocity fields in the atmosphere of the Sun using the Doppler principle, stellar evolution and the Fourier Smoothing of solar and stellar spectra.

I have completed a theortical study of the feasibilty of measuring the solar gravitational red shift, while a NASA SUMMER FACULTY FELLOW at GODDARD SPACE FLIGHT CENTER in Greenbelt, Maryland and a SUMMER VISITOR at the HIGH ALITITUDE OBSERVATORY, NCAR, in Boulder, Colorado. This study was published in SOLAR PHYSICS, (1980).

As a result of the above mentioned study, I have undertaken in cooperation with Dr. A. Keith Pierce of the National Solar Observatory at Kitt Peak, a long-range study to observe solar velocity fields (using the Doppler method) with the goal of separating out the solar gravitational red shift and determining the character of the solar differential rotation and its

possible short-term and secular variations. These observations were made with the McMath telescope and they have been published in SOLAR PHYSICS (1984 & 1985) and ASTRONOMY (in press). This observational program is still in progress.

Preliminary results from observations of a number of strong Fraunhofer lines give a measurment of 1.01 ± 0.03 of the predicted gravitational red shift of 636 m/sec. This determination is about a factor of two more accurate than the best previous determination. Our experience indicates that with further temporal averaging, we can reduce the rms error by about of factor of three and thus be able to quote a result of about 1.00 ± 0.01.

These observations have also shown that the Sun's rotation rate changes its character in periods of time as short as one day. The equatorial velocity has been measured to change by as much as 5% in one day.

Furthermore, our measurements indicate a slow secular change of the average rotation by as much as 2% in about 15 years. This is consistent with observations made by several other observers during this same 15-16 year period since about 1970.

Based on the above mentioned long-range goal, it is essential to obtain an independent set of measurements using another telescope and spectrograph as well as to estimate our systematic error and to increase our data store. **For this reason, I undertook this project to make compariable observations at Sacramento Peak Observatory.**

II. OBJECTIVES OF THE RESEARCH EFFORT:

The objectives of this project were:

1. To obtain measurements of telescope and spectrograph systematic errors by observing with the Vaccum Tower and Big Dome telescopes and spectrographs in direct comparison with the McMath Solar Telescope at Kitt Peak.

2. To extend the set of velocity field data to include at least one more line and if both telescope time and weather permit, to several others.

III. RESULTS TO DATE

I have completed my study of the Fe I 3969Å line and the surrounding profile of the Ca II line. I have compared this profile in absolute intensity from observations taken at the NATIONAL SOLAR OBSERVATORY, KITT PEAK, using the MCMATH SOLAR TELESCOPE to that obtained here at the NATIONAL SOLAR OBSERVATORY, SACRAMENTO PEAK, using the VACUUM TOWER TELESCOPE. The agreement between the two is very good and thus allows me to quote that the systematic error in intensity is less than 1% near the center of the line and less than 2% nearer the wings. This discrepancy is probably entirely due to scattered light from the ESCHELLE spectrograph at the VACUUM TOWER TELESCOPE. See Figure 1.

My Big Dome telescope time has been largely hampered by cloudy weather. Although I have succeeded in obtaining some data with Big Dome, it is far to small a data set to make good comparisons. These observations will be

made by the National Solar Observatory observing staff later in the fall when time permits.

I have completed a set of K I 7699Å center to limb observations along the solar rotation axis at the tower telescope. I have made measurements of the shifts of the this line relative to a nearby Terrestrial O_2 line at 7699.5Å. Figure 2 shows how these observations correspond with those taken at Kitt Peak. Quick inspection indicates that the agreement between the two telescopes and spectrographs is very good thus assuring us that no unknown large systematic errors are occuring.

I have also measured center to limb shifts of K I 7699Å at various angles separated by 5^0 all around the disk. Each center to limb shift was taken in steps of $\mu = .1$ from the center at $\mu = 1$ to the limb at $\mu = 0$ ($\mu = \cos \Delta$). This observing technique gives a two dimensional grid of velocity shifts all over the Sun. I have a similar set for two different observing days. It is my goal to reduce this data set using the computer facilities at Edinboro University of Pennsylvania. I intend to apply to the 1986-1987 MINI GRANT PROGRAM for support of this project.

IV. METHOD OF REDUCTION.

While at Sacramento Peak Observatory, I have written a Fortran Code to obtain the rotational parameters and the gravitational red shift of the Sun from the K I 7699Å data sets. This code will be combined with a graphical data management code written in RS/1, which exists at my home computer facility to reduce the data stored on magnetic tapes.

The velocity in the line of sight, as measured by the Doppler effect, is given by (See Howard and Harvey, 1970)

(1) $$V = V_{rot} \cos B_0 [\sin \emptyset \sin \Delta] + d$$

where the angles $\emptyset$ and Δ uniquely define the position of observation on the Sun in a two dimensional polar coordinate system centered on the solar disc as observed on the sky (See Figure 3).

$\emptyset$ = the angle measured counter-clockwise from Solar North to the point of observation.

Δ = the angle measured on the Sun's disc subtended at the Earth by the point of observation and the center of the disc.

B_0 = the tilt angle of the Sun's rotational axis with respect to the plane of the sky. This angle can also be described as the solar latitude of the center of the disc on the sky.

V_{rot} = the component of differential rotation parallel to the Sun's equator at a point on the Sun.

V = the measured velocity corrected for Earth rotation, Earth orbital motion relative to points on the Sun not at the disc center, and the radial velocity of the Sun due to the Earth's elliptical orbit and the Earth's motion around the Barycenter of the Earth-Moon system.

Following Howard and Harvey (1970), I first assume that the differential solar rotation can be empirically represented by a power series in the sine

of the solar latitude B.

(2) $$V_{rot} = a + b \sin^2 B + c \sin^4 B$$

In addition, following Pierce and LoPresto (1984), I assume a Legendre Polynomial expansion, which has functional orthogonality in the expansion terms and thus avoids inter-parametric dependency of the rotational parameters a, b, and c.

(3) $$V_{rot} = A_0P_0 + A_2P_2 + A_4P_4$$

In both cases, only even powers in the expansion are used, which is mathematically assuming that the Sun's differential rotation is the same in the Northern and Southern hemisphere. The validity of this assumption has never been tested thoroughly and our data set may be enough of a sample to carry out this test. I will do so only after the initial reduction.

Using (2) for illustration, I then solve for the rotational parameters a, b, and c and the gravitational red shift, d, as outlined below.

Re-writing (1) in the form

(4) $$V_i = a_1Z_1 + a_2Z_2 + a_3Z_3 + a_4Z_4$$

where $Z_1 = 1$

$$Z_2 = \cos B_0 \sin \varnothing_i \sin \Delta_i$$

$$Z_3 = Z_2 \sin^2 B_i$$

$$Z_4 = Z_3 \sin^4 B_i$$

and

(5) $$\sin B_i = \sin B_0 \cos \Delta_i + \cos B_0 \sin \Delta_i \cos \varnothing_i$$

I set up a set of conditional equations by summing over all the observations for an observed velocity at each position determined by $\varnothing$ and Δ with the use of equation (4). The least squares method is used to solve for the parameters a, b, c, and d. This gives us four equations and four unknowns. The solutions for a, b, c, and d are obtained by a Gaussian elimination with pivoting.

V. FUTURE PLANS

My future plans are to continue to make high resolution Doppler shift observations of solar velocity fields. Once securing an acceptable measurement of the gravitational red shift (about 1.00 ± 0.01), I intend to monitor the changes in the solar rotation rate. I currently believe that the "observed changes" are due to a variety of chromospheric velocity fields, which when observed, mimic a change in the the rotation rate. A properly disigned on-going observing strategy, with careful spatial coverage on the Sun, should add insight into this problem.

On the other hand, if the changes in rotation are either real or partly real,

a long-term observational program is essential in order to establish how these changes relate to the solar magnetic cycle.

References

1. LoPresto, J. C., THE HALF-WIDTHS OF STELLAR H(ALPHA) PROFILES DEDUCED FROM SPECTROGRAMS OBTAINED WITH THE MCMATH SOLAR TELESCOPE, (1971), P.A.S.P. 83, pp. 674-676.

2. LoPresto, J. C., Chapman, R. and E. A. Sturgis, SOLAR GRAVITATIONAL REDSHIFT, (1980), SOLAR PHYSICS, 66, pp. 245-249.

3. Pierce, A. K. and LoPresto, J. C., (1984), SOLAR ROTATION FROM A NUMBER OF FRAUNHOFER LINES, SOLAR PHYSICS, 93, pp. 155-170.

4. LoPresto, J. C. and Pierce, A. K., (1985), THE CENTER TO LIMB WAVELENGTH SHIFT OF A NUMBER OF FRAUNHOFER LINES, SOLAR PHYSICS, 102, (1985), pp. 21-27.

5. LoPresto, J. C., (1986), THE ROTATION OF THE SUN, ASTRONOMY, (in press).

6. Howard, R. and Harvey, J., (1970), SOLAR PHYSICS, 12, pp. 23-51.

Figure 1.

Center of disc observations. Similar comparisons
are made at postions from μ = 0.1 in steps of 0.1 to 1.

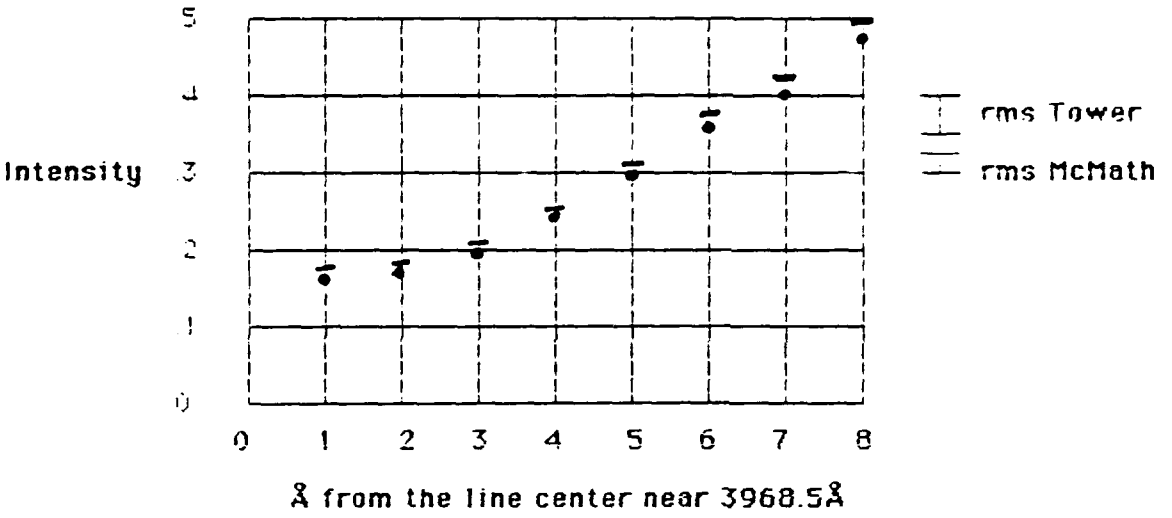

Kitt Peak data (main spectrograph with photomultiplier at McMain)
Sacramento Peak data (Eschelle spectrograph & CCD data at Tower)

The rms errors in both data sets increase by about a factor
of 1.3 from 7 Å to 10Å away from the line center.

Figure 2.

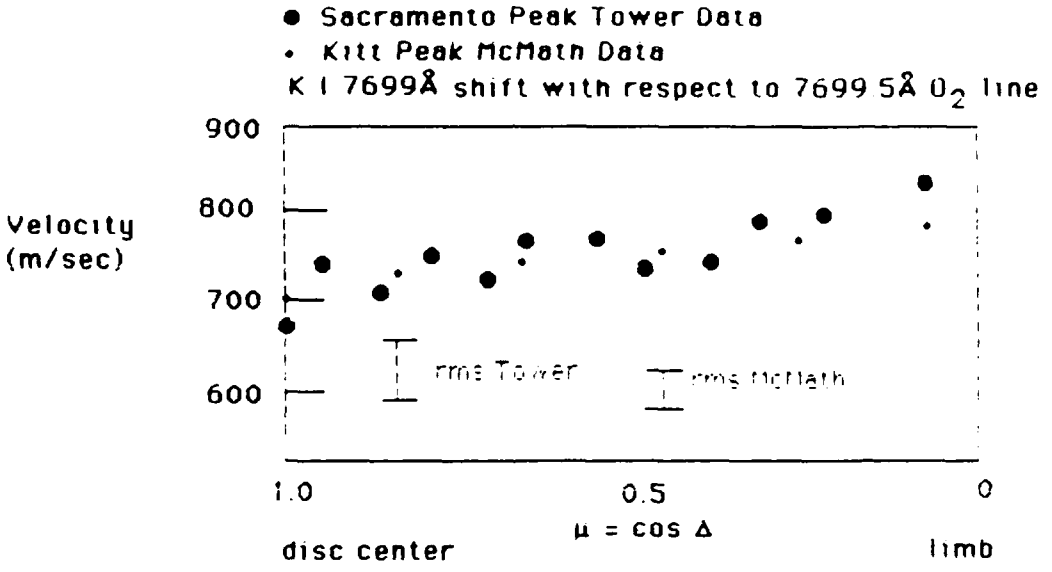
● Sacramento Peak Tower Data
• Kitt Peak McMath Data
K I 7699Å shift with respect to 7699.5Å O_2 line
900
800
700
600
Velocity
(m/sec)
rms Tower
rms McMath
1.0
0.5
0
μ = cos Δ
disc center
limb

Figure 3.
Observation Point on the Solar Disc

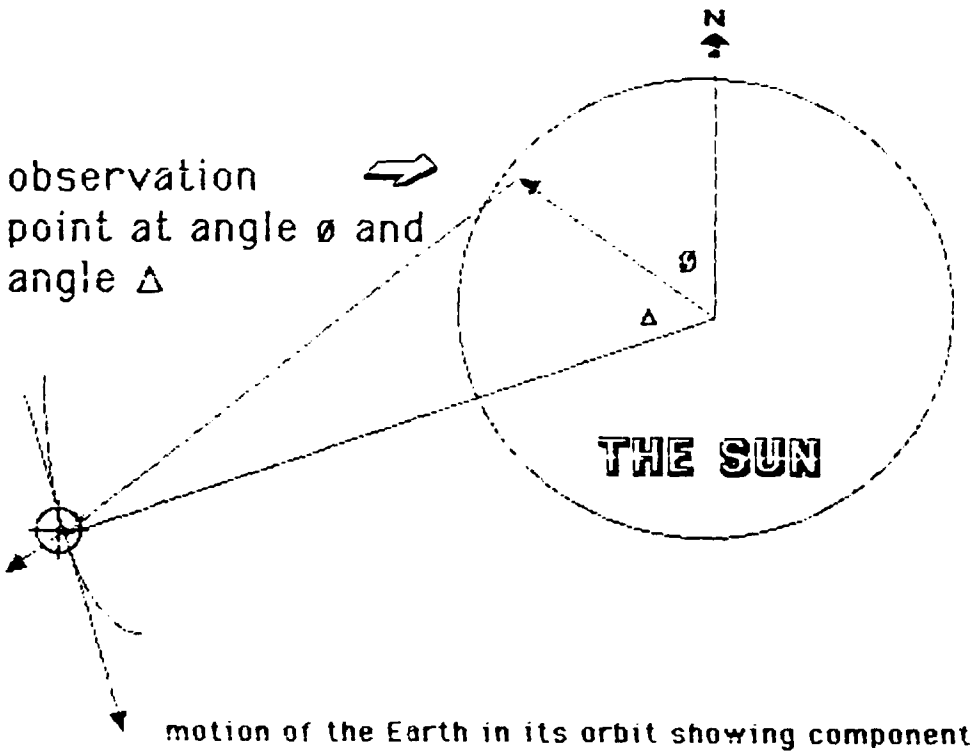

1986 USAF-UES Summer Faculty Research Program
Graduate Student Summer Support Program

Sponsored by the

Air Force Office of Scientific Research

Conducted by the

Universal Energy Systems, Inc.

FINAL REPORT

Visual Problem-Structuring and Hemispheric Processes of the Human Brain

Prepared by:	Stephen L. Loy, Ph.D.
Academic Rank:	Assistant Professor
Department and	Management Department College of Business Administration
University:	Iowa State University
Research Location:	Human Resources Laboratory Ground Operations Branch
USAF Researcher:	Lawrence Reed, Branch Chief
Date:	July 28, 1986
Contract No:	F49620-85-0013

Visual Problem-Structuring and Hemispheric Processes of the Human Brain

by

Stephen L. Loy

ABSTRACT

The possibility of the relationships between right-hemisphere brain functions in visual problem-structuring aids were explored. A theoretical model of the role of hemispheric functions in visual problem structuring is developed and recommendations for testing this model are presented. The literature and theories of hemispheric brain functions, structural modeling, computer-based decision support systems (DSS) are reviewed in the first section of this paper. A theoretical model of the role of hemispheric functions in visual structural modeling is developed in the second section. The model posits that the information processing functions of the hemispheres influence the effective use of a visual problem structuring tool in formulating complex problems.

Acknowledgments

I would like to thank the Air Force Human Resources Laboratory and the Air Force Office of Scientific Research for sponsorship of my research. I would like to thank the members of the HRL/LRG, Dr. Larry Reed, Mike Young, Captain David Barnthouse, and Major Raymond Spaeth, for giving me the opportunity and guidance for this research.

Finally, above all else, I thank my wife, Marianna, for her patience and support through this project even though she could not be here with me.

I. INTRODUCTION: I received my Ph. D. from the College of Business Administration of Texas Tech University. My major area of study was Management Information Systems. My recent research efforts have related to Decision Support Systems and structural modeling.

My summer research effort involved a literature review related to the information processing functions of the two hemispheres of the human brain, problem structuring, and computer-based decision support systems (DSS). From the literature review a tentative theoretical model was developed concerning the ability of a visual problem-structuring aid to support right-hemisphere functions. This theoretical model is an extension of my previous research efforts.

II. OBJECTIVES OF THE RESEARCH EFFORT: The overall objective of the research effort was to investigate theoretical possibility of whether a visual problem-structuring aid can support right-hemispheric functions of the human brain. The problem-structuring aid is based on a Systems Engineering technique known as structural modeling.

My individual objectives were:

(1) A study of the Neuropsychology and Cognitive Science literature about hemispheric functions of the human brain.

(2) Then, to synthesize this literature relevant to decision making and problem structuring and to relate to recent research efforts in visual structural modeling.

(3) From this synthesis, I hoped to develop a theoretical model which could be used to study how decision support aids for right hemisphere functions can be designed and tested.

III. Results of the Research Effort

1. Hemisphericity

A literature search and review of the Neuropsychology and Cognitive Science research was conducted in order to develop basic knowledge of the functions and processes of the hemispheres of the human brain. The result of this review led to the conclusions that right-hemisphere functions are important in problem solving, and that it may be possible to provide computer-based support for those functions. To operationalize this support a visual media to represent holistic views of problem domains could be used.

A review of structural modeling and management information systems was conducted to determine where hemisphericity is relevant to DSS. It was concluded from these reviews was that structural modeling techniques can provide tools to represent problem domains holistically. A visual problem structuring recently tool has been developed which is speculated to support right-hemisphere processes [Pracht, 1986]. If this tool does support right-hemisphere processes in the problem structuring phase of problem

solving, then this tool could provide a needed facility for decision support systems that this currently not available.

From these literature reviews a theoretical model of the relationships between right-hemisphere functions and the use of a visual problem-structuring aid was developed (Figure 1). The basic premises of this model are that the visual problem-structuring aid will affect user problem-understanding and decision quality, and that the affects depend on the level of right-hemisphere abilities regardless of hemispheric dominance. The affects also depend on the level of left-hemisphere abilities. Therefore, when both hemispheres are support in problem solving the result will be enhanced problem understanding and decision quality.

IV. Recommendations

No experiments have been conducted testing the validity of the theoretical model. An experiment should be performed to relate right-hemisphere abilities with the use of a visual problem-structuring aid. The experiment should consider the interdependence of the left- and right-hemisphere abilites. The dependent variables should be user problem-understanding and decision quality in a complex problem environment. From this experiment it should be possible to gain some insight into the interactions between hemispheric abilities and visual problem-structuring aids, and how the interaction affects

problem understanding and decision quality.

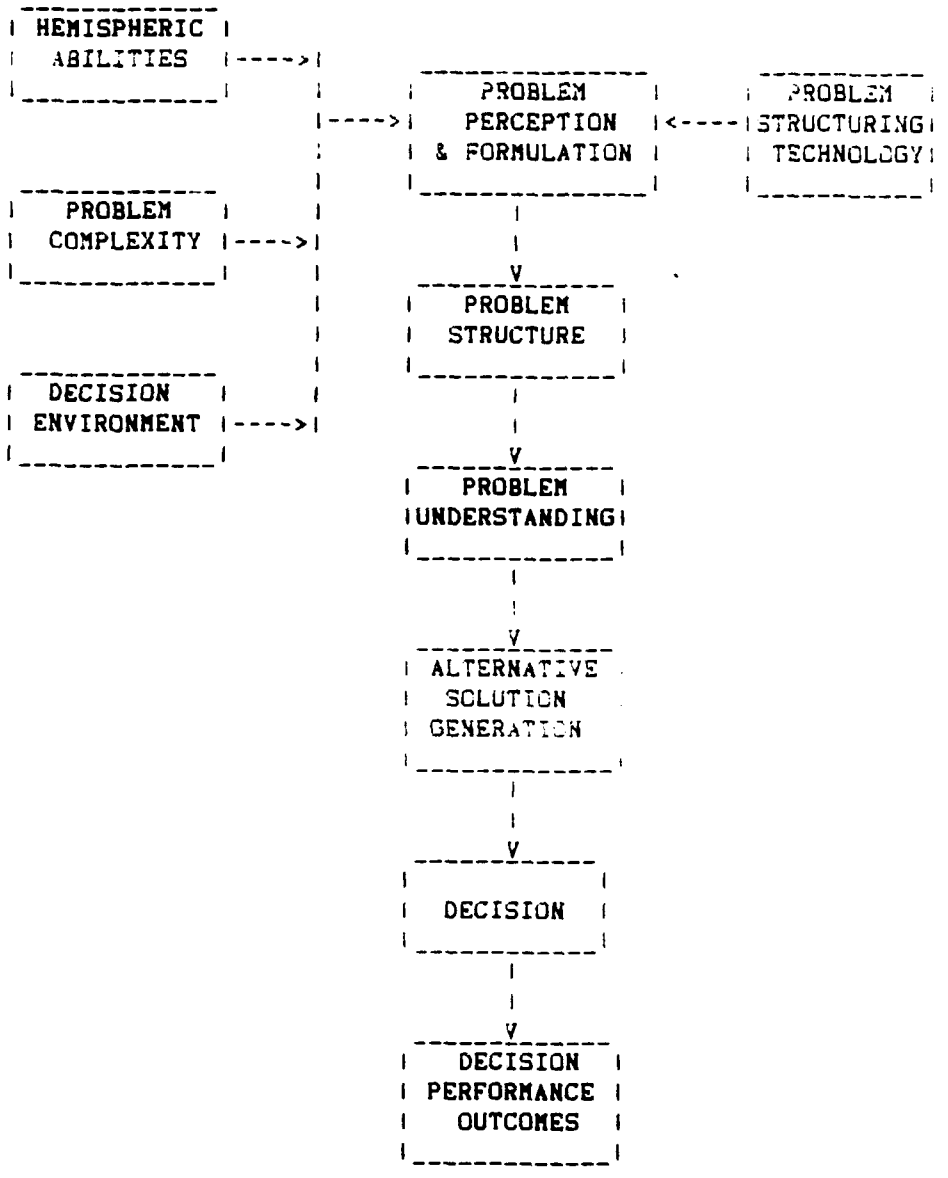

Figure 1: The Research Model

2. Much work remains on enhancing and refining visual problem-structuring aids. These improvements should include the incorporation of structural analysis routines into the basic model building routines. With such refinements, further experiments comparing the affects of analytical decision aids with visual problem-structuring aids, and the combined affects of these aids will be possible. Such experiments may help determine whether DSS can and should support both hemispheres, and what the characteristics those aids should be.

References

Ackoff, R. The Art of Problem Solving. New York, NY: John Wiley & Sons, Inc., 1978.

Alexander, C. Notes on the Synthesis of Form. Cambridge, Ma: Harvard, 1964.

Benbasat, I. and R.N. Taylor. "The Impact of Cognitive Styles on Information Systems Design." MIS Quarterly, vol. 2, no. 2, June 1978, pp. 43-54.

Buehner, L.J. "The Impact of Cognitive Styles and Subject Matter on Instructional Design." AFHRL Technical Report Paper 85-11, Wright-Patterson AFB, 1985.

Burns, J.R. and W.M. Marcy. "Causality: Its Characteristics in System Dynamics and KSIM Models of Socieconomic Systems." Technological Forecasting and Social Change, Vol. 14, 1979, pp. 387-398.

Courtney, J.F. and R.L. Jenson. SLIM Users Manual. Dallas, TX: Business Publications, Inc., 1981. Courtney, J.F., G. DeSanctis, and G.M. Kasper. "Continuity in MIS/DSS Laboratory Research: The Case for a Common Gaming Simulator." Decision Sciences, vol. 14., no. 3, 1983, pp. 419-439.

DeSanctis, G.R. "An Examination of an Expectancy Theory Model of Decision Support System Use." Unpublished DBA dissertation: Texas Tech University, 1982.

DeSanctis, G.R. "Computer Graphics as Decision Aids: Directions for Research." Decision Sciences, vol. 15, no. 4, December 1984, pp. 463-487.

Dumas, R. and A. Morgan. "EEG Asymmetry as a Function of Occupation, Task, and Task Difficulty." Neuropsychology, vol. 13, pp. 219-228.

Franco, L. and R.W. Sperry. "Hemispheric Lateralization for Cognive Processing of Geometry." Neuropsychology, vol. 15, pp. 107, 114.

Forrester, J.W. Principles of Systems. Cambridge, MA: Wright-Allen, 1968.

Greeno, J.G. "The Structure of Memory and the Process of Problem Solving." In R.L. Solso (Ed.) Contemporary Issues of Cognitive Psychology: The Loyola Symposium, New York: Wiley, 1973, pp. 105-133.

Harary, F., R.Z. Norman, and D. Cartwright. Structural Models: An Introduction to the Theory of Directed Graphs. New York, NY: Wiley, 1965.

Hart, L.A. Human Brain and Human Learning. New York, NY: Longman, Inc., 1983.

Herman, N. "The Creative Brain." Training and Development Journal, vol. 10, no. 16, 1981.

Hudetz, W. "A Graphical Interactive Systems Simulation Program for Mini-Computers." In Concepts and Tools Computer-Assisted Policy Analysis, H. Bossei (Ed.). Basel: Burkhauser, 1977.

Jensen, R.L. and D. Cherrington. BML Participant's Manual. Dallas, TX: Business Publications, Inc., 1977.

Kane, J. "A Primer for a New Cross-Impact Language-KSIM." Technological, Forecasting, and Social Change, vol. 4. 1972, pp. 129-142.

Kasper, G.M. "A Conceptual Model and Empirical Analysis of Decision Support Use." Ph.D dissertation: State University of New York at Buffalo, 1983.

Keen, P.G.W. and G.R. Wagner. "DSS: An Executive Mind Support System." Datamation, vol. 25, no. 12, November 1979, pp. 117-122.

Kinsbourne, M. "The Ontogeny of Cerebral Dominance." In Aaronson, D. and R. Reiber (Eds.), Developmental Psycholoqistics and Communications Disorders. New York, NY: New York Academy of Sciences, 1975.

Kolers, P.A., and H.L. Roediger. "Procedures of Mind." Journal of Verbal Learning and Verbal Behavior, vol. 23, no. 4, pp. 425-429.

Kruzic, P.G. "KSIM Techniques for Evaluating Interactions Among Variables. Stanford Research Institiute, Menlo Park, CA., Techical Note OED-16, June 1873.

Langhorst, E.E. "Computer Graphics Aided Interpretive Structural Modeling: A Tool for Conceptualizing Complex Design Problems." Ph.D. dissertation, Purdue Unversity, 1977.

Lendaris, G.G. "Structural Modeling - A Tutorial Guide." Proceedings IEEE-SMCS Internatl. Conf. Cybernetics and Society, 1980, vol. 10, pp. 807-840.

Loy, S.L. "An Experimental Investigation of a Graphical Problem-Structuring Aid and Nominal Group Technique for Group Decision Support Systems." Ph.D. dissertation, Texas Tech University, 1986.

Luria, A. The Working Brain: An Introduction to Neuropsychology. New York, NY: Basic Books, 1973.

Mason, R.O. and I.I. Mitroff. "A Program for Research on Management Information Systems." Management Science, vol 19, 1973, pp. 475-487.

McDermott, J. and J.H. Larkin. "Representing Textbook Physics Problems." Proceeding of the 2nd National Conference of the Canadian Society for Computational Studies of Inteeligence. Toronto, University of Toronto Press, 1978.

McLean, J.M. and P. Shepherd. "The Importance of Model Structure." Futures, vol. 8, February 1976, pp. 40-51.

McLean, J.M. "Getting the Problem Right-A Role for Structural Modeling," in Futures Research: New Directions, H.A. Linstone and W.H. Simmonds (eds.) Reading, MA: Addison-Wesley, 1977, pp. 144-157.

McLean, J.M., P. Shepherd, and R. Curnow. "Techniques for Analysis of System Structure." SPRU Occasional Paper Series No. 1, Science Policy Research Unit, University of Sussex, UK, 1976.

Mintzberg, H., D. Raisinghani, and A. Theoret. "The Structure of 'Unstructured' Decision Processes." Administrative Science Quarterly, vol. 21, 1976, pp. 246-275.

Newell, A. and H.A. Simon. Human Problem Solving. Englewood Cliffs, NJ: Prentice-Hall, 1972.

Ornstein, R.E. The Psychology of Consciousness (2nd ed.). New York, NY: Harcourt Brace Jovanovich, 1977.

Porac, C. and S. Coren. Lateral Preference and Human Behavior. New York, NY: Spinger-Verlag, 1981.

Pracht, W.E. "An Experimental Investigation of a Graphical Interactive Problem Structuring Tool for Decision Support Systems." DBA dissertation, Texas Tech University, 1984.

Pracht, W.E. "GISMO: A Visual Problem Structuring and Knowledge Organization Tool." IEEE Transactions of Systems, Man, and Cybernetics, vol. SMC-16, no. 2, March/April 1986, pp. 265-270.

Pracht, W.E. and J.F. Courtney. "A Visual Interface for Capturing Mental Models in Model Management Systems." Hawaii International Conference on Systems Sciences, 1985.

Reynolds, C. and E.P. Torrence. "Perceived Changes in Style of Learning and Thinking (hemisphericity) Through Direct and Indirect Training." The Journal of Creative Behavior, vol. 12, no. 4, pp. 247-252.

Roberts, F.S., and T.A. Brown. "Signed Digraphs and the Energy Crisis." American Mathematical Monthly, vol. 82, no. 6, 1975, pp. 577-594.

Roberts, F.S. "The Questionnaire Method," in Structure of Decision: The Cognitive Maps of Political Elites, R. Axelrod (ed). Princeton, NJ: Princeton University Press, 1976.

Robey, D. and W. Taggert. "Human Information Processing and Decision Support Systems." MIS Quarterly, vol. 6, no. 2, 1982, pp. 61-73.

Rouse, W.B. and N.M. Morris. "On Looking Into the Black Box: Prospects and Limmits in the Search for Mental Models." Center for Man-Machine Systems Research. Technicial Report no. 85-2, Defense Technical Information Center, Defense Logistics Agency, Cameron Station, Alexandria, VA, May 1985.

Rubensen, R. "The Roles of the Right Hemisphere in Learning and Creativity Implications for Enhancing Problem Solving Ability. The Gifted Child Quarterly, vol. 23, no. 1, 1979, pp. 78-101.

Sage, A.P. "Behavioral and Organizational Considerations in the Design of Information Systems and Processes for Planning and Decision Support." IEEE Transactions on Systems, Man, and Cybernetics, vol. SMC-11, no. 9, September 1981, pp. 640-678.

Schartz, G, R. Davidson, and E. Pugash. "Voluntary Control Patterns of EEG Parietal Asymmetry: Cognitive Concommitance." Psychophysiology, vol. 13, no. 6, 1976, pp. 498-504.

Simon, H.A. The New Science of Management Decision. New York, NY: Harper and Brothers, 1960.

Simon, H.A. "The Architecture of Complexity." General Systems Yearbook, vol. 10, 1964, pp. 63-76.

Simon, H.A. The Science of the Artificial. Cambridge, MA: M.I.T. Press, 1969.

Simon, H.A. The Science of the Artificial (2nd ed.). Cambridge, MA: M.I.T. Press, 1981.

Sprague, R.H. "A Framework for the Development of Decision Support Systems." MIS Quarterly, vol. 4, no. 4, 1980, pp. 1-26.

Tabatoni, P. and P. Jarniou. "The Dynamics of Norms in Strategic Management," in From Strategic Planning to Strategic Management. Ansoff, H.I., R.L. Declerck, and R.L. Hayes (eds.). London: John Wiley and Sons, 1976, pp. 29-38.

Taggert, W. and D. Robey. "Minds and Managers: On the Dual Nature of Human Information Processing and Management." Academy of Management Review, Vol. 6, no. 2, 1981, pp. 187-185.

Taylor, R.N. "Computers and Hemispheric Functioning." Present at seminar, Teachers College, Columbia University, New York, NY, February 1978.

Volkema, R.J. "Problem Formulation in Planning and Design." Management Science, vol. 29, no. 6, June 1983, pp. 639-652.

Wakeland, W. "QSIM2: A Low Budget Heuristic Approach to Modeling and Forecasting." Technological Forecating and Social Change, vol. 9, 1976, pp. 213-229.

Warfield, J.N. "An Assault On Complexity." Battelle Memorial Institute, Columbus, OH, Battelle Monograph No.3, 1973.

Warfield, J.N. "Structuring Complex Systems." Battelle Memorial Institute, Columbus, OH, Battelle Monograph No. 4., 1974.

Warfield, J.N., H. Geschka, and R. Hamilton. Methods of Idea Management. Columbus, OH: Academy of Contemporary Problems, 1975.

Weber, S. "Cognitive Processes Involved in Solving Information Systems (IS) Design Planning." Proceedings of the Sixth International Conference on Computer Systems, Indianapolis, IN, 1985, pp. 305-312.

Witkin, H.A., P.K. Oltman, E. Raskin, and S.A. Karp. Manual for the Embedded Figures Test. Palo Alto, CA: Consulting Psychologist Press, 1971.

Wittrock, M.C. "Education and the Cognitive Processes of the Brain." In Cognitive Processes of the Brain, 1980, pp. 16-102.

Zenhausern, R. "Imagery, Cerebral Dominance, and Style of Thinking: A Unified Field Model." Bulletin of the Psychonomil Society, vol. 12, no.5, 1979.

Zmud, R.W. "Individual Differnces and MIS Success: A Review of the Empirical Literature." Management Science, vol. 25, no. 10, October 1979, pp. 966-979.

1986 USAF-UES SUMMER FACULTY RESEARCH PROGRAM/

GRADUATE STUDENT SUMMER SUPPORT PROGRAM

Sponsored by the

AIR FORCE OFFICE OF SCIENTIFIC RESEARCH

Conducted by the

Universal Energy Systems, Inc.

FINAL REPORT

REVIEW AND EVALUATION OF A REFUELING CAPABILITY ASSESSMENT MODEL

Prepared by:	Nancy I. Lyons
Academic Rank:	Associate Professor
Department and	Department of Statistics
University:	University of Georgia
Research Location:	Gunter A. F. S., Montgomery, Alabama
USAF Researcher:	Captain David King
Date:	August 11, 1986
Contract No.:	F49620-85-C-0013

REVIEW AND EVALUATION OF A REFUELING CAPABILITY ASSESSMENT MODEL

by

Nancy I. Lyons

ABSTRACT

A study was made to determine the necessary features required of a computer simulation model for assessing aircraft refueling capability at the base level. The RCAM model was used as a starting point. The model was tested for accuracy and validity in representing refueling operations. The assumptions, limitations, and the strong and weak points of the model were documented for future reference. The code was studied to identify computer algorithms used to schedule events and to evaluate the related system subprograms. Based on these findings a recommendation was made to retain the RCAM scheduling algorithm and as much as possible of the other parts of the model. Substantial improvements need to be made to the data entry procedures. Several modifications and additions in other areas were identified for further study and consideration. A prototype of the proposed model was prepared for possible demonstration purposes to solicit suggestions from potential users. The prototype is based on the RCAM model with improvements in the output, the addition of personnel, and the addition of a delay summary table.

ACKNOWLEDGEMENTS

I would like to thank the Air Force Systems Command and the Air Force Office of Scientific Research for sponsoring my research. I would like to thank Captain Dave King, Chuck Miller, Willi Hahn, Lieutenant Colonel Ron Nettles, Major Aaron Dewispelare, all of L.M.C., and Sargent Bruce Wilbur, DSDO, Gunter A.F.S. for their help and advice. I would like to express particular thanks to Lieutenant Colonel Doug Blazer for giving me the opportunity and guidance necessary for carrying out the research effort.

Finally I would like to thank all of the staff at the L.M.C. for making my stay in Montgomery an enjoyable experience.

I. INTRODUCTION

I received my doctorate from N. C. State University and have been with the Department of Statistics and Computer Science at the University of Georgia since 1975. A major part of my dissertation research involved writing a computer simulation model to test a new procedure in regression analysis. I have authored several research papers which required writing simulation models in FORTRAN on both main frame and microcomputer systems.

The research project at the AFLMC, Gunter A. F. S. concerned the development of a computer simulation model for a microcomputer to assess aircraft refueling capability. Part of the project was to test and evaluate a previously written capability assessment model written in FORTRAN. Because of my experience in computer modeling in the FORTRAN language, I was assigned to this project.

II. OBJECTIVES OF THE RESEARCH EFFORT

The long range goal of the project is to produce a computer simulation model for assessing aircraft refueling capability at the base level. It should be designed for use on a microcomputer by fuels personnel. Synergy Corporation is currently developing a model (AFCAM) which automates the routine calculations made by fuels personnel to assess fuels capability on a daily basis. The model proposed in this project differs from AFCAM in stressing the importance of the time factor involved in assessing capability. It would be particularly applicable for determining capability to handle surge situations. The RCAM model (Hodgson, 1984) is a discrete time event simulation model

developed for this purpose. It has not received wide acceptance, primarily because it has not been adequately tested or validated. In addition all necessary data must be stored as a permenent data base making the program cumbersome to use.

In order for such a model to receive wide acceptance it must be user-friendly and it must provide information beneficial to fuels management officers. This means not merely determining if fuels has the resources to meet a specific refueling schedule, but also suggesting possible improvements in allocation of resources, or equipment dispatching practices. Output provided should be determined in consultation with fuels personnel in the field. A possible method of soliciting suggestions from a wide audience of potential users is to provide a written functional description of the proposed model. The availability of a prototype of the model, which could be used for demonstration purposes in addition to a written description, would be very beneficial.

The initial objectives of the summer research period were to test and validate the RCAM model. Validation in this context means determining if the simulation accurately represents what is done in practice. The algorithms used to schedule events and handle dispatching of equipment were to be identified. The strong and weak points of the model were to be documented for future reference. Based on these results a recommendation was to be made between retaining the basic RCAM model with improvements, or designing a new model.

A second objective was the preparation of the prototype model based on a modification of RCAM. In developing the prototype there were five

initial requirements set forth.

1. improve the existing output
2. add the facility for taking numbers of available personnel into account in assessing capability
3. add output summarizing the reasons for possible refueling delays
4. remove the random equipment breakdown and repair time
5. remove the Monte Carlo simulation option and summary

Time permitting, modifications to allow interactive data entry were to be outlined.

III. APPROACHES TAKEN

The RCAM model consists of a main driving program and 34 subroutines and function subprograms. The code is difficult to follow from a programmer's standpoint, partly because of the very nature of the process being modeled, but also because the code is not written in structured style. A combination of running test data sets and examination of the code was used to determine how RCAM functions. Most of the test data sets used represented scenarios which pushed refueling operations to capacity. Output was checked by hand calculation for several test runs. The subroutines relating directly to equipment dispatching and monitoring of various fuel levels were flowcharted. These five subroutines were recoded in equivalent structured form and documented. The code in the remaining subprograms was studied to determine algorithms used for scheduling events.

Validation was approached in a similar manner. The methods RCAM uses to handle various refueling operations were discussed with two Air Force personnel experienced in fuels operations--- Capt. David King

and Sgt. Bruce Wilbur. They were also consulted in improving the output and in adding personnel to the prototype model. The delay summary output was patterned after the CAMMP model.

IV. RESULTS

The most important features of the RCAM model are described briefly below. A more detailed description has been prepared and submitted to the Directorate of Supply, AFLMC, Gunter A. F. S.

1. Event Scheduling Methods

Each event, refueler, and aircraft is described by a set of numerical values, or descriptors, which are stored as a row in a real two-dimensional array. By use of four auxiliary arrays, these rows are classified into eight subsets called lists. The members of the list may be ordered according to the value of any one of the numerical descriptors. One of the lists is used exclusively to store events in order of scheduled occurrence. Events are selected one at a time from the top of the list and the simulated time is correspondingly advanced in discrete jumps. Altering the primary status (busy or idle) of each refueler and aircraft is accomplished by reclassifying the corresponding row into the appropriate list. Secondary status is indicated by use of one or more of the descriptors as switches.

2. Dispatching Rules

The rules for determining the type of refueler (hotpit, truck, or hydrant) dispatched to an aircraft are rigid and are part of the model code. The primary criterion for selecting a refueler is based on examination of the fuel levels in the equipment. The user has some

control over the choice of refueler type by specifying a general preference for each aircraft in the data set, but it is limited. For example, the user cannot force aircraft to be refueled by hydrant if trucks are available.

3. Allocation of Resources

The model handles dispatching for each aircraft on a first come first serve basis. As each fuel request is made, equipment is reserved until the request is met or until all available equipment is reserved.

4. Fuel Level Monitoring

Fuel levels are monitored by requiring the user to specify a refill level for each refueler and for bulk fuel supply. When fuel drops below this level, a refill is scheduled. The refill level, especially for trucks, must be chosen carefully. A high refill level may force too many unnecessary truck refills. A low level can force a truck to sit unused because its fuel level is between the refill level and any aircraft fuel requirement.

5. Waiting Aircraft Selection

If fuel request schedules are heavy several aircraft may have to wait for a refueler. Each aircraft is assigned a priority and a maximum time for fuel completion by the user in the data set. When a refueler becomes free the model selects aircraft according to its priority. If two or more waiting aircraft have the same priority, the one that has been waiting longest is selected first. However if any aircraft is close to exceeding its maximum allotted refuel time, it is automatically given the highest priority.

V. TESTING THE MODEL

Several minor errors were discovered in the calculation of output values. Most of these were corrected to reflect the description provided in the original RCAM user's manual. However the definition of refueler turn time and average aircraft wait time are questionable as described and need to be clarified. The frequency of bulk fuel level checks appears to be too low, causing bulk fuel level to become negative due to the discrete nature of the model, and not because of a real lack of bulk fuel. This terminates the program unnecessarily. A potential problem also occurs because of the precision with which a refueler is chosen based on sufficient fuel level. For example, a truck with 2999 gallons of fuel would not be chosen to refuel an aircraft if the requirement is 3000 gallons.

VI. VALIDATION

The following situations were found not to conform to practice:

1. Simultaneous refueling of aircraft by two trucks is not coordinated properly.
2. Aircraft may be fueled partially by truck and completed by hydrant.
3. Available resources are tied up unnecessarily due to the tendency of the model to reserve equipment.
4. If all hydrants are busy, a waiting aircraft lines up at the hydrant with the least fuel, rather than the one that will become free first.

VII. PROTOTYPE

The problems encountered in the validation were either corrected or improved in the prototype model. The model was altered so that it

can reserve at most one idle truck in addition to the current refueler. An option was also added to reserve one busy truck after all other options are exhausted. The history print option, which prints out a step by step description of the process, was improved by printing descriptive phrases in standard fuel terminology, rather than merely a set of codes. The random equipment breakdown and repair time facility was removed as well as the Monte Carlo simulation option, along with all related subprograms and variables.

In the addition of personnel it was assumed that there are a fixed number of shifts per day. The number of available personnel on a particular shift is assumed to be the same throughout the simulation. Supervisors are not taken into consideration, and personnel at fill-stand and supply line posts are stationed permanently. Remaining personnel are assumed to be capable of handling refueling by any of the three types of equipment.

A refueling delay was defined to be any period of time an aircraft sat unattended while waiting for fuel. Lack of hotpit, truck, or hydrant refueler were identified as primary reasons. Lack of personnel to operate the equipment was defined as a secondary reason. At the end of each day of the scenario, a table of all aircraft delays is printed listing the following information:

1. aircraft tail number and type
2. fuel required at time of delay
3. time and length of delay
4. primary and secondary reasons for delay
5. status of the waiting aircraft

VIII. RECOMMENDATIONS

A computer model based on RCAM is applicable to stress situations in which assessment of capability is needed relative to a short time frame, as well as for day to day planning of normal operations. In this context the following observations and recommendations are noted.

The basic scheduling algorithm used in RCAM is sound. It is typical of that used by several accepted computer simulation languages. The related system subprograms are efficiently designed and coded. They provide sufficient flexibility to correct all of the above mentioned problems and make major revisions to other parts of the model. The fuels related subroutines represent a good subdivision of the tasks into related groups. The sequence in which operations are performed is well chosen. Based on these findings the recommendation is that the basic algorithms and approach of the RCAM model be retained with major improvements to be considered in three areas.

The input data base should be separated into three parts. One part should contain fixed specifications of base facilities that do not change. It should remain as a fixed data base, created only initially. The facility to tie into the CFMS data base should be investigated. The data relating to the aircraft fuel request schedule should be in a separate data base, fixed but easily edited. Providing a utility program to aid the user in creating this data set would be worthwhile. The remaining data, specifically those entries which control dispatch rules and allocation and change of resources should be made interactive so the user can experiment with different options. This will require substantial modification and redesign of the subroutines which read

data (INITLZ and DAYREP). The subroutines in the model which provide the facility to change resources could be easily modified for this.

If the model is ever to be used to maximize refueling efficiency, it must anticipate future fuel requests. A substantial revision of the RCAM code will be necessary, both in the input data procedures and in the dispatching process, to provide this facility. It is not clear at this point that maximum efficiency can even be defined. However this possibility needs to be given serious consideration.

A third modification concerns the assumption of fixed drive times between fillstands and aircraft. The model considers time as a limiting factor in addition to resources and fuel. The fixed drive time assumption is the most likely to give inaccurate time estimates. Again the CFMS data base provides information concerning positioning of fillstands and aircraft parking areas which could be used to estimate drive times more precisely. Using this data base would be preferable to requiring the user to enter such information.

Other minor considerations to be made before developing the final model are listed below.

1. The dispatching of equipment should be altered to give the user more control if desired. This requires revision of only one subroutine, DSPTCH.

2. The method of selecting aircraft from those waiting for a refueler should be studied further. Alteration would require modification of only the subroutine SLCT.

3. Frequency of bulk fuel level checks needs to be increased to coincide with each equipment refill. In the same context, the

maximum sustained fuel dispensing rate for the base, given its resources, should be computed and reported. This would require modification of subroutines RFLCMP and RSUPLY.

4. The method of reserving equipment, particularly pertaining to trucks, needs to be studied further in terms of efficiency. Alteration in this respect would require modification of only the subroutine DSPTCH.

5. Based on responses from the field, the output should be improved. Many of the current options of the RCAM model should be eliminated and duplications removed for clarity. The option of providing graphics from packages available on the system should be investigated.

6. A subroutine for converting daily clock time into and from cumulative hours in decimal form needs to be added to facilitate input and output interpretation for the user.

The code for the prototype model is ready. However there was not sufficient time to adequately test the two new options: personnel and delay summary output. More test data sets need to be run before the prototype is released for use. Improvement of the input procedures along the lines discussed for the final model, should be considered if the prototype is to be used successfully as a demonstration tool.

REFERENCES

1. Hodgson, G. M., "Refueling Capability Assessment Model (RCAM): Users', Analysts', and Programmers' Manual." Technical Report, Assistant Chief of Staff, Studies and Analysis, U.S.A.F, July, 1984.

2. McLean, C. S. and King, D. M., "Handbook for the Fuels Management Officer." Technical Report, AFLMC Project No. LS850520, AFLMC, Gunter A.F.S., Al. 36114, November, 1985.

1986 USAR - UES SUMMER RESEARCH PROGRAM

Sponsored by the
AIR FORCE OFFICE OF SCIENTIFIC RESEARCH
Conducted by the
Universal Energy Systems, Inc.

FINAL REPORT

STATISTICAL PATTERN RECOGNITION MODELLING OF VISUAL PERCEPTIONS

Prepared by:	Robert L. Manicke, Ph.D.
Academic rank:	Assistant Professor
Department and University:	U.S. Naval Academy
Research Location:	Armstrong Aerospace Medical Research, Human Engineering Division
USAF Researcher:	Major Lonnie Roberts
Date:	9 August 1986
Contract No:	F49620-85-C-0013

STATISTICAL PATTERN RECOGNITION MODELLING OF VISUAL PERCEPTIONS

by

Robert L. Manicke, Ph.D.

ABSTRACT

This report is divided into two main sections. The first section develops the context and deductions necessary to construct a probability distribution of perceptual stimulus spaces. The second section propounds the notion of perceptual differentiation by prescribing a probabilistic metric model to mimic the orders from a respondent's point pair comparisons.

Specifically, the first section constructs a probabilistic context for the multidimensional scaling method. This context is generated by considering human pattern recognition as a question of estimating the relative multivariate odds that input stimuli can be associated with some known cognitive populations. The last section models paired comparisons of stimuli by differences of stimulus utilities. Distances between stimuli are derived by probabilistic measurements of these utility differences.

ACKNOWLEDGEMENTS

I wish to acknowledge the sponsorship of the Air Force Systems command, Air Force Office of Scientific Research, and the Armstrong Aerospace Medical Research Laboratory. I also wish to thank Major Lonnie Roberts for his strong encouragement and suggestions.

I INTRODUCTION

Most vision researchers, whether researching machine or biological vision, have a common goal of understanding and conceptualizing the general computational nature of visual perception. Experts widely acknowledge that synergism of many subdisciplines (artificial intelligence, psychophysics, statistical decision theory, neurophysiology, pattern recognition theory, etc.) is necessary for progress towards this understanding. Moreover, computational analysis of visual perception is most beneficial when it uncovers conceptual theories or hypotheses that can be empirically tested.

Many hypotheses on perception have been explored. These hypotheses either assume that the stimuli are random in some manner or that the stimuli are fixed and determined. One such hypothesis concerned with random stimuli assumes that perceptual organization determines the perception of a stimulus field and that this process of organization is evident in the characteristics of the reproduction of the stimulus field (Cooper, 1980). An example of a hypothesis concerned with fixed stimuli is that visual image perceptibility and interpretability are not affected by filter center frequency (Kuperman, 1985).

Recently the concept of a proximity measure has emerged as a computational cornerstone for modelling human perception. For visual perception a proximity measure is an index defined over pairs of images that quantifies the degree to which the two objects are alike as perceived by a respondent at the particular time of measurement. Analyses of these proximity measures have been done almost solely under the purview of a technique known as multidimensional scaling (MDS).

For any specific measurement instrument, to date, all MDS computing algorithms assume quite unrealistically that: (1) the data are valid, true and contain no errors; (2) the metric of the ambient modelling space is static; and (3) the representational geometric configuration of the data is independent of

time. It has been shown empirically that respondents perceptual metrics change with time (Shepard, 1964), but no method has been devised to utilize this finding to perceptual data analyses. Moreover, putative modelling spaces are chosen for their mathematical convenience; there does not exist any theoretical or empirical evidence to justify any specific ambient modelling space.

Manicke (1985) generalizes the geometric foundations of MDS by demonstrating criteria and theorems based on the concept of a monotone metrical transform (von Neumann, 1941). The author also develops the criteria necessary to associate any paired comparison perceptual data to a representative class of metrics (1986) and a class of probability measures, thus obviating the need for the first assumption above.

REFERENCES

Cooper, L. A., Recent themes in visual information processing: A selected overview. In R. S. Nickerson (Ed.), Attention and Performance VIII. Hillsdale, N.J.: Lawrence Erlbaum Associates, 1980.

Kuperman, G. G., July 1985, Bandpass Spatial Filtering and Information Content, AAMRL-TR-85-046.

Manicke, R. L., On the Stochastic Geometrical Foundations of Metric Multidimensional Scaling, Journal of Mathematical Social Sciences 9(1985) 53-62.

Shephard, R., Attention and the Metric Structure of the Stimulus Space, Journal of Mathematical Psychology 1(1964) 54-87.

von Neumann, J., Fourier Integrals and Metric Geometry, Transactions of the American Mathematical Society 50(1941) 226-251.

II. OBJECTIVES OF THE RESEARCH EFFORT

The goals of this research are to develop:

(1) criteria and theorems that characterize utility functions of perceptual data sufficiently to allow application to MDS and proximity measures; and

(2) a consistent theory of utility functions as a canonical basis of proximity measures for MDS; and

(3) a model based on past literature and the new results from proposals (1) and (2) that performs dimension reduction, testing of hypothesized dimensions, and analysis of pattern differentiation for prothetic psychophysical perceptions, in particular visual perceptions.

MAIN SECTION
III

THE UNIQUE EXISTENCE OF A PROBABILITY MEASURE FOR HUMAN PATTERN RECOGNITION

INTRODUCTION

In almost all data analyses there exists an implicit statement about the way the observations vary about the fitted value. Sometimes the model for the distribution of errors is given secondary status being completely overshadowed by the output analyses. In other cases, the methodology has not been sufficiently developed to assume an underlying sampling theory. Both of these are sometimes true when the data exhibit multiple dimensions or are extremely difficult to fit. In these cases most data analyst totally ignore an analysis of errors for any acceptable meaningful or meaningless fit of the data. In the case of multidimensional scaling (MDS), the technology of the fitting process has tended to be the methodological raison d'etre. So far, the analyses of proximity (distance-like) measurements has not lent itself to an underlying measure theoretic sampling theory or a final analysis of errors in the fitting process.

After much experimentation and modelling Shepard (1962) concluded that the proximity measures of the data need not be proportional to the distances but only that the data be monotonically related to the distances. That is, if δ_{ij} represents a proximity measure between stimulus i and j, then any metric model of these measurements must assume there exists a monotonic function on the distances in some metric space into the proximity measures, that is,

$$\delta_{ij} = f(d_{ij}) \text{ such that } d_{ij} \leq d_{i'j'} \rightarrow f(d_{ij}) \leq f(d_{i'j'})$$

for all i, i', j, j'

Kruskal (1964) generalized Shepard's model to assess the degree to which the stimulus co-ordinate estimates (in l_p space) $\hat{x}_{ik}$ and $\hat{x}_{jk}$ reproduce the rank order of the data. These are used in estimating the distance d_{ij} by the standard l_p metric:

$$d_{ij} = \left[\sum_k |\hat{x}_{ik} - \hat{x}_{jk}|^p \right]^{1/p} \quad \text{for some } p,$$

and where the rank images or disparities of the data $\hat{\delta}_{ij}$ are computed to closely mimic the distance estimates, subject to the constraint that they be monotonically related to the original data. That is, $\hat{\delta}_{ij}$ is computed as close to $\hat{d}_{ij}$ as possible to still allow

$$\delta_{ij} < \delta_{i'j'} \Rightarrow \hat{\delta}_{ij} \leq \hat{\delta}_{i'j'} \quad \text{for all } i, i', j, j' .$$

Tucker (1960) shows that, where interpoint distance data are realizable for individual subjects, there exists evidence that dimensionality varies across subjects, and that the separate multidimensional spaces of individuals or groups may differ sharply. Shepard (1962) shows that subjects may fluctuate in attention and in doing so may ignore attributes or in some manner distort the psychological attribute space. If an algorithm for combining individual response differences is to be created, the above findings suggest the foundational assumptionals should be general enough to describe inter and intra individual differences (also see Carroll & Chang, 1970).

FOUNDATIONAL NOTIONS

In view of these developments define

> the(psychological) attribute space of a set of stimuli to be the set of all qualities which are perceived by a class of individuals responding across an index of measurement times.

Stimuli possess attributes in a variety of degrees across individuals which can vary intra-individually at different times. They can be nomologically described by the attribute space. The attribute space can be viewed as having a dimension equal to the number of attributes.

Clearly, since each individual could perceive a set of different qualities from other individuals, the original dimension of an attribute space could be enormous. Realistically, some attributes will be common to some class or classes or even to all respondents. Possibly, some attribute will be present to the same degree or at least imperceptibly different for each subject in some stimuli.. So, by construction, an attribute space could contain a large amount of undifferentiated qualitative redundancy.

To establish any dimension reduction technique modelling an attribute space it is necessary to define:

> a differentiable attribute space as the minimal subset of the attribute space on which stimuli are differentiated by the class of respondents responding across the same index of measurement times. (Hereinafter referred to as S_d)

This definition is to be interpreted only for judgemental or perceptual attributes, that is, the type of attributes Stevens (1957) referred to as prothetic psychophysical continua. This leads to the necessity of excluding those measurements of attributes which are psychophysically unrelated to the attribute. For example, colorblind respondent's data on a test of different hues would be excluded. Again, from the attribute space attributes which are measurably impreceptable in each stimulus for the particular class of respondents would be eliminated. It is necessary to consider orders among stimulus pairs, since this is the only way the proximity data can be experimentally realized. Psychologically, it seems reasonable to model values of an order as a variable for either single subject or group scaling, that is, assume at each measurement response the values of the order among stimulus pairs could change. This variability could be related to the stimuli, attributes, or respondents.

Perception theorist seem to believe that order analyzing large numbers of finite finite subsets of points of an attribute scaling space will give clues to charac terizations of the space itself. In von-Neumann and Shoenberg (1941) it is shown that an order does not, in general, determine any unique metric or geometry of the embedding space, even up to a similarity or change of scale. In fact, they show an order can be isometrically embedded into an infinitude of geometries. Hence, any order among stimulus pairs exhibits a class of metric spaces each of which could represent this order. For any order t denote it s class of representative metric spaces by M_t.

Assume that for every dimension of the attribute space of the stimuli, that the respondent is indifferent to some order values of each stimulus about the value given by the response measurement. More precisely, assume the order value of a stimulus for each dimension is only one point of a subset or range of order values that the respondent finds cognitively not differentiable from the other points in the subset. Since these order values are in a one to one correspondence with points in an embedding space, every stimulus is then represented by a subset of points in this embedding space.

Denote the set of points that represents ,across some class of measurement times, the ith stimulus by S_i. Therefore, to measure and model the responses to the stimuli let the attribute space be modelled by

$S = \{p \mid p \in S_i \text{ for any } i = 1,2...n\} = \bigcup_{i=1}^{n} S_i$ where n is the number of stimuli.

In this framework, MDS theorists putatively conjecture there exists a totally ordered set t and a function $h:SxS \to t$. By this paradigm, the orders are induced on SxS by t and h, and for any particular occasion of measurement

h(SxS) is empirically a finite subset of t. Therefore, t may be considered a subset of the positive reals, and (S,h) is a t-metrized or distance space (Blumenthal, 1953).

More generally, MDS techniques attempt to order embed (S,h) into a predefined metric space (M,ρ), that is, these techniques assume that given any pairs of elements of S, Say (p_1,p_2) and (p'_1,p'_2) there exists a function f:S→M such that

$$h(p_1,p_2) \leq h(p'_1,p'_2) \rightarrow \rho(f(p_1),f(p_2)) \leq \rho(f(p'_1), f(p'_2)).$$

MDS techniques usually assume (M,ρ) to be the standard Euclidean space and metric (Torgerson, 1952) or l_p space with standard metric (Kruskal, 1964). Lew (1978) gives examples of possible empirical distance spaces that have no order embedding into E^n for $n \geq 2$ and other examples which have no order embedding into a general Hilbert space. Thus, demonstrating the necessity of considering more general spaces other than E^n or l_p as the pre-defined scaling metric space (M,ρ).

FOUNDATIONAL GENERALIZATIONS

A natural expansion of the previous paradigms can be developed by considering all sets of points $S_i \times S_j$ and assuming each of the cartesian products corresponds uniquely to some order for every dimension of comparison. Precisely, assume for each $S_i \times S_j$ that there exists totally ordered sets: t_k where k =1,2,...,N (where N is the hypothesized largest dimension) and monotonic functions h_k such that

$$h_k: S_i \times S_j \rightarrow t_k \text{ for each } k .$$

Again, for each order let M_{t_k} be the class of metric spaces that represents the order t_k

By construction of S_d there exists subsets of each S_i such that their union is S_d. This can be written as: for all $i=1,2\ldots,n$ there exists an $A_i \subset S_i$ such that

$$\bigcup_{i=1} A_i = S_d$$

Then for any i, $S_i - A_i$ represents points of the stimulus space S_i that are indistinguishable relative to any other stimulus space.

Since the order among stimulus pairs could change at each response to measurement and since the points from the differentiable attribute space jointly represent all stimuli, this implies the set

$\{t|t$ is a respondents order on any dimension at any time $\alpha\}$

could be infinite.

Consider the mapping

$H: \prod_{i=1}^{N} t_{i\alpha} \to \prod_{i=1}^{n} A_{i\alpha}$ given by $H: (t_{1\alpha}, t_{2\alpha}, \ldots, t_{N\alpha}) \to (A_{1\alpha}, \ldots, A_{n\alpha})$

where $A_{k\alpha} \subset A_k$ for the kth stimulus and for some measurement time α.

$A_{i\alpha}$ shall be called the differentiable stimulus space at time α for the ith stimulus, and represents the ith stimulus at time α.

Then the class of possible orders for a respondent of a fixed set of stimuli determines each A_i by $A_i = \bigcup_{\alpha \in T} A_{i\alpha}$ where T is some time indexing set of a respondents possible orders. In this structure, at each occasion of measurement α, a respondent chooses orders $(t_{1\alpha}, t_{2\alpha}, \ldots, t_{N\alpha})$ which determine a subset $A_{i\alpha}$ for each A_i for all stimuli. So at some time α the points of $A_{i\alpha}$ are psychologically indistinguishable relative to the ith stimulus for a respondent.

If indistinguishability or indifference of points was assumed transitive and each $A_{i\alpha}$ had at least one point in common, then all points of A_i would be

indistinguishable for the respondent relative to the ith stimulus, that is, if $\bigcap_{\text{all } \alpha} A_{i\alpha} \neq \phi$, then A_i contains all points of indifference.

Indeed, if transitivity held, any collection of $A_{i\alpha}$'s that had at least one point in common would contain only points of indifference.

ESTABLISHING A UNIQUE PROBABILITY MEASURE ON A DIFFERENTIABLE ATTRIBUTE SPACE.

Since

$$S_d = \bigcup_{i=1}^{n} A_i \text{ and } A_i = \bigcup_{\alpha \in T} A_{i\alpha}$$

then

$$Sd = \bigcup_{i=1}^{n} \bigcup_{\alpha \in T} A_{i\alpha} \text{ where } S_d \text{ is a metric space with a topological and}$$

measurable structure induced by an admissible metric on S.

Multidimensional scaling can be defined abstractly as the quantization and categorization of attribute data into identifiable classes or point sets via the extraction of significant features or attributes of the data from an original background containing redundant and irrelevant detail. Human perception of patterns may be considered as a psychophysiological problem which involves relationships between a person and physical stimuli. When a person perceives similarities, differences, similar differences or different similarities in stimuli, he/she makes an inductive inference and associates this perception with some general concepts or cues which are derived from past experience. Human pattern recognition and classification can be considered as a question of estimating the relative odds that the input stimuli can be associated with one of a set of known statistical populations which depend on past experience and which form the criteria and the a priori information for classifications. Thus, the general problem of human pattern recognition addressed by multidimensional

scaling may be regarded as one of discriminating among input data, not between individual patterns but between statistical populations of stimuli, via the search for features or invariant attributes among members of populations.

Then, it is both empirically and logically reasonable to assume that at any time α a respondent creates instruments which focus on the local variations of their discrimination or detection abilities relative to the stimuli. These devices or "psychometric probability measures" (Falmagne, 1982) can be modelled as measures of the likelihood of a respondent choosing a set of points in each stimulus space (point set population). Thus, for each stimulus i assume the respondent cognitively constructs a probability measure ν_i that determines the likelihood of a class of subsets of A_i. Hence, by construction for each stimulus space $i = 1,\ldots,n$ and at a specific time α

$$\nu_i(A_{i\alpha}) = 1 \text{ and } \nu_i(A_i - A_{i\alpha}) = 0 .$$

Since each stimulus space is covered by subsets representing points of indifference at a specific time, construct a topology F_i for each A_i by letting each $A_{i\alpha} \in F_i$, with finite intersections and arbitrary unions of $A_{i\alpha}$'s also being elements of F_i. Under this topology for each i

$$\bigcup_{\alpha \in T} A_{i\alpha} \text{ is an open cover of } A_i$$

If transitivity of indifference does not hold, it is quite possible any two stimulus spaces may have points in common, that is, for $i \neq j$ possibly $A_i \cap A_j \neq \phi$. Indeed, suppose at some time α: $\nu_i|_{A_{i\alpha} \cap A_{j\alpha}} \neq \nu_j|_{A_{i\alpha} \cap A_{j\alpha}}$

but if for the respondent the ith stimulus was indistinguishable to the jth stimulus then

$$A_{i\alpha} = A_{j\alpha} \text{ and}$$
$$1 = \nu_i(A_{i\alpha}) \neq \nu_j(A_{j\alpha}) = 1$$

Therefore, assume at any time of measurement α, that

$$\nu_i|_{A_{i\alpha} \cap A_{j\alpha}} = \nu_j|_{A_{i\alpha} \cap A_{j\alpha}}$$

To derive any algorithm to help locate an unknown $A_{i\alpha}$ in a pre-specified embedding space $S_d = M$ it is necessary that there exists a unique probability measure on S_d, say ν such that $\nu|_{A_{i\alpha}} = \nu_i$ for any α

To show the unique existence of a probability measure ν given the conditions it is sufficient to assume each $A_{i\alpha}$, for any i and α, is compact. This is reasonable because it can be interpreted as the space of points that represents the ith stimulus at time α is not unbounded in it's interpoint distances, that is, for the respondent the points that are psychologically indistinguishable for the ith stimulus lie in some "small" region made precise by the compact hypothesis. To construct a unique ν based on these hypotheses some probabilistic structure must be defined:

> Let $A_{i\alpha}$ denote a compact topological space (subspace of A_i) and let $C(A_{i\alpha})$ denote the vector space of all continuous functions mapping $A_{i\alpha}$ into the reals for any i and α.

The space $C(A_{i\alpha})$ will be regarded as a normed vector space under the supremum norm:

$$\|g\| = \sup_{y \in A_{i\alpha}} |g(y)|$$

The support of a real function g on the topological space $A_{i\alpha}$ is defined as the closure of the set $\{y | y \in A_{i\alpha}, g(y) \neq 0\}$.
This shall be denoted by supp (g). Let $CK(A_{i\alpha})$ denote the space of continuous functions on $A_{i\alpha}$ with compact support.

The following two theorems can be found in or derived from results in Bourbaki (1974) Topologie Generale, chapters 5-10 or Bourbaki (1965) Integration chapters 1-4 and shall be quoted without justifications.

Theorem 1 Let U be an open covering of a compact toplogical space Y. There exist finitely many C(Y) functions $g_1, g_2, \ldots, g_n$ with the following properties:

(1) $g_i \geq 0$,

(2) $g_1 + \ldots + g_n = 1$,

(3) any of the g_i's has its support contained in a set from U.

Theorem 2 Let g denote a CK(Y)-function on the locally compact space Y and let U denote a collection of open sets covering supp(g). There exist finitely many CK(Y) functions $g_1, \ldots, g_n$ with the following properties:

(1) $g_1 + \ldots + g_n = g$,

(2) any of the function g_i has its support contained in a set from U ,

(3) for $g \geq 0$, $g_i \geq 0$.

Classical probability theory has developed from the foundational axioms and structure propounded by Kolmogorov (1933). Many of the same results have been obtained from the theory given by Radon (1913). Whereas classical probability measures (integrates) classes of sets, Radon probability theory with integrals (measures) of CK(Y) functions generalizes to a larger collection of functions, then measures the same class of sets.

Since every point in S_d is contained in at least one $A_{i\alpha}$ it has a compact neighborhood; namely, any $A_{i\alpha}$ that contains it; hence, S_d is locally compact. A Radon probability measure on a locally compact space S_d is a linear mapping $u: CK(S_d) \rightarrow$ Reals such that for any $g \in CK(S_d)$, $g \geq 0$ implies $u(g) \geq 0$, with total mass equal one (Dieudonne, 1968).

To construct a consistent unique (Radon) probability measure on S_d it is sufficient to demonstrate the following:

Lemma Let $g_1,\ldots,g_n$ be $CK(S_d)$ - functions with $supp(g_k) \subset A_{k\alpha}$ such that $g_1+\ldots+g_n = 0$. Then $u_1(g_1|_{A_{1\alpha}}) + \ldots + u_n(g_n|_{A_{n\alpha}}) = 0$.

Proof: This lemma shall be justified by induction. For $j = 1$ the lemma is obviously true. Suppose it is true for $n = j$ such functions. Now suppose $g_1+\ldots+g_j + g_{j+1} = 0$ with $supp(g_k) \subset A_{k\alpha}$. Then

$$g_{j+1} = -(g_1+\ldots+g_j) \text{ implies}$$

$$Supp(g_{j+1}) \subset supp(g_{j+1}) \cap \bigcup_{i=1}^{j} supp(g_i)$$

$$\subset A_{j+1\alpha} \cap \bigcup_{i=1}^{j} A_{i\alpha} = \bigcup_{i=1}^{j} (A_{i+1\alpha} \cap A_{i\alpha})$$

From theorem 2. g_{j+1} can be written as $g_{j+1} = f_1+\ldots+f_j$ where $supp(f_i) \subset A_{j+1} \cap A_i$. Hence, $(g_1 + f_1) +\ldots+ (g_j + f_j) = 0$ and the support of each $(g_i + h_i) \subset A_{i\alpha}$. From the inductive hypothesis it can be concluded that

$$0 = u_1((g_1 + f_1)|_{A_{1\alpha}}) +\ldots+u_j((g_j + f_j|_{A_{j\alpha}})$$

$$= u_1(g_1|_{A_{1\alpha}}) +\ldots+u_j(g_j|_{A_{j\alpha}})+u_1(f_1|_{A_{1\alpha}})+\ldots+u_j(f_j|_{A_{j\alpha}}).$$

with consistent applications of theorem 2. and diligent algebra this can be shown to equal

$$u_1(g_1|_{A_{1\alpha}}) +\ldots+u_j(g_j|_{A_{j\alpha}}) + u_{j+1}(f_1|_{A_{j+1\alpha}})+\ldots+u_{j-1}(f_j|_{A_{j-1\alpha}})$$

$$= u_1(g|_{A_{1\alpha}})+\ldots+u_j(g_j|_{A_{j\alpha}}) + u_{j+1}(g_{j+1}|_{A_{j+1\alpha}})$$

Now again if the respondent evokes a psychometric probability measure u_i to choose with probability one $A_{i\alpha} \subset A_i$ which represents the points of A_i that are

indistinguishable at the time α relative to the ith stimulus, then the following theorem shows that these u_i's can be combined to form a consistent "overall" probability measure.

Theorem Let S_d be a locally compact space such that $S_d = \bigcup_{i=1}^{n} \bigcup_{\alpha \in T} A_{i\alpha}$, where each $A_{i\alpha}$ is considered an open set of S_d. If for each i there exists a probability measure u_i such that

$$u_i|_{A_{i\alpha} \cap A_{j\alpha}} = u_j|_{A_{i\alpha} \cap A_{j\alpha}} \quad \text{for all } i \neq j,$$

then there exists a unique probability distribution u on S_d such that $u|_{A_{i\alpha}} = u_i$ for all i

Proof: First, let h be an arbitrary $CK(S_d)$ function. By theorem 2, h can be written as $h = h_1 + \ldots + h_n$, where the supports of $h_1 + \ldots + h_n$ are contained in sets $A_{1\alpha}, A_{2\alpha}, \ldots, A_{n\alpha}$ of the open covering of S_d.

But

$$u(h) = u(h_1) + \ldots + u(h_j)$$

$$= (u|_{A_{1\alpha}})(h|_{A_{1\alpha}}) + \ldots + (u|_{A_{n\alpha}})(h_n|_{A_{n\alpha}})$$

$$= u_1(f_1|_{A_{1\alpha}}) + \ldots + u_n(h_n|_{A_{n\alpha}})$$

Hence, any decomposition of h as a sum of $CK(S_d)$ functions with supports contained in sets of the open covering of S_d determines u(h). Hence, at most one measure with the given restrictions can exist.

In order to define u by the above structure it must be shown that any two different decompositions $h = h_1 + \ldots + h_m$ and $h = g_1 + \ldots + g_k$, where $\text{supp}(f_i) \subset A_{i\alpha}$ and $\text{supp}(g_i) \subset A_{i\alpha}$ of the function h give the same result or

$$\nu_1(h_1|_{A_{1\alpha}}) + \ldots + \nu_m(h_m|_{A_{m\alpha}}) = \nu_1(g_1|_{A_{1n}}) + \ldots + \nu(g_n|_{A_{kn}})$$

Let $n=m+k$ and denote $-g_1$ by h_{m+1}, $-g_2$ by $h_{m+2}, \ldots, -g_k$ by h_n. So what must be proved is: if $f_1, \ldots, f_n$ are $CK(S_d)$ functions with $\text{supp}(f_j) \subset A_{j\alpha}$ such that $f_1 + \ldots + f_n = 0$, then $\nu_1(f_1|_{A_{1\alpha}}) + \ldots \nu_n(f_n|_{A_{n\alpha}}) = 0$. Which is exactly a restatement of the lemma.

Discussion and Summary

Since MDS is the modelling of perceptions from paired comparison data into some random abstract geometry, a theoretical basis general enough to develop probabilistic considerations such as sampling space or sampling errors is minimally essential. In the concepts just developed the pair

$$(S_d, \nu)$$

consisting of a locally compact topological space S_d (which is taken to be some admissible metric space) and the (Radon) probability measure ν, S_d is considered a sample space for some MDS experient. The notion is that S_d is the set of possible outcomes of the stochastic experiment of a respondent perceiving pairs of fixed stimuli with ν the distribution of these outcomes, that is, for any ν-measurable set $B \subset S_d$, $\nu(B)$ should be interpreted as the probability of the event that the random outcome falls in point set B.

By considering human pattern recognition as a problem of discriminating between a priori statistical populations representing stimuli (not among individual patterns) through the search for features and invariant attributes a unique probability measure of time oriented stimulus point sets has been shown to exist. This is accomplished by assuming these time oriented point sets representing stimuli are compact and the a-priori psychometric probability functions are consistent across stimulus populations at a fixed time.

1986 USAF-UES SUMMER FACULTY RESEARCH PROGRAM/

GRADUATE STUDENT SUMMER SUPPORT PROGRAM

Sponsored by the

AIR FORCE OFFICE OF SCIENTIFIC RESEARCH

Conducted by the

Universal Energy Systems Inc.

FINAL REPORT

AN EXPERIMENTAL DESIGN TO VERIFY THE AFGL FASCOD2 FOR WATER VAPOR AND CARBON DIOXIDE AT LOW TEMPERATURES AND PRESSURES

Prepared by:	Arthur A. Mason
Academic Rank:	Professor
Department and University:	Department of Physics and Astronomy Space Institute The University of Tennessee
Research Location:	Arnold Engineering Development Center Arnold AFS TN 37389-5000
USAF Researcher:	Dr W. K. McGregor
Date:	August 20, 1986
Contract No:	F49620-85-C-0013

AN EXPERIMENTAL DESIGN TO VERIFY THE AFGL FASCOD2 FOR WATER VAPOR AND CARBON DIOXIDE AT LOW TEMPERATURES AND PRESSURES

by

ARTHUR A. MASON

ABSTRACT

The AFGL FASCOD2 (Fast Atmospheric Signature Code) is a model and computer program for accelerated line by line calculation of spectral transmittance and radiance for atmospheric problems. This summer research project was devoted to designing an experiment to verify the model and programs of FASCOD2 under conditions experienced in test cell environments at altitude, that is, conditions of low temperatures and pressures. Preliminary spectral measurements were made showing satisfactory comparison. A secondary objective evolved during the research: The design and development of a high altitude spectroscopy calibration laboratory for basic infrared measurements of gases of interest to the Air Force.

ACKNOWLEDGEMENTS

It is my pleasure to recognize with appreciation the following organizations and individuals:

The United States Air Force Systems Command and the Office of Scientific Research for Sponsoring the Summer Faculty Research Program;

Universal Energy Systems, Inc. for conducting the program in an efficient and pleasant manner;

The Arnold Engineering Development Center for providing a stimulating environment;

Mr Marshall K. Kingery, The Focal Point at AEDC, for his encouraging efforts in coordinating the program;

Dr Wheeler K. McGregor of Sverdrup Technology, Inc., for suggesting the research topic;

Mr Michael Scott of Sverdrup Technology, Inc., for his dedicated assistance in the laboratory;

Mr Robert Hiers of Sverdrup Technology, Inc., for his knowledgeable coordination of the computer programming.

I. INTRODUCTION

The absorption, emission, and scattering of radiant energy by the constituent gases of a test environment or the atmosphere provide powerful diagnostic techniques for understanding physical processes. The Air Force and its contractors at the Arnold Engineering Development Center have found the science of infrared spectroscopy to be well suited to the task of remotely determining the composition, concentrations, and temperatures of gases associated with the testing and development of propulsion systems. At the same time the refinement of computer simulated spectra by groups such as the Air Force Geophysics Laboratory has contributed much to the planning of measurements and the interpretation of spectroscopic data. The benefits of computer generated spectra are maximized when their applicability is verified for the conditions under which the measurements are to be made.

It is the purpose of this research to plan that verification for a particular case. The AFGL FASCOD2 (Fast Atomospheric Signature Code) is a radiation model and computer program for the accelerated line by line calculation of spectral transmittance and radiance for atmospheric problems. The source of spectral line information may be the AFGL Line-by-Line Compilation of Molecular Spectroscopic Parameters or equivalent line data. Accurate and detailed knowledge not only of the spectral line parameters but also of their temperature and pressure dependence and of atmospheric transmission of radiation is essential for input into the model and database and for correct

interpretation of data. The computer generated spectra of FASCOD2 can be very useful to the engineers and scientists at AEDC if it can be verified that the model predictions match measurements in the test cell environment.

II. OBJECTIVES

A. The primary objective of this research project is to design an experiment to verify the predictions of the AFGL FASCOD2 and AFGL Line-By-Line Compilation under conditions experienced in test cell environments at high altitude - i.e., under conditions of low temperature and low pressure. Specific objectives are:

1. Determine the present status of research in this area,

2. Focus initial studies on water vapor and carbon dioxide as two active infrared gases which are often of dominate importance in acquiring and interpreting infrared spectra. It should be noted that accurate water vapor spectra are important in determining absolute humidity and in determining atmospheric effects on the data from a source to be analyzed. Carbon dioxide spectra provide a remote and sensitive temperature probe but also interfer with source radiation propagated through the atmosphere. Suitable spectral regions of these gases will be selected for study.

3. Design the measuring instruments and techniques needed to evaluate the model under controlled laboratory conditions. The question to be answered is "does FASCOD2 correctly predict the effect of low temperatures and pressures on the spectral line parameters and hence the resulting spectra?"

B. An important secondary objective evolved during the research project: the design and development of a High Altitude Spectroscopy Calibration Laboratory which makes possible the study of the physics of molecular interactions through high resolution infrared measurements of gases in simulated high altitude environments of interest to the Air Force and other government agencies.

III. BACKGROUND OF CURRENT RESEARCH

1. ATTENDANCE AT AFGL WORKSHOPS

The Air Force Geophysics Laboratory presented two workshops: (i) The Tri-Service Cloud Modeling Workship, and (ii) The Review Conference on Atmospheric Transmission Models. These workshops brought me into direct contact with the people and the research most pertinent to the summer project and are briefly summarized here.

Cloud research is focused currently on cloud simualtion models and cloud structure which are important in communications and remote sensing. Active areas of research include: the study of infrared cloud signatures for purposes of detection and identification, examination of transmission windows, reduction of background clutter, and infrared measurements of cloud temperatures. Two emerging areas of cloud researches are: ground based laser soundings and fractal simulation clouds by computer modeling.

Atmospheric transmission research is focused on particulate emission and climatology on the one hand and molecular absorption and emission on the other. Of immediate relevance to this Summer research project was the report of a new version of the atmospheric absorption line parameters compilation (HITRAN database). The structure of the

database has been expanded to allow for additional molecular parameters such as self broadened linewidths, temperature dependence of halfwidths, line shifts and transition moments that extend the capabilities to upper atmospheric comparisons. There were reported several comparisons between observed atmospheric transmissions spectra and calculated spectra but no comparisons of low temperature low pressure laboratory spectra of water vapor or carbon dioxide for comparison with computer generated spectra. The current status of the AFGL atmospheric transmittance and background radiance models, FASCOD 2 and LOWTRAN 6 was discussed. New features in FASCOD include new molecular atmospheric profiles up to 120KM. The adddition of all the aerosol models and diffuse molecular absorption species, new cloud and rain models, a non local thermodynamic equilibrium option for upper atmospheric applications, and a weighting function option for remote sensing problems.

2. BIBLIOGRAPHY

A literature review revealed that few laboratory mesurements have been undertaken on low temperature low pressure water vapor and carbon dioxide infrared radiation and that such measurements would be useful in validating FASCOD 2 in the regimes of interest to AF-AEDC.

The literature review and the workshops stressed the importance of continuum absorption by water vapor in the infrared region. Absorption in the atmospheric windows is usually greater than that predicted on the basis of known intensities, widths, and theoretical line shapes because of continuum absorption. Since communication and remote sensing systems operate in the infrared

windows of the atmosphere, the ability to predict the attenuation within these windows under different atmospheric conditions is of utmost importance. Water vapor continuum is responsible for much of the window absorption in the lower atmosphere, however laboratory measurements at low temperatures to determine the effects of H_2O concentration on the continuum absorption and hence window transmission have yet to be made. Figure 1 illustrates the poor window transmission throughout the near and mid-infrared regions. The bibliography contains some of the references which were examined.

3. THEORY

The transmmittance of radiation through a gas is given by the expression

$$\tau = \exp\left(-\int k(\nu)\, d\nu\right)$$

where k_ν is the absorption coefficient

u is the absorber thickness

The absorption coefficient of a single line is related to the true transmittance of the line (observed with infinite resolving power) by

$$k(\nu) = -\frac{1}{u} \ln \tau$$

To calculate spectral absorption contours for complex absorping optical paths extensive consideration must be given to the spectral line shape, that is to the functional definition of the absorption coefficient. For a single isolated pressure broadened absorption line the absorption coefficient is given by the Lorentz expression.

$$k(\nu) = \frac{S}{\pi} \frac{\alpha_L}{(\nu-\nu_0)^2 + \alpha_L}$$

where S is the line strength or line intensity, α_L is the Lorentz half width, ν_0 is the frequency or Wavenumber of the line center in units of cm^{-1}.

The Lorentz half width is a function of both pressure and temperature:

$$\alpha_L(p,T) = \alpha_L(p_0,T_0)\left(\frac{p}{p_0}\right)\left(\frac{T_0}{T}\right)^n$$

where p_0 and T_0 are standard pressure and temperature, p_0 = latm, T_0=296K. Recent measurements and theory have shown that

$$0.5 \leq n \leq 1.0$$

varying from molecule to molecule and line to line. The FASCOD2 database provides an n for each molecule. The value of n is important since most measurements of α_L are made at room temperature whereas temperatures at high altitudes are some 100K colder. The pressure broadened half width is a function of the absorbing molecules and the quantum states involved in the transition. At sufficiently low pressures, Doppler broadening (thermal motion) dominates and the absorption coefficient is given by

$$k(\nu) = \frac{S}{\alpha_D \pi^{1/2}} \exp\left(-\left[(\nu-\nu_0)/\alpha_D\right]^2\right)$$

where

$$\alpha_D = \frac{\nu_0}{c}\left(2KT/M\right)^{1/2}$$ Doppler Half width

If the Lorentz and Doppler half widths are of the same magnitude a convolution of the two known as the Voight profile is used. In many cases the two half widths do not become equal until pressure and temperatures are those of the mid-stratosphere. FASCOD uses an approximation to the Voight line shape to reduce a prohibitive amount of computational time in performing line by line calculations. The

largest error in determining the Voight half width with this approximation is found to be of the order of 0.02%. Returning to the transmittance for a single spectral line

$$\tau(\nu) = I_\nu / I_0 = \exp\left(-k(\nu)\, u\right)$$

We define the optical depth as the product of the absorption coefficient and the absorber thickness

$$\phi(\nu) = k(\nu)\, u$$

where various units may be used for the absorber thickness,

$$u\ (\text{atm cm}_{STP}) = p\, L\ 273/T$$

$$u\ (\text{gm } H_2O\ \text{cm}^{-2}) = 8.04 \times 10^{-4}\ p\, L\ 273/T$$

$$u\ (\text{molecules cm}^{-2}) = 2.69 \times 10^{19}\ p\, L\ 273/T$$

IV. EXPERIMENT DESIGN

In the design of the experiment to validate FASCOD2 several factors must be considered:

(a) the selection of optimal spectral regions for observing the infrared absorption of water vapor and carbon dioxide;

(b) the selection of altitudes to be simulated, that is, the pressures, temperatures, partial pressures of the infrared active gases, and path lengths which will provide a satisfactory comparison between observed and computed spectra;

(c) the selection of instrumentation for measurement.

The selection of the spectral regions and the environment to be observed, that is (a) and (b), will govern the selection of instrumentation. Therefore synthetic spectra were computer generated

using the AFCL FASCOD 2 and AFCL Line Parameters Compilation for Line by Line calculations to survey the fundamental vibration-rotation bands of H_2O and CO_2 at various altitudes and path lengths. The water molecule fundamental bands are centered at 6.27, 2.74, and 2.66μm; the CO_2 bands are at 15 and 4.3 μm. Altitudes of 6km and 12km were chosen for initial study because their conditions are more readily achievable in the laboratory than those at higher altitudes while at the same time simulating realistic conditions found in the troposphere. Based on the computer simulated spectra all of the fundemental bands are sufficiently intense at altitudes of 6km and 12km to provide a good comparison of FASCOD2 with laboratory measurements. Futher consideration led to the selection of the 2.73 μm region for H_2O and the 4.25 μm region for CO_2. L. D. Nelson has shown that absorption measurements at 2.66 can theoretically be expected to give a valid measurement of water vapor density over a dynamic range of at least four order of magnitude in absolute humidity. Further, in this region the absorption will be more sensitive to water vapor than to liquid water or ice and this is an important factor in the rejection of hydrometeors in the sample volume and possible water and ice on instrument windows. These factors are illustrated in Figure 2. Although the CO_2 band at 15μm is an intense band there are some problems with interference from ozone and water vapor in the atmosphere. This together with the strong temperature dependence of the Planck function in the 4.3μm region made that the region of choice.

Final arguments for selecting these spectral regions for the initial validation are that both H_2O and CO_2 can be observed with a single experimental setup where excellent sources, detectors, windows, etc are available.

Several alternatives were considered in the selection of instrumentaion for measuring the spectra. These included radiometers, grating spectrometers, diode lasers, and Fourier transform spectrometers (FTS). A Nicolet FTS was chosen because of its combination of broad spectral range, moderately high resolution, and availability. The broad spectral range allows the comparison of observation and FASCOD2 over a wide wavenumber interval and consequently an almost unlimited choice for determining the best narrow band on which to base a field instrument for humidity measurements. The theoretical resolution of $0.06cm^{-1}$ is necessary if meaningful comparisons are to be made with the line-by-line calculations of FASCOD.

V MEASUREMENTS

Measurements were made of the near infrared water vapor band at $2.73\,\mu m$ between $3630cm^{-1}$ and $3670cm^{-1}$ and of the CO_2 band of $4.25\,\mu m$ between $2320\ cm^{-1}$ and $2380cm^{-1}$. These measurements were made at room temperature and a total pressure of less than 1 torr using the Nicolet Fourier Transform Spectrometer with a globar source, a pyroelectric detector and a one meter path length. Although these preliminary measurements have as their purpose the evaluation of the instrument, the laboratory observed spectra correspond well with the computer generated spectra of FASCOD2 as can be seen in Figure 3.

VI DESIGN AND ASSEMBLY OF LABORATORY

The final stage of the summer research project involves developing an experimental approach to laboratory measurements at low temperatures and pressures to fit existing requirements and equipment at AF-AEDC. An excellent three meter high vacuum low temperature test cell designed and built for another purpose has been made available for the measurements discussed above.

The cell can be evacuated to pressure of 10^{-6} microns and cooled to temperatures of less than 200K simulating altitudes to 100KM. The cell functions in the following manner. Water vapor at chosen conditions will be introduced into the cell by flowing cold air over ice until saturation is reached. At that time the temperature and concentration of the water vapor are known and spectral measurements will be made for comparision with computer generated FASCOD 2 spectra. The union of this cold cell with the Fourier transform spectrometer and appropriate computational and instrumental components has been initiated. This has required the design of the optical path and the selection of appropriately matched infrared instrument and optical components which assembled will provide a unique and flexible high altitude spectroscopy calibration laboratory.

Since the initial measurements are to be made in the near infrared between 2.5μm and 4.5μm the components are chosen to optimize the signal in this spectral region and minimize all other signals. A high intensity source of radiation is provided by a quartz halogen tungsten filament lamp. The detector is an indium antimonide photovoltaic device responding from 2.0μ to 5.5μ with a $D^* \geq 10^{11}$.

This detector is enclosed in a sidelooking metal dewar operating at liquid nitrogen temperature and views radiation through a sapphire window which has excellent transmission to 5.5μm. The detector mount which has been designed and is being built may require cooling. A calcium fluoride lens collects the radiation emerging from the cold cell and focuses it onto the detector element. The windows isolating the cold cell from the FTS and for the detector housing are optical quality polished calcium fluoride crystals chosen for their excellent environmental characteristics as well as their near 95% transmission in the region of interest. The optical path throught the cold cell is a modified white cell design which provides a 12 meter path length through the absorbing gas chosen as a result of calculations and examinination of computer generated H_2O spectra at simulated 40,000 feet altitude. Because of the design of the cold cell it was not possible to install the multiple path white cell optics at this time although that should be done in the future. The mirrors which direct the radiation through the cold cell are 50mm in diameter with a 3 meter radius of curvative. Figure 4 is a schematic diagram of the system.

The short term thrust of the fellowship research has been the design of a series of measurements to establish the usefulness of FASCOD2 as a planning and diagnostic tool in conjunction with observation in test cell environments. However, the long term value will be the development of this high altitude spectroscopy calibration laboratory which will be used for high resolution infrared measurements of low temperature gases of interest to the Air Force.

VII RECOMMENDATIONS

1. Guidelines for implementing my research.

The design of the laboratory is completed and the necessary components are identified and being brought together. Machining for mounting the detector, connecting the low temperature cell to the spectrometer, and installing windows is underway or completed. The mirrors are to be installed. Vacuum checks are being run on the cold cell. When the assembly of the systems is completed, the optics will need to be aligned and their ability to maintain alignment at low temperatures checked. There will need to be shakedown runs for evaluating the system as a whole and the instrument function for the entire system will need to be determined.

2. Suggestions for Follow-on Research.

When the laboratory is functioning there are two related projects which should be undertaken immediately.

a. The actual measurements of the infrared spectra of water vapor and carbon dioxide at the low temperature and low pressure conditions corresponding to altitudes of 40,000 feet and higher must be made and compared with the computer generated spectra of the AFGL FASCOD2.

b. Measurements of the effects of continuum absorption at low temperatures in the atmospheric windows between 3 and 5 micrometers has not been done and should be done to verify extrapolations of higher temperature experiments which are now used in FASCOD2.

3. Suggestions for Future Research.

Accurate measurement and modeling of radiative transfer is basic to understanding the complex interplay between the chemical, radiative, and dynamical processes that govern the atmosphere or test environments simulating the atmosphere. Valid measurements and effective modeling are dependent on the accuracy to which spectroscopic parameters and their variation with temperature and pressure are known for radiatively active atmospheric gases. The recent NASA Assessment of Present State of Knowledge of the Upper Atmosphere points to major requirements for basic studies in laboratory spectroscopy, including:

a. Line intensities: spectral parameters are needed for several infrared bands of major and trace constituents where data are either totally missing or of poor quality.

b. Line widths: improved knowledge of air broadened half widths and their temperature dependence is needed for nearly all of the optically active atmospheric species;

c. Other requirements: laboratory studies are required for line shapes, accurate integrated intensities and band models, improved models for the temperature and pressure dependence of the water vapor continuum, improved parameters for transitions involved in non-LTE radiative transfer in the upper atmosphere, and more accurate absorption coefficients.

The High Altitude Spectroscopy Calibration Laboratory when completed will be uniquely suited to carrying out many of the above measurements which are of vital interest to the scientific community at large and to the Air Force whose working environment is the atmosphere.

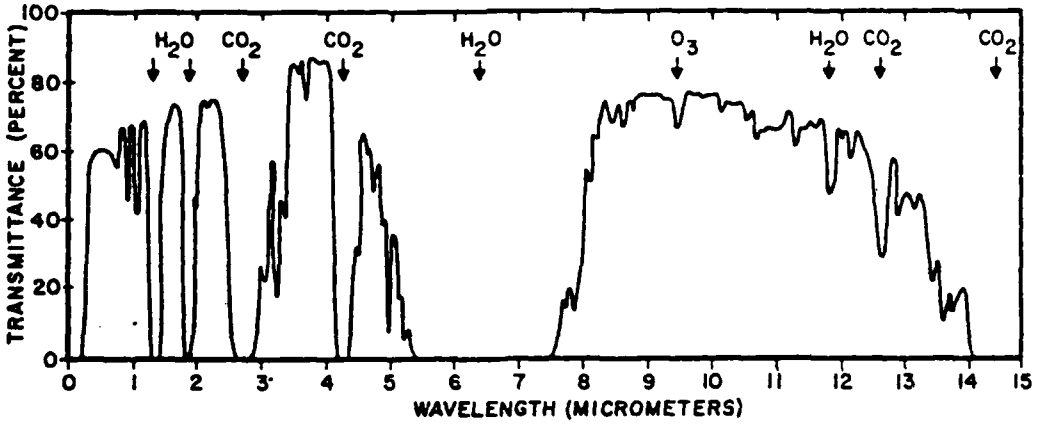

Figure 1. Spectral transmission characteristics of the atmosphere. Arrows identify some spectral regions in which water, carbon dioxide and ozone cause significant transmission loss.

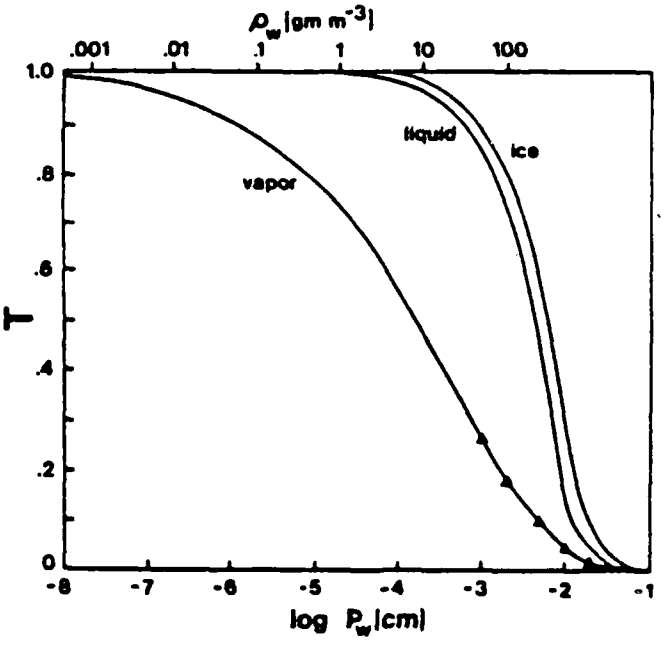

Fig. (2) Water Vapor Transmissivity at 2.665 micrometers

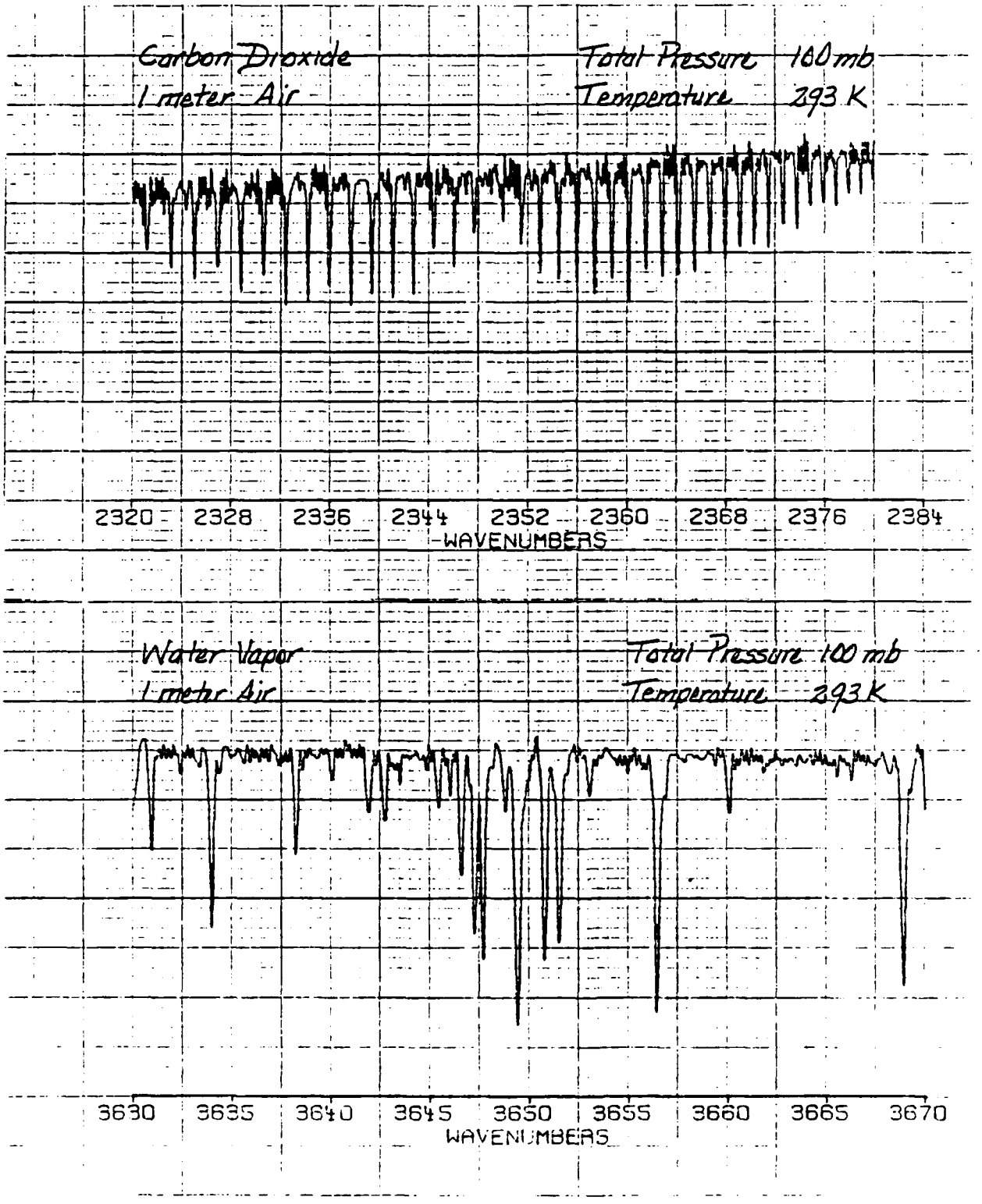

Figure 3. Spectra: H_2O at 2.73 μm & CO_2 at 4.25 μm

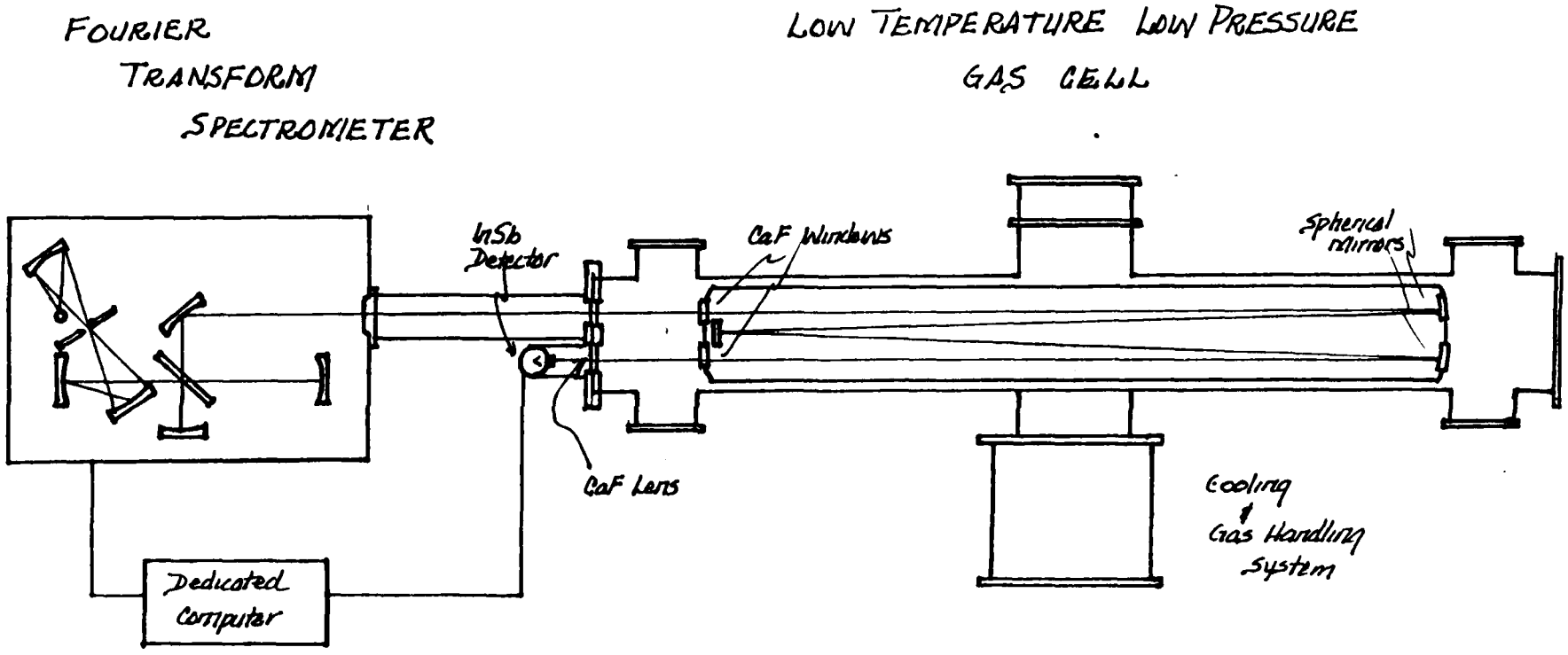

Figure 4. HIGH ALTITUDE SPECTROSCOPY CALIBRATION LABORATORY

REFERENCES

Articles and Reports

1. Clough, S.A. Kneizys, F.X., Shettle, E.P., and Anderson, G.P. Atmospheric Radiance and Transmittance: FASCOD 2 Sixth Conference on Atmospheric Radiation, 1986.

2. Nelson, L.D., Theory, Electro-Optical Design, Testing, and Calibration of a Prototype Atmospheric Supersaturation, Humidity, and Temperature Sensor. AFGL-TR-32-0283

3. Watson, R.T., Geller, M.A., Stolarski, R.S., and Hampson, R.F. Present State of Knowledge of the Upper Atmosphere: An Assessment Report NASA Reference Publication 1162 May 1986.

Conferences and Journal Publications:

1. Conference on Atmospheric Radiation, Fort Collins, Colorado August 7-9, 1972 American Meterological Society

2. Journal of Geophysical Research, Volume 89 No. D4, June 30, 1984 American Geophysical Union

3. Atmospheric Transmission, Robert W. Fenn, Editor Proceeding of SPIE Volume 277 (1981)

Books

1. Deepak, A., Wilkerson, T.D., Rutinke, L.H., Editors Atmospheric Water Vapor, Academic Press, 1980.

1986 USAF-UES SUMMER FACULTY RESEARCH PROGRAM/

GRADUATE STUDENT SUMMER SUPPORT PROGRAM

Sponsored by the

AIR FORCE OFFICE OF SCIENTIFIC RESEARCH

Conducted by the

Universal Energy Systems, Inc.

FINAL REPORT

THE DETERMINATION OF LEAD IN BLOOD

Prepared by:	Curtis W. McDonald
Academic Rank:	Professor of Chemistry
Department and	Department of Chemistry
University	Texas Southern University
Research Location:	USAF Occupational and Environmental Health Laboratory
	Analytical Services Division
	Occupational Chemistry Branch
	Metals Section
USAF Researcher:	Leo Jehl and Doris Tessmer, Collaborators
Date:	July 20, 1986
Contract No:	F49620-85-C-0013

The Determination of Lead in Blood

by

Curtis W. McDonald, PhD

ABSTRACT

Lead in blood is determined at USAFOEHL using an atomic absorption spectrophotometer equipped with a graphite furnace. The low melting point of lead causes its loss due to vaporization at the charring step prior to the measurement of lead. This leads to errors in the method. Ammonium phosphate has been recommended as a matrix modifier to react with lead to form high melting lead phosphate which should permit the utilization of higher charring temperatures. Ammonium phosphate did not prove to be a good matrix modifier. A theory was developed to explain the limited usefulness of ammonium phosphate. The rough surface of the graphite tube at the charring temperature (500°C to 600°C) in an enert argon gas atmosphere is an excellent reducing medium. It appears highly unlikely that the phosphate, which has a pentavalent phosphorus attached to four oxygen atoms, would be stable under such a reducing atmosphere. The lead phosphate would probably decompose to metallic lead which would instantly melt at the charring temperature and begin to vaporize causing a loss of lead.

Acknowledgements

I would like to thank the Air Force Systems Command and the Air Force office of Scientific Research for sponsorship of my research. I would like to express my appreciation to Colonel James C. Rock, the Vice Commander of USAFOEHL and Focal Point of the USAF-UES Summer Faculty Research Program and Colonel Bruce J. Poitrast, consultant in occupational medicine for providing an intellectually stimulating environment for my research. Finally, I would like to thank Leo Jehl and Doris Tessmer of the Metal Section who worked with me daily and shared their limited space and facilities with me.

I. Introduction

I received my PhD from the University of Texas at Austin where I developed a spectrophotometric method for determining the element osmium. I later served as a research associate at the Oak Ridge National Laboratory in Oak Ridge, Tennessee where I developed an extraction method for removing cadmium from aqueous solutions using high-molecular-weight amines.

The United States Air Force Occupational and Environmental Health Laboratory (USAFOEHL) receives blood samples from Air Force personnel throughout the world for blood-lead assays. The laboratory currently uses a stabilized temperature platform furnace (STPF) atomic absorption spectrophotometric method with Zeeman background correction for determining the lead in blood. The method often gives a negative deviation to Beer's Law. This deviation results in some uncertainty in the lead determinations.

My experience in developing analytical methods at the University of Texas at Austin and the Oak Ridge National Laboratory gives me the research background to critically evaluate the USAFOEHL method for the determination of lead in blood and suggest methods for improvement. Because of this research background, I was assigned to work on the blood-lead method in the Metals Section at USAFOEHL.

II. Objectives of the Research Effort

The overall objectives of the Metals Section at USAFOEHL is to determine various metals in air, bulk samples, and biological fluids.

My individual objectives were as follows:

1. Become very familiar with the scientific literature associated with determining lead and other metals in blood and other biological fluids.

2. Acquire the special analytical techniques needed to handle, preserve and analyze biological fluids.

3. Learn to perform the STPF analytical methods which USAFOEHL uses to determine lead in blood and urine.

4. Develop the necessary techniques to routinely perform other analytical methods which USAFOEHL uses to determine metals such as cadmium, mercury, arsenic, tin, silver, and selenium in air and bulk samples.

5. Improve the USAFOEHL method to determine blood-lead by modifying the currently used STPF method.

6. Write a proposal to the Air Force Office of Scientific Research to continue research on the problems associated with determining lead in blood and urine at Texas Southern University.

III. The Determination of Lead

The adverse effects of lead are now well recognized and documented. Lead reportedly interferes with a number of body functions, notably the central nervous system, the hematopoietic system and the kidney (1,2). The quantity of lead in blood may be regarded as a reliable index to the extent of recent lead intake. Therefore, accurate and reliable analytical methods for its determination in blood are very useful in the diagnosis of lead poisoning and monitoring the working environment.

The introduction of atomic absorption spectrophotometry by Walsh in 1955 dramatically changed the method of determining blood-lead (3). Prior to this time, the primary method for determining lead was chelation with dithizone followed by extraction and colorimetry. By 1967, over 5,000 flame atomic absorption instruments were in use throughout the world. These instruments proved to be very good for determining lead in the milligrams per liter range. Due to the high toxicity of lead which has a normal range of 5 to 40 micrograms per deciliter in blood, more sensitive methods were needed. The sensitivity of determining blood-lead was increased to the micrograms per liter level by the development of the graphite furnace by L'vov in 1959 (4,5). The graphic furnace is electrically heated and has undergone a number of advances since it was first introduced by L'vov. Typically, a few microliters of blood are deposited in a graphite tube, or on a tantalum ribbon, a carbon rod or a graphite platform. The blood sample is successively dried, charred and atomized. The concentration of lead is determined during the atomization step.

IV. The USAFOEHL Method for Determining Lead in Blood

In the USAFOEHL procedure for determining lead in blood, the blood samples are removed from the refrigerator and allowed to come to room temperature. The blood sample is mixed gently by inverting the tube 12 to 15 times. Vigorous mixing must be avoided to prevent hemolyzing the blood. A 1.0 mL blood sample is immediately pipetted and diluted with 9.0 mL of 0.1% triton-x-100 surfactant in a 15 mL polypropylene

capped centrifuge tube. The resulting solution is mixed thoroughly for 10 seconds using a Vortex-Genie. A 1.5 mL sample is placed in a plastic cup. The sample is then ready to be measured.

The samples are measured using a Perkin-Elmer-Zeeman Model 5000 atomic absorption spectrophotometer equipped with a HGA-500 graphite furnace and AS-40 autosampler. Pyrolytically coated graphite tubes having grooves to proper position the graphite platform were used with the pyrolytic graphite platforms.

Zeeman Model 5000 Parameters

Wavelength - 283.3 nm

Slit Width - 0.7 nm

Calibration Mode - Peak Area

Current - 10 ma

Intergration Time - 5 Sec

Purge Gas - Argon

HGA Graphite Furnace Parameters

			Ramp	Hold
Step	Function		(Seconds)	
1	Dry	110°C	5	45
2	Char	530°C	5	45
3	Atomize	2300°C	0	7
4	Cleanout	2600°C	1	3
5	Cool	20°C	1	20

V. The Blood-Lead Analysis Problem

The USAFOEHL's problem in analyzing lead in blood is shared by more than 200 laboratories using the graphite furnace technique throughout the world. The problem can be associated with the unusually low melting point of lead (327°C) which causes difficulties when it is determined using graphite furnace techniques. The melting points of other common metals such as copper (1,083°C), iron (1,535°C) and chromium (1,857°C) are much higher. The problem associated with the low melting point of lead occurs during the charring step in the graphite furnace. The charring procedure is carried out to rid the blood sample of the bulk materials associated with the lead and interfere with the final measurement. These include blood cell fragments, anticoagulants, other biomolecules and triton-x-100. Due to the extraordinarily large quantities of these materials in blood, a high charring temperature of at least 900°C is needed to clean the sample.

The charring temperature used at USAFOEHL is 530°C. At this temperature, the charring process is probably not complete. However, a higher charring temperature should not be used to avoid a greater loss of lead due to vaporization. Even at 530°C which is 200°C higher than the melting point of lead, some loss of lead unfortunately does occur due to vaporization. Ideally, no vaporization of lead should occur prior to the atomization step. The loss of lead during the charring step can be attributed at least partially to the failure of the USAFOEHL method to follow Beer's Law.

The highly qualified and experienced USAFOEHL chemists have skillfully manipulated the various instrumental and methodic parameters to make excellent blood-lead analyses using the STPF technique. The most recent certification samples sent from the Center for Disease Control (CDC) were analyzed and in excellent agreement with CDC results. Yet, the failure to follow Beer's Law remains a problem. The analysts feel uncertain about some of the results.

VI. The Use of Matrix Modifiers

The problems associated with the determination of blood-lead using a graphite furnace has been known for about 15 years. During that time, more than 50 research papers and a number of research conferences have been devoted to the problem. Perhaps, the best idea to emerge from this research activity was the addition to blood samples substances called matrix modifiers. The concept of matrix modifiers was initiated by Ediger in 1975 when he recommended the addition of nickel to selenium to improve the determination of selenium (6). Nickel reacts with selenium which has a melting point of only 217°C to form nickel selenide which melts at a much higher temperature. A much higher temperature can now be used to determine selenium. The matrix modifier concept has been applied to blood-lead problems. Subramanian and Meranger recommended the use of $NH_4H_2PO_4$ as a matrix modifier for blood-lead (7). Fernandez and Hilligoss recommended the use of a Mg-$(NH_4)_2HPO_4$ solution as a matrix modifier (8). In both cases, the investigators theorized that lead phosphate which has a melting point of 1,014°C was formed prior to the charring step.

A number of investigators continue to be troubled with the loss of lead during the charring step when $NH_4H_2PO_4$ or Mg-$(NH_4)_2HPO_4$ solutions are added to the blood samples as matrix modifiers. The USAFOEHL chemists and I have tried to use these matrix modifiers to increase charring temperatures with very little success. Even with the Mg-$(NH_4)_2HPO_4$ solution, Fernandez and Hilligoss recommended a charring temperature of only 600°C, far below the temperature necessary to completely char the blood samples (8). There are two possible explanations for the failure of ammonium phosphate's failure to serve as an effective matrix modifier. The lead in the blood sample may not have reacted with the ammonium phosphate to form the high melting lead phosphate. A second possible explanation is that lead phosphate did form but decomposed to metallic lead during the charring process. I believe the second explanation is the case.

The rough surface of the graphite platform at 530°C in an inert gas argon atmosphere is an excellent reducing medium. In my opinion, it is highly unlikely that the phosphate, which has a pentavalent phosphorus atom attached to four oxygen atoms, would be stable in such a reducing atmosphere. It seems likely that the lead phosphate will decompose producing lead oxide (PbO) which will susequently be reduced to lead metal. The metal instantly melts at the charring temperature and begins to vaporize causing a loss of lead.

VII. Recommendations

1. I was not able to find a suitable matrix modifier during my ten week study at the USAFOEHL. A number of other compounds form stable

high melting products with lead. These include selenium, tungstic acid and ammonium molybdate. These compounds should be studied as potential matrix modifiers.

2. Lead is a contaminant in most commercially sold chemicals. It will be very difficult to purchase lead free ammonium molybdate, selenium and tungstic acid. The chemicals should be purchased at the highest possible parity and further purified using ion-exchange and solvent extraction techniques.

References

1. Tsuchiya, K., Handbook on the Toxicology of Metals, Amsterdam, Holland, Elsevier/North Holland Biomedical Press, 1978

2. Dudley, D.M., Critique, Blood Lead Analysis, 1981, Atlanta, Georgia, U.S. Department of Health and Human Services, Center for Disease Control Report, 1982

3. Walsh, A., "The Application of Atomic Absorption Spectra to Chemical Analysis", Spectrochim. Acta, 7, (1955) 108-117

4. L'vov, B.V., "Investigation of Atomic Absorption Spectra by Complete Vaporization of the Sample in a Graphite Cuvette", Inzh. Fiz. Zh., 44 (1959) 2-6

5. L'vov, B.V, "Twenty-Five Years of Furnace AAS", Spectrochim. Acta, 39, (1984) 149-158

6. Ediger, R., "Atomic Absorption Analysis with the Graphite Furnace Using Matrix Modification", At. Absorption Newslett., 3 (1975) 127-130

7. Subramanian, K.S., and J.C. Meranger, " A Rapid Electrothermal AAS Method for Cadmium and Lead in Human Whole Blood", Clin. Chem, 27 (1981) 1866-71

8. Fernandez, F.J., and D. Hilligoss, "An Improved Graphite Furnace Method for the Determination of Lead in Blood Using Matrix Modification and the L'vov Platform", At. Spectrosc., 3 (1982) 61-65

1986 USAF-UES SUMMER FACULTY RESEARCH PROGRAM/

GRADUATE STUDENT SUMMER SUPPORT PROGRAM

Sponsored by the

AIR FORCE OFFICE OF SCIENTIFIC RESEARCH

Conducted by the

Universal Energy Systems, Inc.

FINAL REPORT

COMPATIBILITY OF REINFORCEMENT AND MATRIX PHASES IN COMPOSITE MATERIALS FOR HIGH-TEMPERATURE, AEROSPACE APPLICATIONS

Prepared by: Gopal M. Mehrotra

Academic Rank: Assistant Professor

Department and

University: Materials Science and Engineering Program,
Mechanical Systems Engineering Department,
Wright State University, Dayton, Ohio

Research Location: AFWAL Materials Laboratory (MLLM),
Wright-Patterson Air Force Base, Ohio

USAF Researcher: Mr. K. S. Mazdiyasni

Date: August 25, 1986

Contract No.: F49620-85-C-0013

COMPATIBILITY OF REINFORCEMENT AND MATRIX PHASES IN COMPOSITE MATERIALS FOR HIGH-TEMPERATURE, AEROSPACE APPLICATIONS

by

GOPAL M. MEHROTRA

ABSTRACT

The mutual chemical compatibility of the matrix and reinforcement materials, for ceramic-ceramic and ceramic-intermetallic composites, was analytically evaluated with the help of thermodynamic calculations. In the case of ceramic-ceramic composites, the chemical stability of TiC, AlN, TiB_2, HfC, and ZrC in a matrix of Al_2O_3, ZrO_2 or HfO_2 was evaluated. In the case of intermetallic-ceramic composites, Al_2O_3, TiC, TiB_2, SiC, Si_3N_4, and AlB_{12} were evaluated as reinforcement phases in a matrix of Ni_3Al. More work on analytical and experimental evaluations needs to be done for ceramic-ceramic composites.

In addition, experimental work was initiated to synthesize silicon hexaboride, which has been reported to have very good oxidation resistance up to $\sim$ 1530°C.[1] It was found that the reaction between the silicon and boron powders is sluggish, and that an accurate control of conditions during hot-pressing is necessary. The products of syntheses were characterized by x-ray diffraction (XRD). Further experiments to standardize the conditions for synthesis of SiB_6, and to characterize it by analytical electron microscopy, thermogravimetric analysis (TGA), and differential thermal analysis (DTA) need to be carried out.

ACKNOWLEDGEMENTS

I would like to thank the Air Force Systems Command, the Air Force Office of Scientific Research, and the AFWAL/MLLM Materials Laboratory for the sponsorship of this research. The award of an UES-USAF Summer Fellowship is gratefully acknowledged. I would particularly like to thank several members of the AFWAL/MLLM staff at Wright-Patterson Air Force Base, Ohio: Mr. K. S. Mazdiyasni for giving me the opportunity to do this resarch and his constant support, encouragement, and guidance; Dr. A. P. Katz, Mr. E. E. Hermes, Mr. R. Kerans, and Dr. H. A. Lipsitt, for their interest in my work; Dr. H. Graham for providing access to his library; Mr. Jerry Barlowe of UES, for preparation of graphite dies and assistance with arc melting, and Mr. Joe Henry of UES for his help with microprobe analysis. The help of Lou Henrich in typing this report is gratefully acknowledged.

I. INTRODUCTION:

I received my Ph.D. degree from the Technical University Berlin, West Berlin, Germany; my research work involved thermodynamic studies of binary oxide and oxide-fluoride mixtures. Subsequently, as a post-doctoral fellow, at the University of Pennsylvania and at Arizona State University, I did work on intercalation compounds, diffusion of sulfur in stabilized zirconia, high-temperature oxidation of nickel sulfide, thermodynamic properties of nickel sulfide and iron sulfide, and electrical properties of stabilized zirconia. At the University of Arizona, where I was a visiting lecturer, I was involved in research concerning the stability of ceramic crucibles during vacuum induction melting of nickel base superalloys. My background is, therefore, in the area of high-temperature materials.

The research work at the AFWAL/MLLM Materials Laboratory, Wright-Patterson Air Force Base, involved analytical evaluation of the mutual chemical compatibility of the matrix and reinforcement materials in ceramic-ceramic and ceramic-reinforced intermetallic composites for high-temperature, aerospace applications. The research problem also involved studies on synthesis and characterization of silicon boride, which has been reported to have inherent, good oxidation resistance up to $\sim$ 1530°C.[1]

The research problem at the AFWAL Materials Laboratory was, therefore, well suited to my previous background and experience in the areas of high-temperature materials and thermodynamics. In view of this, I was assigned to study the compatibility of matrix and reinforcement phases in composites for high-temperature applications, and to synthesize and characterize an oxidation resistant compound, SiB_6, which may be useful as a ceramic material in composites.

II. OBJECTIVES OF THE RESEARCH EFFORT:

The overall objective of the research effort was to obtain an understanding of the chemistry at the interfaces of the constituent

materials of a composite during processing, and its relationship with the microstructure and properties of the composite. Specifically, my objectives were:

(1) To screen the ceramic reinforcement materials, on the basis of their chemical compatibility with the matrix materials, for the purpose of making ceramic composites. This was to be accomplished by carrying out thermodynamic calculations and, thereby, evaluating the stability of a reinforcement material in a given matrix. The matrix materials chosen were: ZrO_2, HfO_2, Al_2O_3, and Ni_3Al.

(2) To identify, on the basis of the results of thermochemical evaluation, the systems which would be suitable for further, experimental studies.

(3) To do a thorough literature search on the composites containing silicon boride, reported to have very good oxidation resistance up to 1530°C.

(4) To synthesize and characterize SiB_6.

III. EVALUATION OF CHEMICAL COMPATIBILITY OF REINFORCEMENT AND MATRIX PHASES:

The analytical evaluations are based on the thermodynamic data available in the literature.[2-6] For the ceramic-ceramic composites, the materials chosen for the matrix phase are Al_2O_3, ZrO_2, and HfO_2, having the melting points of 2072, 2700, and 2758°C, respectively. For the reinforcement phase, the materials evaluated are TiC, AlN, TiB_2, HfC, and ZrC which have the melting points of 3140, 2200, 2900, 3890, and 3540°C, respectively. In addition, Al_2O_3, TiC, AlB_{12} SiC, Si_3N_4, and TiB_2 have been evaluated as reinforcement materials for the Ni_3Al matrix.

(a) Ceramic-Ceramic Composites:

(1) TiC as a reinforcement phase in the matrix of Al_2O_3, ZrO_2, or HfO_2.

The reactions between TiC and the various oxide matrix materials can be written as follows:

$$3TiC + 2Al_2O_3 = 3TiO_2 + Al_4C_3 \quad (1)$$
$$TiC + Al_2O_3 = TiO + Al_2O + CO \quad (2)$$
$$TiC + 2Al_2O_3 = TiO_2 + CO_2 + 2Al_2O \quad (3)$$
$$3TiC + Al_2O_3 = 3\underline{Ti} + 2\underline{Al} + 3CO \quad (4)$$
$$3TiC + 5Al_2O_3 = 3 \langle TiO_2 \cdot Al_2O_3 \rangle + Al_4C_3 \quad (5)$$
$$TiC + ZrO_2 = TiO_2 + ZrC \quad (6)$$
$$TiC + 2ZrO_2 = TiO + 2ZrO + CO \quad (7)$$
$$TiC + HfO_2 = TiO_2 + HfC \quad (8)$$

In addition, the chemical reactions between the solid products of a reaction and the matrix or reinforcement phases may also take place, e.g., a reaction between TiC and ZrC leading to the formation of a complex carbide. Such reactions can sometimes result in the formation of low melting phases. However, there are not enough thermodynamic data available for these reactions. Some other reactions can also be written. These have been evaluated to be not feasible.

The feasibility of reactions (1)-(8) has been evaluated using the standard Gibbs energy of formation data[3-6] for the various compounds involved in these reactions. The results of the calculations are given in Table I. In this table, as well as in all the other tables, the values of standard free energy change, $\Delta G°$, for various reactions are in calories. The subscripts in the symbols $\Delta G°_i$ and K_i refer to the reaction number. Thus, $\Delta G°_1$ and K_1, are the standard free energy change and equilibrium constant, respectively, for reaction (1). The results in Table I show that reactions (1) and (5) are not feasible. Reactions (2)-(4) and (7) involve gaseous products (Al_2O, CO, CO_2, and ZrO) and would be driven from left to right if these products were continually

removed from the reaction site. Reactions (6) and (8) would be feasible, if ZrC and HfC form complex carbides with TiC and their activities are low. Therefore, TiC and Al_2O_3 should be compatible with each other, except at very low pressures. Of the three oxide matrix materials considered, HfO_2 appears to be the least compatible with TiC.

TABLE I

Thermodynamic Data for Reactions (1)-(8)

ΔG° Reaction K Reaction	Temperature (°K) 1873	1973	2073
ΔG°_1 K_1	172,538 7.34×10^{-21}	171,020 1.13×10^{-19}	169,502 1.34×10^{-18}
ΔG°_2 K_2	77,015 1.03×10^{-9}	67,444 3.38×10^{-8}	57,873 7.91×10^{-7}
ΔG°_3 K_3	186,515 1.72×10^{-22}	172,464 7.84×10^{-20}	158,413 1.98×10^{-17}
ΔG°_4 K_4	175,373 3.43×10^{-21}	160,512 1.65×10^{-18}	145,651 4.40×10^{-16}
ΔG°_5 K_5	159,700 2.31×10^{-19}	158,464 2.79×10^{-18}	157,228 2.65×10^{-17}
ΔG°_6 K_6	29,027 4.10×10^{-4}	28,801 6.45×10^{-4}	28,575 9.71×10^{-4}
ΔG°_7 K_7	206,501 7.99×10^{-25}	193,933 3.28×10^{-22}	181,365 7.54×10^{-20}
ΔG°_8 K_8	17,586 8.87×10^{-3}	17,550 0.011	17,514 0.014

(2) AlN as a reinforcement phase in the matrix of Al_2O_3, HfO_2, or ZrO_2.

The reactions considered between the reinforcement phase and matrix materials are:

$$4AlN + Al_2O_3 = 3Al_2O + 2N_2 \quad (9)$$
$$2AlN + 2Al_2O_3 = 3Al_2O_2 + N_2 \quad (10)$$
$$4AlN + 3ZrO_2 = 2Al_2O_3 + 3ZrN + 1/2N_2 \quad (11)$$
$$4AlN + 3HfO_2 = 2Al_2O_3 + 3HfN + 1/2N_2 \quad (12)$$

The standard Gibbs energy change and equilibrium constants for the above reactions are given in Table II. As there are no high-temperature data available for the Gibbs energy of formation of HfN, the thermodynamic stability of HfN has been assumed to be the same as that of ZrN. This is reasonable, in view of the fact that the values of heat of formation of HfN and ZrN and of their entropies at 298K are comparable to each other.

TABLE II

Thermodynamic Data for Reactions (9)-(12)

ΔG° Reaction K Reaction	Temperature (°K) 1873	1973	2073
ΔG°_9	174,082	151,687	129,292
K_9	4.85×10^{-21}	1.57×10^{-17}	2.33×10^{-14}
ΔG°_{10}	268,104	249,030	229,956
K_{10}	5.17×10^{-32}	2.59×10^{-28}	5.68×10^{-25}
ΔG°_{11}	-8,850	-10,842	-12,834
K_{11}	10.78	15.89	22.55
ΔG°_{12}	-16,926	-18,228	-19,530
K_{12}	94.44	104.55	114.61

The results shown in Table II indicate that reactions (9) and (10) are not feasible except at very low pressures [lower than $\sim 1.7 \times 10^{-4}$ - 3.7×10^{-3} atm for reaction (9), and 2.7×10^{-8} - 1.5×10^{-6} atm for reaction (10)]. Thus, AlN and Al_2O_3 should be mutually compatible. The values of K for reactions (11) and (12) are large, and therefore, AlN is not compatible with ZrO_2 and HfO_2, especially with HfO_2.

(3) TiB_2 as a reinforcement phase in a matrix of Al_2O_3, ZrO_2 or HfO_2.

We can consider the reactions of TiB_2 with the oxide matrix materials:

$$2TiB_2 + 2Al_2O_3 = 2AlB_2 + 2TiO_2 + Al_2O_2 \quad (13)$$

$$TiB_2 + Al_2O_3 = B_2O_3 + \underline{Ti} + 2\underline{Al} \quad (14)$$

$$TiB_2 + ZrO_2 = TiO_2 + ZrB_2 \quad (15)$$

$$TiB_2 + HfO_2 = TiO_2 + HfB_2 \quad (16)$$

From the available thermodynamic data,[3-6] we can calculate the results given in Table III.

These results show that of the three oxides, HfO_2 is the least compatible with TiB_2, and Al_2O_3 is the most compatible.

TABLE III

Thermodynamic Data for Reactions (13)-(16)

ΔG° Reaction / K Reaction	Temperature (°K) 1873	1973	2073
ΔG°_{13}	222,272	215,900	209,528
K_{13}	1.15×10^{-26}	1.21×10^{-24}	8.10×10^{-23}
ΔG°_{14}	116,107	112,826	109,545
K_{14}	2.83×10^{-14}	3.17×10^{-13}	2.82×10^{-12}
ΔG°_{15}	24,276	24,200	24,125
K_{15}	1.47×10^{-3}	2.08×10^{-3}	2.86×10^{-3}
ΔG°_{16}	14,478	14,338	14,198
K_{16}	0.020	0.026	0.032

(4) ZrC as a reinforcement material in a matrix of Al_2O_3, ZrO_2 or HfO_2.

The reactions between ZrC and the matrix materials can be written as:

$$3ZrC + 2Al_2O_3 = Al_4C_3 + 3ZrO_2 \quad (17)$$

$$3ZrC + Al_2O_3 = 3\underline{Zr} + 2\underline{Al} + 3CO \quad (18)$$

$$ZrC + 2ZrO_2 = 3ZrO + CO \quad (19)$$

$$2ZrC + ZrO_2 = 3Zr + 2CO \quad (20)$$

$$2ZrC + HfO_2 = 2\underline{Zr} + \underline{Hf} + 2CO \quad (21)$$

$$ZrC + HfO_2 = ZrO_2 + HfC \quad (22)$$

The standard Gibbs energy change and equilibrium constants for the above reaction are given in Table IV.

TABLE IV

Thermodynamic Data for Reactions (17)-(22)

ΔG° Reaction / K Reaction	Temperature (°K) 1873	1973	2073
ΔG°_{17}	85,457	84,617	83,777
K_{17}	1.07×10^{-10}	4.23×10^{-10}	1.47×10^{-9}
ΔG°_{18}	188,389	173,768	159,147
K_{18}	1.04×10^{-22}	5.62×10^{-20}	1.66×10^{-17}
ΔG°_{19}	283,684	267,823	251,961
K_{19}	7.86×10^{-34}	2.14×10^{-30}	2.72×10^{-27}
ΔG°_{20}	133,061	124,131	115,201
K_{20}	2.97×10^{-16}	1.77×10^{-14}	7.14×10^{-13}
ΔG°_{21}	130,369	121,669	112,969
K_{21}	6.12×10^{-16}	3.32×10^{-14}	1.23×10^{-12}
ΔG°_{22}	-11,441	-11,251	-11,061
K_{22}	21.60	17.60	14.70

The results of Table IV show that reactions (17)-(21) are not feasible, but reaction (22) is. ZrC will, therefore, not be compatible in a matrix of HfO_2. It is, however, compatible with ZrO_2 and Al_2O_3.

(5) HfC as a reinforcement material.

The reactions between HfC and matrix materials can be written as:

$$3HfC + 2Al_2O_3 = Al_4C_3 + 3HfO_2 \quad (23)$$
$$3HfC + Al_2O_3 = 3Hf + 2Al + 3CO \quad (24)$$
$$HfC + ZrO_2 = HfO_2 + ZrC \quad (25)$$
$$2HfC + ZrO_2 = 2\underline{Hf} + \underline{Zr} + 2CO \quad (26)$$
$$2HfC + HfO_2 = 3Hf + 2CO \quad (27)$$

The calculated thermodynamic data for the above reactions are given in Table V.

TABLE V

Thermodynamic Data for Reactions (23)-(27)

ΔG° Reaction / K Reaction	Temperature (°K) 1873	1973	2073
ΔG°_{23}	119,781	118,371	116,961
K_{23}	1.05×10^{-14}	7.71×10^{-14}	4.66×10^{-13}
ΔG°_{24}	214,636	200,135	185,634
K_{24}	8.98×10^{-26}	6.75×10^{-23}	2.68×10^{-20}
ΔG°_{25}	11,441	11,251	11,061
K_{25}	0.046	0.057	0.068
ΔG°_{26}	150,560	141,710	132,860
K_{26}	2.69×10^{-18}	2.00×10^{-16}	9.81×10^{-15}
ΔG°_{27}	147,867	139,247	130,627
K_{27}	5.56×10^{-18}	3.75×10^{-16}	1.69×10^{-14}

These results show that HfC is compatible with Al_2O_3 and HfO_2. However, some reaction is possible between HfC and ZrO_2.

(b) Ceramic-Intermetallic (Ni_3Al) Composites:

Evaluations for six reinforcement materials, namely, Al_2O_3, AlB_{12}, TiB_2, TiC, SiC, and Si_3N_4 were made on the basis of available thermodynamic data[3-7] for these compounds and Ni_3Al. Due to a lack of space, only some of the results of calculations will be given here.

The upper and lower bounds of the activities of Ni and Al in Ni_3Al have been estimated from the standard Gibbs energy of formation of Ni_3Al.[6-7] These results are given in Table VI.

TABLE VI

Thermodynamic Data for Ni_3Al

T(°K)	$\Delta G°$ (cal/mol)	$a_{Ni}^3 \cdot a_{Al}$	Lower bounds of	
			a_{Ni}	a_{Al}
1000	-34,300	3.18×10^{-8}	5.03×10^{-3}	7.54×10^{-8}
1100	-33,530	2.18×10^{-7}	9.55×10^{-3}	5.17×10^{-7}
1200	-32,760	1.08×10^{-6}	0.016	2.56×10^{-6}
1300	-31,990	4.18×10^{-6}	0.026	9.91×10^{-6}
1400	-31,220	1.34×10^{-5}	0.038	3.18×10^{-5}
1500	-30,450	3.66×10^{-5}	0.053	8.68×10^{-5}

The upper bounds of the activities of Ni and Al in Ni_3Al are 0.75 and 0.25, respectively. All the data in the above table are for stoichiometric Ni_3Al.

(1) Al_2O_3 as a reinforcement phase in Ni_3Al.

Consider the following reaction of Al with Al_2O_3:

$$4Al + Al_2O_3 = 3Al_2O \qquad (28)$$

For this reaction, we calculated the thermodynamic data given in Table VII.

TABLE VII

Thermodynamic Data for Reaction (28)

T(°K)	$\Delta G°$ (cal)	K	Range of P_{Al_2O}
1000	167,350	2.64×10^{-37}	$2.04 \times 10^{-22} - 1.01 \times 10^{-13}$
1200	144,648	4.51×10^{-27}	$5.79 \times 10^{-17} - 2.60 \times 10^{-10}$
1500	110,595	7.67×10^{-17}	$1.63 \times 10^{-11} - 6.69 \times 10^{-7}$

Therefore, reaction (28) is not feasible, except at extremely low pressures. Similar calculations for the reaction leading to the formation of Al_2O_2 have shown that this reaction, too, is not feasible.

Reaction of Ni with Al_2O_3:

$$3Ni + Al_2O_3 = 3NiO + 2Al \qquad (29)$$

For reaction (29), we calculate the data given in Table VIII.

TABLE VIII

Thermodynamic Data for Reaction (29)

T(°K)	$\Delta G°$ (cal)	K	$a^2_{\underline{Al}}/a^3_{\underline{Ni}}$ (min)	a_{NiO} (max)
1000	217,930	2.33×10^{-48}	1.35×10^{-14}	5.57×10^{-12}
1200	214,650	8.01×10^{-40}	1.55×10^{-11}	3.72×10^{-10}
1500	209,730	2.75×10^{-31}	1.79×10^{-8}	2.49×10^{-8}

The above results show that reaction (29) is also not feasible. Therefore, Al_2O_3 appears to be a good candidate as reinforcement material for the Ni_3Al matrix.

(2) AlB_{12} as a Reinforcement Phase in Ni_3Al.

(i) Reaction of $\underline{Al}$ with AlB_{12}

$$5\underline{Al} + AlB_{12} = 6AlB_2 \qquad (30)$$

For reaction (30), calculations yield the data given in Table IX.

TABLE IX

Thermodynamic Data for Reaction (30)

T(°K)	$\Delta G°$ (cal)	$a_{\underline{Al}(eqbm)}$	$a_{\underline{Al}}$ (in Ni_3Al - Lower Bound)
1000	-33,440	0.035	7.54×10^{-8}
1200	-27,484	0.10	2.56×10^{-6}
1500	-18,550	0.29	8.68×10^{-5}

It can be seen from the above table that $a_{\underline{Al}(eqbm)}$, at 1000 and 1200°K, lies between the lower and upper bounds of $a_{\underline{Al}}$ in Ni_3Al. Reaction (30) may, therefore, be feasible. At 1500°K, however, the reaction is not feasible as $a_{\underline{Al}(eqbm)}$ is greater than the upper bound of a_{Al} in Ni_3Al.

(ii) Reaction of Ni with AlB_{12} and AlB_2

$$12\underline{Ni} + AlB_{12} = 12NiB + \underline{Al} \quad (31)$$
$$16\underline{Ni} + AlB_{12} = 4Ni_4B_3 + \underline{Al} \quad (32)$$
$$2\underline{Ni} + AlB_2 = 2NiB + \underline{Al} \quad (33)$$
$$8\underline{Ni} + 3AlB_2 = 2Ni_4B_3 + 3\underline{Al} \quad (34)$$
$$2\underline{Al} + 6\underline{Ni} + AlB_{12} = 6NiB + 3AlB_2 \quad (35)$$

The results given in Table X are obtained from the thermochemical calculations for the above reactions.

TABLE X

Thermodynamic Data for Reactions (31)-(35)

	Temperature (°K)		
	1000	1200	1500
$\Delta G°_{31}$	-429,200	-424,756	-418,090
$a_{Ni,eq\ (max)}$	1.36×10^{-8}	3.18×10^{-7}	7.47×10^{-6}
$\Delta G°_{32}$	-221,600	-215,636	-206,690
$a_{Ni,eq\ (max)}$	8.61×10^{-4}	3.22×10^{-3}	0.012
$\Delta G°_{33}$	-65,960	-66,212	-66,590
K_{33}	2.61×10^{14}	1.15×10^{12}	5.05×10^{9}
$a_{\underline{Al}}/a^2_{\underline{Ni}}$ (max) in Ni_3Al	9.88×10^{3}	9.77×10^{2}	89.0
$\Delta G°_{34}$	-94,080	-94,076	-94,070
K_{34}	3.65×10^{20}	1.36×10^{17}	5.09×10^{13}
$a^3_{\underline{Al}}/a^8_{\underline{Ni}}$ (min) in Ni_3Al	4.28×10^{-21}	1.68×10^{-16}	6.53×10^{-12}
$\Delta G°_{35}$	-231,320	-226,120	-218,320
$(a^3_{\underline{Ni}} \cdot a_{\underline{Al}})$ eq.	5.25×10^{-26}	2.55×10^{-21}	1.24×10^{-16}

The above results show that reactions (31)-(35) are feasible.

On the basis of the evaluations in Table X, one concludes that AlB_{12} will not be a good candidate for reinforcement of the Ni_3Al matrix.

As stated earlier, due to a lack of space, the data obtained from other calculations will not be given here. However, results of evaluations of other materials are as follows; (i) TiB_2 would not be compatible with Ni_3Al, (ii) TiC is a good candidate for reinforcement of Ni_3Al, (iii) No definitive conclusions can be drawn regarding the compatibility of SiC and Si_3N_4 in the Ni_3Al matrix.

IV. LITERATURE SEARCH ON THE REFRACTORY COMPOSITES CONTAINING SiB_6:

The literature search revealed that very little work has been accomplished to characterize SiB_6. Cline[8] synthesized SiB_6 and characterized it using the x-ray diffraction technique. He reported the x-ray data and also the lattice parameters calculated therefrom. The crystal structure of SiB_6 is orthorhombic. Feigelson[1] reported that this compound has very good oxidation resistance up to $\sim$ 1530°C. Rizzo and Bidwell[9] have characterized SiB_4 using the x-ray diffraction technique. Rizzo, et al.[10] also studied the properties of SiB_6 dispersed in a borosilicate matrix and reported that the new refractory is stable in air above 1550°C and has a good thermal shock resistance.

Studies on the composites of SiB_6 and Al_2O_3 or ZrO_2 or HfO_2 are scant. In an application for a patent, the research laboratories of Union Carbide report that the refractory composites containing silicon boride and ZrO_2 or HfO_2, together with some carbonaceous material, have good oxidation resistance due to a protective coating formed on the surface and are impermeable and machineable.[11] It therefore seems desirable to study the oxidation resistance of SiB_6 and its refractory composites.

V. EXPERIMENTS ON SYNTHESIS AND CHARACTERIZATION OF SiB_6:

Several attempts were made to synthesize SiB_6 from silicon and boron powders. The silicon used was crystalline and of 99.99% purity. The boron used was crystalline in some experiments and amorphous in others. Both of the starting materials, silicon and boron were characterized by x-ray diffraction using CuKα radiation. The crystalline boron was determined to be of rhombohedral crystal structure. In the case of amorphous boron, a sharp peak was observed at $2\theta = 28.3°$, indicating the presence of B_2O_3. This, however, is not surprising, in view of the submicron particle size and very high reactivity of amorphous boron which results in its oxidation at the surface. The amorphous boron was therefore handled in a controlled atmosphere dry box. In spite of this, some oxidation of boron was unavoidable.

The approaches taken to synthesize SiB_6 included: (i) Hot-pressing of stoichiometric mixtures of boron and silicon powders, (ii) Arc melting cold compacted stoichiometric powder mixtures, as well as, mixtures containing excess silicon or boron, and (iii) Hot-pressing pre-reacted (at $\sim$ 1200°C) mixtures of boron and silicon powders. The products of synthesis were characterized using x-ray diffraction. An attempt was also made to characterize one of the samples using a scanning electron microscope (SEM) and an energy dispersive x-ray analyzer (EDAX) to obtain a line scan for silicon and a microprobe to quantitatively analyze the sample for Si. Density measurements were also made.

The characterization of the synthesized products by x-ray diffraction revealed the following: (i) there are inhomogeneities in the samples as regards the distribution of phases, (ii) the presence of silicon is easily detectable in almost all the samples, (iii) some boron carbide is formed in the hot-pressed samples as a result of a reaction with graphite die, (iv) other boron silicides are possibly also formed, and (v) occasionally there were peaks (reflections) corresponding to some unidentifiable phases.

Characterization of a sample using SEM, EDAX, and microprobe showed a somewhat inhomogeneous distribution of silicon. Results from quantitative microprobe analysis of Si need to be furthr verified.

A TGA/DTA run on one of the samples was also made. However, due to the inhomogeneities in the composition, no meaningful conclusions can be drawn. More work therefore is needed.

VI. RECOMMENDATIONS:

1. The theoretical screening studies of reinforcement and matrix materials have shown that the constituents of composites of TiC-Al_2O_3, AlN-Al_2O_3, TiB_2-Al_2O_3, HfC-HfO_2, HfC-Al_2o_3, ZrC-Al_2O_3, and ZrC-ZrO_2 will be mutually chemically compatible. Further evaluation, using a similar approach would be helpful in determining other compatible materials for high temperature ceramic composites.

2. Experimental studies on composites whose constituents have been identified as chemically compatible remain to be accomplished. Material/processing/microstructure studies would provide a much needed understanding of the complex behavior of composite materials. Some of these studies must be carried out in an atmosphere of controlled oxygen pressure so as to prevent the oxidation of non-oxide ceramic materials. In the case that reinforcement materials are available in whisker or fiber form, studies of mechanical properties of composites would be very desirable.

3. The work on synthesis of SiB_6 has resulted in an understanding of the problems in synthesizing the compound. Further work in this area needs to be done. In view of the reported good oxidation resistance of this compound, it is recommended that oxidation studies of a well characterized compound be carried out to check the validity of reported good oxidation resistance. Subsequent studies of properties of composites containing SiB_6 are also recommended.

REFERENCES

1. Feigelson, R. S., "Some Physical Properties of Polycrystalline Silicon Boride," Watertown Arsenal Laboratories, Technical Report, WAL-TR-853-1 (May 1962). Cited in Engineering Properties of Ceramics, by J. F. Lynch, C. G. Ruderer, and W. H. Duckworth, Reference No. 774, Technical Report AFML-TR-52, June 1960, Wright-Patterson AFB, OH.

2. CRC Handbook of Chemistry and Physics, 60th ecition, Ed. R. C. Weast and M. J. Astle, CRC Press, 1980.

3. Barin, I. and Knacke, O., Thermochemical Properties of Inorganic Substances, Springer Verlag Berlin/Heidelsberg and Verlag Stahleisen Dusseldorf, 1973.

4. Barin, I., Knacke, O., and Kubaschewski, O., Thermochemical Properties of Inorganic Substances - Supplement, Springer Verlag, Berlin/Heidelberg/New York, and Stahleisen Dusseldorf, 1977.

5. Kubaschewski, O., Metallurgical Thermochemistry, John Wiley and Sons, 1979.

6. Turkdogan, E. T., Physical Chemistry of High Temperature Technology, Academic Press, 1980.

7. Sigli, C. and Sanchez, J. M., "Theoretical Description of Phase Equilibrium in Binary Alloys," Acta. Metal. 33, 1097-1104 (1985).

8. Cline, C. F., J. Electrochem. Soc., 106, 322-325 (1959).

9. Rizzo, H. F. and Bidwell, L. R., J. Am. Ceram. Soc., 43, 550-551 (1960).

10. Rizzo, H. F., Weber, B. C., and Schwartz, M. A., J. Am. Ceram. Soc., 43, 497-504 (1960).

11. Chemical Abstracts, Vol. 75, Abstract No. 132549u, 1971.

1986 USAF-UES SUMMER FACULTY RESEARCH PROGRAM/

GRADUATE STUDENT SUMMER SUPPORT PROGRAM

Sponsered by the

AIR FORCE OFFICE OF SCIENTIFIC RESEARCH

Conducted by the

Universal Energy Systems, Inc.

FINAL REPORT

Empirical Confidence Intervals for a Validity Coefficient Under Range Restriction: An Application of the Bootstrap

Prepared by:	Dr. Jorge L. Mendoza
Academic Rank:	Associate Professor
Department and University:	Department of Psychology Texas A&M University
Research Location:	Air Force Human Resources Laboratory/MOAE Brooks Air Force Base, TX
USAF Researcher:	Malcolm Ree
Date:	July 11, 1986
Contract No.:	F49620-85-C-0013

EMPIRICAL CONFIDENCE INTERVALS FOR A VALIDITY COEFFICIENT UNDER RANGE RESTRICTION: AN APPLICATION OF THE BOOTSTRAP

by

Jorge L. Mendoza

with the assistance of

Darren E. Hart and Amy B.Powell

ABSTRACT

Efron's bootstrap procedure was utilized to develop two computer intensive techniques for constructing confidence intervals on the unrestricted correlation parameter under explicit predictor restriction. One procedure bootstrapped the corrected correlation coefficient to obtain the interval, while the other one relied on the frequency distribution of the applicant test scores to generate the bootstrap confidence interval. The techniques were evaluated using a Monte Carlo procedure. The study assessed the techniques under a number of hypothetical selection situations. The results showed that boostrapping the corrected correlation coefficient is a reliable technique for obtaining confidence intervals for the population correlation under most selection situations.

ACKNOWLEDGEMENTS

We would like to thank the Air Force Human Resource Laboratory at Brooks AFB for sponsoring our research. All laboratory personnel associated with this project went out of their way to accomodate us. The atmosphere at the HRL not only facilitated our research efforts, but also made this summer an enjoyable one. We would also like to thank Malcolm Ree, Toni Wegner, John Welsh, Lonnie Valentine, and Jim Earles for their support and guidance.

I. Introduction

I received my Ph. D. at the University of Oklahoma studying quantitative psychology, statistics, and computer simulation techniques. I have also published a number of articles dealing with the quantitative aspects of personnel selection.

The research problem at the Human Resources Laboratory at Brooks AFB involved estimating the precision of a correlation coefficient that has been corrected for restriction in range. Because of my background in personnel selection and quantitative skills, I was given the assingment.

II. Background

One of the oldest and most common problems in test validation is that of range restriction on the predictor due to explicit selection. Range restriction occurs when predictor and criterion data are available only for the selected group. This is a group that is systematically different from the applicant group mostly because of the organization's selection policy. The restricted variable for which data are missing has generally a restricted variance. Hence, the correlation between the predictor and the criterion in this group underestimates the validity of the test.

Investigators have been concerned with this attenuation problem for some time. Karl Pearson (1903) was the first to provide a procedure to correct for the bias inherent in the selection process. Lawley (1943) relaxed the assumptions necessary for the correction, and Thorndike (1947) is accredited with bringing the procedure to the attention of psychologists. The Pearson correction formula for

explicit selection is

$$r_c = \frac{S_r^2}{S_r^2 + S'^2(1 - r)}$$

The " ' " indicates that the test variance and the correlation were computed in the selected group.

The correction procedure makes two assumptions: a) linearity of the regression of the criterion y on the test x, and b) homoscedasticity of the residual variances. Linn (1968) and Lord & Novick (1968) have pointed out that these assumptions are usually not met in practical settings. In general, departures from linearity tend to deflate the corrected correlation, while lack of homoscedasticity tends to inflate it. The correction is robust to lack of homogeneity of variances, but very sensitive to lack of linearity (Greener and Osburn, 1979). Nevertheless, some (Campbell, 1979; Linn, 1968) have suggested that it may be disadvantageous to adjust the correlation under such conditions.

Greener and Osburn (1979) found that while corrected correlations, for moderate to large unrestricted population correlations, are more accurate than uncorrected ones, they become less accurate as the proportion of selected individuals decreases. Using a Monte Carlo procedure, Brewer and Hill (1969) examined the correction under varying degrees of predictor skewness. They found that correction becomes less accurate as skewness and selectivity increase.

Others have investigated the correction under more general conditions. Alexander, et al (1984) have examined the robustness of the correction procedure when both the predictor and the criterion are

truncated, and found that the procedure undercorrected in most circumstances. Gross and Fleishman (1983) found that when the selection process is incorrectly assumed to be based solely on the predictor, the corrected correlation is highly positively biased, and it is less accurate than the uncorrected correlation.

Olson and Becker (1983) claimed that the correction has the additional assumption of complete truncation, which is generally not met in applied settings. Complete truncation occurs when all of the observations falling above or below a certain point are lost from the applicant sample. Incomplete truncation or attrition, on the other hand, occurs when "it is possible to observe an individual at any point on the test or job performance distribution, but the probability that an observation is lost from the sample is related to test or job performance itself" (Olson & Becker, 1983, p137). It is likely that incomplete truncation more realistically represents practical situations. Incomplete truncation can appear in situations where there is no strict adherence to a cut off score, and/or when the selection is not based solely on the test score.

Although we know much about the performance of r_c , we know little about its standard error and its sampling distribution. Not knowing the sampling distribution has impeded researchers from testing hypotheses or constructing confidence intervals. The traditional sampling theory for the Pearson product moment coefficient is not appropriate for r_c (Forsyth, 1971).

Given the state of the art, it would be desirable to find either a procedure for obtaining confidence intervals on the unrestricted population correlation ρ based on r_c, for situations where we know that r_c does a reasonable job and/or establish a procedure for

obtaining an estimator of ρ that does not make the assumptions of r_c . Until now, the mathematics necessary for doing such a procedure have been prohibitive. But it can now be attempted using Efron's (1979) bootstrap procedure. In this paper we suggest two bootstrap procedures for setting confidence intervals on ρ and evaluate their effectiveness using a Monte Carlo simulation.

Efron's bootstrap procedure is a computer assisted nonparametric method to evaluate the precision of a statistic. The bootstrap procedure is implemented when parametric assumptions cannot be made regarding the population where the observations were drawn. The central feature of the procedure is the repeated generation of bootstrap samples. A bootstrap sample of size n is obtained by sampling at random and with replacement from one's original sample of size n. Each boostrap sample is used to estimate the statistic of interest. Efron & Gong (1983) suggest that 200 boostrap replications are sufficient for most applications. These bootstrap values are then used to estimate population parameters or set confidence interval. Excellent descriptions of the method can be found in Efron & Tibshirani (1986) and Lunneborg (1985). The bootstrap works because the sample data resembles the population from which they were obtained. Its use, of course, requires some degree of confidence in the sample.

III. Objectives

The purpose of the paper is two fold: a) to suggest and evaluate a procedure for constructing confidence intervals on ρ based on r_c ; and, b) to suggest and evaluate a parametric free procedure for

estimating ρ which does not depends on r_c.

IV. Boostrap confidence intervals

Two bootstrap procedures are presented. The first is a procedure for obtaining a confidence interval on ρ using the r_c. The procedure requires two bootstrap samples for each repetition, one from the applicant sample and one from the selected group. The second procedure does not rely on r_c, but instead relies on the applicant frequencies.

Boostrapping the corrected r

The procedure can be summarized as follows:

1) Obtain a bootstrap sample of the applicant sample and compute the test variance $S.^2$

2) Obtain a bootstrap sample of the selected group and compute the correlation r' between the test and the criterion. Also compute the variance S'^2 of the test.

3) Using equation (1) correct r' for range restriction using S and S' to obtain the bootstrap value r_c^* .

4) Repeat 1-3 two hundred times to obtain $r_c^*(1)$, $r_c^*(2)$, . . . , $r_c^*(200)$.

5) Rank order r*(1), ... ,r*(200) and count 5 from the top and 5 from the bottom to establish a 95% confidence interval. Efron (198) calls this method of constructing confidence interval the percentile method.

Bootstrapping using the applicant frequencies

The procedure is summarized below:

1) Obtain the frequency distribution of the test scores for the n applicants. Then, divide the range of test the into k equal intervals (e.g., 0-10, 11-20, 21-30, ... ,91-100) and count the number of individuals in each interval.

2) Obtain a bootstrap sample of the selected group using the applicant frequencies divided by n. For example, if there are 100 applicants in interval I(3) and 500 in the total sample, then we would sample interval I(3) with probability .20. Once I(3) is selected then each individual in the interval has an equal probability of being selected. For I(3), it would be 1/100. This is similar to obtaining a quota sample.

3) Compute the correlation r^* in the bootstrap sample.

4) Repeat 1-3 two hundred times, rank order $r^*(1)$, $r^*(2)$, ... , $r^*(200)$ and construct the confidence interval.

V. THE MONTE CARLO

Under the assumption that the applicant sample resembles a random sample, we wrote a computer program which simulates the hiring process in an organization, to allow us to evaluate the general applicability of the bootstrap procedure to the attenuation problem in the selection paradigm. Given the paradigm, the bootstrap can be applied in a variety of ways. We developed two, both which utilized information from the applicant sample. (See the section on bootstrap.)

The Monte Carlo study investigated the behavior of the bootstrap corrected coefficient r_c^* for a number of bivariate distributions that

represented the joint distribution of the criterion and predictor in the unrestricted population. The computer program sampled from the bivariate normal distribution, the contaminated bivariate normal (this distribution is symmetric but not normal) and from the bivariate gamma distribution, a skewed distribution.

The program started the simulation by drawing a random sample of size n (200) from a given bivariate distribution with correlation ρ. This random sample represented the sample of applicants. Each applicant had a test score and y score. If the individual was selected later by the selection routine, the y score became the criterion score. If, on the other hand, the individual was not selected, the y score for that individual was discarded, resembling the situation where one has only criterion scores for those hired.

The selection routine selected "ns" individuals from the applicant sample according a set of attrition (conditional) probabilities. Table 1 contains the four sets of probabilities used in the study. Note that each set is composed of ten conditional probabilities. These probabilities were chosen to reflect four situations ranging from low-to-high selection and from low-to-high attrition. Next, ten equal intervals were obtained and each interval was then sampled according to its attrition probability. Individuals in the same interval had the same probability of being selected. However, individuals in high-scoring intervals had a higher chance of being selected than those in low-scoring intervals.

After the individuals were selected, the program began the bootstrapping. The program, first, generated a bootstrap sample from the applicant sample and another one from the selected group. Then, it computed the bootstrap corrected correlation r_c^*. This process was

repeated 200 times to generate $r_c^*(1)$, $r_c^*(2)$, ... ,$r_c^*(200)$. By rank ordering the correlations and counting 5 from the top and 5 from the bottom, we identified the lower and upper 95% confidence bounds.

The second bootstrap correlation was obtained utilizing the frequency distribution of the applicant sample. The bootstrap sample was drawn so that it resembled the distribution of the test scores in the applicant sample. This was accomplished by creating ten intervals in both samples and counting the number of applicants that fell into each interval. This process yielded ten intervals in the applicant sample and ten corresponding intervals in the selected group. The sampling proceeded as follows. Suppose that out of 200 applicants, interval I(2) in the applicant sample had 20. Then, we would sample from interval I(2) in the selected group with probability 1/10. We repeated the procedure 200 times and used the median of $r^*(1)$, ... ,$r^*(200)$ as the bootstrap estimate of ρ.

VI. Data Generation

One standard normal and one standard gamma random deviate generator from the Institute of Mathematical Statistical Library were used in the study. The normal routine was used to generate bivariate normal distributions and contaminated normals. We obtained the contaminated normal by mixing two normal distributions with weights .7 and .3. A total of two bivariate normal and two contaminated distributions were utilized in the study. The standard gamma routine was use to generate three standard gamma variables, x_0, x_1, and x_2. By forming the variables $x_0 + x_1$, and $x_0 + x_2$, we obtained the bivariate gamma distribution. This distribution has a linear regression of y on x, but the homoscedasticity assumption does not hold. Two gamma

distributions were used in the study. By reversing the attrition probabilities when we sample from the bivariate gamma, we simulated the effects of a negatively skewed distribution. Two sets of distributions were used, one set had ρ equal .50 and the other had ρ=.33. We sampled 500 times from each distribution for each situation.

VII. Results

Tables 2 and 3 contain the Monte Carlo results. Each table displays in columns 2, 3, and 4 the average correlation for the restricted correlation, the bootstrap correlation (median r^*), and the corrected correlation, respectively. The number within the parentheses in columns 3 and 4 indicate percentage time that the confidence interval included the unrestricted population correlation. Fruthermore, each table displays in column 1 the ratio of the average restricted variance over the average unrestricted variance. The average selection ratio is given in column 5. Table 3 shows the results for ρ = .33, and Table 3 gives the results for .50.

Tables 2 and 3 show that overall the corrected correlation r_c estimated the unrestricted population correlation accurately. The r_c tended to overestimate, however, under high-truncation/low-acceptance, and when the samples were drawn from a skewed distribution, corroborating the results of Brewer and Hill (1969). The r_c-bootstrap confidence interval on ρ performed remarkly well. Even in the worst of the situations, it still covered the correlation 89% of the time, rather than 95%. It was somewhat affected by skewness, but overall it was quite robust.

The median r^* generally underestimated the correlation, especially when the correlation was .33. Overall, it performed better

than the restricted correlation. The confidence interval based on the r*'s unfortunately did not perform well.

Selectivity did not seem to play much of a role in the estimation of ρ or the accuracy of the confidence intervals. Both estimators r_c and median r* performed reasonbly well under highly selective situations as can be seen from Tables 2 & 3. This is somewhat contrary to what Greener and Osburn (1979) observe, but they had complete truncation and we did not. It is possible that the r_c is more robust under incomplete truncation than under complete truncation, since under incomplete truncation it utilizes more information.

VIII. Recommendations

The r_c -bootstrap interval was shown to be robust to incomplete truncation, lack of normality, and lack of homoscedasticity. The study did not investigate, however, the effects of nonlinearity and/or the effects of incorrectly assuming that the selection process is solely based on the predictor. Future studies will have to assess the effects of these conditions on the r_c-bootstrap interval, since these conditions may negatively impact on the stability of the confidence interval. For situations in which these two conditions are not a factor, however, we feel comfortable in recommending the use of the r_c-bootstrap interval. Hence, we recommend that personnel researchers in the U. S. Air Force and other institutions correct their validity coefficients for range restriction, and obtain a confidence interval on the unrestricted population correlation using the r_c -bootstrap method proposed here.

References

Alexander, R.A., Carson, K.P., Alliger, G.M., & Barrett, G.V. (1984). Correction for restriction of range when both X and Y are truncated. Applied Psychological Measurement, 8, 231-241.

Brewer, J.K., & Hills, J. R. (1969). Univariate selection: The effects of size of correlation, degree of skew, and degree of restriction. Psychometrika, 34, 347-361.

Campbell, J.P. (1976). Psychometric theory. In M. Dunnette (Ed.), Handbook of industrial and organizational psychology. Chicago: Rand McNally.

Efron, B. (1979). Bootstrap method: Another look at the jackknife. The Annals of Statistics, 7, 1-26.

Efron, B., & Gong, G. (1983). A leisurely look at the bootstrap, the jackknife, and cross-validation. The American Statistician, 37, 36-48.

Efron, B., & Tibshirani, R. (1986). Bootstrap methods for standard errors, confidence intervals, and other measures of statistical accuracy. Statistical Science, 1, 54-77.

Greener, J.M., & Osburn, H.G. (1979). An empirical study of the accuracy of corrections for restriction in range due to explicit selection. Applied Psychological Measurement, 3, 31-41.

Lawley, D. (1943). A note on Karl Pearson's selection formulae. Royal society of Edinburgh, Proceedings, Section A, 62, 28-30.

Linn, R.L. (1968). Range restriction problems in the use of self-selected groups for test validation. Psychological Bulletin, 69, 795-801.

Lord, F.M., & Novick, M.R. (1968). Statistical theories

of mental test scores. Reading, MA: Addison-Wesley.

Lunneborg, C.E. (1985). Estimating the correlation coefficient: The bootstrap approach. Psychological Bulletin, 98, 209-215.

Olson, C.A., & Becker, B.E. (1983). A proposed technique for the treatment of restriction of range in selection validation. Psychological Bulletin, 93, 137-148.

Pearson, K. (1903). Mathematical contributions to the theory of evolution XI. On the influence of natural selection on the variability and correlation of organs. Philosophical transactions of the Royal Society, London, Series A, 200, 1-66.

Thorndike, R.L. (1950). The problem of classification of personnel. Psychometrika, 15, 215-235.

Table 1

Attrition Probabilities by Test Intervals

	Low-truncation						Low-acceptance			
p1:	.05*	.10	.15	.20	.25	.30	.40	.40	.40	.35

	Moderate-truncation						Moderate-acceptance			
p2:	.01	.01	.01	.01	.05	.10	.30	.60	.60	.55

	High-truncation						Low-acceptance			
p3:	.001	.001	.001	.001	.001	.003	.28	.39	.39	.39

	Low-truncation						High-acceptance			
p4:	.05	.06	.10	.12	.20	.30	.90	.95	.95	.95

* The probability of being selected (and accepting) given that an individual falls within the test range

Table 2

Monte Carlo Results for the Bootstrap when $\rho = .33$

The table displays the average correlation and the percent time that the C.I. contains p, in parentheses.

Distribution	Mean S'^2 / Mean S^2	Restricted correlation	Bootstrap correlation	Corrected correlation	Average selection ratio
	p1: Low-truncation, Low-acceptance				
Normal	.88	.32	.33 (88)	.34 (93)	.28
Mixed	.86	.31	.32 (90)	.34 (94)	.28
- skewed	.67	.29	.30 (89)	.34 (93)	.36
+ skewed	1.23	.33	.31 (93)	.32 (95)	.19
	p2: Moderate-truncation, Moderate acceptance				
Normal	.65	.26	.27 (79)	.33 (93)	.06
Mixed	.73	.27	.29 (85)	.35 (91)	.15
- skewed	.32	.20	.24 (67)	.35 (95)	.38
+ skewed	1.87	.32	.32 (83)	.35 (89)	.05
	p3: High-truncation, Low-acceptance				
Normal	.32	.19	.19 (86)	.41 (90)	.09
Mixed	.35	.19	.20 (82)	.44 (90)	.09
- skewed	.25	.19	.20 (83)	.36 (93)	.26
+ skewed	.65	.16	.19 (86)	.48 (88)	.05
	p4: Low-truncation, High-acceptance				
Normal	.79	.29	.31 (83)	.33 (94)	.40
Mixed	.82	.29	.31 (84)	.32 (91)	.39
- skewed	.45	.24	.29 (77)	.35 (93)	.73
+ skewed	1.76	.30	.34 (92)	.30 (95)	.18

Table 3

Monte Carlo Results for the Bootstrap when ρ = .50

The table displays the average correlation and the percent time that the C.I. contained p, in parentheses.

Distribution	Mean S'^2 / Mean S^2	Restricted Correlation	Bootstrap correlation	Corrected correlation	Average selection ratio
p1: Low-truncation, Low-acceptance					
Normal	.87	.46	.46 (89)	.48 (93)	.28
Mixed	.88	.47	.47 (89)	.50 (92)	.28
- skewed	.70	.43	.46 (87)	.50 (94)	.34
+ skewed	1.12	.48	.47 (94)	.47 (92)	.20
p2: Moderate-truncation, Moderate-acceptance					
Normal	.69	.37	.41 (93)	.49 (93)	.15
Mixed	.83	.39	.44 (86)	.49 (93)	.13
- skewed	.37	.35	.40 (69)	.52 (91)	.32
+ skewed	1.48	.46	.45 (85)	.47 (89)	.06
p3: High-truncation, Low-acceptance					
Normal	.33	.29	.30 (75)	.50 (90)	.09
Mixed	.39	.30	.30 (84)	.52 (89)	.09
- skewed	.28	.32	.33 (72)	.53 (93)	.23
+ skewed	.64	.36	.34 (92)	.53 (95)	.06
p4: Low-truncation, High-acceptance					
Normal	.76	.45	.47 (83)	.50 (92)	.39
Mixed	.84	.45	.47 (84)	.49 (94)	.40
- skewed	.49	.40	.46 (73)	.53 (91)	.68
+ skewed	1.49	.51	.49 (90)	.45 (92)	.21

1986 USAF-UES Summer Faculty Research Program

sponsored by

Air Force Office of Scientific Research

conducted by

Universal Energy Systems, Inc.

FINAL REPORT

Human Factors Analysis of a Microcomputer-Based Maintenance System for Advanced Combat Aircrafts

Prepared by: Shreenivas Moorthy Ph.D., P.E.

Academic Rank: Associate Professor

Department: Electrical Engineering & Computer Science

University: Texas A & I University

Research Location: Air Force Human Resources Laboratory
Logistics and Human Factors Division
Combat Logistics Branch
Wright-Patterson AFB, Ohio

USAF Researcher: Gail A. Hudson

Date: August 8, 1986

Contract No.: F49620-85-C-0013

Human Factors Analysis of a Microcomputer-Based Maintenance System for Advanced Combat Aircrafts

By

Shreenivas Moorthy Ph.D., P.E.

ABSTRACT

Maintenance performed in the present way has resulted in costly losses, both in terms of wasted manpower resources and in terms of the unnecessary replacement of parts. While the combat readiness of the U.S. Air Force is a primary objective of maintenance, such a waste of resources cannot be tolerated. This report analyzes the human factor requirements of the microcomputer-based maintenance system for advanced aircrafts. The analysis is based on applying the state-of-the-art technology, application software, as well as emerging developments in microelectronics. The approach optimizes user interest compatibility with system reliability, availability and maintainability and its performance efficiency characteristics. Recommendations for a significantly improved system from the human factor point of view are highlighted.
Excellent cooperation from various personnel and the organization is deeply appreciated.

ACKNOWLEDGEMENT

I would like to thank the U.S. Air Force Systems Command, the Office of Scientific Research and Universal Energy Systems, Inc. for their sponsorship of this work. The Air Force Human Resources Laboratory provided a highly stimulating environment to facilitate this research. While I am grateful to several members of the Air Force Human Resources Laboratory staff for their support and courtesies, I am particularly indebted to Ms. Gail Hudson, Mr. Robert Johnson and Dr. Donald Thomas for their excellent cooperation, guidance and encouragement; Lt. Jeffery Clay, Capt. Stan Collins, Mr. Bertram Cream and Lt. Dean Orrell for their valuable ideas; Prof. John D'Azzo, Capt. David King and Lt. Col. Stan Levantowicz of AFIT for their suggestions and Prof. Thomas J. Higgins (Professor Emeritus, University of Wisconsin) for his constant support during my work at AFHRL. Finally, I would like to thank my wife Malathi, and my sons Sanjoy, Chetan, and Aditya for their support and encouragement during my tenure at the Air Force Human Resources Laboratory in the Summer of 1986.

I. INTRODUCTION

I received my Ph.D. degree from the University of Sussex (U.K.) in computer control of (Combat Aircraft) power systems. Subsequently, I worked as a post-doctoral research fellow at the Council of Scientific and Industrial Research, New Delhi, India (assigned to Hindustan Aeronautics Ltd., Bangalore, India). There I worked with a team of engineers and scientists in the Department of Avionics to develop a general purpose model for combat aircraft and a pilot training simulator. I have since worked on several projects relating to the development of modeling, simulations and analysis of nuclear power plants; human factor analysis of nuclear power plant control rooms; control room simulation for operator training; and microelectronic universal logic modules for the Combat Development Experimentation Center (U.S. Army). The research work at the Air Force Human Resources Laboratory (AFHRL) was related to human factor analysis, microelectronic system development, and advanced combat aircraft. The problem under investigation at the U.S. Air Force Human Resources Laboratory was therefore similar in many respects to my earlier experience which qualified me for the assignment on human factor requirement analysis of an integrated computer-based maintenance information system.

II. OBJECTIVES

The computer based maintenance system by AFHRL/LRC is known as the Integrated Maintenance Information System (IMIS). The IMIS is presently under development by AFHRL. While the purpose of the IMIS is to aid in the maintenance of combat aircraft, it is also applicable to missile systems and ground-based systems. The reasons for the

development of the IMIS are to:

(1) provide the technician with easy to use technical data,

(2) provide a direct interface with aircraft systems and to interact with the aircraft systems to diagnose faults in the systems, and

(3) provide direct access to other maintenance information systems (maintenance management systems, supply, training, etc.) through a common set of protocols. The basic objectives are to improve the technician's access to information and at the same time eliminate the need for the technician to learn the use of multiple information systems and the need for the AF to provide separate hardware for each information system.

The objective of this human factors requirements analysis was to identify factors that would help to enhance the utility of the micro-computer-based system, by applying current technological advances in the field. In this report an attempt will be made to maximize user/technician and developer interest and involvement compatible with reliability and efficient performance of the system. In my analysis of the human factors requirements, the following objectives have been paramount:

(1) improving the existing Job Performance Aid (JPA) system,

(2) expanding the use of the Portable Computer-Based Maintenance Aid Systems (PCMAS),

(3) having adequate hardware and software interfaces with the airborne and ground based systems to provide information in a consistent way to the maintenance technician,

(4) facilitating maintenance tasks through a library of nonvolatile memory modules with easy accessibility that will render unnecessary either recourse to the cockpit or to the technical manual,

(5) enabling the computer personnel of the AFHRL to maintain its normal system function,

(6) using scenario simulation to devise methods for raising the information utility level of technical orders through encouragement of user participation,

(7) eliminating costly maintenance and user errors,

(8) updating the system by using emerging technology,

(9) rendering the system compatible with modification and expansion as required for future use by a variety of users in a range of situations

(10) increasing the use of knowledge-based expert systems, and

(11) demonstrating the advantages of a modified ADA/AI language.

III. BACKGROUND

Industry's concern with human factors is engendered mainly by expansion in the user population (technicians and computer specialists in regard to IMIS), that includes novices and non-technically trained people, the increasing organizational dependence on interactive systems, and the high performance requirements in critical applications such as combat aircraft maintenance in the U.S. Air Force. Design issues pose conflicting challenges such as: command language vs. menu selection, response time vs. display rates, wording of system messages, on-line tutorials/explanations vs message interrupts, the profusion of hardware options vs compatibility, and pros cons of partcipatory design concepts which need to be addressed effectively in relation to human factors to accomplish a good design. The development of cognitive models of human behavior is expected to provide a positive tool for under-

standing and predicting human performance and good organizing principles for the designers.

Human factors in the modern sense is using what we know about the way people really are to build the required systems and develop techniques to use them. A worthwhile end of the design efforts should be human happiness leading to enhanced productivity by way of increased capability and motivation. This can be accomplished effectively by integration of the right kind of people, right facilities, desired information, good procedures, mental models of technicians, and qualitative reasoning in the programs, and implementing the most relevant feedback from users.

IV. METHODOLOGY

This report seeks to analyze human factor requirements for an improved, user friendly system. The results of the analysis should aid in significant improvement of the system in the following areas:

(1) human-computer dialogue for the user system communications,

(2) steady-state and dynamic graphics,

(3) format and display options,

(4) technical content of the text, and

(5) voice-interaction between system and users.

Each of these have a demonstrable impact on the design of keyboard, techniques for providing technical data with varying difficulty levels, remedial training, and graphics simplification.

The principles of design evolved herein were announced earlier in an unpublished technical evaluation study (Behavioral Technology),

which examined the tasks of:

(1) remove/replace,

(2) deductive troubleshooting, and

(3) modularized illustrated parts breakdown to determine the feasibility of using the information.

The conclusions of the study have subsequently been confirmed by a report (Kern and Hayes) based on a test demonstration of a computer-based maintenance aid system. This has revealed the system's compatibility with minimal technician involvement as well as developer interest. The language for communication preferred by novice users could be based on either conventional programming languages and data base theory or ergonomic analysis and simulation of interaction technology. Either way, user friendliness could be achieved with the help of consistent user interface.

V. ANALYSIS

The use of Job Performance Aids (JPA) based on modern research manuals have not yielded the expected level of improvements. A recent study found that of all the maintenance tasks observed, only 23% were performed without error; and 40% of the line replacement units LRU, which did not need removal or repair were indeed removed and tested for malfunctions. The "new look" technical manuals incorporating the results of recent research required branching for troubleshooting procedures, cross referencing for paper economy, and have resulted in impossibly large manuals. Technicians had to refer to several large manuals to perform on troubleshooting task (Hartung). Users interests were not adequately represented. It was erroneously assumed that research

findings would be sustained when implemented on a large scale. The incorporation of computer-controlled simulation in the training programs has been found to be inadequate (Rouse).

Efforts to implement software in an advantageous combination language ADA/AI were minimal or perfunctory. The development of AI software in ADA for long term benefits of USAF has largely been ignored. Studies are urgently required in the areas of: fifth generation computer systems (FGCS), reduced instruction set computation (RISC), and AI/PROLOG language for personal logic programming station.

Criteria: The overal goal of human factors requirements analysis is to draw on de facto standards, information sources, human factor studies, experiences, opinions and user feedback in order to adapt systems design to the needs of the technician, whose primary function is corrective maintenance: restoring malfunctioning equipment to an acceptable level of functioning. The usability criteria could be summarized as accuracy, understandability, retrievability, relevance, completeness, portability, diagnosability, availability, and flexibility. While these are readily comprehensible, their implementation is hampered by two factors:

(1) the composition of the user population which ranges from the inexperienced technician with limited technical knowledge, to the experienced master-technician, and

(2) the reluctance of the supervisors and trainers to accept new technology.

To overcome these drawbacks, this report takes note of user characteristics; personnel constraints; user interfaces; hardware/ software requirements; dialogue design; voice interaction; emerging

technology and its impact on maintenance, training, and operation.

User Characteristics: The users or maintenance technicians and to a lesser extent, the developers have limited memory retention and a propensity for error, are impatient with error, have no knowledge of data base details, and no desire to remember cryptic computer names; are intolerant of strict and query languages; and are reluctant to deal with the complex logic of questions and answers. They need to know the relevance of previous questions to the present one and to seek a coherent end to any dialogue. Whereas they require a safety net, they will accept only minimal training. They specify their needs in wholly colloquial English and feel insulted or inferior when "high tech" terms are used, and are understandably insulted by rude or impolite reference (Granda and Koch).

System Characteristics: User compatibility of the IMIS can be assured by providing:

(1) easy to discover available choices in explicit compact menus,

(2) prompting messages friendly to users,

(3) system conceptualization in simple terms, and

(4) feedback and logic specifications that are non-intimidating.

The system must be able to resolve user problems dealing with type and location of error, data requirements, input format, and interpretation of system terminology. The system must also incorporate filtering devices to prevent unauthorized access.

User Interfaces: The system should be user accessible and command diversified. It should clearly identify dialogue branching with a

built-in capacity to allow the user to return to any convenient anchor point in the dialogue.

System Hardware: The system hardware should be adequately equipped to perform the following tasks: optimize time, indicate input response and relevance, clear and correct input errors, explain response delay, screen alternate options, present tabular display data, provide data in realistic times, provide flashing and display freeze as relevant to user needs, use standardized alpha-numeric data, provide self-explanatory labeling, and establish scroll and continuity in display for editing use.

System Software: The software must be able to minimize number of displays, eliminate delay, include access priorities, indicate current location, distinguish the nature of system failure, and simplify the task by rejecting unnecessary duplication.

Knowledge Based Systems: Classical approaches in this area include systems employing sophisticated procedural language requiring empirical association and deep knowledge-based systems using propagation to construct behavioral expectation models. A sophisticated knowledge-based system combines both these approaches with minimal assumptions, dramatically reduces the number of rules required to a mere twenty-five, and is thus ideally suited to handling troubleshooting and corrective maintenance functions.

The Language: The IMIS proposal to provide all necessary automation in a single compact user-friendly device should consider studying existing AI languages like LISP or PROLOG and thereby modifying the ADA language to meet AI programming needs.

Dialogue Design: The system dialogue facility should be restricted to a choice list: incorporate command-response consistency, eliminate abbreviation ambiguity, provide short cuts, and accommodate varying levels of user skills.

The dialogue design should be friendly, allow for concentration on application, avoid jargon, and enable correction. Knowledge-based systems stress economies of time, efficient performance and maintenance, handle information needs, identify tasks, use knowledge-based graphics, and allow for human interaction. Such a design can provide answers to questions regarding goals and their achievement, efficiency and ability of the process including alternatives, components interaction, data translation, and knowledge visualization.

Voice Interaction: A display of maintenance operations accessible through a voice recognition system would allow the user to function with both hands and eyes free of restraints in a system incorporating voice interactive maintenance functions.

Emerging Technology: Designers and specification writers of portable computer-based maintenance aid systems (PCMAS) are abreast of technological developments. Evaluation must await actual use. Recommendations in this report (Section VII) will therefore be confined to further exploratory possibilities in this area.

VI. RESULTS AND DISCUSSION

This study confirms the importance of human factors in any computer-based maintenance system. The hardware generally available can be modified without significant effort so as to accommodate a high resolution

flat panel display, optical storage, voice interaction, touch sensitive technology, etc. to meet IMIS needs. Software needs to be streamlined, to be adapted and data preparation to be added, error to be eliminated, equipment to be modified, and receptivity to be changed.

Conferences with the senior personnel of AFHRL have revealed an awareness of the need for improvements in current IMIS programs. I would therefore stress that my final remarks are being made to emphasize the relevance of my findings to future product quality and the ability of the system to adapt to and incorporate future emergent technology.

The findings of my analysis effort may be summarized as thus:

(1) Available data can be better fully utilized.

(2) Personnel and facility utility could be maximized.

(3) Systems requirements could be satisfactorily integrated.

(4) Information set-up should be adequately equipped.

(5) Troubleshooting techniques should be fully compatible with operational requirements.

(6) User involvement is intermittent.

VII. RECOMMENDATIONS

There is considerable agreement in regard to the need for incorporating human factor requirements into the maintenance aid system while keeping pace with technological advances. The questions that remain are the determination of the language of communication, system adaptation, and user training. Many design features and development procedures planned for the IMIS to the extent that has been defined are seen as essential and are included with a view of stressing the value of implementing them. With this in mind, I make the following

recommendations:

(1) Redesign the information to render it concise (text, graphics).

(2) Encourage user participation and active involvement in the development process.

(3) Combine and organize tested information by categories as well as independently.

(4) Arrange troubleshooting walk-through sessions with users to assess the completeness of information.

(5) Arrange debriefing sessions to assess acceptance of the proposed package and to allow for the airing of criticism.

(6) Provide at least three options to accommodate multi-level users, namely:

a) menu listing and test symptoms from which to choose. This focuses on subject modules one by one by asking the user for the results of specific tests and measures till the malfunctioning component is is isolated for users with little experience or familiarity.

b) menu listing of all major modules for which test measurements can be input (as well as test menus) leading to more specific menu listing. The user can input as many different modules as desired. After all values are inputted, the system draws conclusions asking for additional test readings as needed: this is for a reasonably experienced and familiar user.

c) menu listing of major modules: this focuses on the diagnosis of the module selected. An experienced user who does not have to backtrack the diagnosis uses the process of elimination and alternate hypotheses. This is for the well-experienced user. Other options include more flexibility through a facility to review or change

previously inputted data or volunteer new information. The diagnosis then proceeds from the point it left off allows the user to catch and correct input errors, and to change back and forth from system-directed to user-oriented diagnosis.

(7) Incorporate the results of performance analysis and failure mode and fault analysis system analysis.

(8) Use an expert system approach for troubleshooting and corrective maintenance which reads the program input, parses it, constructs a causal model, and generates a set of minimal rules based on knowledge and deductive inference, which works like a realistic human technician.

(9) Caution is advised though, to strike a compromise so as to retain user initiative, motivation, confidence, credibility, and advancement.

(10) Provide flat panel displays, in particular the dc plasma/color displays.

In addition to the above stated recommendations impacting the human factor requirements for a human engineered IMIS, specific suggestions for possible inclusion in the IMIS statement of work are as follows:

(1) Use graphic VLSI/CAD/5G technology and RISC architecture to facilitate more functional capabilities in hardware and to accommodate user-programmable micro-coding such as PROLOG,

(2) Provide video-display terminal (VDT) facility to reduce musculo-skeletal and visual-ocular stress for the frequent user,

(3) Provide output question/answer/consequences of actions on the split screen (Vestiwig et al, Willeges),

(4) Provide voice I/O facility to allow the maintenance technician to have freedom of handling and seeing while executing maintenance tasks,

(5) Use of fifth generation computer technology particularly vital to long term application to IMIS,

(6) Provide software compatibility and maintainability, particularly for host computer systems (UNIX) and the accepted defense system. Computer language ADA could be made to respond faster than C, which in combination with convenient AI/natural query command languages optimizes the utility for a range of users,

(7) Explore further the feasibility and compatibility of using recent advanced techniques (structured tools) for system software developments (separate report by Prof. Gowda),

(8) Investigate further modeling and simulation of typical IMIS system, users, and system functions, to narrow the gap that exists between the reality and the assumptions (possible research project at Texas A&I University), and

(9) Institute further detailed study to investigate IMIS system hardware compatibility with futuristic microelectronic technology development after the 1990s.

Typical examples for search, replacement, concise formats, consistency in location, color-coding, split-screen display, video and voice interaction output philosophy, and their benefits to users were examined and studied but not included in the recommendations for lack of space.

REFERENCES

Antonelli, D. R.: The application of AI to maintenance and diagnostic information system (MDIS), AFHRL-TR-84-25, Boeing Aerospace Co., 1984.

Behavioral Technology Corp.: Draft, A study of the human factor requirements for a computer based maintenance and presentation system, unpublished, report prepared for AFHRL, 1979.

Brookes, R. A.: IMIS portable computer technology survey, AFHRL, Wright Patterson AFB, OH, 1984.

Buffy, T. M., and Waller, R. (Ed.): Design usable text, Academic Press, N.Y., 1986.

Carroll, R.J. et al: Maintenance training simulation, their use, cost, and effectiveness, AFHRL, Brooks AFB, TX, 1984.

Chenzoff, A.P. et al: Advanced man-machine interface concepts for a fully integrated information presentation system, Naval Personnel Research and Development Center, San Diego, CA, 1986.

Chenzoff, A. P. et al: Fully proceduralized job performance aids (draft specifications for organizational and intermediate maintenance), AFHRL-TR-73-43 I, II, III, Advanced Systems Division, Wright Patterson AFB, OH, 1973.

Chenzoff, A. P.: Decision processes and information requirements for integrated diagnostics and battle damage assessment, Naval Personnel Research and Development Center, San Diego, CA, 1985.

Christiansen, J. M.: Design for maintainers conference, AD-A160934, Proceedings of a conference, Naval Air Development Center, CA, 1982.

Computer based military training systems, Royal Air Force Technical cooperation program subcommittee on Non-Atomic military research and development subgroup, Technical Panel UTP-2, U.K., 1980.

Cotton, J. C. et al: Development of speech input/output interfaces for tactical aircraft, AFWAL-TR-83-3073, Wright Patterson AFB, OH, 1983.

Cuff, R. N.: On casual users, International Journal of Man-Machine Studies, vol. 12 (2), 1980.

Dallman, B.: Program for AI application, AI in maintenance, Proceedings of the joint services workshop, (Richardson, Ed.), AFHRL-TR-84-25, Brooks AFB, TX, 1984.

Davis, G. and Stockton, G.: F-16 voice system study, NAECON, Proceedings , IEEE Press, 1983.

Davis, R.: Diagnosis via causal reasoning: Paths of interaction and locality principle, Proceedings of National Conference on AI, 1983.

Dierker, R. J. et al: Role of diagnostics information in electronic job performance aiding, AFHRL/AFSC, Wright Patterson AFB, OH, 1985.

Fiegenbaum and McCordoc: Land of the rising fifth generation, High Technology, vol. 3, no. 6, 1983.

Fifth Generation Project, VLSI application, speech processing, Infotech 1983.

French, J. C. et al: Avionics diagnostics pilot study, AFHRL, Wright Patterson AFB, OH, 1983.

Garbin, C.P. et al: Guidelines: assessing use of information sources and quality of performance at the work site, (Army Research Institute research note), National Training Information Systems, No. AD 125336, US Army Research Institute, Alexandria, VA, 1982.

Granda, T. M.: An application of human factors concepts to an interactive computerized personnel record keeping system, RR-1233, US Army Research Institute, Human factors technical data, 1980.

Gunning, D.: Integrated Maintenance Systems (unpublished), Jan. 1984.

Hartung, W. E.: Personnel electronic aid for maintenance (PEAM), Proceedings of Human Factors Society, 29th annual meeting, (Ed. Swezy), vol. II, 1985.

Johnson, R.: Integrated Maintenance Information Systems: An Imaginary Preview, (AFHRL TP-81-18), Sept. 1981.

Kern, R. P. and Hayes, J. F.: Research findings to aid supervisors and trainers in improving maintenance performance, Army Research Institute, (ARI-RP-83-14), National Training Information Systems No. AD 144655, 1983.

Klass, P. J.: Technique benefits to novice technicians, Aviation Week and Space Technology, Oct. 11, 1982.

Koch, G. G.: User interface design for maintenance trouble shooting expert systems, Proceedings of Human Factors Society, vol. I, 1985.

Kohl, G. and Nassau, S. J.: Symposium on combining human and artificial intelligence: a new frontier on human factors, Metropolitan chapter of Human Factors Society, N.Y., 1984.

Lieberman, H.: Seeing what your process is doing, International Journal of Man-Machine Studies, vol. 21, 1984.

Lorenz, R. O. and Rue, H. D.: Study of causes of unnecessary removals of avionic equipment, Rome Air Development Center, AFSC, Griffis AFB, N.Y., 1983.

Malone, T.: Heuristics for designing enjoyable user interfaces, lessons from computer games, Proceedings of Human Factors in Computer Systems Conference, Gaithersburgh, MD, 1982.

McCann, P. H.: Development of the user-computer-interface, Computers and Education, vol. 7, (4), 1983.

Metz, S. V. et al: Methodology for exploring voice-interactive avionics talks: optimizing interactive dialogue, Proceedings of Human Factors Society, 26th annual meeting, Santa Monica, CA, 1982.

Moorthy, S.: Control Panels and Human Factors, Measurement & Control, Sept. 1983.

Norman, D. A.: Steps toward a cognitive engineering design rules based on analysis of human error, Proceedings of the Conference on Human Factors on Computer Systems, Institute for computer sciences and technology, Gaithersburgh, MD, 1982.

Norman, D. A. and Draper, S. W.: User centered system design: New perspectives on human-computer interaction, Lawrence-Erlbaum Associates, Hillsdale, NJ, 1985.

PCMAS (Portable computer-based maintenance aid system), Intermediate Design Review, May 28, 1986.

Richardson, J. (Ed.): Artificial Intelligence in maintenance, Proceedings of Joint Services Workshop, AFHRL, Wright Patterson AFB, OH, 1984.

Rouse, W.B. and Morris, N.M.: Conceptual design of a human error tolerant interface for complex engineering systems, Proceedings on 2nd IFAC/IFIP/IFCRS/IEA conference -, analysis, design and evaluation of man-machine systems, Verese, Italy, 1985.

Salvendy, G. et al (Ed.): Handbook of human factors: Ergonomics, Wiley, NY, 1986.

Schustack, S.: Variations in C, Microsoft Press, Bellevue, WA, 1985.

Smith, S. L. and Mosier, J. N., (MITRE): A design evaluation checklist for user-system interface software, ESD-TR-358, Hanscom, United States AFB, MA 1984.

Vestewig, R. E. and Propst, F. M.: Speech input and video-disk team up for military maintenance, Speech Technology, vol. 1, 1982.

Warnier, J. D.: Computers and human intelligence, Reston, NJ, 1986.

Willeges, B. H. and Willeges, R. C.: Dialogue design considerations for interactive computer systems, Human Factors Review, (Muckler, Ed.), 1984.

1986 USAF-UES SUMMER FACULTY RESEARCH PROGRAM/

GRADUATE STUDENT SUMMER SUPPORT PROGRAM

Sponsored by the

AIR FORCE OFFICE OF SCIENTIFIC RESEARCH

Conducted by the

Universal Energy Systems, Inc.

FINAL REPORT

Evaluation of a Computer Program to Predict Thermal Retinal Damage from LASER Radiation

Prepared by:	Mary L. Morton-Gibson
Academic Rank:	Associate Professor
Department and	Department of Chemistry/Physics/Geosciences
University:	Lock Haven University of Pennsylvania
Research Location:	USAF School of Aerospace Medicine/RZV Brooks Air Force Base, TX
USAF Researchers:	Lt. Col. Robert M. Cartledge Dr. Ralph G. Allen

Date:	August 29, 1986
Contract No:	F49620-85-C-0013

Evaluation of a Computer Model to Predict Thermal Retinal Damage from LASER Radiation

by

Mary L. Morton-Gibson

ABSTRACT

A computer model of the thermal response and predicted damage to the eye from a LASER assault was examined in some detail. The basic equations and assumptions used in developing the model, the values of the constants used and the method of solution have been determined. The sources of some errors have been identified and an interim solution implemented. Recommendations are made for improving the user-friendliness and flexibility of the program, updating some of the algorithms and program parameters and developing user documentation.

A preliminary simulation indicates that retinal damage due to LASER assault is increased when retinal blood flow is decreased. Since retinal blood flow is markedly reduced during high g load accompanying some flight maneuvers, a parametric study is recommended.

ACKNOWLEDGEMENTS

I would like to express my appreciation to the Air Force School of Aerospace Medicine, The Air Force Office of Scientific Research, and Universal Energy Systems, Inc. for sponsoring my research. I am particularly thankful for the person(s) responsible for finding such a close match between my experience and interests and this project.

Both the professional and support staff of the USAFSAM LASER Lab made me feel welcome. The guidance of Lieutenant Colonel Robert Cartledge and Dr. Ralph Allen is very much appreciated. Stimulating discussions with Mr. Jack Labo and Captain Elmar Schmeisser contributed greatly to my work.

I. Introduction My formal educational background includes a Bachelor of Science in Mechanical Engineering and a Doctor of Philosophy in Physiology and Biophysics with a minor in Engineering, both from the University of Kentucky, Lexington, KY. In addition I was a post-doctoral trainee for three years in the Department of Neurophysiology, University of Wisconsin-Madison, Madison, WI. I also took graduate level courses in Mechanical Engineering and Gross Anatomy at the University of Wisconsin-Madison.

Following the post-doctoral training I did neurophysiological research in the Departments of Ophthalmology and Neurophysiology and taught in the Department of Mechanical Engineering at the University of Wisconsin-Madison. Later I taught in the Department of Physics at The Citadel, The Military College of South Carolina, until moving to my present position. The results of the neurophysiological experiments were used to develop models of basilar membrane motion and neural coding in the visual and auditory systems. My teaching responsibilities have been concentrated primarily in mechanics and the thermal sciences. In the heat transfer classes I taught the use of finite difference methods in the solution of both steady state and transient two dimensional heat transfer problems.

My unique combination of physiological, heat transfer and computer knowledge and experience is what led the

USAFSAM LASER LAB to invite me to work with them on the RETINAL THERMAL MODEL.

II. OBJECTIVES OF THE RESEARCH EFFORT: The RETINAL THERMAL MODEL was originally developed to be used on a large mainframe computer, operating in Batch Mode, which was state-of-the-art at the time the program was developed. Recently, there has been a renewed interest in using the program. The program was modified to be run interactively on a DEC Micro VAX II at the LASER Lab. Unfortunately, no clear documentation exists of (1) what the program was designed to do, (2) the assumptions inherent in the program, or (3) the meaning of the many variables and the values chosen for them. In short, the program was designed for programmers, not users.

Three goals were set for this project;

1) To develop an understanding of the basic assumptions used to develop the model and to relay that information to the personnel interested in using the model.

2) To determine the underlying cause of recently discovered errors in temperature prediction. The model should be revised to eliminate those errors.

3) To make a preliminary prediction of the increased threat of retinal damage due to LASER assault when retinal blood flow is low. This is of concern to Air Force pilots since retinal circulation is markedly reduced during sustained high g load.

III. BACKGROUND: In the early 1970's a computer model to predict thermal injury to the eye following LASER exposure was developed under a United States Air Force Contract (Takata, et al, 1974, Mertz, et al, 1976). The model can be utilized to predict safe exposure levels for virtually any set of LASER parameters. Standards for both military and non-military uses should be frequently evaluated and changed to include new LASER systems as they are developed and implemented.

The model has been used extensively by researchers at The Department of Biomedical Engineering, the University of Texas at Austin (Polhamus, 1980; Welch, et al., 1976; 1979; Welch and Polhamus, 1984). The shape of the temperature profile in the eye, the maximum temperature rise, the maximum temperature and threshold power are predicted reasonably well. The model does not adequately predict the radial profile, particularly for small images.

More recently Zuclich and his colleagues (unpublished data) have found a significant discrepancy in the temperature profile. For the time immediately after the laser application, the model predicts a temperature LESS than normal tissue temperature under some conditions.

IV. DESCRIPTION OF THE RETINAL THERMAL MODEL: The model consists of two models which are used in series to predict damage due to LASER assault:

1) A temperature model is used to predict the temperature distribution in the eye as a function of LASER parameters, spatial coordinates and time.

2) A rate process model is then used to predict damage as a function of the time-temperature history of the tissue. The eye is modeled as a cylinder with symmetry about the central axis. A partial differential equation

$$[\rho\, C]\frac{dv}{dt} = q(z, r, t) + k\left[\frac{1}{r}\frac{\partial v}{\partial r} + \frac{\partial^2 v}{\partial r^2}\right] + \frac{\partial}{\partial z}\left[k\frac{\partial v}{\partial z}\right] \qquad (1)$$

where

v = temperature rise above initial temperature

z = axial distance

r = radial distance

t = time

q = rate of heat deposition from LASER

C = specific heat

k = thermal conductivity

ρ = density

is used to describe the relationship between temperature rise, axial position, radial position, energy input and time. That equation is converted to a set of M by N finite difference equations (14 X 28 equations in the current

version). Those equations must be solved at every successive discrete time increment from zero to the final time of interest.

There are two commonly used types of solutions to the finite difference equations. The EXPLICIT solution is straight forward and simple. Unfortunately, the solution is unstable unless the time step between calculations is quite small. When using an IMPLICIT solution, the time increments between calculations can be much larger, however, each calculation is more complicated and time consuming than individual calculations using an explicit method.

In the RETINAL THERMAL MODEL a hybrid of the two methods is used. The technique is based on an alternating implicit-explicit method developed for the solution of finite difference equations in Cartesian coordinates (Peaceman and Rachford, 1955; Douglas and Gallie, 1955). The method is unique in two ways: (1) The finite difference equations are solved explicitly in the axial direction and implicitly in the radial direction for odd time steps. The procedure is reversed for even time steps. (2) The first time step is small but each successive time increment is larger than the previous one.

Since the equation describing the temperature model is linear, the temperature rise due to multiple pulses can be predicted by adding the rises due to each individual pulse together with appropriate time offsets. In its current form the program can only consider LASER pulses with an instantaneous onset and offset (zero rise and fall times).

Thermal damage is assumed to be an accumulative process that is dependent upon both the magnitude of the temperature rise of the tissue and the duration of that rise. The finite difference version of the damage integral for each segment is:

$$DAMAGE(z,r) = \sum\left[\exp\left\{\ln(C_1) - \frac{C_2}{v(z,v,t)+273.} + \ln(\Delta t)\right\}\right] \quad (2)$$

The constants C1 and C2 are fixed so that when the summation is equal to 1.0, irreversible tissue damage has occurred in a given segment. No damage occurs if the temperature of the ocular media remains below 44 deg C. The damage model is also used to estimate the power levels required to produce damage in a given segment (threshold estimation).

V. PROGRAM CONSTANTS Examination of the program revealed that many of the parameters have been considered to be constants. A selected list of these is summarized in Table I. Of particular concern are the pupil diameter, flow rates, the distance over which damage is assessed and the damage coefficients. Pupil diameter changes under a wide variety of conditions. The blood flow rate to the eye is known to decrease dramatically under high g stress, for example during flight maneuvers. The radial distance over which damage is expected to occur depends greatly on the beam size and the strength of the LASER assault. The source

of the data for damage coefficients is not specified. However, they are identical to the experimental values found for pig skin subjected to controlled burning of JP-4 fuel (Takata, 1974).

TABLE I

Partial list of parameters which are held constant.

TO	Initial eye temperature	37. C
RVL	Radius at which Temperature has returned to TO	0.7 cm
PUPIL	Pupil radius	0.35 cm
CONX(I)	Thermal conductivity of eye media	0.0012 cal(cm sec C)$^{-1}$
VSHX(I)	Heat capacity of eye media	1.0 cal cm^{-3}C^{-1}
SHB	Heat capacity of blood	0.92 cal cm^{-3}C^{-1}
CFLOW	Total blood flow to choriocapillaris	0.024 g(sec)$^{-1}$
XFLOW	Blood flow to tissue surrounding eye	0.001 g cm^{-3}sec^{-1}
CABER	Spherical aberration term in the spread function	-3.0e+6 cm^{-4}nm
RMAX	Radial distance over which damage is assessed	1.0 cm
LESION	Radial extant of small printout steps	0.001 cm

		Temperature	ln(C1)	C2
DAMAGE	Coefficients for damage rate integral	<50deg	149	50,000
		>50deg	242	80,000

The following parameters are also held constant. The values used for each ocular layer maybe found in the referenced tables of Mertz, 1976.

Reflectivity, transmissivity and absorptivity	A-1 and A-2
Thickness of ocular media	A-3
Refractive index	A-7

The number of segments into which the eye is divided is also fixed in the program. In the current version there are 28 axial segments and 14 radial segments. The grid layout in both directions is shown in Table II. Note that near the center in the radial direction the increments are spaced close together. Furthermore, in the very thin pigment epithelium and the choriocapillaris there are 12 axial segments. In both cases the very close spacing occurs in

TABLE II

Current configuration of cylindrical segments.

GRID LAYOUT (AXIAL)

	INITIAL	FINAL
Cornea to Pigment Epithelium	IPA 2	LPA 9
Pigment Epithelium	IPE 10	LPE 15
Choriocapillaris	IPV 16	LPV 20
Choriod	IPC 21	LPC 24
Sclera	IPS 25	LPS 26
Posterior to Sclera	IPT 27	

Note that there are 12 uniform closely spaced increments between #9 and #21. Outside that region the spacing is larger.

GRID SPACING (RADIAL)

The grid spacing in the radial direction consists of 4 uniform closely spaced increments (at the center) surrounded by 9 increasingly larger increments.

the region most likely to be damaged (at the center of the beam in the region of highest absorptivity).

VI. TEMPERATURE ERRORS The initial discovery of temperature prediction errors was made when a NEGATIVE temperature of the eye media was predicted during a simulation of multiple pulse presentations. The temperature predictions for an individual segment were examined at every time step from the onset of the first pulse until after the offset of the last pulse for a variety of stimulus parameters. That examination revealed two things:

1) The temperature predictions were not only negative but were also oscillatory. The predicted temperature initially fell, as anticipated. However, it continued to fall ultimately becoming negative, a highly implausible situation. Furthermore, it eventually began to climb, then continued to alternatly fall and rise.

2) The obviously inaccurate predictions were observed at times far removed from the onset, either during multiple pulse simulations or during very long duration single pulses.

Both of these observations support the likelihood that the solution is unstable. Using an explicit technique, the solution will oscillate if the time step is too large. Recall that the time step is progressively increased from the start of the pulse to the end of the simulation. Therefore, the time step computation was examined.

The initial time step (DT) for multiple pulse presentations is calculated as follows:

$$DT = \frac{4.568 \cdot 10^{-2} DP}{\left(\frac{1.8 \cdot NP}{F}\right)^{0.16} + C} \qquad (3)$$

where

DP = the duration of an individual pulse

NP = number of pulses

F = repetition rate

C = constant which had been set to 1.0.

Each successive time step is increased by the multiplicative factor 1.4. It is readily apparent that the time step can become quite large, particularly when the number of pulses is high and the repetition rate is low.

Decreasing the time step does indeed eliminate the oscillatory behavior. A simple method of making such a reduction is to increase the value of the constant C. That procedure was chosen as an interim solution. Unfortunately, this change dramatically increases the computational time. A method needs to be devised to set the value of C in such a way that a correct solution is assured and the computational time is minimized.

A second factor that contributed to the inaccurate solution is the method used to compute the temperature following the offset of the pulse. There are actually two sets of finite difference equations which represent the partial differential equation (1). The first set contains an energy term and describes the temperature profile during the

time the pulse is on. The second set does not have an energy term and is used after the pulse is turned off. Each set should be treated separately. The time step should be returned to its initial value at the end of the pulse. This change in the program has been made.

VII. EFFECTS OF BLOOD FLOW A brief simulation of the effects of blood flow on retinal damage was performed. Only one LASER wavelength and one set of time parameters were examined. The effects of four different power levels were examined. Four trials of 20 nanosecond pulses were presented at 15 Hz. The wavelength was 532. nanometers. Two blood flow rates were examined; no flow and the constant values normally used by the program (see Table I). The results are tabulated in Table III.

TABLE III

Effects of blood flow on lesion radius.

POWER (MW)	LESION RADIUS (cm)	
	FLOW ON	FLOW OFF
5.0	0.0454	0.0472
0.5	0.0185	0.0197
0.05	0.00658	0.00664
0.005	0.00283	0.00283

The data clearly indicate that lesion size is increased in the absence of retinal blood flow.

VIII. RECOMMENDATIONS

1) The program is currently cumbersome and difficult to use. Furthermore, the documentation is inadequate. The process of making the program run interactively should be completed. A complete user's manual will then be needed. Such manual should include not only detailed instructions for using the model but also explanations of the limitations of the model and the meaning of each of the parameters. Some of the parameters which are now constants should be made variables to be specified by the user (blood flow rates, thermal conductivities, pupil diameter, etc.) Extensive HELP capabilities should be added to make the program easier to use.

2) A set of guidelines must be developed for choosing the maximum allowable time step. The recently devised method of decreasing the time step must be refined in order to assure both accurate results and a reasonable computation time.

3) At present, the model will only handle square pulses, that is, zero rise and fall times. Provisions should be made to handle other temporal shapes.

4) The point spread function used to simulate ocular focusing and optical aberration effects should be examined more closely. The function used currently should be defined and made clear to the user. In addition that function should be compared to more recent formulations of the coherent spread function. The more recent formulation

should either be substituted or the user should be given a choice of the two functions.

5) A comprehensive input data set should be chosen as a test set. This data set should be designed to serve as a benchmark to compare newer versions of the program to the current version. That data set will be particularly valuable when program changes are made or when the program is converted to run on other machines.

6) The program assumes that no damage occurs until the tissue temperature reaches 44 deg Celsius. The repercussions of that assumption should be examined.

7) There are two constants used in the damage model. What is the source of those constants and have there been additional data published in the last fifteen years?

8) In the model the beam radius is defined at the $1/e^2$ intensity point rather than the more commonly used 1/e point. Why was such an unusual choice made?

9) Output routines should be written that allow the user to get files, printouts and plots of the temperature profile as a function of both spatial coordinates and time.

10) Preliminary results indicate that for 532 nm LASER assault, blood flow has a small but significant effect on lesion size. In view of the decrease in retinal blood flow during high acceleration maneuvers, a complete parametric study should be done.

REFERENCES

1. Takata, A. N., L. Goldfinch, J. K. Hinds, L. P. Kuan, N. Thomopoulis and A. Weigandt, "Thermal Model of Laser-Induced Eye Damage", Final report for USAF School of Aerospace Medicine, Brooks AFB, TX, report IITRI-J-TR-74-6324, contract F41609-74-C-0005, IIT Research Institute, Chicago, IL, 1974.

2. Mertz, A. R., B. R. Anderson, E. L. Bell & D. E. Egbert, "Retinal Thermal Model of Laser-Induced Eye Damage: Computer Program Operator's Manual", Final Report for USAF School of Aerospace Medicine, Brooks AFB, Tx, report SAM-TR-76-33, 1976.

3. Welch, A. J., L. A. Prieve, L. D. Forster, R. Gilbert, C. Lee and P. Drake, "Experimental Validation of Thermal Retinal Models of Damage from Laser Radiation", Final report for USAF School of Aerospace Medicine, Brooks AFB, TX, report SAM-TR-79-9, contract F33615-76-C-0605, Bio-Medical Engineering Laboratory, UT, Austin, TX, 1979.

4. Welch, A. J. and G. D. Polhamus, "Measurement and Prediction of Thermal Injury in the Retina of the Rhesus Monkey", IEEE Trans. on Biomed. Engr., V31, pp 633-644, 1984.

5. Polhamus, G. D., "In Vivo Measurement of Long-Term Laser Induced Retinal Temperature Rise", IEEE Trans. on Biomed. Engr., V27, pp 617-622, 1980.

6. Welch, A. J., L. A. Priebe, G. D. Polhamus and G. D. Mistry, "Limits of Applicability of Thermal Models of Thermal Injury", Final report for USAF School of Aerospace Medicine, Brooks AFB, TX, report UT-TR-77-11, contract F41609-76-C-0005, Biomedical Engineering Laboratory, UT, Austin, TX, 1976.

7. Peaceman, D. W. and H. H. Rachford, Jr, "The Numerical Solution of Parabolic and Elliptic Differential Equations", JSIAM, V3, pp28-41, 1955.

8. Douglas, J, Jr and T. M. Gallie, Jr, "Variable Time Steps in the Solution of the Heat Flow Equation", Proc Amer Math Soc, V6, 1955.

9. Takata, A., "Development of Criterion for Skin Burns", Aero Med, pp634-637, 1974.

1986 USAF-UES SUMMER FACULTY RESEARCH PROGRAM/

GRADUATE STUDENT SUMMER SUPPORT PROGRAM

Sponsored by the
AIR FORCE OFFICE OF SCIENTIFIC RESEARCH
Conducted by
Universal Energy Systems, Inc.

FINAL REPORT

CHLAMYDOMONAS PHOTOTAXIS AS A SIMPLE SYSTEM FOR TESTING THE EFFECT OF DRUGS ON VISION

Prepared by: Dr. Rex C. Moyer
Academic Rank: Professor of Biology
Department: Biology Department
University: Trinity University

Research Location: Opthamology Branch,
Clinical Sciences Division
School of Aerospace Medicine
Brooks Air Force Base, Texas 78235-5301

USAF Researcher: Dr. John Taboada

Date: August 22, 1986

Contract No. F49620-85-C-0013

CHLAMYDOMONAS PHOTOTAXIS AS A SIMPLE SYSTEM FOR TESTING THE EFFECT OF DRUGS ON VISION

by

Rex C. Moyer, Ph.D.

ABSTRACT

The major goal of this program is to develop, refine, and characterize the phototaxis system in **Chlamydomonas reinhardti** and then employ it in the goal of finding and quantifying the effect of drugs which may enhance dark or color vision in pilots. A major problem associated with the testing of drugs which may affect vision in animals or man is that the drugs may affect more than one tissue, organ, or organ system. The advantage of first testing the effect of the drugs on the ability of a phototactic alga such as **Chlamydomonas** to swim toward the light is the inherent simplicity of the system in which the investigator can control the variables. **Chlamydomonas** is a simple, single-celled alga whose phototaxis apparatus biochemically mimics the fundamental vision system of man.

Major emphasis of our research team, Ms. Angela Braun, Dr. Taboada and Dr. Moyer has been the simplification of the procedure for producing phototactic cells and improve the method for measuring phototaxis. Eight Strains of **Chlamydomonas reinhardtii** were placed under phototaxis-inducing conditions and the growth and phototactic ability of the strains compared in different phases of their growth curves. Various means of measuring phototaxis were investigated. We were successful in simplifying and shortening the procedure for developing phototactic cells and in developing a simple and rapid method for quantifying the phototactic ability of algae cells to any wavelength of light between 400 and 700 nanometers.

Because of the large amount of data generated and the size limitation of the final report, the final reports of Ms. Braun and Dr. Moyer have been cooperatively blended to provide enough space to include all of the figures and legends.

ACKNOWLEDGEMENT

I would like to thank the Air Force Systems Command, the Air Force office of Scientific Research, and Universal Energy Systems for providing me the opportunity to participate in a valuable research experience at the Clinical Sciences Division, School of Aerospace Medicine, Brooks Air Force Base, Texas. My thanks are particularly directed to Dr. John Taboada and Sergeant Mario Villanea of the Laser Spectroscopy Clinical Application Laboratory and Robotic Vision Laboratory Opthamology Branch for their help and for making my brief stay very pleasant as well as informative and productive.

My thanks also to Capt. Paul Barnicott, and Sgt. Raul Canales, Flight Medicine Branch, Clinical Sciences Division, Brooks AFB for their permission and aid in the use of their model ZBI Coulter Counter and Diluter. I also wish to thank Ms. Bonnie Fridley for aid in the use of the Aerospace Library and Mr. Joe Franzello (Aeromedical Library) for performing a computer search on phototaxis in algae.

My thanks to Angela Braun AFOSR-UES graduate student research collaborator for her excellent technical assistance. My thanks also to Trinity University personnel, Ms. Sylvia Stewart, Biology Department Secretary for typing, to Mr. Jesse Villalobos, Biology Department, for purchase of chemicals and equipment and for helping to set-up algae culturing apparatii, to Mr. Tom Nixon, physical plant, for set-up of lighted incubators and environmental chambers, to Ms. Sophia Wu, Thorman Laboratory, for other technical assistance, and to Ms. Beth Burgener, Biology Department, for washing glassware. My thanks to Dr. Tom Koppenheffer, Chair of the Biology Department and Dr. Ed Roy, Dean of the Division Science, Mathematics and Engineering for their continuing support of my research.

My personal thanks to Dr. John Taboada, Clinical Science Division, Brooks AFB, for being an excellant research collaborator.

I. INTRODUCTION

I have been a microbiologist since 1957. I have done research on bacteria, yeasts and filamentous fungi, and viruses as well as higher plants and animals. Thus I am well equipped to provide breadth and depth of experience to any project requiring the use of microorganisms. Prior to 1985 I had no experience working with algae, but this experience was gained during my 1985 AFOSR-UES Summer Faculty Fellowship when this research project was initiated. I also have a range of experience and knowledge of higher plants as well as many professional contacts in this area which will be useful in Phase III of this research. I also have had experience in working with retinoids which will be useful in Phase III. I have not had experience in optics, or lasers, nor in instrumentation but this deficiency is abrogated by my Air Force research colleague, Dr. John Taboada who qualifies as an expert in these and other fields as well. I have a well equipped microbiology research laboratory at Trinity University, only 12 miles from Dr. Taboada's laboratory and thus our two laboratories together can adaquately address research projects in optics, biophysics, and microbiology, and botanical sciences. I also have access to a Trinity University student labor force which can be useful.

II. OBJECTIVES OF THE RESEARCH EFFORT

The major goal of this 1986 Summer Fellowship is to develop phototaxis in **Chlamydomonas reinhardtii** algae in order to find and quantify the effect of drugs which may enhance dark or color vision in man.

The overall research plan has three component phases:

Phase I. Establish Phototaxis System using **Chlamydomonas reinhardtii**.

Phase II. Refine and Characterize the Phototaxis System; Isolate a Collection of Phototaxis Mutants.

Phase III. Testing the Effect of Drugs on Phototaxis in **Chlamydomonas reinhardtii.**

Phase I was completed during my 1985 Summer Faculty Research Fellowship. Phase III is to be accomplished in the future and Phase II is my goal for my 1986 Fellowship and my 1985 Minigrant. Phase II

had four goals: (1) Simplify the procedure for producing phototactic cells; (2) Develop methods for the synchronization of the growth of **Chlamydomonas**; (3) Improve the laser doppler method for measuring phototaxis; and (4) Isolation of temperature-sensitive phototaxis mutants.

III. MATERIALS AND METHODS

A. Cultures:

1. ***Chlamydomonas reinhardtii*** strains CC-124, CC-125, CC-1009, CC-1010, CC-654, CC-656, CC-1101, and CC-1102 were obtained from Dr. Elizabeth Harris, Chlamydomonas Genetics Center, Duke University, Durham, N.C. A brief description of each stain is presented below:

   CC-124 wild type mt^- Levine strain from original wild type strain 137c.

   CC-125 wild type mt^+. Levine strain from original wild type strain 137c.

   Both 124 and 125 have two gene mutations (nit-1 and nit-2) in the nitrate reductase activity and cannot use nitrate as a nitrogen source.

   CC-1009 wild type mt^- (UTEX 89)

   CC-1010 wild type mt^+ (UTEX 90)

   CC-654 Ebersold #191 lnp mt^- (phototaxis mutant)

   CC-656 Ebersold #187 y-1 lnp mt^- (phototaxis mutant)

   CC-1101 ey mt^- eyespotless mutant from Hartshorne.

   CC-1102 ey mt^+ eyespotless mutant from Hartshorne.

B. Culture Media:

1. Trace Elements mix (1000x) from Elizabeth Harris, personal communication.

Trace Element	Weight (g)	ml dist H_2O
Na_2 EDTA	50.0	250
$ZnSO_4.7H_2O$	22.0	100
H_3BO_3	11.4	200
$MnCl_2.4H_2O$	5.06	50
$FeSO_4.7H_2O$	4.99	50
$CoCl_2.6H_2O$	1.61	50
$CuSO_4.5H_2O$	1.57	50
$(NH_4)\ MO_7O_{24}.4H_2O$	1.10	50

Dissolve each salt in distilled or deionized water as indicated. Disodium EDTA must be dissolved in boiling water. Prepare $FeSO_4$ last since it oxidizes in solution. Mix all solutions except EDTA. Bring the mixed salts solution to a boil and then add the Na_2 EDTA solution. The mixture should turn green. When all the salts are dissolved, cool the solution to 70°C. Keeping the temperature at 70°C, adjust the pH to 6.7 with 80-90 ml of hot KOH (20%). Standardize the pH meter at 70°C also. Do not use NaOH to adjust the pH.

Let final solution stand for 1-2 weeks in a cotton stoppered flask. Shake the solution once a day. The solution should turn purple and leave a rust-brown precipitate. After two weeks, filter the solution through 2 layers of whatman #1 filter paper. Refrigerate or freeze in convenient aliquots.

2. Concentrated Beijerinck's solution:

Salt	wt (gl)
NH_4Cl	100
$MgSO_4 \cdot 7H_2O$	4
$CaCl_2 \cdot 2H_2O$	2

3. Concentrated Beijerinck's without nitrogen.

Salt	wt (g/l)
$MgSO_4 \cdot 7H_2O$	4
$CaCl_2 \cdot 2H_2O$	2

4. Concentrated phosphate.

Salt	wt (g/l)
K_2HPO_4	288
KH_2PO_4	144

5. Media Formulations

Constituent	HSA	Modified Foster	NMM
Conc. Beijerinck's	5 ml	5 ml	--
Conc. Beijerinck's -N	-	-	5 ml
Conc. Phosphate	5 ml	5 ml	1 ml
Trace Elements	1 ml	1 ml	1 ml
Sodium acetate $\cdot (3H_2O)$	2.0 gm	2.0 gm	2.0 gm
Bacto-tryptone	-	2.0 gm	-
Agar*	15 gm	15 gm	-
Distilled water	990 ml	q.s.1 liter	q.s.1 liter

* Agar Conc. - ordinary agar plates 15 gm/l
agar slants 20 gm/l

suspension was inoculated into 50 ml of previously sterilized HSA broth in 250 ml side-armed Erlenmeyer flasks. The cultures were incubated at 22°C in a oscillatory shaker at 64 cycles/min. 20 cm under 4 Sylvania 40W--cool white bulbs. The turbidity of the culture was measured at intervals by spectrophotometry at 600 nm of the culture in the side arm of the flask using sterile HSA broth blank to adjust the abosrbance to zero. This culture was incubated from 0-70 hours depending upon the experiment.

3. Induction of gametogenesis.

Shake cultures in HSA broth were harvested at various times after they were initiated and converted to gametes by nitrogen deprivation as follows. Cultures were aseptically poured into sterile 50 ml centrifuge tubes and centrifuged at room temperature for 5 minutes at full speed in an International Model HN centrifuge. The green cell pellets were resuspended in 10 ml NMM broth medium and again centrifuged under the same conditions. The pellets were washed one more time with NMM. The cell pellet was again resuspended in 10 ml of NMM broth and inoculated into 40 ml of NMM broth. The cultures were incubated at 22°C at 64 rev/min as discribed above. The vegetative cells were converted to gametes by 24 hours under these conditions (Foster et al. 1984).

C. Tests for Bacterial Contamination.

To determine if bacteria were contaminating the algal cultures, 0.1 ml of algal material was aseptically pipeted onto a Blood Agar and Brain-Heart Infusion Agar. The inoculum was spread over the surface with the aid of glass "hockey sticks." The plates were incubated at room temperature (20-25°C) and duplicates at 37°C. Cultures are examined daily for bacterial growth. The algae do not grow on these media.

E. Algal cell counts. Cell counts were made both by direct cell count with Model ZBI Coulter Cell Counter and a Model WRD.Z Coulter Diluter housed in the Clinical Chemistry Branch. 1.0 ml of culture suspension was removed at time intervals and transported immediately to Brooks AFB for cell counting. Culture samples were

diluted in Isoton Solution either at 1:100 or 1:500 using the following formula:

$$\text{DF (Dilution Factor)} = \frac{\text{ml of sample + ml diluent}}{\text{manometer sample size x ml of sample}}$$

$$\text{For 1:100 dilution} = \frac{0.1976 \text{ ml} + 19.76 \text{ ml}}{0.5 \text{ ml} \times 0.1976 \text{ ml}} = \frac{19.9576}{0.0988} = 202$$

$$\text{For 1:500 dilution} = \frac{0.04 \text{ ml} + 19.76 \text{ ml}}{0.5 \text{ ml} \times 0.04 \text{ ml}} = \frac{19.8}{0.02} = 990$$

Thus the coincidence corrected algal cell count x the DF yields the number of cells/ml in the shake culture.

F. Measurement of Phototaxis. Four different methods have been tested for measuring algal cell phototaxis.

1. Argon laser

An argon laser (Spectra Physics 164) with a continuous output of 200 mW at 476.2 nm (blue light) and a beam diameter of 1 mm was used to photostimulate the cells. The cells to be tested for phototaxis are drawn into a 100 l capillary tube. The Argon laserbeam is directed through the open end of the capillary tube. Phototactic cells collect either at entrance meniscus (positive phototaxis) or at the exit meniscus (negative phototaxis). This procedure was of limited use because only one sample could be run at a time and each sample required up to 10 minutes of exposure.

2. Slide Projector/Filter Method.

This procedure was set up at Trinity University and therefore saved a trip to Brooks to measure phototaxis. A model 3689 "GK" Delineascope slide projector (American Optical Company, Buffalo, N.Y.) with a 750 watt DDB lamp was used as a light source. In the slide mounting were placed filters mounted between 2" x 4" glass plates. The filters are referred to as "roscolene" filters and were purchased from Rosco Laboratories, Port Chester, New York. Roscolene filter numbers 819, 851, 854, 855, 866, 874, and 877 were prepared and tested. The spectrum of light transmitted by each filter is on file. In general the filters transmitted a wave length "window" of about

100 nm. The algae are pulled into a 100 µl capillary tube, the end sealed with parafilm, and placed 2 cm from the exit of light. A thermometer is placed on the stand holding the capillary tubes. The temperature in the light path generally rises to about 30°C. The algae, depending upon the strain, will migrate toward or away from the light within 10 minutes. However, there is never a 100% attraction of cells to one meniscus or the other, and thus the population is neither completely phototactic or photophobic. About 16 capillaries can be tested at one time.

3. Diffraction Grating Method.

   This technique was set up to determine the effect upon phototaxis of each of the spectral wavelengths at one time. This was done by exposing a capillary tube filled with an algal suspension to the complete visible light spectrum. The visible spectrum was generated by using a standard 35 mm slide projector with a opaque slide with a 1 mm slit. The visible light passing through the slit was directed onto diffraction grating taken from a spectrophotometer. The spectral light generated was focused on a platform constructed to hold up to 20 capillaries.

4. Helium Neon Laser/Spectrophotofluorometer Method.

   An Aminco-Bowman spectrophotofluorometer was modified by removing one lamp and substituting a Helium Neon laser (Hughes Aircraft Co. model 322 5H-PC) with a continuous output of 10 mW and 632.8 nm red light and beam diameter of 1 mm. The laser beam was directed via mirrors through a 10 mm cuvette containing the suspension of algae. The beam directed through the swimming cells and partially becomes reflected back through mirrors to a detector. The detector was connected to an oscilloscope whose pattern reflected the movement of the cells.

5. Spectrophotometer Method.

   A Bio-Tech Spectrophotometer with a wave-length scan from 400 nm to 700 nm was used in conjunction with the side-armed Erlenmeyer culture flasks as described above. This procedure was eventually adopted because it could assess growth of the

culture as well as the organisms phototactic response to all wavelengths of light between 400 and 700 nm. The spectrophotometer was warmed up and a wavelength selected. The tests were performed in a darkened room. The culture to be tested was removed from the shaker (in the light), mixed, the culture broth dumped into the side-arm and the side-arm placed in the spectrophotometer light path. A reading was taken immediately to obtain an absorbance at the selected wavelength due solely to the turbidity of the organisms and not influenced by phototaxis. Absorbance readings were taken at 30 seconds intervals for a total of 4 minutes. As the phototactic organisms accumulated in the light path the absorbance increased. The absorbance of a non-phototactic culture would not increase except slightly due to some settling of the culture.

IV. RESULTS

A. Growth, of algal cultures and the role of the medium and possible contaminants.

As indicated in our Brief Report of Effort, the growth of the algal cultures were initially only 20% of what was obtained during my 1985 SFRP fellowship. The possible reasons for this were many, but included the age and source of medium constituents, possible microbial contaminants, and lighting and temperature requirements which at that time were different from last year. The problems of the poor growth was solved and was due to some component of the medium since a newly prepared medium did result in good growth. However, during this time the Environmental chamber was repaired and optimal lightening installed. Due to the number of manipulations the cultures are put through in order to develop phototactic gametes according to the Foster et al procedure, bacterial and fungal contaminants do occur and we have detected them, but we could not detect any contaminants in our stock cultures. In general, the contaminants that do occur are not great in number and (with the exception of 1-3 recent examples) do not significantly affect the growth of the algal cultures.

B. Growth Characteristics of the Algal Cultures.

The major goal of our SFRP fellowship was to simplify and shorten the procedure required to produce phototactic cells. In order to accomplish this, it was necessary to characterize the growth and phototaxis of the eight Chlamydomonas cultures at all of the stages required by the Foster et al procedure. The growth component of this goal has been accomplished, but the characterization of the phototaxis of these cultures has been completed for only the vegtative cells of two strains. The study of the phototaxis of the vegetative cells for the other six strains and of the cells after they have been induced for gametegonesis will have to be accomplished during the tenure of the mini-grant.

Because the Coulter Cell Counter is located at Brooks AFB and the cultures are grown and turbidities measured at Trinity University, it was generally attempted to assess the growths of the algal liquid cultures by OD600 rather than cells/ml, especially when it was important to collect data rapidly. When it was necessary to relate the growth of a strain to cells/ml, this could be done easily with a standard curve relating cell number to turbidity at 600 nm. Figs. 1 and 2 describe this relationship for all algal strains growing in HSA liquid shake 18 hour cultures. The points were derived by diluting all eight cultures at undiluted, 1:2, 1:4, and 1:8 in sterile HSA broth and determining the turbidity at 600 nm. One ml of each dilution was transferred to a sterile capped tube and transported to Brooks for cell counts. All cultures and dilutions were counted at 1:100 dilution. Raw counts were corrected for coincidence. Mean cell volumes on all cell samples were also determined.

Fig. 1 provides the turbidity/cell number for strains 125, 654, and 1009.

Fig. 2 provides the relationship for strains 124, 656, 1010, 1101, and 1102. Comparison of these relationships suggests that all of the different strains do not fit the same line. Strains 1010, 1101, and 1102 fall into a similar group, as do 124 and 656 and do 125, 654, and 1009. These latter groups are more heterogeneous, however.

In order to attempt to ascertain the meaning of these varied turbidity-cell number relationships, the turbidity which is equivalent to 1 million cells was estimated from Figs 1 and 2. These are presented below along with the mean cell volumes provided by the Coulter Counter. These mean cell volumes represent the average of 24 individual measurements for each strain.

RELATIONSHIP BETWEEN TURBIDITY, CELL NUMBER, AND MEAN CELL VOLUME

Strain No.	OD600 Equivalent to 10^6 CEIls	Mean cell Volume
1010	0.07	124
1101	0.10	174
1102	0.11	171
656	0.19	197
124	0.25	188
125	0.47	184
654	0.66	270
1009	0.81	277

This data shows a positive correlation between the turbidity of one million cells and the mean cell volume. This would suggest that the turbidity (OD600) of a culture is a strong function of cell volume as as well of cell number. This would also suggest that there would be little correlation between *a* growth curve determined by turbidity and one determined by cell counts. As shown in the growth curves presented in Figs 3, 4, and 5, this indeed appears to be the case.

Fig. 3 shows one of two growth curves of strains 124, 125, 654, 656, 1009, 1010, and 1101 in which growth was assessed by measuring culture turbidity at 600 nm over the 220 hours of the experiment. At 90 hrs culture incubation time, the cultures were shifted to nitrogen-free media which induces gametogenesis. All of the strains reach maximum stationary phase of growth by 24 hours in liquid shake culture. In these runs, all of the cultures reached a maximum OD_{600} of about 0.9 - 1.0 except for 1010 which reached an OD_{600} of 1.8 and 125 which reached a maximum OD_{600} of 0.6. Strain 125, which reached the lowest turbidity in this growth curve, also had the lowest initial turbidity, of only 0.13.

As shown in Fig. 4, which was a repeat growth curve of Fig. 3, shows strain 125 to reach the highest stationary phase turbidity (OD_{600} = 1.34) and in this second case the starting turbidity was 0.24. Finally, Fig. 5 shows a growth curve of vegetative cells in HSA broth, but in which the cell number was recorded vs. time instead of OD_{600}. In this experiment, strain 125 reached the highest cell count. In this experiment also, the maximum stationary phase was reached in 24 hrs by strains 124 and 654 but required 48 hrs for strains 125, 656, 1010, 1101, and 1102. Strain 1009 required 72 hrs to reach maximum cell numbers per ml. These three growth curve experiments demonstrate that the growth characteristics of the eight algal strains are quite unique and that there are a number of factors which govern the growth of these cells which are at present unknown.

The remainder of the Results are presented in the report of Ms. Angela Braun, the graduate student assistant on the project.

V. DISCUSSION

Please see Angela Braun's report.

VI. RECOMMENDATIONS

Please see Angela Braun's report.

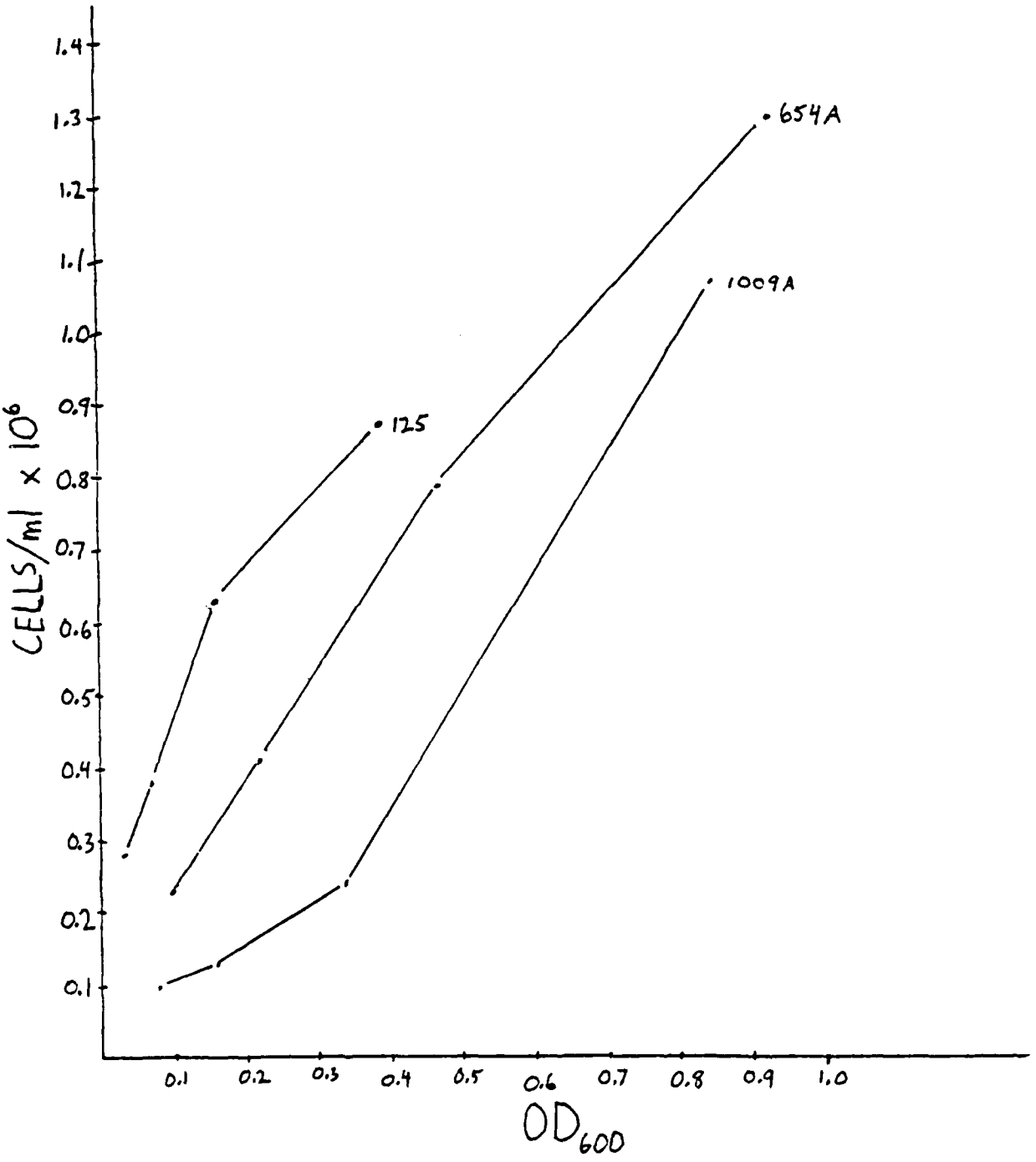

FIG. 1: Relationship between cell number and turbidity at 600 nm for C. reinhardtii strains 125, 654, and 1009.

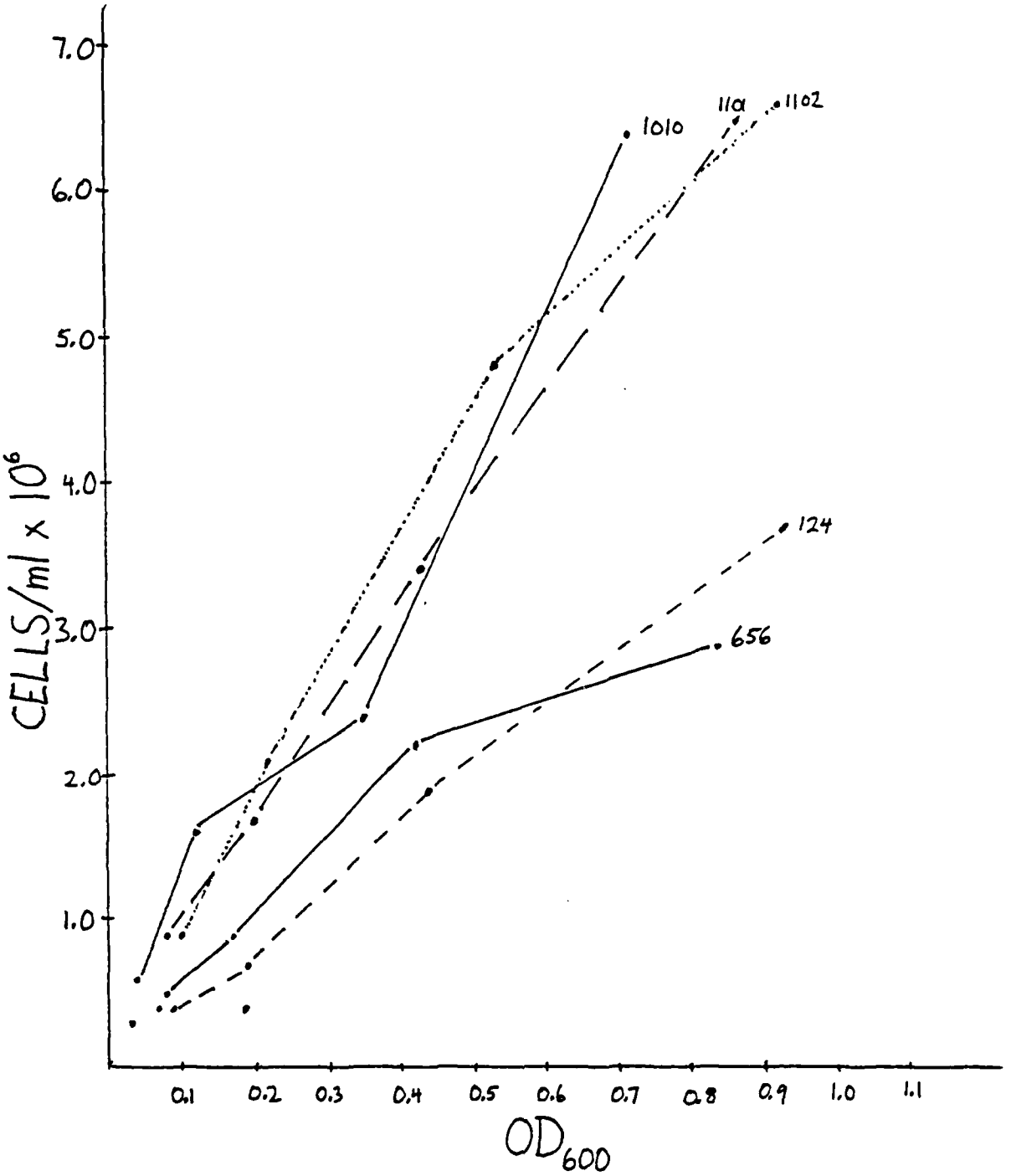

FIG. 2: Relationship between cell number and turbidity at 600 nm for C. reinhardtii strains 125, 654, and 1009.

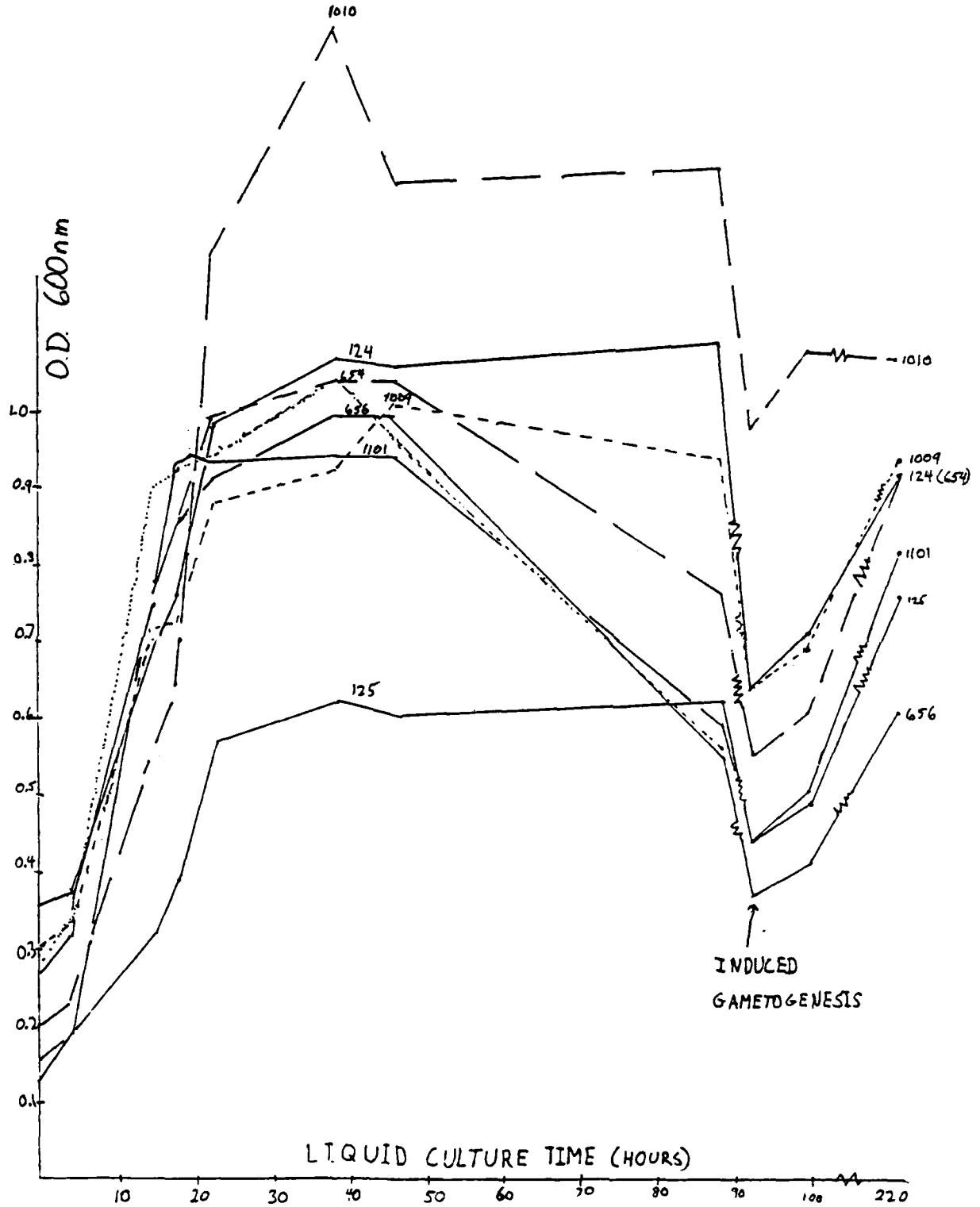

FIG. 3: Growth curves of C. reinhardtii strains 124, 125, 654, 656, 1009, 1010, and 1101 in liquid shake culture in HSA broth.

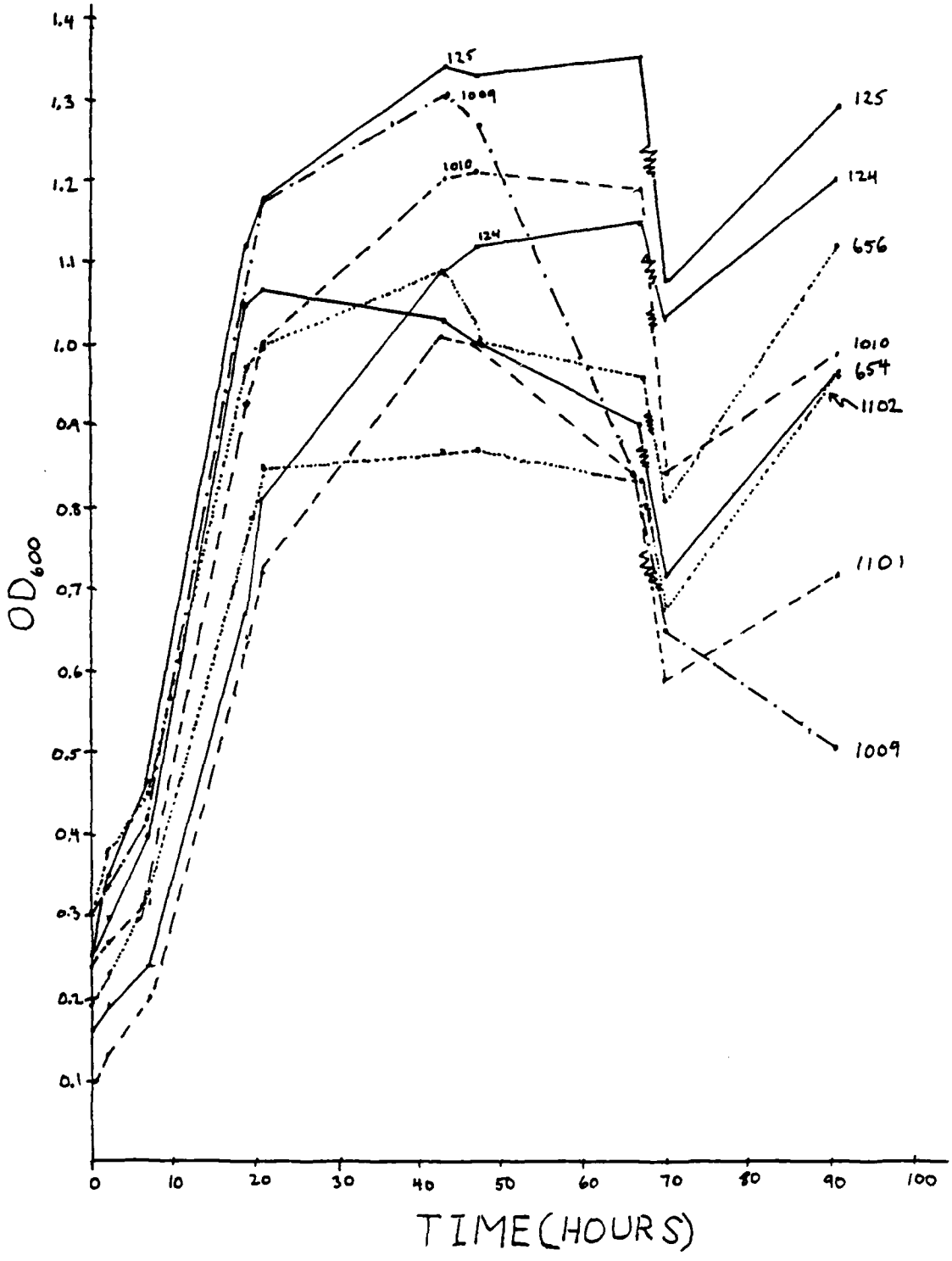

FIG. 4: Growth curves of C. reinhardtii strains 124, 125, 654, 656, 1009, 1010, 1101 and 1102 in liquid shake culture in HSA broth.

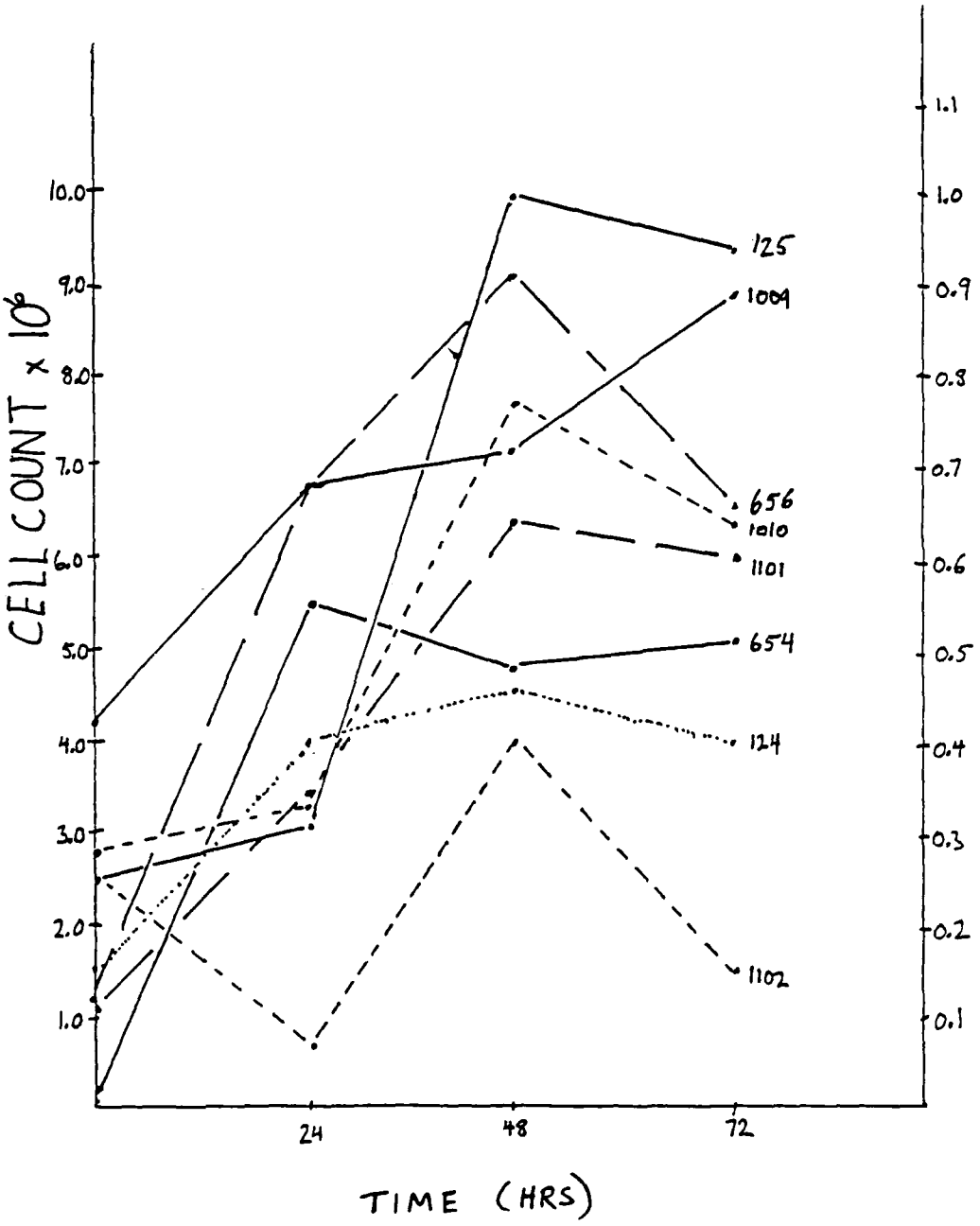

FIG. 5: Growth curves of C. reinhardtii strains 124, 125, 654, 656, 1009, 1010, 1101, and 1102 in liquid shake culture in HSA broth.

1986 USAF-UES SUMMER FACULTY RESEARCH PROGRAM/

GRADUATE STUDENT SUMMER SUPPORT PROGRAM

Sponsored by the

AIR FORCE OFFICE OF SCIENTIFIC RESEARCH

Conducted by the

Universal Energy Systems, Inc.

FINAL REPORT

An Investigation of the Utility of Computational Fluid Dynamics in the Prediction of Structural Active Cooling

Prepared by:	V. Dakshina Murty
Academic Rank:	Associate Professor
Department and	Mechanical Engineering
University:	University of Portland
Research Location:	Flight Dynamics Laboratory, Wright Patterson Air Force Base, Ohio, 45433, AFWAL/FIBE
USAF Researcher:	Mr. Michael E. Pajak
Date:	September 26, 1986
Contract No:	F49620-85-C-0013

An Investigation of the Utility of Computational Fluid Dynamics in the Prediction of Structural Active Cooling

by
V.Dakshina Murty

ABSTRACT

The finite element method is used to analyze forced convection heat transfer problems that are of interest in the evaluation of heat exchanger effectiveness. Towards this end, the transient, incompressible Navier-Stokes equations together with the energy equation are solved using the Galerkin's variational scheme for spatial descretization and the Crank-Nicholson method for time variation. Partial results in the form of plots of isotherms and streamlines for various values of the Peclet number are presented for two problems. They are --- forced convection in a 180 degree channel and forced convection through a rectangular offset pin array.

ACKNOWLEDGMENTS

The author would like to thank the Air Force Office of Scientific Research for offering him the Summer Faculty Fellowship at the Wright Patterson Air Force base. The author wishes to express his deep appreciation to Mr. Mike Pajak for being his sponsor and also helping him in many ways, both professionally and personally. Thanks are also due to Dr. Don Paul not only for suggesting the topic for the research but also for frequent consultations. It has indeed been a pleasure to have been associated with them. A special note of thanks to the entire staff of the FIBE group of AFWAL for making the author feel completely at home amongst them and making the summer a truly enjoyable and professionally rewarding experience.

I. INTORUDCTION:

I received my Ph.D from the University of Texas, Austin studying the applications of the finite element methods to the solution of Non-Newtonian fluid flow and heat transfer problems. I continued in this area at University of Portland where I have been teaching for the last five years. A major effort of my dissertation was to develop a general purpose finite element computer package to analyze computational fluid dynamics and heat transfer problems. A significant portion of my research thus focussed on the analysis of forced and free convection heat transfer phenomena.

The structures group at the Flight Dynamics Lab has been interested in evaluating the performance of actively cooled structures. Because of my background and interest in Numerical fluid flow and heat transfer, I have become involved in this basic research effort of analyzing complex heat transfer mechanisms which include boundary layer separation, heat transfer augmentation, stability of the flow structure, etc. and also numerical methods in the CFD field.

In the past few years there has been an increasing demand for compact and high performance heat exchangers due to their importance in aerospace and automobile vehicles, cooling of electronic equipment, space vehicles, and artificial organs. The consequence has been the development of several types of compact heat exchangers examples of which

are pin-fin heat exchanger, offset-fin heat exchanger, plain-fin heat exchanger. To evaluate the performance of these, one needs to know the heat transfer characteristics as functions of the flow parameters. Until recently this was done experimentally. However, with the advent of high speed supercomputers it has been possible to analyze them computationally.

Among the computational techniques used to solve continuum problems the finite difference and the finite element are the most common methods. Of the two, the finite difference method is older and simpler and hence is used commonly in fluid flow problems. However, despite its slight complexity the finite element method offers distinct advantages over the finite difference method. These include a sound mathematical foundation in the form of variational methods, ability to accurately model curved surfaces, relative ease with which the boundary conditions can be modelled, and the elegant physical interpretation which can be given to the resulting equations. As a result, despite its infancy the finite element method has become quite popular in computational fluid dynamics and heat transfer.

II. OBJECTIVES OF THE RESEARCH EFFORT:

As noted already, the usual method of determining the effectiveness of heat exchangers is through expreriments. This could be quite expensive since each new set of conditions may lead to a new experiment. With the advent of high speed computers, it is now possible to use CFD tools to perform the same task. In addition to being relatively inexpensive, the use of numerical solutions would add increased flexibility and also provide an efficient mechanism to study basic fluid flow and heat transfer phenomena. This investigation is aimed at studying the feasibility of use of the finite element method in the evaluation of heat exchangers.

In the rest of the report the methodology and the details of the computer code NONFLAP are described followed by the numerical results and recommendations for future work.

III. GOVERNING EQUATIONS AND FORMULATION:

The equations that govern convection heat transfer are the conservations of mass, linear momentum and energy. They are as follows:

$$\frac{\partial u_i}{\partial x_i} = 0 \qquad (1)$$

$$\rho\left[\frac{\partial u_i}{\partial t} + u_j \frac{\partial u_i}{\partial x_j}\right] = -\frac{\partial p}{\partial x_i} + \hat{f}_i + \frac{\partial \tau_{ij}}{\partial x_j} \qquad (2)$$

$$\rho C_p\left[\frac{\partial T}{\partial t} + u_j \frac{\partial T}{\partial x_j}\right] = k \frac{\partial^2 T}{\partial x_j \partial x_j} \qquad (3)$$

with a constitutive equation for a Newtonian fluid of the form

$$\tau_{ij} = \mu \left(\frac{\partial u_i}{\partial x_j} + \frac{\partial u_j}{\partial x_i} \right) \tag{4}$$

In the above equtaions it has been assumed that the fluid is incompressible, and the flow is two dimensional (plane or torsionless axisymmetric) and laminar. Generation of heat due to viscous dissipation has been neglected. To complete the mathematical description of the problem, a set of boundary and initial conditions is needed. A suitable set of such conditions are as follows:

$$\begin{aligned} u_i &= f_i(s) \qquad \text{on } S_u \\ t_i &= \tau_{ij}(s) n_j(s) \qquad \text{on } S_t \end{aligned} \tag{5}$$

for the hydrodynamic part and

$$\begin{aligned} T &= g(s) \qquad \text{on } S_T \\ q_i(s) n_i(s) &= h(s) \qquad \text{on } S_q \end{aligned} \tag{6}$$

for the thermal part and intial conditions of the form

$$\begin{aligned} u_i &= \hat{u}_i(t) \\ p &= \hat{p}(t) \\ T &= \hat{T}(t) \end{aligned} \tag{7}$$

The above equations complete the continuum description of the problem. A descrete analogue of the above is obtained using the Galerkin's variational statement. This can be done by taking the inner products of the continuity, linear

momentum, and the energy equations with pressure, velocity, and temperature. The resulting set of equations are

$$\int_V \delta p \, \frac{\partial u_i}{\partial x_i} \, dV = 0 \tag{8}$$

$$\int_V \rho \left[\frac{\partial u_i}{\partial t} + u_j \frac{\partial u_i}{\partial x_j} \right] \delta u_i = -\int_V \frac{\partial p}{\partial x_i} \delta u_i + \int_V \delta u_i \left(\frac{\partial \tau_{ij}}{\partial x_j} \right) \tag{9}$$

$$\int_V \rho C_p \left(\frac{\partial T}{\partial t} + u_j \frac{\partial T}{\partial x_j} \right) \delta u_i = \int_V k \frac{\partial^2 T}{\partial x_i \partial x_i} \delta T \tag{10}$$

The diffusion terms in equations (9)-(10) can be reduced using Green's theorem as follows:

$$\int_V \rho \left[\frac{\partial u_i}{\partial t} + u_j \frac{\partial u_i}{\partial x_j} \right] \delta u_i + \int_V \tau_{ij} \frac{\partial \delta u_i}{\partial x_j} = -\int_V \frac{\partial p}{\partial x_i} \delta u_i + \int_{S_t} \tau_{ij} n_j \delta u_i \tag{11}$$

$$\int_V \rho C_p \left[\frac{\partial T}{\partial t} + u_j \frac{\partial T}{\partial x_j} \right] \delta T + \int_V k \frac{\partial T}{\partial x_j} \frac{\partial \delta T}{\partial x_j} = \int_{S_q} k \frac{\partial T}{\partial x_j} n_j \delta T \tag{12}$$

Equations 9, 11, 12 complete the variational statement of the problem.

The spatial descretization of the problem is obtained by dividing the domain into a number of subregions called the finite elements and approximating the dependent variables over each element by means of suitable interpolation functions.

$$\begin{aligned} u_i &= \underset{\sim}{\phi}^T(x,y) \, \underset{\sim}{u}_i(t) \\ p &= \underset{\sim}{\psi}^T(x,y) \, \underset{\sim}{P}(t) \\ T &= \underset{\sim}{\Theta}^T(x,y) \, \underset{\sim}{T}(t) \end{aligned} \tag{13}$$

If the above equation is substituted into 9, 11, 12 the following set of matrix equations is obtained (see Gartling [1] for details).

$$[\hat{\underline{\underline{C}}}]\{\dot{\underline{q}}\} + [\underline{\underline{C}}(\underline{q}) + \underline{\underline{K}}]\{\underline{q}\} = \{\underline{F}\} \qquad (14)$$

where

$$[\hat{\underline{\underline{C}}}] = \begin{bmatrix} \underline{\underline{0}} & \underline{\underline{0}} & \underline{\underline{0}} & \underline{\underline{0}} \\ \underline{\underline{0}} & \underline{\underline{0}} & \underline{\underline{0}} & \underline{\underline{0}} \\ \underline{\underline{0}} & \underline{\underline{0}} & \underline{\underline{0}} & \underline{\underline{0}} \\ \underline{\underline{0}} & \underline{\underline{0}} & \underline{\underline{0}} & \underline{\underline{0}} \end{bmatrix},$$

$$\underline{\underline{C}} = \begin{bmatrix} \rho \underline{\varphi}\underline{\varphi}^T \underline{u} \frac{\partial \underline{\varphi}^T}{\partial x} & \rho \underline{\varphi}\underline{\varphi}^T \underline{v} \frac{\partial \underline{\varphi}^T}{\partial y} & \underline{\underline{0}} & \underline{\underline{0}} \\ \rho \underline{\varphi}\underline{\varphi}^T \underline{u} \frac{\partial \underline{\varphi}}{\partial x} & \rho \underline{\varphi}\underline{\varphi}^T \underline{v} \frac{\partial \underline{\varphi}}{\partial y} & \underline{\underline{0}} & \underline{\underline{0}} \\ \underline{\underline{0}} & \underline{\underline{0}} & \underline{\underline{0}} & \underline{\underline{0}} \\ \underline{\underline{0}} & \underline{\underline{0}} & \underline{\underline{0}} & \rho c \left[\underline{\varphi}\underline{\varphi}^T \underline{u} \frac{\partial \underline{\varphi}}{\partial x} + \underline{\varphi}\underline{\varphi}^T \underline{v} \frac{\partial \underline{\varphi}}{\partial y} \right] \end{bmatrix}$$

$$\underline{\underline{K}} = \begin{bmatrix} \mu 2 \frac{\partial \underline{\varphi}}{\partial x} \frac{\partial \underline{\varphi}^T}{\partial x} & \mu \frac{\partial \underline{\varphi}}{\partial y} \frac{\partial \underline{\varphi}^T}{\partial x} & \frac{\partial \underline{\varphi}}{\partial x} \underline{\psi}^T & \underline{\underline{0}} \\ \mu \frac{\partial \underline{\varphi}}{\partial x} \frac{\partial \underline{\varphi}^T}{\partial y} & \mu 2 \frac{\partial \underline{\varphi}}{\partial y} \frac{\partial \underline{\varphi}^T}{\partial y} & \frac{\partial \underline{\varphi}}{\partial y} \underline{\psi}^T & \underline{\underline{0}} \\ -\gamma \frac{\partial \underline{\varphi}^T}{\partial x} & -\gamma \frac{\partial \underline{\varphi}^T}{\partial y} & \underline{\underline{0}} & \underline{\underline{0}} \\ \underline{\underline{0}} & \underline{\underline{0}} & 0 & k \left[\frac{\partial \underline{\Theta}}{\partial x} \frac{\partial \underline{\Theta}^T}{\partial x} + \frac{\partial \underline{\Theta}}{\partial y} \frac{\partial \underline{\Theta}^T}{\partial y} \right] \end{bmatrix}$$

$$\{\underline{q}\}^T = \{\underline{u}^T \quad \underline{p}^T \quad \underline{T}^T\}$$

The time dependent set of matrix equations are solved by the Crank-Nicholson method.

Since the above set of equations is nonlinear, an iteration scheme is needed. In this investigation, Picard's method is used with the starting iterate being that of creeping flow and pure thermal diffusion solutions. The iterative procedure is stopped when the following convergence criterion is satisfied for temperature: for j^{th} iteration

$$\max \left\{ |T_i^{(j-1)} - T_i^{(j)}| \,/\, |T_{max}^{(j-1)}| \right\} \leq 10^{-2} \qquad (16)$$

$1 \leq i \leq$ No. of Nodes

with

$$T_{max}^{(j-1)} = \max_{1 \leq i \leq \text{No. of nodes}} |T_i^{(j-1)}|$$

A similar criterion is used for the velocities and temperature also.

The above features are incorporated into a general purpose finite element program NONFLAP (Non Newtonian Fluid Analysis Program). The program has several desirable features such as a versatile grid genartor, dynamic storage capability, frontal solution technique, Penalty method (see Murty [2] for details), etc. For brevity the details are not presented; the reader may consult Murty [3] and Harlan [4]. The research described in this report was conducted using NONFLAP.

IV. NUMERICAL RESULTS:

In this section computational results for two problems are presented. They are convective heat transfer analysis in

a rectangular offset pin heat exchanger and leading edge cooling of an aircraft.

The physical problem, the computational domain and the mesh for the first

problem are shown in Fig. 1.

A plot of the streamlines and isotherms for various values of Peclet number is shown in Fig. 2. For all the values of the Peclet number, the Reynolds number is constant. It can be seen that since the Reynolds number was quite low the streamlines are almost symmetric about the horizontal centerline. The highest value of Peclet number used in this study was 54.0 and it can be seen that the due to the coarseness of the mesh the thermal boundary layer has not been resolved effectively.

The physical description and the computational domain for the aircraft leading edge cooling problem are shown Fig. 3. The corresponding streamlines, isobars, and isotherms are shown in Fig. 4. The effect of boundary layer separation on the isotherms can be seen easily.

From the above two examples it can be concluded that the finite element method offers a viable alternative to expensive and cumbersome experimentation to study the characteristics of heat exchangers. In addition to being relatively inexpensive, numerical methods offer flexibility for studying the effect of the variation of different flow parameters, dimensions, and boundary conditions on the

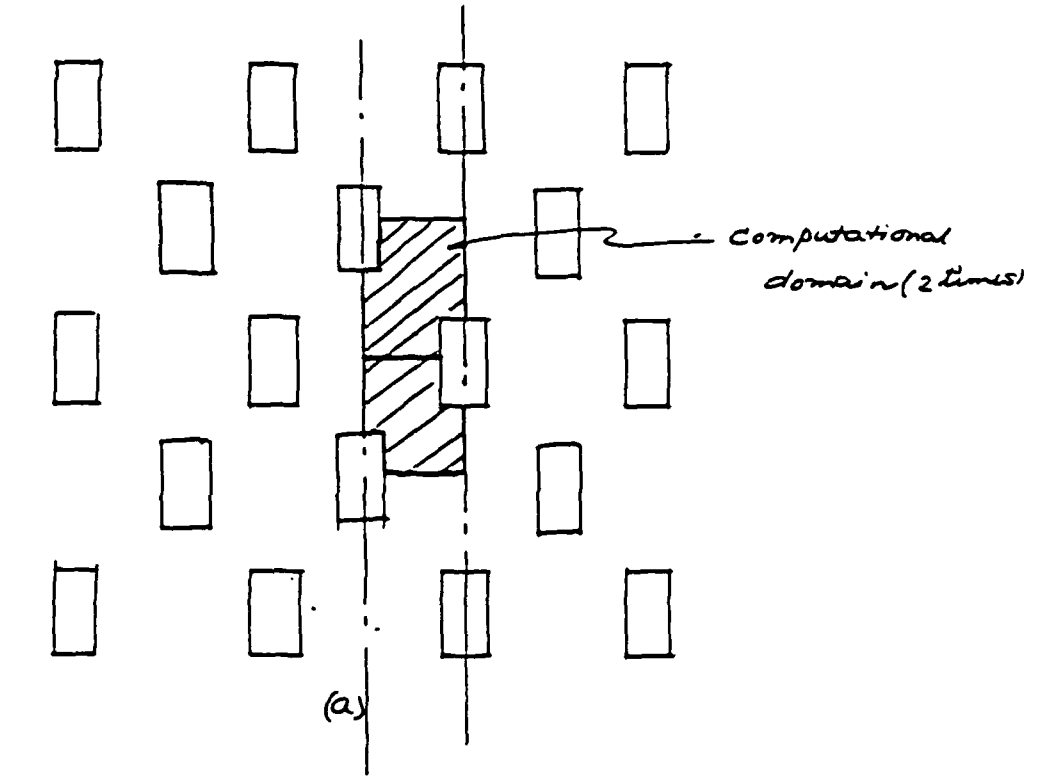

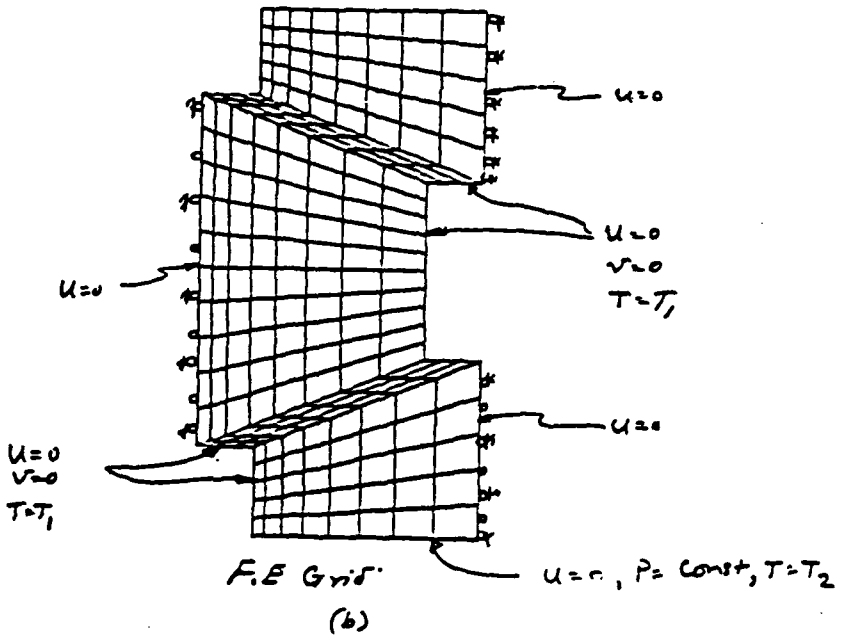

Figure 1: Rectangular offset pin heat exchanger
a) Computational domain b) F.E. mesh

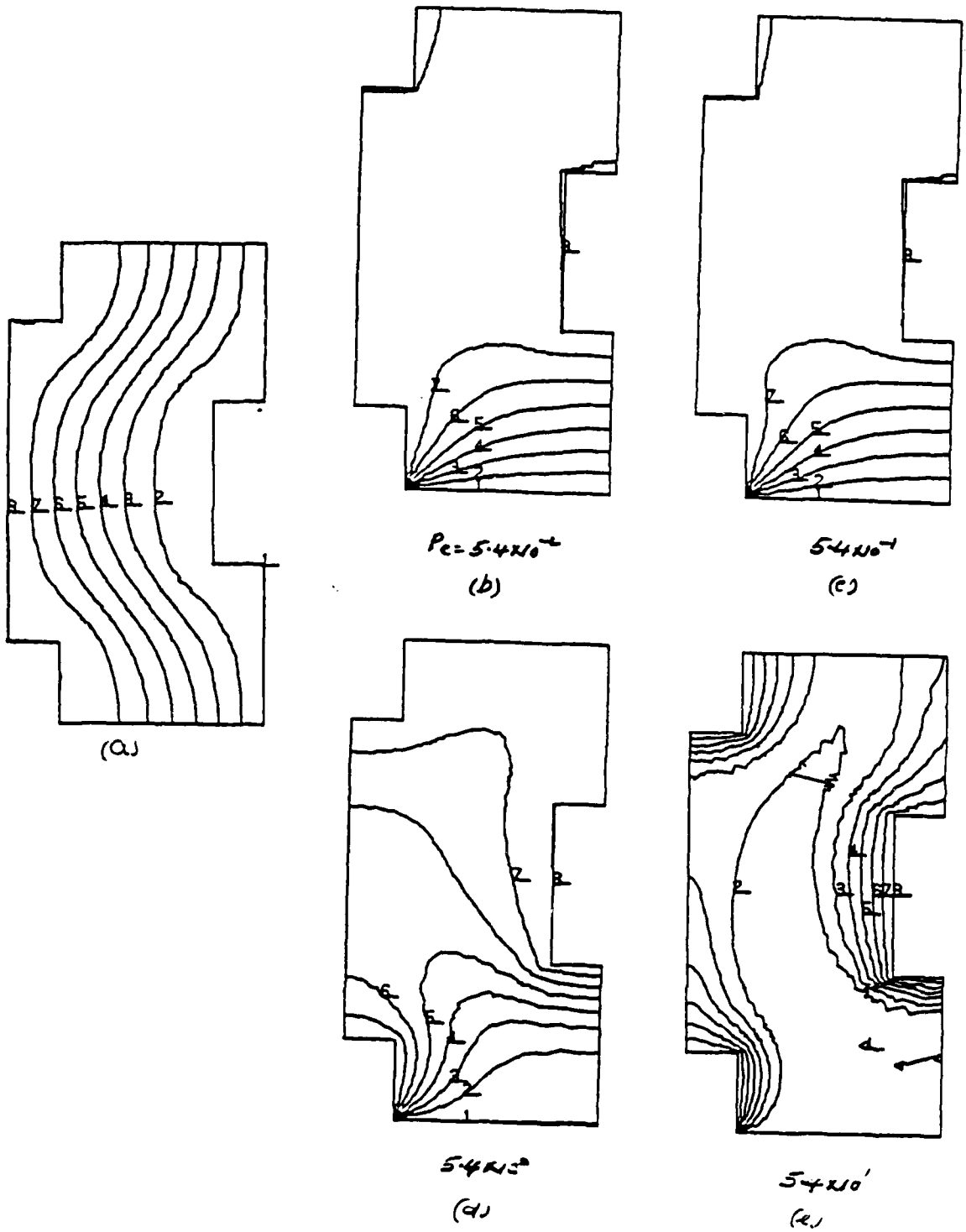

Figure 2: a) Streamlines (b) – e) Isotherms, for rectangular offset fin problem

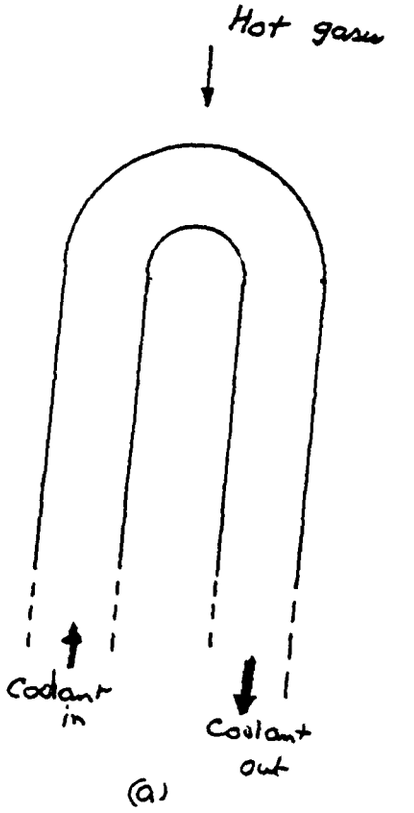

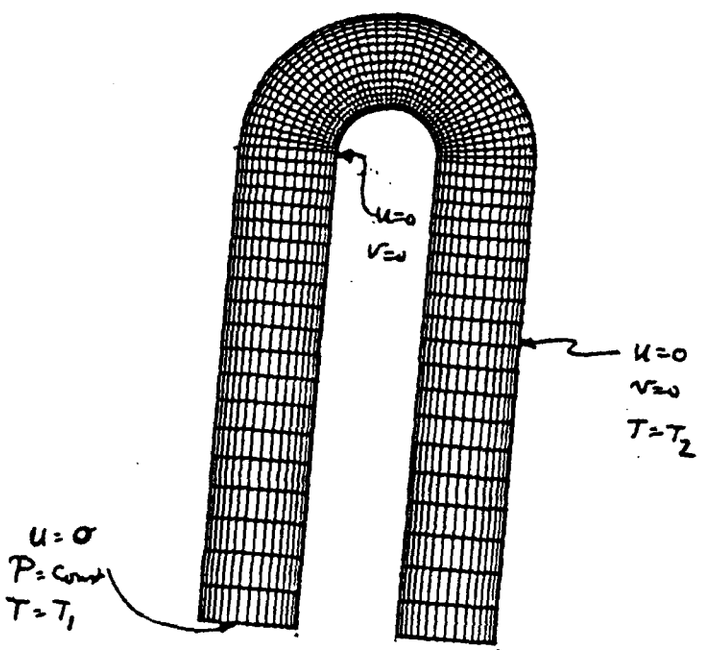

Figure 3: 180° channel problem (a) Physical problem.
(b) Computational mesh.

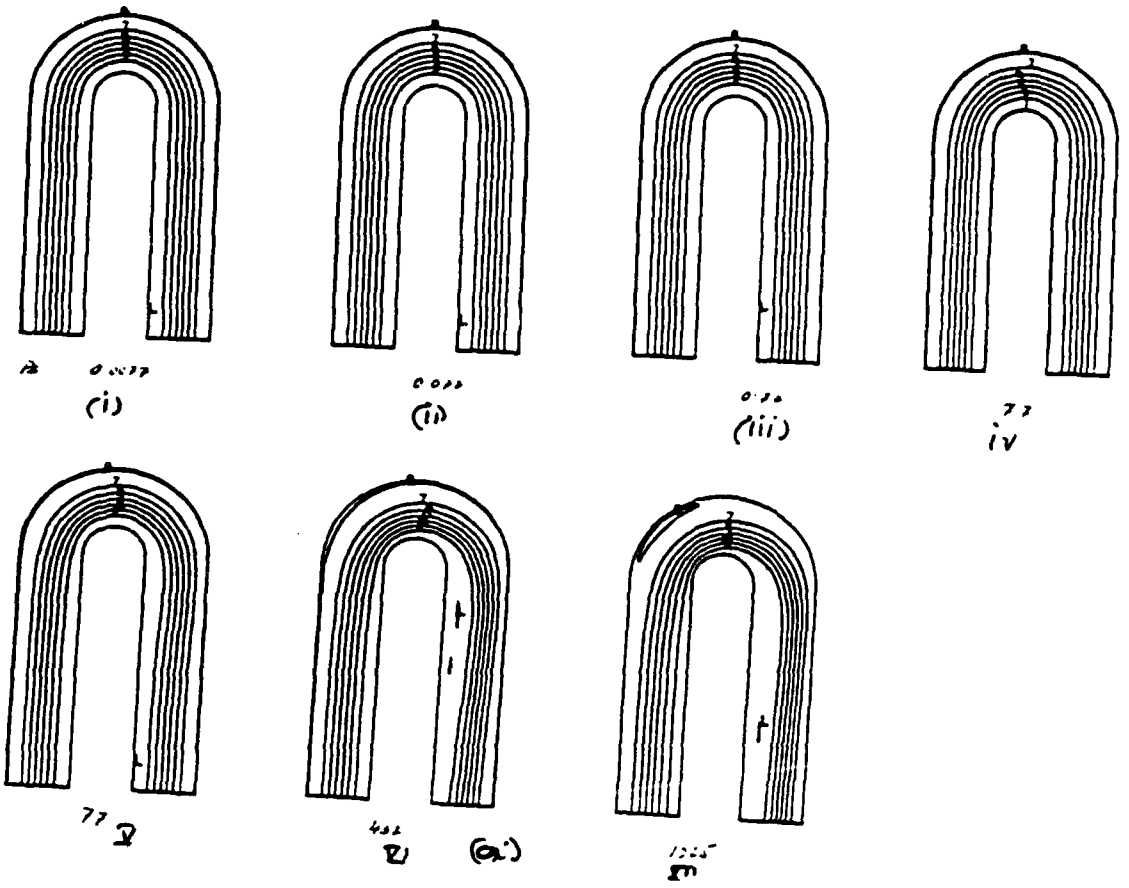
(i)
(ii)
(iii)
iv
(a)
(b)

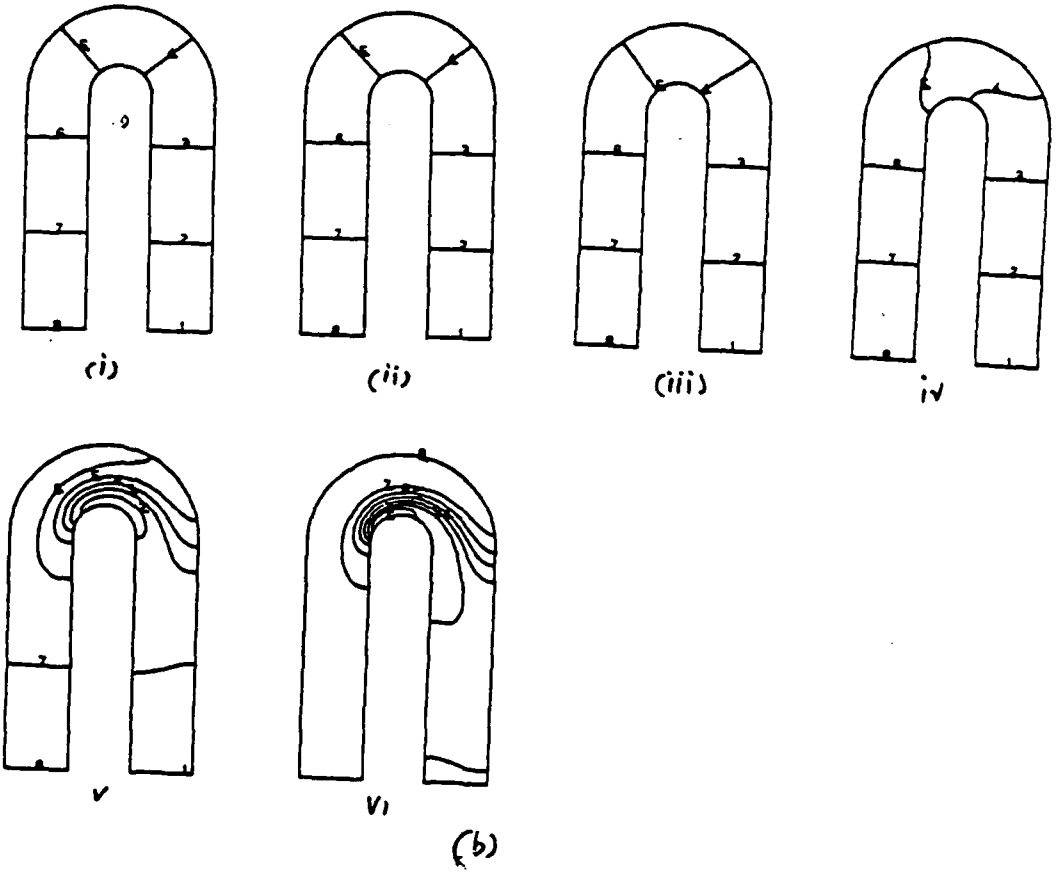
(i)
(ii)
(iii)
iv
v
vi
(b)

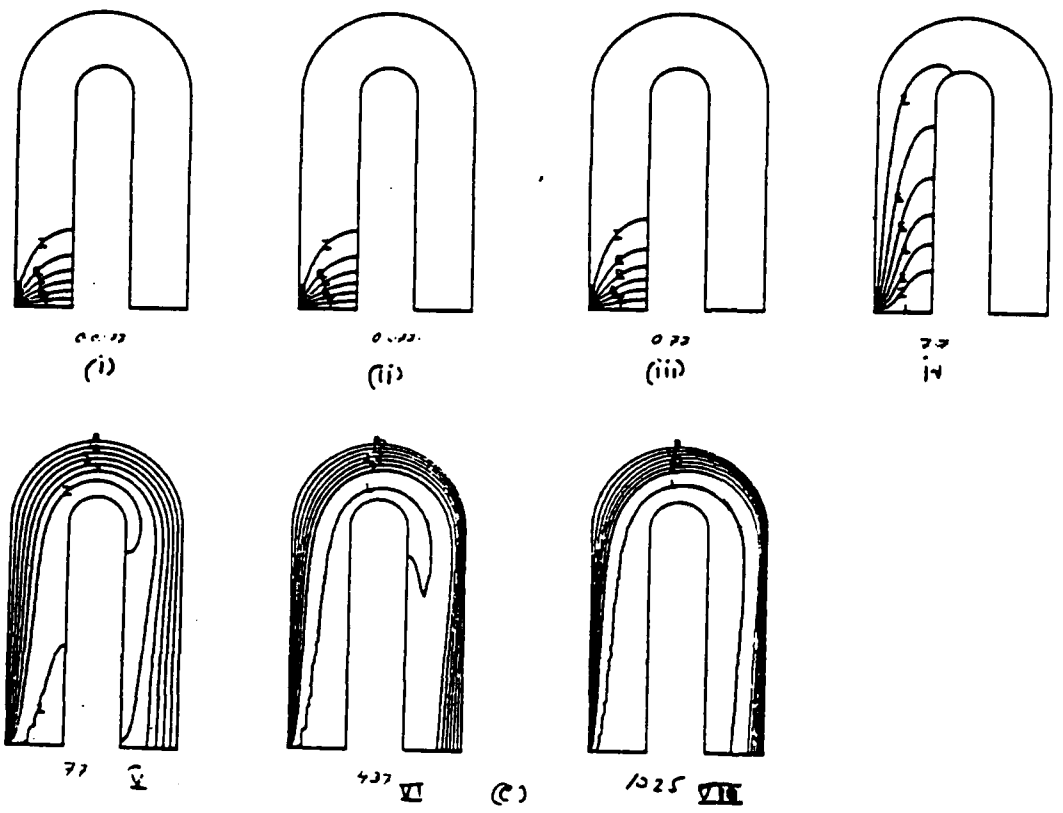

Figure 4: a) Streamlines (b) Isobars (c) Isotherms for 180° channel flow problem

(i) Re = 0.0077
ii = 0.077
iii = 0.77
iv = 7.7
V 77
VI 437
VII 1025

performance of heat exchangers.

V. RECOMMENDATIONS:

It can be seen from this work that computational fluid mechanics provides a very powerful tool to analyze fluid flow phenomena which would be very expensive via experiments. Because of the reasons mentioned in the preceding sections the finite element method is a very efficient tool that can be successfully used in the solutions of these problems. From the examples solved it can be concluded the groundwork has been laid; however, much work needs to be done. In the study of pin-fin and rectangular offset fin geometries, it is of interest to model several rows rather than a single one and study the effect of interacting boundary layers and flow separations. A numerical study of a single row with periodic boundary conditions to simulate fully developed flow can be performed, and the results compared with results from several rows. Because of the use of gaseous coolants in the area of active cooling of aircraft structures, the effects of compressibility (albeit subsonic) are extremely important. This could be the next step of this research. Forced convection heat transfer with phase change is not only of importance from a practical point of view, but also is very challenging, theoretically and numerically. This is the next logical step.

Phase change problems in porous media, with applications in such diverse fields as heat pipes, oil exploration,

geological modelling, agriculture etc., lead to the intriguing field of stability of flow phenomena, such as the classical Rayleigh Benard problem in porous media with different boundary conditions. The next step after this would logically be to investigate fully three dimensional phenomena such as secondary flows on which there is vast experinemtal evidence.

In conclusion it can be said that computational fluid dynamics with applications to forced convection heat transfer is a very challenging and fertile area in which to do basic research.

NOMENCLATURE

t = time
x_i = coordinate directions
u_i = velocity component in direction x_i
ρ = density
p = pressure
T = temperature
μ = coefficient of dynamic viscosity
k = coefficient of thermal conductivity
τ_{ij} = stress tensor
Pr = Prandtl number = $c_p\mu/k$
R = Reynolds number = $\rho VD/\mu$
$R \cdot Pr$ = Peclet number
Nu = Local Nusselt number
$\overline{Nu}$ = Average Nusselt number
c_p = specific heat
$\underline{\phi}$ = vector of nodal point unknowns
$\underline{\Phi}, \underline{\Psi}, \underline{\Theta}$ = vectors of shape functions for velocity, pressure, and temeprature

REFERENCES

1. Gartling, D.K., "Convective Heat Transfer Analysis by the Finite Element Method", Computer Methods in Applied Mechanics and Engineering, Vol. 12, 1977, pp. 365-382.

2. Murty, V.D., "The Solution of Free Convection Problems in Closed Regions Using a Penalty Finite Element Method", Proceedings of the Third International Conference on Numerical Methods in Thermal Problems, University of Washington, Seattle, Aug. 2-5, 1983.

3. Murty, V.D., NONFLAP user's manual, in preparation.

4. Harlan, Jon, User's Manual for Post Processor for NONFLAP, in preparation.

1986 USAF-UES SUMMER FACULTY RESEARCH PROGRAM

Sponsored by the

AIR FORCE OFFICE OF SCIENTIFIC RESEARCH

Conducted by the

Universal Energy Systems, Inc.

FINAL REPORT

A Model for a Coordinated System of Parallel Expert Systems for Autonomous Satellites

Prepared by:	Richard W. Nau
Academic Rank:	Professor of Mathematics and Computer Science
Department and University:	Math Department, Carleton College
Research Location:	AFWL/SIR
USAF Researcher:	Capt. Robert J. Millar
Date:	September 5, 1986
Contract No:	F49620-85-C-0013

A Model for a Coordinated System of Parallel Expert Systems for Autonomous Satellites

by

Richard W. Nau

ABSTRACT

The problem of a coordinated system of expert systems for use in achieving autonomy for satellites was studied and an appropriate model obtained. Design goals for independence, flexibility and robustness were outlined. Object oriented representations for both experts and physical systems were developed and organized into a coherent hierarchy consisting of a coordinating root node, functional groupings and individual systems. Specification of expert systems as objects, communication protocols between the systems, rules within the systems and amenability to parallelism were demonstrated.

ACKNOWLEDGEMENTS

I wish to express my gratitude to Capt. Robert J. Millar for suggesting this topic, continually directing me toward clarity and generality and creating the research environment at AFWL/SIR; to Capt. Mike Tebo for many valuable discussions and suggestions; to my wife, Sharol, for her typing, editorial and encouraging support during the summer; and to the Air Force Systems Command, the Office of Scientific Research and the Weapons Lab for their sponsorship.

I. INTRODUCTION

Background

The author's previous experience with expert systems consisted of working on a team at Carleton College that produced The Statistical Consultant, an expert advisor on the use of statistical methods; attending week long workshops at Carleton, TI in Austin and CDC in Minneapolis; conducting a senior seminar on AI and delivering several invited lectures on expert systems and related topics.

My interest in parallelism, although less intense, goes back to the summer of 1970 at NASA when we were considering the design of, languages for, and applications of the Illiac IV. Since then I have been able to keep apace by reviewing several new books on parallelism.

My work on aerospace applications includes designing mathematical models for a cabin pressurization system and advanced radomes (the Boeing Company), an analysis of the convergence of methods for extracting aerodynamic coefficients from flight test data (NASA) and the analytical determination of the dynamic response of a dirigible subject to crosswinds (Sheldahl).

USAF Research Area

The Information Systems Research group at the Air Force Weapons Laboratory was experienced in Artificial Intelligence and its applications, had developed expert system tools and applied them to meaningful problems. My own research interests and approach to problem solving corresponded to and complemented those of the group.

II. OBJECTIVES OF THE RESEARCH EFFORT

The aim of the autonomous satellite program is to replace, as

much as possible, the ground support for satellites by corresponding on-board systems. This will be accomplished over approximately a decade in several incremental stages.

An overall design is needed which can accommodate various levels of autonomy in different subsystems but still can adapt to improvements in hardware, software and systems analysis as they occur.

The purposes of this particular research effort were to:

1. Establish a priori design principles which a coordinated system of expert systems should satisfy.

2. Survey existing and proposed software and parallel hardware appropriate to the problem to become familiar with their strengths and weaknesses.

3. Design a generic logical model for a coordinated system of expert systems which would include means for resolving differences between the system goals and those of individual experts.

4. Determine an appropriate representation for interacting expert systems built upon this logical model.

5. Apply the logical model to a typical satellite system to demonstrate and test the feasibility of the model.

III. DESIGN GOALS

The major difficulty that the designer of a large system, which is to be implemented over a long period of time, faces is that many of the decisions which are likely to be made early in the design cycle will be based upon current details of the problem domain and upon

available technology.

This is an chronic problem in applications of artificial intelligence resulting in many systems which are brittle, i.e. they may work well for the particular narrow set of circumstances around which they were built but cannot accommodate much in the way of deviations or generalizations.

Add to this the fact that computers, especially parallel computers, are passing through rapid phases of increases in capabilities and experimentation .

In particular it would be a mistake to design future autonomous satellites by simply tacking expert systems based upon the current state of AI and computers on to existing satellite systems. Rather, an approach should be taken which allows for changes in both the AI techniques as well as the computer hardware.

Thus the approach was to consider first the desirable design goals resulting in our design paradigm. The following is a list of the more important goals determined.

1. Understandability. The system as a whole should be understandable not only by the system designer but also by those who will be responsible for implementing portions of it and those who will make decisions about it. Each component of the system should be transparent; one should be able to understand the input, output and the transformation performed. Exactly how it accomplishes its job need not be visible and, in fact, could be changed without having any external effects.

2. Integrity. The system should model closely how a system of real experts would interact. As a whole it should be coherent and work together. It should be able to check and test itself. One should be able to comprehend each component in a consistent manner and how it contributes to the whole.

3. Flexibility. At the uppermost levels the design should transfer to other systems of expert systems. All but a few components at the lowest level should be transportable directly to satellites with entirely different purposes. The design should allow for evolution in satellite and computer hardware, in AI techniques and in other software systems. In particular, it should not be irretrievably dependent upon present modes of designing expert systems or today's parallel computers, both of which are early stages of development. It should allow for an early implementation and a growth through levels of autonomy.

4. Robustness. The system should be reprogrammable. It should adapt to whatever resources are available to it and should resist or adjust to changes in its physical environment. It should degrade gracefully but be recoverable.

5. Verifiability. As much as the state-of-the-art allows, the following should be verifiable: Each expert should respond correctly without interfering with other experts. The system of experts should make continual, definite progress towards its goals.

6. Direction. It should give guidance to the design of future systems of experts.

IV. LOGICAL MODEL

Organizational Structure

A single top-level coordinator is in charge of the entire system. It receives the goals and ascertains that the goals are being met. It resolves conflicts between major subsystems and between the mission goals and the subsystem goals. As such a node is a potential bottleneck, so much as possible executive functions will be relegated to other objects such as subsystem supervisors or special executives. In particular, communication between subsystems or with the outside world is not generally channeled through this root node.

At the next to the top level, there are functional classes of expert systems. The expert systems themselves are at the tertiary level with other systems that they control or communicate with below that.

Object Representation

The fundamental representation selected as being the most consistent with the design goals and the logical organization is that provided by objects.

Different descriptions of object-oriented programming use slightly different terms. The following list of definitions draws upon common usage but emphasizes terms most suited to our purposes. For a thorough exposition of object-oriented programming see [5 and 7].

Object: Everything from a bit through an entire system can be regarded as an object. The essential characteristic is that objects are independent modules. Other objects are only aware of

what other objects can do, how to communicate with them, but not how they operate. It is possible to change completely the way an object meets its specification without having any effect on anything else. The main objects in our application will be expert systems, other physical and computational systems, data structures, sensors, etc. An example of an object could be a verbal clock. You can ask what time it is, and it will tell you what time it is. But internally whether it is digital or uses gears or burning ropes you have no idea.

Class: An object which is a group of similar objects.

Hierarchy: A root class which may have subclasses which may in turn have subclasses and so on down to some primitive objects.

Inheritance: The ability of an object to derive variables, procedures, rules, etc. from its mother class.

Object-oriented programming consists of naming objects, specifying what they do, defining their communication protocols and refining the objects until they're ultimately expressible in terms of fundamental objects provided.

Message Passing

Progress is made by sending messages to objects and receiving messages from objects. The system as a whole can be regarded as an object which would be sent initial values and goals and would eventually respond by exerting some effect on the environment. The set of allowable messages constitutes the language of inter-communication for the objects in the system. The response of an object is completely determined by the message sent to it and its

internal state. Each object is aware of all the objects that it can receive messages from as well as all messages it can receive. It also knows all the messages it can send and to whom it can send them.

For our purposes, sending a message comprises the following:

1. Identifying the objects to which the message is to be sent.

2. Specifying the operation to be performed.

3. Passing along any additional information needed.

4. Accepting the reply returned, if any.

Classification of Messages

Various kinds of messages are possible. For our use, the following list and discussion is intended to be inclusive.

1. Announcement. A message sent to a potentially interested set of objects about the status of some variables.

2. Reply. A directed response to an object which had previously made a request. The requester may or may not still be interested.

3. Request for Information. The requester desires information from another object. In general, the receiver may or may not have a responsibility to reply. A low level object may have the obligation to reply.

4. Request for Action. A suggestion or recommendation to another object that a particular action in its repertoire be taken. If the recipient doesn't have any reason not to, the action will be taken. Degrees of strength may be indicated, e.g. "I strongly

suggest that. . ."

A request that must be obeyed is a command. The commander assumes control over the commandee. Failure to react is cause for alarm.

Issues Related to Message Passing

1. Reception. The above description emphasizes sending a message. A corresponding viewpoint and procedure is implicit for receiving messages as well.

2. Data Sharing. Note that the only form of communication is through message passing. In particular, there are no global references possible, one object cannot affect another object's internal data, and updating of data structures must be accomplished by sending a message to the object in charge of that data.

3. Acknowledgements. An important design issue is whether or not each message sent should be immediately acknowledged. For longer hauls and for longer messages, e.g. files, acknowledgement is certainly worthwhile. For other, shorter, incidental messages sent to a busy receiver, waiting for the acknowledgement may not be worth the time. Therefore part of the protocol of the message will be whether an acknowledgement is required, not required but expected, or not expected at all.

4. Waits. In many instances, after a request is made, the requester cannot proceed much longer in that direction without receiving a reply. This may be more frequent for requests for information than for requests for action which may be merely advisory.

An indefinite wait is a potential source of deadlock and should be avoided. A wait for a while, making use of a local timer, could be built into an object's rule base. If the situation were critical and no reply were received after a reasonable wait, a complaint would be sent to a responsible supervisor who would take charge.

5. Buffering. The existence and control of buffers is an operating systems issue and will not considered to be part of the definition of the objects themselves.

6. Interrupts. On the other hand, an object could be continually monitoring its input stream and if the occasion arose would terminate some of its processes in favor of others.

V. APPLICATION

Satellite Autonomy

It is planned that within ten years most of the operational function for satellites that are presently accomplished by ground-based computer systems or human experts will be done on-board. The satellite would receive initialization and goals originally from the ground but should be able to proceed for months on its own receiving new instructions from the ground only for major changes in plans. On-board functions will exist for redundancy, reconditioning, planning and adjusting to degradation. The result will be more effective satellites requiring less expenditure of human effort.

Organization of the Expert Systems

As described above, an object-oriented model is most appropriate for this problem. The root object would be responsible for seeing

that progress is made toward the overall mission goals and resolving conflicts among subsystems or between mission goals and subsystem goals. Major supervisors would exist for the health, resources, data and decision-making classes. The expert systems themselves would be members of these classes. Descriptions of these classes follow.

Health and Welfare Class

This includes all monitoring, testing, diagnostic and repair functions for all components both physical and computational. As the mission cannot be accomplished without maintaining a reasonable degree of health, management of the functions should be at a high level and integrated early into the system design. Another reason for clustering all such functions is the fact that faults are frequently interdependent; for example what appears to be a thermal fault could actually be a fault in an electrical or computer system.

Resource Management Class

At any point in the mission, resource management is important. Either there's an abundance of resources, in which case they all need to be put to as much productive use as possible, or there's a shortage, in which case as much has to be accomplished as possible without endangering the mission or the survivability of the satellite. Thus, resource management should also be at this high level.

Examples of particular kinds of resources that need management include physical resources such as propellant, thermal energy and electrical power; computational resources such as processors and memory; geometrical resources such as attitude, platforms and pointing directions; communication links and special instruments. Use of time and ordering, which could be regarded as resources, more appropriately

fits in the decision making category below.

Data, Telemetry and Command Class

This area is responsible for the management, validation and transmission of data. It includes the gathering and distribution of data from sensors; the storage to and retrieval from databases; communication with ground stations or other satellites; the passing of commands to actuators; conversion of telemetric information and control of special processes, e.g. for pattern recognition or fast Fourier transforms. Because of the essential, pervasive nature of these functions, this general area also deserves high position in the organization.

Decision-Making Class

In addition to the main coordinator and supervisors, several special executives are identifiable including

1. planners, e.g. for maneuvers;

2. schedulers, e.g. of experiments; and

3. optimizers, especially across other subsystems.

Many of these are spin-offs from the top coordinating node. Most of the command sequences would be generated in this area such as for navigation and the mission.

An Orbitkeeping Scenario

To appreciate the applicability of this model, consider the following example.

Orbitkeeping refers to the occasional checking and maneuvers needed to maintain the satellite's orbit within some prescribed bounds. Let OrbitKeeper[1] be an object appointed this task. OrbitKeeper will accept a request to check to see if an orbitkeeping maneuver is required and, if so, to take appropriate action. The request may originate from either a PeriodicScheduler whose job it is to watch the Clock and periodically make such requests of objects with responsibilities similar to OrbitKeeper's or from AMonitor who, due to the sounding of an Alarm, has reason to suspect that orbitkeeping may be required. OrbitKeeper simultaneously sends requests to OrbitPredictor and CurrentBounds. OrbitPredictor is requested to return predicted values of the parameters describing the orbit. OrbitPredictor may, in turn, use other objects, such as OrbitDeterminer, for this purpose. As OrbitPredictor may have recently responded to other requesters, such as EclipsePredictor, it may respond immediately or it may choose to recompute the predicted Ephemeris. For its part, CurrentBounds returns the current, acceptable bounds on the orbit parameters. These values are not static but may have been set by some MissionPlanner who has decided that either broader bounds are allowable or that narrow bounds are needed or by some Optimizer who is performing a balance between costs and risks. Whether or not the values returned from the OrbitPredictor are within the bounds provided by CurrentBounds, OrbitKeeper so informs the requester if such a response is required. If the values are not within bounds, a request for action will be sent to ManeuverPlanner who will consult with OrbitGoals and send a request

[1]As is the custom in object-oriented programming, the names of objects will be capitalized with internal capital letters used for readability.

for action to the Scheduler who will ultimately send a request for a specific burn duration, direction and timing to Thrusters.

A specification of the structure and function of the object OrbitKeeper in an object specification language might be:

```
Object:  OrbitKeeper
Class:  Supervisor
Senders:  PeriodicScheduler, AMonitor
Receivers:  OrbitPredictor, CurrentBounds,
            ManeuverPlanner
In:  response-desired, values, bounds
Out:  status
Task:  ((Par (Ask OrbitPredictor Values)
             (Ask CurrentBounds Bounds))
        (Cond ((Within Values Bounds)
               (Cond (Response-desired
                      (Reply Sender  Status T))))
               (T (Par (Cond (Response Desired
                              (Reply Sender Status NIL))
                  (Request Maneuver Planner
                   Strongly)))))
```

where Class indicates the class that the object OrbitKeeper is a member of, Senders designates other objects that may call upon OrbitKeeper, Sender is the particular sender who invoked OrbitKeeper, Receivers are those objects that OrbitKeeper initiates message passing with, and In and Out are lists of input and output parameters. Amenability to parallelism is also indicated by the function Par. A more thorough specification should include types of the parameters, acknowledgements, definition of within, etc.

Additional Comments on the Example

1. The description of the task here is essentially a single rule. In other cases it might involve a combination of forward and backward rules, an entirely different representation of an expert system on no expertise at all.

2. Other systems such as for attitude control, although more time critical, would be similar to OrbitKeeper and could make use of some of the same objects.

3. Orbit control could inherit values as well as meta- rules as a member of the class of supervisors.

4. If computing resources were being controlled, initially an object from the class of resource managers would be consulted to obtain the facilities needed.

5. Bottlenecks could develop at several objects. This could be handled deliberately through rules or by scheduling, pipelining or replication.

VI. RECOMMENDATIONS

To obtain a coherent but flexible, specifiable though robust design for a coordinated system of expert systems, an object-like approach should be taken. This will allow for each expert system as well as physical components and non-expert systems to be developed in independent yet consistent modules.

First, a high level specification language should be designed. Tools for its implementation and related auxiliary tools should be designed and written providing consistency across subsystems. The overall design including all of the major subsystems, their functions and communication protocols should be specified in this language.

To gain better insight and to establish that this approach will work, prototypes should be written early both for the overall system and for at least one of the typical subsystems down to a language dependent level.

To demonstrate that the logical model applies to coordinated systems of experts generally, a completely different application should be selected and prototypes written for it as well.

REFERENCES

1. Douglas, R., "A Qualitative Assessment of Parallelism in Expert Systems," IEEE Software, May 1985; pp. 70-81.

2. Ekman, D., "Orbit Control Software for Communications Software," Computer, April, 1983; pp. 43-51.

3. Erman, L., London, P. and Fickas, S., "The Design and an Example Use of Hearsay-III," IJCAI, 1983; pp. 409-415.

4. Evans, D. and Gajewski, R., "Expanding Role for Autonomy in Military Space," Aerospace America, Feb., 1985; pp. 74-77.

5. Goldberg, A. and Robson, D., Smalltalk-80, the Language and Its Implementation, Addison-Wesley, 1983.

6. Grenander, S., "Toward the Fully Capable AI Space Mission Planner," Aerospace America, Aug., 1985; pp. 44-46.

7. Stefik, M. and Bobrow, D., "Object-oriented Programming: Themes and Variations," The AI Magazine, Vol. 6, 4., Winter 1986, pp. 40-62.

8. Vegdahl, S., "A Survey of Proposed Architectures for the Execution of Functional Language," IEEE Transactions on Computers, Vol. C-33, No. 12, Dec. 1984, pp. 1050-1071.

9. Vere, S., "Deviser: An AI Planner for Spacecraft Operations," Aerospace America, April, 1985; pp. 50-53.

1986 USAF-UES SUMMER FACULTY RESEARCH PROGRAM/

GRADUATE STUDENT SUMMER SUPPORT PROGRAM

Sponsored by the

AIR FORCE OFFICE OF SCIENTIFIC RESEARCH

Conducted by the

Universal Energy Systems, Inc.

FINAL REPORT

$CO_2(001)$ VIBRATIONAL TEMPERATURES IN THE 50 TO 150 KM ALTITUDE RANGE

Prepared by:	Dr. Henry Nebel
Academic Rank:	Associate Professor
Department and University:	Physics Department, Alfred University
Research Location:	Air Force Geophysics Laboratory, Infrared Technology Division, Infrared Dynamics Branch.
USAF Researcher:	Dr. Ramesh D. Sharma
Date:	8 August 1986
Contract No:	F49620-85-C-0013

CO_2(001) VIBRATIONAL TEMPERATURES IN THE 50 TO 150 KM ALTITUDE RANGE

by

Henry Nebel

ABSTRACT

Vibrational temperature profiles as functions of altitude have been obtained for the (001) state of carbon dioxide in the atmosphere by considering various excitation and de-excitation mechanisms for the CO_2(001) state and the first excited vibrational state of N_2. The resulting profiles have been used to calculate infrared radiance from the 4.3 micron (ν_3) band of CO_2 through the atmosphere in a limb-viewing geometry. The resulting radiance is compared with data from the Spectral Infrared Rocket Experiment (Stair, et. al., 1985). Although the calculated radiance is in good agreement with the data at 50 km, it is up to two orders of magnitude lower than the data at altitudes of 60 to 100 km. Thus additional processes and refinements must be considered. Recommendations for further work are included in this report.

ACKNOWLEDGEMENTS

I would like to thank the Air Force Systems Command and the Air Force Office of Scientific Research for sponsorship of this research. I would also like to thank Dr. Ramesh D. Sharma of the Air Force Geophysics Laboratory for suggestion of the problem and for continued guidance during the course of the work. I also thank Dr. Richard Picard of AFGL for guidance in the use of the computer facilities at AFGL.

Finally, I greatly appreciate the assistance of Dr. Peter Wintersteiner of Arcon Corporation. Dr. Wintersteiner helped me in more ways than I can possibly enumerate. This research would not have been possible without his assistance.

I. INTRODUCTION: I spent the summers of 1983 and 1984 at the National Center for Atmospheric Research in Boulder, Colorado analyzing data from a limb-sounding infrared detector which flew on the Nimbus 7 satellite. Part of that time was spent considering non-equilibrium conditions in the atmosphere, i.e. situations where local thermodynamic equilibrium may not be assumed to apply. This generally occurs in the upper atmosphere (above 60 km). I spent the summer of 1985 at NASA's Langley Research Center in Hampton, Virginia considering these non-equilibrium conditions from a theoretical point of view. In particular, my research group at Langley was interested in how one does radiative transfer calculations in non-equilibrium atmospheres and how this might affect the analysis of limb-sounding data referred to above. During that summer I spent a week at the Air Force Geophysics Laboratory (AFGL) in order to study a non-equilibrium model developed at AFGL.

The research problem at AFGL for this summer involved use of the same non-equilibrium radiative transfer model. Thus my previous experience made me well suited to pursue this problem. My research at AFGL has involved further in-depth study of the theoretical aspects of non-equilibrium conditions in the atmosphere.

II. OBJECTIVES: My objective was to calculate the night-time vibrational temperature profile of the asymmetric stretch (ν_3)

mode of excitation of carbon dioxide (4.3 micron band) in the upper atmosphere. This was done using a high-altitude radiative transfer model for non-equilibrium conditions in the atmosphere. The model was developed at AFGL and includes a computer code for calculating populations of excited states of molecules under non-equilibrium conditions. My objective was to study this model, familiarize myself with the associated computer code, and write additional code which would permit calculation of excited state population as a function of altitude for the 4.3 micron band of carbon dioxide under quiescent night-time conditions. The results may then be used to calculate infrared emission and transmission through the atmosphere for comparison with experimental data. The model allows application to limb-viewing geometry or any other line-of-sight path desired. The path chosen will of course depend upon the particular data set one is trying to explain.

III. APPROACH: I began by familiarizing myself with a program called RAD, developed at AFGL by Dr. Ramesh D. Sharma of AFGL and Dr. Peter Wintersteiner of Arcon Corporation. This program calculates vibrational temperatures in non-equilibrium regions of the atmosphere based on collisional interactions, absorption of earthshine and airglow, and spontaneous emission. The model had previously been applied to the bending (ν_2) mode of excitation of carbon dioxide (15 micron band). I then set up the kinetic equations required to treat the 4.3 micron band. A

new subroutine was written to solve a 2x2 matrix equation, yielding the population densities of the pertinent excited state of CO_2 and the first vibrational state of N_2, which has about the same energy. The population densities are then used to calculate vibrational temperatures of the excited states in question. These vibrational temperatures are then used as input to another program called NLTE, also developed at AFGL (Sharma et. al., 1983). This program calculates infrared emission and transmission through the atmosphere. The total radiance thus calculated can then be compared with experimental data.

IV. <u>THEORETICAL DEVELOPMENT</u>: The 4.3 micron pure vibrational state of CO_2 lies at 2349 cm^{-1} above ground, and the first vibrational state of the nitrogen molecule lies at 2331 cm^{-1} above ground (see Figure 1). Because these two states are so close in energy, there will be rapid transfer of vibrational quanta between the two. Thus any calculation designed to determine the excited state density for the CO_2 level must also consider the nitrogen level. I have considered the major excitation and de-excitation mechanisms for each of these states under quiescent night-time conditions.

For the CO_2 state we have the following processes:

Spontaneous emission:

$$CO_2(001) \longrightarrow CO_2(000) + h\nu$$

Earthshine pumping:

$$CO_2(000) + h\nu \longrightarrow CO_2(001)$$

V-V transfer with N_2:

$$CO_2(001) + N_2(0) \rightleftharpoons CO_2(000) + N_2(1) + 18cm^{-1}$$

V-T transfer to $CO_2(030)$:

$$CO_2(001) + M \rightleftharpoons CO_2(030) + M + 346cm^{-1}$$

V-T transfer with oxygen atoms:

$$CO_2(001) + O \rightleftharpoons CO_2(000) + O + 2349cm^{-1}$$

V-V transfer with O_2:

$$CO_2(001) + O_2(0) \rightleftharpoons CO_2(010) + O_2(1) + 128cm^{-1}$$

For the N_2 state we have the following processes:

V-V transfer with CO_2:

$$CO_2(001) + N_2(0) \rightleftharpoons CO_2(000) + N_2(1) + 18cm^{-1}$$

V-V transfer with O_2:

$$N_2(1) + O_2(0) \rightleftharpoons N_2(0) + O_2(1) + 775cm^{-1}$$

V-T transfer with M (N_2 or O_2):

$$N_2(1) + M \rightleftharpoons N_2(0) + M + 2331cm^{-1}$$

V-T transfer with oxygen atoms:

$$N_2(1) + O \rightleftharpoons N_2(0) + O + 2331cm^{-1}$$

Rate constants for the above reactions have been obtained from Degges (1971), Houghton (1969), and Taylor (1974). Each of the two excited states is assumed to have a population density which is constant in time. Thus the sum of the excitation rates is set equal to the sum of the de-excitation rates for

each state. The result is two coupled linear equations in the densities of the excited states in question. These equations are combined to form a 2x2 matrix equation which is solved by the computer code yielding the population densities of the $CO_2(001)$ state and the $N_2(1)$ state. The vibrational temperatures are then calculated by means of the formulas

$$CO_2(001)/CO_2(000) = \exp(-h\nu/kT_{001})$$

and

$$N_2(1)/N_2(0) = \exp(-h\nu/kT_{N2})$$

where T_{001} and T_{N2} are the vibrational temperatures of the $CO_2(001)$ state and the $N_2(1)$ state respectively, and ν is the frequency associated with the transition in each case.

The computer program requires as input for the calculation an "initial guess" vibrational temperature profile. A series of iterations is then performed to approach the final vibrational temperature profile for the $CO_2(001)$ state. Two different initial guess profiles were used, one lower than the expected profile and one higher than that expected. The goal here is to obtain the same final profile regardless of the form of the initial guess.

The calculation can be done for a single line within the 4.3 micron band, or for the entire band including all lines. Line

parameters have been obtained from the AFGL line tape (Rothman, et. al., 1983) and these have been used as input for the calculation. The full band calculation takes considerably more computer time than the single line calculation; thus it is a definite advantage if one can achieve accurate results using a single line.

V. RESULTS: Several computer runs were made with twelve iterations for the full band and also for a single strong line (R 14) within the band, using both of the initial guess vibrational temperature profiles. In each case, the single line result does not differ appreciably from the full band result. They are within 2 or 3 degrees K of one another for the entire altitude range considered (40-150 km). Thus preliminary results have been obtained using the single line calculation with 40 or 50 iterations depending on the initial input profile. Figure 2 shows the final vibrational temperature profiles obtained for the CO_2(001) state using each of the two initial guess profiles. The two final profiles converge toward one another and, as can be seen in Figure 2, they are within about 5 degrees of one another at all altitudes after 40 and 50 iterations. Of course, one would hope for closer convergence, but for the purpose of preliminary results this is condidered adequate.

The upper of the two final profiles has been chosen as input

for the NLTE program which calculates infrared emission and transmission through the atmosphere for various viewing geometries. The upper profile has been chosen because it extends to 150 km whereas the lower profile is only available up to 130 km. The additional 20 km might be important in terms of calculating total emission in a limb-viewing line-of-sight path. This has been done using the NLTE program for various tangent heights (see Figure 3), considering the most abundant isotopic form of carbon dioxide ($^{12}C^{16}O_2$) labeled 626, and also the most important minor isotopic form ($^{13}C^{16}O_2$) labeled 636. The results are presented in Table 1 along with experimental results from the Spectral Infrared Rocket Experiment, or SPIRE (Stair et. al., 1985). Although the calculations are in good agreement with the SPIRE data at 50 km, they are less than the experimental values from 60 to 100 km. In fact, the calculated result is two orders of magnitude lower than the experimental result at 80 km. Thus these preliminary results do not adequately explain the SPIRE data. Further refinements are required and additional processes must be considered.

VI. <u>RECOMMENDATIONS</u>: It is recommended that the following refinements be implemented in any extension of this research:

a) Extension of one of the input profiles to 150 km.

b) Full band calculations with 40 or 50 iterations to obtain the final vibrational temperature profiles for the $CO_2(001)$ state.

c) A literature search for more recent values of the rate constants for the reactions listed in (IV). The values used for the calculations reported here date from 1974 and earlier.

d) Consideration of hot bands which might contribute appreciably to the emission in the 4.3 micron band. The programs have the facility to accomplish this.

e) Consideration of the first excited state of the O_2 molecule as an unknown population density. This state has been considered to be in thermodynamic equilibrium which may not be a valid assumption. Inclusion of this state would require solution of a 3x3 matrix equation.

f) Consideration of other trace isotopic forms of the CO_2 molecule in addition to 626 and 636.

TABLE 1

Tangent Height (km)	Calculated Radiance (watts/cm²sr) 626	636	sum	Experimental Radiance (from SPIRE data) (watts/cm²sr)
50	8.69×10^{-7}	6.18×10^{-8}	9.31×10^{-7}	$8\text{-}9 \times 10^{-7}$
60	5.81×10^{-8}	5.25×10^{-9}	6.34×10^{-8}	$1\text{-}2 \times 10^{-7}$
70	2.44×10^{-9}	7.34×10^{-10}	3.17×10^{-9}	$4\text{-}6 \times 10^{-8}$
80	3.29×10^{-10}	2.76×10^{-10}	3.57×10^{-10}	$3\text{-}5 \times 10^{-8}$
90	2.66×10^{-10}	1.53×10^{-10}	4.19×10^{-10}	$1\text{-}3 \times 10^{-8}$
100	2.83×10^{-10}	6.09×10^{-11}	3.44×10^{-10}	$.8\text{-}2 \times 10^{-8}$

REFERENCES

Degges, T. C., "Vibrationally Excited Nitric Oxide in the Upper Atmosphere", Appl.Opt. 10, 1856 (1971).

Houghton, J. T., "Absorption and Emission by Carbon-Dioxide in the Mesosphere", Quart. J. Roy. Meteor. Soc. 95, 1 (1969).

Rothman, L. S., R. R. Gamache, A. Barbe, A. Goldman, J. R. Gillis, L. R. Brown, R. A. Toth, J. M. Flaud, and C. Camy-Payret, "AFGL Atmospheric Absorption Line Parameters Compilation: 1982 Edition", Appl. Opt. 22, 2247 (1983).

Sharma, R. D., R. Siani, M. Bullitt, and P. P. Wintersteiner, "A Computer Code to Calculate Emission and Transmission of Infrared Radiation Through a Non-Equilibrium Atmosphere", AFGL-TR-83-0168 (1983).

Stair, A. T., R. D. Sharma, R. M. Nadile, D. J. Baker, and W. F. Greider, "Observations of Limb Radiance With Cryogenic Spectral Infrared Rocket Experiment", J. Geophys. Res. 90, 9763 (1985).

Taylor, R. L., "Energy Transfer Processes in the Stratosphere", Can. J. Chem. 52, 1436 (1974).

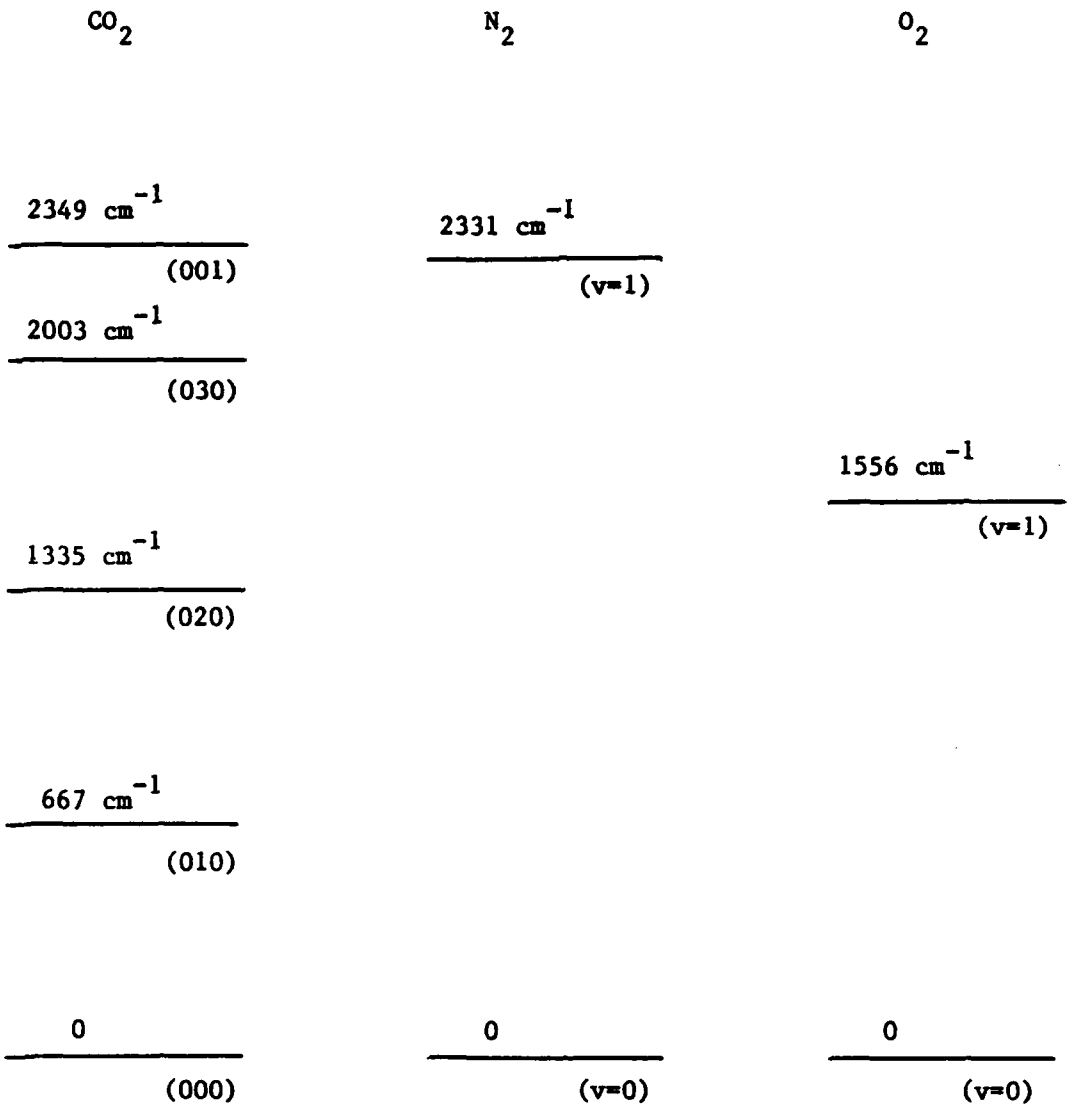

Figure 1. Low-lying vibrational levels of CO_2, N_2, and O_2.

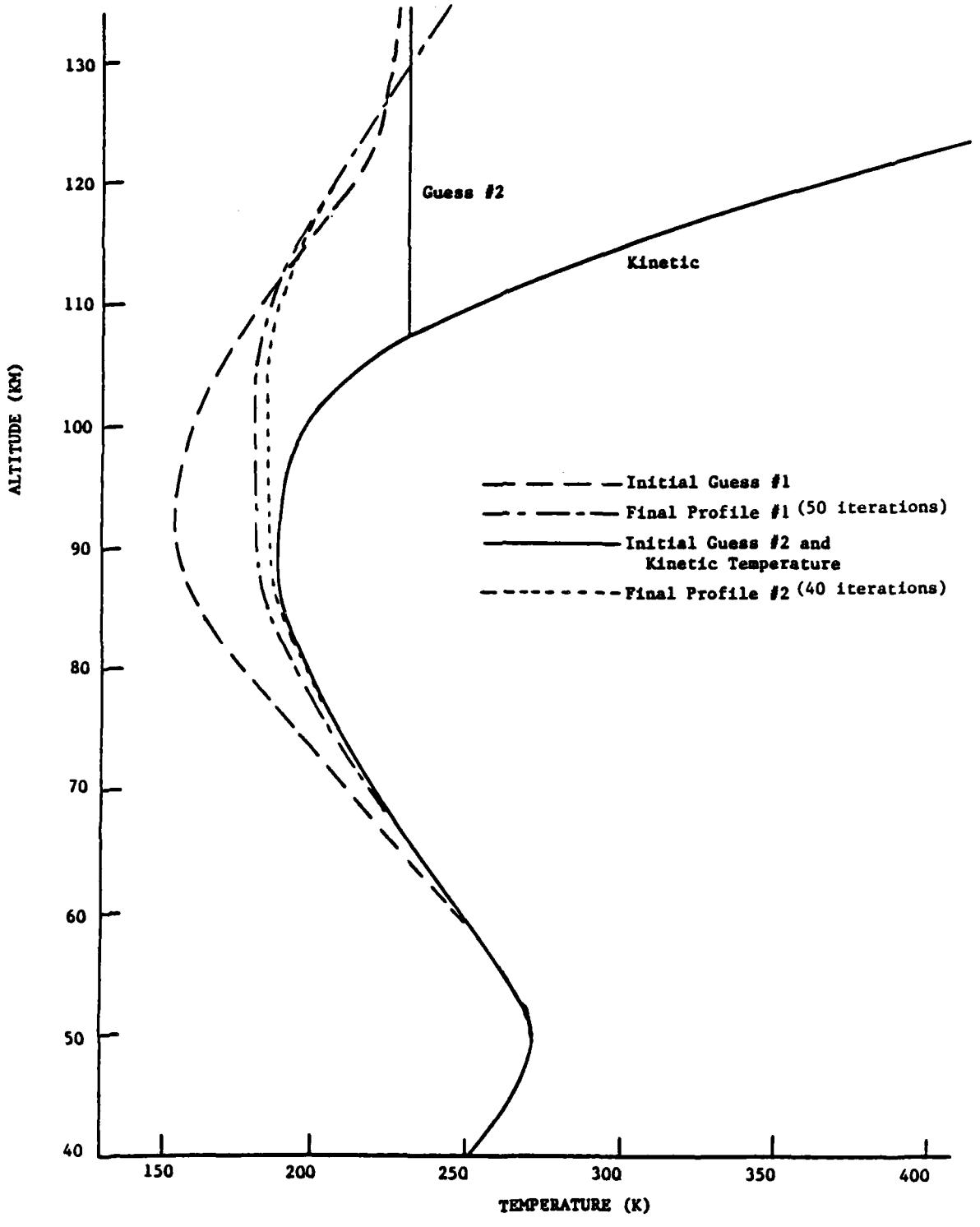

Figure 2. Initial and final vibrational temperature profiles for $CO_2(001)$.

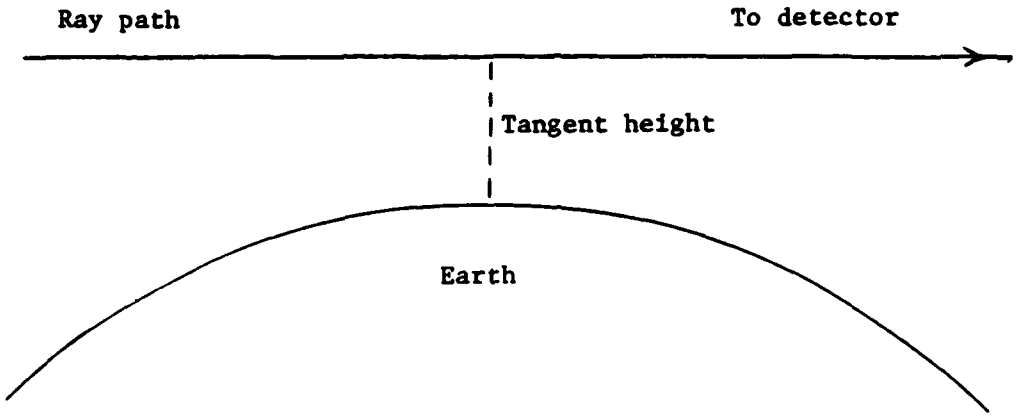

Figure 3. Limb-viewing geometry. The tangent height is the shortest distance between the ray path and the earth.

1986 USAF-UES SUMMER FACULTY RESEARCH PROGRAM/

GRADUATE STUDENT SUMMER SUPPORT PROGRAM

Sponsored by the

AIR FORCE OFFICE OF SCIENTIFIC RESEARCH

Conducted by the

Universal Energy Systems, Inc.

FINAL REPORT

A Study of the Finite Element Method in Limited Area Weather Prediction Modeling

Prepared by:	Robert M. Nehs
Academic Rank:	Associate Professor
Department and University:	Department of Mathematics, Texas Southern University
Research Location:	Geophysics Laboratory, Atmospheric Sciences Division, Atmospheric Prediction Branch, Hanscom AFB
USAF Researcher:	Dr. Samuel Yee
Date:	September 20, 1986
Contract No:	F49620-85-C-0013

A Study of the Finite Element Method in Limited Area Weather Prediction Modeling

by

Robert M. Nehs

ABSTRACT

A preliminary study of the use of finite element techniques in limited area atmospheric models was performed. This included a survey and summarization of the basic theory and programming procedures employed in finite element approximations. Attention was then focused on the fully operational Canadian model, particularly on the development of the finite element grid scheme. A key component of this is a 2-dimensional nonuniform rectangular grid which contains a subregion of high resolution. An alternative grid, consisting of a combination of rectangular and trapezoidal elements, was developed. This grid contains fewer elements in the over-all domain while maintaining the same high resolution over the area of interest. A finite element program to solve a Poison equation using a simplified version of either grid scheme was written. Runs were made with both grid types and the results were compared at the grid points within the high resolution area. The errors at most of these points were smaller for the new grid. More extensive tests should be conducted; however, these preliminary results indicate that further investigation of the new grid scheme is warranted.

ACKNOWLEDGMENTS

I would like to thank the Air Force Systems Command and the Air Force Office of Scientific Research for their sponsorship of this project. I am grateful for the excellent facilities, ample support and valuable assistance available at the Geophysics Laboratory. Don Chisolm's encouragement and prompt responses to our requests were greatly appreciated. The USAF research colleague, Samuel Yee, initially suggested this particular project and contributed several important ideas to our work. In particular, the new grid scheme outlined in Section 5 was developed during one of our conversations.

Special recognition should be made of the contributions of Cornell Wooten, my graduate student research assistant, to this project. The work could not have progressed as far as it has without his valuable help.

Finally, I wish to thank my wife, Marge, and my children, Gwendolyn and Jonathan, for their patience and support during the ten week period.

I. INTRODUCTION: I received my Ph.D. from the University of Houston in the field of algebraic topology. However, recently my interests have expanded to include the area of applied mathematics; in particular, finite difference equations. Furthermore, I have had some training in computer programming.

One of the research areas at the Geophysics Laboratory involves the use of limited area mathematical models in weather prediction. Currently they are using a model based on finite difference approximations. There is some interest in determining whether finite element techniques could be used to develop a better model. It was suggested that, with my mathematical and programming background, I could begin a preliminary investigation of this question.

II. OBJECTIVES OF THE RESEARCH EFFORT: The over-all goal of our project was to make a preliminary examination of the practicability of using the finite element method in a limited area atmospheric model.

Our individual goals were:

1. to study the basic theory of finite element approximations,
2. to survey current applications of finite element techniques in local weather models, and
3. to develop a simple finite element program.

III. The Finite Element Method: We began our study of the finite element method with a survey of some of the literature in this area ([1] through [7]). The following is a brief synopsis of the basic finite element procedure.

The finite element method has developed rapidly over the past 30 years as a technique for solving a wide variety of problems in engineering, physics and mathematics. The first step of the process consists of covering the domain of the problem with a grid, or mesh, formed by partitioning the region into small non-overlapping pieces called elements. Local approximations (shape functions) of the solution are defined over each element and these are patched together to

form global approximating functions (basis functions). The basis functions $T_1, T_2, \ldots, T_n$ are generally piecewise polynomials which are zero over most of the elements.

The next step is to determine the coefficients in the expression

$$U = \sum d_i T_i \qquad (1)$$

so that the function U is, in some sense, the best approximation to the solution. In many problems this leads to a matrix equation

$$S \cdot D = C, \qquad (2)$$

where S is an n x n matrix, D and C are n x 1 vectors. The unknown coefficients $d_1, d_2, \ldots, d_n$ in (1) form the vector D, while the terms of S and C involve integrals of expressions containing the basis functions or their derivatives. Integrations are performed over individual elements and usually require numeric procedures. After the arrays S and C are determined, the system in (2) is solved for $d_1, d_2, \ldots d_n$. The size of the mathematical system is determined by the number of basis functions which, in turn, is related to the number of elements in the mesh.

For one dimensional problems in which the domain R is an interval, the grid is formed by a partition of R into subintervals. The simplest basis functions in this case are piecewise linear functions having the value 1 at one of the partition points and 0 at the rest. These are known as roof functions.

Rectangles and triangles are the most popular elements for two dimensional problems. A rectangular domain R may be subdivided by lines parallel to the sides of R into a grid consisting of rectangles. The rectangular mesh is said to be uniform when the lines are equally spaced and, therefore, the elements are congruent. The shape functions for rectangular elements are often products of pairs of one dimensional shape functions. For example, products of linear shape functions produce the bilinear shape functions, $a + bx + cy + dxy$ (known also as roof functions).

Triangular elements are useful in the approximation of boundaries of irregular domains. More complex elements, including those with curved sides, are formed by isoparametric transformations. This technique involves non-singular mappings of some standard element, such as a rectangle or triangle, into the domain.

The main advantage of the finite element method is the flexibility it offers through the choice of elements and shape functions. Furthermore, the resulting algebraic system will often generate a positive definite symmetric matrix containing numerous zeros. The disadvantages generally arise from the complexity of the method. The numeric procedures usually require a large storage capability and a considerable number of calculations. Moreover, questions concerning the accuracy and stability associated with a particular finite element scheme cannot be answered easily.

In recent years there has been a lively debate as to the relative merits of the finite element method and the older finite difference method. The situation is complicated by the fact that comparisons of results depend upon so many factors. These include the nature of the problem, the grid used for the domain, the numeric procedures employed in the program, the design of the computer and the criteria used in evaluation of the results. Similar difficulities arise when different finite element schemes are compared with each other. Generally, the use of more complex elements or higher order shape functions will increase the rate of convergence of the method at the cost of increased computer requirements. The question of which is the best scheme, or even a satisfactory one, for a particular problem is one that requires further study and experimentation.

IV. Finite Element Procedures in Limited Area Weather Models: In order to gain a perspective about finite element modeling of meteorological phenomina, a study of the Canadian limited area finite element model was attempted. Several papers were examined. The following is a summary of our readings.

The Canadian model was a culmination of years of study and the piecing together of several parts into an over-all model. Many have made contributions to the study; however, since we were mainly interested in the application of the finite element method, we studied the papers of only a few individuals.

Our primary interest was the configuration of the mesh used in the model. Staniforth and Mitchell [8] studied the efficiency of using the finite element method to solve the shallow-water equations, essentially a barotropic model. They used vorticity and divergence as predictive variables, rather than the velocity components, and they employed a semi-implicit time discretization. The basis functions used for interpolation were the 2-dimensional roof functions. The equations were solved on a uniform rectangular grid.

Later Staniforth and Mitchell [10] generalized this model by using a nonuniform rectangular mesh. The grid had one area of particularly fine resolution, the rest of it consisted of coarser resolutions. Methods were given for approximating elliptic boundary-value problems; however, we were primarily interested in the mesh itself. Experiments were performed using several mesh configurations having a uniformly high resolution over the entire domain. They found that, "the forecast produced on a uniformly high resolution mesh can be essentially reproduced for a limited time over the specific area of interest by a variable resolution mesh configuration at a fraction of the computational cost." [12] Noise problems were eliminated by smoothly varying the resolution away from the area of interest. They concluded that this is a workable strategy for the limited area/time numerical weather prediction problem.

Meanwhile, Staniforth and Daley [9] were formulating a baroclinic model for the vertical discretization of the sigma coordinate system. They wanted to combine the baroclinic model with the barotropic model in [10] in order to create a three dimensional limited area model. The three dimensional model was realized by Staniforth and Daley in [11]. The moister equations were included in this model to enhance accuracy.

V. A Finite Element Model: At the suggestion of our research colleague, we considered possible alternatives to the variable rectangular grid described in the previous section. We felt that the flexibility of the finite element method had not been fully utilized in such limited area models. Figure 1 displays a simple version of the grid scheme that we developed as a possible alternative. Square ABCD represents the high resolution area which is covered by a uniform rectangular mesh. The rest of the domain is partitioned by two surrounding layers of trapezoidal elements. Square EFGH was placed so that $A_2/A_1 = A_3/A_2$, where A_1, A_2 and A_3 are the areas of the elements in different layers (see Figure 1).

Next we wanted to compare this configuration with an analogous nonuniform rectangular grid in which ABCD is covered by an identical high resolution grid. Our grid contains fewer elements and, therefore, will require less storage and fewer computations. In order to compare the

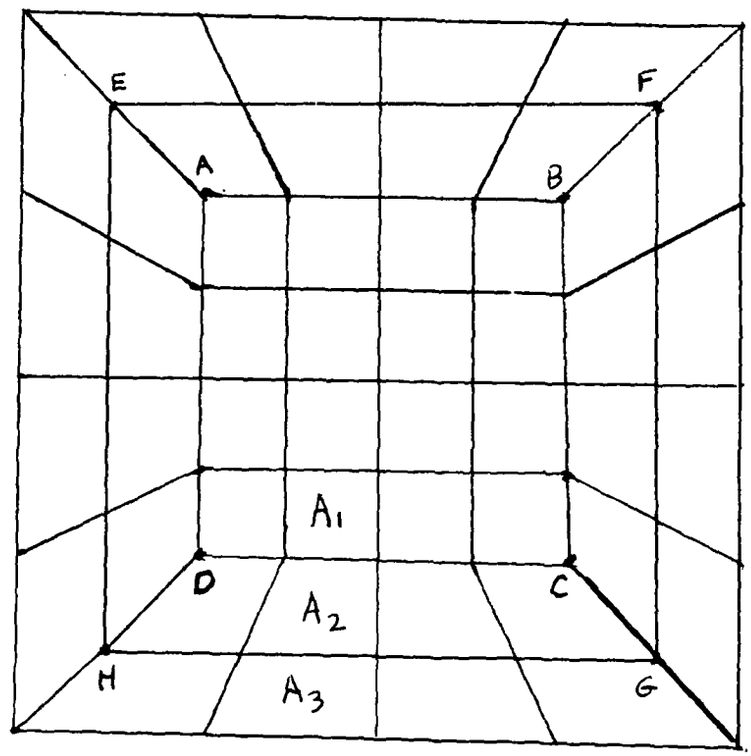

Figure 1. Finite Element Grid

accuracy, a finite element program was written in which either grid could be employed with bilinear shape functions. A simple time independent problem was choosen for the program;

$$u_{xx} + u_{yy} = f(x)$$
$$u = g(x) \text{ on the boundary .} \qquad (3)$$

We ran the program with both grids using $f(x) = \sin(\pi x)$ and $g(x) = 0$ in (3). Utilizing the analytic solution to this problem, the results for both grids were compared at the grid points within the high resolution area ABCD. The rectangular grid gave rather uniform results, the percent error at all these grid points ranged from 1.25% to 1.36%. The results from the new grid were not as good at the corner points A,B,C and D but were better at the interior points. (The percent error at each corner was 2.8%, at the rest of the boundary points it ranged from .2% to 1.5% and at the interior points from .5% to .7%.) These initial results were encouraging but time did not permit a more extensive series of tests. However, we do feel that further investigation of the new grid scheme is justified.

Many of the components of our program are modifications of procedures found in Akin [1] . The program employs a subroutine which generates the initial mesh data for the rectangular grid. However, the corresponding data for the new grid must be supplied as input.

VI. Recommendations: 1. In order to facilitate further study, a subroutine should be developed which would generate the initial mesh data for this type of grid.

2. There should be further testing of this grid, including runs with different functions f and g in (3). Also, the question of where the intermediate square EFGH should be placed needs to be examined further. It would be important to determine, if possible, which location produces the best (in some sense) results.

3. The next step would be the investigation of a similar grid which has a higher resolution. This would involve a finer mesh (more squares) over ABCD and additional trapezoidal layers (more intermediate squares of the type EFGH).

4. The use of this grid scheme for time dependent problems should then be studied extensively. This will introduce questions of stability and numeric procedures for time discretization. The work would begin with a simple initial value problem but should eventually lead to more complex dynamic systems; for example, the shallow-water equations.

5. We also feel that comparisons should be made with models based upon finite difference approximations only.

REFERENCES

1. Akin, J.E., Application and Implementation of Finite Element Methods, New York, Academic Press (1980)

2. Chari, M.V.K. and P.P. Silvester, Finite Elements in Electrical and Magnetic Field Problems, New York, John Wiley and Sons, Inc. (1980)

3. Davis, A.J., The Finite Element Method, A First Approach, Clarendon Press, Oxford (1980)

4. Huebner, K., The Finite Element Method for Engineers, New York, John Wiley and Sons, Inc. (1975)

5. Lapidus, L. and G.F. Pinder, Numerical Solutions of Partial Differential Equations in Science and Engineering, New York, John Wiley and Sons, Inc. (1982)

6. Strang, G. and G.J. Fix, An Analysis of the Finite Element Method, New York, Prentice-Hall (1973)

7. Wait, R. and A.R. Mitchell, Finite Element Analysis and Applications, New York, John Wiley and Sons, Inc. (1985)

8. Staniforth, A.N. and H.L. Mitchell, "A Semi-Implicit Finite Element Barotropic Model," Mon. Wea. Rev., 105, pp. 154-169 (1977)

9. Staniforth, A.N. and Roger W. Daley, "A Finite Element Formulation for the Vertical Discretization of Sigma Coordinate Primitive Equation Models," Mon. Wea. Rev., 105, pp. 1108-1118 (1977)

10. Staniforth, A.N. and Hershell L. Mitchell, "A Variable Resolution Finite Element Technique for Regional Forecasting with the Primitive Equations," Mon. Wea. Rev., 106, pp. 439-447 (1978)

11. Staniforth, A.N. and Roger W. Daley, "A Baroclinic Finite Element Model for Regional Forecasting with the Primitive Equations," Mon. Wea. Rev., 107, pp.107-121 (1979)

12. Staniforth, A.N., "The Application of the Finite Element Method to Meteorological Simulations-A Review," International Journal for Numerical Methods in Fluids, 4, pp. 1-12 (1984)

1986 USAF-UES SUMMER FACULTY RESEARCH PROGRAM/

GRADUATE STUDENT SUMMER SUPPORT PROGRAM

Sponsored by the

AIR FORCE OFFICE OF SCIENTIFIC RESEARCH

Conducted by the

Universal Energy Systems Inc.

FINAL REPORT

Issues Related to Lithium and Lithium-Hydride Thermal Storage Spheres

Prepared by:	Douglas L.R. Oliver
Academic Rank:	Assistant Professor
Department:	Mechanical Engineering, University of Toledo; Toledo Ohio.
USAF Researcher:	Elliot Kennel, AFWAL/POOS-3, Wright-Patterson Air Force Base.
Date:	28, August, 1986.
Contract No:	F49620-85-C-0013

Issues Related to Lithium and Lithium-Hydride Thermal Storage Spheres

by

Douglas L.R. Oliver

ABSTRACT

Several issues related to the use of lithium and lithium-hydride spheres for space based thermal storage systems are investigated. These issues include: hydrogen diffusion rates through an outer shell of silicon carbide, the structural integrity of a silicon carbide shell, and heat transfer rates from the spheres. A numerical heat transfer code has been developed and tested to predict the heat transfer rates from the spheres with phase change and variable thermal properties.

ACKNOWLEDGMENTS

I wish to thank Elliot Kennel of the Areo Propulsion Laboratory at WPAFB for proposing this project. In addition, credit is due to Drs. L. C. Chow and J. N. Chung for suggestions made during the course of this research. This research was funded by the Air Force Office of Scientific Research.

I. INTRODUCTION

For space based thermal storage systems it is desirable to minimize the total system weight. To accomplish this, materials with relatively high thermal capacities should be used. The thermal capacity is the total enthalpy gained due to a temperature rise divided by that temperature rise. Thus, materials with high specific heats and a phase change will tend to have high thermal capacities.

A proposed thermal storage material with a high thermal capacity, in the temperature range from 300 K to 1200 K, is lithium-hydride or lithium enriched lithium-hydride. One of the proposed methods of containing the liquid lithium-hydride is in a spherical silicon carbide shell (see Fig. 1). In this work several issues related to the use of lithium and lithium-hydride spheres for thermal energy storage with a temperature range of 300 K to 1200 K are investigated. The issues covered in the report are: hydrogen diffusion rates through a thin silicon carbide outer shell, the structural integrity of that outer shell, and the heat transfer rates to the lithium-hydride sphere.

To address these issues, both analytical and numerical analyses were performed. The two issues related to the silicon carbide outer shell were addressed with the aid of analytic models derived from mass transport theory (hydrogen diffusion), and elastic theory (structural integrity). The heat transfer issue was addressed with the aid of a numerical code which was developed and tested for this purpose.

My background as a numerical modeler specializing in transport processes qualified me to develop the heat transfer model used in the following analyses. In addition, the general knowledge regarding stress analysis required to investigate the structural integrity of the

silicon carbide shell is possessed by most mechanical engineers.

II. OBJECTIVES OF THE RESEARCH EFFORT

The objective of this effort is to address three issues related to the use of lithium or lithium-hydride spheres as a space based thermal storage system. First, the diffusion rates of free hydrogen through the silicon carbide shell are to be estimated. Second, the structural integrity of the SiC shell is to be discussed. Most importantly, the heat transfer rates from a lithium and a lithium-hydride sphere are to be estimated.

III. DIFFUSION RATES OF H_2 FROM LiH SPHERES

Hydrogen is often a very mobil element. As the temperature increases the dissociation pressure of LiH increases exponentially. With this rapid rise in the dissociation pressure it is important that the free hydrogen not be allowed to diffuse from the sphere. SiC is a good material for limiting the diffusion of hydrogen. The following analysis demonstrates how the diffusion rates of hydrogen may be estimated for SiC and other shielding materials.

The diffusion of H_2 from a LiH sphere that is enclosed by a SiC shell may be predicted by knowing the permeability "P" of the SiC shell, and the dissociation pressure "D" of the LiH at a given temperature. In Figure 2 the permeabilities are given with units of [cm^2 (stp) mm] / [cm^2 hour $atm^{1/2}$]. The cm^3 (stp) units are the volume of gaseous H_2 at 300 K and 1 atm. The dissociation pressures are plotted as a function of temperature on Fig. 3. The net flow rate due to diffusion from the sphere is given by:

$$Flux_{(net)} = Area\ P\ D^{1/2}/L$$

$$= 4(\pi)\ r^2\ P\ D^{1/2}\ /L$$

where "L" is the shell width in mm.

Example:

The net flux of H_2 from a 1.5cm radius sphere at 1200 K with a 0.1mm thick shell of SiC_β is given by:

Diffusion Rate = 4 (π) $(1.5cm)^2(2atm)^{1/2}(10^{-4}cm^3(stp)\ mm)/(cm^2$ hour $atm^{1/2})/(.1mm)$

$= 0.04\ cm^3(stp)$ / hour

$= 1.6x10^{-6}$ moles / hour (or $3.2x10^{-6}$ gr / hour).

The preceding example illustrates that if the spheres are to be exposed to elevated temperatures for short periods of time, only a thin layer of SiC is required for hydrogen containment. The above analysis assumed that the SiC_β shell remained intact with no cracks due to rupturing. The structural integrity of the SiC shell is considered in the next section.

IV. STRUCTURAL INTEGRITY OF THE SILICON CARBIDE SHELL

In a weightless environment, liquid LiH is expected to wet the surface of the solid SiC outer shell. Thus, as the LiH becomes denser as it solidifies it will likely form a thick hollow spherical shell. When the LiH sphere is reheated, the outer surface will melt first. Upon melting, LiH has a large increase in volume. With this large volumetric expansion it is important to ensure that the outer shell of SiC is not ruptured before the inner shell of LiH melts. The following simple analysis uses elastic theory to make a preliminary investigation of the required thickness of the SiC containment shell to insure the structural integrity of the sphere.

An elastic analysis might be overly conservative with respect to

the thickness required to prevent rupture of the shell. However, a simple elastic analysis may be used as a first approximation of the required shell thickness. The assumptions used in the analysis are:

small displacements,

- the SiC shell is a thin shell,
- the LiH forms a thick shell with a single void in the center,
- the LiH shell is rigid,
- thermal effects (other than phase change expansion) areneglected.

A thin shell analysis of the SiC shell (according to Equations 2.4.4 and 2.2.7 of Pressure Vessel Design by J.F. Harvey) yeilds:

$$dr = [P\ r^2(1 - \nu)] / [2\ t\ E_{SiC}],$$

$$\sigma_{SiC} = (P\ r) / (2\ t),$$

where 't' is the thickness of the SiC shell, 'dr' is the thickness of the incremental expansion of the SiC shell due to melting of the LiH, 'P' is the resulting pressure, and 'r' is the outer radius of the LiH sphere.

If σ_{SiC} is taken to be the tensile strength of SiC (25,000 Psi), then:

$$dr/r = (1-\nu)\ \sigma_{T,\ SiC} / E_{SiC}$$

The modulus of elasticity for SiC is about 61,000,000 Psi, and Poissons ratio is about 0.18, thus:

$$dr/r = 3.e\text{-}4$$

With this small potential for expansion of the SiC shell, (about 0.1% of the volume of the sphere), the LiH shell must rupture immediately to guarantee that the SiC shell will not rupture. A thick shelled analysis may be perfomed on the (assumed rigid) LiH shell to investigate what conditions will lead to a rupture of the LiH shell

before the SiC shell ruptures.

From Equation 208 of Theory of Elasticity by Timoshenko & Goodier:

$$\sigma_{max} = [3P\, r^3] / [2\,(r^3 - a^3)]$$

where 'a' is the inner radius of the LiH shell.

If the total mass of LiH in the sphere is assumed to be such that the SiC shell is completly filled when the LiH is in a liquid state, a mass balance yeilds:

$$(a/r)^3 = 1 - \rho_L / \rho_S$$

If σ_{max} is taken to be the compressive strength of LiH (14,000 to 28,000 Psi for cold pressed LiH), then:

$$P = 2/3\, \sigma_{C,\,LiH}\, \rho_L / \rho_S$$

also (from above):

$$P = 2\, t\, \sigma_{T,\,SiC} / r.$$

Thus, if there is an equal propensity for either the SiC shell or the LiH shell to rupture:

$$t/r = 1/3\, [\sigma_{C,\,LiH} / \sigma_{T,\,SiC}]\, (\rho_L / \rho_S).$$

Taking:

$$\sigma_{C,\,LiH} = 20{,}000 \text{ Psi},$$

$$\sigma_{T,\,SiC} = 25{,}000 \text{ Psi},$$

$$\rho_L = .54 \text{ gr/cc}, \quad \rho_S = .75 \text{ gr/cc},$$

thus, $t/r = .19$.

With $t/r = .19$ about 40% of the total volume of the sphere will be for the SiC shell. Thus the majority of the total weight will be attributed to the SiC shell.

Again, it should be emphasized that this was an elastic analysis. An elastic/plastic analysis which included thermal stresses, might result in a different mass ratio of SiC to LiH. However, the use of an elastic analysis does indicate that SiC shells might not result in an optimum gross weight for the spheres.

In the preceeding analysis the large stresses were the result of the large density changes associated with the melting of LiH, and the brittle nature a crystaline LiH. A brittle material might not allow the expanding liquid on the heated surface of the sphere to expand into the void in the center of the sphere. On the other hand, pure lithium is a very soft metal which does not expand as much as LiH does. A soft material could be forced into the void as the liquid on the outer surface of the sphere expands on melting. Thus, lithium spheres would probably have less propensity to rupture the external containment shell.

One disadvantage of lithium as a thermal storage material is that it has a thermal capacity (between 300 K and 1200 K) that is about 50% of the thermal capacity of LiH. This will be discussed further in the next section.

V. HEAT TRANSFER FROM A LITHIUM-HYDRIDE AND A LITHIUM SPHERE

Accurate estimations of the heat transfer from a sphere which undergoes a change of phase requires a numerical simulation. Analytic solutions to general phase change problems have not been developed. The literature contains several potential numerical schemes which may be used to estimate the heat transfer rates from bodies which experience a phase change. Due to the large temperature difference expected (about 900 degrees Kelvin), the thermal properties of both

lithium and lithium-hydride will vary significantly inside the sphere. No numerical procedure was found which could accurately model heat transfer, with phase change, from spheres where the thermal properties varied with the temperature. Thus, a numerical code SPH THERK was developed and tested for this purpose.

The code SPH THERK is an explicit, finite difference code which is capable of modeling transient heat transfer with a phase change. It is a one dimensional code using spherical or rectangular coordinates. This code is capable of modeling temperature dependent thermal conductivity and specific heat. Currently this code is limited to constant densities for both the solid and liquid phases.

To gain confidence in the implementation and encoding of a numerical code the results should be compared with the results of analytic solutions, other computer codes, or experiments. Several analytic solutions to heat transfer problems with phase change have been implemented to verify the code SPH THERK. These analytic solutions represent special cases of the more general solution domain of SPH THERK.

The first of these analytic verification problems is designed to test the ability of SPH THERK to predict the net enthalpy gain (loss) with time for a sphere experiencing a phase change. The analytic solution for this problem is based on the work of A.M. Soward. In this work, Soward proposes a solution to a phase change problem in a sphere which is initially at the fusion temperature. This solution assumes that the thermal properties are constant, and that the change in the enthalpy due to phase change is much greater than the change of enthalpy due to temperature change. The details of the Soward solution

have been omitted from this work due to space considerations. Equation 2.16a of Soward was used for this comparison.

Two simulations were made for comparison with the work of Soward; one for thawing of a LiH-like substance and one for freezing of the same substance. On Figure 4 the enthalpy gained (lost) by a sphere is illustrated for comparison with the solution of Soward. In both cases the two models compare favorably.

The second verification problem is designed to test the ability of SPH THERK to model heat transfer with phase change where the relative effects of the latent heat of fusion are less than in the above problem. In addition, this verification problem will test the ability of SPH THERK to model heat transfer with a variable thermal conductivities, and where the initial temperature is not the fusion temperature. The analytic solution used for this verification is based on the work of Cho and Sunderland, which proposes an analytic solution for heat transfer in a semi-infinite slab with a phase change and a variable thermal conductivity. (In the course of implementing the analytic solution of Cho and Sunderland a mistake was found in Equation 43 of their work. Equation 43 needed to be revised to be in conformance with Equation 24 of their work. The revised version of Equation 43 was confirmed with Dr. Sunderland.)

On Figure 5 the phase change location for a hypothetical substance is plotted for comparison with the solution of Cho and Sunderland. Two grid mesh sizes were used to demonstrate the effects of mesh size. As the mesh size is increased, an approximation used in SPH THERK, (which neglected the sensible energy in estimating the spatial change in the phase change location), resulted in a "stair-step" like appearance for

the location of the phase change. This effect becomes less noticeable as the mesh size is reduced. Even with the coarse grid size used in the simulation, the location of the phase change front predicted by SPH THERK is in adequate agreement with the analytic model of Cho and Sunderland.

No analytic solution was found which could be used to test the ability of SPH THERK to accurately model heat transfer with variable specific heats in the presence of a phase change. For this reason such an analytic solution was developed, (Oliver). This solution is similar to that of Cho and Sunderland, with the exceptions that the initial temperature is assumed to be the fusion temperature, and the effects of variable specific heats have been included. On Figure 6 the phase change location has been plotted for freezing of a LiH-like substance. The agreement between the predictions of the analytic solution and those of SPH THERK is good, (less than 1% difference for larger times).

Based on the above set of verification problems it is believed that the numerical code SPH THERK can adequately model one dimensional heat transfer problems in rectangular and spherical coordinates, with a phase change, and variable thermal properties where the densitiy is assumed uniform.

The heat transfer rates from a lithium-hydride and a lithium sphere has been modeled with the numerical code SPH THERK. The spheres were assumed to be hollow to account for the density differences between the two extreme temperatures. Large variations may be found in the literature for thermophysical properties of both lithium-hydride and lithium. References which include data pertaining to thermophysical properties for either lithium of lithium-hydride include: Anderson et

al., Touloukian and Ho, Maroni et al., and Shpil'rayn, et al. Shpil'rayn et al. appears to be the best source for LiH and Li,LiH thermophysical property data. For the heat transfer simulations of Li and LiH spheres the following properties were used:

Lithium-Hydride:

Inner radius: 69% of the outer radius,

Density: 790 kg/(m^3),

Melting temperature: 956 K, Heat of fusion: 2.7 MJ/kg,

Liquid Phase: $k = [1.2 + .003\ K^{-1}(T-956\ K)]$ W/(m K),

$c = [8290. - .4\ K^{-1}(T-956\ K)]$ J/(kg K),

Solid Phase: $k = [3.5 - .01\ K^{-1}(T-956\ K)]$ W/(m K),

$c = [8000. + 6.1\ K^{-1}(T-956\ K)]$ J/(kg K).

Lithium:

Inner radius: 55% of the outer radius,

Density: 535 kg/m^3,

Melting temperature: 454 K, Heat of fusion: 380. kJ/kg

Liquid Phase: $k = [39.1 + .025\ K^{-1}(T-454)]$ J/(m K),

$c = 4200.$ J/(kg K), (constant),

Solid Phase:

$k = [73.6 + .071\ K^{-1}(T-454\ K)]$ W/(m K),

$c = [4230. + 4.37\ K^{-1}(T-454\ K)]$ J/(kg K).

The enthalpy gained by the spheres with time has been plotted on Fig. 7 and Fig. 8. The time scale has been scaled to allow for estimations for heat transfer to spheres with an arbitrary radius. The time scale is proportional to the square of the radius. For example, Figures 7 and 8 are scaled for a sphere with a 1cm radius. If the sphere had a radius of 2cm, the time required to gain the same enthalpy (on a per kilogram basis) would be four times as great.

The lithium sphere takes only about a half of a second to come to a near equilibrium state, the lithium-hydride sphere requires about fifty seconds to come to a near equilibrium state. The lithium sphere responds more rapidly for two reasons: the thermal conductivity of lithium is much higher than it is for lithium-hydride, also the thermal capacity of lithium is about half of that for lithium-hydride.

The above analysis neglected the effects of density variation. The effect of including thermal expansion could result in either an increase or a decrease in the thermal response time. The reasons for this ambivalence are complex, and are not dealt with in this work. However, it is expected that Figures 7 and 8 adequately predict the heat transfer to the spheres for a preliminary analysis.

From a thermophysical perspective, LiH spheres have the advantage of a large thermal capacity (about 8 MJ/kg from 300 K to 1200 K). The disadvantages of LiH spheres are: the brittle nature of solid LiH, the potential for hydrogen diffusion from the sphere, and its large expansion upon melting. The advantages of a lithium spheres are: lithium does not expand much upon melting, it is a soft metal, and it has a high thermal conductivity. The disadvantage of lithium is that it has only about half of the thermal capacity of LiH.

It is possible that a Li,LiH solution will offer the optimum combination of thermal properties and mechanical properties. However, there is very little data on Li,LiH solutions in the English language literature. Shpil'rayn et al. (a text in Russian) appears to be one of the most thorough reveiws of Li,LiH properties.

VI. RECOMENDATIONS

Based on the above analyses, the optimum thermal storage material

for the temperature range of 300 K to 1200 K might be a solution of lithium and lithium-hydride. Lithium has the advantage of being a soft material which does not expand greatly on melting. In addition, lithium has a high thermal conductivity, and hydrogen diffusion from pure lithium is not an issue. The advantages of lithium-hydride is that it has a large thermal capacity. A solution of lithium and lithium-hydride might offer an optimum combination of a soft material, with a high thermal capacity.

One problem associated with the use of a solution of lithium and lithium-hydride is that the complexity of the system is increased. The addition of the second species results in a variable phase diagram and the potential for an inhomogeneous sphere. For example, as a hot Li,LiH sphere is cooled, the lithium-hydride will solidify first (probably at the outer edge of the sphere). Thus, the Li,LIH sphere could be inhomogeneous and non-isotropic with LiH at the outer surface and Li at the inner surface.

The net effects of such a solution are not clear. As pointed out earlier, there is little published data (in English) on lithium, lithium-hydride solutions. Shpil'ryan et al. appears to be the best source on the thermophysical properties of this solution. If serious work on lithium, lithium-hydride solutions is contemplated, it is recommended that an English translation of this text be obtained.

There appears to be a large degree of variability in certain of the thermophysical properties of both lithium and lithium-hydride. Some of this variability appears to be due to differences in the condition of the material (i.e. cold pressed, crystaline etc.). It is recommended that the important thermophysical properties of lithium and lithium-

hydride (or their solutions) be independently confirmed before any thermal storage design is finalized.

FIG. 1

Schematic of the Thermal Storage Spheres.

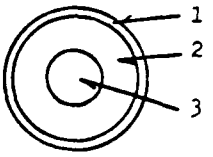

1 - SiC outer shell
2 - LiH or Li shell
3 - void
(not to scale)

FIG. 2

Tritium Permeability in Metals & SiC, From Fig. 6 of Causey et al.

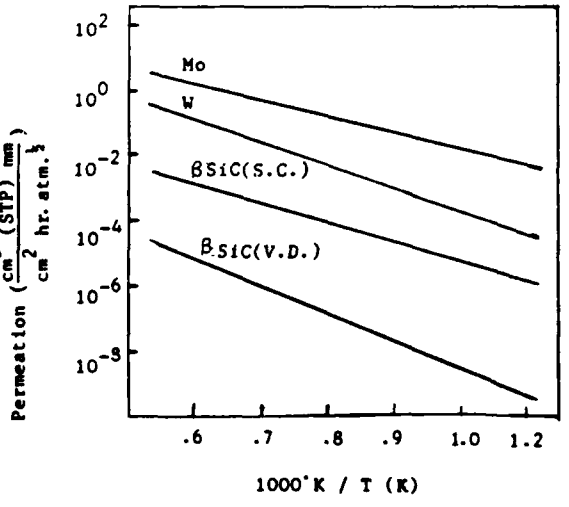

FIG. 3

Hydrogen Pressure for LiH.

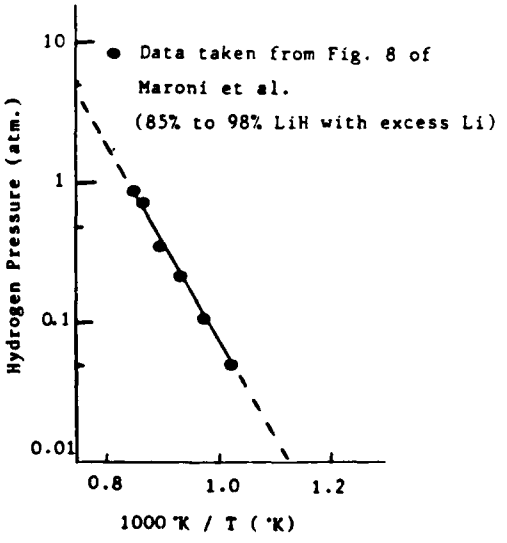

FIG. 4

Freezing and Thawing of a Sphere / Comparison with the Analytic Solution of Soward.

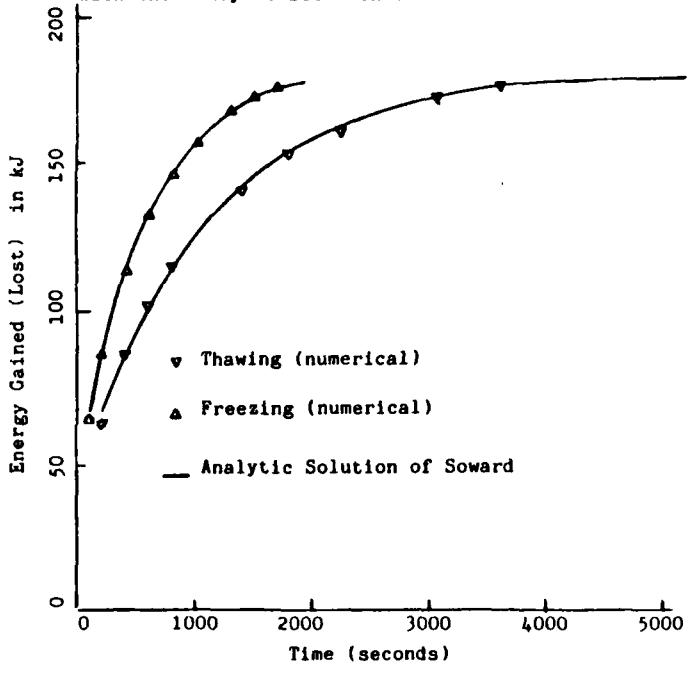

FIG. 5

Thawing of a Hypothetical Substance, Comparison with Cho & Sunderland.

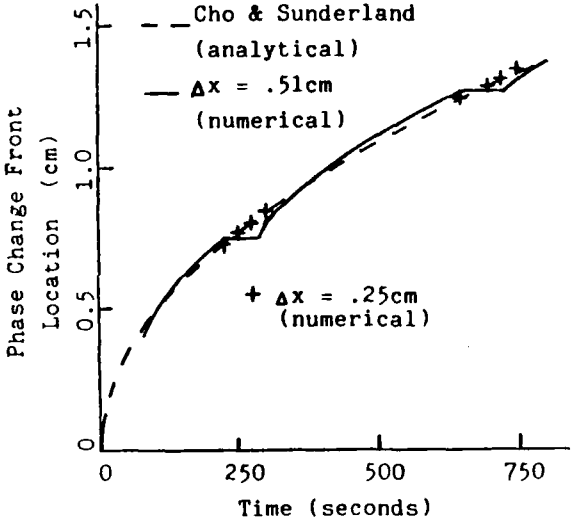

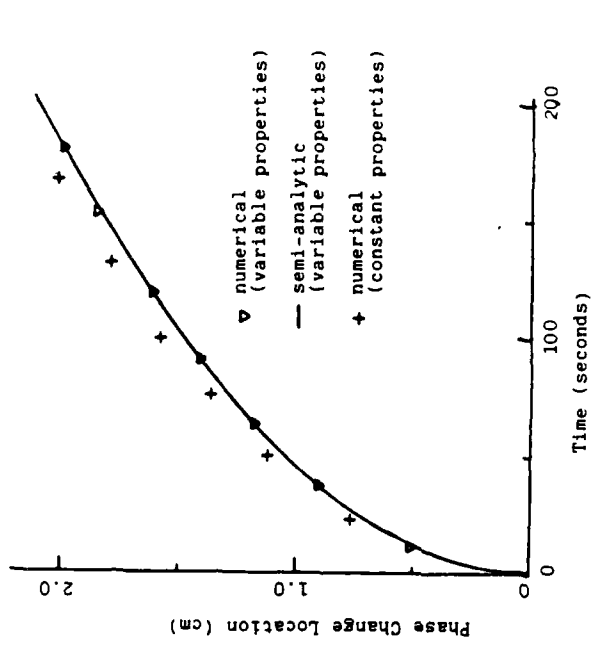

FIG. 6
Freezing of Lithium-Hydride: Phase Change Location

FIG. 7

Thawing of a Lithium Sphere.

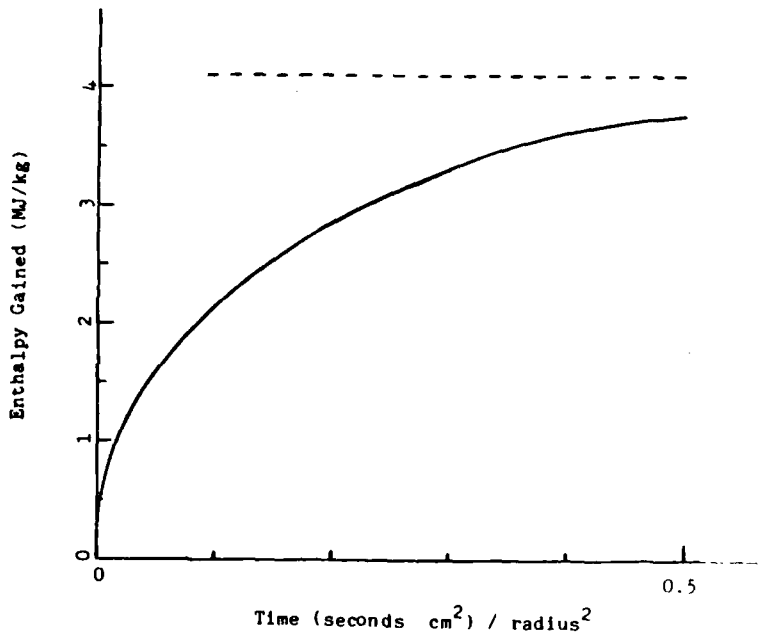

FIG. 8

Thawing of a Lithium-Hydride Sphere.

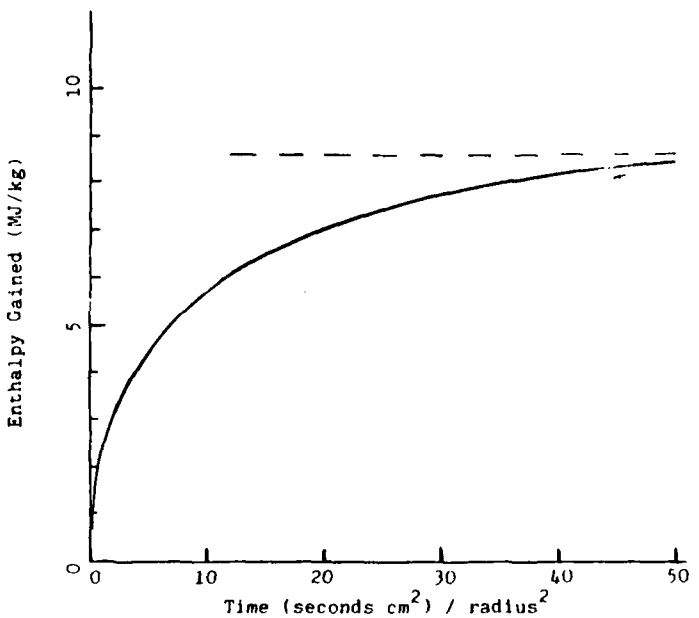

REFERENCES

1) Anderson, R.V., D. Bost, and W.R. Determan, 'Space-Reactor Electric Systems: Subsystem Technology Assessment,' ESG-DOE-13398, Rockwell International / Energy Systems Group, 1983

2) Causey, R.A. et. al. 'Hydrogen Diffusion and Solubility in Silicon Carbide,' Amer. Ceramic Soc. vol. 61, n 5-6, pp 221-225. 3) Cho, S.H. and J.E. Sunderland, 'Phase Change Problems with Temperature-Dependent Thermal Conductivity,' ASME, J. Heat Trans., vol. 96, pp. 214-217, 1974.

4) Harvey, J.F., Pressure Vessel Design; Nuclear and Chemical Applications, D. van Nostrand Co. Toronto, 1963.

5) Maroni, V.A. E.J. Cairns, and F.A. Cafasso, 'A Review of the Chemical, Physical, and Thermal Properties of Lithium that are Related to its Use in Fusion Reactors', ANL-8001, Argonne National Lab., 1973.

6) Oliver, D.L.R, 'A Phase Change Problem with Temperature Dependent Thermal Conductivity and Specific Heat,' to be published.

7) Shpil'rayn, E.E. et. al. Thermopysical Properties of Hydride, Deutride, Lithium Tritide and their Solutions with Lithium: A Handbook, (in Russian), Moscow, 1983.

8) Soward, A.M. 'A Unified Approach to Stefan's Problem for Spheres and Cylinders,' Proc. R. Soc. Lond. A373, pp. 131-147, 1980.

9) Timoshenko, S.P. and J.N. Goodier, Theory of Elasticity, 3rd ed. McGraw-Hill, New York, 1970.

10) Touloukian, Y.S. and C.Y. Ho, Thermophysical Properties of Matter, volumes 1 and 4, IFI/Plenum Data Company, 1979.

1986 USAF-UES SUMMER FACULTY RESEARCH PROGRAM

GRADUATE STUDENT SUMMER SUPPORT PROGRAM

Sponsored by the

AIR FORCE OFFICE OF SCIENTIFIC RESEARCH

Conducted by the

Universal Energy Systems, Inc.

FINAL REPORT

A NETWORK TUTOR BASED ON THE HEURISTIC OF POLYA

Prepared by:	Philip D. Olivier
Academic Rank:	Assistant Professor of Electrical Engineering
Department and University:	Division of Engineering, The University of Texas at San Antonio
Research Location:	The Air Force Human Resources Laboratory, Training Systems Division, Intellegent Systems Branch
USAF Researcher:	Dr. Philip D. Gillis
Date:	September 10, 1986
Contract No:	F49620-85-C-0013

A NETWORK TUTOR BASED ON THE HEURISTIC OF POLYA

by

Philip D. Olivier

ABSTRACT

This report describes the core of an Intelligent Tutorial system designed to help students learn basic circuit and network theory at a level taught to sophomore Electrical Engineering students. The tutorial strategy is taken from the heuristic of George Polya, in that the student is asked to answer questions about the problem at hand, and these questions are inspired by the questioning procedure suggested in Polya's HOW TO SOLVE IT. In a very real sense the student is lead through the design of the solution procedure in much the same way that students are lead through the "invention" stage of writing an essay in other CAI programs. In addition to helping the student develop a plan of attack for a particular problem the tutor described here also monitors his/her answers and attempts to diagnose the students weaknesses. It is hoped that the student not only learns some network theory but also internalizes the procedure used to elicit the answers. The tutor described here initially asks the student several questions about the solution to determine whether or not the student has successfully solved the problem. When errors are detected the tutor asks deeper questions.

ACKNOWLEDGMENTS

I would like to take this opportunity to acknowledge and thank the Air Force Human Resources Laboratory at Brooks Air Force Base for their hospitality and support. I would like to especially thank Lt.C. Hugh Burns and Dr. Philip Gillis of the Intelligent Systems division for making my stay enjoyable and productive.

I. INTRODUCTION:

The area of Intellegent Computer Aided Instruction is going to grow very rapidly in the near future. This growth is due to several factors, amoung them are: 1) the scarcity of highly trained instructors in critical areas, 2) the infinite patience that a computer posseses, 3) the reduction in price of powerful processors, and 4) the need to provide on-site on-the-job training to technicians in factories, on flight lines and in space. However the cost of these systems needs to be reduced before they will make a significant impact on elementary, secondary, or college education.

Several Intelligent Tutorial Systems (ITSs) have been built to teach computer programming languages (LISP, PASCAL), history, economics, and medical diagnosis to name a few areas. However, none of them seem to be based on the tutorial heuristic of Polya. The Artificial Intelligence (AI) community pays tribute to Polya and his work on heuristic but they do not seem to use his work (see Newell's paper). It has been my experience as a teacher that I have intuitively used Polya's approach to guide my students through problems that they have found difficult.

Some ITSs have evolved from domain specific expert systems. This seems reasonable, since it should require an expert in an area to teach the material. However this seems to be a very expensive building block especially if there is no real need for a stand-alone expert system in the domain. Another expense that seems unnecessary is

caused by the authors of ITSs who insist on building the system from ground zero. By this I mean that ITS authors seem to not only design the computer program but to design the complete curriculum and instructional environment. While this may produce the optimal ITS product it seems to reduce the availability of this technology. Further, I beleive that it is too early in the development of ITSs to be concerned with the devleopment of 'optimal' systems. We must be concerned with good, useful systems.

The remainder of this report is organized as follows: Section II describes the objectives of my research on Intellegent Computer Aided Instruction; Sections III, IV and V describe the details of this work. Section VI briefly describes three smaller projects that I worked on while at the Air Force Human Resources Laboratory (AFHRL). Section VII concludes this report with several recommendations.

II. OBJECTIVES OF THE RESEARCH EFFORT:

This research effort attempts to show that Polya's approach to tutoring is mechanizable and to show that the cost of producing ITSs can be reduced if one builds on an existing curriculum. This is true, at least, if the system is going to augment, rather than replace, a traditional classroom environment. The system that has been built can best be described as an Instructor's Associate or as an Intellegent Computer Grader/Tutor.

The benefits of an Instructor's Associate ITS are

-More efficient feedback for the student,

-Lower workload for the instructor,

Copied from Polya's HOW TO SOLVE IT, 1973.

HOW TO SOLVE IT

UNDERSTANDING THE PROBLEM

First.
You have to *understand* the problem.

What is the unknown? What are the data? What is the condition? Is it possible to satisfy the condition? Is the condition sufficient to determine the unknown? Or is it insufficient? Or redundant? Or contradictory?

Draw a figure. Introduce suitable notation.

Separate the various parts of the condition. Can you write them down?

DEVISING A PLAN

Second.
Find the connection between the data and the unknown. You may be obliged to consider auxiliary problems if an immediate connection cannot be found. You should obtain eventually a *plan* of the solution.

Have you seen it before? Or have you seen the same problem in a slightly different form?

Do you know a related problem? Do you know a theorem that could be useful?

Look at the unknown! And try to think of a familiar problem having the same or a similar unknown.

Here is a problem related to yours and solved before. Could you use it? Could you use its result? Could you use its method? Should you introduce some auxiliary element in order to make its use possible?

Could you restate the problem? Could you restate it still differently? Go back to definitions.

If you cannot solve the proposed problem try to solve first some related problem. Could you imagine a more accessible related problem? A more general problem? A more special problem? An analogous problem? Could you solve a part of the problem? Keep only a part of the condition, drop the other part; how far is the unknown then determined, how can it vary? Could you derive something useful from the data? Could you think of other data appropriate to determine the unknown? Could you change the unknown or the data, or both if necessary, so that the new unknown and the new data are nearer to each other?

Did you use all the data? Did you use the whole condition? Have you taken into account all essential notions involved in the problem?

CARRYING OUT THE PLAN

Third.
Carry out your plan.

Carrying out your plan of the solution, *check each step.* Can you see clearly that the step is correct? Can you prove that it is correct?

LOOKING BACK

Fourth.
Examine the solution obtained.

Can you *check the result?* Can you check the argument?
Can you derive the result differently? Can you see it at a glance?
Can you use the result, or the method, for some other problem?

(5)

steps are listed below. The student must:

1) Understand the problem,
2) Devise a plan to solve the problem,
3) Carry out the plan,
4) Look back and summarize the solution process.

Step one, Understanding the problem, is confusing to some students because they say "If I understood the problem I would not need to solve it". However, Polya does not mean to 'understand the solution', he means to understand what needs to be calculated and what tools are at hand to calculate with. Until this step is completed it is inappropriate for the student to search for solution templates (i.e. gratuitously worked problems).

Step two, devising the plan, involves deciding how to combine the available formulae and methods to the problem. At this point it is often very useful for the student to find a similar problem and use its result. (I.e. find a solution template.)

Step three, carrying out the plan, normally involves using standard mathematical tools such as algebra and calculus to convert the plan into a formula and then perhaps into a number.

Step four, looking back over the solution, is where the details are separated from the general method of the solution in preparation for using this solution to help solve some future problem. If students never look back over their work they will be limited to using only the worked examples in the text for guidance and these are often too limited in scope to be useful when attacking

large real-world problems. In the field of Mathematics the last step is institutionalized by labelling certain results as 'THEOREM's and requiring students to memorize the more useful solutions (the 'PROOF's).

Experience indicates that good students tend to be good problem solvers and therefore intuitively use a variation of this procedure. Experience also indicates that mediocre students try to skip step 2 (devising a plan) and don't even think about step 4 (looking back). Any ICAI product based on Polya's heuristic will have to coerce the poorer students into paying attention to these steps.

IV. Knowledge Representations

Most work and thought in any AI project goes into deciding how the knowledge about the domain is best represented. Several knowledge representation schemes have been tried and they will now be discussed. Before presenting the knowledge representations the types of knowledge that are needed will be presented. These are

-Circuit theory knowledge

-Knowledge of the expert solution

-Ancillary tool knowledge

The Circuit theory knowledge is usually in the form of equations and/or procedures. This immediately brings up the tradeoff between procedural and declarative representations. Take, for example Ohm's law, v=Ri, where v is the voltage across a resistor of resistance R and i is the current through the resistor. This equation is really three equations as far as a student is concerned. Which equation is determined by what is known and what is to be

calcualted; i.e v=Ri is used when v is needed and R and i are known (directly or indirectly), i=v/R is used when i is needed and v and R are known and finally R=v/i is used when R is needed and v and i are known. This is a classic example of this tradeoff. A student must either memorize all three equations (a purely declarative representation) or the basic equation must be memorized along with the procedure to derive the other two equations (a declarative and procedural representation). Scientific and Engineering theories try to emphasize the procedural knowledge at the expense of declarative knowledge. That is, a student is supposed to memorize less than derive. However, in trade-schools this emphasis is reversed. (As a matter of fact textbooks on basic electricity for use in trade-schools present these three equations as "Ohm's three laws".) For the representation in the ITS a declarative representation is adopted.

Each equation is represented as a list along with a specification of what is calcualted by the equation and what information is required for the calculation.

Knowledge of the expert solution can be captured from the instructor or it can be generated by the system. Obviously it is quicker to build an authoring shell that captures the solution from the instructor. It is just as obvious that such a shell will require an instructor of high ability. From my experience as an instructor it is necessary to work the assigned problems so capturing the solution from the instructor is the chosen approach. The instructor will be asked the same high level questions as

the student and only when there are differences will the program delve deeper.

The ancillary knowledge, such as knowledge of mathematics, can be built in by using a system similar to MACSYMA or REDUCE. These programs do symbolic mathematical manipulation at a level of a good graduate student in mathematics. They can symbolicly solve problems in algebra, calculus and differential equations. Once a calculation is started intermediate and final answers can be compared to the answers generated by this type of program. A streamlined version needs to be developed so that it can be incorporated into this type of ITS.

V. State of the System

Currently the tutoring program, written in XLISP for IBM compatible computers, can ask students questions about certain problems taken from Strum and Ward's book. The student's answers are compared to the instructor's answers and if the answers disagree then some help is provided to the student. The students answers are preserved in a 'history' file so that systematic errors can be discovered (this algorithm is yet to be designed) and appropriate remediation can be provided.

The questions that the student must answer concern the GOAL of the problem, what information is GIVEN in the problem, what EQUATIONS are key to the solution, what METHODS are key to the solution, what the ANSWER to the problem is, and what UNITS the answer is in.

The current version is limited in that it cannot handle problems that involve several answers, and it cannot

yet help the student find the correct combination of equations that will relate the unknown to the given through several intermediate quantities. Another way of saying this is that the program cannot yet help the student derive a complicated formula from several basic formulas.

The XLISP code for this program is now presented.

```
;7-8-86

(print '(----------------------------------NETWORK TUTOR-----------------------------
(print '(-----------------------------------------by-----------------------------------
(print '(--------------------------------Philip D. Olivier-----------------------------
(print '(-----------------------------------June 1986-------------------------------

(print '(This program is an Intelligent Tutorial system designed to help
students learn basic network theory on the level of Strum and Ward s book.  The
student is assumed to have read the appropriate chapter in the textbook.  It is
not assumed that the student has completely mastered nor memorized the
information.  This program will pose problems for the student to solve and
monitor the students answers to questions about the problems.  Based on a
comparison of the students work to that of an expert the program will attempt
to diagnose the cause of the students errors as well as alter its own
questioning strategy.  The questioning strategy is taken from that of Polya s
Heuristic))

;For each chapter the domain specific knowledge is contained in the
;list EQUATIONS which is made of sublists according to the following format:))

;equation:equation#:quantities:validity:component))
;(where))
;equation stands for the equation))
;equation# is the equation number in the text [sometimes this is NONE]))
;quantities is a list that contains the names of the circuit variables
;and or parameters that are related by the equation))
;-----possible entries are))
;-------- CURRENT  CHARGE  ENERGY  VOLTAGE  POWER  RESISTANCE))
;-------- INDUCTANCE  CAPACITANCE  FLUX  PERIOD  SECONDARY*VOLTAGE))
;-------- PRIMARY*CURRENT  MUTUAL*INDUCTANCE  FREQUENCY HERTZ))
;-------- FREQUENCY RADIAN  EFFECTIVE*VALUE  RMS*VALUE))
;-------- UNIT*STEP*RESPONSE  UNIT*RAMP*RESPONSE  UNIT*DELTA*FUNCTION))
;-------- UNIT*RECTANGULAR*PULSE))
;validity refers to the range of validity of the equation possible
;entries are))
;-------- DEFINITIONS  THEOREMS  LINEAR  NONLINEAR  ALL  TIME*VARYING))
;component usually refers to the type of circuit componet ie ))
;-------- RESISTORS  INDUCTORS  CAPACITORS  TRANSFORMERS  OPAMPS))
;however it can be FUNCTIONS if the equation defines a function))

;the following function finds the equation number for a given
;equation

(defun equationnumber? (equations equation)
       (setq newequations 'nil)
       (dolist (x equations number)
              (cond ((equal equation (caar x))
                     (setq newequations (append newequations x))
                     (print (car (cdr (x))))
       )      )     )

;the following function finds the quantities that are related by the
;given equation
(defun equationquantities? (equations equation)
       (setq newequations 'nil)
       (dolist (x equations quantities)
              (cond ((equal equation (caar x))
                     (setq newequations (append newequations x))
                     (setq message '(relates))
```

```
                        (print (append message (car (nthcdr 2 x))))
        )       )       )

;the following function finds the range of validity for the given
;equation
(defun equationvalidity? (equations equation)
        (setq newequations 'nil)
        (dolist (x equations validity)
                (cond ((equal equation (caar x))
                        (setq newequations (append newequations x))
                        (setq message '(has validity type))
                        (print (append message (car (nthcdr 3 x))))
        )       )       )

;the following function finds the type of component that the equation
;refers to
(defun equationcomponent? (equations equation)
        (setq newequations 'nil)
        (dolist (x equations type)
                (cond ((equal equation (caar x))
                        (setq newequations (append newequations x))
                        (setq message '(this equation refers to the following
                                component[s]))
                        (print (append message (car (nthcdr 4 x))))
        )       )       )

;this function finds the equation given the equation number
(defun numberequation? (equations number)
        (setq newequations 'nil)
        (setq message '(the equation[s] with the given number
        is [are]))
        (dolist (x equations newequations)
                (cond ((equal number (caar (cdr x)))
                        (setq newequations (append newequations x))
                        (print (append message (list (car x))))
        )       )       )

;this function finds the equations that involve a given quantity
(defun quantityequation? (equations quantity)
        (setq newequations 'nil)
        (setq message '(the equations that refer to))
        (setq message (append message (list quantity) '(are:)))
        (print message)
        (dolist (x equations newequations)
                (cond ((member quantity (car (nthcdr 2 x)))
                        (setq newequations (append newequations x))
                        (print (caar x))
        )       )       )

;this function finds the equations that pertain to a given component
(defun componentequation? (equations component)
        (setq newequations 'nil)
        (setq message (list '(the following equations pertain to)))
        (setq message (append message component '(are:)))
        (print message)
        (dolist (x equations)
                (cond ((member component (car (nthcdr 4 x)))
                        (print (caar x))
                        (setq newequations (append newequations x))
        )       )       )
```

```
(print '(GOAL?))
(setq goal (read))
(setq history (append history (list (list 'GOAL goal))))
(if (member goal (assoc 'GOAL currentsolution))
        't
        (and (print '(please re-read the problem and answer again))
                (setq goal (read))
                (setq history (append history (list (list 'GOAL goal))))
                (if (member goal (assoc 'GOAL currentsolution)) 't
                        (and (setq message '(the correct goal is))
                                (print (append message (cdr (assoc 'GOAL
                                                currentsolution))))))))

(print '(GIVEN?))
(setq given (read))
(setq history (append history (list (list 'GIVEN given))))
(if (member given (assoc 'GIVEN currentsolution))
        't
        (and (print '(please re-read the problem and anwer again))
                (setq given (read))
                (setq history (append history (list (list 'GIVEN given))))
                (if (member given (assoc 'GIVEN currentsolution)) 't
                        (and (setq message '(the given information is))
                                (print (append message (cdr (assoc 'GIVEN
                                                currentsolution))))))))

(print '(EQUATIONS NEEDED))
(setq equationsneeded (read))
(setq history (append history (list (list 'EQUATIONSNEEDED equationsneeded))))
(cond ((equal equationsneeded '?)
        (and (quantityequation? equations goal)
                (quantityequation? equations given)
                (componentequation? equations goal)
                (componentequation? equations given)
                (print '(EQUATIONS NEEDED))
                (setq equationsneeded (read))
                (setq history (append history (list (list 'EQUATIONSNEEDED
                equationsneeded))))))))
(if (member equationsneeded (assoc 'EQUATIONS currentsolution))
        't
        (and (setq message '(the needed equation is))
                (print (append message (cdr (assoc 'EQUATIONS
                                currentsolution))))
              ))

(print '(METHODS NEEDED))
(setq method (read))
(setq history (append history (list (list 'METHODS method))))
(if (member method (assoc 'METHODS currentsolution))
        't
        (and (setq message '(how do you relate))
                (setq message (append message (cdr (assoc 'GOAL
                currentsolution)) '(and) (cdr (assoc 'GIVEN currentsolution))))
                (print message)
                (setq method (read))
                (setq history (append history (list (list 'METHODS method))))
                (if (member method (assoc 'METHODS currentsolution))
                        't
                        (and (setq message '(Appropriate methods are))
                                (setq message (append message (cdr (assoc
```

```
;this function finds the equations that have a given validity
(defun validityequation? (equations validity)
        (setq newequations 'nil)
        (setq message (list 'the 'following 'equations 'are validity))
        (print message)
        (dolist (x equations)
                (cond ((member validity (car (nthcdr 3 x)))
                        (print (caar x))
                        (setq newequations (append newequations x))
        )       )       )

;the following function prints a problem from the list of problems in
;the chapter
(defun printequations (equations)
        (print '(the equations in this chapter are:))
        (dolist (x equations)
                (print (car x))))

(defun printproblem (x)
        (print '(-----------------------------------------------------------------------
        (print x)
        (print '(-----------------------------------------------------------------------


;THE MAIN PROGRAM STARTS HERE

(print '(Hi I will be helping you today.  What is your name?))
(setq name (read))
;needs to check student base for existing record to append this record to
(setq history (list (list 'NAME name)))

;the following question should be answered by analyzing the student model
(print '(what chapter do you wish to work on?))
(print '(1: CHAPTER 1))
(print '(2: CHAPTER 2 [NOT YET AVAILABLE]))
(print '(3: CHAPTER 3 [NOT YET AVAILABLE]))
(print '(4: CHAPTER 4 [NOT YET AVAILABLE]))
(print '(TYPE YOUR CHOICE 1 THRCUGH 4))
(setq ans (read))
(setq history (append history (list (list 'CHAPTER ans))))
(cond ((= 1 ans) (load "chapter1"))
        ((= 2 ans) (load "chapter2"))
        ((= 3 ans) (load "chapter3"))
        ((= 4 ans) (load "chapter4"))

(dolist (x problems)
(print '(your next problem is))
(setq x (car problems))
(printproblem x)
(setq currentproblem x)
(setq history (append history (list (list (car x)))))
(setq currentsolution (car solutions))
(setq solutions (cdr solutions))
(setq problems (cdr problems))

(print '(YOU WILL NOW BE ASKED SOME QUESTIONS ABOUT THE PROBLEM:))
(print '(IF YOU DO NOT KNOW THE ANSWER THEN TYPE ?))

(setq answer 'nil)
```

```
                                    'METHODS currentsolution))))
                                   (print message)
                                  ))))

(print '(ANSWER?))
(setq answer (read))
(setq history (append history (list (list 'ANSWER answer))))
(if (member answer (assoc 'ANSWER currentsolution))
        't
        (and (setq message '(please check for typographical errors))
                (print message)
                (setq answer (read))
                (setq history (append history (list (list 'ANSWER answer))))
                (if (member answer (assoc 'ANSWER currentsolution))
                        't
                        (and (setq message '(possible answers are))
                                (setq message (append message (cdr (assoc
                                    'ANSWER currentsolution))))
                                (print message)))))

(print '(UNITS?))
(setq answer (read))
(setq history (append history (list (list 'UNITS answer))))
(if (member answer (assoc 'UNITS currentsolution))
        't
        (and (setq message '(please check for spelling errors))
                (print message)
                (setq answer (read))
                (setq history (append history (list (list 'UNITS answer))))
                (if (member answer (assoc 'ANSWER currentsolution))
                        't
                        (and (setq message '(possible units are))
                                (setq message (append message (cdr (assoc
                                 'UNITS currentsolution))))
                                (print message)))))

dolist (x history)
        (print x))

;the following questions need to be asked in the debugging process
;DO YOU NEED TO FORMALIZE AND SOLVE AN INTERMEDIATE PROBLEM?
;DO YOU KNOW A PROBLEM RELATED TO THIS ONE?
;DO YOU NEED TO MAKE ADDITIONAL ASSUMPTIONS? [DO NO UNLESS ABSOLUTELY
;NECESSARY
;HAVE YOU USED ALL THE INFORMATION PROVIDED?
;LOOK AT THE UNKNOWN!!!!
;CARRY OUT YOUR PLAN
;CAN YOU CHECK YOU ANSWER ON A SIMPLER SITUATION?
```

VI. Other projects

I worked on three smaller projects while at AFHRL. These were

1) Helping to install a version of LISP on AFHRL's new VAX 8600 computer

2) Investigate the usefullness of XLISP 1.4 on both the VAX 8600 and on the IBM PCs.

3) To construct an annotated bibliography on Parallel processing and its impact on ICAI.

Comments concerning XLISP can be found in next section on recommendations. The annotated bibliography on Parallel processing is still in progress.

VII. RECOMMENDATIONS:

I have several recommendations, they are:

1) XLISP is a reasonable dialect of LISP that is almost COMMON LISP. It works pretty well on the IBM PCs. It is very slow on the VAX. Its slowness is due to the fact that it is an interpreter that is written in C. It therefore cannot be compiled. I wrote and ran a small parsing program in XLISP and used it on some data that Dr. Philip D. Gillis had. The XLISP program was much smaller than the corresponding SNOBALL program that Dr. Gillis has used to do a similar analysis. In spite of its small size the execution time on the VAX was much longer than the execution time of the SNOBALL program on a UNIVAC. In spite of this I think it is very useful to have a version of LISP that runs on both the PCs and on the VAX. This is especially useful for training purposes. It is also

important to note that XLISP is in the public domain and therefore is FREE.

2) Due to the extreme slowness of XLISP, however, I do recommend that AFHRL obtain a license for CONMMON LISP for the VAX. This will allow for the exchange of software with the quickly growing 'COMMON LISP' world.

3) Parallel processing is very likely to be very influential in ICAI. Parallel processing will be indispensible especially when multimedia ICAI products become available. Not only will a separate processor be essential to control each media device but the coordination of the many devices will compound the information processing problem. As Kurt van Lehn pointed out ICAI tools to enhance cooperative learning are likely to become important. Each participant in any cooperative learning exercise will likely need his/her own processor and these processors will have to interact, thus producing a distributed processing environment.

4) I feel that I have demonstrated that a new approach to the construction of ITS systems can place more of them in use more quickly and that the experience gained from their use can be used to help build more optimal systems in the future. However, more work needs to be done to verify this.

5) A small subset of REDUCE or MACSYMA needs to be developed to solve typical problems in network theory to allow the ITS to do a 'fine grain' analysis of the students work.

REFERENCES

1. Anderson, J. R. and B. J. Reiser, "The LISP Tutor", BYTE, pp. 159-175, April 1985.

2. Betz, D., "XLISP: An Experimental Object Oriented Language", Version 1.4, 1984.

3. Joobbani, R. and Talukdar, S., "An expert system for understanding Expressions from Electric Circuit Analysis", Proceedings of the 9th International Joint Conference on Artificial Intellegence, 18-23 August 1985, Los Angeles, CA.

4. Newell, A., "The Heuristic of George Polya and its Relation to Artificial Intelligence", International Symposium on the Methods of Heuristic, University of Bern, Bern Switzerland, September 1980.

5. Polya, G., HOW TO SOLVE IT, Princeton, New Jersey, Princeton University Press, 1973.

6. Strum, R. D., and J. R. Ward, ELECTRIC CIRCUITS AND NETWORKS Englewood Cliffs, New Jersey, Prentice-Hall, 1985.

7. Woolf, B., "Context Dependent Planning in a Machine Tutor", Dissertation, University of Massachusetts, 1984.

1986 USAF-UES SUMMER FACULTY RESEARCH PROGRAM/

GRADUATE STUDENT SUMMER SUPPORT PROGRAM

Sponsored by the

AIR FORCE OFFICE OF SCIENTIFIC RESEARCH

Conducted by the

Universal Energy Systems, Inc.

FINAL REPORT

Oxidative Stability and Related Studies of Silahydrocarbons

Prepared by:	Harvey L. Paige
Academic Rank:	Associate Professor
Department and:	Department of Chemistry
University:	Alfred University
Research Location:	Air Force Wright Aeronautical Laboratories Materials Laboratory Non-Structural Materials Branch Lubricants and Fluids Group
USAF Researcher:	C. E. Snyder
Date:	September 26, 1986
Contract No:	F49620-85-C-0013

Oxidative Stability and Related Studies of Silahydrocarbons

by

Harvey L. Paige

ABSTRACT

The oxidative stability of a series of seven alkyl tri(octyl)silanes, generically called silahydrocarbons, differing by branching and unsaturation of the five-carbon alkyl group, was studied using differential scanning calorimetry. It was found that there is a reproducible difference between the various compounds. Unsaturated silahydrocarbons are less stable to oxidation at elevated temperatures than are saturated analogs. A normal pentyl group on the silicon results in a slightly more stable compound than various branched isomers.

The mass spectra of the seven silahydrocarbons were studied to determine if fragmentation patterns would provide insight into the mechanism of oxidation. Attempts were also made to isolate intermediates in the oxidation of the silahydrocarbons. These studies are incomplete.

Acknowledgements

I would like to thank the Air Force Systems Command and the Air Force Office of Scientific Research for sponsorship of this work. The Materials Laboratory at Wright-Patterson Air Force Base provided the material and human resources necessary to carry out the work with minimum difficulty. It is not possible to list all the individuals to whom I feel indebted for the warm welcome and working assistance in the Materials Laboratory. I am especially indebted to C. E. Snyder for his suggestions, assistance and thoughtful counsel. Valuable assistance was also provided by L. J. Gschwender of the Materials Laboratory, and G. Fultz, D. E. Miller, and M. A. Stropki, all of the University of Dayton Research Institute.

Special thanks are due my wife, Ruth, and my son, Eugene, and daughter, Eva, for permitting the disruption of normal family life so that I could work in the Materials Laboratory on this project.

I. Introduction

My graduate research at Duke University involved the synthesis and characterization of a number of organosilicon-nitrogen-boron compounds. Included in those studies was some thermal analysis of selected compounds, which work was later continued at the USDA Agricultural Research Service Laboratory in Philadelphia.

The research problem at the Materials Laboratory at Wright-Patterson Air Force Base involved a study of the thermal properties of silahydrocarbons in an oxygen atmosphere by differential scanning calorimetry. The object of this work was to find a rapid method for the assessment of oxidative stabilities of potential silahydrocarbon fluids.

Because of my experience with organosilicon compounds and with thermal analysis, I was assigned to work on the oxidative stability of silahydrocarbons at the Materials Laboratory.

II. Objectives of Research Effort

The Lubricants and Fluids Group is responsible for the evaluation of compounds which may be used as lubricants or hydraulic fluids. The candidate compounds may be submitted by manufacturers or vendors, or they may be synthesized at the Materials Laboratory. In all cases the goal is finding lubricants which have a longer liquid range, lower flammability, and a favorable temperature-viscosity curve, all while functioning in working situations at least as well as currently used materials.

In order to discharge its responsibilities efficiently and reliably, there is a continual evaluation of new technologies for conducting tests. The major portion of my effort was the evaluation of differential scanning calorimetry as a method for assessing the oxidative stability of some model silahydrocarbons.

A secondary goal of my work was obtaining mass spectra of the model compounds and determining whether mass spectral data could be correlated with reactivity with oxygen.

As a consequence of early results, a third objective, identifying intermediates in the oxidation of silahydrocarbons, was included in the project.

III. Oxidative Stability of Silahydrocarbons

A series of silahydrocarbons (alkyl tri(octyl)silanes) synthesized in the Materials Laboratory was studied by differential scanning calorimetry. The compounds and their internal designations were:

$(C_8H_{17})_3Si-R$

ML086-20	R = $CH_2CH_2CH_2CH_2CH_3$
ML086-61	R = $CH_2CH_2CH(CH_3)_2$
ML086-139	R = $CH(CH_3)CH_2CH_2CH_3$
ML086-140	R = $CH{=}CH\ CH_2CH_2CH_3$
ML086-146	R = $CH_2CH_2CH_2CH{=}CH_2$
ML086-162	R = $CH_2CH{=}CH\ CH_2CH_3$
	and $CH_2CH_2CH{=}CH\ CH_3$
ML086-166	R = $CH_2CH(CH_3)CH_2CH_3$

Based on previous work in the laboratory, a sample of ML086-20 was heated from ambient to 300°C at a rate of 10°/min in an atmosphere of 500 psi oxygen. This heating rate resulted in a vigorous oxidation reaction which burned the aluminum sample pan and precluded temperature and energy measurements. Decreasing the rate of heating to 5°/min resulted in a controlled oxidation reaction and quite reproducible temperature and energy measurements. Hereafter this process will be referred to as a temperature scan.

In addition to the temperature scan, previous work had also included measurements under isothermal conditions in an atmosphere of 500 psi oxygen. Exposure to 125° for 5 hours resulted in no measurable reaction, but at 150° a reaction was noted after only 3 hours. If the reaction time was extended to 24 hours, there was no measurable reaction beyond that seen in 5 hours. Consequently, the procedure used was 5 hours at 150° and 500 psi oxygen. This will be referred to as an isothermal run.

Numerous temperature scans were run on the seven model compounds. The DuPont 9900 Thermal Analyzer and associated computer provided information on the onset of reaction and the temperature at which the reaction was the most exothermic. It also provided a record of the operator-selected start and stop points. All of these points are indicated in Fig. 1.

Some of the data from the various runs is summarized in Table 1 and shown graphically in Fig. 2.

Table 1. Temperature of Onset of Oxidation and Energy of Oxidation Reaction

Silahydrocarbon Number	Onset Temperature Celsius	Energy J/g
ML086-20	194 +/- 1	8.5 +/- 1.1
ML086-61	192 +/- 0	7.8 +/- 1.6
ML086-139	188 +/- 1	9.2 +/- 0.6
ML086-140	172 +/- 4	6.7 +/- 3.1
ML086-146	178 +/- 1	118. +/- 0.5
ML086-162	146 +/- 6	10.8 +/- 0.8
ML086-166	190 +/- 1	8.5 +/- 0.3

The dark lines in Fig. 2 represent the mean temperatures and the shaded area spans +/- one standard deviation. These data show that the compounds with saturated C-5 groups oxidize at a higher temperature than those with an unsaturated C-5 group. Within the saturated group, the highest temperature is required for the normal C-5 and the temperature decreases for the branched C-5 as the methyl group is moved from the gamma, to the beta, to the alpha position. Among the unsaturated groups, the highest temperature for the onset of oxidation is for the double bond in the delta position with an only slight decrease for the double bond in the alpha position. The much lower temperature for the onset of oxidation for the double bond in the beta and gamma positions is partly a consequence of the shape of the curve, which is, in turn, partly a consequence of the fact that the sample is a mixture. Fig. 3 is a composite of temperature-energy curves for single samples of the seven compounds. It illustrates the difference between the saturated and unsaturated compounds, as well as the qualitatively different curve in the case of the mixture, ML086-162.

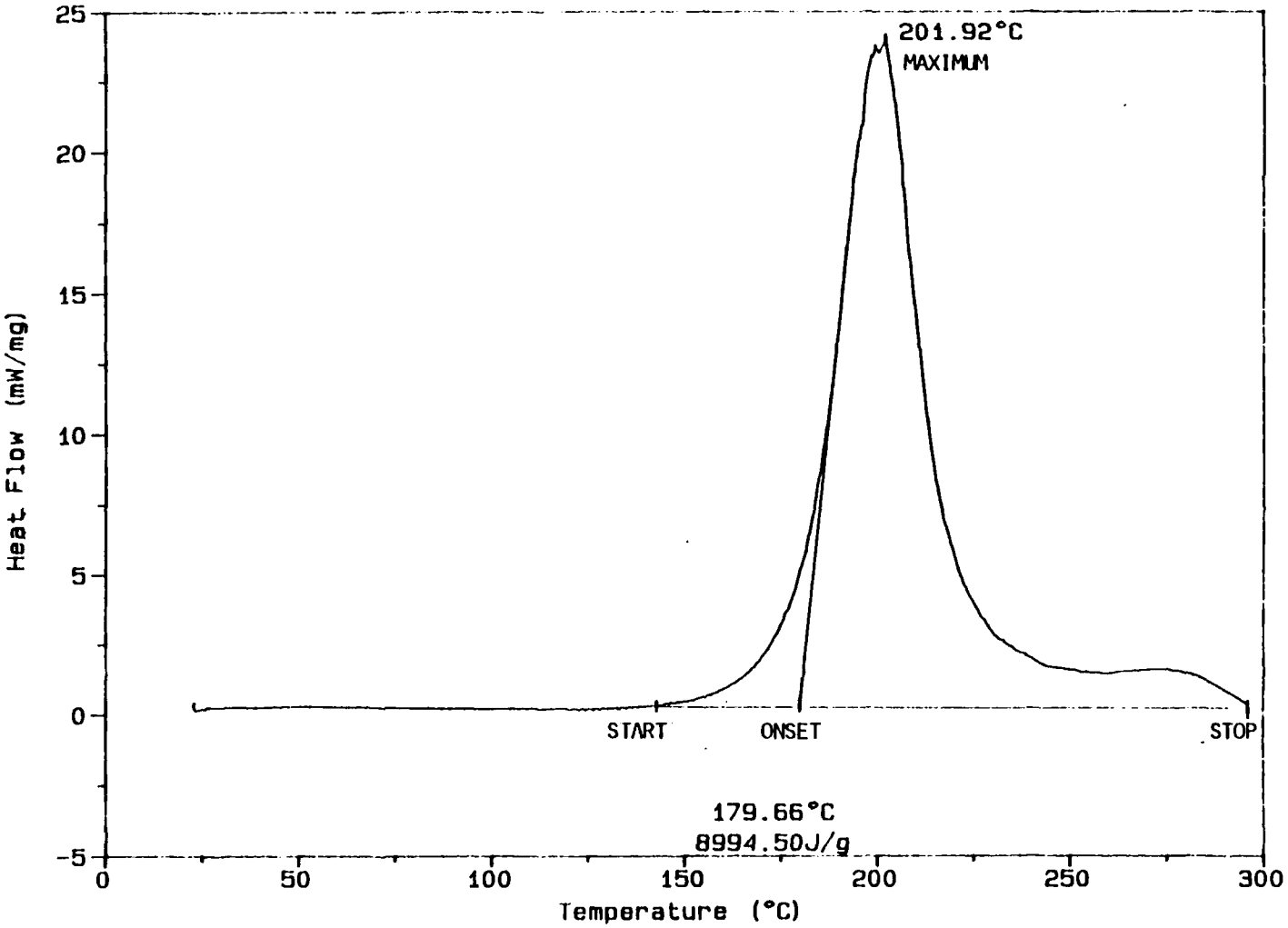

FIGURE 1. ILLUSTRATION OF START, ONSET, MAXIMUM, AND STOP TEMPERATURES

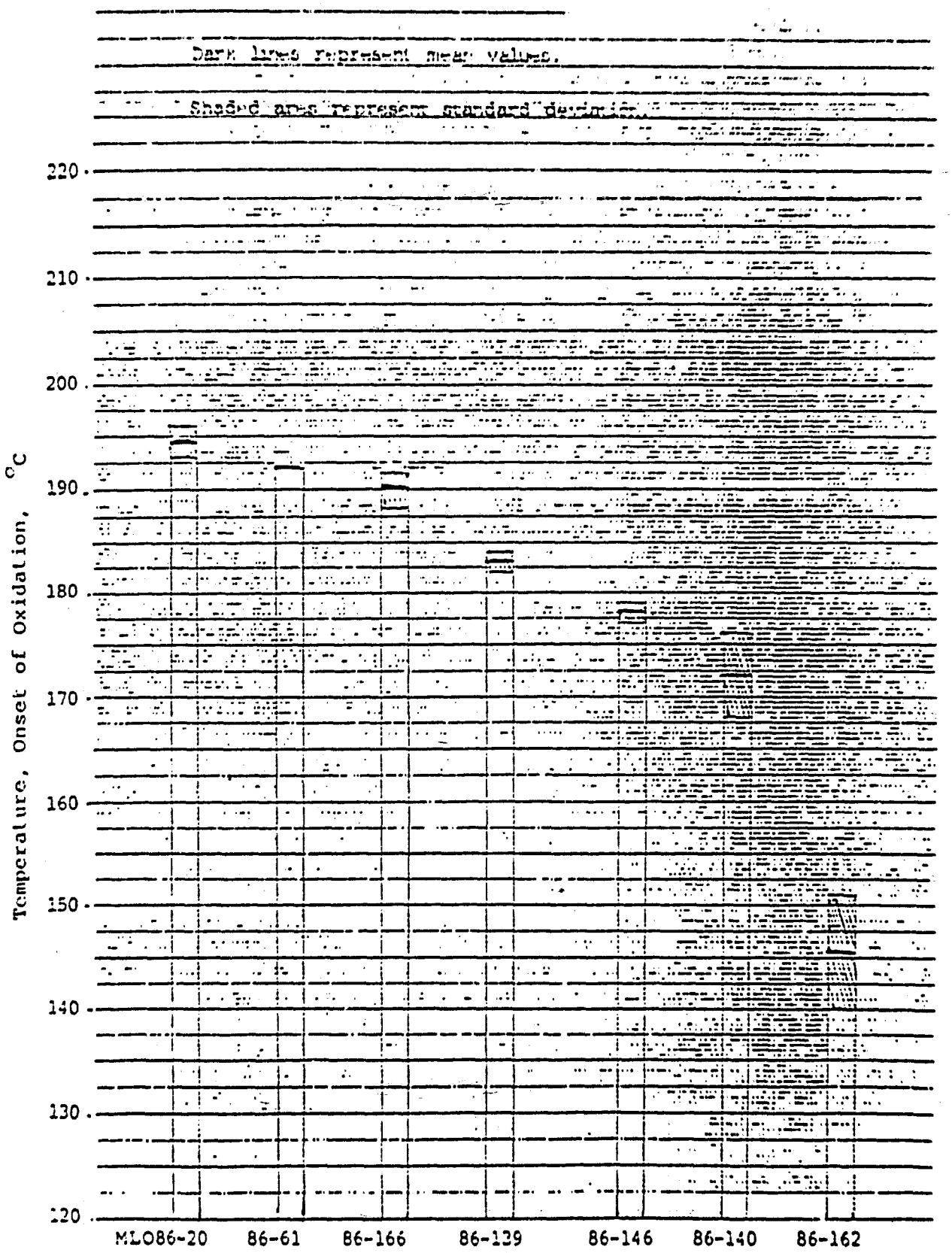

Figure 2. Temperature of Onset of Oxidation of Various Silahydrocarbons

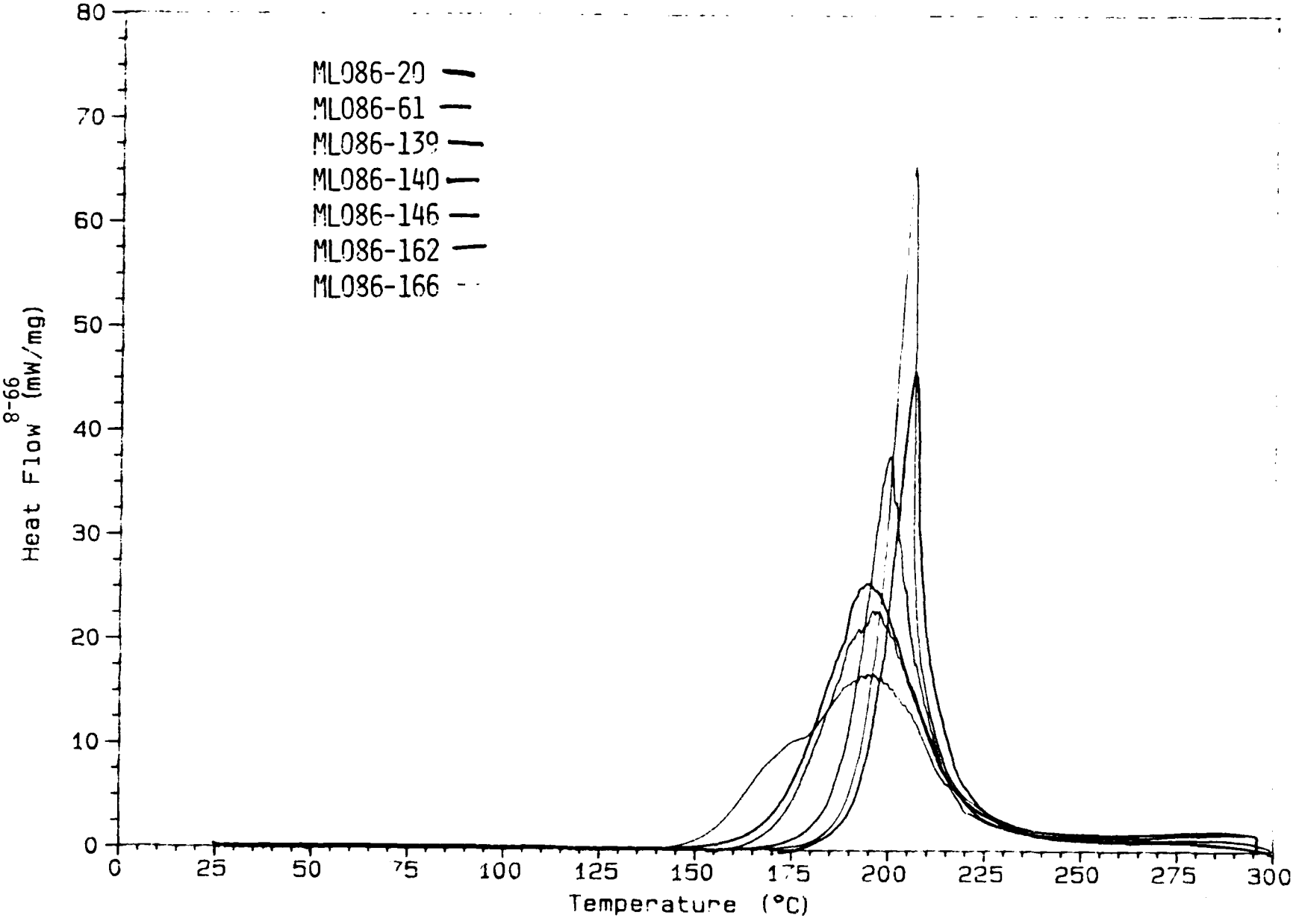
ML086-20
ML086-61
ML086-139
ML086-140
ML086-146
ML086-162
ML086-166
Heat Flow 8-66 (mW/mg)
Temperature (°C)
0
10
20
30
40
50
60
70
80
0
25
50
75
100
125
150
175
200
225
250
275
300

An antioxidant used in lubricating oils, E-702, was added to each of the seven compounds at a concentration of 0.5%. Temperature scans were run on these seven samples. It was found that the saturated compounds all reacted with considerable vigor, so much so that the aluminum sample pans were burned. The unsaturated compounds reacted much less vigorously with only ML086-146, the C-5 group with the delta double bond, showing a sufficiently rapid oxidation to prevent measurement of temperature and energy, and none of the reactions sufficiently vigorous to burn the aluminum sample pan. In all cases, the oxidations occurred at higher temperatures than with the corresponding oil without the antioxidant.

Data in Table 2 were all estimated, due to the inability of the computer to give results for some of the samples with antioxidant. Graphs of the heat flow vs. temperature from which this data is derived are included as an Appendix to the AFWAL/MLBT copy of this report.

Table 2. Temperature of Onset of Oxidation of Silahydrocarbon and Silahydrocarbon with Antioxidant E-702

Silahydrocarbon Number	Onset Temperature Celsius	Onset Temperature with Antioxidant
ML086-20	191	209
ML086-61	192	207
ML086-139	189	208
ML086-140	171	193
ML086-146	178	202
ML086-162	147	166
ML086-166	187	209

It was also found that the time required for the onset of oxidation in an isothermal run was increased by the addition of E-702 antioxidant. The estimated onset temperatures in the isothermal runs are given in Table 3. Due to uncertainty in the net onset time (onset time less the time for the ramp to 150° C.) in four of the samples without antioxidant, maxima in the heat flow-time curves are also given in Table 3. These data were not available for all of the samples with antioxidant because the maximum in the curves appeared beyond the time limit of the experiment.

Table 3. Times of Onset and Maximum Energy Flow for Silahydrocarbons with and without Antioxidant

Silahydrocarbon Number	Silahydrocarbon Onset Minutes	Silahydrocarbon Maximum Minutes	Silahydrocarbon with Antioxidant, Onset Minutes
ML086-20	62	147	258
ML086-61	48	108	221
ML086-139	18	100	138
ML086-140	18	48	108
ML086-146	20	53	150
ML086-162	18	27	28
ML086-166	37	118	194

(times given include time to reach 150°)

Statistical analysis of the data in Tables 2 and 3 is included in the AFWAL/MLBT copy of this report. They show correlations between onset temperatures and the times for reactions to occur at 150°C. These and other results support the idea that differential scanning calorimetry data can be a measure of oxidative stability.

IV. Mass Spectra of Silahydrocarbons

Mass spectra of all seven silahydrocarbons were obtained in the Materials Laboratory as strip chart spectra and from Ultrasystems of Irvine, California as a digital output. In no case was a molecular ion found, in spite of lowering the ionizing voltage. Both formats showed a great similarity among the spectra of the seven compounds. In all cases, the four highest mass peaks with significant intensity represented:

the loss of a C-5 radical (m/e = 367)

the loss of a C-8 radical (m/e = 323 or 325)

the loss of a C-5 radical and a C-8 alkene (m/e = 255)

the loss of a C-8 radical and a C-5 alkene (m/e = 213)

The relative intensities of the 4 peaks in the spectra are given in Figures 4a and 4b. It is noted that there is a wide variation of relative intensities from one compound to the next. The compound with the alpha methyl group, ML086-139, was the only saturated compound to lose the C-5 group in preference to the C-8 group. The other saturated compounds were quite similar (see Figure 4a). In the case of the unsaturated compounds, the situation was quite different in that none of the unsaturated

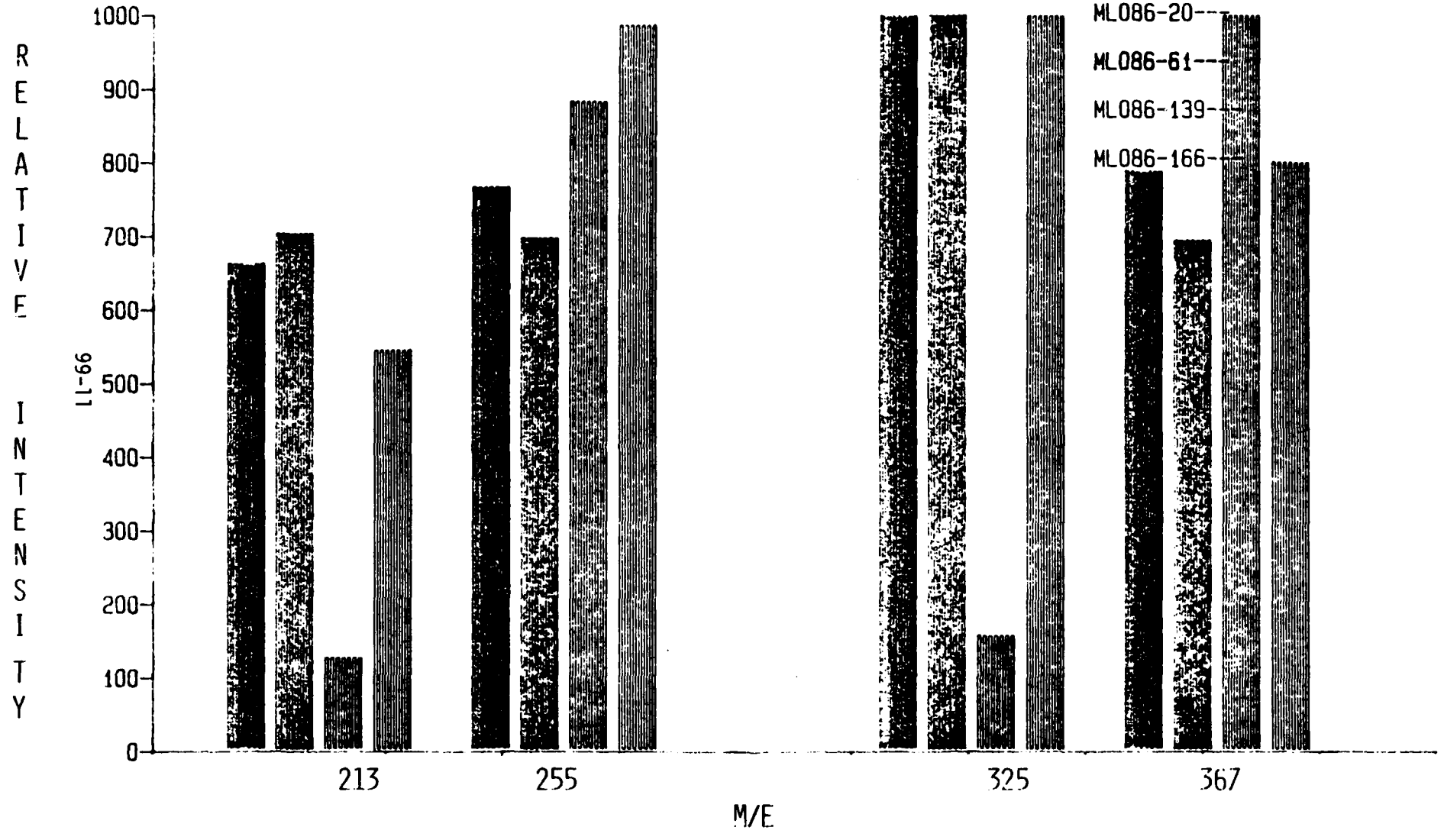

FIGURE 4A. RELATIVE INTENSITIES OF SELECTED PEAKS IN MASS SPECTRUM OF SILAHYDROCARBONS

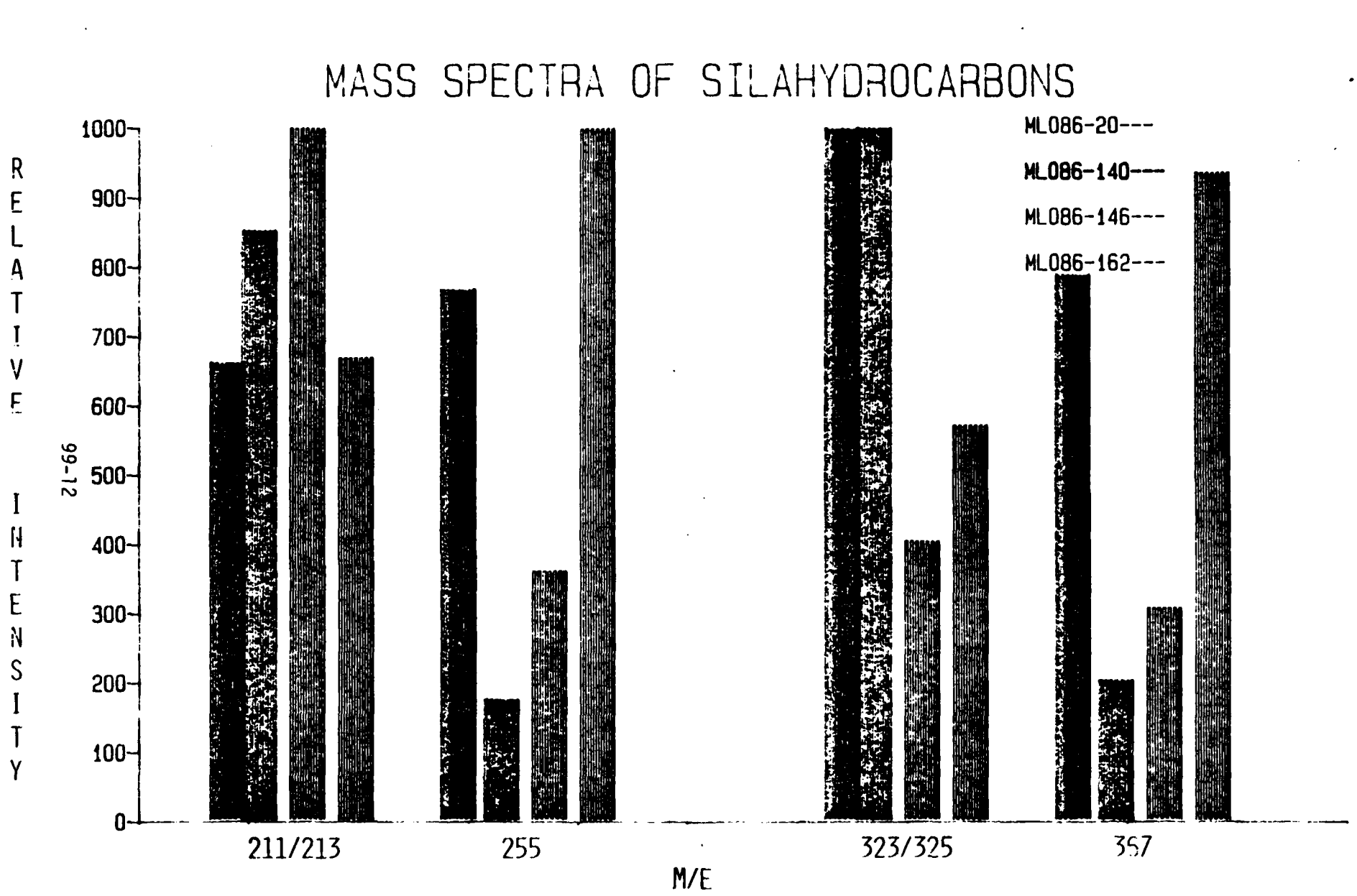

FIGURE 4B. RELATIVE INTENSITIES OF SELECTED PEAKS IN MASS SPECTRUM OF SILAHYDROCARBONS

isomers resembled the saturated straight chain C-5 compound. The mixed beta and gamma unsaturated compounds preferentially lost a C-5, and nearly as often lost C-5 and C-8 fragments. The alpha unsaturated compound tended to lose one or two C-8 fragments. The delta unsaturated compound had a strong tendency to lose two C-8 fragments and a lesser, almost equal tendency to lose a single C-5 or C-8 fragment.

Generally in the mass spectra of silanydrocarbons (tetra(alkyl)silanes) the larger alkyl group is preferentially lost. Such was not always the case in this series of compounds. These results can be rationalized to a point. The loss of the alpha methyl C-5 group of ML086-139 results in a secondary radical, $CH(CH_3)CH_2CH_2CH_3$, which is more stable than the primary radicals resulting when any of the other Si-C bonds are broken. In the case of the beta unsaturated C-5 group, one isomer in ML086-162, breaking the Si-C bond results in an allyl radical, another more stable species. It is possible, but highly speculative, that the alpha unsaturated compound, ML086-140, preferentially loses a C-8 because pi interactions between the double bond and the silicon d-orbitals strengthens that Si-C bond.

Also of interest in the mass spectra of the seven silanydrocarbons is the pattern of metastable peaks. These peaks are a result of ion fragmentation after acceleration, but before completing the path through the magnetic field. Because the relationship between the metastable ion and the parent and daughter ions is known (mass-metastable = mass-daughter^2/mass-parent), the parent and daughter ions can generally be determined.

In the present situation, the schematic representation is as follows:

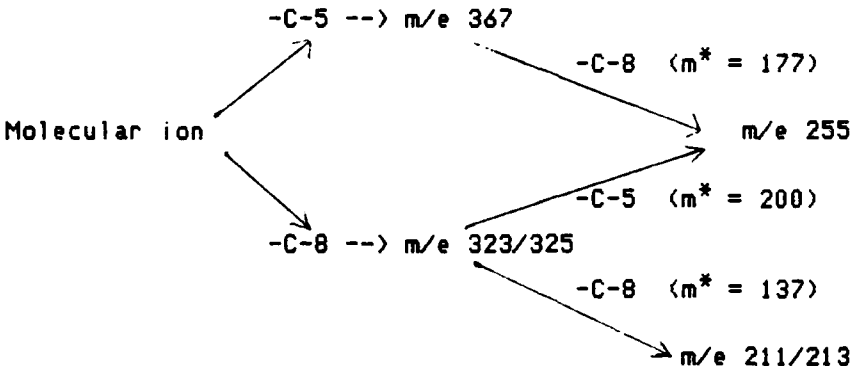

An evaluation of the spectra shows the metastable peaks can be categorized as large (L), medium (M), small (S), and absent (A), as given in Table 5.

Table 5. Metastables in Silahydrocarbon Mass Spectra

Number	~137	~177	~200
ML086-20	M	M	M
ML086-61	S	S	S
ML086-139	A	L	S
ML086-140	S	A	A
ML086-146	L	S	A
ML086-162	S	L	A
ML086-166	S	M	L

Careful consideration of these results supports the conclusions based on the relative intensities of the four highest-mass peaks. The conclusion that the C-5 group of ML086-140 does not easily fragment from the molecule is supported. Likewise, in the the case of ML086-139, the conclusion that C-5 leaves, followed by a C-8, rather than a C-8 followed by C-5 is supported by the relative intensities of the relevant metastable peaks. The only other case where the C-5 fragment seems to be lost first is ML086-162. In this case, the metastable intensities show that the loss of C-5 followed by the loss of C-8 is most likely, the loss of successive C-8's is less likely, and the loss of a C-8 followed by a C-5 is unlikely.

In the above descriptions, the first fragment is lost as a radical and the second as a neutral alkene, thus leaving a hydrogen on silicon. This is seen as the favored process in the fragmentations, particularly when a C-5 leaves ML086-139 or a C-8 is lost from ML086-20, 61, 140, or 166. It is, however, not the exclusive process. The significance of these results remains to be determined.

Complete mass spectral data is attached to the AFWAL/MLBT copy of this report.

V. Intermediates in the Oxidation of Silahydrocarbons

It was recognized early in the project that the isothermal treatment of the silahydrocarbons resulted in only a limited oxidation of the fluid. This was demonstrated by the fact that a temperature scan following isothermal treatment at 150° C, even for 24 hours, still showed a significant exothermic reaction. Attempts to quantify the relative magnitudes of reaction in the isothermal and temperature scan modes were only partially successful, due to the large uncertainty in the computed data.

Some of the liquid or semisolid products of isothermal reactions were analyzed by infrared spectrophotometry. Although there was an indication of a carbonyl band, and possibly an Si-O-Si band, the results were inconclusive. Attempts were made to partially react larger samples of ML086-20 with oxygen in a large pressure reactor. These reactions either gave the starting material back or the silahydrocarbon was oxidized completely to silicon dioxide and, presumably, carbon dioxide and water. A trial with ML086-139, however, appeared to be more useful to the study. The infrared spectrum showed substantial carbonyl and Si-O-Si, plus some OH. The acid number was measured and found to be 38 mg/g. Surprisingly, the differential scanning calorimeter gave a lower onset and maximum temperature during a temperature scan than did an unstressed sample. The gas chromatogram revealed that about 90% of the "product" was starting material, but that there were at least two additional compounds present. An effort to identify the other products by gas chromatography/mass spectrometry is incomplete as of the date of this report.

Records of gas chromatographic and infrared analyses of the product of the partial oxidation are attached to the AFWAL/MLBT copy of this report.

VI. Recommendations

The work described in this report supports the use of differential scanning calorimetry as a screening method for oxidative stability of lubricants and other oils. In order to permit confident routine use, it will be necessary to correlate the results using this method with other measures of oxidative stability. It will also be necessary to demonstrate that the method is applicable to a larger range of base fluids and compounded fluids.

The mass spectrometric results indicate that multiple factors are involved in the fragmentation of the molecular ions and in further fragmentation of the initial fragments. Spectra of additional pure substances should be obtained, particularly one wherein the largest alkyl group has an alpha double bond. In the absence of the double bond, the larger alkyl group should be preferentially lost. If this is not the case, it would support the suggestion that there are pi interactions between the carbon-carbon double bond and the silicon d orbitals.

Much is left to be done on the gentle oxidation of silahydrocarbons and the identification of the oxidation products. Samples of various silahydrocarbons should be treated with oxygen at various temperatures for various lengths of time. It may also be useful to vary the pressure of oxygen. Samples of the gaseous products as well as the liquid products should be analyzed.

References

1. Blaine, R. L., "Thermal Analytical Characterization of Lube Oils and Greases," NLGI Spokesman, June, 1976.

2. Gschwender, L. J., C. E. Snyder, Jr., D. R. Anderson, and G. W. Fultz, "Determination of Storage Stability of Hydraulic Fluids for Use in Missiles," J. Amer. Soc. Lub. Eng. 40 (1984) 659-662.

3. Ihrig, P. J., "Electron Impact Formation of the Phenalenium Cation. Mass Spectral Rearrangements of Organosilanes," Diss. Abstr. Int. B, 30 (1969) 1041.

4. Onopchenko, A., E. T. Sabourin, and D. A. Danner, "Mass Spectra of Some High Molecular Weight Tetra(alkyl)silanes," Org. Mass Spect., 20 (1985) 505-510.

5. Snyder, C. E., Jr., L. J. Gschwender, C. Tamborski, G. J. Chen, and D. R. Anderson, "Synthesis and Characterization of of Silahydrocarbons, a Class of Thermally Stable Wide-Liquid-Range Functional Fluids," ASLE Trans, 25 (1982) 299-308.

6. Tamborski, C., G. J. Chen, D. R. Anderson, and C. E. Snyder, Jr., "Synthesis and Properties of Silahydrocarbons, A Class of Thermally Stable, Wide Liquid Range Fluids" Ind. Eng. Chem. Res. Dev. 22 (1983) 172-178.

1986 USAF-UES SUMMER FACULTY RESEARCH PROGRAM

Sponsored by the

AIR FORCE OFFICE OF SCIENTIFIC RESEARCH

Conducted by the

Universal Energy Systems, Inc.

FINAL REPORT

Cleansing of Bone-Marrow by Lymphokine Activated Killer Cells (LAK-Cells)

Prepared by:	Parsottam J. Patel; DVM, PhD
Academic Rank:	Associate Professor
Department, School and University:	Department of Microbiology School of Medicine Meharry Medical College
Research Location:	Wilford Hall USAF Medical Center Lackland Air Force Base, TX 78236
USAF Research:	Col. Richard N. Boswell
Date:	September 25, 1986
Contract No.:	F49620-85-C-0013

Cleansing of Bone-Marrow by Lymphokine Activated Killer Cells (LAK-Cells)

by

Parsottam J. Patel; DVM, PhD

ABSTRACT

Lymphokine Activated Killer (LAK) cells are targeted lymphocytes that kill tumor cells while not harming normal cells. The purpose of this study was to test the hypothesis that LAK cells from the patient, or allogeneic donor, can be added *in vitro* to bone-marrow to kill the tumor cells and not harm the normal bone-marrow stem cells. LAK cells were generated from normal bone-marrow using the techniques similar to that used for generating LAK cells from normal peripheral blood leucocytes. Whether these LAK cells would be able to lyse tumor cells, without harming the normal stem cells remains to be determined. If successful, this approach could provide the basis for *in vitro* treatment of bone-marrow for autologous transplantation. In other series of experiments, sera from lupus erythematosis and HTLV-III (AIDS) patients were screened for the presence of anticardiolipin antibodies. More than 90% of lupus and about 60% HTLV-III patients showed the presencce of anticardiolipin antibodies of IgG class as detected by ELISA (Enzyme Linked Immunosorbent Assay) test.

ACKNOWLEDGEMENT

Acknowledgement is made of the Air Force Systems Command, the Air Force Office of Scientific Research and Universal Energy Systems for the sponsorship of my research. Project Supervisor was Col. Richard N. Boswell, Dept. of Medicine, Wilford Hall Hospital to whom appreciation is expressed for an exciting and stimulating Summer Research Fellowship. Associate investigators, to whom I am indebted, were Lt. Col. R. Houck, Maj. Gerald L. Messerschmidt, Maj. James M. Thompson, Maj. Richard S. Leff, Maj. Robin Brey, and Lt. Col. Mary Brown. Because of space constrains, many sargents in Bone-marrow Transplantation and HLA-Laboratory have not been named specifically, their courtesy and help were never-the-less greatly appreciated. Dr. T. Boldt, Department of Medicine, University of Texas Health Science Center provided me the opportunity to learn the LAK technology. Kathy Comsack was most courteous and helpful during my experiments at the South-West Foundation. Special thanks are extended to Dr. Bryce Hartman and Dr. Blouse for the considerations and enthusiastic support in the conduct of the Summer Research Fellowship.

I. INTRODUCTION

From the discussions during pre-summer visit it was felt that only one project may not fully occupy the time during the Summer Research Fellowship Program. For this reason, we decided to work simultaneously on two different projects, viz.

(A) Cleansing of bone-marrow by lynphokine activated killer (LAK) cells, and

(B) Screening of sera from patients suffering from lupus erythematosis for antibodies to cardiolipin.

A. Cleansing of Bone-Marrow by LAK Cells

Bone-marrow transplantation is a commonly used treatment to cure patients with disseminated malignancy. Use of patients own marrow (autologous transplantation) is possible if the malignancy does not inolve the marrow space. However, if the marrow is infiltrated by tumor, allogeneic transplantation is required because autologous marrow transplatation cannot be performed without some sort of purging. Allogeneic transplantation is risky in this setting and often fails in patients with solid tumors, Without transplantation all of these patients eventually succumb to their malignancies.

Tumor purging is the process of removing tumor cells from the bone marrow. Several different methods have been

described for this purpose; the methods utilizing monoclonal antibodies being the most common. Eventhough, such an approach can successfully be used to purge marrow, it is very expensive and cumbersome. Chemotherapeutic purging has also been used with some success but it is nonspecific and has a tremendous deletarious effects on normal stem cells.

There is a great deal of interest in recently described LAK cells. The incubation of normal mouse or human lymphocytes in the presence of lymphokine Interleukin-2 (IL-2) results, after several days, in the generation of activated lymphoid (LAK) cells that could lyse fresh, noncultured natural killer (NK) cells resistant primary and metastatic cells but will not harm normal cells (1-4). The lysis of tumor cells could easily be measured in 4-hour chromium release assays. Some of the currently known important properties of LAK cells are listed in Table 1. (See Ref. 4).

Our hypothesis is that LAK cells may be capable of destruction of tumor in the marrow, without harming the normal stem cells. If this is the case, it would than be possible to purge the marrow and perform autologous transplantation in patients with tumor metastatic to bone-marrow. We, therefore, established the following initial goals for the summer research program:

1. To adopt the technique of generating LAK cells from normal peripheral blood leukocytes and bone-marrow cells.

1. To adopt the technique of generating LAK cells from normal peripheral blood leukocytes and bone-marrow cells.

2. To determine the effect of LAK cells on normal bone-marrow stem cells.

3. To determine if LAK cells could be used to successfully eliminate tumor cells deliberately spiked into normal marrow cells.

B. Screening of Sera for Anticardiolipin Antibodies

The purpose of this study was to screen the sera from patients suffering from systematic lupus erythematosis (SLE) for antibodies to cardiolipin employing a recently developed (5) sensitive test that makes use of Enzyme Linked Immunosorbent Antibody (ELISA) technique.

II. EXPERIMENTAL METHOD/APPROACH

A. Generation of LAK Cells. Venous blood was collected into heparinized venoject tubes from healthy adult individuals. The diluted blood samples were subjected to Ficoll-paque (Pharmacia, Sweden) density gradient centrifugation (6) to separate white mononuclear cells (MNC). In the case of bone-marrow cells, frozen bone-marrow samples from normal healthy individuals were quickly thawed in a 37° C waterbath and then subjected to Ficoll-paque

separation. The MNC were washed 3x in Hanks Balanced Salt Solution (HBSS). The final cell pellet was resuspended in a complete RPMI 1640 medium, passed through 200 mesh nylon screen and the cell concentration adjusted to a 1 x 106 cells/ml. The composition of complete culture medium was as follows:

RPMI 1640 Culture Medium		96ml
Normal Human (AB) Serum *		2ml
Gentamycin	50 µg/ml	1ml
Glutamin	200 mM/ml	1ml

* Deactivated for 30 minutes at 56° C temperature

The MNC were cultured in 50 ml aliquots in 250 ml tissue-culture disposable flasks to which recombinant IL-2 (generously donated by the Cetus Corporation) was added at a concentration ranging from 0 to 2,000 units/ml of cell suspensions. The flasks were incubated at 37° C in a humidified Co_2 incubator for a desired length of time. At the end of the incubation period, the cells were harvested by centrifugation, washed 2x in HBSS, counted and the viability determined. The tumoridal activity of these effector (LAK) cells generated was determined in a 4 hr chromium release assay using K-562 target cells as described below.

B. ^{51}Cr Release Assay.

Labelling target cells with ^{51}Cr K-562 target cells actively growing in culture were used as target cells.

A 5 ml suspension of K-562 target cells at a density of 10^6 cells/ml was washed 2x. The final pellet was resuspended in 0.5 ml complete medium to which 200 μCi ^{51}Cr was added. The cell suspension was incubated at 37° C for 1 hour on a rocker. At the end of incubation, cells were washed 3x in complete medium, counted and resuspended at a density of 10^5 cells/ml.

^{51}Cr -labelled K-562 were incubated with effector cells at a desired range of effector: target ratios. Triplicate test combinations were assayed in 200 ml complete medium in round-bottomed 96-well plates. After a brief centrifugation to enhance cell contact, the plates were incubated at 37° C in 5% CO_2 atmosphere for 4 hours. 75 μl aliquots of supernatant was removed from each well and counted for 1 minute in a gamma counter (Packard Instruments, Illinois, USA).

The % specific lysis of K-562 targets was calculated as follows:

$$\% \text{ specific lysis} = \frac{ER - SR}{TR - SR} \times 100$$

where,

ER = mean ^{51}Cr K-562 targets during incubation with effector cells (CPM)

SR = spontaneous release of ^{51}Cr from K-562 targets during incubation in 200 ul CM alone

TR = total release of ^{51}Cr as determined by lysing K-562 target with 0.1 N Hcl

C. Measurement of Anticardiolipin Antibodies By An Enzyme-Linked Immunosorbent Assay (ELISA).

Antibodies to cardiolipin were analyzed according to the method publlished by Loizou et al. (5) as decribed below.

Cardiolipin (27 ul) at a concentration of 49 ug/ml in ethanol was added to flat-bottomed titertek polystyrene plates and coated onto the plate surface by evaporation. Plates were then blocked to prevent non-specific binding of immunoglobulins by the addition of 110 ul of Phosphate Buffered Saline containing 10% Fetal Calf Serum (PBS/FCS) for 2 hr at room temperature. They were then washed four times with 120 ul PBS, soaking for 2 min between each wash. Serum samples (100 ul) diluted 1:100 in PBS/FCS (in triplicate) was added to test wells and 100 ul of PBS/FCS was added to the blank control wells. The plates were incubated for 1 hr at room temperature and washed four times with PBS. First antibody (100 ul) goat antihuman IgG diluted 1:4000 in PBS/FCS was added to each well and the plates were again incubated for 1 hr at room temperature and then washed four times as before. The alkaline

phosphatase-conjugated second antibody (rabbit anti-goat IgG) was diluted 1:1000 in PBS/FCS and 100 µl aliquots were added to each well and incubated for 1 hr at room temperature, after which time the plates were again washed four times with 120 µl/well PBS; p-nitrophenyl phosphate (1mg/ml) was prepared immediately before use in diethanolamine buffer (pH 9.8) and 100 µl aliquots were added to each well and the plates were incubated in the dark at 25° C for 1 hr.

The reaction was stopped by the addition of 3M NaOH (50 µl) to all wells and the optical absorbance of each well was read at 405 nm with a Titertek Multiscan (Flow Laboratories, Irvine, CA).

III. RESULTS

Activation of human peripheral blood lymphocytes with IL-2 to produce LAK has been well documented in the published reports (4). As a first step, I wished to reproduce these results at the Wilford Hall Laboratory. Accordingly, I culutred MNC from normal healthy donors in the presence of 2,000 units recombinant IL-2 per ml of cell suspension for a total period of 4 days. The LAK effector cells so generated were then tested for their tumoricidal activity against ^{51}Cr-labeled K-562 cultured target cells. As can be seen from results presented in Table 1, MNC cultured without IL-2 were ineffective in lysing chromium-labeled K-562 target

cells at a lower Effector:Target cell ratio. Culturing MNC in the presence of IL-2 resulted into generation of activated cells that lysed a significantly high percentage of target cells at E:T ratios ranging from 25 to 75. The percent specific lysis of target cells at E:T ratio of 100 was lower than E:T ratio of 75, indicating that maximal specific lysis was achieved at E:T ratios between 75 and 100.

The next experiment was performed to study the effect of concentration of recombinant IL-2 on cultured MNC to generate LAK and to determine the effect of varying the time the cells are kept in culture. MNC were cultured in the presence of reccombinant IL-2 ranging from 0 - 2,000 units/ml and tested for their tumoricidal activity on day 3 through day 5. Only results obtained on day 4 in culture are presented in Figure 1, as maximum lysis was seen at this particular time point. Once again MNC cultured in the absence of recombinant IL-2 failed to generate any significant level of effector cells. Marginal or no significant differences were observed in the generation of effector cells among cultures activated with 500 - 2,000 units/ml of recombinant IL-2. However, on an average maximum lytic activity was achieved in cultures stimulated with 1000 units/ml of IL-2. Hence, it was decided to use this concentration of IL-2 for all the future experiments.

The next step was to determine if the effector cells could be generated by culturing bone-marrow cells with recombinant IL-2 in a fashion similar to peripheral MNC. Cryopreserved bone-marrow cells were first subjected to Hypaque-ficoll density gradient separation. The separated cells were then cultured either without any addition of IL-2 or in the presence of 1000 units/ml recombinant IL-2. To ascertain the appropriateness of cultural conditions, cultures of peripheral MNC were also set up simultaneously. The tumoricidal activity of effector cells were treated in a standard 4 hour assay on days 3 - 5 of cultures. Results are presented in Table 2. Effector cells from control cultures (without IL-2) showed no significant lytic activities at E:T ratios tested. (Results not shown) considerable effector activity, as indicated by high percent specific lysis, was generated in bone-marrow cultures at days 4 and 5. The levels of which were comparable to those obtained in cultures of peripheral MNC.

The K-562 cell line that was used so far as a target in chromium release assays is sensitive to similar <u>in vitro</u> lysis by natural killer (NK) cells (2, 4). It could be argued that at least part if not all, of the lytic activity seen so far may be attributable to lysis of target cells by NK cells. Eventhough, trivial levels of effector activity in control cell cultures (cultures without added IL-2), in particular at lower E:T ratios argue against this possibility; it does not completely rule out a possible role

for NK cells. Hence, in the next experiment, a new cell line, viz. Daudi, was also used as target cells in addition to the ususal K-562 cells. Daudi is a transformed target cell line that is resistant to lysis by NK cells. Results are presented in Table 3. As can be seen, results obtained with K-562 cell lines were quite reproducible. However, unfortunately the results with Daudi as target cells had many problems. In case of Daudi, the spontaneous chromium release was 2180 cpm (versus 780 cpm in case of K-562) and the total chromium release was 2470 cpm (as compared to 4280 cpm for K-562) making these results of little or no meaning. The main reason for high spontaneous chromium release appeared to be due to the fact that the Daudi cell line was just pulled out from a stock that was in a cryopreserved state over a long period of time, and the cell line was not given enough time to adapt to a continual cultural environment. No further progress was possible with this series of experiments beyond this point for a number of reasons:

(1) The bone-marrow lab in which I was working had to be physically relocated at another location. All the tissue culture equipment (including hoods and incubators) had to be moved and recalibrated.

(2) The Co_2 incubator that I was working with started showing signs of malfunctioning after relocation.

(3) The Daudi cell line was kept in continuous culture, but yet it was not ready to be used as a target cell line when the program ended. One of the reasons being that the Daudi line we obtained was grown in fetal calf serum. For our experiments we had to switch to normal AB human serum as a supplement to grow these cells. This considerably slowed down the growth of Daudi cells in the beginning.

During this program I had the opportunity to work and train two techicians about all different phases of work involved ppin generation and testing the LAK cells. It is hoped that at least some aspect of this work will be continued at the Wilford Hall Laboratory.

Testing Of Sera For The Presence Of Anticardiolipin Antibody

Control sera were obtained from 80 healthy subjects and tested for anticardiolipin antibodies of IgG class. The optical absorbance (OA) at 405 nm, value obtained was 11.5 ± 0.28 (mean ± S.E.M.). The blank value, estimated in triplicate on each plate, was obtained by identical treatment of wells using 100 µl PBS-FCS, in place of serum. The average blank value obtained was 0.06 for all the determinations made.

Sera from 80 patients suffering from lupus erythematosis and 60 patients suffering from HTLV-III infections (AIDS patients) were screened for anticardiolipin antibodies of

IgG class. The results were calculated and expressed in terms of Binding Index, as calculated:

$$BI = \frac{OA\ (Test\ Sample) - O\ A\ (Blank)}{OA\ (Control\ Sera) - OA\ (Blank)}$$

A BI value of greater than 3 was considered as a positive reaction. Based on these criteria, more tha 90% of lupus patients and approximately 60% of HTLV-III patients were found positive for the anticardiolipin antibodies.

During this investigative part I had the opportunity to work with two staff physicians at Wilford Hall Hospital: Dr. Robin Brey of the Neurology Department and Dr. R. Houk, Chief, Rheumatology/Immunology Services. This technique has been adopted for future investigational use at Wilford Hall Hospital Laboratory and we also hope to have a publication from the results obtained so far.

Recommendations

It is evident, from the results presented, that LAK cells could be successfully generated from bone-marrow using an experimental approach similar to that published for peripheral blood leucocytes. Much work, however, remains to be done. Optimal cultural conditions in terms of length of incubation, concentration of IL-2, number of bone-marrow cells to be cultured must be established before any further

experiments are done. Also one needs to compare results between the cultures of whole bone-marrow versus Ficoll-hypaque separated bone-marrow cells. Once this is done, experiments should be performed to determine the effects of LAK cells on normal bone-marrow stem cells. Based on our knowledge about LAK cells, it could be predicted that LAK cells should have no harmful effect on normal bone-marrow stem cells, however, this remains to be established. If this turns out to be the case, then the experiments should be performed in which bone-marrow is spiked with a known number of transformed cells, and the ability of LAK cells to successfully eliminate these transformed cells investigated. If successful, these studies could form a basis for the in vitro treatment of patients bone-marrow for autologous transportation.

All the serum samples from lupus erythematosis and HTLV-III patients available at the time at Wilford Hall Hospital were completed for testing of anticardiolipin antibody of IgG class. Similar studies need to be done to determine the presence of anticardiolipin antibodies of other Ig classes, in particular IgM and IgA, in these patients and then an attepmt should be made to establish relationships among anticardiolipin antibody and other clinical conditions. The finding that of all the HTLV-III patients tested, approximately 60% were found positive for the presence of anticardiolipin antibody appears to be of significant clinical interest. These studies should be continued, and

the relationship between anticardiolipin antibodies with other clinical features of the disease be established. This could potentially be useful in better management and treatment of the disease.

REFERENCES

1. Yvon, I., T.A. Wood, P. Spiess, and S.A. Rossenberg. "In Vitro growth of murine T-cells. The isolation and growth of lymphoid cells infiltrating syngeneic solid tumors." J. Immunol. 125: 238-245, 1980.

2. Rosenstein, M., I. Yvon, Y. Kaufman and S. A. Rosenberg. "Lymphokine activated killer cells: lysis of fresh syngeneic NK-resistant murine tumor cells by lymphocytess cultured in Interleukin-2." Cancer Res. 44: 1946-1953, 1984.

3. Laffreniere, R. and S. A. Rosenberg. "Successful immunotherapy of murine experimental hepatic metastases with lymphokine activated killer cells and recombinant interleukin-2." Cancer Res. 45: 3735-3741, 1985.

4. DeVita, V. T., S. Hellman, and S. A. Rosenberg. "Adoptive immunotherapy of cancer using lymphokine activated killer cells and recombinant interleukin-2." Imp. Adv. Oncol. 9: 55-81, 1986.

5. Loizou, S., J. D. McCrea, A. C. Rudge, R. Reynolds, C. C. Boyle and E. N. Harris. "Measurement of anticardiolipin antibodies by an enzyme-linked immunosorbent assay (ELISA): standardization and quantitation of results." Clin. Exp. Immunol. 62: 738-745, 1985.

6. Boyum, A. "Isolation of mononuclear cells and granulocytes from human blood." Scand. J. Clin. Lab. Invest. 21 suppl. 97: 77-89, 1968.

TABLE 1

Characteristics of Murine Lymphokine Activated Killer (LAK) Cells

1. LAK cells are generated by incubation in interleukin-2 (IL-2).

2. Peak lysis is observed between 3 and 6 days after onset of incubation in IL-2.

3. Fresh, noncultured, NK-resistant primary and metastatic tumor cells are lysed but not normal cells.

4. Syngeneic, allogeneic, and xenogeneic tumor cells are lysed. (Murine LAK lyse human tumors, and vice versa.)

5. Frequency of LAK precursor lymphocyte is about 1:5000 splenocytes as measured in limiting dilution assays.

6. Precursor of the LAK cell is a non-B, non-T lymphocyte (Thy-1 negative, Ia negative, surface Ig negative ; thus is a "null" lymphocyte).

7. Precursor LAK lymphocyte bears asialo-GM1 antigen.

8. LAK effector cell (resulting from incubation in IL-2) is Thy-1. Thus LAK cells are probably "primitive" cells in the T-lymphocyte lineage.

9. LAK cells bear cytolysin granules. Lysis can be inhibited by anti-LFA-1 monoclonal antibody and is partially inhibited by anti-Lyt-2 antibody.

TABLE 2

Generation Of LAK From Normal Human Peripheral Mononuclear Cells.

Effector: Target (K-562 Cells) Ratio	% Specific Lysis	
	Control Cells*	IL-2 Activated Cells*
25	7	32
50	18	55
75	32	89
100	54	54

* MNC were cultured for 4 days either in the presence of 2000 units of recombinant IL-2/ml (IL-2 activated cells) or without any addition of IL-2 (control cells).

TABLE 3

Generation Of LAK From Bone-Marrow Cells.

Source of Cells Cultured*	E:T Ratio (K-562)	% Specific Lysis Day 3	Day 4	Day 5
	20	12	42	40
Peripheral Blood	40	18	58	62
	80	43	82	84
	20	32	52	50
Bone-Marrow	40	48	74	72
	80	61	76	82

* Peripheral Blood MNC or Bone-Marrow cells were cultured for the number of days indicated in the presence of 1000 units IL-2/ml.

TABLE 4

Generation Of LAK Cells From Bone-Marrow Cells **

	% Specific Lysis			
	K-562 Target Cells		Daudi Target Cells	
E:T Ratio	Control *	IL-2 Activated	Control*	IL-2 Activated
20	18	53	42	62
40	20	69	69	62
80	42	92	73	52

* No IL-2

** Bone-marrow cells were cultured without IL-2 (control cells) or in the presence of 1000 units/ml IL-2 for a period of four days. The effector LAK cells so generated were assayed for their tunoricidal activity using ^{51}Cr-labeled K-562 or Daudi cell lines.

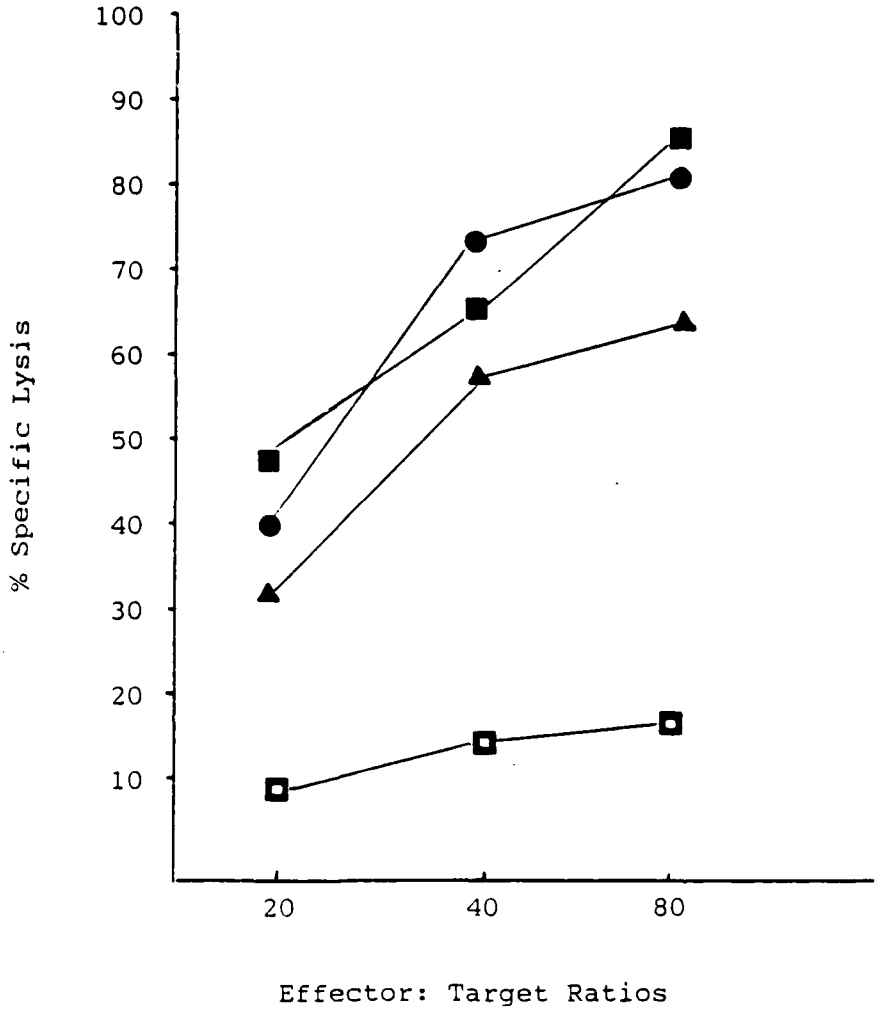

Figure 1. Dose Response Analysis Of IL-2 On Generation Of LAK Cells.

MNC obtained from peripheral blood cells were cultured without (□——□) IL-2 or in the presence of 500 units/ml IL-2 (▲——▲); 1000 units/ml IL-2 (■——■) or 2000 units/ml of IL-2 (●——●) for a period of 4 days. The tumoricidal activity of effector cells so generated was determined at E:T ratios indicated using ^{51}Cr labeled K-562 target cells.

1986 USAF-UES SUMMER FACULTY RESEARCH PROGRAM/

GRADUATE STUDENT SUMMER SUPPORT PROGRAM

Sponsored by the

AIR FORCE OFFICE OF SCIENTIFIC RESEARCH

Conducted by the

Universal Energy Systems, Inc.

FINAL REPORT

All Aromatic Rod-Like Polymers Based on Intramolecular Cycloadditions: Model Compound Study

Prepared by: Robert A. Patsiga

Academic Rank: Professor

Department and University: Chemistry, Indiana University of Pennsylvania

Research Location: Materials Laboratory, Polymer Branch AFWAL/MLBP

USAF Researcher: Dr. Fred E. Arnold

Date: August 26, 1986

Contract No. F49620 85-C-0013

All-Aromatic Rod-Like Polymers Based on Intramolecular Cycloadditions: Model Compound Study

by

Robert A. Patsiga

ABSTRACT

Attempts were made to prepare three aryl-substituted diene-yne compounds. These compounds were to serve as model structures for study of cyclization-aromatization ability which could be extended to curing of thermally stable polymers. A precursor ketone, 1,3-diphenyl-1-propynone, and its hydrobrominated product were prepared. However, an attempt to perform a Wittig reaction on the bromoketone resulted in dehydrobromination. Another precursor ketone, vinylphenyl ketone, underwent polymerization when an attempt was made to perform a Wittig reaction on it. Coupling of trimethylsilyl acetylene with benzoylchloride and condensing lithium acetylide with benzaldehyde were unsuccessful in producing 1-phenyl-1-propynone. Recommendation is made that aldehyde structures be utilized in the syntheses because of their greater disposition to undergo the Wittig reaction.

Acknowledgments

I wish to express my gratitude to the Air Force Systems Command of the Air Force Office of Scientific Research for sponsoring my research. The summer research opportunity was worthwhile for me and I hope my contribution to the totally-aromatic polymer project will be of value. I wish to thank my immediate supervisor, Dr. Fred Arnold as well as fellow researchers, Dr. Loon-Seng Tan and Bruce Reinhardt for helpful guidance. Also I extend my appreciation to Dr. Richard VanDuesen, Polymer Branch Chief for providing and overseeing a smooth operating structure within which it was a pleasure to work.

I. Introduction

Robert A. Patsiga received the Ph.D. degree from the State University of New York College of Environmental Science and Forestry. Following the graduate degree he had two years of experience in industry and one year of post doctoral research. All of these experiences were in the area of polymer synthesis. During the next twenty years in college and university teaching he continued research in emulsion polymerization and block copolymer synthesis. In 1983-84 he spent a sabbatical leave at Virginia Polytechnic Institute and State University where he carried out research in isocyanate-epoxy polymers.

The Materials Laboratory at Wright-Patterson Air Force Base has been engaged for several years in the synthesis of new, thermally stable polymers. Dr. Patsiga's background in polymer synthesis was considered to be complimentary to this project.

Totally aromatic or heterocyclic aromatic units have proven to be reliable building blocks in thermally stable polymers. From a theoretical and practical point of view, the preparation of linear polymers composed of phenylene rings, I, as repeating units are an ideal objective in this field.

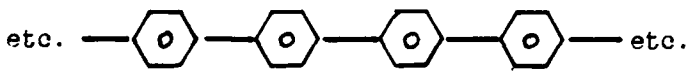

I

Unfortunately, in the past a number of difficulties have been encountered in attempts to prepare polyphenylenes. Often crosslinked (and therefore insoluble) material accompanied synthetic attempts. Also some polymerization methods resulted in

incorporation of undesirable units (for example, N=N-) along the backbone of the polymer chain. Previous syntheses of the polyphenylene structure have also been impeded by the low solubility of high molecular weight material. Thus, there is a need for a polymeric system which can remain soluble or meltable at high molecular weight and can be "cured" to give a totally aromatic polyphenylene structure. Further requirements are that the curing process should not result in the formation of volatile by-products and no additional reagents or catalysts (residues of which may later adversely effect polymer properties) should be used.

One approach to the problem of polyphenylene synthesis that has been taken at the Air Force Materials Laboratory is the attempted preparation of certain conjugated alkene-alkyne systems which can undergo intramolecular cyclization to give an aromatic structure.

II. Objective of the Research Effort

The overall objective of the all-aromatic polymer project was to prepare diene-yne model compounds which could be studied for their cyclizing ability. Specifically, attempts were made to prepare compounds II, III, and IV. It is hoped that these compounds will cyclize to form the aromatic structures indicated in the equations.

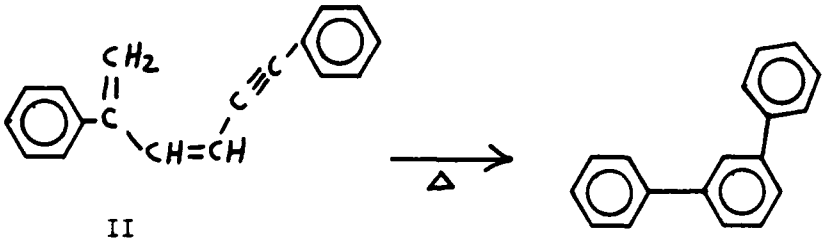

II

Eq. 1

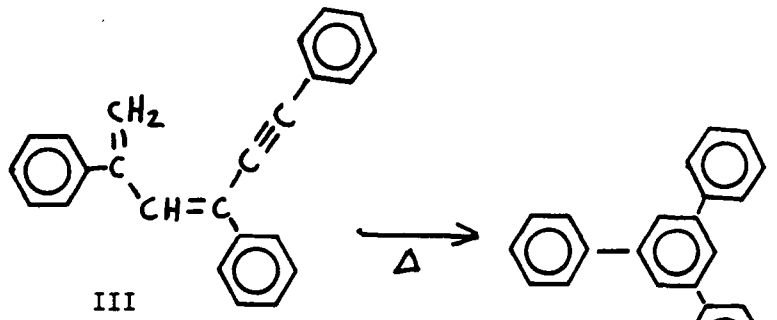

III

Eq. 2

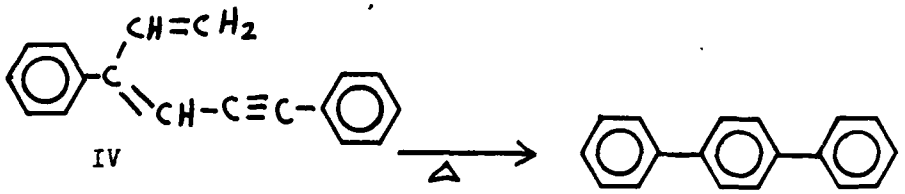

IV

Eq. 3

Compounds II, III, and IV are model structures which would represent the repeating unit in a precursor polymer. Structure IV would give rise to a para-polyphenylene, while II and III would lead to a meta configuration in the polymer.

The steps planned for the synthesis of compounds II-IV are shown in Scheme 1 and 2.

III. Attempted Synthesis of 1,5-Diphenyl-3,5-hexadien-1-yne (Compound II)

The success achieved in coupling an acid chloride with a monosubstituted acetylene (see section IV) prompted an investigation into the preparation of the silylated ketone VII in Scheme 1. The value of this ketone is due to its easy conversion to the free terminal acetylene IX.

The procedure of Tohda, et al. (1) was followed; with certain variations in procedure also explored in some trials.

Scheme I

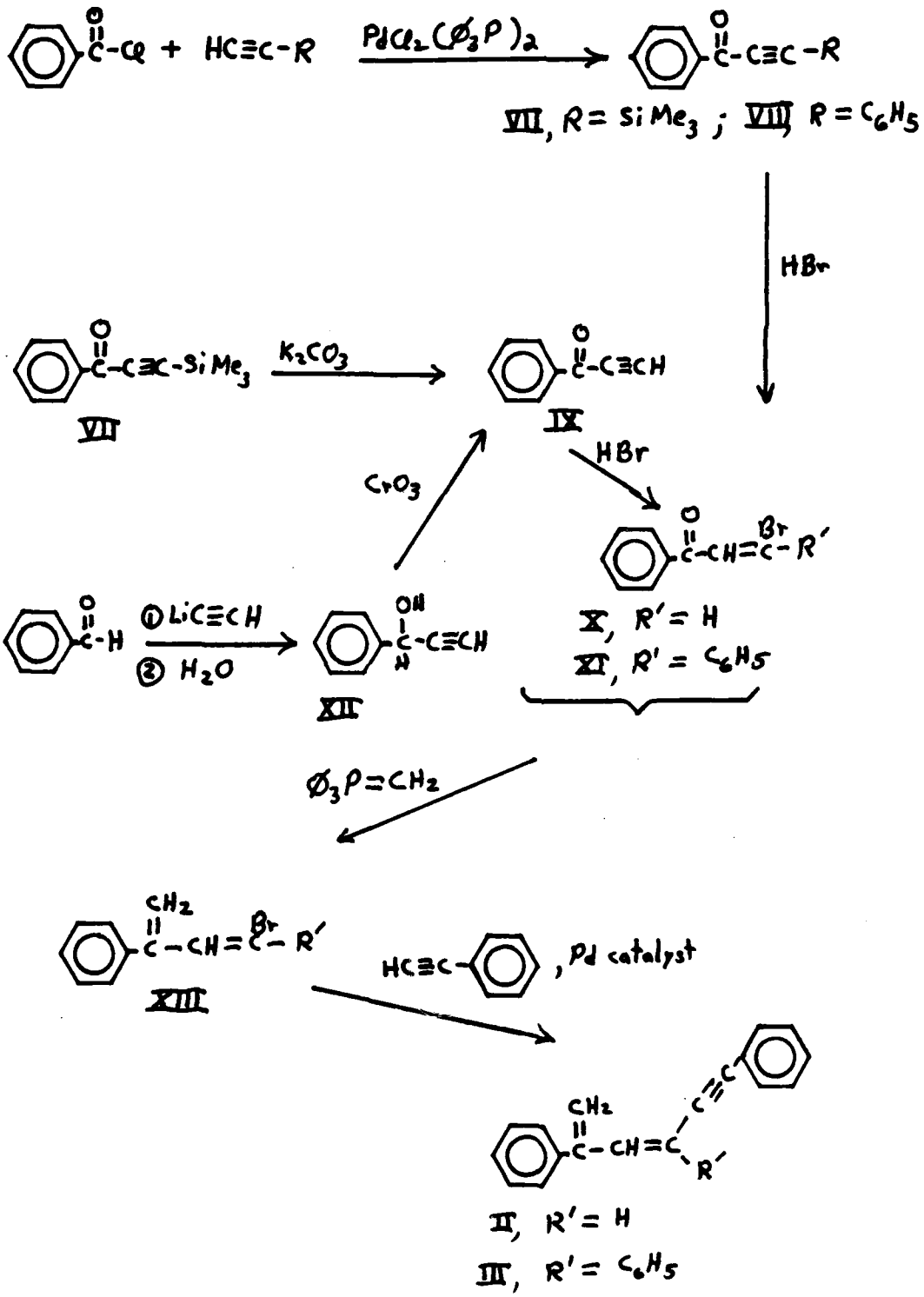
PdCl2(Ø3P)2
VII, R = SiMe3 ; VIII R = C6H5
HBr
K2CO3
VII
IX
HBr
CrO3
X, R' = H
XI, R' = C6H5
① LiC≡CH
② H2O
XII
Ø3P=CH2
XIII
HC≡C-
, Pd catalyst
II, R' = H
III, R' = C6H5

Scheme 2

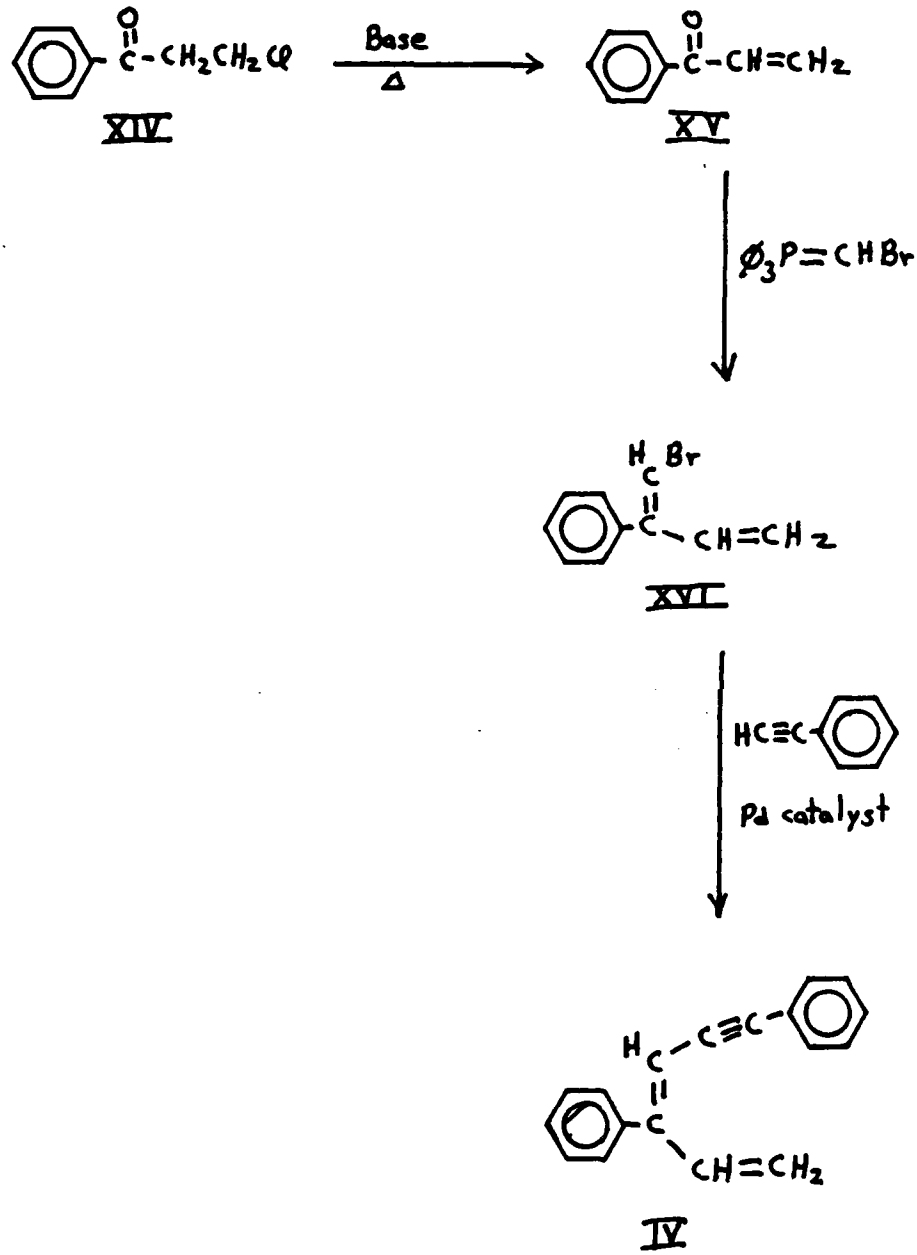

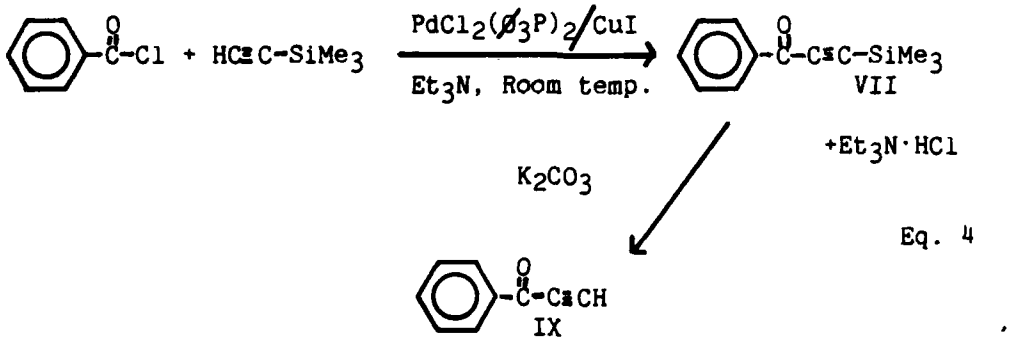

Eq. 4

Four attempts were made on a 0.05 mole scale. These are summarized as follows:

Trial*	Procedure	Results
1-8	Procedure of Tohda, et al. followed except rxn mixture chromatographed without filtration of $Et_3N \cdot HCl$. Vac. dist. liquid.	Middle cut at 0.3mm, 83-90° gave 2.16g clear, colorless liquid. GC-Mass spec. indicates Ø CO-C≡CSiMe$_3$ plus two two other components. %C=71.24, %H=6.89. Calc.=71.28, 6.93.
1-5	As above except $Et_3N \cdot HCl$ filtered from rxn. mixture (106% recovered). Col. chrom. then vac. dist.	Upon exposure to air the mixture slowly darkens and tar-like solid precipitates. Only a few drops liq. could be collected from dist.
1-8	Acid chloride in Et_3N added slowly to HC≡CSiMe$_3$/ catalyst/Et_3N. Filtration (111% $Et_3N \cdot HCl$), Col. chrom., vac. dist.	Upon exposure to air the mixture slowly darkens and tar-like solid precipitates. Only a few drops liq. could be collected from dist.
1-26	HC≡CSiMe$_3$ added (syringe) slowly to Ø COCl/catalyst/ Et_3N. Filtration (105% $Et_3N \cdot HCl$).	Filtrate again turns dark with tar even in refrigerator at 8°.

Except for the first trial in which approximately thirty percent yield was achieved, this synthetic route proved to be difficult and nearly fruitless. The one successful trial gave material whose spectral and elemental analyses agreed closely with expected values. However, GC suggested the presence of some

impurity (two other components) and the material appeared to be unstable. This was indicated by the gradual darkening from a clear, colorless liquid to dark amber brown over a few days. A tar-like deposit also formed. Logue and Moore (2) do not mention that ketone VII should be unstable. However, they do describe darkening and precipitate formation from solutions of the cuprous acetylide, CuC $CSiMe_3$. Thus, although our procedure is somewhat different from that of Logue and Moore, this same cuprous acetylide may be forming and for some reason not coupling with the acid chloride.

An alternate route to ketone IX (Scheme 1) was attempted. This approach involved the condensation of lithium acetylide with benzaldehyde, followed by oxidation of the product alcohol, XII. These steps were used by

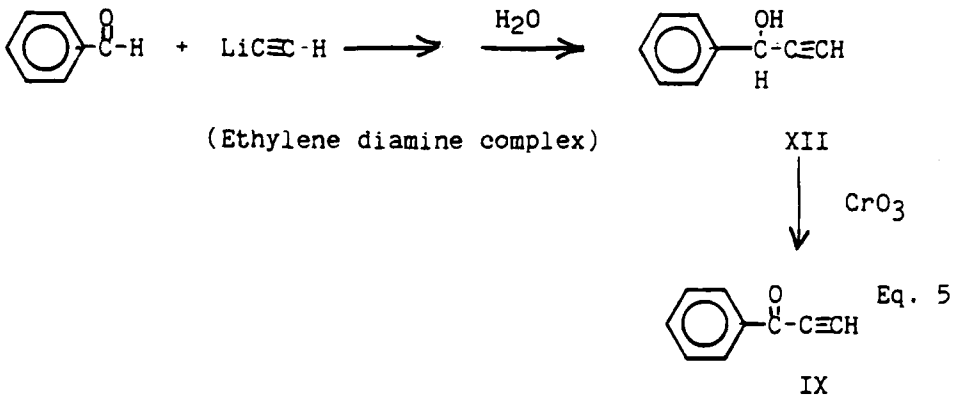

Harris and Belty (3) to prepare bis-acetylenic ketones. However, they prepared the lithium acetylide <u>in situ</u> by reaction of acetylene with butyllithium. Our approach was to use the solid, commercially available ethylene diamine complex of lithium acetylide. This has been shown (4) to give high yields of ethynyl carbinols with ketones.

The procedure of Harris and Belty was followed (0.3 mole scale) except for the use of the solid acetylide-ethylene diamine complex. No product corresponding to alcohol XII could be isolated (Properties: see ref. 5 and 6). Upon concentration of the ether extracts of the reaction mixture, there was obtained by filtration a series of solids (three could be distinguished) melting from 122° to 240°. The highest melting solid (about 1/5 of the isolated mass) contained 72.5% carbon, 6.73% hydrogen, and surprisingly, 8.9% nitrogen. Vacuum distillation of the filtrate (amounting to about 50% of the isolated mass) gave benzaldehyde (5%), benzyl alcohol (12%-IR and NMR match) and an unknown liquid residue. The proton NMR of this liquid showed absorptions at 10.05 δ (sing.), 8.4 δ (sing.), 8-7 δ (mult.), 5.3 δ (weak sing.), 4.0 δ (strong sing.). The mass spectrum gave a parent peak mass at 133 amn with fragments suggesting the presence of nitrogen.

Thus, except for the isolation of benzyl alcohol and unreacted benzaldehyde, the major products of this reaction could not be identified. The presence of nitrogen in the product materials indicates that the ethylene diamine is somehow participating in the reaction. This rules against the use of this acetylide complex in condensation with aldehydes.

IV. Attempted Synthesis of 1,3,5-Triphenyl-3,5-hexadien-i-yne (Compound III)

The first step in the sequence (Scheme 1) is the preparation of ketone VIII. The method of Tohda, et al. (1) was used to couple benzoyl chloride with phenyl acetylene. The reaction is

catalyzed by a combination of cuprous iodide and $PdCl_2[(C_6H_5)_3P]_2$ in amounts on the order of 0.1 mole percent. Enough triethyl amine is used to

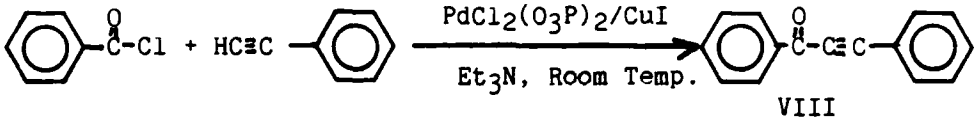

VIII

$+Et_3N \cdot HCl$ Eq. 5

act as a solvent as well as to neutralize the HCl produced. About twelve percent solids were used in the initial reaction mixture.

When the catalyst combination was added to the acid chloride-alkyne solution a fourteen degree exotherm was observed (0.15 mole scale). The mixture was allowed to stir overnight at room temperature under a blanket of nitrogen. The reaction mixture was then quenched with methanol and then concentrated by heat and vacuum. The residue was then treated with water-cyclohexane and the water layer discarded. The cyclohexane solution was dried, again concentrated, and the residue was chromatographed on a silica gel column using cyclohexane.

Two trials gave yields of 37 and 70 percent. There appeared to be considerable loss of material on the silica gel column. Improvements could easily be made in this part of the procedure. The product melts at 42-45° (Lit.: 49-50°). The IR and NMR spectra agree with the structure for 1,3-diphenylpropynone (VIII). [IR: 3000-3100 cm^{-1} (aryl C-H); 2211 cm^{-1} (C≡C); 1725 cm^{-1} (C=O); NMR: medium multiplet at 8.3 δ; strong multiplet at 7.7 δ]. Mass

spectral analysis gave a parent peak of 206 amu as expected for ketone, VIII.

The next step in the sequence was addition of HBr across the triple bond of ketone, VIII to form the bromo-ketone, XI. Grob and Cseh (7) used HBr in various

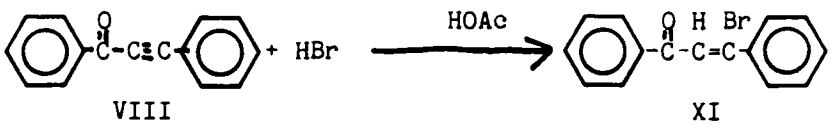

VIII XI Eq. 6

forms in reaction with aryl acetylenes (HBr/HOAc, HBr/DMF, $HBr/CHCl_3$ and gaseous HBr). Adams and Theobald (8) bubbled dry HBr through an acetic acid solution of aryl propiolic acids to prepare β-bromo-β-phenylacrylic acids. For the present work, commercial, 30% HBr in acetic acid was used.

The most successful procedure was to dilute the ketone with 2/1 (v/v) $CHCl_3$/HOAc to give a 25% solids solution. The stirred solution (N_2 blanket) was cooled to -20° and one equivalent of HBr/HOAc solution was added (5-10 min.) by syringe. The mixture was allowed to warm to room temperature over a two hour period. The reaction mixture was then poured into ice water, washed with 2% $NaHCO_3$ and ultimately the organic residue was chromatographed (silica gel-CH_2Cl_2/cyclohexane, 50/50). Evaporation of solvent gave 84% yield of product having: 62.69% C, 3.90% H, 27.29% Br (Calcd.: 62.74% C, 3.86% H, 27.83% Br). The mass spectrum gave doublet parent peaks at 286 and 288 amu as expected for the bromoketone XI. Gas chromatography showed two peaks in a ratio of about 2:1 (the larger peak having the longer retention time).

This is no doubt due to the two geometric isomers possible for XI.

In spite of it being an isomer mixture, it was decided to perform a Wittig reaction on XI in order to prepare the bromo-diene, XIII.

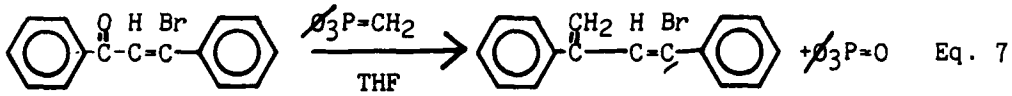

XI XIII Eq. 7

The ketone was added to the ylide at -78° (N_2 blanket) and the mixture was allowed to stir and reach room temperature overnight. This was followed by warming at 60° for two hours. Filtration followed by concentration of the filtrate gave a red oil whose NMR and IR spectra matched that for ketone, VIII. This was corroborated by the mass spectrum which gave a molecular ion mass of 206 amu.

Thus, it appears that the alkylidene phosphorane (ylide) is sufficiently basic to cause dehydrobromination. Future syntheses are likely to require carrying out the Wittig prior to addition of HBr across the triple bond.

V. Attempted Synthesis of 1,4-Diphenyl-3,5-hexadien-1-yne (Compound IV)

As indicated in Scheme 2, the first step in the synthetic sequence was the preparation of vinylphenyl ketone, XV. This ketone is unstable in that it readily polymerizes. Therefore, vinylphenyl ketone must be prepared the same day it is to be used in the Wittig synthesis of the bromodiene, XVI. The most satisfactory procedure was found to be the dehydrochlorination of

β-chloropropiophenone in the molten state using potassium carbonate as base. A small amount (ten mole percent) of

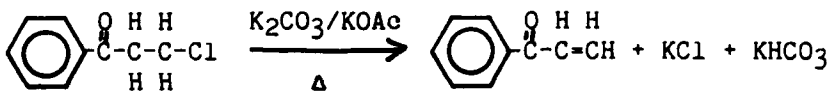

Eq. 8

potassium acetate was also added as a base which may have greater solubility in the molten ketone. However, it is quite likely that this is not necessary (a thorough study to optimize this reaction was not made).

The procedure involved heating the dry reactants in a short path distillation apparatus. The distilled vinylphenyl ketone was collected and stored at 0°. Distillation occurred at 75-77°, 1.5 mm Hg pressure. A 68% yield was obtained on a 0.1 mole scale reaction. The NMR spectrum of the distillate showed multiplets at 8.05 δ and 7.6 δ, a series of four dublets at δ 6.6, 6.3, 6.0 and 5.8 and three singlets at δ 7.3, 7.2, and 7.0. The IR spectrum showed the expected absorptions at 3058 cm^{-1} (sp^2 CH), 1674 cm^{-1} (C=O), and 1000-990 cm^{-1} ($=CH_2$).

For use in the Wittig reaction, the bromoalkylidene phosphorane, $\not{\phi}_3P{=}CHBr$ was prepared according to the procedure of Wolinsky and Erickson (9). The Wittig reaction was performed as described by Masakatsu and Kuroda (10). The freshly prepared vinylphenyl ketone was added as a

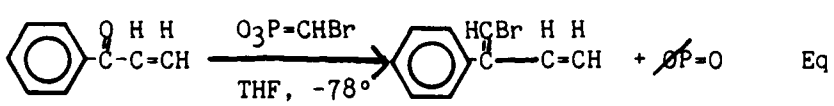

Eq. 9

THF solution to the ylide at -78°. The mixture was allowed to warm up to room temperature overnight. When ether was added to

the reaction mixture a large mass of sticky solid precipitated. This material exhibited an IR and NMR spectrum nearly identical to a previously prepared sample of polyvinylphenyl ketone. Other than solvents, no volatile material could be distilled from the reaction mixture.

Here again, the basic nature of the ylide caused a side reaction (polymerization) to occur in preference to the Wittig reaction.

One attempt at performing the above Wittig reaction on β-chloropropiophenone with the intention of dehydrochlorinating as a following step, was also unsuccessful. Again, copious quantities of polymer were obtained along with starting material and compounds resulting from substitution of the chlorine.

IV. Recommendations

If Wittig reactions are required in the synthesis of diene-yne compounds, consideration must be given to the basic nature of the ylides used and whether base-sensitive functional groups are present in the carbonyl substrate. The ylides are likely to dehydrobrominate vinyl bromides and initiate anionic polymerization of certain vinyl ketone (as is the case with vinylphenyl ketone). In Scheme 1 it may be preferable to perform the acetylene coupling on bromo ketones X or XI (the last step shown in Scheme 1) prior to the Wittig step.

Another feature of the Wittig reaction is that it takes place sluggishly with many ketones. Aldehydes react more readily and should produce fewer side reactions. For example, compound II might be prepared by the sequence:

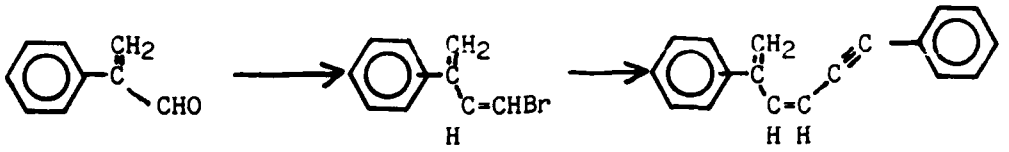

II

The first step would involve a Wittig reaction on an aldehyde, presumably a more facile process.

Similarly, compound IV might be prepared from the same starting aldehyde as shown by the following series of reactions:

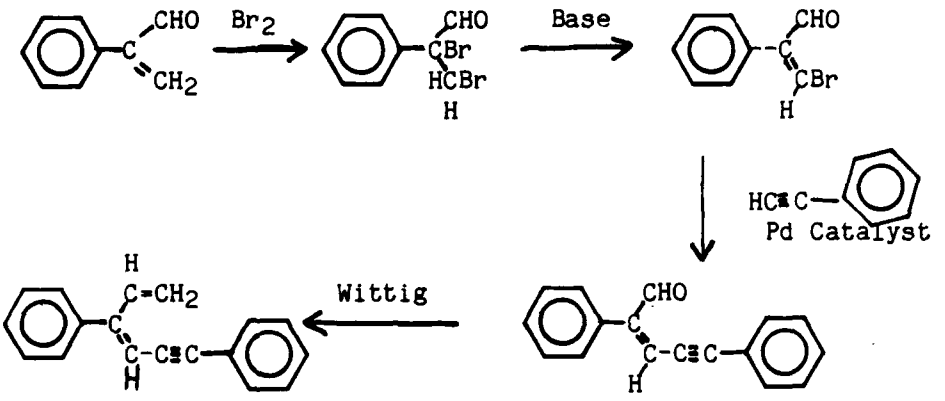

References

1. Tohda, Y., K. Sonogashira, and N. Hagihara, Synthesis, (1977), 777.
2. Logue, M. W. and G. L. Moore, J. Org. Chem., 40, (1975), 131.
3. Harris, F. W. and M.W. Beltz, Prepr. ACS Div. Polym. Chem., 27(1), (1986), 114.
4. Beumel, O. F. and R. F. Harris, J. Org. Chem., 29, (1964), 1872.
5. Campbell, K. N., B. K. Campbell and L. T. Eby, J. Am. Chem. Soc., 60, (1938), 2882.
6. Jones, E. R. H. and J. T. McCombie, J. Chem. Soc., (1942), 733.
7. Grob, C.A. and G. Cseh, Helv. Chim. Acta., 47, (1964), 194.
8. Adams, R. and C. W. Theobald, J. Am. Chem. Soc., 65, (1943), 2208.
9. Wolinsky, J. and K. I. Erickson, J. Org. Chem., 30, (1965), 2208.
10. Matsumoto, M. and K. Kuroda, Tetr. Lett., 21, (1980), 4021.

1986 USAF-UES SUMMER FACULTY RESEARCH PROGRAM/

GRADUATE STUDENT SUMMER SUPPORT PROGRAM

Sponsored by the

AIR FORCE OFFICE OF SCIENTIFIC RESEARCH

Conducted by the

Universal Energy Systems, Inc.

FINAL REPORT

Computer Software Executable Image Efficiency In Real-time LIDAR Applications

Prepared by:	Martin A. Patt
Academic Rank:	Associate Professor
Department and University:	Department of Electrical Engineering, University of Lowell
Research Location:	Geophysics Laboratory, Optical Physics Division
USAF Researcher:	Dr. Donald Bedo
Date:	1 August 1986
Contract No:	F49620-85-C-0013

Computer Software Executable Image Efficiency In Real-time LIDAR Applications

by

Martin A. Patt

ABSTRACT

A study comparing the efficiencies of executable-image codes generated for a real-time LIDAR application was performed for three computer source languages: C, FORTRAN, and BASIC. Programs were compiled and executed under the VMS operating system on a Digital Equipment Corporation VAX-11/780 Mainframe Computer.

ACKNOWLEDGMENTS

I would like to thank the Air Force Systems Command and the Air Force Office of Scientific Research for sponsorship of my research. In order to be meaningful, scientific research must be conducted in an intellectually stimulating environment. The Geophysics Laboratory provided this environment. The genuine support and encouragement of the following members of the Optical Physics Division at AFGL is hereby acknowledged with gratitude.

Dr. Donald Bedo
Mr. Robert Swirbalus
Dr. Donald Fitzgerald
Mr. Steven Alejandro
Lt. Michael Estes

The enthusiastic assistance provided by Mr. Mark W. Lisee, my research assistant, is acknowledged with many thanks.

- M. A. P.

I. INTRODUCTION

In August of 1984, a team of dedicated scientists and engineers working out of the Optical Physics Division at AFGL successfully launched a balloonborne laser radar system for observations of atmospheric backscatter from high altitude(2). Data acquired during this flight is unique in that it represents the only existing set of high-altitude backscatter data. Simultaneously under development at AFGL is a ground-based (but mobile), coherent, pulsed, Doppler CO2 lidar system housed in a modified 12m semi trailer. The pulsed Doppler system is designed to evaluate techniques for the acquisition and real-time interpretation of atmospheric windfield structure as well as aerosol attenuation and concentrations over long path lengths(1). Experiments simultaneously utilizing both the ground-based and balloonborne lidars are expected to begin as early as the summer of 1987. To facilitate and enhance these combined experiments, a Digital Equipment Corporation VAX-11-730 digital computer will be housed in the semi trailer to perform some real-time signal processing which might allow for reconfiguring of the instruments while experiments are in progress. It has been suggested that this processing time might be reduced by selecting a software source language which bests fits this application.

II. OBJECTIVES OF THE RESEARCH EFFORT

This summer-research effort has been devoted to a comparative study of the applicability of three source languages: C, FORTRAN, and BASIC, with the objective of determining which of these may prove most suitable for this signal-processing application. Care has been taken to obtain "best" programs in each of the source languages. Failure to have done so would have resulted in a comparison of the suitability of programmers rather than languages. To this end, all source programs have been subjected

to careful scrutiny and review by a team of conscientious analytical programmers.

III. BACKGROUND

Electromagnetic energy is scattered by gas molecules of the atmosphere and also by its particulate or droplet constituents. In the case of energy at the optical and near-optical wavelengths generated by lasers, such scattering is sufficient to permit application of the radar principal to observations of the atmosphere itself. Even in the visibly "clear" atmosphere backscattered signals from gases and suspended particles at ranges of several kilometers may readily be detected with laser "radars", or "lidars", of modest performance. It is accordingly possible to detect the presence and location of particulate clouds or layers and, by tracking inhomogeneities in particle concentration, to determine atmospheric structure and motion. In addition, this capability of obtaining returns from distant atmospheric volumes provides, from a single location, an extended path along which the effects of atmospheric absorption may be determined. In this way, by using energy at specific wavelengths, resonant absorption may be used to make range-resolved measurements of the quantity of a particular absorptive gas along the path(5).

The basic radar principle of remote atmospheric probing by lasers is called LIDAR, from the acronym Light Detection And Ranging. This term was first applied to pulsed light techniques using conventional sources by Middleton and Spilhaus(6). The anticipated application of an earth-orbiting Doppler lidar to the measurement of tropospheric wind fields on a global scale has provided recent impetus to the measurement of atmospheric aerosol volume backscatter coefficients. When known as a function of altitude (at least up to the tropopause) at a number of globally-distributed locations, these backscatter coefficients can be instrumental in weather prediction as well as in studies of

large aerosol particle formation, transport, and removal processes. Although there is now a large body of information regarding atmospheric aerosol backscatter coefficients in the visible region, there is quite a bit less at CO2 laser wavelengths thus far(4).

Fitzjarrald(3) in 1985 pointed out that a high-altitude experiment can suffer from a lack of effective real-time display of results which, if available, could be used to guide the operation of the experiment in progress. A flexible real-time display system was developed at the NASA Marshall Space Flight Center to provide for the display of line of sight information for either signal intensity or velocity. These could be displayed on a color monitor as the flight progressed to check on the operation of the system, so that a timely response could be made either to adjust the system or change the aircraft flight track.

IV. DESCRIPTION OF THE BALLOONBORNE LIDAR DATA

The balloonborne lidar data initially tested as part of this summer research effort was restricted to high-gain ultraviolet data. The data may be thought of as framed in the following way. Each lidar "shot" (there were ten per second) yields five minor frames of sixty-four twelve-bit data words. Each of the five minor frames has the following format.

twelve-bit data word	Contents
0	Minor frame sync (decimal 856)
1	Minor frame number (0 to 4)
2	Major frame counter (appears in first minor frame only)
3	open
4 - 63	Sixty consecutive 12-bit data words (instrument counts)

Thus there are sixty data words per minor frame, and 300 data words per major frame (lidar shot). Each of these sixty 12-bit data words has the following bit configuration.

Bit position from the right	Contents
11	Even parity
10	FIFO Status (Empty=0)
9	Least-significant bit
0	Most-significant bit

V. PROCESSING APPLIED TO THE BALLOONBORNE LIDAR DATA

For the first comparative test of executable-image efficiencies, the balloonborne data was processed in the following way. Ten major frames of data were decoded, examined and averaged. The results were cleaned(8,9) and then displayed as a plot of average instrument count vs. range bin. Since there are ten "shots" per second, this represents one second of measured data. Each minor frame was checked for proper synchronization as well as proper reporting of the major and minor-frame counters. Inconsistencies resulted in rejection of the entire major frame.

To generate a meaningful comparison of executable image efficiencies, the test was run with a number of different data sets. The percentage of "good" data varied from set to set. The data sets were organized as sequential files with one minor frame per record. This file organization was selected to allow the FORTRAN software to read data efficiently without the need for "direct access" (random access). Random access had been considered for the purpose of speeding up the FORTRAN by allowing it to skip over bad data (the C software does not require special file structuring to do this). This approach was later abandoned when it was found that the overhead of record management and the four-to-one increase in file-size would not be outweighed by a significant improvement in speed in this application.

VI. RESULTS AND CONCLUSIONS

In tests performed with actual balloon telemetry data, the C and FORTRAN ran with nearly equal speed (as measured by C.P.U. times), the C software being slightly faster. Both ran approximately five times faster than the equivalent BASIC software. Results obtained by processing a number of "made up" data sets are summarized in the chart which follows. It must be pointed out that the data structure was purposely set up to accomodate the FORTRAN, allowing the FORTRAN program to read efficiently from the data file (by structuring one minor frame per record rather than one data word per record). Further, the volume of terminal output was kept as small as possible because the FORTRAN was found to be slower than C on output. Tests revealed that the C software would have beat the FORTRAN by a factor of two had these concessions not been granted. The apparent superiority of C in this kind of real-time processing is due in part to its inherent efficiency, allowing for better utilization of modern computer architectures.

C.P.U. TIME TO PROCESS TEN LIDAR SHOTS (MAJOR FRAMES)
AS A FUNCTION OF PERCENT-GOOD DATA

Percent-good	C	FORTRAN	BASIC	MACRO
100	2.1 sec.	2.6	12.5	1.0
90	2.0	2.5	12.0	1.0
80	2.0	2.4	11.5	1.0
70	1.9	2.3	10.9	1.0
60	1.9	2.2	10.4	1.0
50	1.8	2.1	9.9	0.9
40	1.7	2.1	9.4	0.9
30	1.7	2.0	8.9	0.9
20	1.6	1.9	8.4	0.9
10	1.6	1.8	7.9	0.9
0	1.5	1.7	7.3	0.8

VII. RECOMMENDATIONS

AFGL maintaines a substantial investment in computer hardware. At its main computer center, there is a Control Data Corp. CYBER-750 (Operating System: NOS 2.2) as well as a Digital Equipment Company VAX-11/780 (Operating System: VMS 4.4). Although both systems have compilers for both the FORTRAN and Pascal languages, the FORTRAN compilers are used almost exclusively. There is no C compiler available on either CYBER or VAX machines. Both Pascal and C (but not FORTRAN) provide the advantage of speedy software development usually associated with highly structured languages. Of the two, C is the more general and versatile language.

It is recommended that:

(1) A C-compiler be acquired for the VAX-11/780, and that some new AFGL software being developed for the VAX be written in the C-language. Programs written in C for the VAX are readily linked with existing FORTRAN subroutines - users with a substantial investment in existing FORTRAN routines would not be placed at a disadvantage.

(2) A short course should be taught (possibly by the system programmers at A.F.G.L.) to help potential users migrate to the C-language.

REFERENCES

Conference and Journal Publications:

1. S. B. Alejandro and D. R. Fitzgerald, "AIR FORCE GEOPHYSICS LABORATORY'S (AFGL) MOBILE CO2 DOPPLER LIDAR", Topical Meeting on Optical Remote Sensing of the Atmosphere Sponsored by the Optical Society of America and the U.S. Army Research Office, at Incline Village, Nevada, 1985

2. D. E. Bedo and R. A. Swirbalus, "ATMOSPHERIC BACKSCATTER OBSERVATIONS FROM A BALLOONBORNE LIDAR", 13th International Laser Radar Conference, Toronto, Ontario, Canada, 1986

3. D. E. Fitzjarrald, "PRELIMINARY RESULTS FROM 1984 AIRBORNE LIDAR WIND MEASUREMENTS", Topical Meeting on Optical Remote Sensing of the Atmosphere Sponsored by the Optical Society of America and the U.S. Army Research Office, at Incline Village, Nevada, 1985

4. Menzies, Kavaya, Flamant, and Haner, "ATMOSPHERIC AEROSOL BACKSCATTER MEASUREMENTS USING A TUNABLE COHERENT CO2 LIDAR" (Applied Optics, 1-Aug-84) Vol.23, No.15

Textbooks:

5. R.T.H. Collis and P.B. Russell "LIDAR MEASUREMENT OF PARTICLES AND GASES BY ELASTIC BACKSCATTERING AND DIFFERENTIAL ABSORPTION"; E. D. Hinkley, Ed., "Laser Monitoring of the Atmosphere", TOPICS IN APPLIED PHYSICS, Vol. 14 (Springer-Verlag, 1976) Ch.4

6. W.E.K. Middleton and A.F. Spilhaus, "Meteorological Instruments" (University of Toronto Press, Toronto 1953)p.208

Final Reports:

7. Visidyne, Inc., "ABLE INTERFACE CONTROL DOCUMENT/REVISION C", Contract F19628-81-C-0165, Air Force Geophysics Laboratory, 1984

8. M. W. Lisee and M. A. Patt, "Computer Software Development in a Study of Executable Image Efficiency", Contract F49620-85-C-0013, Air Force Geophysics Laboratory, 1986

Reports:

9. M. A. Patt and M. W. Lisee, "Cleaning Telemetry Data Handbook", Contract F49620-85-C-0013, Air Force Geophysics Laboratory, 1986

1986 USAF-UES SUMMER FACULTY RESEARCH PROGRAM

Sponsored by the

AIR FORCE OFFICE OF SCIENTIFIC RESEARCH

Conducted by the

Universal Energy Systems, Inc.

FINAL REPORT

A BIOMECHANICAL STUDY OF ANTHROPOMORPHIC HEAD-NECK SYSTEMS

Prepared by:	Jacqueline G. Paver
Academic Rank:	Research Assistant Professor
Department:	Biomedical Engineering Department
University:	Duke University
Research Location:	AAMRL/BBM
	Wright-Patterson Air Force Base
USAF Researcher:	Dr. Ints Kaleps
Date:	September 22, 1986
Contract No.:	F49620-85-C-0013

A BIOMECHANICAL STUDY OF ANTHROPOMORPHIC HEAD-NECK SYSTEMS

by

Jacqueline G. Paver

ABSTRACT

Hybrid II, modified Hybrid II, and Hybrid III anthropomorphic manikin head-neck assemblies were studied. Preparations were made to measure the kinematic and dynamic responses of these mechanical head-neck assemblies to abrupt decelerations imparted to the base of the neck by a pendulum test apparatus according to existing DOT specifications for Part 572 dummy compliance testing and recommended procedures for Hybrid III compliance testing. The actual execution of these tests is planned for the upcoming year. Measurements were made of the geometric and inertial properties of the pendulum and the modified Hybrid II and Hybrid III test specimens. The measured geometric and inertial properties and pendulum test performance standards were then analyzed to determine inputs for both the Articulated Total Body (ATB) Model and the AAMRL Head-Spine Model (HSM). Data sets, which represent the Hybrid II head-neck system, were developed for the HSM and ATB Model. Simulations of the Hybrid II pendulum tests were performed and compared to experimental results in order to validate these data sets. More modeling work still needs to be done. Some additional tuning of the Hybrid II data sets is suggested. Modified Hybrid II and Hybrid III data sets need to be developed and validated.

ACKNOWLEDGEMENTS

I would like to express my appreciation to the Air Force Systems Command, the Air Force Office of Scientific Research, and Universal Energy Systems for sponsorship of my research. I thank Dr. Ints Kaleps for his guidance, encouragement, and criticism of my research. I also thank the BBM staff, especially Dr. Eberhardt Privitzer and Louise Obergefell for their assistance and patience with modeling tasks and Capt. Gary Chestnut for his assistance with the experimental aspects of this project. Several members of the SRL staff deserve special recognition and thanks; these include Dick White, Jennifer McKenzie, Jeff Setticerri, Jeff Eastup, and Gene McGregor. Dr. Bob Beecher of UDRI was also very helpful with the anthropometric aspects of this study. Overall, the laboratory proved to be a very stimulating and enjoyable work environment.

In addition, appreciation is expressed to Steve Goldner of Humanoid Systems and James Blaker of the Transportation Research Center of Ohio for their technical assistance.

I. INTRODUCTION

I received my Ph.D. from Duke University in December, 1985. My dissertation was entitled, "The Biomechanics of Head and Neck Injury and Protection." The ultimate goal of my research was to provide a rational tool for optimum helmet design. As a graduate student, I trained in an extensive and well-equipped laboratory specifically designed for testing and modeling the mechanical properties of biological tissues and their anthropomorphic analogs. During this period, I developed a head-neck injury model by modifying the Calspan CVS Model to incorporate a helmet and more realistic neck based upon measurements of the viscoelastic responses of unembalmed human cervical spines and a variety of helmet types to dynamic compression loading. As a research associate at Duke University, I worked on a grant with the Industrial Safety Equipment Association (ISEA). The goal of the ISEA project was to perform research to: (1) develop justification for the test specifications in a proposed standard for hardhats for use in environments that require a high level of lateral protection; and (2) develop a helmet test system as described in the proposed standard.

The research problem at AARML/BBM involved an investigation of the geometric, inertial, and mechanical properties of the head-neck systems of several anthropomorphic dummies. Both experimental work and computer simulation were included in this research effort. The problem under investigation at AAMRL/BBM was, therefore, very similar to the problems I had studied at Duke University. Because of this similarity, I was assigned to work at AAMRL/BBM.

II. OBJECTIVES OF THE RESEARCH EFFORT

One goal of the AAMRL/BBM research program is to develop a durable, servicable, and biofidelic anthropomorphic dummy head-neck system with repeatable and reproducible biomechanical responses. Another goal is to develop data sets for the Articulated Total Body (ATB) Model and the AAMRL Head-Spine Model (HSM) which accurately predict the head-neck kinematics and dynamics of existing dummies in crash environments. To accomplish these goals, it was desired to measure, analyze, and simulate the kinematic and dynamic responses of Hybrid II, modified Hybrid II, and Hybrid III mechanical head-neck assemblies to abrupt decelerations imparted to the base of the neck by a pendulum test apparatus.

My individual objectives were:

(1) to measure the geometric and inertial properties of the modified Hybrid II and Hybrid III head-neck systems and the pendulum test apparatus

(2) to setup the test apparatus and instrumentation to measure the desired responses of these mechanical head-neck assemblies according to existing DOT specifications for Part 572 dummy compliance testing and recommended procedures for Hybrid III compliance testing

(3) to analyze the measured geometric and inertial properties and pendulum test performance standards to determine inputs for both the HSM and the ATB Model.

(4) to compare simulations of the pendulum tests to experimental results to verify the assumptions used to define the head and neck structures and validate the HSM and ATB Model data sets.

III. RATIONALE

In recent years, there has been an increasing awareness of both the serious consequences that can occur with head and neck injuries and the effectiveness of biomechanical studies to reduce the likelihood of these injuries. Two sources of information about head and neck injury and prevention are: (1) experiments with human surrogates; and (2) analysis of mathematical models. Information from dummy tests is limited. The use of inanimate devices reduces the repeatability problems associated with animals and cadavers but raises questions as to biofidelity. Attempts to improve human surrogate biofidelity are well documented. When a new manikin design is incorporated into a crash test program, data bases are generated which describe their geometric and inertial properties and mechanical behavior. Performance evaluations are conducted to ensure uniformity of results among different specimens and laboratories. Compliance tests are developed. Mathematical modeling is an accepted technique of scientific research. Once validated by comparison with experimental results, mathematical models are useful, economical, and versatile engineering tools. They can, in lieu of direct experimentation with actual physical systems, evaluate the effects of varying parameters on the responses of systems to a wide variety of input conditions. In particular, with validated data sets for the Hybrid II, modified Hybrid II, and Hybrid III head-neck systems, any environment or test, where the head and/or neck is in jeopardy, could be simulated.

It was expected that the proposed systematic study of the geometric, inertial, and kinematic and dynamic properties of mechanical head-neck assemblies would provide useful information to those interested in injury prevention and crashworthiness.

IV. BACKGROUND

Experimental Studies

Hybrid II, modified Hybrid II, and Hybrid III mechanical head-neck assemblies were chosen as specimens for this study.

The Hybrid II was the first GM dummy design to have acceptable repeatability and good durability and serviceability. The Hybrid II head-neck assembly is a fairly simple system. The head is a hollow aluminum casting, with a rear cap to allow access to the instrumentation inside. This instrumentation consists of a mutually orthogonal array of three uniaxial accelerometers; this array is mounted at the head CG. Both pieces of the head are covered with a rubber skin. The neck is a right circular cylinder of butyl rubber. It is solid, except for a small hole through the middle. Metal plates are molded into each end to facilitate head-neck and the neck-thorax attachment.

The AAMRL modified Hybrid II accommodates a load cell, for measuring neck axial and shear loads and moments about the occipital condyles, and a nodding joint at the occipital condyles. These modifications required alterations of both the head and the neck. A large hole was cut in the transverse bulkhead, the load cell and nodding joint were added between the base of the head and the top of the molded neck, and the accelerometer array was mounted on top of the load cell. Also, the solid molded neck was shortened in order to keep the overall height the same as that specified by DOT for Part 572 dummies. Another modification is the use of head accelerometers and an aluminum mounting plate unlike the devices supplied by Humanoid Systems. These modifications are significant and will probably alter the bending properties and overall performance of the head-neck system.

The Hybrid III head-neck system is a measurable improvement over the Hybrid II and modified Hybrid II systems in terms of component biofidelity in frontal impacts. The Hybrid III design represents state-of-the-art knowledge of human geometry, weight, inertia, and biomechanical response. The head is a hollow two-piece precision casting of 356 aluminum with T6 heat treatment. The thickness of the vinyl skin is specified and closely controlled to assure biomechanical fidelity and repeatable head response in hard-surface impacts. As in the modified Hybrid II, a load cell and nodding joint connect the head and neck. The molded neck is constructed of alternate layers of aluminum and 75-durometer (shore hardness) butyl rubber elastomer; the rubber layers are asymmetric to give different responses in flexion and extension. A steel cable runs through the center of the neck to provide axial strength. An adjustable bracket connects the neck to the thorax. The AAMRL Hybrid III dummy was modified to include head accelerometers and a steel mounting plate, unlike the devices supplied by Humanoid Systems, and an occipital condyle pin replacement, which permits attachment to the three-potentiometer unit. These modifications should not significantly alter the bending properties and performance of the head-neck system.

The head-neck pendulum test consists of a pendulum drop. At the bottom of the pendulum's swing, the arm impacts a block of honeycomb; this produces a near-square wave pendulum deceleration pulse. The head-neck system, which is mounted to the end of the pendulum, does not undergo any impact. The environmental test conditions, instrumentation requirements, and test procedures (including the pendulum geometric and inertial properties and strike plate deceleration pulse and impact velocity) are specified. For the Hybrid II dummy, the head rotation, chordal displacement of the head center of gravity, and maximum allowable

head acceleration are also specified. Hybrid II test procedures and performance standards are described in the Code of Federal Regulations, Title 49, Part 572. For the Hybrid III dummy, the moments at the occipital condyles and D-plane rotation are specified by recommended Hybrid III test procedures and performance standards, which are based on the General Motors Calibration Test Procedure, evaluation testing performed by the Transportation Research Center of Ohio for the NHTSA Vehicle Research and Test Center, and the Society of Automotive Engineers (SAE) Engineering Aid #23, written by the Dummy Testing Equipment Working Group. Currently, there are no DOT specifications for Hybrid III compliance testing.

The instrumentation used in a typical pendulum test consists of piezoresistive accelerometers, a six-axis load cell, a three-potentiometer device or high-speed 16mm camera, and a velocimeter with a photocell sensor. A triaxial accelerometer measures the pendulum arm deceleration 65.25 inches from the pivot point of the pendulum along the pendulum arm centerline. Three single-axis accelerometers measure the Hybrid II head accelerations. A two- or three-potentiometer unit or a high-speed 16mm camera measures head rotation and displacement data in order to obtain a complete description of head motion in the mid-sagittal plane. A six-axis load cell measures forces and moments at the modified occipital condyle pin of the Hybrid III manikin. A velocimeter-photocell device measures the pendulum velocity just prior to impact.

Theoretical Studies

Two types of mathematical models were selected for this study: (1) an internal body structure model; and (2) a whole-body gross-motion simulator model. Internal body structure models have been successfully

implemented at AAMRL for military applications (e.g., the dynamic responses of head-spine subsystems to +Gz accelerations). Numerous applications of whole-body gross-motion simulator models, involving automobile, pedestrian, and motorcycle crash victims, are documented in the literature.

Description of the Head-Spine Model

The Head-Spine Model (HSM) is a three-dimensional computer model which represents the human body by a collection of rigid bodies connected by deformable elements (Belytschko et al., 1976). The deformable elements can be beam elements, spring elements, hydrodynamic elements, or elastic surfaces. The rigid bodies generally represent bones (e.g., the head, vertebrae, pelvis, and ribs); the deformable elements represent soft tissues (e.g., viscera, ligaments, and intervertebral discs).

The mathematical model is a matrix structural analysis program. The program integrates the equations of motion in time, either implicitly or explicitly. The analysis accommodates large displacements of the rigid bodies, nonlinear material properties, and viscous forces.

The data base defines the structure to be modeled. It consists of the geometric and inertial properties of the rigid bodies, the geometric, inertial, and material properties of the deformable elements, the connectivity data, boundary conditions, constraints, and global coordinate system definition. The model inputs are defined in a separate subroutine called ICIF that is linked with the code prior to execution.

Description of the Articulated Total Body Model

The Calspan three-dimensional Crash Victim Simulator (CVS) Model is a digital computer program developed at Cornell Aeronautical Laboratory (McHenry and Naab, 1967) for the DOT for the study of human and dummy

dynamics during automobile crashes. Originally, its validity was determined from comparisons of predicted responses with those measured in sled tests and full-scale automobile crash tests using anthropometric dummies (McHenry and Naab, 1967; Bartz, 1972). The formulation, however, was of sufficient generality to allow application of this model to problems involving other impact environments. The Articulated Total Body (ATB) Model is a modified version of the CVS which accommodates specific Air Force applications such as vibration loading, encumberance effects on crewman performance, and ejection from disabled aircraft (e.g., retraction, head-canopy impacts, windblast, parachute-opening shock).

The primary component of this program is the body dynamics model. The body dynamics model contains and solves the equations of motion and constraint. These equations are formulated from Euler's rigid body equations of motion with Lagrange-type constraints. This model differs from most other three-dimensional occupant models, which are formulated from Lagrange's equations of motion. Variation of the number of segments and joints is permitted within the formulation. In most applications, the crash victim is represented by fifteen rigid body segments connected by fourteen joints. The resulting simultaneous first-order ordinary differential equations are solved using a Vector Exponential Integrator. The three-dimensional rotational equations are integrated using quaternions (also known as Euler Parameters).

V. SFRP RESEARCH

As part of the SFRP at AAMRL, Paver and Doherty conducted experimental and theoretical studies of the Hybrid II, modified Hybrid II, and Hybrid III dummy head-neck assemblies and the Part 572 and recommended Hybrid III dummy head-neck compliance tests. Measurements were made of the geometric and inertial properties of the test specimens and apparatus. Mounting plates, test fixtures, and apparatus modifications were made. All transducers were wired; some were calibrated. The test specimens and apparatus were assembled for the Part 572 tests. A test plan was written. The measured geometric and inertial properties and Part 572 pendulum test specifications were analyzed to determine inputs for both the HSM and the ATB Model. Data sets which represent the Hybrid II head-neck system were developed for the HSM and ATB Model. The pendulum test was simulated to validate these data sets.

Experimental Studies

The inertial properties of the dummy head and neck segments were determined experimentally using balsa wood holding boxes, a C & S electronic scale, a moment table, a Space Electronics Model #KGR1000-3 Mass Properties Torsion Pendulum, a Hewlett-Packard HP85 microcomputer, and a Micro Control Systems perceptor three-dimensional digitizer linked tc the AAMRL Perkin Elmer computer. The scale was used to determine the segment-box weight to the nearest 0.01 lbs. The moment table, which had two parallel knife edges, was used to measure the segment-box center of gravity (CG) location. One knife edge was placed on the scale and the other on a fixed stand. With the scale tared to zero, the first moment about the fixed blade edge was read directly from the scale. Then, using

the known distance between the knife edges, the exact location of the CG of the segment-box combination was calculated. The torsion pendulum was used to determine the moment of inertia of the segment-box combination about its CG. By performing this task with the segment-box in six different orientations, the inertia tensor elements at the CG were determined. Using these tensor elements and data obtained from the perceptor, the principal moments of inertia, and the direction cosines of the respective principal axes were determined. The effects of the box were removed and the inertial properties of the segment were calculated relative to specified points on the segment.

The geometric and inertial properties of the pendulum were also measured. The weight was determined with a high-capacity scale. A knife edge was used to measure the CG location. The torsion pendulum and HP85 microcomputer were used to determine the relevant moment of inertia. Although the pendulum was designed using the Part 572 specifications as a model, some differences exist. The estimated effects of the differences were negligible with respect to the dynamics of the head-neck system.

Simulating the Part 572 Head-Neck Pendulum Test with the Head-Spine Model

An HSM data set, which represents the Hybrid II head-neck system, was developed. The Part 572 head-neck pendulum compliance test was simulated to validate this data set. Since the head is connected directly to a cylindrical rubber neck and the base of the neck is connected directly to the pendulum arm during a test, the corresponding HSM was made up of two elements. A rigid body represented the head; a beam element represented the neck. The pendulum arm was not explicitly defined; the boundary conditions of the node at the base of the neck were made to reflect the presence of the pendulum.

For this simulation, it was necessary to describe the geometric and inertial properties of the head separately from those of the neck. Since the Part 572 specification requires that the head and neck properties be defined by the SAE Recommended Practice J963 (i.e., the head and upper neck are lumped together; the upper torso and lower neck are lumped together), this data was inappropriate. Instead, values for these parameters were abstracted and/or derived from Hubbard and McLeod (1977) and the Hybrid II Performance Evaluation Report (1973), where the geometric and inertial properties of the head are described separately from those of the neck.

The coordinate system was defined so that the positive x axis was the A-P direction, the positive y axis was the L-R direction, and the positive z axis was the S-I direction. The pendulum arm was free to rotate about the y axis only. Since the response is measured only from the time of impact to the time the head returns to the pre-impact position, the end of the pendulum (i.e., the base point) does not rotate during the test. The motion of this point was modeled as a pure translation in the x direction; no translations in the y and z directions or rotations about the x or z axes were allowed for this point. All other points were allowed to translate and rotate in the x-z plane.

A trapezoidal acceleration pulse with a 20 G constant peak acceleration was the excitation for the model. This pulse complied with Part 572. The initial condition was the pendulum strike plate impact velocity specified in Part 572. These two quantities were not included in the data set itself; they were inputs to the subroutine ICIF. This subroutine is called by the model after it reads the data set.

The data set was tuned to make the HSM head-neck response comply with the Part 572 head-neck pendulum test performance standards. Part 572 specifies the response in three ways: head rotation vs. time, chordal displacement vs. time, and peak head acceleration. Since the inertial properties of the Hybrid II head and neck are well documented, these constants remained fixed; they were not used to tune the data set. The stiffness and damping of the neck, however, are not as well documented. The values used initially for axial, bending, and torsional stiffness and damping were calculated from a material specification abstracted from a Sierra blueprint. The response of the model did not comply with Part 572 using these initial values; it was necessary to increase the amplitude and decrease the period of the response. The material properties of the neck were varied in a systematic manner to bring the response of the model into compliance with Part 572. It was discovered that a decrease in the bending stiffness increased both the amplitude and the period of the motion. A decrease in the bending damping increased the amplitude but had little effect on the period. Changes in the axial and torsional stiffness and damping had no effect on the performance of the head-neck system in bending. The final data set resulted in the correct period of rotation but slightly low amplitudes. The peak head acceleration was also slightly low. Both of these deficiencies may have resulted from the fact that the input acceleration pulse was trapezoidal, with a 20 G constant peak acceleration; actual acceleration pulses show a peak of 25-30 G's. These deficiencies may also have resulted from the initial condition specification; the actual neck velocity should be higher than the pendulum strike plate velocity. A more realistic excitation and initial condition would give the head a higher-amplitude rotation and higher peak accelerations.

Simulating the Part 572 Head-Neck Pendulum Test with the ATB Model

ATB data sets, which represent the Hybrid II head-neck system, were developed. The Part 572 head-neck pendulum test was simulated to validate these data sets. Initially, three segments were defined. Ball-and-socket joints were specified between the head and neck and between the neck and pendulum. A pin joint was specified between the pendulum and the vehicle. The geometric and inertial properties of the Hybrid II head and neck and the joint characteristics of the neck were abstracted from operational data sets at AAMRL/BBM. The pendulum geometric and inertial properties and joint characteristics were measured or estimated.

Two types of ATB simulations were performed. The first type were full-drop simulations where time zero represented the initial release of the pendulum. The second type were simulations of only the impact phase where time zero was the time just prior to the impact of the pendulum against the aluminum honeycomb.

The full-drop simulations were used to determine the relative angular orientation and velocity of the head and neck with respect to the pendulum just prior to impact. It was discovered that the time to impact and the initial striking velocity could be varied by changing the joint viscous coefficient of the pendulum pivot. The required simulation time varied from 750 to 1250 msec, depending on the specified impact velocity. Only the final 150 msec corresponded to the impact phase.

The impact phase simulations revealed a problem in the specification of the pendulum-honeycomb contact. Three approaches were considered:

(1) The pendulum was defined as a segment with an attached ellipsoid and the honeycomb was defined as a plane. Plane-ellipsoid contact resulted.

(2) The pendulum was defined as a segment with an attached plane and the honeycomb was defined as an ellipsoid. Plane-ellipsoid contact resulted.

(3) The pendulum acceleration specified by Part 572 was input by defining the pendulum as the vehicle and attaching the neck to the vehicle. No contacts were defined.

Since the contact forces were defined in terms of the penetration between contact surfaces and since the strike plate was located at a distance almost equal to the major axis length of the pendulum ellipsoid, contact was not observed at the right point in space if the dimensions of the pendulum and honeycomb were defined correctly. Hence, both the amount of penetration and the contact time were low. One fix for this problem was to make the contact ellipsoid attached to the pendulum or honeycomb large enough so that the minor axis occurred at the strike plate location. This resulted in unrealistic graphics which were later modified in the AMRLVIEW input deck.

VI. RECOMMENDATIONS

The following are recommendations for future experimental studies:

(1) Execution of modified Hybrid II and Hybrid III pendulum tests according to existing DOT specifications for Part 572 dummy compliance testing and recommended procedures for Hybrid III compliance testing. Some tests will be designed to assess the effects of three-potentiometer devices, in two different mounting configurations, on head-neck kinematics and dynamics.

(2) Expansion of the test program to include other impact directions and deceleration profiles to obtain a comprehensive evaluation of the manikin head-neck responses.

The following are recommendations for future theoretical studies:

(1) Continue tuning the proposed Hybrid II data sets.

(2) Develop and validate data sets of the modified Hybrid II and Hybrid III head-neck systems. As a preliminary effort, the data sets would not contain detailed representations of every part of the neck. Instead, the effects of the nodding blocks, central cable, and the layered construction of the Hybrid III neck would be lumped together.

(2) Develop and validate data sets which incorporate the occipital condyle nodding joint into the neck description. This joint is part of both the modified Hybrid II and III head-neck systems. Experimental determination of the torque-angle characteristics of the joint will be required.

(3) Develop and validate Hybrid III data sets which incorporate the layered aluminum-butyl rubber construction of the neck.

REFERENCES

1. Bartz, J.A.: Development and Validation of a Computer Simulation of a Crash Victim in Three Dimensions. Proceedings of the 16th Stapp Car Crash Conference, SAE PAPER #720961, 1972.

2. Belytschko, T.; Schwer, L.; Schultz, A.: A Model for Analytical Investigation of Three-Dimensional Head-Spine Dynamics. NTIS Report #AD-A025-911, April 1976.

3. Hubbard, R.P.; McLeod, D.G.: Geometric, Inertial, and Joint Characteristics of Two Part 572 Dummies for Occupant Modeling. Proceedings of the Twenty-First Stapp Car Crash Conference, SAE PAPER #770937, 1977.

4. McHenry, R.R.; Naab, K.N.: Computer Simulation of the Crash Victim -- A Validation Study. Proceedings of the 10th Stapp Car Crash Conference, SAE PAPER #660792, 1967.

5. Miller, J.S.: Performance Evaluation of the General Motors Hybrid II Anthropomorphic Test Dummy, NTIS Report #PB-224-005, Department of Transportation Report #DOT-HS-800-919, September 1973.

1986 USAF-UES Summer Faculty Research Program/
Graduate Student Summer Support Program

Sponsored by the
Air Force Office of Scientific Research
Conducted by
Universal Energy Systems, Inc.
Final Report

Automatic Program Generation from Specifications

Prepared by:	Alex Pelin
Academic Rank:	Associate Professor
Department and	Department of Mathematical Sciences
University:	Florida International University
Research Location:	Weapons Laboratory
	Kirtland AFB, NM.
USAF Research:	Captain Robert Millar
Date:	September 29, 1986
Contract No.:	F49620-85-C-0013

AUTOMATIC PROGRAM GENERATION FROM SPECIFICATIONS USING PROLOG

by

Alex Pelin

ABSTRACT

A framework was built for an expert system which generates PROLOG programs from formal specifications. The system was able to generate correct programs for sorting problems. The program generator was written in PROLOG.

The specifications were presented as equations. Work was done on validating the specifications and we obtained important results in this field. There are, however, problems in translating equations into PROLOG clauses. More research needs to be done in this area.

Several heuristics were also developed for the program generator which can enable it to solve a larger class of problems.

The system uses correct rules, but it proves neither the correctness nor the termination of the generated programs. It can be augmented to do this by using the theorem prover ITP. More research needs to be done in this area, particularly in developing programs that use induction.

ACKNOWLEDGEMENTS

I would like to thank the Air Force Systems Command and the Air Force Office of Scientific Research for the sponsorship of my research.

During the 10 week period that I spent at the Weapons laboratory, I had the necessary resources to pursue interesting research topics. I would like to thank the Chief Scientist, Dr. Gunther, and his staff, for doing everything in their power to create a productive research environment. Thanks are also due to the S.I. Division for their support.

I am especially grateful to Captain Robert Millar for many interesting discussions and for always being ready to help; and to my assistant, Michael Slifker, for implementing many of the programs discussed in this report.

I would also like to thank Captain Michael Tebo, Brian Kennedy and Dr. Richard Nau for their help.

Finally, I would like to thank my wife, Mary Lou, and my children, Dan and Lydia, for keeping me company during my stay in Albuquerque.

I. Introduction

I received my Ph.D. from the University of Pennsylvania studying the equivalence of recursive procedures. I was very interested in using equations to characterize properties of recursive programs. While pursuing graduate studies at the University of Pennsylvania, I worked closely with Dr. Noah Prywes. He had an ONR Grant to build an automatic program generator. His group built MODEL, a program generator that produced PLI code from input/output specifications. After I obtained my Ph.D. I was consultant for the project and I investigated methods for handling recursive specifications. Later I became interested in abstract data types. They provide a way of defining data structures as sets of terms which satisfy certain properties. The properties are expressed as equations or conditional equations. I was interested in building an automatic program generator which took as input the following specifications: the descriptions of the input and the output data types, the input/output relation and a set of tests,transformations which could be used in constructing the program. Since equations are a convenient way of describing properties of the data, I investigated methods for dealing with equations. I obtained theoretical results pertaining to a generalization of the term rewriting method which transforms equations into rewrite rules.

I taught a course in automated reasoning at Temple University in which I used ITP, an interactive theorem prover. I became interested in PROLOG since its statements can be seen both as commands and descriptions. Research at the Weapons Laboratory involved building an automatic program generator that produced PROLOG programs from specifications. I was interested in finding out if PROLOG was suitable for this task, and in investigating various heuristics that can be used in building automatic program generators. The problems under investigation at the Weapons Laboratory were a natural continuation of research which I began during my graduate studies at the University of Pennsylvania, and which continued at Temple University.

For this reason I was assigned to work on building an expert system for generating programs at the Weapons Laboratory.

II. Objectives of the Research Effort

The goal of the field of automatic programming is to automate the software development cycle. The chief reason for this is that while the need for software and software engineers, is growing exponentially, the productivity of the software industry is rising very slowly. Today, this productivity problem has reached crisis proportions ([1]).

Expert systems are now considered as tools for improving software development techniques and programmer productivity.

We feel that expert systems can be used in automatic programming, especially in its most challenging task, which is to create programs that generate other programs.

My individual goals were:

1. To create a program generator which takes as input the following specifications:
    a) A description of the input data type.
    b) A description of the output data type.
    c) A set of transformations.
    d) A set of tests.
    e) A relation between the input and the output data items.

The program generator had to take as input, the above specifications and create a program which transforms an item of the input data type into an item of the output data type, such that the two items are related as described in part (e) of the specifications.

In constructing the program, the generator will use only the transformations and the tests allowed by the specifications.

2. To investigate methods for validating the specifications that are fed into the program generator.

3. To develop heuristics for generating programs from transformations and tests.

4. To study how suited PROLOG is as a language for writing program generators.

III. Abstract Data Types

Abstract data types were introduced in the computer science field by tne ADJ groups ([3]) as a way of defining data structures that is independent of implementation. An abstract data type is a collection of domains and operators. A typing function relates the operators to the domains. The typing function t associates a non-empty sequence of domains with each operator. If t (0) = < s1, s2,....., sn, s> then 0 is an operator which takes as input n arguments t1 of the type s1, t2 of type s2,....., tn of type sn; and its output is of type (sort) s. We write t (0) = s1 x s2 x .... x sn → s. For example, the data type list of natural numbers has three domains: Natural numbers (abbreviated nat), list of natural numbers and boolean which we abbreviate as bool. The typing function t is given by the equations: t (T) = t (F) = → bool, t(le) = nat x nat → bool, t (succ) = nat → nat, t (0) = → nat, t (Λ) = → list, t (add) = list x nat → list. This means that T and F are constants of the boolean type, le is an operator which takes as input two natural numbers and outputs a boolean value succ is the successor function on the set of natural numbers, 0 is the natural number zero, Λ is the empty list, and add creates a new list by adding a natural number to an existing list.

The semantics of the data type is given by a set of equations or conditional equations. For example, the following equations define the semantics of le.

le (n,n) = T

le (n,m) = T → le (n, succ (m)) = T

le (n,m) = T → le (succ (m), n) = F

Figure 1

The set of terms is obtained from the set of operators in the usual way by repeatedly applying the operators. More exactly, the set of terms is given by productions S → 0 (S1, ..., Sn) for all operators 0 with signature t (0) = s1 x .... x sn → s. In our case the set of terms is generated by the

productions N → 0, N → succ (N), B → T, B → F, B → le (N,N) L → Λ , L → add (L,N), where N generates all natural numbers, B generates all the boolean values, and L generates all lists. A data type is a collection of domains together with a set of equations that must be satisfied by the terms of those domains.

We use the data types described above as descriptions for the input and the output data types. It is very easy to write a PROLOG program which checks if a string belongs to a data type as specified above. Handling the equations that constitute the semantics of the data type is difficult in any programming language.

IV. Tests and Transformations

The tests are predicates which are defined on the set of data items. The tests are defined in a hierarchal way. For example, test P may be defined in terms of test Q, and test R may be built on top of P. We do not allow test P to be defined in terms of test Q, and test Q is defined as a function of test P. The tests must be total, (i.e. for any data item d, P(d) is either true or false.)

The tests can be defined in a recursive fashion as seen in the following example:

1. SORTED (Λ)
2. SORTED (add (Λ , n))
3. le (m,n) = F → ¬SORTED (add (add (a, m),n)
4. le (m,n) = T → SORTED add (add (a,m), n) = SORTED (add (a,m))

Figure 2

The test SORTED is defined for data items of type list. It is built on top of test le and it contains the recursive rule 4. The sign ¬ denotes negation.

The transformations are also described by equations. A transformation can be seen as part of the data type. For example, we can define the transformation inv which takes as input a list, and outputs a list in which the last two elements are inverted.

The equations which describe inv are:

1. inv (Λ) = Λ
2. inv (add (Λ,n)) = add (Λ,n)
3. inv (add (a,m),n) = add (add(a,n),m)

Figure 3

Further on we will use the notation n for SUCC(SUCC... (SUCC(O))...)) where SUCC operator occurs n times, and we will use [] for Λ. For the list add (add(L,m),n) we will write [L,m,n]. This way the terms of the data domains are easier to read. We note that there is a big difference between tests and transformations. A transformation, being part of the definition of the data type, preserves the equations in the data type. In fact, we must add (4) to the set of equations that define the data type.

inv (L) = L (4)

Then we know that the lists [1,2] and [2,1] are equal under this definition. On the other hand, tests are only functions on strings and as such, they do not preserve the equality relation. Thus SORTED([1,2]) is true, but SORTED ([2,1]) is false. We intend to create a library of built-in data types, some of which have already been created.

This way the typical user can select the data types, the tests, the transformations and the input/output relation from the library.

The generated programs depend not only on the input data types, but on the set of tests and transformations. The algorithm for sorting an array in which we are allowed to switch only adjacent pairs, is different from the sorting program in which we have transformations for exchanging the contents of any locations in the array.

We plan to build an interface which hides the equational definitions of the data types, tests, transformations and input/output relations from the user. He can make his requests through English-like commands.

At the same time the sophisticated user can define data types, tests and transformations. We want to construct a program generator that behaves like a computer system into which most users enter programs in high-level languages, but at the same time supports system programming for those who desire to write them. The input/output relation in all cases that we considered so far was i=0. This means that 0 is derived from i by using the transformations in the set of transformations.

V. Heuristics

Given the descriptions of the input and output data types, the sets of tests and transformations and the input/output relation, the program generator can pursue its goal of constructing a program in two ways. The first way is to use heuristics. This means that it tries certain strategies which may or may not work. We will describe one heuristic that was implemented in our program generator.

In the case of sorting a list, the input data type is the one described in Section III, the tests are le and SORTED, the transformation is inv and the output data type is SORTED list. This means that 0 is a SORTED list if 0 is a list and SORTED (0) is true. The input/output relation is i=0.

The program generator splits rule 4 of figure 2. into two rules.

5. le (m,n) =T, SORTED (l,m) $\rightarrow$ SORTED ([L,m,n])
6. le (m,n) =T, $\neg$ SORTED ([L,m]) $\rightarrow$ SORTED ([L,m,n])

Figure 5

In this approach the program generator focusses on rule 3 of Figure 2 and rule 6 of Figure 5.

These two rules are of the form C (t) $\rightarrow \neg$ SORTED (t), where C is a conjunction of tests. The system tries to find a transformation or a sequence of transformations T such that C (T (t)) is no longer true. In our system the search for a transformation or a sequence of transformations T is rather primitive. A more sophisticated approach would take into account

the periodicity of the transformations and would also rank the equations of the form C (t) $\Rightarrow \neg$ SORTED (t). Our system ranks them in two categories: reductions, and recursive rules. Rule 3 of Figure 2 is a reduction while rule 6 is a recursive rule, since $\neg$ SORTED occurs on both sides of the implication sign. The reductions have higher priority than the recursive rules. This methadology requires some theorem proving, since in order to pick a transformation T we must check that C (T(t)) is false. In our system we have the theorems listed in a file. In the future we plan to use the interractive theorem prover ITP.

More heuristics are described in [8]. The program generator must have more heuristics since these methods tend to generate solutions faster.

PROLOG has a built-in goal-searching mechanism that implements the backward chaining method. It also has a built-in backtracking mechanism. The trouble is that it is very hard to control backtracking in PROLOG. Another problem is that due to the goal structure set in PROLOG the statements A,B: - C and B,A: - C are not equivalent. This puts an additional burden on the program generator.

The second way of generating programs is by using theorem proving. This method requires more advanced features than PROLOG has to offer. The interactive theorem prover ITP can be used and augmented for this purpose.

One difficulty is that the theorem provers are slow. This method is worth exploring, but needs more background work before it can be implemented.

VI. Data Type Validation

Data type validation is an important problem for the user. The user may want to know, for example, if the operation le defined in Figure 1. is complete (i.e., if for all natural numbers m and n le (m,n) evaluates to either T or F). In general terms the data validation problem is the following: given a set of items T together with the equations E that define them, and a property P expressed as a disjunction of equations (or inequations), does the property P follow from the set of terms T

and equations that define the data type? This problem can be seen as a particular case of theorem proving.

Handling equations is a difficult problem, and since the set of terms T is involved, we need some induction mechanism. Some theoretical results were obtained in this area ([7]) but the approach that we developed requires more background work before it can be implemented. The problem is very important and there are few tools available.

Knuth and Bendix [4] devised an algorithm for handling equations. Pelin and Gallier [6,7] expanded the algorithm to include conditional equations. They also removed some of the restrictions imposed by Knuth and Bendix.

VII. Recommendations

1. We finished implementing the skeleton of an automatic program generator which constructs programs from input/output specifications. The system can generate sorting programs from the input specifications. At this stage it can deal with lists. It can sort a list with or without eliminating duplications. It can be extended to cover the case of arrays. We would like to get the generator to output such programs as mergesort and quicksort. In order to do this the knowledge base must be expanded. More heuristics, like the ones described in [8] must be implemented.

Program modules which create a transformation space must also be built. This way, when a transformation (or sequence of transformations) T is needed which satisfies a certain property P, we can get it from that space.

Another task is to develop routines to create solution spaces for certain classes of problems. In some cases, when no strategy works, it is necessary to build a solution space and search through it.

The above topics involve some theoretical development but are basically programming tasks. It would not be difficult for a good programmer to implement many of the above concepts.

2. Another question studied was the usefulness of abstract data types in the automatic program generation process. Abstract data types provide a general method for specifying data structures that is independent of implementation. At the same time they are difficult to handle and to define both by the user and by the system. As far as the user is concerned, an interface can be built between him and the data types. He may also use the built-in tests and transformations.

The automatic program generator MODEL [9] uses such an interface. This task requires time, but the tools necessary to accomplish it are available.As far as the system is concerned, the equations that define the data type are not easy to handle. If we need to do theorem proving on abstract data types we may need induction, which is not easy to implement. The validation of the data types is another thorny problem. These problems require development on both the theoretical and the implementation level. If, however, we want to build a program from specifications, we must give precise specifications to the program generator. The abstract data types give a method for such specifications. There are programs which handle abstract data types such as REVE [5] and OBJ [2]. We can incorporate some of the methods used in those programs or we may try to use some of the constructs developed by Pelin and Gallier [7].

3. The last question addressed here is the suitability of PROLOG as a language for automatic program generation. While PROLOG has certain features that are convenient such as: backward chaining; descriptive statements; and backtracking, it also has many disadvantages. These are: inability to control backtracking; few data structures; and due to its built-in goal strategy, the order of the statements is crucial. However, we don't see any decisive advantages from switching to LISP or to PASCAL. While there are cases in which PASCAL or LISP would be more convenient, the converse is also true.

We intend to have our specifications independent of the language of the program generator. At the same time it would be interesting to investigate the construction of a program generator that generates parallel algorithms. We can modify the generator to output code in parallel PROLOG ([10]). This is a longer term project, but it is worthwhile in light of the tremendous developments that have taken place in parallel architecture.

# #

References

1. Frenkel, L., "Toward Automating the Software Development Cycle," Communications of the Association for Computer Machinery 28 (1983), pp.578-589.
2. Goguen, J. and Tardo, J., OBJ-0 Preliminary Users Manual, UCLA, Semantics and Theory of Computation Report No.10, (1977).
3. Goguen, J., Thatcher, J., Wagner, E. and Wright, J., "Initial Algebra Semantics and Continuous Algebras," Journal of the Association for Computer Machinery 24 (1977), pp.68-95.
4. Knuth, D. and Bendix, P., "Simple Word Problems in Universal Algebra," Computational Problems in Abstract Algebra, Pergamon Press (1970), pp.263-297.
5. Lescanne, P., "Computer Experiments with the REVE Term Rewriting System Generator," Proc. 10th Conference on Principles of Programming Languages, (1983).
6. Pelin, A. and Gallier, J., "Solving Word Problems in Free Algebras Using Complexity Functions," Proc. of the Conference on Automated Deduction (1984), Springer Verlag, pp.476-495.
7. Pelin, A. and Gallier, J., "Building Exact Computation Sequences," to appear in Theoretical Computer Science.
8. Pelin, A., Prabhakaran, N. and Slifker, M.: "Automatic Program Generation from Specifications" to appear in Proc. 3rd Conference on System Research, Informatics and Cybernetics.

9. Prywes, N., Shi, Y., Stymanski, B. and Tseng, J.: "Supersystem Programming with Model," Computer 19 (1986), pp.50-60.
10. Shapiro, E., "Concurrent Prolog: A Progress Report," Computer 19 (1986), pp.44-58.

1986 USAF-UES SUMMER FACULTY RESEARCH PROGRAM/

GRADUATE STUDENT SUMMER SUPPORT PROGRAM

Sponsored by the

AIR FORCE OFFICE OF SCIENTIFIC RESEARCH

Conducted by the

UNIVERSAL ENERGY SYSTEMS, INC.

FINAL REPORT

ELECTROCHEMISTRY IN ROOM TEMPERATURE MOLTEN SALT SYSTEMS

Prepared by: Bernard J. Piersma

Academic Rank: Professor of Chemistry

Department and University: Department of Chemistry, Houghton College

Research Location: The Frank J. Seiler Research Laboratory
FJSRL/NC
USAF Academy
Colorado Springs, CO 80840-6528

USAF Researcher: Dr. John S. Wilkes

Date: August 8, 1986

Contract No: F49620-85-C-0013

ELECTROCHEMISTRY IN ROOM TEMPERATURE MOLTEN SALT SYSTEMS

by

Bernard J. Piersma

ABSTRACT

Electrochemical behavior in 1-methyl-3-ethylimidazolium chloride/aluminum chloride molten salts at 25C using cyclic voltammetric, steady-state potentiostatic and rotating disk electrode techniques was investigated for several systems. Ferrocene was chosen for study since its oxidation-reduction behavior is essentially reversible and not influenced by the Lewis acidity (i.e. chloride concentration) of the melt. Compounds studied for possible electrode reactions in batteries using molten salts included CuCl and $CuCl_2$ and several sulfur compounds; sulfur, Na_2S, S_2Cl_2, and CS_2. Finally an electrochemical investigation of carbonium ion formation in neutral (equimolar amounts of MeEtImCl and $AlCl_3$) and slightly acidic (mole fraction of $AlCl_3$ greater and one half) melts was initiated with studies of 2-Cl-propane, 1-Cl-butane, 2-Cl-butane, 1-Cl-2-Methylpropane and 2-Cl-2-Methylpropane.

ACKNOWLEDGEMENTS

The author is pleased to acknowledge with appreciation the support of this research effort under the Faculty Summer Research Program by the Air Force Systems Command, Air Force Office of Scientific Research. in addition, the author wishes to acknowledge the support of AFOSR under the University Resident Research Professor Program in 1981-82 during which time much of this study was initiated. The assistance of Mr. Rodney Darrah with arrangements for the FSRP program at UES is appreciated.

The author is grateful for the direction and encouragement of Dr. John Wilkes and for helpful discussions with Lt Col Chet Dymek. The support services of Mr. Fred Kibler who always knew where to find what was needed or could make it, Mr. Jeff Boon who synthesized the MeEtImCl and purified the $AlCl_3$ and Mr. Lloyd Pflug who did the G.C. - Mass Spec. analyses are appreciated. The patience of Missy Landess with my typing requests and handwriting and the assistance of Tomi Quigley in preparing diagrams are much appreciated.

Finally, the author is thankful for the support and encouragement of his family, Pris, Ben, Jay, and Joy, for willingly accepting all the travel and changes in normal routine required for this summer program.

I. Introduction

After receiving a B.A. in chemistry from Colgate University, I studied physical chemistry at St. Lawrence University for two years, receiving an M.S. and did thesis work on chemical kinetics and mechanism studies in nonaqueous solutions. My professional training in electrochemistry was received at the University of Pennsylvania where I received the PhD degree in 1965. My thesis work with Professor J. O'M. Backris was an investigation of the electrode kinetics and mechanisms of anodic oxidation of hydrocarbons in aqueous solutions primarily using s. ady-state potentiostatic techniques. Graduate courses in electrode kinetics and the electrical double layer which I took from Prof. Bockris became the basis of his two volume work with A. N. Reddy, Modern Electrochemistry.

In order to learn about transient and perturbation techniques for studying electrochemical process and the structure of the double layer, I worked for about two years after my graduation from Penn. with Sigmund Schuldiner at the U.S. Naval Research Laboratory in Washington as a NAS-NRC Postdoctoral Resident Research Associate. For the last 15 years I have taught at a liberal arts undergraduate college in a sponsored half-time teaching, half-time research position with research interests in the stability of materials under physiological conditions and the electrochemical processes that occur at cardiac pacemaker electrodes.

For the 1981-82 school year, I was on sabbatical and recieved a grant from the USAFOSR as a University Resident Research Associate at the Frank J. Seiler Research Laboratory to study electrochemical processes in a recently developed room-temperature molten salt system. One major technical report resulted from that effort, Electrochemical Survey of Selected Cations and Electrode Materials in Dialkylimidazolium Chloroaluminate Melts.(1) Work on several other reports was not completed in my one year tenure as a URRP. A primary objective for this summer was to complete these projects.

II. Objectives of the Research Effort

The summer program was discussed with Dr. John Wilkes during the presummer trip to FJSRL in April and three project areas were outlined. These are listed below in order of priority of research effort to be expended.

A. Completion of three projects remaining from my 1981-82 URRP program at FJSRL as follows:

1. The electrochemistry of Cu(I) and Cu(II) in 1-Methyl-3-Ethylimidazolium chloroaluminate (MeEtImCl - $AlCl_3$) molten salts.

2. The electrochemistry of sulfur in MeEtImCl - $AlCl_3$ molten salts. This project was extended to include sodium sulfide, sulfur monochloride, and carbon disulfide.

3. The electrochemistry of Ferrocene in MeEtImCl - $AlCl_3$ molten salts.

These projects were to be completed by the preparation of technical reports following some experimental studies, particularly in neutral (equi-molar quantities of MeEtImCl and $AlCl_3$) melts.

B. Some novel aspects of organic electrochemistry in room temperature molten salts.

Friedel-Crafts Reactions in acidic MeEtImCl - $AlCl_3$ melts (mole fraction of $AlCl_3$ greater than one half) had been briefly explored at FJSRL.(2) Carbonium ions appeared to be stable in acidic melts but were not found in basic melts. It was suggested, from this study, that the alkylation of benzene may very likely proceed via a "σ-complex" intermediate.

We developed the following objectives:

1: To study Friedel-Crafts type reactions in neutral MeEtImCl-$AlCl_3$ melt and to determine whether carbonium ions can be electrochemically generated and detected.

2. To study the mechanisms of acylation and alkylation in neutral MeEtImCl-$AlCl_3$ melt and attempt to detect "σ-complexes" electrochemically and to identify intermediates and products.

3. To examine other reactions by adding different Lewis bases to react with carbonium ions produced in the MeEtImCl-$AlCl_3$ melts.

4. To explore other possibilities for electro-organic chemistry in the MeEtImCl-$AlCl_3$ melts.

C. Elucidation of the electrochemistry required to produce high energy density secondary batteries has continued to be a primary research objective at FJSRL. If time permitted we planned to continue

studies of specific cathode and anode reactions. The objective was to study the electrochemistry of oxidation-reduction couples, specifically Cd/Cd(II), Zn/Zn(II), and Br_2/Br^-, that may be of practical significance for the development of batteries using the room temperature MeEtImCl-$AlCl_3$ molten salt system.

III. Electrochemistry of Ferrocene in MeEtImCl-$AlCl_3$ melts.

The electrochemical behavior of Ferrocene (bis(cyclopentadienyl)iron) was examined using the techniques of cyclic voltammetry, rotating disc electrode voltammetry and steady-state potentiostatic voltammetry. Detailed studies in basic (mole fraction of $AlCl_3$ equal to 0.4) and in acidic (mole fraction of $AlCl_3$ equal to 0.6) had been completed previously (under the URRP program in 1981-82). Similar studies were made in exactly neutral melt (0.50 mole fraction of $AlCl_3$) by obtaining a maximum in the electrochemical window (about 4.0 volts) before Ferrocene was added.

A technical report has been completed and the following conclusions were reached:

A. Ferrocene undergoes a reversible one-electron process in MeEtImCl-$AlCl_3$ melts which is not influenced by the Lewis acidity of the melt. The $E_{p/2}$ potential was +0.403 ± 0.005 volts versus an aluminum wire in 0.60 melt, irrespective of the melt composition.

B. Kinetic parameters derived from cyclic voltammetric and steady-state potentiostatic measurements indicate that a step following

electron transfer is rate limiting (in the Tafel region) both for oxidation of Ferrocene and for reduction of Ferricenium ion. A mechanism is proposed which is consistent with the kinetic parameters and desorption is suggested as the rate limiting step for both oxidation and reduction.

C. Comparison of steady-state currents at a given potential in the Tafel region for Ferrocene oxidation in basic and acidic melts indicates that the reaction rate is not influenced by melt composition. The standard heterogeneous rate constnats determined from rotating disc measurements support this conclusion.

D. Ferrocene reacts chemically with acidic melts by a process that appears to be second order in Ferrocene. Ferrocene is stable in basic and neutral melts.

IV. Electrochemistry of Cu(I) and Cu(II) in MeEtImCl-$AlCl_3$ melts.

Similar experimental techniques were used to study the redox behavior of copper. Detailed studies had been completed previously in basic and acidic melts. Some measurements were made in basic and acidic melts, particularly to check on the values of diffusion coefficients, but the primary effort was to study Cu(I) and Cu(II) in exactly neutral melt. A technical report is in preparation and the following conclusions were made:

A. Cu(II) is stable in basic MeEtImCl-$AlCl_3$ melts and Cu(I) is stable in acidic MeEtImCl-$AlCl_3$ melts. In neutral and slightly acidic

melts two Cu(II) and two Cu(I) species can be detected electrochemically.

B. Cu(II) reacts chemically in neutral or slightly acidic melts by an apparent second order reaction. In more acidic melts Cu(II) is rapidly reduced to Cu(I).

C. Cu deposition was observed at all melt compositions studied. This represents an unusual case of metal deposition from basic melts.

D. Kinetic parameters for Cu(II) reduction and Cu(I) oxidation were derived and reaction mechanisms were proposed which are consistent with the measured parameters. The suggested mechanisms require strong adsorption of both Cu(I) and Cu(II) species.

E. For melt conditions under which convective diffusion limitations could be obtained (Cu(II) in basic and neutral melts), diffusion coefficients calculated were consistent with those reported for copper in other room temperature melts.

V. Electrochemistry of Sulfur, Na_2S, S_2Cl_2, and CS_2 in MeEtImCl-$AlCl_3$ melts.

No further experimental work was required for this project. Some of the data obtained previously was reanalyzed and some additional calculations were carried out. A technical report has been prepared with the following conclusions:

A. The electrochmical behavior of sulfur and sulfur compounds is significantly different in room temperature MeEtImCl-$AlCl_3$ melts than

in $NaCl-AlCl_3$ melts. Important differences are lack of solubility of Na_2S and marked irreversibility of redox behavior in the room temperature melts.

B. The presence of sulfur species in the melts extends the electrochemical windows, particularly by increasing the overpotential for aluminum deposition in acidic melts.

C. Kinetic parameters were derived and reaction mechanisms proposed for oxidation and reduction of sulfur and sulfur monochloride in neutral and acidic melts. Sulfur and S_2Cl_2 probably form similar species in the melt and undergo similar electrochemical processes.

D. Diffusion coefficients and standard heterogenous rate constants were determined for some of the sulfur species at different melt compositions.

E. Sulfur and the sulfur compounds examined here are probably not suitable as battery cathodes in $MeEtImCl-AlCl_3$ melts.

VI. Electrochemical Investigation of Carbonium Ions Formed in $MeEtImCl-AlCl_3$ Melts.

To determine whether stable carbonium ions could be formed and electrochemically detected in neutral melts, exactly 0.50 $MeEtImCl-AlCl_3$ melts were prepared by adjusting the acidity (by addition of solid $AlCl_3$ or solid MeEtImCl) until a maximum electrochemical window was obtained. Several chloroalkanes were selected (including 2-Cl-propane, 1-Cl-butane, 2-Cl-butane, 1-Cl-2-

methylpropane, and 2-Cl-2-methylpropane) to yeild carbonium ions of differing stabilities, added to solutions of neutral melt and examined for electrochemical activity by cyclic voltammetry. In general 150-200 mg of organic compoud were added to 16 g of neutral melt to yield a concentration of about 150 mM in the organic species.

After the CV (cyclic voltammetric) studies in neutral melt, the solutions were made very slighly acidic by addition of solid $AlCl_3$ and again examined by CV. Finally the acidic melts were made neutral by addition of solid MeEtImCl to determine whether carbonium ions would remain stable in neutral melt after being formed in acidic melt for those compounds which were unreactive in neutral melt.

A summary of the CV data determined from these studies is presented in Table I. We have not had sufficient time to account for the multiple cathodic and anodic peaks observed. We believe that carbonium ions are formed from 1-Cl-2-methylpropane and 2-Cl-2-methylpropane in neutral melt but not from 2-Cl-propane, 1-Cl-butane, or 2-Cl-butane. Rearrangements might be expected after carbonium ion formation and could account for some additional CV peaks, however, this area will require considerably more work. In general no oxidation peaks were observed until after reduction occured, which would be expected of carbonium ions.

Previous work at FJSRL(2) demonstrated that alkylated benzenes were produced by reactions with several chloroalkanes. We added benzene to neutral melt containing 2-Cl-2-methylpropane and observed its effect on the CV curves. The cathodic peak at -1.35 V disappeared on addition of

benzene (approximately 150 mM benzene added), with no other changes over a four hour period. When an additional amount of benzene was added (approximately five times the amount of 2-Cl-2-me-propane) the cathodic peak at -1.03V also disappeared. This work should be followed up with product-analysis studies to verify that benzene is in fact reacting with carbonium ions.

No additional CV peaks were observed with the addition of benzene to 2-Cl-2-me-propane in neutral melt, thus our initial attempts to electrochemically detect "σ-complexes" was not successful. We did, however, as noted previously, observe an effect of benzene addition on the CV curves, which might suggest that "σ-complexes" formed in this case are not electrochemically active. More work is necessary at this point.

VII. Recommendations

A. The study of copper in neutral melt led to the conclusion that two Cu(I) species and two Cu(II) species were present. It would be of interest to attempt to identify these species, e.g., Cu(I) can be examined by NMR spectroscopy. This could be important to help establish the proposed mechanisms for the oxidation-reduction processes.

B. Organic electrochemistry in room temperature molten salts is a virtually unexplored area. We have seen that chloroalkanes give multiple reduction and oxidation CV peaks in neutral melts, presumably due to carbonium ion formation by removal of the chloride ion. More

work should be done to identify these species that undergo reduction and oxidation.

C. Several chloroalkanes, with selection partly based on availability at the lab, were examined with the intent of producing carbonium ions of different stabilities. Some differences were observed, e.g., 2-Cl-2-methylpropane developed considerable electrochemical activity in neutral melt while the other compounds studied did not. It would be of interest to look at another series of chloroalanes under carefully controlled conditions of melt acidities which could give a wider range of carbonium ion stabilities. I recommend a study of the eight isomers of chloropentane in neutral and slightly acidic MeEtImCl-$AlCl_3$ melts.

D. Friedel-Crafts acylation reactions were reported(2) and one of our objectives was to examine the proposed mechanism for acylation of benzene. We were able to observe some effect of the addition of benzene on the CV curves for 2-Cl-2-Me-propane in neutral melt, presumably due to formation of a "σ-complex." Our brief look indicates that further work along this line cold be very helpful in establishing the proposed reaction mechanism. The use of several substrates to form different "σ-complexes" could be very helpful.

E. Time did not permit an investigation of the scope of reactions that could be carried out in the MeEtImCl-$AlCl_3$ melts. It is recommended that a research effort be continued in this area.

F. Objective 3 under section II is important to the mission of FJSRL, but time did not permit any work in this area. Research is

definitely needed in this area for the development of high energy density batteries, and it is strongly recommended that priority be placed in this area.

REFERENCES

1. Piersma, B. J. and Wilkes, J. S., FJSRL-TR-82-0004, September 1982.

2. Boon, J. A.; Levisky, J. A.; Pflug, J. L.; and Wilkes, J. S., J. Organic Chemistry, 51, 480 (1986).

3. Luer, G. D. and Bartak, D. E., J. Organic Chemistry, 47, 1238 (1982).

TABLE I

Solution	Cathodic Peaks			Anodic Peaks			Notes
	$E_{p,c-1}$	$E_{p,c-2}$	$E_{p,c-3}$	$E_{p,a-1}$	$E_{p,a-2}$	$E_{p,a-3}$	
1. 2-Cl-Propane/ slightly acidic melt	-0.40V	-0.80V	-1.65V	--	--	--	A
2. 2-Cl-Propane/ 0.50 (after being acidic)	--	-0.85	-1.60	--	--	--	B
3. 1-Cl-Butane/ slightly acidic melt	-0.33	-1.58	-1.68	1.23	1.53	--	C
4. 1-Cl-Butane/ 0.50 (after being acidic)	-0.35	-1.58	--	1.21	1.58	--	D
5. 2-Cl-Butane/ slightly acidic melt	-0.33	-1.50	--	1.20	1.58	--	E
6. 2-Cl-Butane/ 0.50 (after being acidic)	-0.35	-1.10	--	1.20	1.58	--	F
7. 1-Cl-2-Me-Propane/ 0.50 melt	--	-1.0	--	--	--	--	G

TABLE I (Cont.)

8. 1-Cl-2-Me-Propane/ slightly acidic melt	--	-1.80	-1.50	--	--	--	H
9. 1-Cl-2-Me-Propane/ (after being acidic)	--	-1.50	--	--	--	--	I
10. 2-Cl-2-Me-Propane/ 0.50 melt	-0.32	-0.99	-1.55	1.23	1.61	1.84	J
11. 2-Cl-2-Me-Propane/ slightly acidic melt	-0.35	-1.00	-1.55	1.11	1.55	--	K
12. 2-Cl-2-Me-Propane/ 0.50 (After being acidic)	-0.32	-1.03	-1.35	1.20	1.56	1.75	L
Triphenyl methyl chloride/ 0.52 BPC (Luer & Bartak)-3	+0.10	--	--	0.17	0.85	2.1	

Notes:

A: No redox behavior in 0.50 melt. $E_{p,c-1}$ is a shoulder on peak $E_{p,c-2}$. Al deposition at ~-0.75V and Al stripping at -0.13V.

B: No oxidation observed.

TABLE I (Cont.)

C: No redox behavior in 0.50 melt. $E_{p,c-1}$ has a shoulder at -0.20V. Al deposition at -0.7V and Al stripping at +0.03V.

D: $E_{p,c-1}$ has a shoulder at -0.20V. Anodic peaks are not present without prior reduction.

E: No redox behavior in 0.50 melt. $E_{p,c-1}$ has a shoulder at -0.20V. Al deposition at -1.35V and Al stripping at 0.00V.

F: Oxidation current anodic to $E_{p,a-2}$ but no defined peaks.

G: Product at $E_{p,c-2}$ is irreversibly absorbed, and with continued cycling, $E_{p,c-2}$ varies from -1.0 to -1.35V. No anodic peaks observed.

H: Position and height of cathodic peaks are very dependent on melt acidity. No oxidation observed.

I: No oxidation observed.

TABLE I (Cont.)

J: Anodic peaks are not present without prior reduction. After ~24 hours, the anodic peak $E_{p,a-3}$ is not present.

K: Anodic peaks are not present without prior reduction.

L: There is an additional anodic peak before $E_{p,a-1}$ at 0.95V.

1986 USAF-UES SUMMER FACULTY RESEARCH PROGRAM/

GRADUATE STUDENT SUMMER SUPPORT PROGRAM

Sponsored by the

AIR FORCE OFFICE OF SCIENTIFIC RESEARCH

Conducted by the

UNIVERSAL ENERGY SYSTEMS, INC.

FINAL REPORT

EFFECTS OF ACCELERATION STRESS UPON BLOOD LIPID LEVELS

Prepared by:	Leonard Price, Ph.D.
Academic Rank:	Professor
Department and	Department of Chemistry
University:	Xavier University of Louisiana
Research Location:	USAF School of Aerospace Medicine, Brooks AFB, TX, Clinical Sciences Division, Clinical Pathology Branch
USAF Researcher:	Dr. Harvey A. Schwertner
Date:	July 25, 1986
Contract No:	F49620-85-C-0013

EFFECTS OF ACCELERATION STRESS UPON BLOOD LIPID LEVELS

BY

LEONARD PRICE

ABSTRACT

Serum total cholesterol and triglyceride concentrations of two individuals were measured after daily exposures to high gravitational forces (+Gz) simulating aerial combat maneuvers. The post-acceleration cholesterol levels were significantly higher (40-95%) than the normal resting levels. Serum cortisol levels were higher than the resting levels. This agrees with previous studies which have shown significant increases in serum cortisol levels after acceleration stress. Cortisol and total cholesterol values were significantly correlated ($r = 0.614$, $p < 0.05$) in one of the individuals of this study. Since cortisol is a hormone which influences lipid metabolism, there may be a causal relationship between the increased cortisol levels produced by acceleration stress and increased lipid levels. The lipid levels in the two subjects after acceleration exceeded the 90th percentile for the population as a whole. As such, they could be at high risk for subsequent coronary heart disease if they are exposed to high G-forces on a frequent basis.

An ancillary study was conducted to develop an electrophoretic method to rapidly separate and quantitate serum high density lipoprotein (HDL) subfractions HDL_2 and HDL_3. Serum levels of one of these subfractions may be a better predictor of coronary heart disease than total cholesterol. Serum α-lipoproteins isolated by affinity chromatography were separated into a number of subfractions by polyacrylamide gel electrophoresis. These subfractions were marked by the usual lipoprotein stains, and by filipin, a fluorescent, naturally occurring antibiotic which, reportedly, binds specifically to cholesterol. Identification and quantification of these HDL subfractions remain to be accomplished.

ACKNOWLEDGMENTS

I would like to thank the Air Force Systems Command and the Air Force Office of Scientific Research for sponsorship of this research. Special thanks to Dr. Harvey Schwertner, my Effort Focal Point, for his generous assistance and guidance. I would like to also thank personnel of the Acceleration Effects Laboratory, Crew Technology Division, the Clinical Radioassay Function, Epidemiology Division, and the Lipids Evaluation Function, Clinical Sciences Division for their support in this research.

I. INTRODUCTION.

I received the Ph.D. degree in chemistry (organic) from Notre Dame University in 1962. I studied and conducted research in biochemistry at Rice University (1968-69), Louisiana State University Medical School (1977), and at Tulane University Medical Center (Summers 1981, 1982, 1983). In addition, I have taught university organic chemistry for 25 years, biochemistry for 15 years, and performed research in a wide range of areas including organic synthesis, biochemical analysis and mechanisms.

II. OBJECTIVES OF THE RESEARCH EFFORT.

Pilots flying high-performance aircraft are repeatedly exposed to high sustained G-forces during aerial combat maneuvers. Since both cortisol and physical stress are elevated during high G-forces, and since both cortisol and physical stress have been shown to be associated with elevated lipids levels (1), we sought to determine if lipid levels are elevated in subjects exposed to high G-forces. In addition, we measured serum cortisol concentrations in order to determine if the cholesterol increases are related to the increases in this particular stress hormone.

A complementary goal of this research was to develop an electrophoretic method to rapidly separate serum high density lipoproteins (HDL) into HDL_2 and HDL_3 subfractions, and to rapidly quantitate HDL_2 and HDL_3 cholesterol in these subfractions. The measurement of serum HDL_2 cholesterol may be a better indicator of coronary heart disease than total HDL (2).

To accomplish these goals, the following objectives were established:

1. Obtain serum samples from individuals prior to and after their exposure to an established protocol of daily +Gz accelerations simulating aerial combat maneuvers.
2. Determine serum cortisol and total serum cholesterol in these serum samples and determine whether the cholesterol levels are related to the cortisol levels. Also, determine whether they increase with increase in G-force.
3. Separate serum high density lipoproteins (HDL) from other serum lipoproteins, and develop an electrophoretic technique to separate the HDL into subfractions HDL_2 and HDL_3. Identify the HDL subfractions with lipid stains or with fluorescent filipin which has been reported to bind specifically to cholesterol (3).

III. +Gz ACCELERATION PROTOCOL AND ANALYTICAL METHODOLOGY.

As part of an ongoing, independent study, two military volunteers were subjected to daily +Gz acceleration on the human centrifuge for a one week training period and for a two week test period. The acceleration protocol included the drawing of a pre-acceleration fasting blood sample on Monday morning prior to acceleration exposure. On Monday, Wednesday, and Friday, volunteers were exposed, unprotected, to rapid and gradual onset of +Gz acceleration to the maximum tolerable +Gz level (4.5-9G). On Tuesday and Thursday, they were exposed, but protected, to more exhaustive aerial combat maneuvers (SCAM, 4.5-9G) and were required to perform specific tracking tasks.

A post-acceleration blood sample was withdrawn from each subject about 15 minutes after each acceleration period. Serum samples were stored at -20°C (about 3 weeks) until analyzed for total cholesterol, triglyceride, and cortisol concentrations. Serum cortisol concentrations were determined by radioimmunoassay. Cholesterol and triglyceride levels were determined by enzymatic methods.

IV. SERUM CORTISOL, CHOLESTEROL, AND TRIGLYCERIDE LEVELS AFTER EXPOSURE TO +Gz ACCELERATION.

In the first subject, a 40-year-old male, serum cholesterol levels increased from a normal 158 mg/dl to 281 mg/dl (approximately 78%) after exposure to +Gz acceleration. The cholesterol remained elevated for the duration of the experiment (Table 1, Fig.1). These elevations are the likely result of the chronic daily exposure to +Gz forces, and are the first reported observations of a rise in serum cholesterol associated with +Gz acceleration. The cortisol levels also appear to be elevated in the first subject, however, cortisol baseline levels were not taken prior to G-force exposure. Previous studies (4, 5) however, have shown that increases in cortisol levels do occur as a result of +Gz acceleration. More importantly, a statistically significant correlation ($r = 0.614$, $n = 11$, $p < 0.05$) was found to exist between cortisol and cholesterol concentrations (Fig. 3). Triglyceride concentrations were also elevated, but varied widely.

The second subject also had elevated cholesterol levels, however, the increases were less pronounced than for the first subject. With this subject, the cholesterol concentration increased from a baseline value of 148 mg/dl to 186 mg/dl after the first acceleration test. The cholesterol values remained

elevated through the completion of the experiment, but were less variable than the values for the first subject (Table 1, Fig. 2). The cortisol levels were also lower than for the first subject. Even though the cortisol and cholesterol levels were elevated after exposure to +Gz forces, there was no significant correlation between them. The differences in absolute cholesterol values between the two subjects could be due to age differences (40 versus 21). Some of the differences in could also be due to the fact that some individuals can tolerate stress and others cannot. In other words, some individuals can be classified as responders and others respond to a lesser extent.

V. ELECTROPHORETIC DETERMINATION OF SERUM HIGH DENSITY LIPOPROTEIN (HDL) SUBFRACTIONS HDL_2 AND HDL_3.

Electrophoretic methods were examined for the purpose of developing a rapid clinical method for the analysis of HDL subfractions. Serum samples were fractionated into α-lipoprotein (HDL) and β-lipoprotein (LDL) components with commercially prepared heparin-agarose affinity chromatography columns (Isolab, Inc.). The HDL component was subjected to a number of electrophoretic techniques to separate, identify, and quantitate its subfractions.

A. Agarose Gel Electrophoresis.

Agarose gel electrophoresis has been used to separate serum lipoproteins into patterns showing two lipoprotein bands in the "α zone" of the electrophoretogram (10). The bands were not identified as HDL subfractions. However, we conducted a number of agarose gel electrophoretic analyses of total serum samples and HDL and LDL components isolated by affinity chromatography. Various slab agarose gel plates (0.3 to 2% agarose in Tris barbital buffer, pH 8-9) about 3 mm thick were prepared. Before electrophoresis, serum or lipo-

protein samples were mixed with lipid pre-stains or the fluorescent, natural product filipin, which supposedly binds specifically to cholesterol-containing lipoproteins. The electrophoresis was conducted in closed horizontal chambers in the Tris buffer for 1-2 hours at a constant voltage of 5-6 V/cm. Lipid stained and filipin-treated electrophoretic patterns of α-lipoproteins gave only a single broad band in the HDL region, and even a broad band in the LDL region, which indicates that affinity columns only partially purified the α fraction. We checked the effects of pH between 7.2 and 8.6. In general, the lower pH resulted in slower lipoprotein migration.

B. Polyacrylamide Gel Electrophoresis.

In the polyacrylamide gel studies, a wide range of parameters were modified. The concentration of the acrylamide as well as the degree of cross-linking has been found to be critical. In general, the higher the degree of cross-linking the greater the number of HDL subfractions. A polyacrylamide concentration of 5% with 0.04% cross-linking, and 0.1M sodium phosphate buffer (pH 7.2) gave best resolution of HDL bands. Filipin-treated serum samples were also electrophoresed in slab and tube polyacrylamide gels. However, filipin has not proven to be specific for cholesterol-containing lipoproteins, since fluorescence has appeared in the zone where albumin is expected.

C. Lipid and Lipoprotein Stains.

We have evaluated a number of lipid staining reagents for specificity and sensitivity. Those studied were Sudan Black, Oil Red-O, and filipin. Filipin has been used in anatomical pathology as a fluorescent, cholesterol specific stain. This is the first time it has been used for quantification of lipoprotein cholesterol levels. In these studies, Sudan Black was found to be more specific than Oil-Red-O in that it did not bind to albumin. Filipin

appeared to have sensitivities equal to that of Sudan Black. Some tests were also made to use cholesterol oxidase reagents to specifically stain the lipoprotein cholesterol. This is perhaps the most specific stain.

VI. RECOMMENDATIONS.

In this study, we have shown that exposure to high G-force results in significant increases in cholesterol and triglyceride. In addition, we have provided some evidence that the lipid increases could be the result of increased cortisol levels which accompany the intense physical stress of acceleration. The cholesterol levels of the two subjects studied here had cholesterol levels which exceeded the 90th percentile for their age bracket. With such levels, they are in the high risk group for developing coronary disease.

Since this study involved only two subjects, we feel that further studies should be performed in order to determine whether other individuals exposed to G-forces also experience elevated levels of serum cortisol and cholesterol, and whether there is significant correlation between the two levels.

Since the human centrifuge is capable of producing exact quantifiable levels of G-force, we recommend that further studies be conducted which more closely show the association between G-force, stress intensity, cholesterol concentration, and cortisol concentration. The study would not only have important health implications for pilots of high performance aircraft, but would also be of importance to the population as a whole. Studies identifying changes in individual lipoproteins would also be important, as would studies of other lipid fractions such as the free fatty acids. Other endocrine hormones besides cortisol should also be examined.

It is also recommended that serum high density lipoprotein (HDL), and subfractions HDL_2 and HDL_3 concentrations be determined before and after subjects are exposed to +Gz acceleration. It should be of interest to determine which lipoprotein component is responsible for the observed increases in total serum cholesterol. Studies have suggested that cholesterol associated with these lipoproteins are better indices of the risk of coronary heart disease than total cholesterol (6-9).

Efforts to separate and identify serum high density lipoproteins into subfractions HDL_2 and HDL_3 should continue. Various electrophoretic techniques have been employed, but results have not been consistent. Cellulose acetate electrophoresis on pre- or post-stained slides did not prove promising. Polyacrylamide gel electrophoresis (slabs or tubes) of chromatographically prepared α-lipoproteins produced a number of lipoprotein fractions. Results varied with pH, concentration and degree of cross-linking of the gel. The effect of higher pH (abaove pH 8) upon resolution of HDL subfractions should be explored. There should also be an examination of the effect of pre-staining upon the separation of HDL into subfractions. Pre-staining may alter migration rates of lipoproteins and, thus, impede their resolution. Finally, an attempt should be made to resolve the α-lipoprotein fraction (isolated on an affinity column) by high performance liquid chromatography (HPLC). This method would permit the evaluation of several parameters in the effectiveness of resolving HDL subfractions.

TABLE 1. SERUM CORTISOL, CHOLESTEROL, AND TRIGLYCERIDE LEVELS OF SUBJECTS EXPOSED TO +Gz ACCELERATION

NO.	DATE	DAY	IDENTIFICATION	TOTAL CHOLESTEROL	CORTISOL	TRIGLYCERIDE
0	---	---	Pre-G Baseline	158	---	---
1	5-5-86	Monday	PGB-1G-11 Baseline	281	23.3	206
2	5-5-86	Monday	PGB-1G-11 Post G	294	22.3	223
3	5-7-86	Wednesday	PBG-1G-13 Post G	274	16.7	156
4	5-8-86	Thursday	PBG-1G-14 Post G	241	16.2	307
5	5-9-86	Friday	PBG-1G-15 Post G	252	12.3	117
6	5-12-86	Monday	PBG-1G-21 Baseline	281	17.8	332
7	5-12-86	Monday	PBG-1G-21 Post G	294	19.4	208
8	5-13-86	Tuesday	PBG-1G-22 Post G	277	22.2	238
9	5-14-86	Wednesday	PBG-1G-23 Post G	229	12.5	226
10	5-15-86	Thursday	PBG-1G-24 Post G	234	15.6	163
11	5-16-86	Friday	PBG-1G-25 Post G	273	10.3	273
00	---	---	Pre-G Baseline	148	---	62
12	6-2-86	Monday	PBG-2G-31 Baseline	186	12.3	102
13	6-2-86	Monday	PBG-2G-31 Post G	195	16.6	301
14	6-3-86	Tuesday	PBG-2G-32 Post G	194	6.8	113
15	6-4-86	Wednesday	PBG-2G-33 Post G	195	8.7	198
16	6-5-86	Thursday	PBG-2G-34 Post G	185	-	160
17	6-6-86	Friday	PBG-2G-35 Post G	180	9.4	159
18	6-9-86	Monday	PBG-2G-41 Post G	199	11.0	108
19	6-10-86	Tuesday	PBG-2G-42 Post G	205	13.8	240
20	6-12-86	Thursday	PBG-2G-43 Post G	185	-	95
21	6-13-86	Friday	PBG-2G-44 Post G	175	-	296
22	6-13-86	Friday	PBG-2G-45 Post G	170	12.3	179

a See test for +Gz acceleration protocol. Statistical comparison between serum cortisol and total cholesterol: First subject, $n = 11$, $r = 0.6138$, $p < 0.05$; Second subject, $n = 8$, $r = 0.103$, insignificant.

b mg/dl.

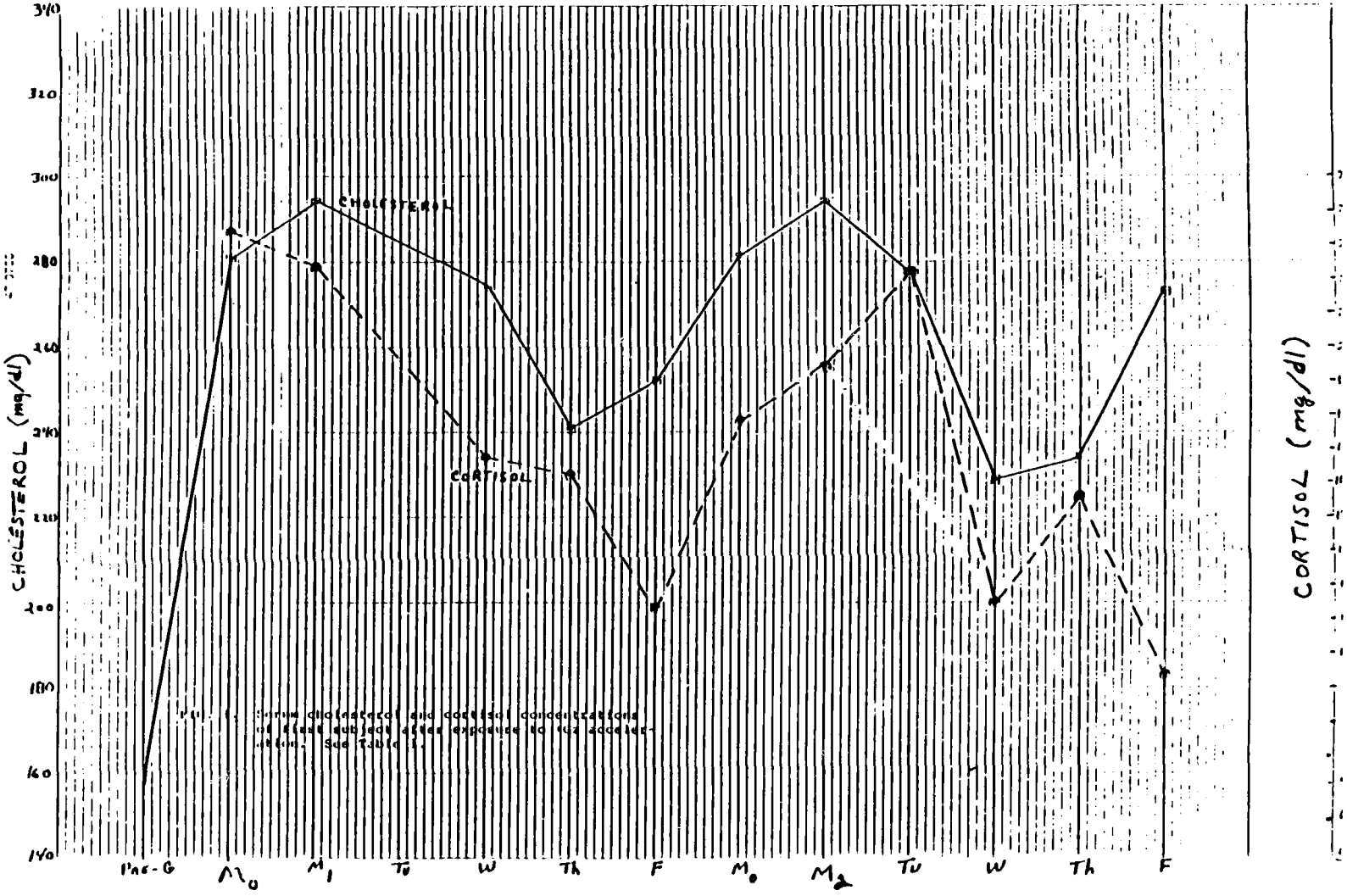

Fig. 1. Serum cholesterol and cortisol concentrations of female subject after exposure to ice accident. See Table 1.

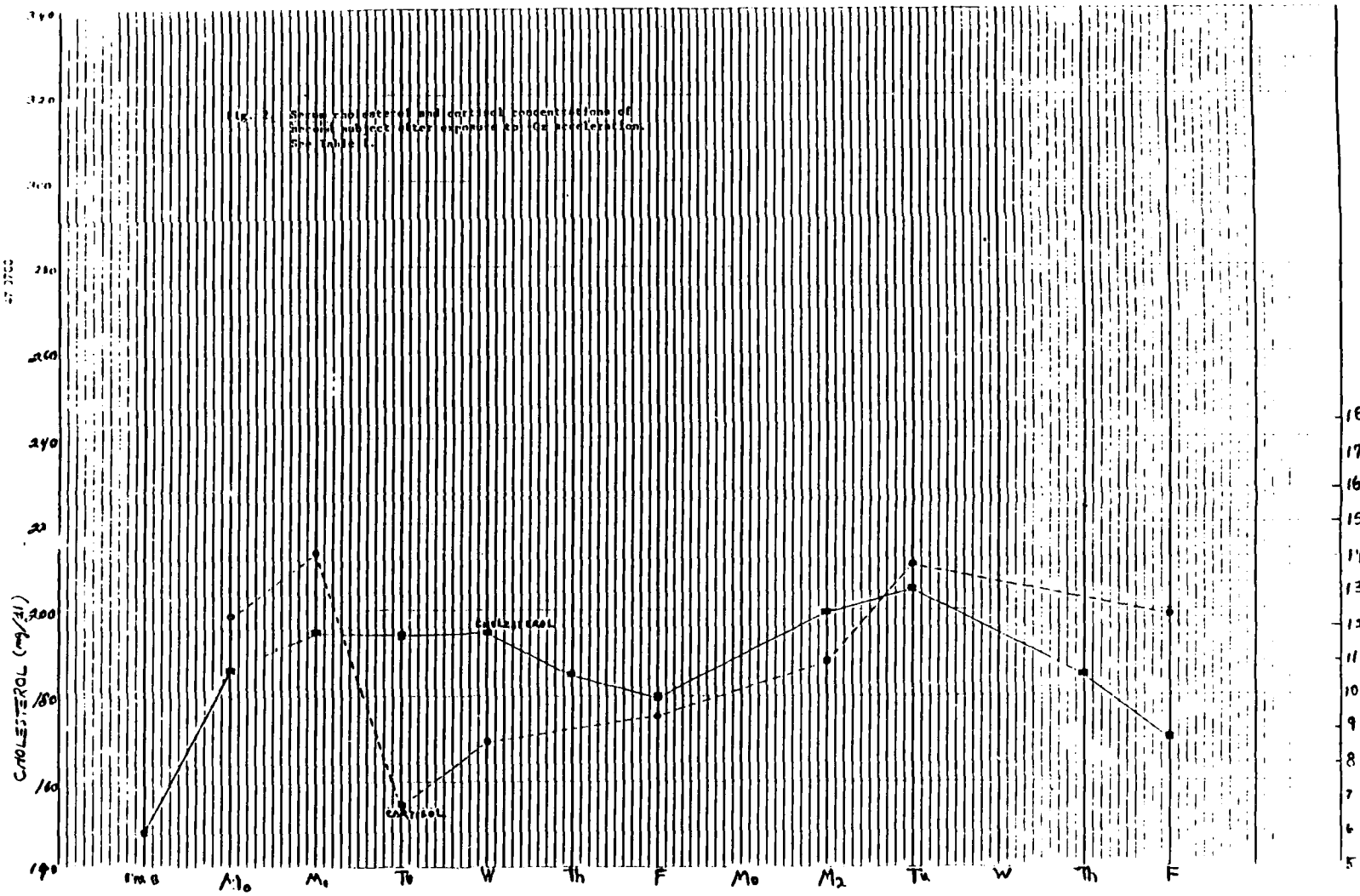
CHOLESTEROL (mg/dl)
CORTISOL (mg/dl)
CHOLESTEROL
CORTISOL
Pre-G
M10
M1
T6
W
Th
F
M8
M12
Tu
W
Th
F

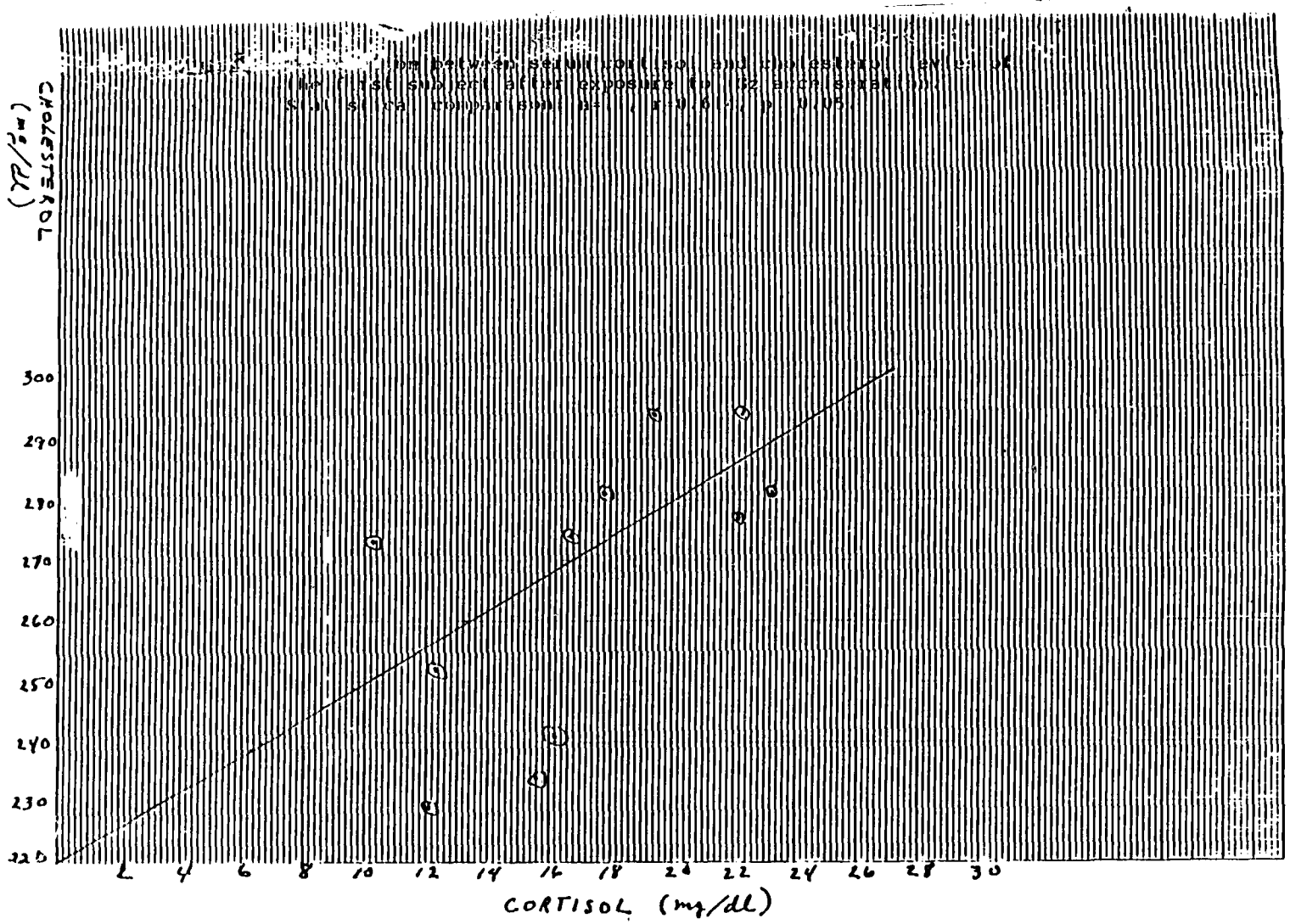
CHOLESTEROL (mg/dl)
300
290
280
270
260
250
240
230
220
2
4
6
8
10
12
14
16
18
20
22
24
26
28
30
CORTISOL (mg/dl)

REFERENCES

1. Schwertner, H.A. and Torres, Linda, et. al., Clinical Sciences Division, USAF School of Aerospace Medicine, Brooks AFB, Texas 78235-5000.

2. Miller, N.E. and Hammett, F., "Relation of Angiographically Defined Coronary Artery Disease to Plasma Lipoprotein Subfractions and Apolipoproteins," British Medical Journal, 282 (1981) 1741-44.

3. Howard, S.K., "Platelet-Mediated Cholesterol Accumulation in Cultured Aortic Smooth Muscle Cells," Science, 227 (1985) 1243-45.

4. Mills, F.J. and Marks, V., "Human Endocrine Responses to Acceleration Stress," Aviation, Space, and Environmental Medicine, 53 (1982) 537-40.

5. Vernikos-Danellis, J. and Dallman, M.F., "Hormonal Indices of Tolerance to +Gz Acceleration in Female Subjects," Aviation, Space, and Environmental Medicine, 49 (1978) 886-89.

6. Gordon, T., Castelli, et. al., "High Density Lipoprotein as a Protective Factor Against Coronary Heart Disease," American Journal of Medicine, 62 (1977) 707-14.

7. Kannel, W.B., et. al., "Cholesterol in the Prediction of Atherosclerotic Disease. New Perspectives Based on the Framingham Study," Ann. Intern. Med., 90 (1979) 85-91.

8. Tan, M.H., et. al., "Serum High Density Lipoprotein Cholesterol in Patients with Abnormal Coronary Arteries," Atherosclerosis, 37 (1980) 187-8.

9. Miller, N.E., et. al., "Relation of Angiographically Defined Coronary Artery Disease to Plasma Lipoprotein Subfractions and Apolipoproteins," Clinical Chemistry, 282 (1981) 1741-43.

10. Papadopoulos, N.M. and Kintzios, J.A., "Determination of Human Serum Lipoprotein Patterns by Agarose Gel Electrophoresis," Annl. Biochem, 30, (1969) 421-26.